

(200)

R290

no. 81-355



3 1818 00070416 1

PROCEEDINGS OF THE SYMPOSIUM ON MINERAL DEPOSITS OF THE
PACIFIC NORTHWEST

GEOLOGICAL SOCIETY OF AMERICA, CORDILLERAN SECTION MEETING
AT CORVALLIS, OREGON, MARCH 20-21, 1980

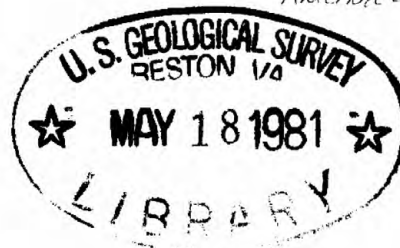
Edited by

Miles L. Silberman, Cyrus W. Field, and Anne L. Berry

U.S. Geological Survey

Open-File Report

81-355



313-113

This report is preliminary and has not been
reviewed for conformity with U.S. Geological Survey
editorial standards.

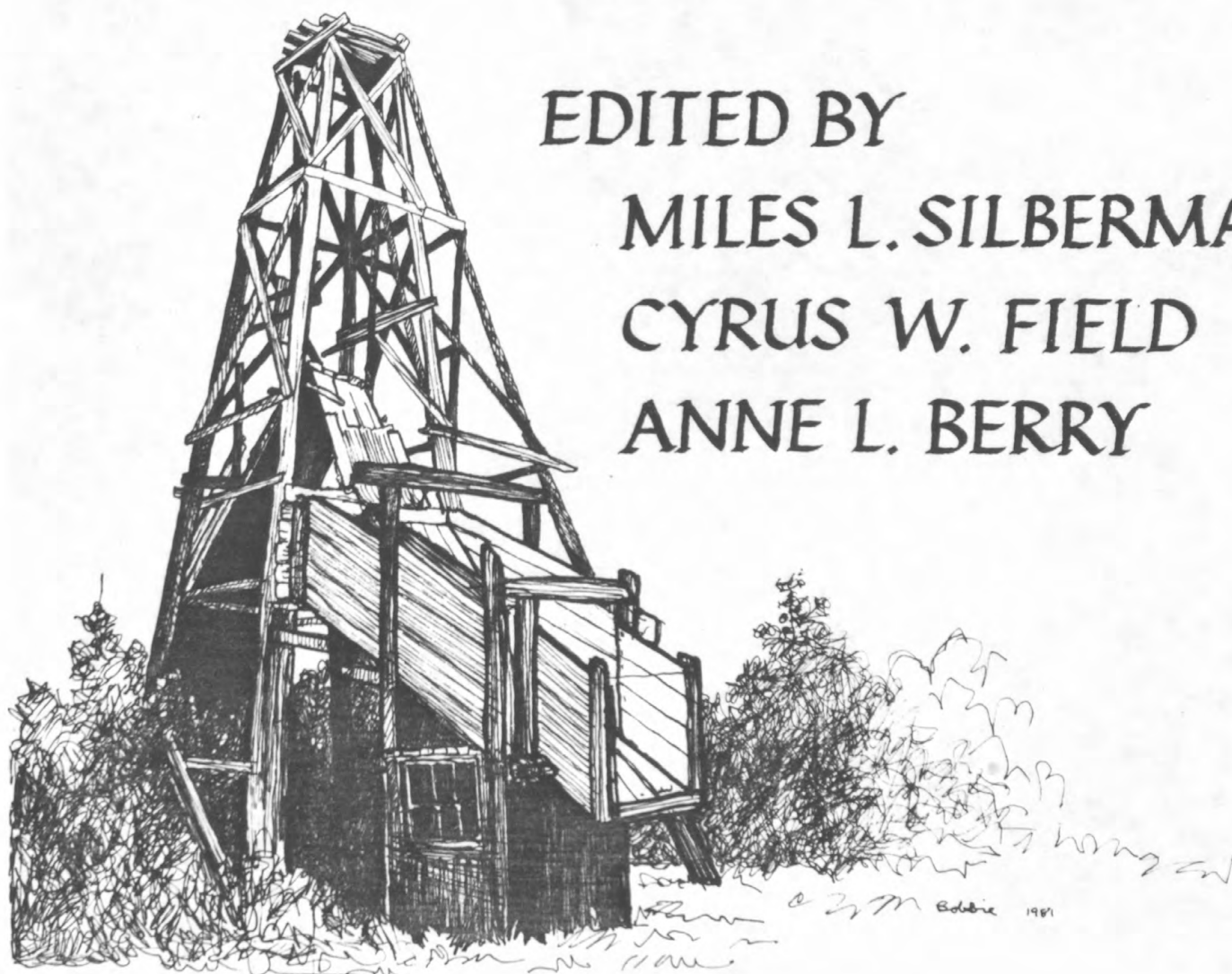
**PROCEEDINGS
OF THE SYMPOSIUM ON
MINERAL DEPOSITS
OF THE
PACIFIC NORTHWEST – 1980**

EDITED BY

MILES L. SILBERMAN

CYRUS W. FIELD

ANNE L. BERRY



INTRODUCTION

The following collection of 29 papers and abstracts was presented at a symposium on Mineral Deposits of the Pacific Northwest. This symposium consisted of four one-half day sessions held in conjunction with the 1980 Cordilleran Section meeting of the Geological Society of America at Oregon State University in Corvallis, Oregon. These papers and abstracts cover a broad spectrum of detail and breadth over a geologically complex terrain that extends from California northward through British Columbia to northwestern Alaska. Although the central theme was invariably concerned with metallization, the scientific emphasis varied appreciably according to the professional interests of the individual contributors. This emphasis not only included traditional geologic studies ranging from detailed investigations of single ore deposits, or of mining districts, to large-scale regional syntheses, but also of topical considerations such as geochronology, geophysics, geothermometry, mineralogy and phase equilibria, petrochemistry, plate tectonics, and radiogenic and stable isotope geochemistry that are relevant to processes of ore genesis as well as to potentially useful methods of exploration. Among the specific types of mineral occurrences considered were epithermal and mesothermal deposits of mercury and precious metals; contact metasomatic deposits of molybdenum, tungsten, and base metals; placer gold; porphyry-type deposits of copper and molybdenum; strata-bound deposits of uranium and base and precious metals; and volcanogenic massive sulfide deposits.

Several contributors attempt to relate the occurrences of specific types of mineral deposits to tectonic domains or to type and evolution of associated magma systems, and two others attempt to summarize genetic implication of the distributions of skarn and strata-bound types of mineral deposits throughout the western United States. Mineral deposits of hydrothermal origin clearly served as an unintentional theme to this symposium, as underscored by the paper concerning The Geysers geothermal area of west-central California. This apparent metallogenetic "excess" is attributable to the cordilleran locale of the Pacific Northwest, and not to editorial bias exercised by the co-conveners of this symposium.

The participants of this symposium, both the contributors and the audience, represented a cross-section of the geologic profession that is concerned with mineral deposits, and with interests ranging from esoteric considerations of ore genesis to the more pragmatic considerations of exploration. They were comprised of members from the academic, governmental, and industrial sectors, and in many cases their contributions were co-authored by individuals from two or more of these communities. As co-conveners of this symposium, we are particularly gratified at the response given to these technical sessions, both from the contributors and from the audience, which numbered more than 300. In order to make these papers and abstracts available without an intolerably long delay, we decided at an early date to publish them collectively as a U.S. Geological Survey Open-File Report. We selected this semiformal method of publication to expedite the printing and distribution of these papers because of the timely

nature of many of these contributions that are in rapidly advancing fields of study.

We wish to express our sincere thanks to the organizers of the Cordilleran Section meeting in Corvallis, Oregon; especially to co-chairmen George H. Keller and Robert S. Yeats of the local committee and E. Julius Dasch and Erwin Suess of the technical program, for providing the opportunity and assistance that enabled us to convene this symposium. We gratefully acknowledge the able assistance of John Derr, of the staff of technical reports unit of the U.S. Geological Survey in Menlo Park, California, for the assembly of this volume with a minimum of delay or difficulty. Lastly, we wish to extend our sincerest appreciation to the contributors of this volume, both for the high quality of their presentations at the symposium and for their cooperation in meeting the deadlines of manuscript submittal. The success of this volume is directly the result of our contributors and of those who have assisted us in this publication effort.

Miles L. Silberman
U.S. Geological Survey
345 Middlefield Road
Menlo Park, California 94025

Cyrus W. Field
Department of Geology
Oregon State University
Corvallis, Oregon 97331

Anne L. Berry
U.S. Geological Survey
345 Middlefield Road
Menlo Park, California 94025

TABLE OF CONTENTS

1. Isotopic geochemistry of stratiform zinc-lead-barium deposits, Red Dog Creek and Drenchwater Creek areas, northwestern Brooks Range, Alaska-----I. M. Lange, W. J. Nockleberg, J. T. Plahuta, H. R. Krouse, B. R. Doe, Uldis Jansons	1
2. Geology of the BT Claim Group, southwestern Brooks Range, Alaska -----M. W. Hitzman	17
3. Magnetic expression and mineralization of some Tertiary plutons of Prince William Sound and the Alaska Peninsula, southern Alaska (abs.)-----J. E. Case	29
4. Geology update of the Quartz Hill molybdenum property near Ketchikan, Alaska (abs.)-----P. R. Smith	31
5. Genesis of gold vein mineralization in an Upper Cretaceous turbidite sequence, Hope-Sunrise district, southern Alaska-----P. A. Mitchell, M. L. Silberman, J. R. O'Neil	33
6. Kennecott-type copper deposits, Wrangell Mountains, Alaska--an update and summary (abs.)-----E. M. MacKevett, Jr., A. K. Armstrong, R. W. Potter, II, M. L. Silberman	50
7. Metallogenic and tectonic significance of oxygen isotope data and whole-rock potassium-argon ages of the Nikolai Greenstone, McCarthy quadrangle, Alaska-----M. L. Silberman, E. M. MacKevett, Jr., C. L. Connor, Alan Matthews	52
8. Placer gold deposits, Mt. Hayes quadrangle, Alaska-----Warren Yeend	74
9. Rock geochemistry, geology and genesis of the Guichon Creek batholith in British Columbia, Canada, as it relates to Highland Valley ore deposits-----W. J. McMillan, Z. Johan	84
10. Geology, petrology, and geochemistry of the Jersey, East Jersey, Heustis, and Iona porphyry copper-molybdenum deposits, Highland Valley, British Columbia-----J. A. Briskey, C. W. Field, J. R. Bellamy	106
11. The Island copper porphyry copper-molybdenum deposit, Vancouver Island, British Columbia (abs.)-----P. L. Fahey	127
12. Lead isotope models for the genesis of carbonate-hosted Zn-Pb, shale-hosted Ba-Zn-Pb, and silver-rich deposits in the northern Canadian Cordillera-----C. I. Godwin, A. J. Sinclair, B. D. Ryan	129

13.	Possible nonsubduction associated porphyry ore deposits, Pacific Northwest-----T. L. Robyn, L. F. Henage, V. F. Hollister	153
14.	Geology and ore deposits of the St. Helens mining district, Washington (abs.)-----R. P. Ashley, R. C. Evarts	166
15.	Geology and mineralization of the Washougal mining district, Skamania County, Washington-----Alexander Shreiner, Jr., R. J. Shepard	168
16.	New concepts of regional geology and uranium exploration in northeastern Washington-----E. S. Cheney	176
17.	Hydrothermal alteration and mineralization at the Blackbutte mercury mine, Lane County, Oregon-----R. E. Derkey	188
18.	Volcanogenic massive sulfide deposits in ocean-crust and island-arc terranes, northwestern Klamath Mountains, Oregon and California-----R. A. Koski	197
19.	The Silver Peak volcanogenic massive sulfide, northern Klamath Mountains, Oregon-----R. E. Derkey	213
20.	Kuroko type mineralization at the Red Ledge deposits, Idaho-----A. P. Juhas, T. P. Gallagher	223
21.	Kuroko type copper-gold mineralization at the Iron Dyke mine, Oregon-----A. P. Juhas, P. S. Freeman, R. S. Fredericksen	236
22.	Geology of the Little Boulder Creek deposit, Custer County, Idaho (abs.)-----J. C. Balla, R. G. Smith	246
23.	Stratiform mineralization and origin of some of the vein deposits, Bunker Hill mine, Couer d'Alene district, Idaho-----M. R. Vulimiri, E. S. Cheney	248
24.	Stable isotopic investigation of hydrothermal ore fluids in massive sulfide deposits of the West Shasta Cu-Zn district, California-----W. H. Casey, B. E. Taylor	261
25.	Genesis of gold-bearing quartz veins of the Alleghany district, California (abs.)-----A. S. Radtke, R. W. Wittkopp, Chris Heropoulos	278
26.	Origin of hydrothermal fluids responsible for gold deposition, Alleghany district, Sierra County, California-----Brian Marshall, B. E. Taylor	280
27.	Subsurface intrusive rocks at The Geysers geothermal area, California-----Alexander Shreiner, Jr., G. A. Suemnicht	294
28.	An overview of tungsten, copper and zinc-bearing skarns in western North America-----L. D. Meinert, Rainer Newberry, M. T. Einaudi	303

29. Paleozoic stratabound lead-zinc-copper deposits in the western
United States-----Half Zantop

328

TABLE OF CONTENTS

- Ashley, R. P., and Evarts, R. C., Geology and ore deposits of the St. Helens mining district, Washington (abs.), 14
- Balla, J. C., and Smith, R. G., Geology of the Little Boulder Creek deposit, Custer County, Idaho (abs.), 22
- Briskey, J. A., Field, C. W., and Bellamy, J. R., Geology, petrology, and geochemistry of the Jersey, East Jersey, Heustis, and Iona porphyry copper-molybdenum deposits, Highland Valley, British Columbia, 10
- Case, J. E., Magnetic expression and mineralization of some Tertiary plutons of Prince William Sound and the Alaska Peninsula, southern Alaska (abs.), 3
- Casey, W. H., and Taylor, B. E., Stable isotopic investigation of hydrothermal ore fluids in massive sulfide deposits of the West Shasta Cu-Zn district, California, 24
- Cheney, E. S., New concepts of regional geology and uranium exploration in northeastern Washington, 16
- Derkey, R. E., Hydrothermal alteration and mineralization at the Blackbutte mercury mine, Lane County, Oregon, 17
- Derkey, R. E., The Silver Peak volcanogenic massive sulfide, northern Klamath Mountains, Oregon, 19
- Fahey, P. L., The Island copper porphyry copper-molybdenum deposit, Vancouver Island, British Columbia (abs.), 11
- Godwin, C. I., Sinclair, A. J., and Ryan, B. D., Lead isotope models for the genesis of carbonate-hosted Zn-Pb, shale-hosted Ba-Zn-Pb, and silver-rich deposits in the northern Canadian Cordillera, 12
- Hitzman, M. W., Geology of the BT Claim Group, southwestern Brooks Range, Alaska, 2
- Juhas, A. P., Freeman, P. S., and Fredericksen, R. S., Kuroko type copper-gold mineralization at the Iron Dyke mine, Oregon, 21
- Juhas, A. P., and Gallagher, T. P., Kuroko type mineralization at the Red Ledge deposit, Idaho, 20
- Koski, R. A., Volcanogenic massive sulfide deposits in ocean-crust and island-arc terranes, northwestern Klamath Mountains, Oregon and California, 18

- Lange, I. M., Nockleberg, W. J., Plahuta, J. T., Krouse, H. R., Doe, B. R., and Jansons, Uldis, Isotopic geochemistry of stratiform zinc-lead-barium deposits, Red Dog Creek and Drenchwater Creek areas, northwestern Brooks Range, Alaska, 1
- MacKevett, E. J., Jr., Armstrong, A. K., Potter, R. W., II, and Silberman, M. L., Kennecott-type copper deposits, Wrangell Mountains, Alaska--an update and summary (abs.), 6
- Marshall, Brian, and Taylor, B. E., Origin of hydrothermal fluids responsible for gold deposition, Alleghany district, Sierra County, California, 26
- McMillan, W. J., and Johan, Z., Rock geochemistry, geology and genesis of the Guichon Creek batholith in British Columbia, Canada, as it relates to highland Valley ore deposits, 9
- Meinert, L. D., Newberry, Rainer, and Einaudi, M. T., An overview of tungsten, copper and zinc-bearing skarns in western North America, 28
- Mitchell, P. A., Silberman, M. L., and O'Neil, J. R., Genesis of gold vein mineralization in an Upper Cretaceous turbidite sequence, Hope-Sunrise district, southern Alaska, 5
- Radtke, A. S., Wittkopp, R. W., and Heropoulos, Chris, Genesis of gold-bearing quartz veins of the Alleghany district, California (abs.), 25
- Robyn, T. L., Henage, L. F., and Hollister, V. F., Possible nonsubduction associated porphyry ore deposits, Pacific Northwest, 13
- Shreiner, Alexander, Jr., and Shepard, R. J., Geology and mineralization of the Washougal mining district, Skamania County, Washington, 15
- Shreiner, Alexander, Jr., and Suemnicht, G. A., Subsurface intrusive rocks at The Geysers geothermal area, California, 27
- Silberman, M. L., MacKevett, E. M., Jr., Connor, C. L., and Matthews, Alan, Metallogenic and tectonic significance of oxygen isotope data and whole-rock potassium-argon ages of the Nikolai Greenstone, McCarthy quadrangle, Alaska, 7
- Smith, P. R., Geology update of the Quartz Hill molybdenum property near Ketchikan, Alaska (abs.), 4
- Vulimiri, M. R., and Cheney, E. S., Stratiform mineralization and origin of some of the vein deposits, Bunker Hill mine, Couer d'Alene district, Idaho, 23
- Yeend, Warren, Placer gold deposits, Mt. Hayes quadrangle, Alaska, 8

Zantop, Half, Paleozoic stratabound lead-zinc-copper deposits in the
western United States, 29

Isotopic geochemistry of stratiform zinc-lead-barium
deposits, Red Dog Creek and Drenchwater Creek areas,
northwestern Brooks Range, Alaska

I. M. Lange, University of Montana
W. J. Nokleberg, U.S. Geological Survey
J. T. Plahuta, University of Montana
H. R. Krouse, University of Calgary
B. R. Doe, U.S. Geological Survey
Uldis Jansons, U.S. Bureau of Mines

ABSTRACT

Stratiform and volcanogenic zinc-lead-barium deposits occur within the pelagic Kagvik sequence in the Red Dog Creek and Drenchwater Creek areas in the DeLong Mountains and Howard Pass quadrangles. The sulfide deposits occur together with barite, tuff, sandstone, shale, chert, and keratophyre flows and sills. The three main occurrences of the stratiform zinc-lead-barium deposits in the Red Dog Creek area are: (1) thinly-bedded stratiform sulfide minerals in organic-rich Mississippian shale and chert; (2) massive sulfide vein and breccia fillings in Mississippian shale; and (3) massive stratiform barite lenses and nodules in chert and shale of the Siksikpuk Formation. The Drenchwater Creek area has only the first type. Sulfide-bearing zones of up to several thousand meters long occur in both areas with up to 19.5 percent Zn, 9.5 percent Pb, and locally more than 150 ppm Ag. Radiolaria from sulfide-bearing chert indicate in the Red Dog Creek area a Mississippian age of sulfide deposition. K/Ar ages of 319 ± 10 m.y. and 330 ± 17 m.y. obtained from biotite in keratophyre associated with sulfide-bearing tuff and chert in the Drenchwater Creek area indicate a Mississippian age of sulfide deposition.

Sulfur isotope analyses of sulfur-bearing minerals from the Red Dog Creek area indicate that a combination of sea water sulfate and deep-seated sulfur was probably the source of the barite sulfate whereas sulfur in the sulfide minerals may have had a deep-seated source. Sulfur isotope values for sphalerite and galena are similar in vein and stratiform occurrences. Using sulfur isotope geothermometry, sphalerite-galena pairs yield paleotemperatures of between 115° and 305° C. Lead isotope analyses of galena from both the Red Dog Creek and Drenchwater Creek areas yield Triassic model ages of approximately 200 m.y. Lead isotope data from both areas approximate typical orogene, i.e., Andean-type arc, or mature island-arc values and exclude ocean floor rifting for the generation of lead. The isotopic, petrologic, and field data indicate the stratiform zinc-lead-barium deposits in the Red Dog Creek and Drenchwater Creek areas formed during a short-lived period of Mississippian submarine volcanism in either an incipient Andean-type arc, or mature island arc environment.

INTRODUCTION AND GENERAL GEOLOGY

Significant stratiform zinc-lead-barium deposits occur in the Red Dog Creek and Drenchwater Creek areas in the northwestern Brooks Range, Alaska (Tailleur, 1970; Nokleberg and Winkler, 1978a, b; Plahuta, 1978; Plahuta and others, 1978; Nokleberg and others, 1979a, b; Nokleberg and Winkler, 1981). The deposits consist of sphalerite, galena, pyrite, marcasite, and barite that occur in an unnamed unit of Mississippian age that contains chert, shale, and sparse tuff, tuffaceous sandstone, keratophyre and andesite. These Mississippian rocks are part of the Kagvik structural sequence (Churkin and others, 1979) which also includes chert and shale of the Permian Siksikpuk and Triassic Shublik Formations, and graywacke and mudstone of the Cretaceous Okpikruak Formation. The Mississippian to Triassic rocks of the Kagvik sequence are interpreted by Churkin and others (1979) as a oceanic sequence that was deposited southward of a continental shelf on which was deposited carbonate platform rocks of the Lisburne Group of Mississippian age, and sandstones of the Sadlerochit Formation of Triassic age. The Red Dog Creek and Drenchwater Creek areas are about 120 km apart, near the western and eastern margins of the east-west striking Kagvik sequence which forms the lowest structural sequence in this region (Churkin and others, 1979).

The major bedrock unit in the Drenchwater Creek area is the Kagvik sequence which occurs in various thrust plates (fig. 1A). The overall structure is characterized by west-northwest-striking thrust plates that dip moderately south. No stratigraphic unit is fully exposed in the Drenchwater Creek area because of intense folding, faulting, and shearing. Because of this intense deformation, the thickness and lateral extent of the various units are variable (fig. 1A). Intermediate to mafic tuff, tuffaceous sandstone, keratophyre flows, and andesite sills or flows locally occur in the Kagvik sequence. Only intermediate tuff, tuffaceous sandstone, and keratophyre flows are shown in Fig. 1A. The locations of the other igneous rocks are shown by Nokleberg and Winkler (1979b, 1981). The stratiform zinc-lead-barium deposits occur mainly in hydrothermally altered chert, shale, tuff, and tuffaceous sandstone either adjacent to or near submarine keratophyre flows. The Mississippian age of the rocks hosting the stratiform sulfide deposits is based on K/Ar ages of 319 ± 10 m.y. and 330 ± 17 m.y. obtained from biotite in keratophyre adjacent to sulfide-bearing tuff and chert (Nokleberg and Winkler, 1981). Stratigraphic thickness of the exposed part of the Mississippian unit is about 200 m.

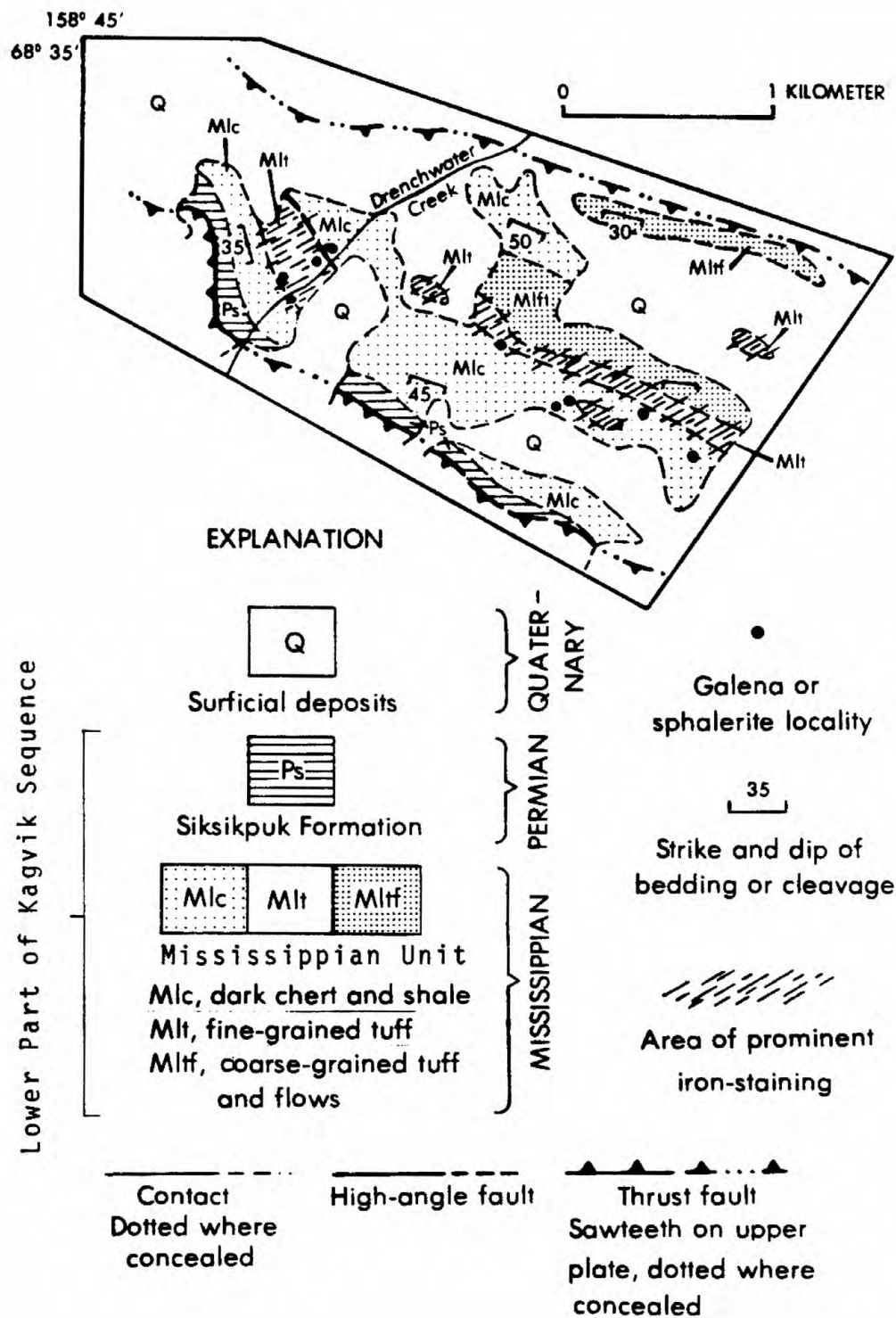
The major bedrock units in the Red Dog Creek area are the Kagvik sequence, clastic rocks of presumable Devonian age, and carbonate rocks of the Lisburne Group all of which occur in various thrust plates (fig. 1B). The portion of the Kagvik sequence containing stratiform zinc-lead-barium deposits is exposed through a window in overlying thrust plates which are warped into a broad north-south trending antiform centered along Red Dog Creek (Plahuta, 1978). The Kagvik sequence is intensely deformed and occurs in northeast-striking thrust plates that dip gently northwest or southeast. In this area, the Mississippian unit consists of a lower member of thinly-interbedded dark chert and limestone, and an upper member of very dark graphitic shale, chert, tuff, and keratophyre. The stratiform deposits occur mainly in the upper member of the Mississippian unit in the Kagvik sequence. Some sulfide deposits may be hosted in the lowest part of the Siksikpuk Formation; however, extensive thrusting, and the lack of precise age control precludes exact determination of the age of the host rock at the top of the sulfide deposits. The Mississippian age of the dark chert and shale hosting the stratiform sulfide deposits is based on identification of radiolaria by D. L. Jones and B. K. Holdsworth (written commun., 1979). Identifications were made on radiolaria extracted from samples of sulfide-bearing chert and shale, and from chert and shale layers within the zone of stratiform sulfide deposits. Stratigraphic thickness of the Mississippian unit is about 130 m. Barite is locally abundant near the contact with the overlying Siksikpuk Formation. The contact between the Mississippian unit and the Siksikpuk Formation in the Red Dog Creek area apparently reflects a change from strongly reducing to moderately oxidizing depositional conditions. The conformably overlying Permian Siksikpuk Formation consists of interbedded locally siliceous shale, and chert. Barite is widespread as disseminations and beds, and is most prevalent near the base of the formation. Stratigraphic thickness of the Siksikpuk Formation is about 170 m.

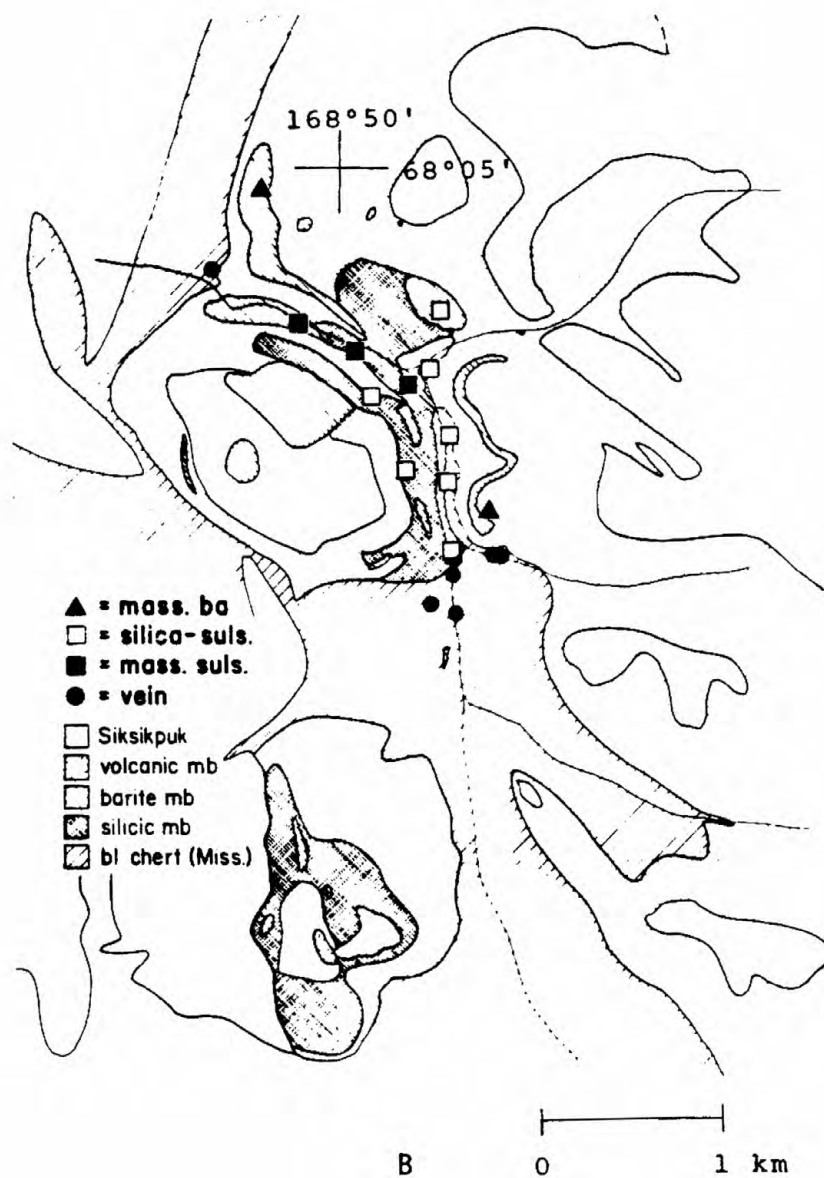
ZINC-LEAD-BARIUM DEPOSITS

Drenchwater Creek Area

The three main occurrences of stratiform zinc-lead-barium deposits in the Drenchwater Creek area are: (1) disseminated sulfide minerals and sparse barite in chert, shale, tuff, and tuffaceous sandstone; (2) disseminated to massive sulfide minerals and sparse barite in quartz-rich rock; and (3)

Figure 1. Simplified geologic maps of the Drenchwater Creek and Red Dog Creek area, northwestern Brooks Range, Alaska. A. Simplified geologic map of the Drenchwater thrust plate. Geology modified from Nokleberg and Winkler (1978b; 1981). B. Simplified geologic map of the Red Dog Creek area showing location of samples for sulfur isotope studies. Geology modified from Plahuta (1978).





extremely sparse disseminated to massive sphalerite and galena in veins crosscutting cleavage in brecciated chert and shale. Selected rock samples contain from less than 200 to more than 10,000 ppm Zn, 15 to more than 15,000 ppm Pb, 150 to more than 5,000 ppm Ba, and less than 0.5 to more than 150 ppm Ag. The deposits are restricted to a 6- to 30-m-wide zone in the Drenchwater thrust plate that extends eastward along strike from Drenchwater Creek for about 1,830 m (fig. 1A).

Chert, shale, tuff, and tuffaceous sandstone contain up to 45 modal percent sphalerite, up to 15 modal percent galena, up to 7 modal percent pyrite and marcasite, and up to 1 modal percent barite. The predominant constituents of chert and shale are recrystallized quartz, and kaolinite replacing feldspar. The predominant constituents in tuff and tuffaceous sandstone are altered volcanic rock fragments, feldspar replaced by kaolinite and quartz, pumice lapilli replaced by kaolinite, sericite, and montmorillonite, quartz, and carbonate.

The quartz-rich rock contains up to 35 modal percent sphalerite, 15 modal percent galena, 5 modal percent pyrite and marcasite, and 2 modal percent barite. The predominant constituent is medium-grained quartz showing excellently developed hexagonal outlines containing concentric growth zones rich in galena. This rock is probably a primary chemical precipitate, analogous to that of siliceous sulfide layers of the Kuroko deposits in Japan.

Sulfide and sulfate minerals crystallized during sedimentation rather than during later epithermal replacement. Sphalerite, galena, pyrite or marcasite, and sparse barite occur primarily as disseminated grains in undeformed host rock. The disseminated occurrence of sulfide and sulfate minerals and the lack of vein replacement features preclude epigenetic replacement of host rock by sulfide and sulfate minerals. Fragments of fine-grained feldspar, pumice lapilli, and mafic volcanic rocks in chert, shale, and tuff are commonly replaced by aggregates of kaolinite, montmorillonite, sericite, chlorite, actinolite, calcite, quartz, fluorite, and prehnite. The occurrence of disseminated sulfide minerals and barite in hydrothermally altered chert, shale, tuff, and tuffaceous sandstone either adjacent to or near keratophyre strongly suggests that zinc-lead-barium mineralization coincided with submarine volcanism and hydrothermal alteration.

Red Dog Creek Area

The three main occurrences of the stratiform zinc-lead-barium deposits in the Red Dog Creek area are: (1) thinly-bedded stratiform sulfide minerals in organic-rich Mississippian shale and chert; (2) massive sulfide-rich vein and breccia fillings in silicified Mississippian shale; and (3) massive stratiform barite lenses and nodules in chert and shale of the Siksikpuk Formation. The stratiform deposits are further subdivided into three types: (1) quartz-rich rock with several percent sulfides and barite; (2) massive sulfide and quartz lenses with several percent barite; and (3) barite and quartz lenses with up to several percent sulfide minerals. Chert and shale, within and adjacent to the stratiform deposits in the Mississippian unit, are locally intensely altered hydrothermally and replaced by aggregates of kaolinite, montmorillonite, sericite, chlorite, calcite, and quartz.

The quartz-rich rock is a vuggy aggregate of interlocking fine- to medium-grained quartz crystals that commonly contain concentric hexagonal growth bands. Interstitial areas between quartz grains and zones within the

growth bands commonly contain up to several percent sulfide minerals and barite. Sphalerite is generally about twice as abundant as galena, and pyrite and marcasite are present in only trace amounts. The quartz-rich rock forms massive layers up to several tens of meters thick that are conformable with the enclosing strata. The quartz-rich rock is probably a primary chemical precipitate, analogous to that of siliceous sulfide layers of the Kuroko deposits.

The massive sulfide and quartz lenses range from two- to five-m thick and have horizontal dimensions greater than 300 m. Sphalerite is two to three times more abundant than galena; pyrite and marcasite are very minor. Chalcopyrite and bornite occur in trace amounts. The sulfide minerals typically form fine-grained aggregates that are intimately intergrown with zoned quartz. Locally the massive sulfide and quartz lenses contain sparse indistinct layers rich in sphalerite or galena. Hexagonal growth bands occur in quartz and contain zones rich in sulfide minerals and barite. Five representative samples from the massive sulfide and quartz lenses average 19.5 percent Zn, 9.5 percent Pb, 0.02 percent Cu, 0.14 percent Cd, and 3.7 oz Ag/ton. Field relations and textural similarities between the massive sulfide quartz lenses, quartz-rich rock, and barite and quartz lenses suggest more or less simultaneous crystallization with greater sulfide deposition near the massive sulfide-rich veins.

Vein deposits are found intermittently exposed along the channel of Red Dog Creek in silicified chert in the northern part of the study area (fig. 1B). The veins are up to 1 m wide, strike north, and dip steeply east or west. Local cross-fractures adjacent to veins consist of a breccia containing a cement of sulfide minerals and clasts of chert and shale. The dominant vein sulfide minerals are sphalerite, pyrite, and marcasite and usually occur as alternating colloform bands. Lesser amounts of galena are paragenetically later than sphalerite, pyrite, and marcasite. Barite has been found only in three veins where it is the dominant constituent in association with sphalerite and trace amounts of pyrite. Sphalerite and barite are generally coarse-grained. Contacts between veins and wall rock are sharp. Pervasive silicification, defined by recrystallization and replacement of chert and shale by medium-grained quartz-rich rock, occurs adjacent to veins. Quartz is not a major or minor component within the veins.

The massive stratiform barite lenses in the Siksikpuk Formation attain thicknesses of greater than 50 m, and occur either distal to, or over the zone of stratiform sulfide mineralization. Soft sediment slump structures and sedimentary breccias occur within the lenses, and carbonaceous-rich layers locally define bedding. The rock varies from fine- to coarse-grained, and normally contains subequal amounts of barite and quartz as intimate intergrowths. Sulfides are usually absent, but may comprise up to 10 percent of the rock as subequal amounts of sphalerite and galena. The barite lenses also locally contain subordinate amounts of pyrite and marcasite.

The occurrence of sphalerite, galena, pyrite, marcasite, and barite as disseminated grains suggests that sulfide and sulfate deposition coincided with sedimentation. As in the Drenchwater Creek area, a sea-floor volcanogenic source for the zinc-lead-barium mineralization is suggested by: (1) proximity of stratiform sulfide deposits to keratophyre; (2) hydrothermal alteration; and (3) proximity of stratiform sulfide deposits to massive sulfide-rich veins which, because of their large dimensions and location in the center of the area of stratiform mineralization, possibly represent a vent and source for the hydrothermal fluids from which were deposited the sulfide

minerals.

LEAD ISOTOPE ANALYSES

Lead isotope analyses were performed on samples of disseminated galena from the Red Dog Creek and Drenchwater Creek areas, and on one sample of vein galena from the Red Dog Creek area (table 1). The analyses were performed using the surface emission (silica gel) ionization technique and the ratios should be within 0.1 percent of absolute values. The lead isotope ratios are extremely similar between both areas, and between both types of disseminated and vein deposits. Using the synthesis of Doe and Zartman (1979) on lead isotopes and geologic environments, and field and petrologic data, the data from the Red Dog Creek and Drenchwater Creek areas show generation of lead in either a Phanerozoic mature island arc setting, in a typical orogene i.e., an Andean-type arc setting, or possibly a back-arc type of intracratonic basin. The lead isotope ratios from the two areas in the northwestern Brooks Range are similar to lead isotope ratios from the Kuroko-type massive sulfide deposits (Doe and Zartman, 1979) which are interpreted as having formed in a mature island arc setting. The data are also closely similar to some data on ores from the Upper Permian Kupferschiefer of Europe in an intracratonic basin environment (Wedepohl and others, 1978), although quite different from most leads in intracratonic basins. The lead isotope data from the two areas in the northwestern Brooks Range specifically exclude generation of lead either in an oceanic spreading environment or probably in a cratonic environment according to the synthesis of Doe and Zartman (1979). The Stacey-Kramer model lead ages of both the Red Dog Creek and Drenchwater Creek areas also yield nearly identical values of about 200 m.y. These ages are younger by 100 to 150 m.y. than the Mississippian age of strata hosting the disseminated zinc-lead-barium deposits in both areas.

SULFUR ISOTOPE ANALYSES

Sulfur isotope analyses were performed on sulfide and sulfate minerals from both the Red Dog Creek and Drenchwater Creek areas (table 2). Fifty-five mineral concentrates, prepared by hand-picking and heavy liquid separation methods, from 23 locations at the Red Dog Creek area, and five mineral concentrates from three locations at the Drenchwater Creek area were examined. Hand-picking and heavy liquids were used in mineral separations. The purity of the mineral separates generally exceeded 95 percent. The sulfide minerals were converted to SO_2 for mass spectrometric analysis by reaction with CuO at 900°C . Barite was reduced to H_2S by boiling in a mixture of HI , H_3PO_2 , and HCl . The H_2S was precipitated as CdS , converted to AgS , and combusted to SO_2 with CuO at 900°C . Reproduction of $\delta^{34}\text{S}$ values is ± 0.2 . The sulfur isotope data is given in Table 2 and the data is plotted in Figure 2.

The range of sulfur isotope data for sphalerite for the Red Dog Creek area is very restricted, showing $\delta^{34}\text{S}$ means near 0. Values of $\delta^{34}\text{S}$ are $+0.7$ for siliceous sphalerite, $+0.5$ for massive sphalerite, and $+1.0$ for vein sphalerite. Galena $\delta^{34}\text{S}$ values are isotopically lighter than sphalerite. Pyrite $\delta^{34}\text{S}$ values range from a low of -16.6 to a high of $+3.6$. Pyrite generally is also isotopically lighter than coexisting sphalerite and therefore not in isotopic equilibrium with sphalerite.

Paragenetically, pyrite crystallized both earlier and later than other sulfides in both the massive sulfide and quartz-sulfide deposits. Early-crystallized pyrite, generally with a colloform habit, was followed by isotopically heavier sphalerite. Galena generally crystallized simultaneously

Table 1. Galena Lead Isotope Analyses,
M. H. Delevaux, analyst

<u>Sample</u>	<u>$^{206}\text{Pb}/^{204}\text{Pb}$</u>	<u>$^{207}\text{Pb}/^{204}\text{Pb}$</u>	<u>$^{208}\text{Pb}/^{204}\text{Pb}$</u>
Red Dog 78ARD-1 (vein)	18.414	15.602	38.254
Red Dog RD-63B (dissem.)	18.409	15.598	38.238
Drenchwater 77ANK-13H	18.428	15.609	38.351

Table 2 . Sulfide and Barite $\delta^{34}\text{S}$ Values,
H. R. Krouse, analyst.

Sample	pyrite	sphalerite	galena	sp-gn	T°C*	barite
Red Dog Creek						
<u>Siliceous</u>						
26-2		1.6	-2.6	4.2	135 ⁰	13.1**, 12.0**
28-2a	-0.2					7.8**
28-2b	-0.2					7.3**
28-3		-0.4	-5.2	4.8	115 ⁰	15.8, 16.5
28-8	-16.6		-1.0			26.7, 10.8**
28-17		0.9	-1.3	2.2	305 ⁰	16.2, 18.2
RD-57		-1.5	-4.6	3.1	210 ⁰	
RD-62		2.5				
RD-89		1.2				
<u>Massive</u>						
28-9		0.6				0.1**
28-12	-3.2	2.4				
28-13		0.9	-7.2	8.1	27 ⁰	
28-16	-1.9	-1.1				
RD-68		-0.5				
<u>Vein</u>						
25-16		0.3				17.4
26-8a		1.6	-1.0	2.6	255 ⁰	17.2, 8.6**
26-8b			0.2**			18.6**
27-2	3.6	1.7				
28-4		1.4				
28-6		0.8	-3.5	4.3	140 ⁰	
28-14a	2.5	2.5				
28-14b	-0.1					0.3**
28-15	-13.5	-1.2				
<u>Massive Barite</u>						
27-1						17.4
28-10						14.2
RD-38						27.8
Drenchwater Creek						
77ANK116A		4.8				
77AN 13F			-1.7			
77ANK13Ha		0.7				2.4**
77ANK13Hb		0.9				

* = using data of Rye and Ohmoto, 1979

** = trace amounts associated with sulfides

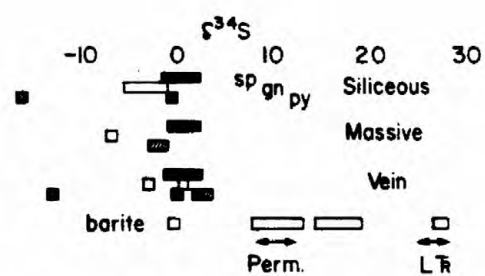


Figure 2.--Graph showing $\delta^{34}\text{S}$ values of sulfide minerals and barite at the Red Dog Creek area, northwestern Brooks Range, Alaska.

with or possibly slightly later than sphalerite, and is isotopically lighter than sphalerite (table 2). Evidence for early pyrite includes atoll and island structures of pyrite in sphalerite and galena, and truncation of growth-zoned pyrite by massive sphalerite. Paragenetically late pyrite occurs in veinlets that crosscut all other sulfide minerals.

As many as four groups of barite can be distinguished isotopically (table 2, fig. 2). Paragenetically early barite in quartz-sulfide deposits occurs along with sulfide minerals in hexagonally zoned quartz crystals. Sphalerite and galena occur interstitially around the quartz crystals, and later-crystallized barite occurs in voids and fractures cutting the interstitial sphalerite and galena.

Temperatures of deposition for sphalerite-galena pairs are calculated using the sulfur isotope analyses and the fractionation data of Ohmoto and Rye (1979). Depositional temperatures vary from 115° to 305° C (table 2) for contiguous sphalerite and galena.

SULFUR ISOTOPE MODEL

Any model for the mineralization process at the Red Dog Creek and Drenchwater Creek areas must be compatible with the following isotopic and geological observations: (1) $\delta^{34}\text{S}$ values for galena and particularly sphalerite are similar in the vein and both types of stratiform sulfide deposits. (2) $\delta^{34}\text{S}$ values for sphalerite have a narrow range and cluster around 0. (3) Sphalerite is generally isotopically heavier than pyrite. (4) At least two generations of pyrite formed, one earlier than, and the other after the crystallization of sphalerite. (5) Barite is texturally and temporally associated with the other sulfide minerals and exhibits up to four groups of $\delta^{34}\text{S}$ values ranging from -0.3 to +27.8 (fig. 2).

Models involving bacterial reduction of sea water sulfate as the sole source of sulfur for both sulfides and barite were considered and rejected because the depositional temperatures are apparently much too high for this process. Another possible model consists of reduction of sea water sulfate into an ore-forming solution by reaction with Fe+2-bearing components in rocks at temperatures above 250° C (Mottl, 1976). This model is appealing because it explains many of the observed isotopic features in the two areas. The resulting barite would range from Permian or Mississippian sea water sulfate $\delta^{34}\text{S}$ values (+9.6 to +13.0) to $\delta^{34}\text{S}$ values heavier than sea water sulfate (Thode and Monster, 1965). The resulting sulfur isotopic fractionation between coexisting sulfide and barite is usually smaller than predicted equilibrium $\delta^{34}\text{S}$ values. This situation occurs at Red Dog Creek. However, while explaining the barite $\delta^{34}\text{S}$ values, the model does not explain the narrow range of sphalerite $\delta^{34}\text{S}$ values which cluster around 0.

Our preferred model incorporates the mixing of two sulfur-bearing solutions and attempts to explain both the wide range of barite $\delta^{34}\text{S}$ values and the narrow range of sphalerite $\delta^{34}\text{S}$ values. A possible model for mineralization follows. Early, isotopically light pyrite and quartz crystallized during inorganic reduction of sea water sulfate at temperatures of at least 250° C. Subsequent hydrothermal mineralization, resulting in the formation of sphalerite, galena, barite, and late pyrite, might have been caused by the mixing of two sulfur-bearing solutions at the site of stratiform mineralization, adjacent to where vents discharged hydrothermal fluids onto the sea floor. One solution contained sea water sulfate with $\delta^{34}\text{S}$ values of perhaps +16 to +18, and the other solution, derived from a deep-seated source,

contained H_2S with about a $\delta^{34}S$ value of 0. The sulfide minerals crystallized from the solution with a $\delta^{34}S$ value of 0, and some of the barite crystallized from sea water sulfate. However, during the mixing of the solutions in the "plumbing system" beneath the forming deposit, some H_2S was oxidized to SO_4^{2-} . The mixing of this SO_4^{2-} with sea water sulfate led to the observed $\delta^{34}S$ range of +7.3 to +18.6 in later-crystallizing barite.

The barite with $\delta^{34}S$ values of +0.1 and +0.2 (table 2) occurs in very minor amounts and is associated with sphalerite that is only slightly heavier isotopically. Apparently this barite formed from oxidized H_2S without any contamination from sea water sulfate. The occurrence of the isotopically heaviest barite, with a $\delta^{34}S$ value of +27.8 (sample RD-38, table 2) occurs at a distance of 1.5 km east of the center of the stratiform sulfide deposits in the Red Dog Creek area. This isotopically heavy barite presumably formed primarily from sea water sulfate without any sulfur from a deep-seated source.

This model is compatible with: (1) the occurrence of much of the isotopically lighter barite in small amounts with sulfide minerals; (2) the occurrence of most of the isotopically heavier barite in massive lenses with minor to no sulfide minerals; (3) the paragenetic occurrence of most of the isotopically heavier barite either prior to or after sulfide minerals; and (4) the relatively narrower ranges and lower values of $\delta^{34}S$ for sphalerite, galena, and pyrite and marcasite which would be derived from a deep-seated source. Alternatively, the barite in the Permian Siksikpuk Formation with $\delta^{34}S$ values of +16 to +18 may also have been derived from Permian evaporite sulfate which would be heavier than contemporaneous Permian sea water sulfate with average $\delta^{34}S$ values of about +10 (Thode and Monster, 1965). However, the absence of Permian evaporite deposits in this region, and the inapplicability of this mechanism for the Mississippian stratiform sulfide deposits preclude this source of sulfur.

GEOLOGIC SETTING OF STRATIFORM ZINC-LEAD-BARIUM DEPOSITS

Field and petrologic data indicates that sulfide and sulfate mineral deposition was stratiform and volcanogenic, meaning the deposits formed simultaneously with, or just after sedimentation and submarine volcanism. Volcanic exhalations, including both magma and hydrothermal fluids, mixing with and heating sea water, were the source of the mineralizing fluids. Continued circulation of hydrothermal fluids generated during submarine volcanism altered the volcanic rocks, volcanoclastic rocks, and chert and shale. Lead isotope data suggest generation of lead in either a mature island arc, or average orogene i.e., an Andean-type arc environment, and also suggest extreme similarity of lead to the Kuroko-type massive sulfide deposits of Japan. Sulfur isotope data indicate: (1) extremely similar $\delta^{34}S$ values for sphalerite and for galena for both disseminated and vein occurrences in both areas; (2) a magmatic source for sulfide sulfur; (3) depositional temperatures between 115° C and 305° C; and (4) compatibility of a model involving mixing of various proportions of sulfur from sea water sulfate and magmatic H_2S to form barite.

The data indicate the stratiform zinc-lead-barium deposits in the Red Dog Creek and Drenchwater Creek areas formed during a short-lived period of Mississippian submarine volcanism. The sulfide and sulfate mineral deposition and the submarine volcanism most likely occurred in an ocean basin adjacent to a continental platform in an incipient Andean-type arc environment or in a mature island arc environment. Metal-laden hydrothermal fluids were

discharged onto a low energy deep ocean floor during submarine eruption of keratophyre and andesite. The massive sulfide-rich veins may represent hydrothermal conduits for discharge of metal-laden hydrothermal fluids. The hydrothermal fluids spread out along the sea floor during discharge to form the disseminated stratiform zinc-lead-barium deposits that are stratigraphically adjacent to or enclosed in chert, shale, tuff, tuffaceous sandstone, and keratophyre. The sedimentary, volcanoclastic, and volcanic rocks of the Mississippian unit of the Kagvik sequence were extensively hydrothermally altered adjacent to the hydrothermal and volcanic vents during discharge and spreading of hydrothermal fluids.

REFERENCES CITED

- Churkin, M., Jr., Nokleberg, W. J., and Huie, C., 1979, Collision-deformed Paleozoic continental margin, western Brooks Range, Alaska: *Geology*, v. 7, p. 379-383.
- Doe, B. R., and Zartman, R. E., 1979, Plumbotectonics and the Phanerozoic, in Barnes, H. L., ed., *Geochemistry of Hydrothermal Ore Deposits*, 2nd edit., New York, John Wiley, p. 22-70.
- Mottl, M., 1976, Chemical exchange between sea water and basalt during hydrothermal alteration of the oceanic crust: Harvard University, Ph. D. thesis.
- Nokleberg, W. J., and Winkler, G. R., 1978a, Geologic setting of stratiform zinc-lead mineralization, Drenchwater Creek area, Howard Pass quadrangle, western Brooks Range, Alaska [abs.]: *Geological Society of America Abstracts with Programs*, v. 10, no. 3, p. 139.
- 1978b, Geologic setting of the lead and zinc deposits, Drenchwater Creek area, Howard Pass quadrangle, western Brooks Range, Alaska: U.S. Geological Survey Open-File Report 78-70C, 16 p.
- 1981, Stratiform zinc-lead deposits in the Drenchwater Creek area, Howard Pass quadrangle, northwestern Brooks Range, Alaska: U.S. Geological Survey Professional Paper 1209, in press.
- Nokleberg, W. J., Plahuta, J. T., Lange, I. M., and Grybeck, Donald, 1979a, Volcanogenic zinc-lead mineralization in pelagic sedimentary rocks of late Paleozoic age, northwestern Brooks Range, Alaska [abs.]: *Geological Association of Canada Abstracts with Programs*, v. 4, p. 21.
- 1979b, Volcanogenic zinc-lead-barite deposits in pelagic rocks of late Paleozoic and early Mesozoic age, northwestern Brooks Range, Alaska [abs.]: *Geological Society of America Abstracts with Programs*, v. 11, no. 7, p. 487-488.
- Ohmoto, Hiroshi, and Rye, R. O., 1979, Isotopes of sulfur and carbon, in Barnes, H. L., ed., *Geochemistry of Hydrothermal Ore Deposits*, 2nd edit., New York, John Wiley, p. 509-567.
- Plahuta, J. T., 1978, Geologic map and cross sections of the Red Dog prospect, DeLong Mountains, northwestern Alaska: U.S. Bureau of Mines Open-File Report 65-78, 11 p, scale 1:20,000.

- Plahuta, J. T., Lange, I. M., and Jansons, Uldis, 1978, The nature of mineralization at the Red Dog prospect, western Brooks Range, Alaska [abs.]: Geological Society of America Abstracts with Program, v. 10, no. 3, p. 142.
- Thode, H. G., and Monster, J., 1965, Sulfur isotope geochemistry of petroleum evaporites, and ancient seas: American Association of Petroleum Geologists Memoir 4, p. 367-317.
- Tailleur, I. L., 1970, Lead-, zinc-, and barite-bearing samples from the western Brooks Range, Alaska, with a section on Petrography and mineralogy, by G. D. Eberlein and Ray Wehr: U.S. Geological Survey open-file report, 16 p.
- Wedepohl, K. H., Delevaux, M. H., and Doe, B. R., 1978, The potential source of lead in the Permian Kuperschiefer Bed of Europe and some selected Paleozoic mineral deposits in the Federal Republic of Germany: Contributions to Mineralogy and Petrology, v. 65, p. 273-281.

Geology of the BT Claim Group, southwestern Brooks
Range, Alaska

M. W. Hitzman, Stanford University

INTRODUCTION

The BT claim group is in the central portion of the Ambler district of the southwestern Brooks Range, approximately 350 km east of Kotzebue and west of the trans-Alaska pipeline. The claims contain three fault-bounded blocks of metamorphosed mixed pelitic, volcanic and carbonate strata of upper Devonian to Mississippian age. Two major folding events have deformed the area, both with associated synkinematic metamorphism. Significant sulfide mineralization is present along two separate horizons. The BT sulfide horizon contains a stratiform, pyritic massive sulfide within a felsic metavolcanic sequence. Jerri Creek horizon mineralization occurs with banded, chemically precipitated metasediments in a carbonate rich host rock. Neither of these occurrences could be classified as typical Kuroko-type volcanogenic massive sulfides since they are not spatially related to a volcanic vent area and have strike lengths of several kilometers. The regional geological setting of the Ambler district suggests that sulfides were deposited in a rifted continental margin rather than a convergent plate margin which is the tectonic setting envisioned for most volcanogenic massive sulfides.

REGIONAL GEOLOGY

Volcanogenic massive sulfide deposits of the Ambler district are contained within a folded sequence of pelitic schists with minor metacarbonate and metavolcanic rocks. Federal land withdrawals artificially bound the mineralized area on three sides. This sequence has been dated as late Devonian to early Mississippian on the basis of fossils in dolomitic marble on the BT claims (Hitzman, 1978), Pb-Pb dates from the BT sulfide horizon (Smith and others, 1978) and U-Pb zircon ages from regionally extensive metavolcanic units (Dillon and Pessel, 1979). The Ambler district mineralization forms a narrow, 5 km wide belt within the Ambler schist belt that strikes roughly east to west along the southern flank of the Brooks Range. The schist belt contains folded pelitic and carbonate metasediments which range in age from early Paleozoic to upper Devonian.

Metavolcanic rocks are volumetrically a minor constituent of the Ambler schist belt. They consist of highly potassic metarhyolites (Kelsey, 1979; Kelsey and others, 1980) and tholeiitic metabasalts (Smith and others, 1978; Nelsen, 1979; Kelsey and other, 1980); no intermediate igneous rocks, such as island-arc andesites are associated with the volcanogenic package hosting the sulfide occurrences. Other features common to convergent plate margins, such as coarse clastic sediments and melange structure are also absent in the Ambler schist belt. Detailed mapping in the schist belt by Anaconda Company geologists indicates that sedimentation and the distribution of volcanic rocks may have been controlled by a series of east to west striking structures, probably grabens.

The schist belt is bounded on the north by the Baird group carbonates of probable upper Devonian age (C. Mayfield, pers. comm, 1979) which are overlain, and structurally intercalated with, thrust sheets of Devonian Hunt's Fork shale and Mississippian Lisburne Group carbonate rocks (Mayfield and Talleur, 1978). Basement of the central Brooks Range in this area is poorly known but apparently consists of metasediments intruded by several granitic plutons, now displaying a gneissic texture. The plutons yield Proterozoic to Paleozoic U-Pb zircon ages (Dillon and Pessel, 1979).

To the south, the Ambler schist belt adjoins the upper Devonian Cosmos Hills terrane which contains a narrow platform sequence of subtidal to intertidal

metacarbonate rocks overlying metasediments (Hitzman, 1979). This terrane is overthrust on its southern edge by the Angayucham metabasalt, a sequence of ocean floor basalts with minor chert and limestone, which has undergone prehnite/pumpellyite grade metamorphism. These rocks are correlative with the ophiolitic sequence recognized in the western Brooks Range (Roeder and Mull, 1978) and range in age from upper Devonian (Fritts, 1970) to Jurassic (D. Jones, pers. comm. 1979).

The Devonian paleogeography of the southern Brooks Range was apparently dominated by topographically high blocks receiving carbonate sedimentation, separating troughs filled by fine-grained pelitic sediments and the minor volcanic rocks. Oceanic crust probably adjoined the southernmost block, the Cosmos Hills terrane. The bimodal nature of the volcanic suite containing the sulfide deposits combined with the lack of evidence for a Devonian convergent plate margin either to the north or south of the schist belt suggests that during the late Devonian the southwestern Brooks Range was a tensional environment; a rifted continental margin is probably the best model.

STRUCTURE AND METAMORPHISM

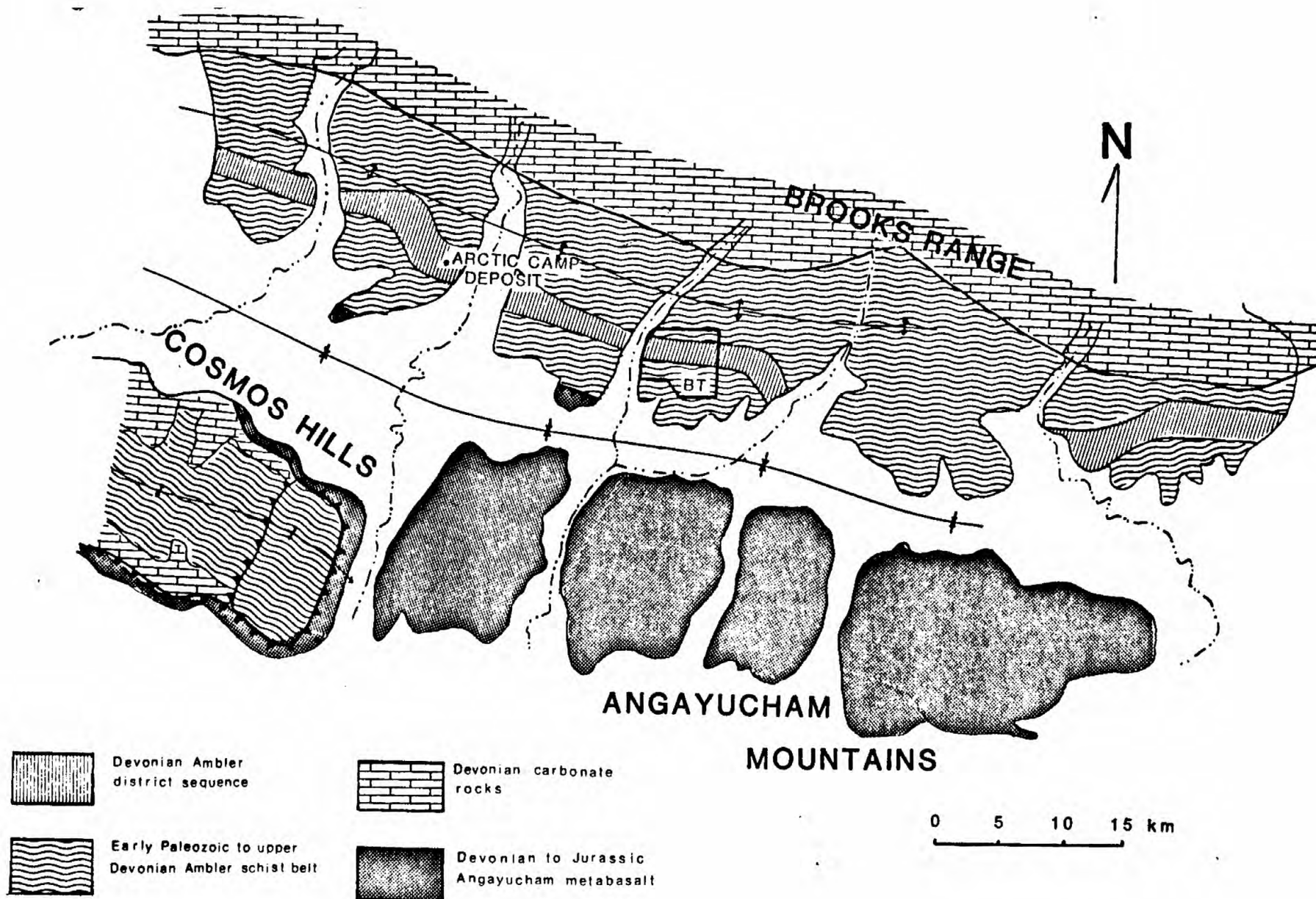
The structural history of the Ambler schist belt is complex, with three major deformational episodes recognized (Hitzman, 1978). An early period of isoclinal folding (F 1) with north-south axes is poorly understood and only locally important. Isoclinal folding (F 2) along an east to west axis associated with synkinematic metamorphism produced the dominant schistosity of the schist belt. The schistosity is axial planar to folds of this generation and is generally parallel to bedding; it is defined by an intense, penetrative fabric and synkinematic growth of upper greenschist to blueschist mineral assemblages. The age of this event is controversial; K-Ar dates on minerals of these assemblages (Turner and others, 1979) suggest it occurred in the late Triassic to Jurassic. Cretaceous deformation (F 3) broadly arched the Ambler schist belt on east-west axes and produced a major thrust belt in the central Brooks Range. Synkinematic metamorphism accompanying this deformation produced retrograde low greenschist assemblages including abundant helicitic albite porphyroblasts.

LITHOLOGIES IN THE BT AREA

The dominant rock type in the area is a well foliated, brown weathering pelitic schist. White mica and granoblastic quartz, the dominant constituents, form well segregated bands. Mica layers contain up to 10 modal percent graphite and accessory chlorite, clinozoisite, epidote, actinolite, sphene and garnet; finely disseminated pyrite is often present. Porphyroblasts of albite helicitically enclosing mica bands are common. The pelitic schist is presumably the metamorphosed equivalent of a fine grained clastic sediment, probably a mudstone or siltstone.

Calcareous metasedimentary rocks are grey weathering, foliated to massive, and often display relict bedding. Most of these rocks are calcareous schists containing nearly equal modal percentages of anhedral calcite and granoblastic quartz. White mica is a major constituent; it is poorly segregated and defines a poor foliation. Epidote, clinozoisite, actinolite, sphene, apatite, tremolite, and pyrite are accessory minerals. Thin massive carbonate lenses are also present. Prior to metamorphism these rocks were probably sandy limestones and and calcareous siltstones.

Mafic metavolcanic rocks are generally green to grey weathering with a massive to well foliated texture. Actinolite, epidote and chlorite are the



Generalized Geologic Map of the Eastern Ambler District

Southwestern Brooks Range, Alaska

FIGURE 1

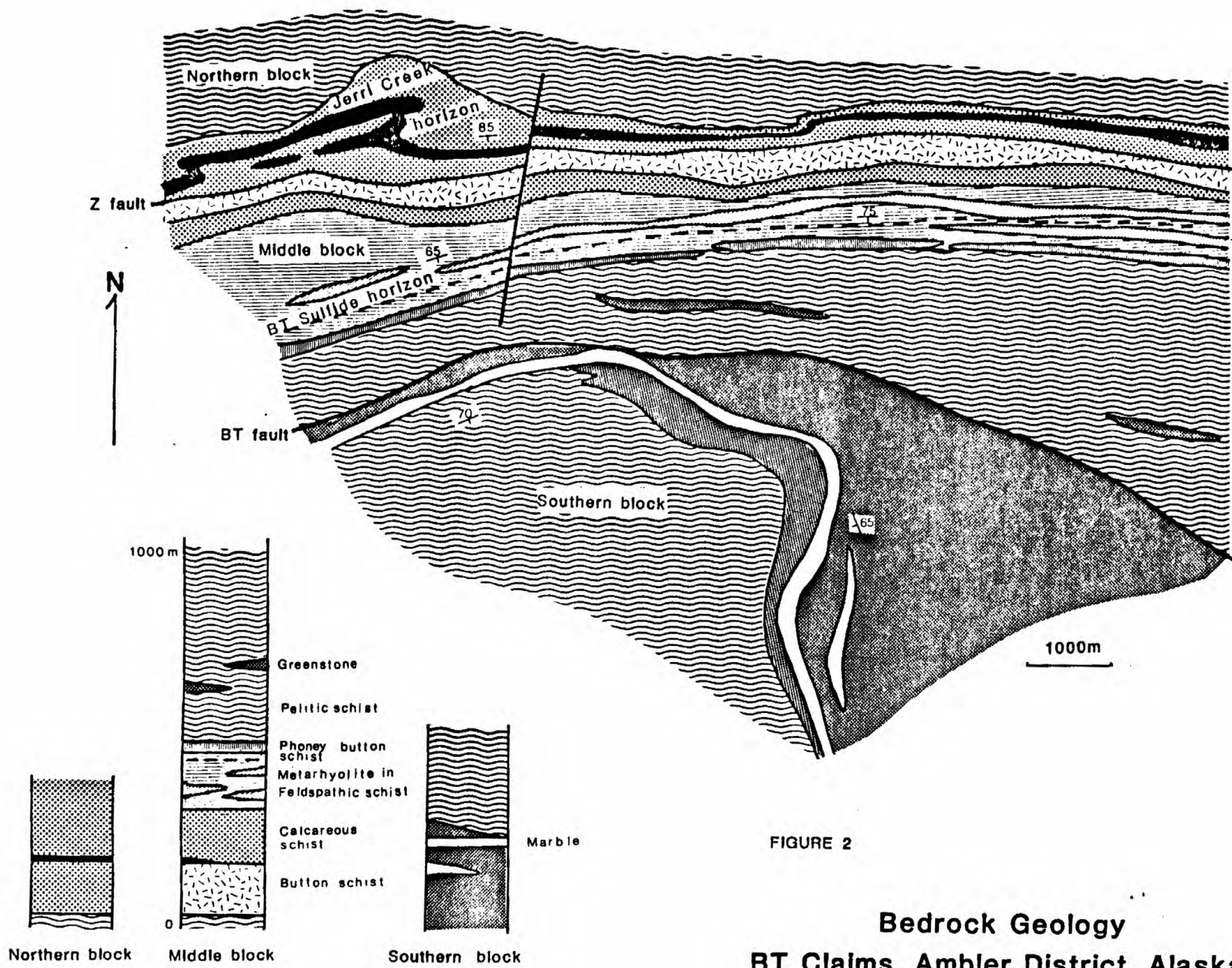


FIGURE 2

Bedrock Geology
BT Claims, Ambler District, Alaska

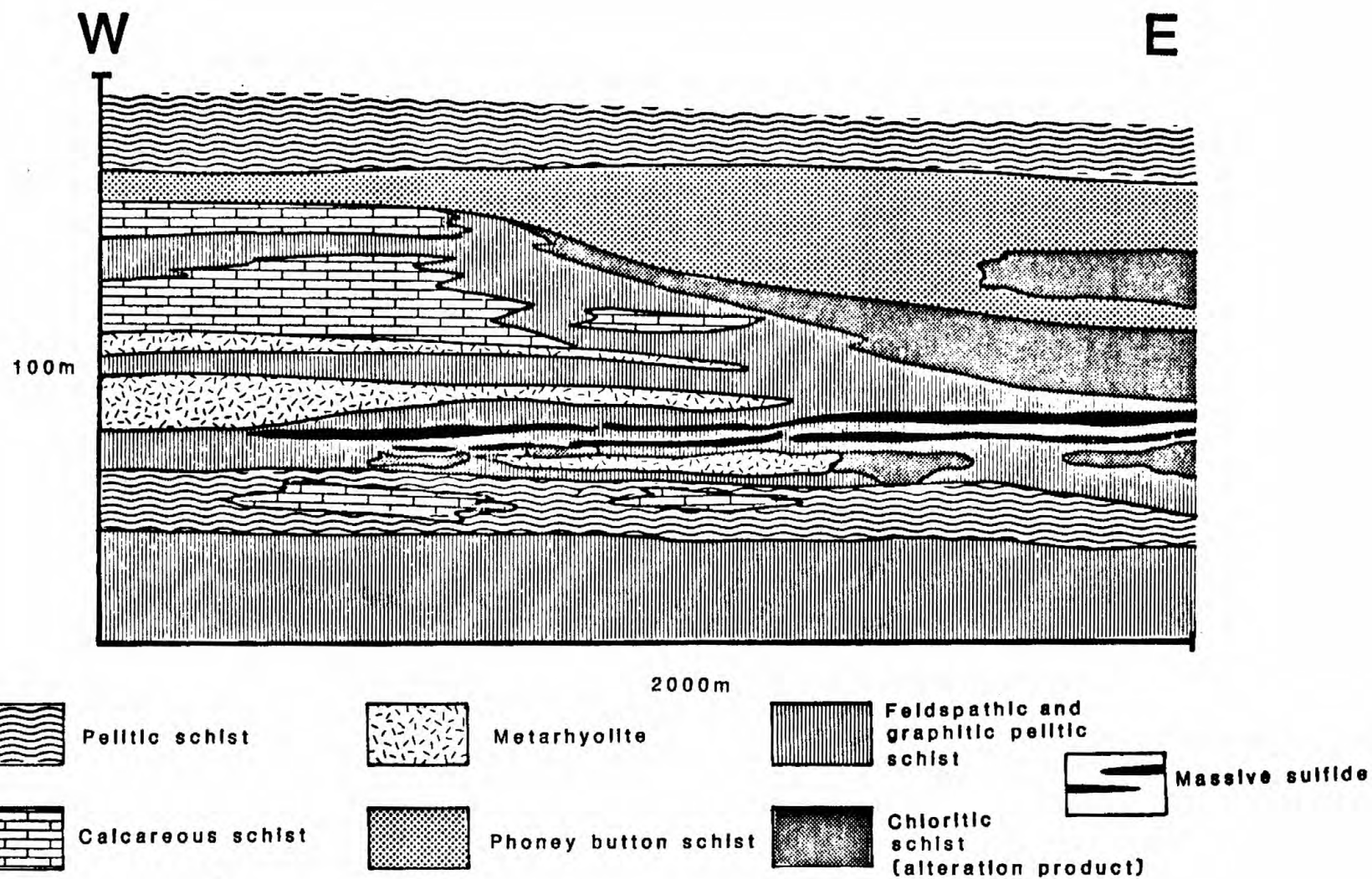


FIGURE 3

Generalized Long Section - BT Massive Sulfide Horizon

dominant constituents of the rocks; quartz, sphene, albite and garnet are common accessories. Albite is particularly common in well foliated greenstones and forms anhedral porphyroblasts up to 8 mm in diameter. Massive greenstones may contain glaucophane. The well foliated greenstones were probably tuffaceous sediments; massive greenstones represent metamorphosed sills and flows.

The BT claims contain three distinct metarhyolite horizons. All are resistant to weathering, poorly foliated to massive and tan to cream on weathered surfaces. The 'button' schist is a porphyritic metarhyolite containing blastophenocrysts of microcline and quartz. The microclines are subhedral to euhedral and may attain a diameter of 3 cm. Crystals which have not been partially recrystallized to white mica and quartz often display relict resorption channels. Wiltse (1975) suggests that the microcline replaced volcanic sanidine. Quartz blastophenocrysts, or 'eyes' may reach 1.5 cm in diameter. Morphology of the quartz eyes is variable; bipyramidal habits are characteristic of certain layers within the button schist while other layers display rounded shapes with excellently preserved relict resorption channels. The groundmass of the button schist is composed of quartz and white mica with accessory biotite, pyrite and zircon; porphyroblasts of albite helicitically preserve the poorly developed foliation. Massive white mica segregations in button schist east of the BT area have been described as recrystallized pumice fragments (Kelsey, 1979). The button schist has a strike length of approximately 30 km in the central Ambler district. It maintains a relatively constant thickness of 200 m in the BT area. It is possible to divide the button schist unit into layers, each with distinctive modal percentages of microcline and quartz blastophenocrysts as well as accessory minerals; tops of layers are more commonly micaceous than their bases. Near the top and bottom of the unit, thin metasedimentary lenses often separate distinctive button schist layers. The relict textures, combined with the field relations, suggest that the button schists represent metamorphosed rhyolitic pyroclastic flows emplaced in a subaqueous environment.

The second felsic metavolcanic unit, metarhyolite, lacks the abundant blastophenocrysts of the button schist. Rare rounded quartz eyes and small euhedral microcline blastophenocrysts are present in some layers but are not easily discernible in hand specimen. Granoblastic quartz, white mica and porphyroblastic albite are the dominant minerals; sphene, pyrite and biotite are common accessories. The rock is highly recrystallized but poorly foliated. Metarhyolite occurs as discrete lenses with strike lengths exceeding 3000 m and thicknesses of 6 to 35 m intercalated with metasediments, dominantly feldspathic schist.

'Phoney' button schist is the third felsic metavolcanic unit. It contains sparse blastophenocrysts of microcline up to 1.5 cm in diameter and few quartz eyes. The groundmass is generally well recrystallized. Unlike the button schist and metarhyolite, the lower portion of the phoney button schist often has a highly chloritic groundmass. The phoney button schist occurs as discrete lenses up to several thousand meters long and 5 to 50 m thick. Lenses of the unit are known to crop out for a strike length of 25 km. Both the metarhyolite and the phoney button schist are believed to have formed similarly to the button schist.

Silicic metavolcanics are often intercalated with feldspathic schists. They are white to yellowish green in outcrop and well foliated. Granoblastic quartz and white mica are the dominant constituents and are well segregated. White mica layers contain abundant porphyroblasts of albite and accessory pyrite and sphene. Highly graphitic pelitic schist is commonly finely interlayered with the feldspathic schists, which are probably felsic tuffs and altered metarhyolites.

STRATIGRAPHY

The units in the BT area strike nearly east to west and dip steeply south; the sequence, comprising three blocks, does not appear to be inverted. Isoclinal drag folds (F2) in calcareous schist along the northern edge of the claims are the only major folds on the claim block. The sequence is separated into a northern and middle block by the Z reverse fault, which formed concurrently with isoclinal folding. The BT reverse fault separating the middle and southern blocks, postdates isoclinal folding and is probably related to Cretaceous deformation (F3).

The northern fault block grades upward from pelitic to calcareous schists and marbles. The Jerri Creek sulfide horizon forms a distinctive marker unit within these calcareous schists. Fossils preserved in dolomitic lenses in the calcareous schists indicate that the paleoenvironment was at least locally subtidal.

In the middle fault block the stratigraphically lowest exposed unit is pelitic schist which is overlain by the button schist sequence. Overlying the button schist is 150 to 200 m of calcareous schist with minor feldspathic and pelitic schist lenses. This is followed by a 600 m section of intercalated feldspathic, pelitic and calcareous schists and metarhyolite containing the BT massive sulfide horizon. The mixed schist section is capped by phoney button schist which marks the cessation of felsic volcanism in the BT area. Overlying units are dominated by pelitic schist containing thin lenses of mafic metavolcanic rocks.

Discontinuous lenses of sulfide bearing metasediments lithologically similar to Jerri Creek horizon rocks are present above the button schist sequence suggesting the sequences in the northern and middle fault blocks are stratigraphically equivalent. Mapping to the west of the BT claims (Proffett, 1975) indicates that there is approximately 1,200 m of reverse displacement on the Z fault. This requires a rapid facies change between the fault blocks and suggests the metavolcanic rocks of the middle block were deposited in a trough bound by a shallow carbonate bank.

Lithologies in the southern fault block are not correlative with those of the northern and middle blocks. Pelitic schist is the dominant lithology and is underlain by distinctive albite-rich greenstones and clean marbles. Felsic metavolcanic rocks, feldspathic schists and calcareous schists are absent.

SULFIDE MINERALIZATION

Two significant sulfide bearing horizons have been located on the BT claim group. A number of minor occurrences are also present.

BT Massive Sulfide Horizon

The BT sulfide horizon consists of one to two layers of stratiform massive to semi-massive sulfide, each averaging 1.5 m thick. These layers are known from drilling to extend 2,000 m along strike and 300 m downdip. Mapping has revealed that similar mineralization extends approximately 10 km to the west along the same stratigraphic horizon; surface exposure is insufficient to determine whether it is continuous or a series of lenses.

Mineralization occurs in a complex sedimentary sequence at the top of the metarhyolite section. A fine grained, pyritic metarhyolite forms the footwall to mineralization in the eastern portion of the drilled area; it grades into feldspathic schist to the west. The sulfidic layers are enclosed by feldspathic and highly graphitic pelitic schists. These lithologies

extend upsection to the contact with the phoney button schist except in the western portion of the drilled area where a thin, pyritic metarhyolite and calcareous schists are intercalated with feldspathic schist.

The feldspathic and pelitic schists in the mineralized section contain anomalously high modal percentages of chlorite compared to similar lithologies elsewhere in the BT area. The chlorite rich zone forms a blanket above and below the sulfide horizon throughout the drilled area, although occurrences of abundant chlorite are spotty and tend to be concentrated in several poorly defined zones. There are no distinct pipelike bodies of chlorite. Mapping suggests that irregular chloritic zones extend at least 5 km to the west along the sulfide horizon. The mineralized section also contains minor glaucophane and chloritoid which are rare in other BT feldspathic and pelitic schists. Some of the feldspathic schists contain relict quartz eyes indicating that they may have originally been rhyolitic flows. Siderite, a rare mineral at BT, occurs in calcareous schists of the mineralized section. These relations suggest that the zones directly below and above the BT mineralization were hydrothermally altered. Such alteration generally involves the addition of SiO_2 , MgO and FeO (Ijama, 1974; Utada and others, 1974; Franklin and others, 1975; Large, 1978; Larson, 1979); the zoning of minerals may be complex and is not well understood. The presence of chlorite as well as siderite, glaucophane and chloritoid is consistent with the addition of MgO and FeO ; the presence of excess SiO_2 is difficult to establish due to the high modal percentage of quartz normally present in these rocks.

Massive ore consists of 5 to 12 cm thick beds of pyrite with subsidiary chalcopyrite and red-brown sphalerite which often occurs in thin bands; chalcopyrite usually forms irregular pods. Silver is present in tennantite and a variety of sulfosalts. Pyrite occurs as a groundmass mineral similar in size to chalcopyrite and sphalerite (.5 to 2 mm in diameter) and as euhedral porphyroblasts (up to 4 cm in diameter). Disseminated sulfides, dominantly pyrite, occur in feldspathic and graphitic pelitic schists between massive sulfide layers. Barium is present as cymrite, a hydrous barium aluminum silicate, and is restricted to zones of disseminated sulfides. Current work has failed to detect a coherent metal zonation.

The apparent lack of a nearby rhyolitic thickening and their lateral extent would normally lead to the classification of BT mineralization as a 'distal' volcanogenic massive sulfide (Large, 1977). However, the chloritic alteration and the relatively high $\text{Cu/Pb} + \text{Zn}$ ratios are characteristics of 'proximal' deposits (Large, 1977). The long strike length of mineralization, the alteration mineralogy and the metal ratios suggest that the deposit may have formed as a number of sulfide lenses above an extensive pyroclastic zone that was undergoing variable alteration.

Jerri Creek Horizon

Sulfide mineralization also occurs in the Jerri Creek horizon within calcareous schist of the northern fault block. This horizon extends across the claim block and has been mapped for several kilometers to the east and west. The horizon is 10 to 20 m thick and contains intercalated feldspathic, calcareous and graphitic pelitic schist with lenses of a compositionally banded rock. This banded rock is composed of layers of fine grained quartz (tan weathering), actinolite and epidote with minor garnet, calcite and apatite (dark green weathering), quartz and epidote with minor actinolite, garnet, and calcite (pale green weathering) and quartz, garnet and calcite (red to pink weathering). Individual bands are .5 to 2 cm thick and have sharp contacts; quartz rich bands may be up to 1 m thick.

Both feldspathic schists and compositionally banded rock contain sulfides (pyrite greater than sphalerite and chalcopyrite). Lead anomalies over the zone indicate probable galena. The sulfides are disseminated and fine grained (up to 5 mm). Minor lateral variation exists in both total sulfide content and ratios between the various ore minerals.

The compositionally banded rock may be the metamorphosed equivalent of cherty, and Fe and Mg carbonate-rich chemical sediments. The uniform nature of mineralization and the lack of extensive metavolcanic lithologies suggest that Jerri Creek mineralization may have formed in conjunction with chemical sedimentation. If this is the case, the mineralization may be an example of Sato's (1972) type III brine deposits which are hypothesized to form from dilute high temperature solutions which are lighter than seawater and therefore relatively mobile. The stratigraphic equivalence of the button schist and Jerri Creek mineralization suggest the button schist eruptive event may have been a source of such brines.

ACKNOWLEDGEMENTS

Petrographic investigations were carried out at the University of Washington and Stanford University. Support for the project, and permission to publish the results, were provided by the management of the Anaconda Company. David Heatwole, John Proffett, David Dobson and Jeanine Schmidt are thanked for their encouragement, assistance and discussion during the course of this work.

REFERENCES

- Dillon, J.T., and Pessel, G.H., 1979; Tectonic Significance of late Devonian and late Proterozoic U/Pb zircon ages from metaigneous rocks, Brooks Range, Alaska (abst.): Geol. Soc. of Amer., Cord. Secn, San Jose, Cal., April, 1979, Abst. w. Prog., v. 11, #3, p. 75.
- Franklin, J.M., Kasarda, J., and Poulsen, K.H., 1975; Petrology and chemistry of the alteration zone of the Mattabi massive sulfide deposit: Econ. Geol., V. 70, p. 63-79.
- Fritts, C.E., 1972; Geology and geochemistry of the Anguyucham Mountains, northwestern Hughes quadrangel and vicinity, arctic Alaska: unpublished Alaska Div. of Geol. Surveys Report #43.
- Hitzman, M.W., 1978; Geology of the BT claim group, southwestern Brooks Range, Alaska; unpublished M.S. thesis, Univ. of Washington, Seattle.
- _____, 1979; Geology of the Cosmos Hills, Alaska: unpublished Anaconda Co. Report, Anchorage, Alaska.
- Ijima, A., 1974; Clay and zeolitic alteration zones surrounding deposits in the Hokuroko district, northern Akita, as submarine hydrothermal products, in Ishihara, S., ed., Geology of Kuroko deposits, Mining Geology Spec. Issue # 6, Soc. of Mining Geol. of Japan, p. 267 - 290.
- Kelsey, G.L., 1979; Petrology of metamorphic rocks hosting volcanogenic massive sulfide deposits, Ambler district, Alaska: unpublished M.S. thesis, Ariz. State Univ., Tempe, Ariz.
- Kelsey, G.L., Glavinovich, P.S., and Sheridan, M.F., 1980; High-potassium meta-rhyolites associated with volcanogenic sulfides, Ambler district, northwest Alaska, (abst.): Geol. Soc. of Amer., Cord. Secn., Corvallis, Oregon, March, 1980, Abst. w. Prog., v. 12, # 3, p. 114.
- Large, R.R., 1977; Chemical evolution and zonation of massive sulfide deposits in volcanic terrains: Econ. Geol., V. 72, p. 549 - 572.
- Larsen, P.B., 1977; The chemistry and mineralogy of the alteration pipe of the Precambrian Bruce volcanogenic massive sulfide deposit, Yavapai County, Ariz. (abst.): Geol. Soc. of Can., Ann. Mtg., Vancouver, B.C., April, 1977, Prog. w. Abst., v. 2, p. 31.
- Mayfield and Talleur, I.L., 1978; Bedrock geology map of the Ambler River quadrangle, Alaska: U.S. Geological Survey Open-File Report # 78 - 120 - A, 1 sheet, 1:250,000.
- Nelsen, C.J., 1979; The geology and blueschist petrology of the western Ambler schist belt, southwestern Brooks Range, Alaska: unpublished M.S. thesis, Univ. of New Mex., Albuquerque.
- Proffett, J.M., 1975; Geologic Mapping of the Z claims and adjacent area: unpublished Anaconda Co. Progress Report.
- Roeder, D., and Mull, C.G., 1978; Tectonics of Brooks Range ophiolites, Alaska; Amer. Assoc. of Petrol. Geol. Bull., V. 62, p. 1696 - 1713.
- Sato, T., 1972; Behaviors of ore-forming fluids in seawater; Mining Geology, V. 22, p. 31-42.
- Smith, T.E., Webster, G.D., Heatwole, D.A., Proffett, J.M., Kelsey, G and Glavinovich, P.S., 1978; Evidence of mid-Paleozoic depositional age of volcanogenic base-metal massive sulfide occurrences and enclosing strata, Ambler district, northwest Alaska, (abst.): Geol. Soc. of Amer., Cord. Secn., Tempe, Ariz., March, 1978, Abst. w. Prog., v. 10, #3, p. 148.

- Turner, D.L., Forbes, R.B., and Mayfield, C.F., 1978; K-Ar geochronology of the Survey Pass, Ambler River and eastern Baird Mountains quadrangles, Alaska: U.S. Geological Survey Open-File Report # 78 - 254, 41pp.
- Utada, M., Minato, H., Ishikawa, T., and Yoshizaki, Y., 1974; The alteration zones surrounding Kuroko-type deposits in Nishi-Aizu district, Fukushima Prefecture, with emphasis on the analcime zone as an indicator in exploration for ore deposits: in, Ishihara, S., ed., Geology of Kuroko Deposits, Mining Geology Special Issue #6, Soc. of Mining Geol. of Japan, p. 267 - 290.
- Wiltse, M.A., 1975; Geology of the Arctic Camp prospect, Ambler River quadrangle, Alaska: Alaska Div. of Geol. and Geophys. Surveys, Open-File Report # 60, 41 pp.

Magnetic expression and mineralization of some Tertiary
plutons of Prince William Sound and the Alaska Peninsula,
southern Alaska

J. E. Case, U.S. Geological Survey

MAGNETIC EXPRESSION AND MINERALIZATION OF SOME TERTIARY PLUTONS OF PRINCE WILLIAM SOUND AND THE ALASKA PENINSULA, SOUTHERN ALASKA

Case, J. E.; U.S. Geological Survey, 345 Middlefield Road, Menlo Park, CA. 94025

Granitoid plutons (59-34 m.y.) intrude deformed flysch of Mesozoic and Cenozoic age in the Prince William Sound region (Chugach terrane). Travis Hudson and others postulated that some of the early Tertiary (50-60 m.y.) granitoid plutons of the Chugach terrane are of anatectic origin, partly on the basis of scarcity of mineral deposits typical of subduction-related magmatic arcs. The magnetic susceptibility of the plutons is low, generally less than 0.0001 emu/cm^3 , and most plutons have virtually no aeromagnetic expression, although small positive anomalies occur over some. The few plutons having small positive anomalies probably were emplaced through thick sequences of magnetic mafic igneous rocks. The near absence of aeromagnetic anomalies, geochemical anomalies, and known mineral deposits over Tertiary plutons of the Seward and Blying Sound quadrangles suggests that absence of aeromagnetic anomalies over other plutons of the Chugach terrane would indicate a low probability for occurrence of economic mineral deposits.

In marked contrast, some Tertiary granitoid plutons of the Chignik and Sutwick Island quadrangles, Alaska Peninsula, intrude moderately deformed Mesozoic and Cenozoic sedimentary and volcanic rocks, and many are associated with copper and molybdenum deposits. Tertiary igneous rocks of the Alaska Peninsula are thought to represent a subduction-related magmatic arc. Most plutons cause conspicuous positive aeromagnetic anomalies ranging from several hundred to 1700 gammas. Magnetic susceptibilities are variable, but many are in the range $0.001\text{-}0.003 \text{ emu/cm}^3$. Because positive aeromagnetic anomalies occur over plutons known to be mineralized, positive anomalies over other plutons constitute reconnaissance exploration guides.

(Courtesy of the Geological Society of America, 1980)

Geology update of the Quartz Hill molybdenum property
near Ketchikan, Alaska

P. R. Smith, U.S. Borax and Chemical Corporation

GEOLOGY UPDATE OF THE QUARTZ HILL MOLYBDENUM PROPERTY NEAR KETCHIKAN,
ALASKA

SMITH, Patrick R., U.S. Borax And Chemical Corporation, E. 5603
Third Avenue, Spokane, Washington 99206

In 1974 a major stockwork molybdenite deposit was discovered by U.S. Borax in Southeastern Alaska. The discovery was a direct result of a regional stream sediment exploration program. The deposit is related to a porphyritic quartz monzonite of Miocene age referred to as the Quartz Hill stock.

Felsic-intrusives of the Quartz Hill complex are chemically and mineralogically similar and consist of quartz, K-feldspar, albite, and minor biotite. Due to the lack of compositional variation the classification of the felsic rock units is based primarily on textural characteristics. Porphyries account for over 90 percent of the Quartz Hill stock. The sequence of rocks present within the Quartz Hill stock from oldest to youngest is as follows: quartz monzonite porphyry, biotite quartz monzonite, porphyritic quartz monzonite, quartz latite porphyry, porphyritic quartz latite, quartz feldspar porphyry, and fine-grained quartz monzonite. Mineralization is present within each of the above units although significantly weaker after emplacement of the quartz latite porphyry. Volcanic type breccias have been noted in three localities and large xenoliths of the gneissic country rock are common at depths of 1000 feet or more.

The textural and structural features of the rocks express a shallow environment of emplacement. The thin gneissic roof capping on the top of Quartz Hill suggests that erosion has exposed the uppermost portion of the stock.

The Quartz Hill ore body as drilled to date is a tabular to umbrella shaped stockwork within the intrusive complex and contains more than 700 million tons of ore.

(Courtesy of the Geological Society of America, 1980)

Genesis of gold vein mineralization in an Upper Cretaceous
turbidite sequence, Hope-Sunrise district, southern Alaska

P. A. Mitchell, Exxon Minerals USA

M. L. Silberman, U.S. Geological Survey

J. R. O'Neil, U.S. Geological Survey

GENESIS OF GOLD VEIN MINERALIZATION IN AN UPPER CRETACEOUS TURBIDITE SEQUENCE, HOPE-SUNRISE DISTRICT SOUTHERN ALASKA

A Preliminary Report

By Peter A. Mitchell, Miles L. Silberman, and James R. O'Neil

INTRODUCTION

The Hope-Sunrise mining district is situated in the Kenai Mountains of southern Alaska, approximately 45 km southeast of Anchorage (fig. 1). The district is located within the westernmost portion of the Valdez Group sedimentary sequence, which is comprised predominantly of turbidite deposits formed during Late Cretaceous subduction.

The mineral deposits of the Hope-Sunrise mining district are low-tonnage, high-grade occurrences. Mining within the district was most intense between 1910 and 1930. During these years several small properties were active, however, only one mine, the Lucky Strike, had significant production. The Lucky Strike mine produced more than 50,000 troy ounces of gold.

GEOLOGIC SETTING

Regionally, the Valdez Group sedimentary sequence is dominated by quartzofeldspathic to feldspatholithic sandstone and siltstone, with minor conglomerate, claystone, limestone and calcareous sedimentary rocks, tuff and bedded chert. These units have been metamorphosed to the chlorite zone, and locally to the biotite zone, of the greenschist facies as defined by Miyashiro (1973) (Tysdal and Case, 1979).

Sandstone Petrography

The sandstones of the Hope-Sunrise district are subquartzose to nonquartzose (detrital quartz 50 percent of all detrital constituents) rocks rich in volcanic lithic fragments. They are compositional graywackes (unstable rock fragments feldspar grains), but in general are not textural graywackes (primary matrix 15 percent). The average mode of the sandstones studied, $Q_{20}F_{24}L_{56}$, plots within the feldspatholithic field, which is denoted by the shaded area of figure 2.

The Valdez sandstones of the Hope-Sunrise district are compositionally unstable and immature. Texturally, the mean sandstone is comprised of 88 percent framework grains, 10 percent primary matrix, and 2 percent authigenic phyllosilicate and rare carbonate cement (fig. 2). No zeolite minerals were identified either by optical or X-ray diffraction techniques.

A petrographic analysis of these 19 sandstone samples indicates that the sedimentary rocks were derived from a volcanic arc provenance (Mitchell, 1979). The dominance of felsite and hypabyssal rock fragments suggest a supracrustal volcanic or volcanoclastic source terrane that was comprised chiefly of rhyolite to dacite

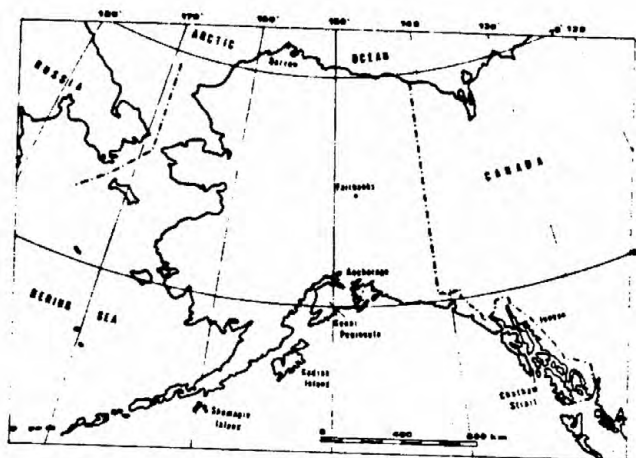


Fig. 1.—Map of Alaska and adjacent areas, with inset map of the Kenai Peninsula showing the study area, and major towns and roads.

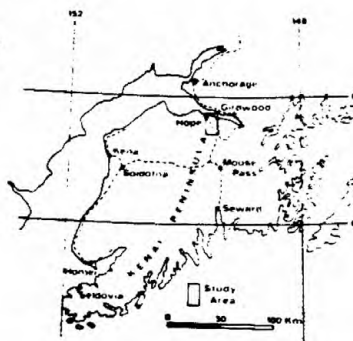
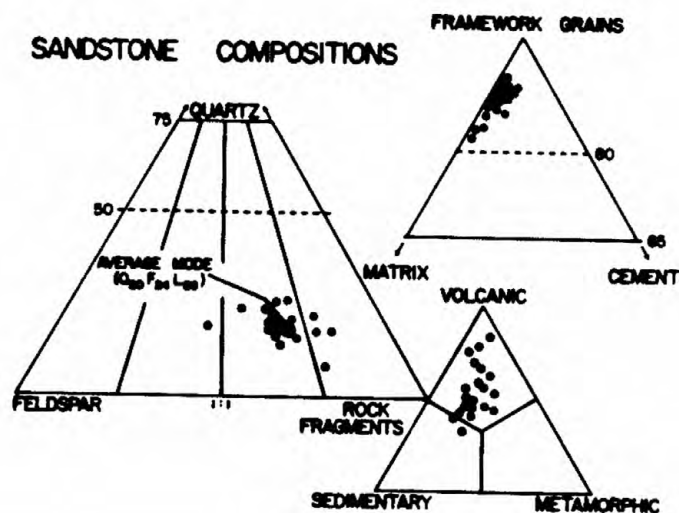


Figure 1.—Map of Alaska and adjacent areas, with inset map of the Kenai Peninsula showing the Hope-Sunrise district (study area) and the major towns and roads.



	% QUARTZ (Q)	% FELDSPAR (F)	% LITHIC (L)
MEAN	20.4	24.2	55.4
RANGE	8-27	11-43	36-72
STANDARD DEVIATION	4.2	4.1	8.5

C = TOTAL POLYCRYSTALLINE QUARTZOSE GRAINS, V = TOTAL VOLCANIC LITHIC GRAINS, P = TOTAL PLAGIOCLASE FELDSPAR GRAINS

	C/Q	P/F	V/L
MEAN	0.34	0.62	0.58
RANGE	0.19-0.59	0.50-0.97	0.35-0.80
STANDARD DEVIATION	0.09	0.13	0.14

MODAL ANALYSES OF 19 VALDEZ SANDSTONES

Figure 2.--Composition diagram and salient statistics for 19 Valdez Group sandstones.

lithologies, but included minor basalt and andesite. A relative major contribution of sedimentary and metasedimentary detritus implies that the volcanic arc was being actively eroded. Plutonic rock fragments are a minor phase, but suggest the incipient unroofing of subjacent plutons.

Intrusive Rocks

In coastal southern Alaska, major intrusive events occurred during the Paleocene to Late Eocene time (60 to 43 m.y., Hudson and others, 1979) and again in early Oligocene time (37 to 35 m.y., Lanphere, 1966). The composition of the central mass of these intrusive bodies ranges from granodiorite to granite. The only intrusive rocks exposed within the Hope-Sunrise area are narrow (~3 m), fine-grained dikes, that were intruded by ~53 m.y. B.P. Compositionally the dikes are either tonalite, granodiorite, or alkali granite.

Structure

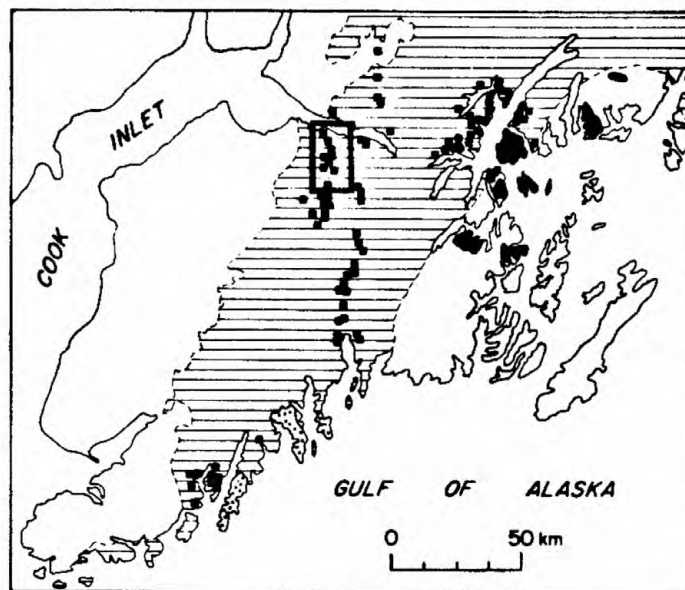
A detailed structural analysis of the Hope-Sunrise district (Mitchell, 1979) suggests that folding began shortly after sediment deposition, producing two broad, arcuate, open folds and a weak axial plane cleavage. As deformation continued, the limbs of these early folds were deformed additionally by the development of small, closely spaced isoclinal folds that were accompanied by pervasive axial plane slaty cleavage oriented ~N. 20° E. Folding accounted for over 40 percent horizontal shortening, increasing the overall thickness of the sedimentary prism to greater than >10 km. Shearing and faulting began late during isoclinal folding and minor movement has continued to the present, but without major displacement on any known fault. Post-folding stress release produced a penetrative joint system oriented west-northwest and north.

Mineralization

Gold mineralization hosted by the sedimentary rocks of the Valdez Group has a pronounced spatial distribution concentrated along a north south belt that may be related to deep-seated structures, variations in lithology, and regional geothermal gradients (fig. 3). The deposits are primarily fissure fillings in which native gold is hosted by a quartz calcite gangue (Tuck, 1933). Gold veins within the Hope-Sunrise district are narrow, that is, generally less than 10 cm, and persist for only a few meters along strike, though the larger veins may exceed 1 m in width and may be laterally continuous for more than 100 m along strike and dip.

Quartz Veins

The oldest veins identified within the Hope-Sunrise district are thin, irregular quartz veins that in general parallel the regional cleavage. These barren, veins are common throughout the district and are believed to be related to the metamorphism that followed the main stages of regional deformation. Metamorphic segregation quartz is milky, fine-grained and massive, and typically is free of sulfide and iron oxide minerals.



HOPE - SUNRISE DISTRICT



VALDEZ GROUP



GOLD LODE DEPOSITS

IGNEOUS ROCKS



± 35 M.Y.B.P.



± 50 M.Y.B.P.

Figure 3.--Distribution of gold lode deposits and occurrences within the Valdez Group sedimentary sequence that is exposed on the Kenai Peninsula, Alaska.

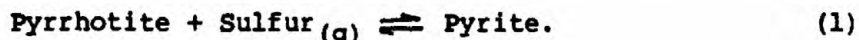
A second type of vein is comprised of milky to blue-gray mineralized quartz usually accompanied by calcite. These veins are coarse-grained and commonly vuggy, contain prominent sulfide and iron oxide minerals, and are typically sheared or brecciated. Joints, faults and mineralized quartz veins cross-cut the regional cleavage and metamorphic segregation quartz veins.

Vein mineralogy

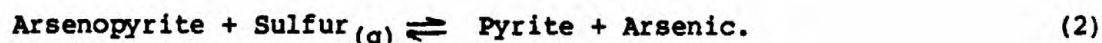
The principal gangue minerals, quartz and calcite, are locally accompanied by alkali feldspar (albite + orthoclase). Zoning of the gangue minerals is common in many of the larger veins, however, quartz is always the earlier mineral and is generally more abundant. Locally base metal sulfides are spatially associated with the calcite, or are found along the quartz-calcite interface. Minor amounts of arsenopyrite, pyrite, sphalerite, hemimorphite(?), galena, gold, silver, and locally pyrrhotite occur in all of the major veins, but disseminated wall-rock mineralization is rare. Arsenopyrite is the most abundant sulfide phase present in the veins, and gold is the most common precious metal.

GEOCHEMISTRY

The presence of arsenopyrite and pyrite in all of the mineral assemblages restricts the sulfur fugacity to a relatively narrow range. The lower limit of sulfur fugacity is established by the coexistence of pyrite and pyrrhotite (fig. 4). Pyrrhotite is a minor phase and is not always present, thus in general the fugacity of sulfur remained at or above the reaction:

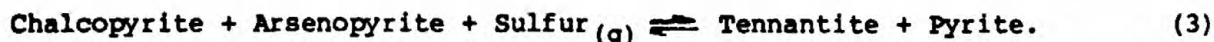


The upper limit of sulfur fugacity is set by the reaction



The assemblage pyrite + arsenic is not known within the district, and consequently the fugacity of sulfur must be below the upper limit established by equation (2).

The possible variations in sulfur fugacity are further restricted by the presence of copper as chalcopyrite, although these restrictions are speculative, since copper is present only locally. Nonetheless it is important to note that chalcopyrite is the only copper species that was identified. Since tennantite is not present, the upper limit of sulfur fugacity must be less than that needed to cause the reaction



Further, reaction (3) must lie at a sulfur fugacity intermediate to reactions (1) and (2) (fig. 4).

Mineral Assemblages and Metamorphic Grade

The mineral assemblages of the veins provides an upper temperature limit for mineralization. The presence of pyrite with arsenopyrite establishes an upper temperature limit of 491°C (Clark, 1960), from the invariant point pyrrhotite + pyrite + arsenopyrite + a member of the orpiment-realgar solid solution series $[As_xS_{(1)}]$, (fig. 4).

Additional, although uncertain, constraints on the temperature of hydrothermal vein formation are suggested by the regional metamorphic grade of the sedimentary sequence. Although metamorphic grade in the Valdez Group varies somewhat, the rocks exposed within the Hope-Sunrise district have been metamorphosed to very low-grade greenschist facies. Their metamorphic grade is established by the pervasive presence of tri-octahedral septachlorite (Deer and others, 1971). Low-grade greenschist facies metamorphism occurs between 300°C and 425°C (Winkler, 1976; Miyashiro, 1973). We believe that the early metamorphic segregation quartz veins were probably deposited at these temperatures. However, preliminary fluid inclusion filling temperatures suggest that the mineralized quartz veins were deposited at significantly lower temperatures.

Fluid Inclusion Temperatures

Fluid inclusion filling temperatures are available from only two samples, one from a mineralized quartz vein, and one from a calcite vein occurring within a mineralized dike (table 1).

The quartz contains very small, liquid-rich inclusions with variably sized gas bubbles. Homogenization took place in the liquid phase, and filling temperatures vary from 168°C to 219°C, averaging 191°C. No daughter minerals were observed, suggesting at most moderate salinity. In general, salinities of fluid inclusions in epithermal ore deposits similar to those at Hope are less than 2 weight percent (Nash, 1972). Vugs, open spaces, and common drusy quartz crystals lining cavities in mineralized veins attest to their shallow depth of emplacement, hence no pressure corrections for the fluid inclusion filling temperatures were made.

The fluid inclusions in the calcite sample are also small. Filling temperatures range from 100°C to 155°C, and appear to fall into two groups, one from 100°C to 136°C, and another from 150°C to 155°C. These limited data suggest that late-stage calcite may have precipitated during two stages, at somewhat different temperatures. The gas bubbles are small, occupying one eighth to one tenth of the inclusion volume. No daughter minerals were observed in the calcite fluid inclusions.

STABLE ISOTOPE RESULTS

Four quartz vein samples were chosen for a preliminary stable isotope evaluation. These samples include three mineralized veins (including the sample upon which the fluid inclusion filling temperatures were determined) and one metamorphic segregation vein (table 2). The δD of fluid inclusion waters of the three mineralized quartz veins averages -106 ± 6 per mil, which is about the same value as modern meteoric water in this area (-110 per mil; Taylor, 1974). These data strongly suggest that the source of the mineralized hydrothermal fluid was

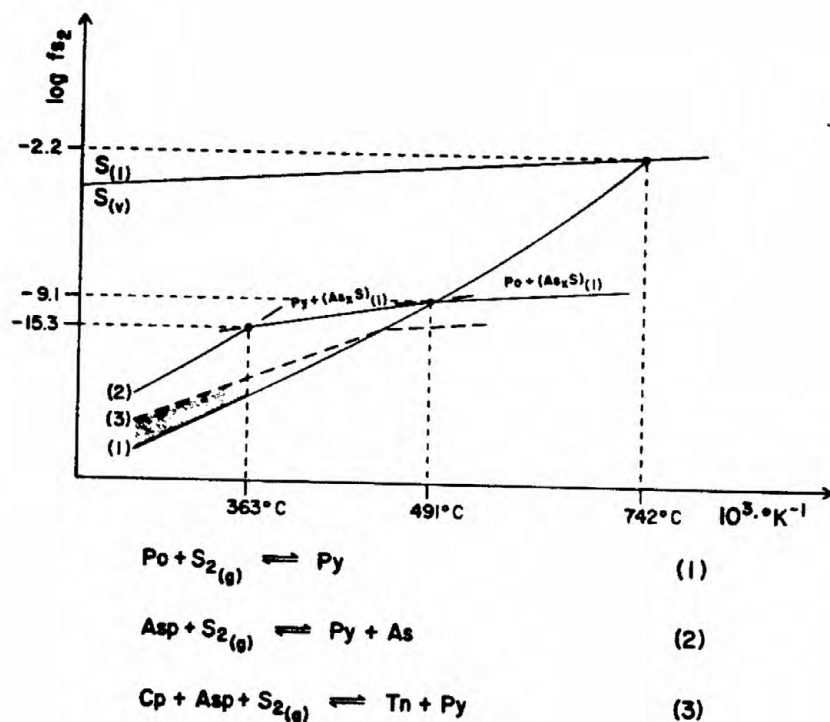


Figure 4.--Temperature (T)-sulfur fugacity (f_{S_2}) diagram showing the possible range in T- f_{S_2} suggested by equations 1-3. The thermodynamic data was taken from Clark (1960), and Barton and Skinner (1979). The Sulfur condensation curve is represented by the line $\text{S}_{(v)}-\text{S}_{(l)}$.

Table 1.--Preliminary fluid inclusion filling temperatures for mineralized quartz and calcite veins of the Hope-Sunrise district

FLUID INCLUSION DATA

<u>VEIN TYPE</u>	<u>PRESSURE (BARS)</u>	<u>FILLING TEMPERATURE (MEAN °C)</u>	<u>STANDARD DEVIATION</u>
QUARTZ	1-25	191	16.7
CALCITE	1-10	137	12.4
GROUP A	—	153	2.3
GROUP B	—	129	7.5

Table 2.--Stable isotope data for hydrothermal and metamorphic segregation quartz from the Hope-Sunrise district

STABLE ISOTOPE DATA (VEIN QUARTZ)			
<u>SAMPLE</u>	<u>ORIGIN</u>	$\delta^{18}\text{O} \text{ ‰}$ (QUARTZ)	$\delta \text{ D } \text{ ‰}$ (FLUID INCLUSION)
1	HYDROTHERMAL	+16.2	-100
2 *	HYDROTHERMAL	+17.1	-101
3	HYDROTHERMAL	+16.6	-117
4	METAMORPHIC SEGREGATION	+19.9	—

* (fluid inclusion sample)

dominantly meteoric water. Assuming that meteoric water was the source of the ore fluid, and using the meteoric water equation, $\delta D = 8\delta^{18}O + 10$ (Craig, 1961), the original $\delta^{18}O$ of the meteoric water is calculated to be -14.5 per mil.

The average $\delta^{18}O$ of the three mineralized quartz samples is $+16.6 \pm 0.3$ per mil (standard error). Utilizing the quartz-water fractionation relationship of Bottinga and Javoy (1973) and the average fluid inclusion filling temperature of $191^\circ C$, we calculate that main stage quartz was in equilibrium with an aqueous fluid whose $\delta^{18}O$ was +1.3 per mil. Water with an original $\delta^{18}O$ of -14.5 per mil could attain a $\delta^{18}O$ of +1.3 per mil by isotopic exchange with the silicate minerals of the sedimentary and metamorphic host rocks at elevated temperatures.

Thermal waters of meteoric origin usually undergo an oxygen shift of a few per mil toward higher $\delta^{18}O$ from exchange with "heavier" oxygen in their host rocks (Taylor, 1974; White, 1974). Shifts of as large as +16.8 per mil have been documented for such fluids in epithermal vein deposits hosted by sedimentary and low-grade metamorphic rocks in central Nevada (O'Neil and Silberman, 1974). The shift in $\delta^{18}O$ in our samples is about +16 per mil, and is within the range of the shift identified in the Nevada deposits hosted by wall rocks similar to those at Hope. No isotopic data presently exists for the host rocks in the Hope-Sunrise district, but low-grade metamorphic rocks of this composition are usually in the range of +8 to +18 per mil (Taylor, 1974; O'Neil, 1979). In order to undergo an oxygen shift of approximately 16 per mil from exchange with the wall rocks, the water to rock ratio must have been very small (O'Neil and Silberman, 1974). The fact that so much isotopic exchange is inferred to have taken place between the water and the host rocks implies that other components of the mineralized veins, such as the metals, sulfur and carbon, may have originated in the wall rocks. Additional geochemical and isotopic analyses are necessary to confirm this suggestion.

No δD analyses from fluid inclusions are available for the metamorphic segregation quartz. The $\delta^{18}O$ of the metamorphic segregation quartz has a slightly heavier value than the mineralized quartz (table 2). Based on an assumed lower greenschist facies metamorphic temperature of $350^\circ C$ and the quartz-water fractionation relationship of Bottinga and Javoy (1973), we calculate that the metamorphic segregation quartz was in isotopic equilibrium with water of $\delta^{18}O$ of +11 per mil. This fluid appears to be richer in ^{18}O than the ore fluid, and is within the oxygen isotopic composition range identified with water of metamorphic origin +5 to +25 per mil (Taylor, 1974). The fluids in equilibrium with metamorphic quartz thus appear to be of different oxygen isotopic composition from those in equilibrium with the mineralized quartz. However, additional data, principally δD analyses of inclusions waters of the metamorphic quartz have to be obtained to confirm origin of these fluids suggested by our interpretation.

Sulfur Isotope Results

The preliminary results of sulfur isotope analyses were obtained from two samples (table 3). The arsenopyrite of sample 1 occurs in a mineralized quartz vein, whereas the pyrite of sample 2 occurs in siltstone adjacent to metamorphic segregation quartz sample no. 4 (table 2). Since the available sulfur isotope data is so restricted and only individual mineral rather than total sulfur data are available (Rye and Ohmoto, 1974) conclusions concerning the genesis of the mineralization are obviously very speculative. However, we believe some discussion is warranted.

Table 3.--Sulfur isotope data for two sulfide minerals from the Hope-Sunrise district

SULFUR ISOTOPE DATA			
Sample	Mineral	Origin	$\delta^{34}\text{S}$ per mil
1	Arsenopyrite	Hydrothermal quartz vein	-0.14
2	Pyrite	Disseminated in meta-siltstone	+7.69

The pyrite sample has a $\delta^{34}\text{S}$ similar to that derived from ocean water sulfates, (Rye and Ohmoto, 1974) perhaps by diagenetic or metamorphic reduction. The arsenopyrite sample has a $\delta^{34}\text{S}$ value of close to zero, which would normally be interpreted as igneous sulfur. However, we suggest that kinetic effects on sulfur isotope fractionation may better explain the difference in $\delta^{34}\text{S}$ between metamorphic and mineralized vein sulfides. If the sulfur was diffusing out of the wall rocks, along with other components of the ore, as we suggest on the basis of our interpretation of the oxygen and deuterium data, then preferential enrichment of the light sulfur isotope, ^{32}S , may have occurred in the mineralized sample. Our data suggest that an enrichment of 8 per mil between the wall rock and vein sulfide must have occurred. Although fractionation of ^{32}S between pyrite and arsenopyrite is not known, it is unlikely that it is this large at 200°C (Friedman and O'Neil, 1977, fig. 46). Enrichment of 14 per mil in ^{32}S was documented in the East Tintic district, Utah, where diffusion controlled the distribution of sulfides adjacent to lode deposits (Jensen, 1967) during mineralization.

POTASSIUM-ARGON AGES

Potassium-argon ages were obtained from two hydrothermally altered and mineralized dikes. Muscovite, separated from an alkali granite dike cut by thin mineralized quartz veins gave a K-Ar age of 53.2 ± 1.6 m.y. (sample 1, table 4). A whole rock sample of an intensely altered dike recrystallized to an assemblage of muscovite, quartz, carbonate, chlorite and albite gave an age of 52.7 ± 1.6 m.y. (sample 2, table 4). The latter dike is strongly brecciated, cut by mineralized quartz-carbonate veins and contains disseminated arsenopyrite (Mitchell, 1979). From these data we infer that hydrothermal alteration and mineralization occurred during earliest Eocene time.

Table 4.--Potassium-argon ages for two hydrothermally altered and mineralized dikes of the Hope-Sunrise district

<u>SAMPLE</u>	<u>LITHOLOGY</u>	<u>MINERAL</u>	<u>ORIGIN</u>	<u>AGE (m.y.)</u>
1	ALKALI GRANITE DIKE	MUSCOVITE	HYDROTHERMAL ALTERATION	53.2 \pm 1.6
2	ALKALI GRANITE DIKE (?)	WHOLE ROCK	HYDROTHERMAL ALTERATION	52.7 \pm 1.6

DISCUSSION

Gold lode mineralization occurred, at least locally, in the Valdez Group sedimentary rocks during early Eocene time. The auriferous veins formed from fluids of dominantly meteoric origin, and were localized by steeply dipping west-northwest and north trending joint and fault systems. These structures generally cross-cut the regional cleavage that developed during penetrative deformation of the sedimentary prism as it was accreted to the North American continent. Accretion probably was accomplished during Late Cretaceous to Early Tertiary time (MacKevett and Plafker, 1974; Byrne, 1978). Small plutons intruded the sedimentary prism between 60 and 43 m.y. ago (Hudson and others, 1979). These intrusions are part of the Sanak-Baranoff belt of plutonic rocks, and are believed to be of anatectic origin (Hudson and others, 1979). The plutons are undeformed, and must have been intruded after accretion. In the Kenai Peninsula, potassium-argon ages of these plutonic rocks range from 59 to 55 m.y. B.P. (Tysdal and Case, 1979). Granitic dikes, similar to the ones that were hydrothermally altered in the Hope-Sunrise district occur throughout the Kenai Peninsula, and are probably the same age and origin as the plutons. Thermal effects of the accretion process probably led to high-grade metamorphism and partial melting of the lower parts of the accretionary prism after it was joined to the continent (Hudson and others, 1979). We suggest that lower grade metamorphism occurred in the upper parts of the prism generating the greenschist facies mineral assemblage and the cleavage localized metamorphic segregation quartz. During late stages of the thermal evolution of the area, temperatures waned, and the structures that cut regional cleavage opened after stress, caused by accretionary vergence of the terrane was released, perhaps during regional uplift. This allowed access of meteoric water, which formed small hydrothermal circulation cells. The meteoric-water-dominated fluid dissolved silica, carbon, sulfur, and metals from the unstable volcanic component in the sedimentary prism and deposited them as auriferous lodes in the open structures. Thus, hydrothermal mineralization occurred late in the accretionary history of the Valdez Group sedimentary sequence, as a result of metamorphic-hydrothermal processes whose later stages were dominated by the influx of meteoric water.

An unanswered question in this proposed model is why the fluids generated by prograde metamorphism shortly after accretion did not result in solution of ore components from the volcanic material deeper in the prism and their deposition in quartz veins localized along regional cleavage in the shallower, lower grade zones of the greenschist facies meta-sediments - a process which Henley and others (1976) propose for lode deposits in the Otago area of New Zealand. The cleavage localized quartz in the Kenai peninsula is notably barren. It may be that a declining temperature regime was necessary, and that open structures were required, and these may not have been present to the required extent until post-accretionary uplift was taking place.

REFERENCES

- Barton, P. B., Jr., Skinner, B. J., 1979, Sulfide mineral stabilities, in Barnes, H. L., ed., *Geochemistry of hydrothermal ore deposits*, (2nd ed.): New York, John Wiley and Sons, p. 278-403.
- Bottinga, Y. And Javoy, M., 1973, Comments on oxygen isotope geothermometry: *Earth and Planetary Science Letters*, v. 20, p. 250-265.
- Byrne, T., 1978, Early Tertiary demise of the Kula-Pacific spreading center: *Geological Society of America Abstracts*, v. 10, p. 98.
- Clark, L. A., 1960, The Fe-As-S system: phase relations and applications: *Economic Geology*, v. 55, p. 1345-1381 and 1631-1652.
- Deer, F. R. A., Howie, R. A., and Zussman, J., 1971, *An introduction to the rock-forming minerals*: New York, John Wiley, 528 p.
- Friedman, Irwin, and O'Neil, J. R., 1977, Compilation of stable isotope fractionation factors of geochemical interest, in Fleischer, M., ed., *The data of geochemistry*: U.S. Geological Survey Professional Paper 440-KK, 57 p.
- Haas, J. L., Jr., 1971, The effect of salinity on the maximum thermal gradient of a hydrothermal system at hydrostatic pressure: *Economic Geology*, v. 66, p. 940-946.
- Henley, R. W., Norris, R. J., and Paterson, C. J., 1976, Multi stage ore genesis in the New Zealand geosyncline. A history of post metamorphic lode emplacement: *Mineralium Deposita*; II, 180-196.
- Hudson, Travis, Plafker, George, and Peterman, Zell, E., 1979, Paleogene anatexis along the Gulf of Alaska margin: *Geology*, v 7, p. 573-577.
- Ingerson, Earl, 1947, Liquid inclusions in geologic thermometry: *American Mineralogist*, v. 32, p. 375-388.
- Jensen, M. L., 1967, Sulfur isotopes and mineral genesis, in Barnes, H. L., ed., *Geochemistry of hydrothermal ore deposits*: New York, Holt, Rinehart and Winston, p. 143-165.
- Lanphere, M. A., 1966, Potassium-argon ages of Tertiary plutons in the Prince William Sound region, Alaska, in *Geological Survey research 1966*: U.S. Geological Survey Professional Paper 550-D, p. D195-D198.
- MacKevett, E. M., Jr., and Plafker, George, 1974, The Border Ranges fault in south central Alaska: *U.S. Geological Survey, Journal of Research*, V. 2, p. 323-329.
- Mitchell, P. A., 1979, *Geology of the Hope-Sunrise (Gold) mining district, north-central Kenai Peninsula, Alaska*: Stanford, Calif., Stanford University, M.S. thesis, 123 p.
- Nash, J. T., 1972, Fluid inclusion studies of some gold deposits in Nevada, in *Geological Survey research 1972*: U.S. Geological Survey Professional Paper 800-C, p. C15-C19.

- Nash, J. T., 1976, Fluid-inclusion petrology--data from porphyry copper deposits and applications to exploration: U.S. Geological Survey Professional Paper 907-D, 16 p.
- O'Neil, J. R., 1979, Stable isotope geochemistry of rocks and minerals, in, Jager, E., and Hunziker, J. C., eds., Lectures in Isotope Geology: Berlin, Springer-Verlag, p. 235-263.
- O'Neil, J. R., and Silberman, M. L., 1974, Stable isotope relations in epithermal Au-Ag deposits: Economic Geology, v. 69, no. 4, p. 902-909.
- Rye, R. O., and Ohmoto, Hiroshi, 1974, Sulfur and carbon isotopes and ore genesis: A review: Economic Geology, v. 69, p. 826-842.
- Taylor, H. P., 1974, The application of oxygen and hydrogen isotope studies to problems of hydrothermal alteration and ore deposition: Economic Geology, v. 69, p. 843-883.
- Tuck, Ralph, 1933, The Moose Pass-Hope district, Kenai Peninsula, Alaska: U.S. Geological Survey Bulletin 849-I, p. 469-530.

Kennecott-type copper deposits, Wrangell Mountains, Alaska--
an update and summary

E. M. MacKevett, Jr., U.S. Geological Survey
A. K. Armstrong, U.S. Geological Survey
R. W. Potter, II, U.S. Geological Survey
M. L. Silberman, U.S. Geological Survey

KENNECOTT-TYPE COPPER DEPOSITS, WRANGELL MOUNTAINS, ALASKA--AN UPDATE AND SUMMARY

MACKEVETT, E. M., Jr.; ARMSTRONG, A. K.; POTTER, R. W., II;

SILBERMAN, M. L.; U.S. Geological Survey, Menlo Park, CA 94025

Kennecott-type deposits are stratabound, massive, copper-sulfide-rich lodes confined to the partly dolomitic intertidal, supratidal and sabhka facies of the lower 130 m of the Late Triassic Chitistone Limestone, which disconformably overlies Nikolai Greenstone and is paraconformably overlain by open-marine carbonate rocks. The Nikolai consists of altered tholeiitic basalt with an intrinsic copper content of 155 ppm. Both units are part of the allochthonous Wrangellia terrane. Ore bodies at Kennecott are localized along the fault-truncated limb of a syncline as long, thin, upward-tapering, plunging wedges. Solution collapse breccias occur near many deposits. Sulfide ore phases of the $\text{CuS-Cu}_2\text{S}$ system generally exceed oxide ore 3 to 1. High copper and sulfur, low iron content, important by-product silver, minor gangue, and generally sharp wall-rock contacts characterize ore. Malachite and azurite are widely distributed throughout all known deposits, and extend to the deepest workings. Fluid inclusion and mineralogic studies, corroborated by oxygen isotope measurements, suggest that ore formed at temperatures of $90^\circ \pm 10^\circ\text{C}$. The deposits probably reflect filling of voids and caverns subsequent to karstification, with copper derived from the Nikolai. Limited sulfur isotope data permit derivation of sulfur from algal mat decay or evaporite sulfate alteration. Whether ore formed during the interval marked by the paraconformity in the lower Chitistone or during later alteration and weak metamorphism of the Nikolai, concomitant with accretion of Wrangellia, is not known.

(Courtesy of the Geological Society of America, 1980)

Metallogenic and tectonic significance of oxygen isotope
data and whole-rock potassium-argon ages of the Nikolai
Greenstone, McCarthy quadrangle, Alaska

M. L. Silberman, U.S. Geological Survey

E. M. MacKevett, Jr., U.S. Geological Survey

C. L. Connor, U.S. Geological Survey

Alan Matthews, Hebrew University

METALLOGENIC AND TECTONIC SIGNIFICANCE OF WHOLE-ROCK POTASSIUM-ARGON
AGES OF THE NIKOLAI GREENSTONE, MCCARTHY QUADRANGLE, ALASKA

M. L. Silberman*, E. M. MacKevett Jr.*, C. L. Connor*, Alan Matthews**

ABSTRACT

The Middle and (or) Late Triassic Nikolai Greenstone, part of the allochthonous terrane of Wrangellia, is typically altered and locally metamorphosed to prehnite-pumpellyite facies with chlorite and epidote as the most common secondary minerals. Intrinsic copper content averages 155 ppm, and two types of concentrations of copper in the Nikolai are common: (1) native copper fillings of amygdules and rubble zones near flow tops, and (2) veins and thin replacement zones that contain native copper and copper-iron sulfides in quartz-epidote or calcite gangue in faults and fractures. Oxygen isotope data from quartz and epidote from three copper-bearing veins yield calculated ore fluid temperatures of approximately 200°C and $\delta^{18}\text{O}$ of approximately +1 per mil in agreement with a metamorphic-segregation origin of these deposits, as suggested by Sinclair (1977).

Seven K-Ar ages of chloritized greenstone, including those adjacent to veins fall on an initial argon diagram with a zero intercept and a slope which yields an isochron age of 112 ± 11 m.y. The ages define a Cretaceous thermal-metamorphic episode which is responsible for alteration and mineralization. The episode is younger than a major Jurassic orogeny, accompanied by granitic intrusion, in the area, and appears to be unaffected by minor granitic intrusion in the middle to late Tertiary. We believe the Cretaceous event is related to accretion of Wrangellia to its present relative position in North America. This age of accretion agrees with stratigraphic and structural evidence cited by other workers.

INTRODUCTION

The Nikolai Greenstone, a thick sequence of tholeiitic, dominantly subaerial basalt flows exposed in the Wrangell Mountains and nearby areas of southern Alaska and the Yukon Territory (fig. 1) forms an important part of the allochthonous terrane of Wrangellia. On the basis of paleomagnetic data (Hillhouse, 1977), Wrangellia is believed to have formed at low latitudes, within 15 degrees of the equator, and to have been tectonically transported to its present position (Jones and others, 1977). Allochthonous terranes with lower Mesozoic stratigraphy similar to that of Wrangellia in the McCarthy quadrangle, are juxtaposed against different lower Mesozoic and older rocks from southern Alaska to Vancouver Island and possibly in the Hell's Canyon area of Oregon-Idaho, and are believed to be the disrupted remnants of a once coherent sub-continental block (Jones and others, 1977). In the McCarthy

*U.S. Geological Survey, Menlo Park, CA 94025.

**Hebrew University, Jerusalem, Israel.

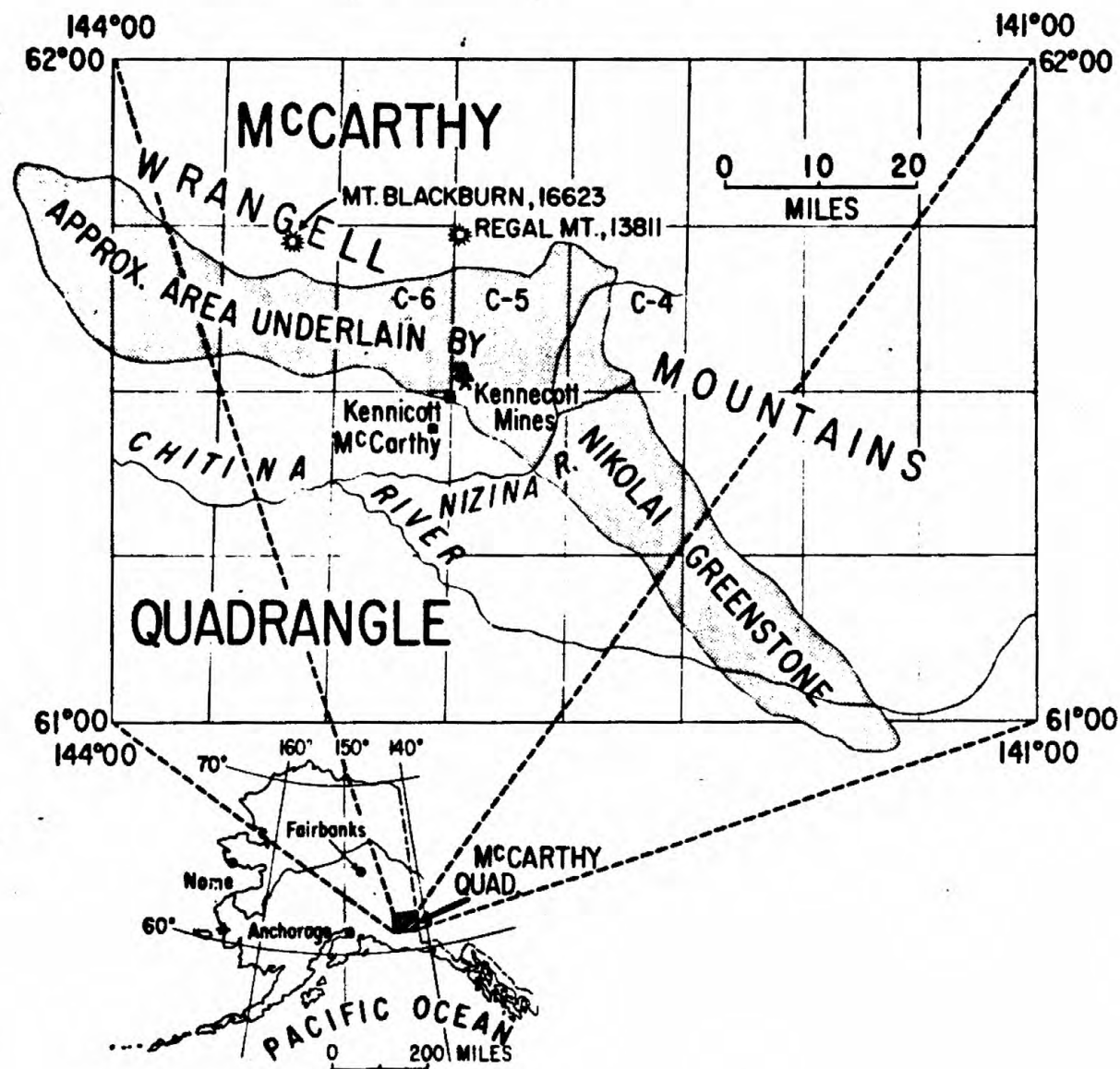


Figure 1.—Maps showing location of McCarthy quadrangle, the Wrangell Mountains and the distribution of the Nikolai Greenstone.

area, emplacement of Wrangellia appears to have been accompanied by frictional heating, which caused alteration and (or) low grade metamorphism of the Nikolai Greenstone, and the generation of copper-bearing vein deposits related to fluids of metamorphic-segregation origin. These veins are localized along pre-existing structures. This report includes preliminary stable isotope data which bear on the conditions of origin of the deposits and on the alteration/metamorphism of the greenstone, and K-Ar whole rock ages which we believe date the time of arrival of Wrangellia to its present position relative to adjacent terranes.

WRANGELLIA AND THE GEOLOGY OF THE WRANGELL MOUNTAINS

The oldest rocks known in Wrangellia in the Wrangell Mountains and elsewhere consist of slightly metamorphosed upper Paleozoic sedimentary and volcanic rocks (fig. 2), believed to represent an upper Paleozoic Island arc, formed largely on oceanic crust (MacKevett, and others, 1977; MacKevett, 1978). The upper Paleozoic rocks are unconformably overlain by more than 3000 m of Triassic subaerial tholeiitic flows and minor subaqueous pillow lavas of the Nikolai Greenstone. Fossils in underlying and overlying rocks indicate that the Nikolai Greenstone flows were extruded in the Middle and (or) Late Triassic (MacKevett, 1978). The Nikolai is disconformably overlain by thin, inner platform carbonate rocks, the Chitistone and Nizina Limestones of Late Triassic age. Thick sequences of Triassic basalts and overlying platform carbonate are a distinctive characteristic of all terranes believed to be part of Wrangellia (Jones and others, 1977). These carbonate rocks were deposited in a marginal sea which developed in the Late Triassic and persisted into the Late Jurassic. Late Triassic and Jurassic sedimentary rocks deposited in this basin include shales and impure cherts of the McCarthy Formation of Late Triassic and Early Jurassic age. A major orogeny began in the Wrangell Mountains in Late Jurassic time and probably culminated in the Early Cretaceous. Orogenic activity included thrust faulting, folding, formation of conglomerates and intrusion of granitic rocks of the Chitina Valley Batholith and related bodies (mostly in the western and southern parts of the quadrangle, not shown on figure 2) which give late Jurassic K-Ar ages (MacKevett, 1978).

Lower and Upper Cretaceous sedimentary rocks unconformably overlie the Jurassic and older sedimentary and volcanic rocks and the Jurassic granitic rocks. The Cenozoic history of the area is dominated by the extrusion of volcanic rocks of the Wrangell Lava which is widely distributed in the northern part of the quadrangle and gives K-Ar ages of between about 3 and 10 m.y. (MacKevett, 1978).

Hypabyssal granitic and intermediate intrusions related to the Wrangell volcanic activity occur throughout the quadrangle and give K-Ar ages between about 14 and 7 m.y. (MacKevett, 1978; E. M. MacKevett and M. L. Silberman, unpub. data, 1980). No major deformation accompanied this Tertiary igneous activity.

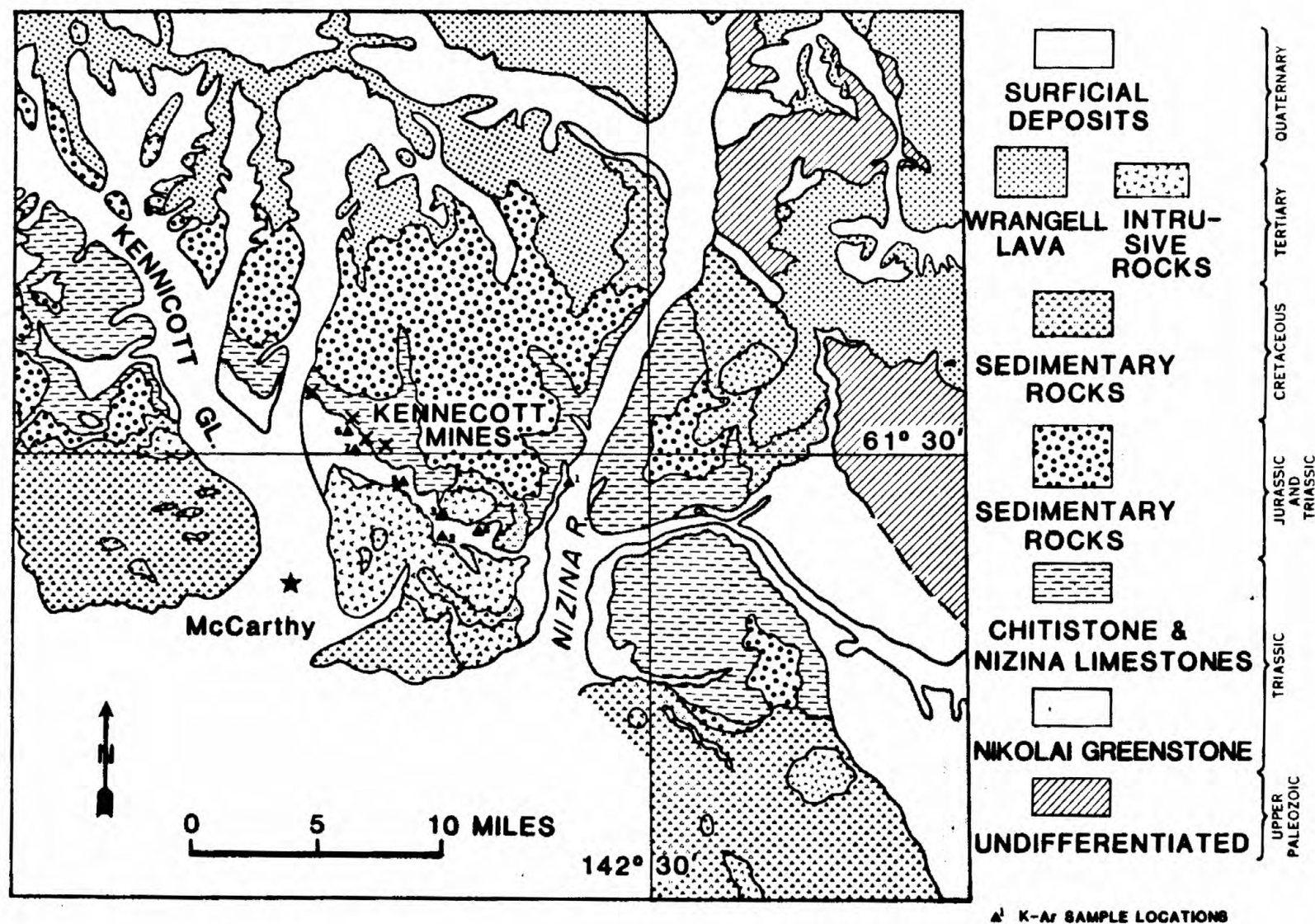


Figure 2.—Generalized geology of part of the McCarthy quadrangle, Alaska.

The lower Mesozoic rocks of the McCarthy area summarized in the stratigraphic column of figure 3 are characteristic throughout Wrangellia (Jones and others, 1977), and contrast strongly with those of adjacent terranes. Later Mesozoic and younger superjacent strata differ from area to area, suggesting that Wrangellia shared its post-early Mesozoic history with adjacent terranes (Jones and others, 1977).

Characteristics of the Nikolai Greenstone

The Nikolai Greenstone, as exposed in the McCarthy quadrangle (fig. 1), is mostly subaerial, porphyritic, tholeiitic basalt, consisting dominantly of intermixed pahoehoe and aa flows which are characteristically amygdaloidal, and between 0.2 and 15 m in thickness. Locally it exceeds 3900 m in cumulative thickness (MacKevett, 1970; 1978). The basalt is mostly fine-grained, containing phenocrysts of labradorite and augite and sparse olivine in an intergranular groundmass composed chiefly of plagioclase and augite. Primary minerals in order of decreasing abundance are plagioclase, augite, relict olivine, opaque minerals, sphene and apatite (MacKevett, 1971). Nikolai basalts are generally slightly quartz normative tholeiites, with some having olivine in the norm (MacKevett and Richter, 1974). The chemical analysis (table 1) is an average of 39 samples of the Nikolai Greenstone collected in the region.

Most of the Nikolai basalts have been altered or metamorphosed locally to prehnite-pumpellyite facies assemblages. The most common secondary minerals are, in order of decreasing abundance: chlorite, iron oxides, epidote, clay minerals, sericite, prehnite, serpentine minerals, pumpellyite, quartz and zeolites. Most of the amygdules in the basalt now contain chlorite + calcite, the rest are rich in chalcedonic quartz and epidote. A few contain zeolites, prehnite or native copper (MacKevett, 1971; 1978). Primary volcanic textures are preserved despite the pervasive nature of the alteration/metamorphism.

Mineralization in the Nikolai Greenstone

The Nikolai Greenstone is intrinsically rich in copper. The mean copper content in 140 Nikolai Greenstone samples from the McCarthy quadrangle is 157 ppm (MacKevett and Richter, 1974). Small copper concentrations of economic and subeconomic grade are common in the Nikolai and are of two main types: (1) thin veins and narrow replacement zones and genetically affiliated deposits such as small pods and local disseminations which are characteristically localized along faults and fractures. The veins are small, from a few centimeters to approximately a meter in width and are rarely traceable for more than 200 m along strike. Mineralogy of these deposits consists largely of bornite, chalcopryite, minor chalcocite and native copper, with quartz, calcite and epidote as the chief gangue minerals (Bateman and McLaughlin, 1920; MacKevett, 1976). A few veins contain some sphalerite and galena or less commonly stibnite and realgar or molybdenite. Minor amounts of

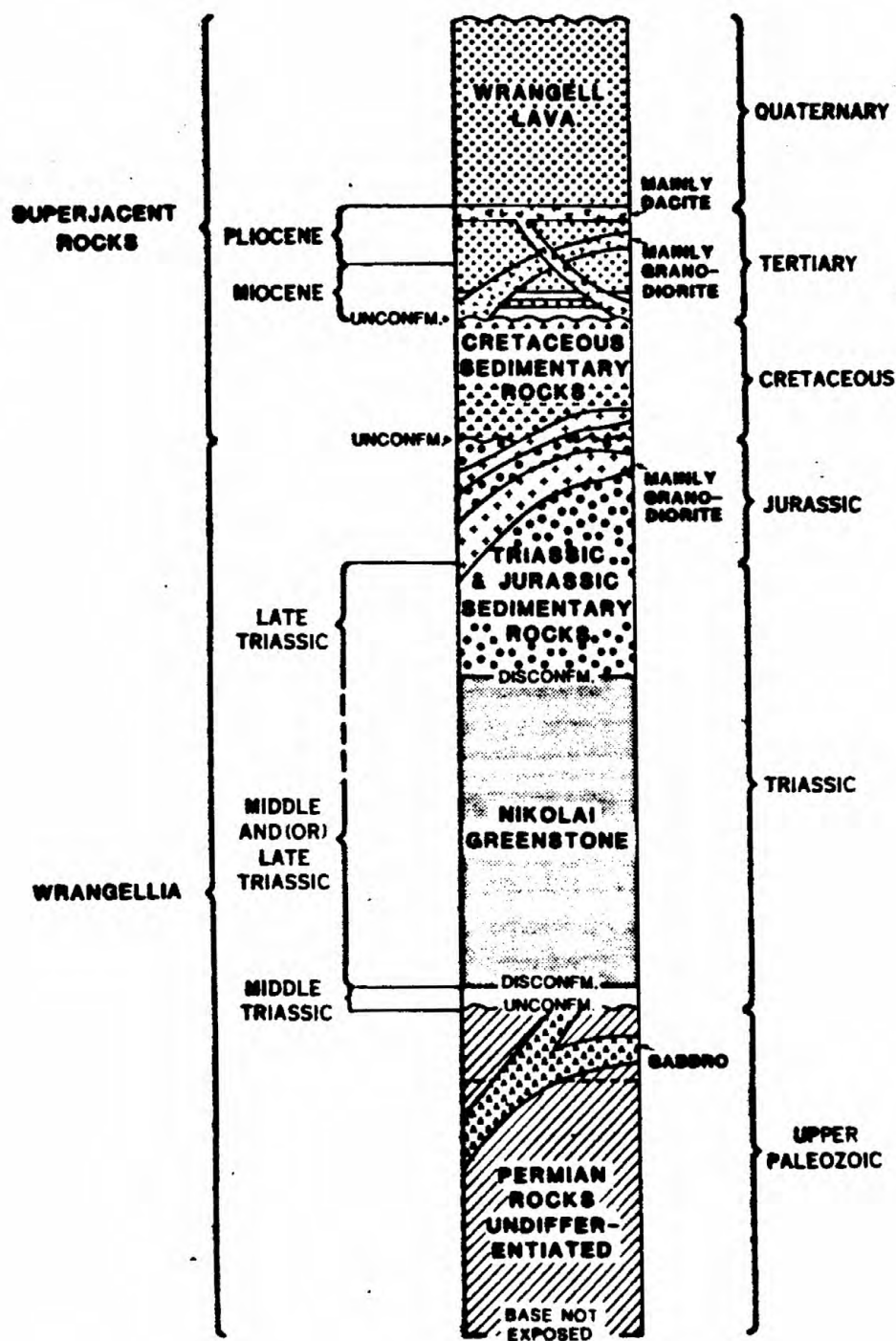


Figure 3.—Stratigraphic column for the Wrangell Mountains in the McCarthy quadrangle.

Table 1.--Chemical composition and CIPW norms for "average" Nikolai Greenstone

[From MacKevett and Richter, 1974.]

Oxide	Weight percent	CIPW norms	
SiO ₂	47.90	Qtz	0.91
Al ₂ O ₃	14.50	Or	2.84
Fe ₂ O ₃	5.20	Ab	26.25
FeO	6.40	An	24.25
MgO	6.90	Wo	7.50
CaO	9.40	En	17.20
Na ₂ O	3.10	Fs	5.48
K ₂ O	.48	Mt	7.55
H ₂ O ⁺	3.76	Il	2.66
TiO ₂	1.40	Ap	.38
P ₂ O ₅	.16	Cc	1.23
MnO	.18		
CO ₂	.54		
Sum	99.92	Sum	96.25
Differentiation index 30.0. Irvine and Barager classification (1971), tholeiitic basalt.			

silver and some gold are also present in some deposits (MacKevett, 1976). (2) The second major type of occurrence consists of native copper as fillings in amygdules or in brecciated or rubbly upper zones of certain flows. A few flows contain broad but erratic disseminations of finely particulate native copper (Bateman and McLaughlin, 1920; MacKevett, 1976). The veins and associated deposits of the type (1) occurrence were believed by MacKevett (1976) to be products of hydrothermal processes related to Late Jurassic or Tertiary plutonic activity that affected the area. MacKevett (written commun., 1980) in particular believes that veins containing stibnite, realgar, molybdenite and most of the gold are geologically related to the Tertiary intrusions.

The calcite - quartz - epidote mineralogy of many of the veins and in the adjacent wall rocks along with chlorite and other minerals characteristic of low grade metamorphism suggest to us that the origin of the veins might be related to metamorphic-hydrothermal process that caused segregation of the intrinsically high copper content of the basalt into fractures and shear zones. The veins, where we have seen them, lack selvages or zones that differ in mineralogy from the greenstone itself suggesting to us that little or no temperature differences existed between the veins and their wall rocks. The shear zones were more permeable than the surrounding unbroken rock and probably represented areas of collection of heated waters which had dissolved copper from the wall rocks. The native copper concentrations of the type (2) occurrences are believed to be related either to terminal stages of the original magmatic activity - deuteric alteration and mineralization, or to metamorphism where copper was concentrated in hydrated parts of the lava pile (MacKevett, 1976).

Sinclair (1977) described a copper deposit hosted by the Nikolai Greenstone in the White River area of the southwest Yukon Territory that has many similarities to those in the Nikolai in the McCarthy quadrangle. The deposit consists of copper sulphide minerals and native copper in amygdules, rubble zones, cross cutting fractures and local disseminations in the Nikolai, which is metamorphosed to prehnite-pumpellyite facies mineral assemblages. He suggests that the ore fluids were derived by metamorphic dehydration with some component originating from connate waters derived from the underlying upper Paleozoic sedimentary rocks. We will attempt to show a similar origin for the small copper-containing vein deposits in the Nikolai Greenstone in McCarthy area.

STABLE ISOTOPE RESULTS

We performed standard oxygen isotope analyses on samples of the Nikolai Greenstone and on veins contained within it. The data (table 2) include oxygen isotopic composition of quartz and epidote separated from grab samples of three mineralized veins that cut the upper part of the Nikolai Greenstone near the Kennecott mines. Trace element chemical data for these veins are listed in table 3. The veins are composed mostly of quartz and epidote with minor amounts of disseminated bornite, chalcopyrite and native copper. Oxygen isotopic composition of 5 whole rock samples of the Nikolai Greenstone, including two samples taken adjacent to quartz epidote veins are listed in table 4. Our objectives in this study are to determine the origins of the ore fluids and the temperatures of vein formation, as well as the origin of fluids in equilibrium with the alteration/metamorphic mineral assemblage of the Nikolai Greenstone and its temperature of metamorphism. Fluid inclusions are present in the quartz of the veins, but their small size precluded quantitative measurement of filling temperatures. Isotopic fractionation of oxygen between quartz and epidote as a function of temperature has not yet been determined experimentally or calculated from theoretical considerations, although experimental studies in the system zoisite-water are presently in progress (Alan Matthews, unpub. data, 1980).

Table 2.--Oxygen isotope composition of quartz and epidote from copper bearing veins in Nikolai Greenstone

[Delta values are reported in parts per mil.]

Sample number	Location	$\delta^{18}\text{O}$ for quartz	$\delta^{18}\text{O}$ for epidote	Δ^1
E3	Erie Mine	+16.5	+7.2	+9.3
9	Bonanza Mine	+16.1	+6.0	+10.1
18	Bonanza Ridge	+15.7	+7.4	+8.3

¹Average fractionation ($\delta\text{Q} - \delta\text{Ep}$) = +9.2 per mil.

Table 3.--Partial chemical analyses for trace elements in quartz-epidote veins of the Nikolai Greenstone

[Reported in ppm.]

Sample number	Width of vein (in cm)	Ag ¹	Co ¹	Cr ¹	Cu ¹	Ni ¹	Pb ¹	Sr ¹	Zn ²	As ³	Sb ²
E3	10	30	15	70	>20,000	15	N(10)	1,500	10	N(10)	L(1)
18	1	.5	30	150	300	50	N(10)	500	15	N(10)	N(1)
9	30	2	15	70	5,000	30	10	3,000	10	20	N(1)

¹Semi-quantitative spectrographic analyses, results reported in the series 1, 1.5, 2, 3, 5, 7, 10 and so on. N = Not detected at limits of detection given in parenthesis, L = detected, but below limit of determination, at or below value shown. Analyst: E. L. Mosier.

²Zn and Sb by atomic absorption analytical methods. Analysts: R. M. O'Leary and J. A. Criswell.

³As by colorimetric analytical method. Analyst: R. M. O'Leary.

Table 4.--Oxygen isotope composition of typical whole-rock
Nikolai Greenstone samples

[Delta values are reported in parts per mil.]

Sample number	Location	$\delta^{18}\text{O}$	Average $\delta^{18}\text{O}$
N1	Nikolai Creek	+10.7	
18A ¹	Bonanza Ridge	+9.6	
8	Bonanza Mine	+8.1	9.5 \pm 0.4 ²
9A ¹	Bonanza Mine	+9.1	
11C	Bonanza Mine	+10.1	

¹Adjacent to quartz-epidote vein.

²Standard error.

We have estimated the temperatures of formation of the quartz-epidote veins in the Nikolai from comparison with published data on oxygen isotope fractionation between quartz and epidote in natural environments where the temperature of equilibration is known from independent evidence (Taylor and O'Neil, 1977; Heaton and Sheppard, 1977). The results of our temperature estimates, and calculations based on these temperatures of the ore fluid oxygen isotopic composition are listed in table 5. Our calculations suggest that the veins were deposited at approximately 200°C from a fluid of $\delta^{18}\text{O} = 1$ per mil. Preliminary results of the zoisite-water oxygen isotope fractionation experiments suggest that this temperature estimate is accurate (Alan Matthews, unpub. data, 1980).

The +8 to +11 per mil, oxygen isotope composition of the greenstone samples (table 4), lies within the range of $\delta^{18}\text{O}$ reported for the upper parts of ophiolite sequences that were metamorphosed at temperatures between about 50°C and 350°C by the action of heated sea water, (Spooner, and others, 1974; 1977; Heaton and Sheppard, 1977). We lack $\delta^{18}\text{O}$ data for individual minerals from the greenstones, so it is not possible to calculate metamorphic equilibration temperatures.

Table 5.--Calculated temperature and fluid oxygen isotope composition for copper bearing quartz-epidote veins in Nikolai Greenstone

[Delta values are reported in parts per mil.]

Approximate temperature of fractionation	$\delta^{18}\text{O}$ (quartz)	$\delta^{18}\text{O}$ (epidote)	$d_q - d_{ep}$
Assume linear relationship between $d_q - d_{ep}$ and $1/T^2$ (Urey, 1947; Bigeleisen and Mayer, 1947) and use published data on quartz and epidote oxygen isotopic fractionation from natural environments where temperature is known. Extrapolate linear relationship to measured Nikolai quartz-epidote fractionations to calculate temperature, and use Bottinga and Javoy (1973) quartz-water fractionation to calculate ore fluid $\delta^{18}\text{O}$.			
480° to 550°C (Osgood Mts., Nevada, scarce data of Taylor and O'Neil, 1977)	+13.6 +14.0	+8.1 +9.3	+5.5 +4.7
	Average		+5.1
340° to 400°C (Quartz-epidote veins in Troodos Complex, Cyprus, data of Heaton and Sheppard, 1977)	+9.5 +6.4	+3.4 .0	+6.1 +6.4
	Average		+6.3
Sample number	Calculated temperature (°C)	Calculated $\delta^{18}\text{O}$ ore fluid	
9	170	-1.1	
18A	230	+3.4	
E3	190	+1.3	
	197	Average	+1.2

Because the mineral assemblages of our greenstone samples collected in the vicinity of the Kennecott mines area (fig. 2) do not vary with distance from quartz-epidote veins, we believe that no large temperature differences existed between the veins and their wall rocks when the veins were emplaced. The temperature limits for zeolite facies metamorphism are about 100°C to 300°C (Miyashiro, 1973; Winkler, 1976); we consider this a reasonable range of temperatures for formation of the quartz-epidote veins as well as for the greenstone mineral assemblage.

Plagioclase and chlorite are the dominant minerals in the Nikolai Greenstone samples. Spooner and others (1977) suggest that the muscovite-water oxygen isotope fractionation relationship with temperature could be used to approximate oxygen isotopic alteration of basalts and greenstones since oxygen isotopic fractionation between muscovite and water is intermediate between that of chlorite-water, and feldspar-water (Taylor, 1974). Using the oxygen isotope fractionation vs. temperature relationship for muscovite-water from Bottinga and Javoy (1973) and the temperature calculated for the formation of the quartz-epidote veins, we estimate that the oxygen isotopic composition of the fluid in equilibrium with the metamorphosed greenstones (average $\delta^{18}\text{O} = +9.5$ per mil) was +4 per mil. At 200°C, the temperature considered most likely for the formation of the veins, a shift of the fluid oxygen isotope composition to heavier $\delta^{18}\text{O}$ would be required if the same fluids were involved in metamorphism of the basalt and formation of the veins. If the fluids were using the fractures that now localize the veins as channelways, and then diffused out into the wall rocks during the metamorphic process, and the water to rock ratio was relatively low (<1), an oxygen shift to higher values would be expected (O'Neil and Silberman, 1974; Spooner and others, 1977).

Although our calculated isotopic compositions of the fluids are based on several assumptions, we believe that it is possible for the same fluid that generated the quartz-epidote veins to be involved in metamorphism of the basalts. The low temperature of vein formation results in a calculated ore fluid composition that would essentially be dominated by "modified connate" water (Taylor, 1974). Thus, on the basis of available, albeit incomplete, stable isotope data, our interpretation is that the copper bearing vein deposits in the Nikolai Greenstone could have formed by the process suggested by Sinclair (1977). Further support for that process is given by the results of the K-Ar age determinations.

K-Ar AGE DETERMINATIONS

Seven samples of the Nikolai Greenstone were chosen for whole rock K-Ar age determination from near the vicinity of the Kennecott Mines (fig. 2; table 6). The samples were ground to -60 +100 mesh, but were otherwise untreated. The mineral assemblage of the samples is typical of the metamorphosed Nikolai Greenstone. The dominant minerals in all samples are chlorite and altered plagioclase with subordinate amounts of the other common minerals of the greenstone. The K-Ar ages range from 91 to 131 m.y., and although the ages tend to cluster somewhat in any given area, they are apparently unaffected by proximity to the late Tertiary hypabyssal, Wrangell Lava-related, plutons in the region, which give K-Ar ages of 7 to 15 m.y. (M. L. Silberman and E. M.

MacKevett Jr., unpub. data, 1980). This episode of Tertiary magmatism apparently was unaccompanied by other than very local thermal effects. One sample, no. 18A (table 6) was collected immediately adjacent to one of the quartz-epidote veins of table 2 (sample no. 18).

Of particular importance is the lack of any significant age difference between the sample collected adjacent to the quartz-epidote vein and those collected long distances away from any veins. If the veins were emplaced significantly later than metamorphism of the basalt, for example in the late Tertiary as a hydrothermal effect of intrusion of the Wrangell plutons as suggested by Bateman and McLaughlin (1920), then we should have obtained a younger age from the vein wall rock sample. K-Ar age studies have documented that volcanic wall rocks adjacent to hydrothermal vein deposits formed at temperatures similar to those calculated for the Nikolai veins yield wall rock ages that are reset to the age of mineralization if this process is significantly younger than the age of the host rocks (Silberman and others, 1972; Ashley and Silberman, 1976; Morton and others, 1977). We interpret our age results to indicate that metamorphism and quartz-epidote veining were nearly simultaneous. These age data support our conclusions based on our stable isotope data, which suggest to us that the same fluids responsible for deposition of the quartz-epidote veins were also involved in metamorphic recrystallization of the Nikolai Greenstone.

Range in the individual ages is relatively large, perhaps due to local differences in metamorphic temperature history, but is unrelated to potassium content of the samples. We plotted the K and Ar analytical results on an initial argon diagram (Shafiqullah and Damon, 1974) to examine the systematics of the data (fig. 4). On this type of diagram the slope of a regression line through the points is proportional to the age of crystallization of the system and the intercept on the argon axis indicates whether there is extraneous argon, or argon loss in the samples. The use of isochron analysis has the implicit assumption that all of the plotted samples contain non-radiogenic argon of the same composition at the time of metamorphic recrystallization (Shafiqullah and Damon, 1974; Turner and others, 1979). Because all of our samples come from a restricted area, and are of similar mineralogy, this assumption, for this particular case, is probably valid.

The slope of the regression line through the points and its statistical uncertainty yield an isochron age of 112 ± 11 m.y., and an intercept of zero. These relations indicate that there has been no loss of argon from the samples since crystallization of the present mineral assemblage in the middle Cretaceous. Agreement of the "slope" age and the average age of the samples is another indication that a true crystallization event has been dated (Shafiqullah and Damon, 1974). We conclude that the Nikolai Greenstone crystallized to its present mineral assemblage during a thermal episode in the middle Cretaceous and has been essentially unaffected by significant argon loss since that time.

The age of formation of the Nikolai Greenstone, Middle and (or) Late Triassic, would by the time scale in use by U.S. Geological Survey (Geologic Names Committee, 1980) be about 210 to 220 m.y. Two other regional thermal events, besides the original volcanic extrusion, could have affected the Nikolai Greenstone. The first was caused by intrusion of the granitic rocks

Table 6.--K-Ar ages of whole rock Nikolai Greenstone samples

Location number (fig. 2)	Field number	Location	K ₂ O (percent) ¹	Age (m.y.)
1	Swan	Swan Lake	0.448	90.9 \pm 4.5
2	N1	Nikolai Creek	.531	105 \pm 5
3	N2 ²	Nikolai Creek	.285	111 \pm 6
4	N4	Nikolai Creek	.814	109 \pm 6
5	18A ³	Bonanza Ridge	.268	120 \pm 6
6	8	Bonanza Ridge	1.29	131 \pm 7
7	11C	Bonanza Ridge	.932	113 \pm 6

¹All K O analyses by Paul Klock, U.S. Geological Survey, Menlo Park, CA.

²Sample N2, argon analysis run at U.S. Geological Survey, Menlo Park, CA. Analysts: M. L. Silberman and C. L. Connor. Other samples run by Teledyne Isotopes, Westwood, NJ. Analyst: Georgiana Kalechitz.

³Adjacent to quartz-epidote vein.

of the Chitina Valley batholith into the Wrangell terrane in the late Jurassic (MacKevett, 1978). The metamorphism of the Nikolai Greenstone is clearly younger than that. The second thermal event, the Late Tertiary intrusion of the Wrangell Lava related plutons appears to have had no effect on the Nikolai K-Ar ages.

Granitic rocks also occur in the northern part of the Wrangell terrane in the eastern Alaska Range. Two large composite plutons of greater than 100 km² outcrop area, with associated hydrothermal alteration and porphyry copper and molybdenum occurrences, and smaller satellitic plutons have given ages of 80 to 120 m.y. (Richter and others, 1975; Silberman and others, 1977). These granitic rocks occur in the Nabesna quadrangle and the northeastern part of the McCarthy quadrangle, over 80 km distant from the nearest dated Nikolai Greenstone sample. No granitic rocks of this age have been found elsewhere in

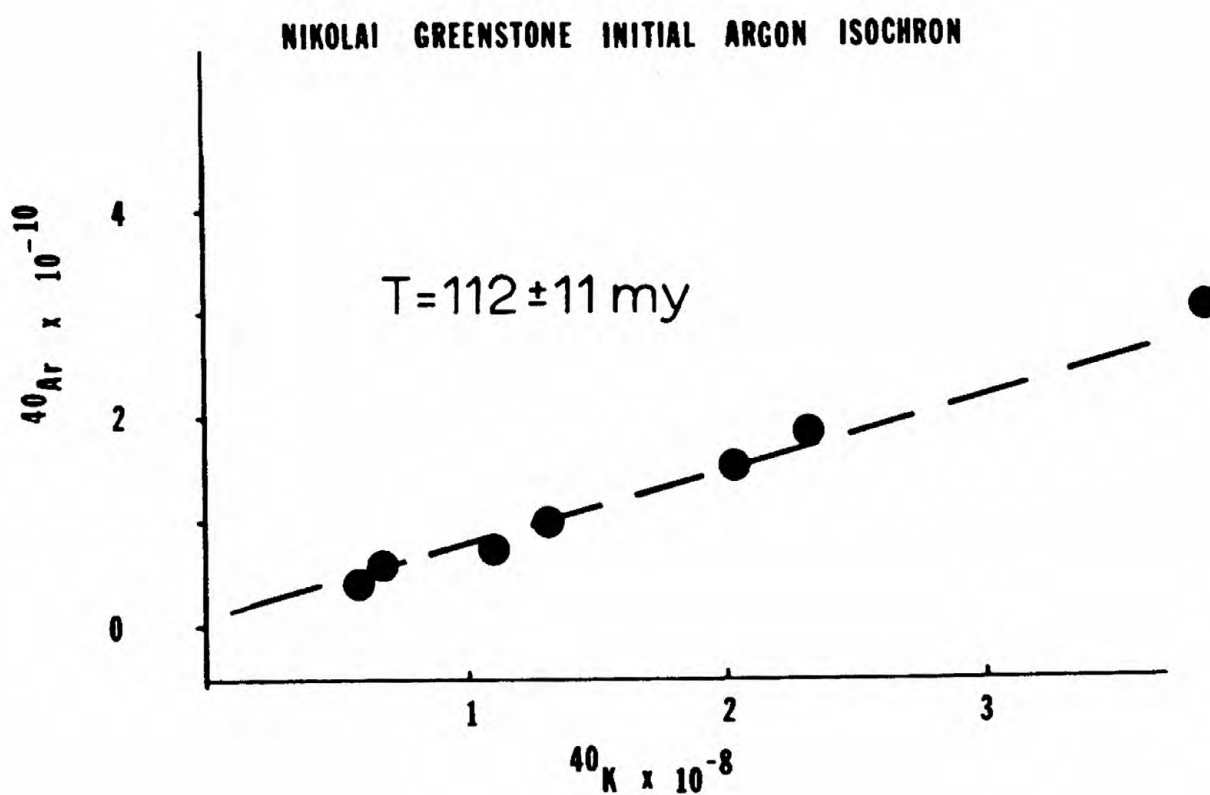


Figure 4.--Initial argon diagram for Nikolai Greenstone whole rock K-Ar data.

the McCarthy quadrangle, and it is our opinion that thermal effects of these plutons could not have possibly have affected our Nikolai K-Ar results. However, plutons of this age do have bearing on the limits for age of accretion of the Wrangell terrane in southern Alaska.

DISCUSSION

Jones and Silberling (1979) believe that the bulk of tectonic activity that formed the accretionary mosaic of disparate terranes in southern Alaska, including Wrangellia (fig. 5), occurred in the middle to late Cretaceous. The arrival of Wrangellia to its present relative position in southern Alaska represents only part of a very complex and poorly understood history of deposition, tectonic transport, accretion, and large-scale structural juxtaposition. Figure 5 illustrates just a few of the over 25 discrete tectonostratigraphic terranes that make up southern and central Alaska (Jones and Silberling, 1979). Approximate limits on the time of arrival of Wrangellia to its present relative position are based on widespread and locally intense deformation of Upper Jurassic and Lower Cretaceous flysch deposits that are exposed throughout southern Alaska (fig. 5). Stratigraphic and structural studies by Csejter and St. Aubin (1980) in the Talkeetna Mountains demonstrate that upper Paleozoic and Triassic rocks of the Wrangell terrane are thrust over severely deformed argillite and graywacke. Granitic plutons intrude the deformed sedimentary rocks, are undeformed themselves, and give Late Cretaceous to Paleocene K-Ar ages (Csejter and others, 1978; Csejter and St. Aubin, 1980).

Additional constraints on the timing of juxtaposition of Wrangellia and adjacent terranes comes from the granitic plutons in the Nabesna area. These middle and upper Cretaceous plutons are part of the Nutzotin-Chichagof belt of plutonic rocks, one of five such belts in southern and southeastern Alaska defined by Hudson (1979b), who believes that they may represent parts of magmatic arcs, although — "the data are inconclusive or simply too scarce for a definitive interpretation" (Hudson, 1979b, p. 231). The plutons that form the Nutzotin-Chichagof belt intrude rocks of three different terranes, including Wrangellia, the Alexander terrane and the Gravina-Nutzotin sedimentary and volcanic belt (Berg, 1972; Hudson, 1979a). In the northern part of the Nutzotin-Chichagof plutonic belt, the granitic rocks, including the plutons near Nabesna, are large complex epizonal bodies that intrude Wrangell terrane rocks, rocks of Precambrian(?) to upper Paleozoic and lower Mesozoic age assigned to the Alexander terrane, and sedimentary and volcanic rocks of the middle Jurassic to lower Cretaceous Gravina-Nutzotin belt, which positionally overlie rocks of the two older terranes (Berg, 1972).

If these plutons represent a magmatic arc, then the arc developed on a basement composed of disparate terranes that were juxtaposed, or were reasonably close to each other by at least Early Cretaceous time, and were intruded together by Middle Cretaceous time (Berg, 1972).

Regional structural, stratigraphic, and plutonic history in southern Alaska thus suggests that juxtaposition of several of the tectonostratigraphic terranes, including Wrangellia, occurred by Late Jurassic — Early Cretaceous

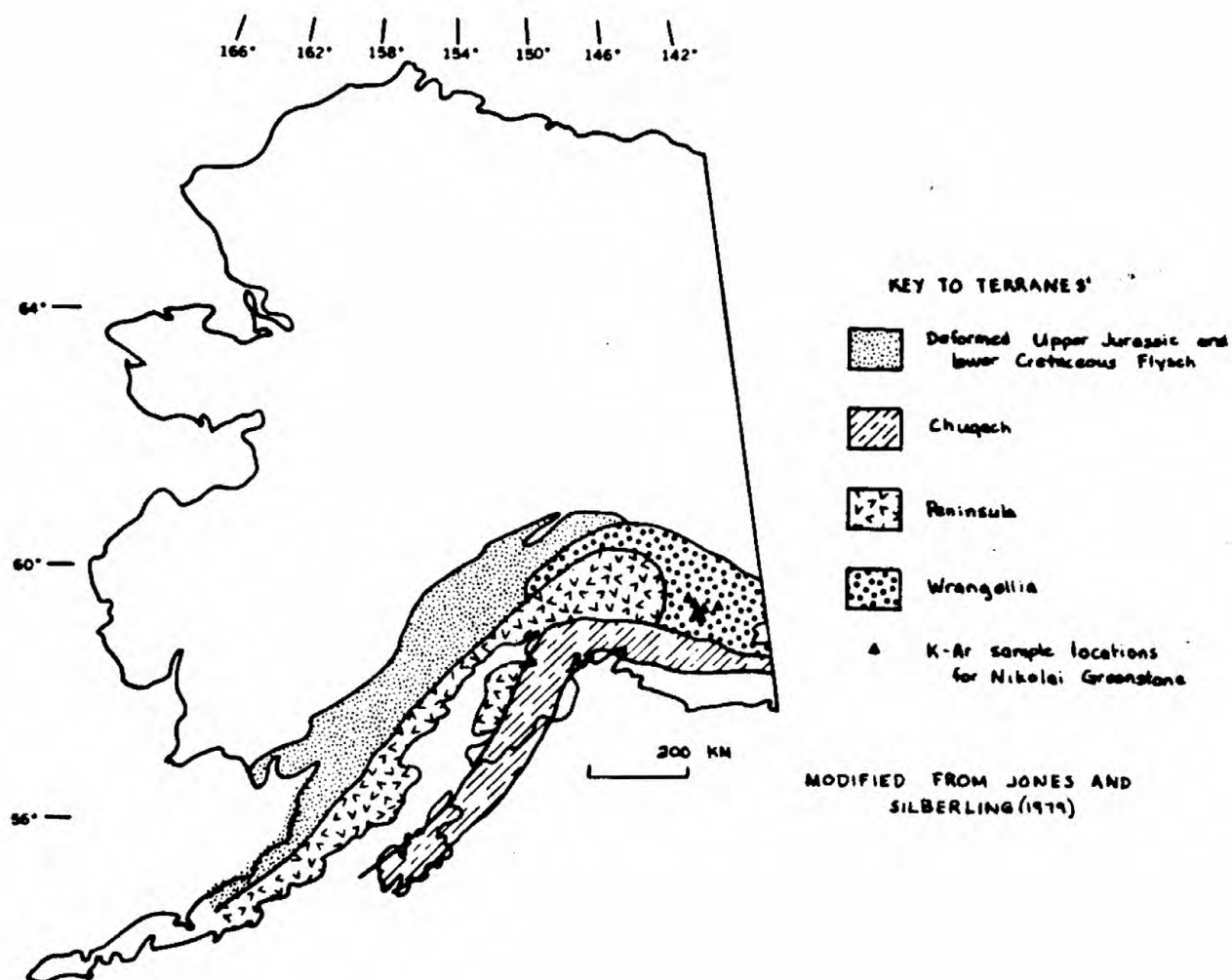


Figure 5.--Map showing distribution of selected Mesozoic terranes in southern Alaska, including Wrangellia.

or Late Cretaceous-Paleocene time. We believe that the 112 m.y. recrystallization age for the Nikolai Greenstone in the McCarthy area resulted from heating of the terrane caused by accretion of Wrangellia to its present relative position. The McCarthy area is some distance away from the boundaries of Wrangellia, and is unlikely to have been affected directly by thermal effects of Cretaceous plutonism. Alteration/metamorphism of the Nikolai, and copper mineralization that appears to be of metamorphic segregation origin, from ore fluid derived by upward migration of evolved connate waters from the underlying upper Paleozoic sedimentary rocks, appear to have occurred during the process of accretion.

This report documents two important points. The first, discussed by Berg (1979) is that the process of accretion itself may give rise to certain types of mineral deposits, or result in modification of pre-existing mineral deposits. The second is that it may be possible to determine the age of accretion of allocthanous terranes by application of conventional K-Ar geochronology to low grade metamorphic, or altered rocks. By extending this reasoning, it may be possible to determine the age of accretion by dating the gangue minerals of certain types of mineral deposits, such as fracture-and shear-controlled base metal sulphide deposits, if by geologic mapping and isotopic work they can be related to metamorphic remobilization and concentration of ore metals. We plan on testing this technique further in areas where independent evidence constrains the timing of accretion in greenstone-bearing allochthonous terranes, such as the Chugach and Prince William terranes.

REFERENCES

- Ashley, R. P., and Silberman, M. L., 1976, Direct dating of mineralization at Goldfield, Nevada, by potassium-argon and fission-track methods: *Economic Geology*, v. 71, p. 904-924.
- Bateman, A. M., and McLaughlin, D. H., 1920, Geology of the ore deposits of Kennecott, Alaska: *Economic Geology*, v. 15, p. 1-80.
- Berg, H. C., 1972, Gravina-Nutzotin belt-tectonic significance of an upper Mesozoic sedimentary and volcanic sequence in southern and southeastern Alaska: U.S. Geological Survey Professional Paper 800-D, p. D1-D24.
- Berg, H. C., 1979, Significance of geotectonics in the metallogenesis and resource appraisal of southeastern Alaska: in Johnson, K. M., and Williams, J. R., eds., *The United States Geological Survey in Alaska: Accomplishments during 1978*: U.S. Geological Survey Circular 804-B, p. 116-118.
- Bigeleisen, Jacob, and Mayer, M. G., 1947, Calculation of equilibrium constants for isotopic exchange reactions: *Journal of Chemical Physics*, v. 15, p. 261-267.
- Bottinga, Y. and Javoy, M., 1973, Comments on oxygen isotopes geothermometry: *Earth and Planetary Science Letters*, v. 20, p. 250-265.
- Bottinga, Y. and Javoy, M., 1975, Oxygen isotope partitioning among the minerals in igneous and metamorphic rocks: *Review of Geophysics and Space Physics*, v. 13, p. 401-418.
- Csejtey, Béla, Nelson, W. H., Jones, D. L., Silberling, N. J., Dean, R. M., Morris, M. S., Lanphere, M. A., Smith, J. G., and Silberman, M. L., 1978, Reconnaissance geologic map and geochronology, Talkeetna Mountains quadrangle, northern part of Anchorage quadrangle and southwest corner of Healy quadrangle, Alaska: U.S. Geological Survey Open-File Report 78-558A, scale 1:250,000.
- Csejtey, Béla, and St. Aubin, D. R., 1981, Evidence for northwesterward emplacement of Wrangellia in the northern Talkeetna Mountains, southern Alaska, in Albert, N. R. D., and Hudson, Travis, eds., *The United States Geological Survey in Alaska: Accomplishments during 1979*: U.S. Geological Survey Circular 804-B, [in press].
- Geologic Names Committee, 1980, Major Geochronologic and chronostratigraphic units, subdivisions in use by the U.S. Geological Survey: A draft of proposed time scale, 2 p.
- Heaton, T. H. E., and Sheppard, S. M. F., 1977, Hydrogen and oxygen isotope enriched for sea-water-hydrothermal alteration and ore deposition, Troodor complex, Cypress, in *Volcanic Processes in ore genesis*, Institution of Mining and Metallurgy and Geological Society of London, p. 42-57.

- Hillhouse, J. W., 1977, Paleomagnetism of the Triassic Nikolai Greenstone, McCarthy quadrangle, Alaska: *Canadian Journal of Earth Sciences*, v. 14, no. 11, p. 2578-2592.
- Hudson, Travis, 1979a, Calc-alkaline plutonism along the Pacific rim of southern Alaska: U.S. Geological Survey Open-File Report 79-953.
- Hudson, Travis, 1979b, Mesozoic plutonic belts of southern Alaska: *Geology*, v. 7, p. 230-234.
- Irvine, T. N., and Baragar, W. R. A., 1971, A guide to the classification of the common volcanic rocks: *Canadian Journal of Earth Sciences*, v. 8, p. 523-548.
- Jones, D. L., Silberling, N. J., and Hillhouse, J. W., 1977, Wrangellia--A displaced terrane in northwestern North America: *Canadian Journal of Earth Sciences*, v. 14, no. 11, p. 2565-2577.
- Jones, D. L., and Silberling, N. J., 1979, Mesozoic stratigraphy, the key to tectonic analysis of southern and central Alaska: U.S. Geological Survey Open-File Report 79-1200, 41 p.
- MacKevett, E. M., Jr., 1970, Geology of the McCarthy B-4 quadrangle, Alaska: U.S. Geological Survey Bulletin 1333, 31 p.
- 1971, Stratigraphy and general geology of the McCarthy C-5 quadrangle, Alaska: U.S. Geological Survey Bulletin 1323, 35 p.
- 1976, Mineral deposits and occurrences in the McCarthy quadrangle, Alaska: U.S. Geological Survey Miscellaneous Field Study Map, MF-773B, scale 1:250,000, 2 sheets.
- 1978, Geologic map of the McCarthy quadrangle, Alaska: U.S. Geological Survey Miscellaneous Investigations Series Map I-1032, scale 1:250,000.
- MacKevett, E. M., Jr., Albert, N. R. D., Barnes, D. F., Case J. E., Robinson, Keith, and Singer, D. A., 1977, The Alaskan mineral resource assessment program: Background information to accompany folio of geologic and mineral resource maps of the McCarthy quadrangle, Alaska: U.S. Geological Survey Circular 739, 23 p.
- MacKevett, E. M., Jr., and Richter, D. H., 1974, The Nikolai Greenstone in the Wrangell Mountains, Alaska, and nearby regions: *Geologic Association of Canada, Cordilleran Section Programme with Abstracts*, p. 13, 14.
- Miyashiro, Akiho, 1973, *Metamorphism and Metamorphic Belts*: George Allen and Unwin, Ltd., Great Britain, 492 p.
- Morton, J. L., Silberman, M. L., Bonhan, H. F., Jr., Garside, L. T., and Noble, D. C., 1977, New K-Ar ages of volcanic rocks, plutons and ore deposits, central and western Nevada, eastern California: *Isochron/West*, no. 20, p. 19-29.
- O'Neil, J. R., and Silberman, M. L., 1974, Stable isotope relations in epithermal ore deposits: *Economic Geology*, v. 69, p. 902-909.

- Richter, D. H., Lanphere, M. A., and Matson, N. A., Jr., 1975, Granitic plutonism and metamorphism, eastern Alaska Range, Alaska: Geological Society of America Bulletin, v. 86, p. 819-829.
- Shafiqullah, M., and Damon, P. E., 1974, Evaluation of K-Ar isochron methods: *Geochemica et Cosmochimica Acta*, v. 38, p. 1341-1358.
- Silberman, M. L., Chesterman, C. W., Kleinhampl, F. J., and Gray, C. H., Jr., 1972, K-Ar ages of volcanic rocks and gold-bearing quartz-adularia veins in the Bodie mining district, Mono County, California: *Economic Geology*, v. 67, p. 597-604.
- Silberman, M. L., Morton, J. L., Cox, D. C., and Richter, D. H., 1977, K-Ar ages of disseminated copper and molybdenum mineralization in the Klein Creek and Nabesna plutons, eastern Alaska Range, in Blean, K. M., ed., *The United States Geological Survey in Alaska: Accomplishments during 1976: U.S. Geological Survey Circular 751-B*, p. B54-B56.
- Sinclair, A. J., 1977, The White River copper deposit, southwestern Yukon (Abs): Geological Association of Canada, Program with Abstracts, v. 2, p. 49.
- Spooner, E. T. C., Beckinsale, R. D., Fyfe, W. S., and Smewing, J. D., 1974, O^{18} enriched ophiolitic meta basic rocks from E. Liguria (Italy), Pindos (Greece), and Troodos (Cyprus): *Contributions to Mineralogy and Petrology*, v. 47, p. 41-62.
- Spooner, E. T. C., Beckinsale, R. D., England, P. C., and Senior, A., 1977, Hydration, O^{18} enrichment and oxidation during ocean floor hydrothermal metamorphism of ophiolitic meta basic rocks from E. Liguria, Italy: *Geochemica et Cosmochimica Acta*, v. 41, p. 857-871.
- Taylor, B. E., and O'Neil, J. R., 1977, Stable isotope studies of metasomatic Ca-Fe-Al-Si skarns and associated metamorphic and igneous rocks, Osgood Mountains, Nevada: *Contributions to Mineralogy and Petrology*, v. 63, p. 1-49.
- Taylor, H. P., Jr., 1974, The application of oxygen and hydrogen isotope studies to problems of hydrothermal alteration and ore deposition: *Economic Geology*, v. 69, no. 6, p. 843-883.
- Turner, D. L., Forbes, R. B., and Dillon, J. T., 1979, K-Ar geochronology of the southwestern Brooks Range, Alaska: *Canadian Journal of Earth Sciences*, v. 16, p. 1789-1804.
- Urey, H. C., 1947, The thermodynamic properties of isotopic substances: *Journal of Chemical Society*, p. 562-581.
- Wenner, D. B., and Taylor, H. P., Jr., 1971, Temperatures of serpentinization of Ultra mafic rocks based on O^{18}/O^{16} fractionation between coexisting serpentine and magnetite: *Contributions to Mineralogy and Petrology*, v. 32, p. 165-185.
- Winkler, H. F. G., 1976, *Petrogenesis of metamorphic rocks* (4th ed.): New York, Springer-Verlag, 334 p.

Placer gold deposits, Mt. Hayes quadrangle, Alaska

Warren Yeend, U.S. Geological Survey

PLACER GOLD DEPOSITS, MT. HAYES QUADRANGLE, ALASKA

by

Warren Yeend

Placer gold deposits have been worked discontinuously in the Mt. Hayes quadrangle since the early 1900's. The area was initially studied by Walter Mendenhall (1905) of the U.S. Geological Survey and more recently by A. W. Rose (1965, 1967), of the Alaska Division of Mines and Minerals. The Slate Creek district has had the most activity with gold production in excess of 100,000 ounces. During the summer of 1979 four different properties in the southern half of the quadrangle were being worked; Quartz Creek, Slate Creek, The Big Four, and Broxson Gulch (fig. 1). The Slate Creek district is 7 kilometers south of the Alaska Range crest and 35 kilometers east of the Richardson Highway.

Quartz Creek

The Placer is in a dissected alluvial fan at the mouth of Quartz Creek. The deposit is a poorly sorted, boulder and cobble gravel with angular to rounded clasts; bedding is crude. Boulders are present to 30 cm (1 ft) in diameter. Most of the deposit is made up of granular to sand size, angular chips of blue gray slate. A pebble count showed the following percentages.

Blue gray slate	46	Plutonic mafic igneous	2
Metavolcanic	28	Limestone	8
Plutonic nonmafic igneous	14	White quartz	2.

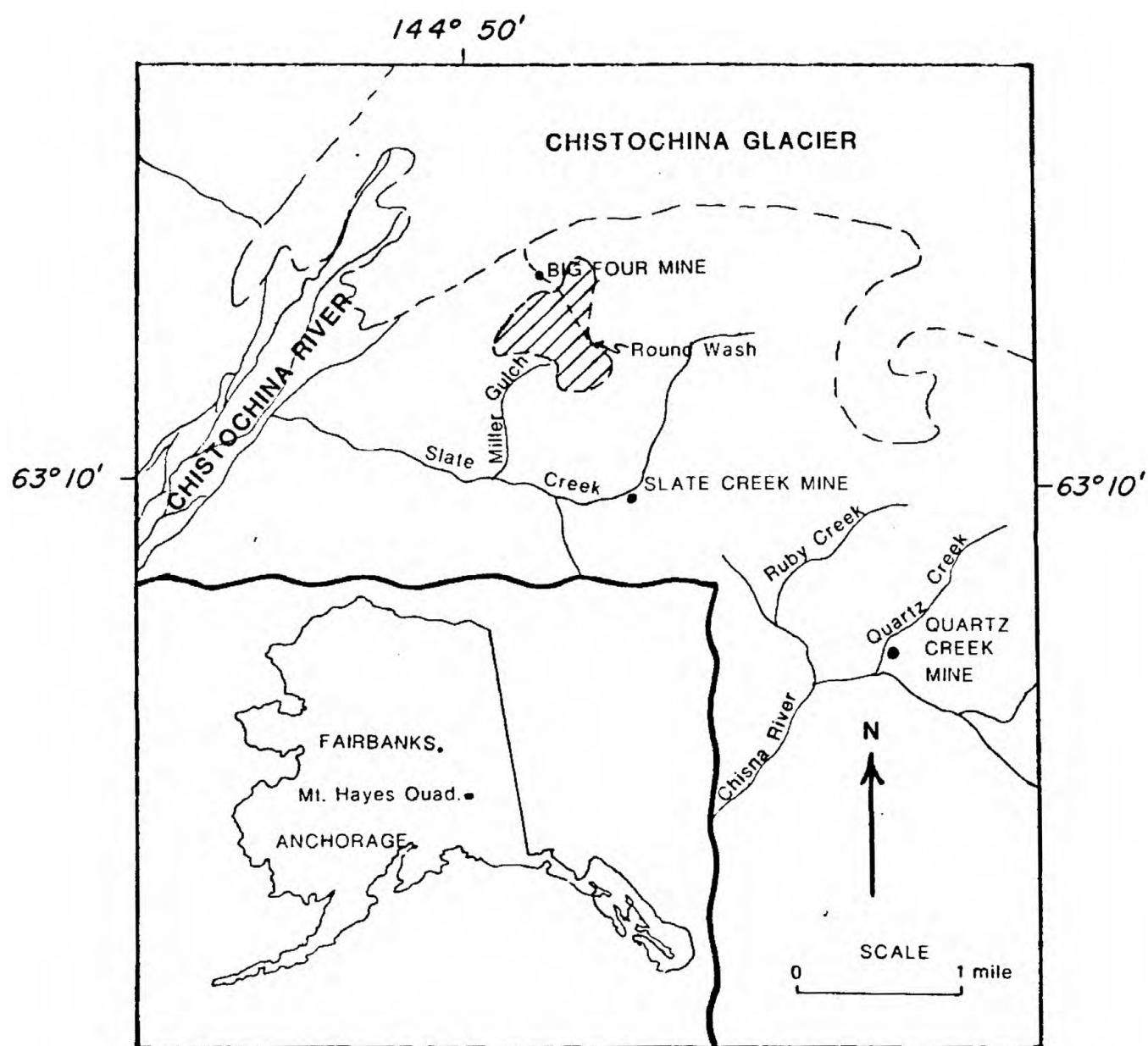


Figure 1. Index map of the Slate Creek area.

The operators report the presence of abundant black sand, both magnetic and nonmagnetic. The best "pay" is in boulder zones on false bedrock which may be a slate-granule bed. Blue-gray very angular slate fragments are generally elongate and are very common. Bedrock is exposed at one place in the fan and the "pay" is generally good on the bedrock. The gold is very flattened, rarely more than 3 mm, and more commonly 1 mm or less in diameter. There are 2 gold varieties, bright yellow and an orange-brown thought to be a result of adhering impurities. The largest nugget found was about 7 mm across and 1.5 mm thick heavily coated with quartz and iron oxide.

A panned concentrate near the fan mouth produced 14 gold fragments, all less than 1 mm across. The fragments were iron stained with adhering minerals of quartz, hornblende and chlorite. The gold from this one pan weighed 4.5 mg and would give a value of \$14.22 per cubic yard at \$500 per ounce price. Other heavy minerals in the concentrate were:

magnetite -- 70 percent, amphibole, pyrite, chlorite, epidote, garnet, zircon, and ilmenite.

As a rough estimate the alluvial fan may be 10 to 15 m thick and contain 600,000 m² of gravel.

Slate Creek

The mine on Slate Creek is the largest operation in the Quadrangle, employing 13 people. The deposit is a combination, alluvial and colluvial fan with admixed drift. It occurs in the valley of Slate Creek where the creek changes flow direction from southwest to northwest. The gravels currently being mined are on the east side of the valley of Slate Creek and would seem to represent an Ancestral Slate Creek which is deeper than the present Slate Creek valley. The gold-bearing gravel is exposed in a cut which extends 12 m (40 ft) below the original land surface and exploratory drilling indicates

bedrock to be 9 m (30 ft) deeper still. The gravel includes an abundance of well rounded granitic boulders and cobbles most likely derived from Tertiary conglomerate, termed "round wash" by the miners, which is exposed capping the high hills north of the Slate Creek mine. A pebble count from the tailings revealed the following percentages.

Greenstone	37	Volcanic	-3
Felsic plutonic	30	Schist	-1
Slate	18	Sandstone	-1
Quartz	6	Hornfels	-1
Ultramafic	2	Chert	-1

A conglomerate resembling the round wash is exposed in the Slate Creek valley in the vicinity of the placer mine. It seems clear that the conglomerate here is in fault contact with older rocks. A fault plane was observed on the north side of the Slate Creek valley just down stream from the mining operations. It strikes N75°W dips 76° to the south. The rake of slickensides in the fault plane plunge 25°E. Chlorite schist and granitic boulders in the conglomerate here resemble those in the round wash conglomerate exposed on the upland surface to the north. A few sandstone and siltstone beds with large clasts of biotite up to 7 mm across were observed on the northside of Slate Creek downstream from the mine site.

The gold recovered is both brassy yellow and copper colored, some flakes with adhering quartz and iron oxide. The largest nugget recovered is 5.6 gms (1/5 ounce), about 8 mm in diameter. Approximately a dozen nuggets of this size had been recovered during the summer -- many are equidimensional, rounded with battered edges. The concentrate contains abundant black sand and presents a problem in trying to separate the fine gold. Approximately 85 percent of the gold passes a 20 mesh screen.

A panned concentrate containing one small "color" of gold obtained from the gravels in the Slate Creek just upstream from the mine contained the following heavy minerals:

magnetite	30 percent	epidote	less than 10 percent
ilmenite	10 percent	zircon	less than 10 percent
pyrite	10 percent	garnet	less than 10 percent
chlorite	10 percent	amphibole	less than 10 percent.

Platinum minerals have been reported from the gravels in the area (Chapin, 1919).

The north side of Slate Creek has faceted spurs with glacial erratics approximately 46 to 61 m (150 to 200 ft) above the canyon floor. It seems clear that during the Wisconsin, ice pushed up into the Slate Creek drainage from the Chistochina River valley and dammed Slate Creek. The deposition of till has modified the topography and altered the flow of Slate Creek.

The Big Four

The Big Four Mine is situated at the mouth of a steep gully hanging several hundred feet about the floor of the recently deglaciated Chistochina valley. It is a most picturesque setting with glaciers and the snowed-capped Alaska Range in the distance. The mine camp is directly on the lateral moraine. Gravels coming down the gully most likely piled up against the ice when the gully drainage was blocked. The gravel in the gully is almost exclusively derived from the round wash conglomerate outcropping in the headwater regions of the gully. The gravel is poorly sorted with a few boulders up to 30 cm (1 ft) in diameter; 15 cm (6-in.) boulders common, is gray-brown in color, and has rounded to subangular clasts. A pebble count

from the mine tailings revealed the following percentages:

schist	24	argillite	13
greenstone	22	quartz	6
granitic	10	diorite	6
volcanic	9	conglomerate	2
gabbro	8.		

The gold recovered has rounded edges is flattened and has some small nuggets 8 mm in diameter. The gold is generally oxide coated and rarely shiny. A panned concentrate from the gully produced 1 gold fragment 1.3 mm in diameter with adhering quartz. Heavy minerals in the concentrate include: magnetite 65 to 70 percent, ilmenite 30 percent and garnet, zircon, epidote and pyrite in lesser percentages.

Broxson Gulch

The placer mine is located at the mouth of a small tributary of an east fork of Broxson Gulch approximately 65 km west of Slate Creek.. The placer is an alluvial fan containing well rounded boulders and cobbles of rock types that are present in the gold-bearing Tertiary(?) conglomerate. A pebble count of coarse clasts in the fan produced the following: Granite - 42 percent, volcanic - 40 percent, gneiss - 5 percent, ultrabasic - 4 percent, quartz - 5 percent, greenstone - 2 percent, schist - 1 percent, and volcanic breccia - 1 percent.

The center of the fan has been mined down to bedrock and the tailings shoved out into the floodplain of Broxson Gulch. There appear to be several axes of fans, one dissected into another. A panned concentrate at the mine site produced 50 to 60 percent magnetite, ilmenite, garnet and zircon in

quantities greater than 10 percent each and lesser amounts of epidote, pyrite, sphene and rock fragments. From the panned concentrate 13 gold fragments were recovered, the largest 3 mm in diameter. Several gold grains possessed a partial silvery gold coating. The gold recovered from this small sample is equivalent to a value of \$16.00 per cubic yard at \$500 per ounce.

Exposed at the mine site is a probable fault contact, juxtaposing Tertiary(?) conglomerate and granite. At the head of the small tributary blue-gray Tertiary(?) conglomerate which contains well rounded cobbles and pebbles and a few boulders with a preponderance of granitic clasts is exposed. It appears to have been faulted in as a narrow band or wedge. The small tributary stream may owe its position to the location of the bounding faults.

Gold Source--The Round Wash

The "Round Wash" is a term applied by the early miners to the coarse boulder deposit capping the upland surfaces at the head of Miller Gulch (fig. 1). It is, in fact, a conglomerate, several hundred feet thick dipping gently to the northwest and resting unconformably on older argillite. Although never actually mined, portions of the conglomerate are under claim.

The unit is a coarse conglomerate with boulders up to 30 cm (1 ft) in diameter of quartz and granite. Schist and gabbro clasts make up a large part of the rock. The matrix is commonly coarse grained and in places resembles a "salt and pepper" sandstone with abundant quartz. It is occasionally greenish in color. Clasts of aragonite(?) are present on the weathered surface. The overall color of the rock is maroon to green. The boulders are well rounded and are common on the weathered upland surface. Quartz and granitic boulders, being more resistant to weathering than the more mafic constituents, appear to

be in higher concentration on the weathered surface than they really are in outcrop. A pebble count of the deposit revealed the following percentages:

chlorite schist	27	quartz monzonite	4
gabbro	20	quartz	2
granodiorite	18	chlorite epidote schist	1
meta diabase	13	diabase	1
meta gabbro	6	rhyodacite	1
amphibolite	6	limestone	1.

Several pans produced a concentrate containing 10 gold fragments, the largest 3.5 mm across. The gold fragments were all heavily tarnished primarily with iron oxide and with adhering impurities, primarily quartz. The gold from 4 pans equaled 8.5 mg in weight. Other "heavies" in the concentrate include the following:

magnetite	60 percent
ilmenite	30 percent
zircon	less than 10 percent
rock fragments	less than 10 percent
garnet	less than 10 percent.

It seems clear that the immediate source of the gold mined at the Slate Creek, Quartz Creek, Miller Gulch, and Big Four properties is the "Round Wash" conglomeratic deposit. All the gold-bearing streams head in areas that either now or most certainly in the recent past contain this gold-bearing conglomerate. This deposit is identical to conglomerate in surrounding areas that have associated sandstone and siltstone beds from which fossil plants have been collected. Although no precise identification of the plants have

yet been made, they are most certainly Tertiary, and might very likely be early Tertiary.

Gold from Tertiary conglomerate was panned in low concentrations as far as 50 km west of Slate Creek! It is only by virtue of the concentrating powers of the Pleistocene and Holocene streams that gold derived from Tertiary conglomerate now occurs in economic or near economic grade.

References

- Chapin, Theodore, 1919, Platinum-bearing auriferous gravels of Chistochina River: U.S. Geological Survey Bulletin 692, p. 137-141.
- Mendenhall, W. C., 1905, Geology of the central Copper River region, Alaska: U.S. Geological Survey Professional Paper 41, 133 p.
- Rose, A. W., 1965, Geology and mineral deposits of the Rainy Creek area, Mt. Hayes quadrangle, Alaska: Alaska Division of Mines and Minerals Geologic Report 14, 51 p.
- , 1967, Geology of the upper Chistochina River area, Mt. Hayes quadrangle, Alaska: Alaska Division of Mines and Minerals Geologic Report 28, 39 p.

Rock geochemistry, geology and genesis of the Guichon
Creek batholith in British Columbia, Canada, as it relates
to Highland Valley ore deposits

W. J. McMillan

Z. Johan

Rock Geochemistry, Geology and Genesis
of the Guichon Creek Batholith in British Columbia, Canada
as it Relates to Highland Valley Ore Deposits

W.J. McMillan and Z. Johan

Introduction

This paper highlights one part of a joint study of Canadian Cordilleran porphyry copper deposits by the B.C. Ministry of Energy, Mines and Petroleum Resources and the Bureau de Recherche Géologique et Minière of France. Geological mapping, grid sampling and major and minor element analyses were done by MEMPR; detailed mineralogy, isotopic analyses and microprobe analyses by BRGM. Other parts and more detailed results of the study will be published in a volume titled "Porphyry Copper Deposits in their Magmatic Context", being prepared for the 26th Geological Congress in Paris.

General Setting

The Guichon Creek batholith lies at the south end of the Cordilleran Intermontane belt (Figure 1). Late Triassic island arc (Gabrielse and Reesor, 1974) volcanic and plutonic rocks in this belt comprise a northwest-trending linear zone that extends from southern British Columbia into southwestern Yukon territory. Volcanic rocks and intrusions in the zone have both calc alkalic and alkalic affinities but both the Guichon Creek batholith and adjoining volcanic rocks are calc alkalic (Figure 2).

The batholith intrudes and metamorphoses late Triassic (Carnian and perhaps Norian) volcanic and sedimentary rocks of the Nicola group. However, isotopic ages from the batholith of 202 ± 8 Ma (K/A) and 205 ± 10 (Rb/Sr) are almost synchronous with suggested ages for Carnian time (Armstrong, 1978). Also, felsic volcanic rocks interlayered in Carnian Nicola group rocks south of the batholith (McMillan, 1977) might be extrusive equivalents of late phases of the batholith. This seems reasonable because Northcote (1969) presented evidence that early, more even grained, batholithic phases were mesozonal whereas late, porphyritic phases were epizonal. The batholith probably fed volcanism and subsequently intruded the lower part of its comagmatic volcanic pile.

Initial strontium ratios are primitive ($\text{Sr}^{87}/\text{Sr}^{86} = 0.7025$ to 0.7046), like those from modern island arcs. The magma was probably derived either from partial melting of upper mantle material or from recycled oceanic crust.

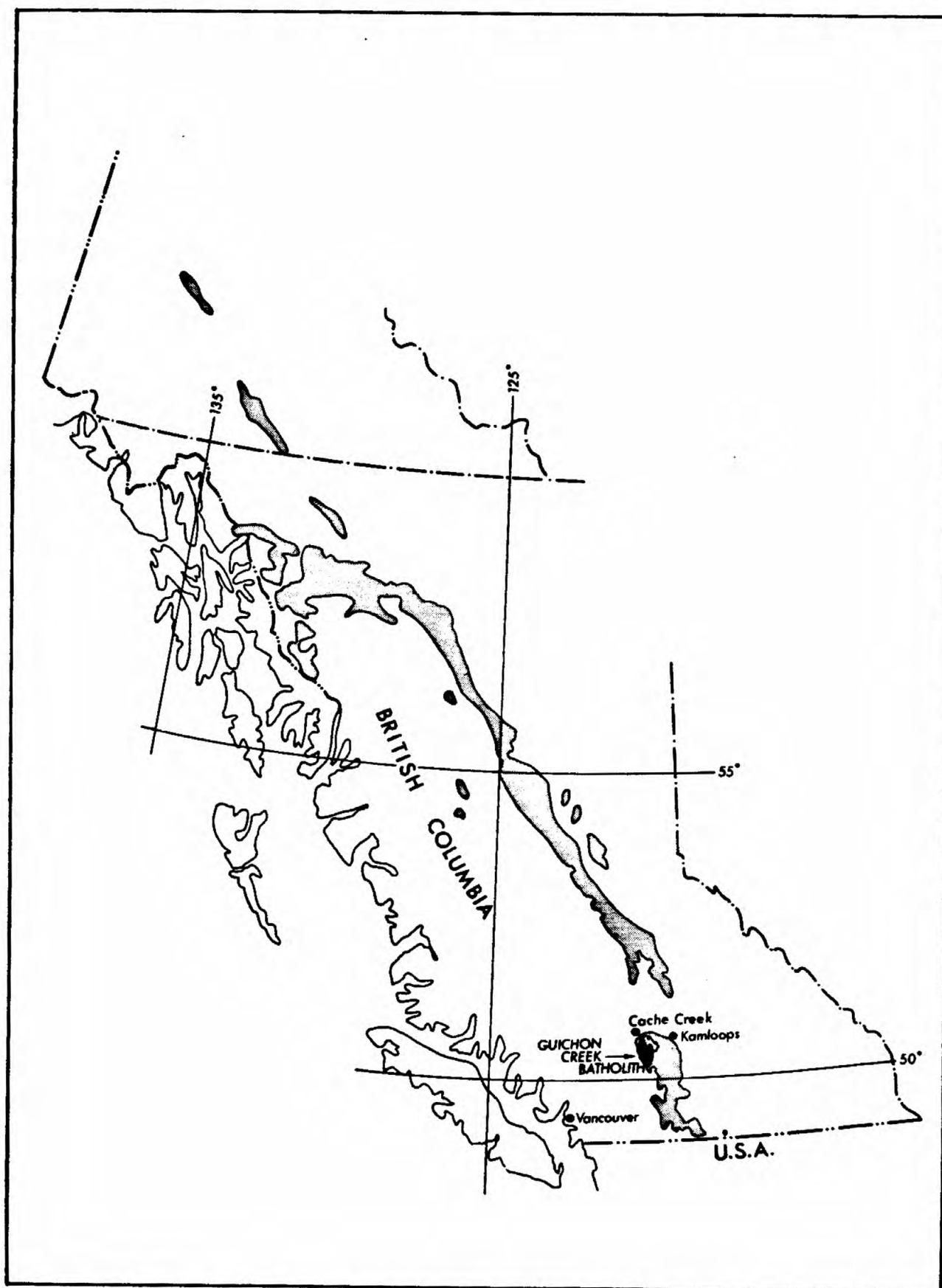


Figure 1 Distribution of Triassic Volcanic and Plutonic Rocks in the Canadian Cordillera.

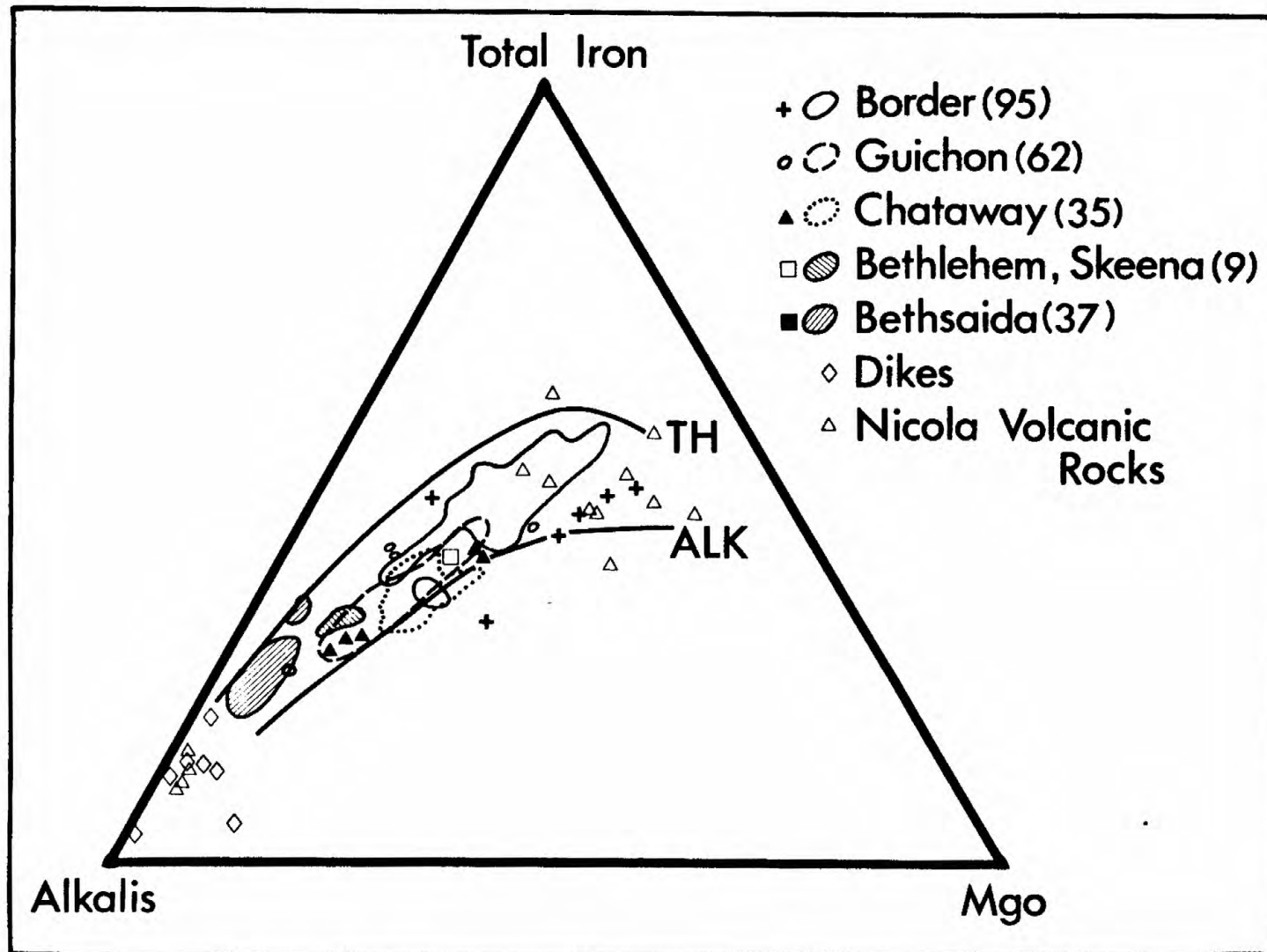


Figure 2 AFM projection for rocks of the Guichon Creek batholith and Nicola volcanic rocks showing their calc-alkaline affinities. Lines A and B (Kuno, 1968) limit thoeitic and alkaline domains respectively.

Strong northerly elongation suggests that the emplacement of the batholith was controlled by basement structures. Interpretation of a gravity survey shows that the pluton spreads out from a root zone under Highland Valley (Ager et al., 1973). This suggests that the intrusion was localized at the junction of basement structures. Reactivation of the regional structures during(?) and several times after emplacement of the batholith not only imposed a north and northwest fault pattern on the batholith but also influenced the distribution of younger sedimentary and volcanic rocks in the area (Carr, 1962; McMillan, 1976). These structures localized ore deposition and swarms of porphyry dikes were emplaced along them.

Geology of the Guichon Creek Batholith

The oldest rocks of the batholith lie at its borders and the youngest in its center (Figure 3). Large areas in the batholith have distinctive mineral compositions and textures; these have been termed "phases". From oldest to youngest they are the Border (formerly Hybrid), Highland Valley, Bethlehem and Bethsaida phases (Northcote, 1969). Within or between phases, mappable subdivisions were called "varieties"; thus the Highland Valley phase consists of the Guichon and Chataway varieties and a mixed zone between Bethlehem and Bethsaida phases is the Skeena variety.

Contacts between phases are generally gradational and rarely chilled; locally, however, they crosscut. Contacts between the older Border and Highland Valley phases are gradational. Younger Bethlehem and Bethsaida phases seem to cut the older phases but, again, contacts can be gradational. Evidently, successive phases were injected before the preceeding phase was completely solidified (Northcote, 1969; McMillan, 1976).

Episodic, volumous dike emplacement began after intrusion of the Bethlehem phase. The Bethlehem, South Seas and Krain ore deposits lie in a swarm of north-trending dikes with associated explosion breccias (Carr, 1960), that cut Bethlehem and older rocks north of Highland Valley. Texturally and chemically (this study; Briskey and Bellamy, 1976; Briskey, 1980) these dikes have Bethlehem affinities. They were generated at the end of Bethlehem phase emplacement and are related to the first major period of ore formation in the batholith. Younger dikes and plugs that trend both parallel to the older dike swarm and northwestward, occur in and south of Highland Valley. They represent both Bethsaida phase magma and related, more evolved later stage magmas. The largest ore deposits in the batholith were deposited during and after their emplacement.

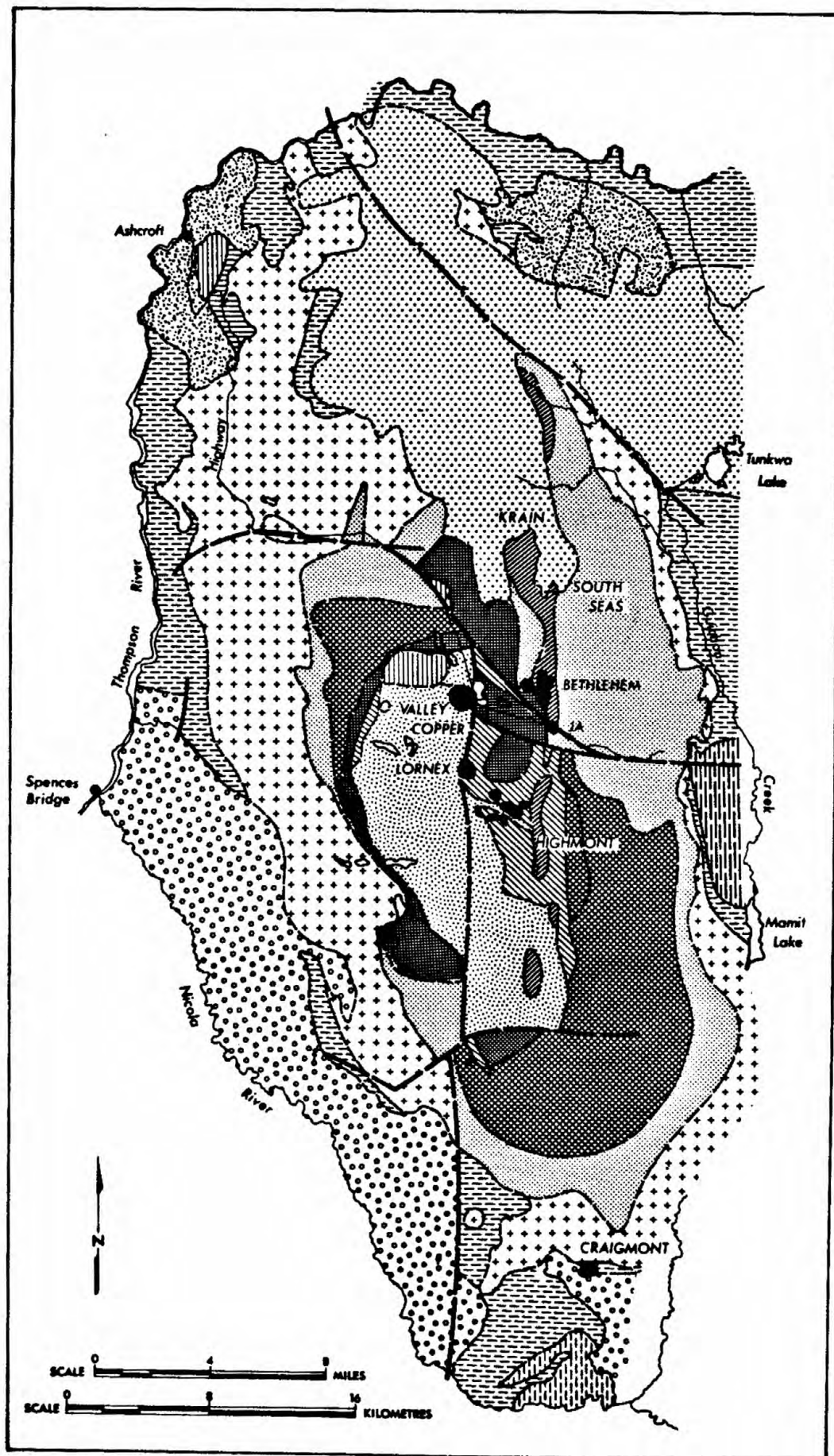


Figure 3 Simplified geology of the Guichon Creek batholith in south central British Columbia.

LEGEND

TERTIARY

 VOLCANIC AND SEDIMENTARY ROCKS

CRETACEOUS (?)

 VOLCANIC AND SEDIMENTARY ROCKS

JURASSIC

 SEDIMENTARY ROCKS

INTRUSIVE ROCKS OF THE BATHOLITH

 BETHSAIDA PHASE*

 SKEENA VARIETY

 BETHLEHEM PHASE

HIGHLAND VALLEY PHASE

 CHATAWAY VARIETY

 GUICHON VARIETY

 BORDER PHASE

INTRUSIVE ROCKS OF UNCERTAIN AFFILIATION

 GUMP LAKE PHASE

 COYLE 'GRANITE'

UPPER TRIASSIC

 VOLCANIC AND SEDIMENTARY ROCKS

SYMBOLS

ORE DEPOSITS, IMPORTANT PROSPECTS

AREAS WITH SWARMS OF PORPHYRY DYKES

FAULTS: MAPPED, INFERRED



*DESIGNATION OF GRANITIC UNITS AS PHASES OR VARIETIES FOLLOWS THE USAGE OF NORTHCOTE (1969).

Petrology

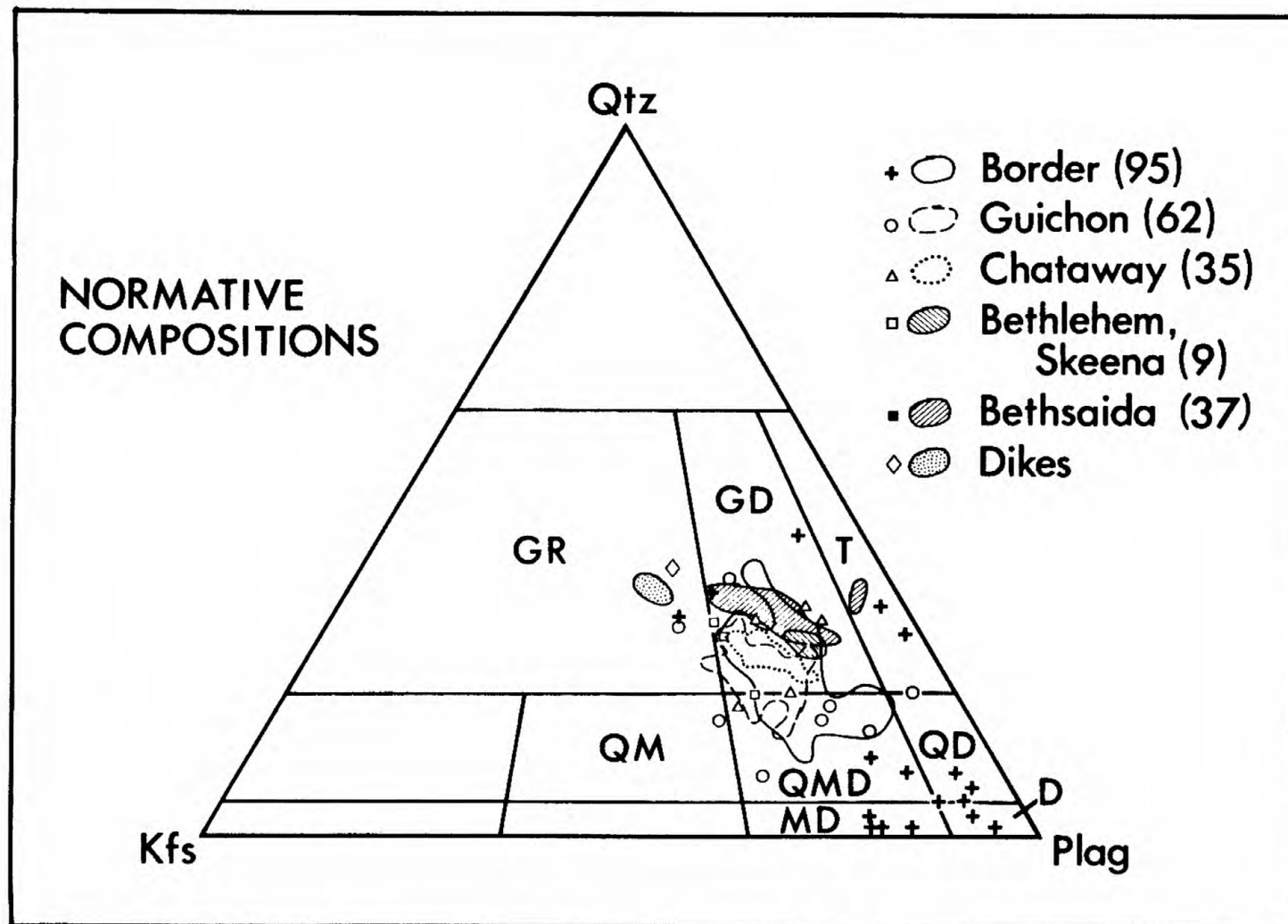
Rocks of the batholith are composed of varying proportions of plagioclase, amphibole, biotite, quartz and potassic feldspar with ubiquitous accessory magnetite, apatite and sphene. In the oldest rocks, amphibole is locally cored by pyroxene; in the youngest rocks biotite may be the only ferromagnesian mineral. The rocks are over-saturated with respect to quartz, hypersthene normative and equivalent to an andesitic rock series (Johan and McMillan, 1980). From border to core, normative compositions range from diorite or quartz diorite through quartz monzodiorite to granodiorite. Late stage porphyry dike compositions extend into the granite field (Figure 4). Older phases are medium grained and relatively equigranular, younger phases are coarser and porphyritic.

Border phase rocks have inclusions of Nicola volcanic and sedimentary rocks. Locally, interaction with these inclusions has produced hybrid amphibolite to monzonitic zones. Granitoid basic inclusions also occur and can be so abundant that they form breccias. In these instances, subangular basic inclusions float in a matrix of Border phase quartz diorite.

The basic inclusions consist of plagioclase, clinopyroxene, orthopyroxene and amphibole; some have subordinate amounts of biotite. Accessory minerals are abundant magnetite, sphene and apatite. Plagioclase crystals are either unzoned or have diffuse, subtle zoning (An_{47} to An_{44}). Crystallization of amphiboles took place under elevated water pressures in the magma and orthopyroxene-clinopyroxene pairs, according to the method described by Wells (1977), give an estimated temperature of $890^{\circ}C$. These basic inclusions are interpreted to be cumulates formed at depth during crystallization of the Guichon Creek batholith.

In rocks of the Border phase and Guichon variety zoning in plagioclase crystals is simple and normal. Compositions range from An_{48} in core zones to as low as An_{10} at borders. In Chataway variety rocks, zoning also looks simple but the microprobe revealed some internal reverse zoning. The most calcic zone measured was An_{44} and most crystal borders were about An_{31} . In all these phases, small plagioclase crystals associated with interstitial quartz-potassic feldspar are more sodic (An_{10} to An_{15}).

Plagioclase in Bethlehem phase, Skeena variety and Bethsaida phase rocks have partly resorbed cores enclosed in a more calcic corona, then a region of complex oscillatory zoning and, finally, normally zoned rims. In Bethlehem phase and Skeena variety, cores are up to An_{42} and rims generally about An_{30} , although some rims and small interstitial crystals range down to An_{10} . In Bethsaida phase, cores are more calcic and range to An_{50} , rims are as low as An_{13} .



GUICHON CREEK BATHOLITH

Figure 4 Normative compositions of intrusive phases of the batholith projected onto the Pl-Q-Kf diagram.

There is obviously a distinct change in conditions of plagioclase crystallization after the Chataway variety. Conditions in the older phases (Border and Highland Valley) were similar to one another but differed from those in the younger phases (Bethlehem and Bethsaida).

Plagioclase crystallization traits, therefore, divide the rocks of the batholith into two series: the older phases (Border and Highland Valley) and the younger phases (Bethlehem and Bethsaida).

Major Element Geochemistry

There is a clear calc alkalic differentiation trend shown by an AFM plot for rocks of the batholith (Figure 2). Some samples lie slightly below the boundary line separating the calc alkaline and alkaline fields but no evidence of a second, alkaline magma exists. Iron depletion due to early crystallization of magnetite in the cumulate phase may explain these samples.

Most oxides from all the phases of the batholith have smooth evolution curves when plotted against SiO_2 or Larson Differentiation Index. As well, the distribution of Mn between biotite and hornblende in rocks of the batholith also shows a smooth evolution curve which indicates near-equilibrium conditions in each phase and a single source magma. In sum, all the phases derive from a single source magma.

Alkalis, however, are not simply distributed. Total alkalis plotted against SiO_2 fall largely in the calc alkaline field in the domain of high alumina basalt (Kuno, 1968). When K_2O is plotted against Larson Differentiation Index, trends for older phases and those for younger phases as well as dikes are discontinuous; they define two separate trends (Figure 5). Plotting alkalis versus lime on a ternary plot (Figure 6) also shows a discontinuity. Dikes are included in the interpretation because there is field and chemical evidence that they are late stage differentiates from the Bethlehem and Bethsaida phases (McMillan, 1976; Briskey and Bellamy, 1976). If dikes are ignored, the discontinuity is less evident and the evolution appears to be trondhjemitic (Olade, 1976). Essentially, the discontinuity results because many rock samples from the younger phases are deficient in K_2O relative to samples of the most evolved older phase rocks (Chataway variety).

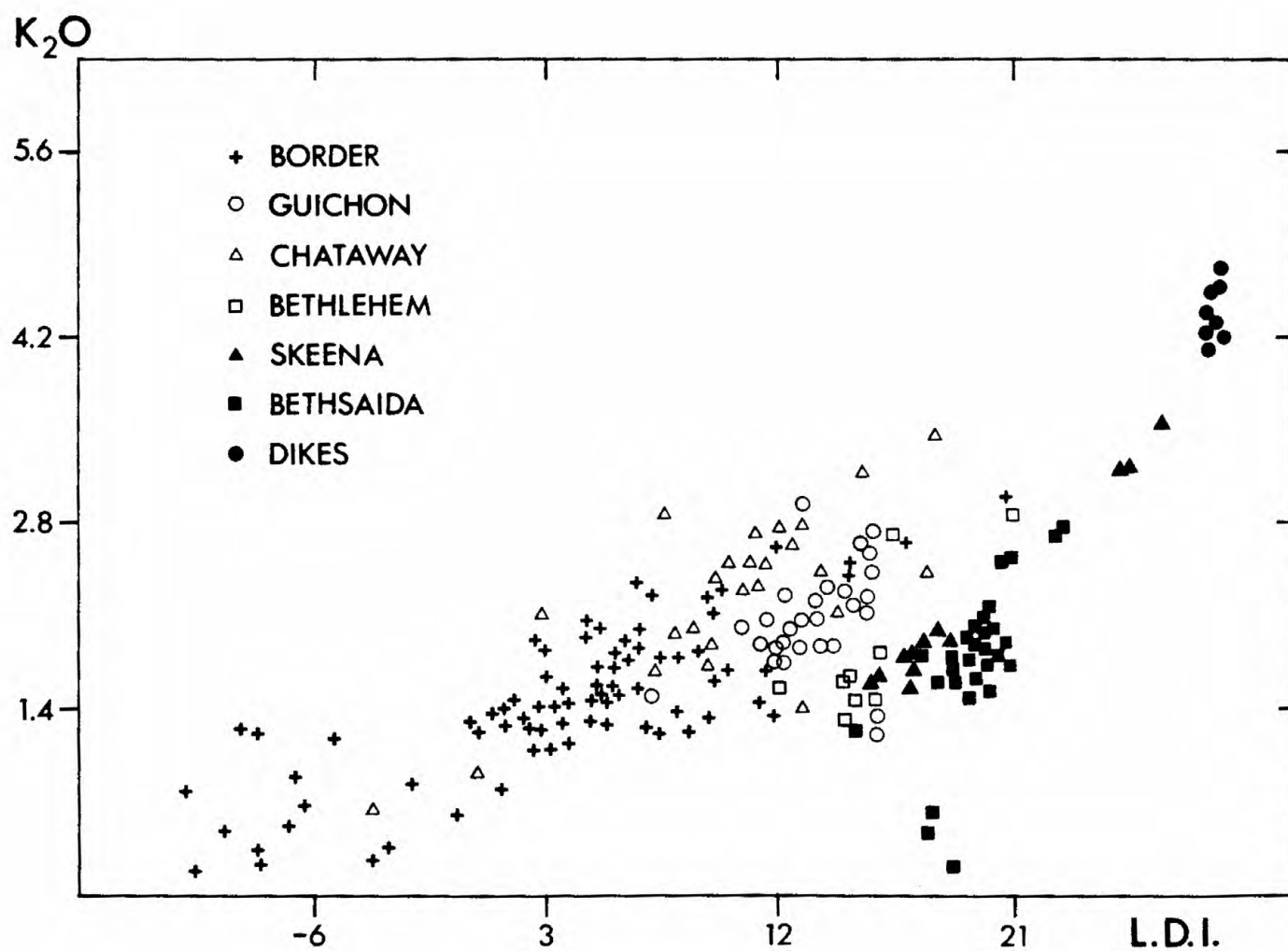


Figure 5 Plot of K_2O versus Larson Differentiation Index for intrusive rocks of the batholith.

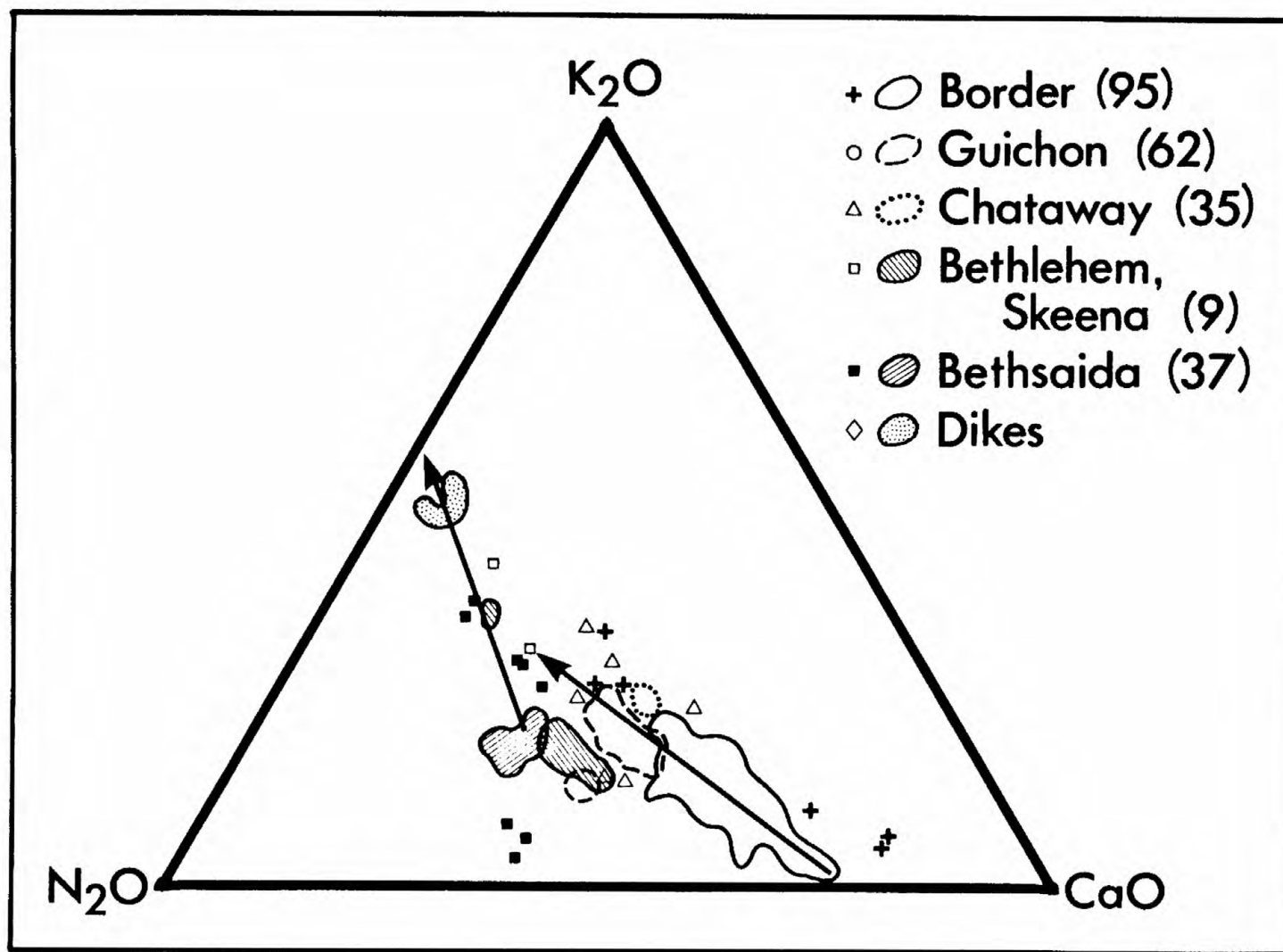


Figure 6 Evolution of the batholith represented on a K_2O - Na_2O - CaO diagram (values in weight percent). Note the discontinuity in evolutionary trends between the older phases and the younger phases.

Minor Element Geochemistry

Minor elements in the batholith form three main groups. Some, primarily Co, Cr and Ni, are influenced by ferromagnesian mineral trends and have smooth evolution curves indicative of a single source magma. Zinc roughly follows this group but its distribution is complicated by its affinity for sulphur. Others, particularly those with large ionic radius, Ba, Sr, Pb, Cs and Li, are influenced by Na, K and Ca. Consequently, their abundances are controlled by cumulate crystallization (Johan and McMillan, 1980). The third group, most notably Rb, Cu and Zr, show a discontinuity between the older and younger phases. Arsenic levels are relatively unchanged with differentiation whereas those of silver and mercury decrease slightly; halides have more complex patterns (Figure 7).

As a test, Cl was measured with the microprobe in biotites from various phases. Biotites in Highland Valley phase rocks averaged 1300 ppm whereas those in Bethlehem phase averaged 600 ppm and those in Bethsaida phase only 380 ppm. A plot of Cu versus Cl plus F (Figure 8) yielded straight line relationships for older phases and a separate straight line for younger phases, therefore both Cu and halide distribution were affected by the same mechanism.

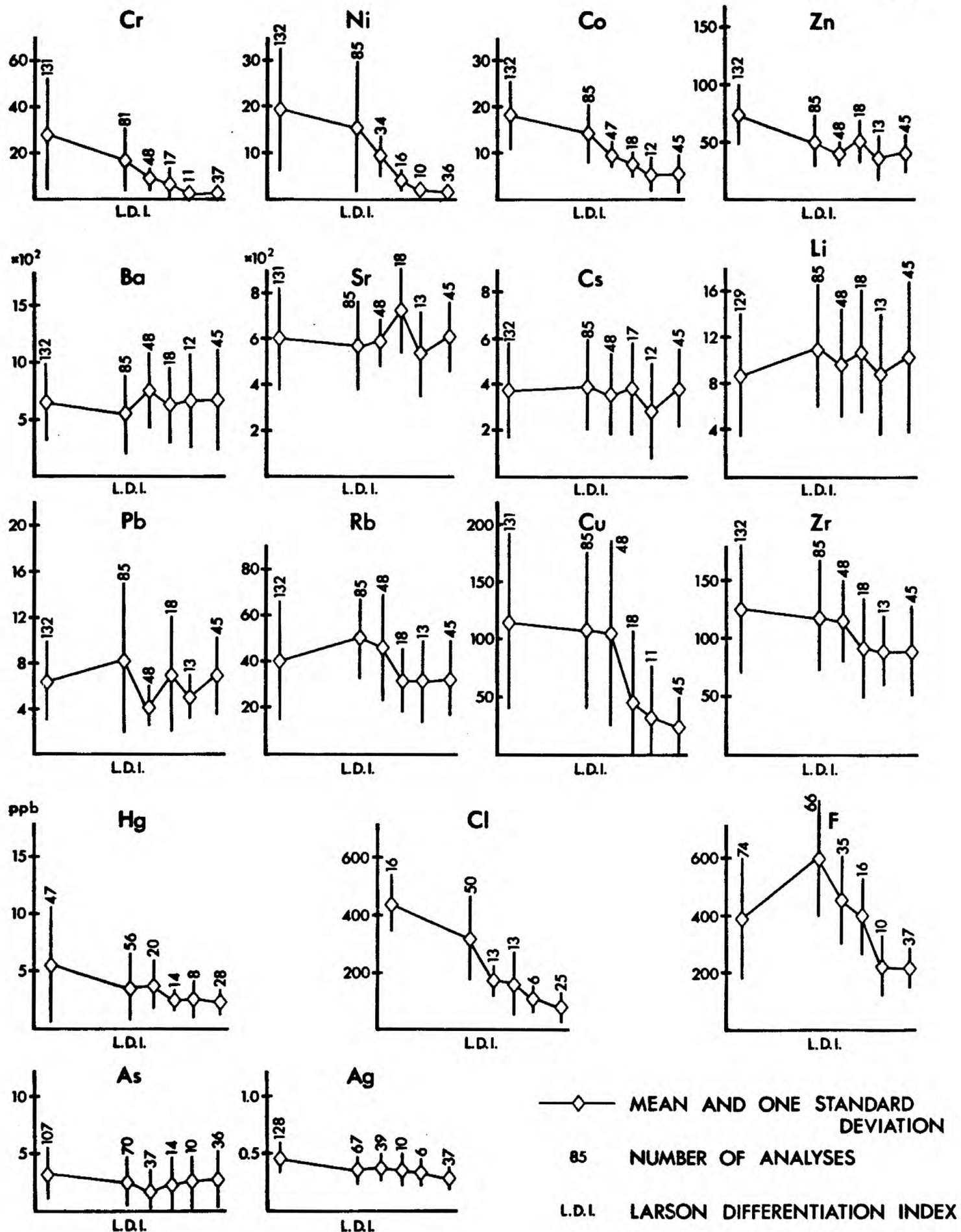
Summary and Discussion

All the phases of the Guichon Creek batholith evolved from a single source magma. However, petrologic and chemical data show a discontinuity between the older and the younger phases of the batholith. A model to account for the mineral and chemical changes follows:

1. The source magma is calc-alkaline and of andesitic composition.
2. Evolution of the phases was controlled by cumulate crystallization. Separation of plagioclase, amphibole and magnetite occurred under conditions of high partial pressure of water. Biotite in cumulates is interpreted to have begun to crystallize when a fluid phase separated in the magma.
3. Crystallization of all the phases began at depth but was completed at intrusive levels.
4. The discontinuity in evolutionary trends between the older and younger phases marks the separation of a fluid phase.

Several lines of evidence led to development of the model. In all phases cores of plagioclase crystals have similar compositions; in the older phases zoning is simple but in the younger phases core zones are partially resorbed and, outward, complex oscillatory is followed by normal zoning. Concentrations of alkalis and several trace elements

Figure 7 Trace element variations plotted as a function of Larson Differentiation Index for intrusive phases of the batholith. In each diagram phases and varieties from lowest LDI to highest are: Border, Guichon, Chataway, Bethlehem, Skeena and Bethsaida.



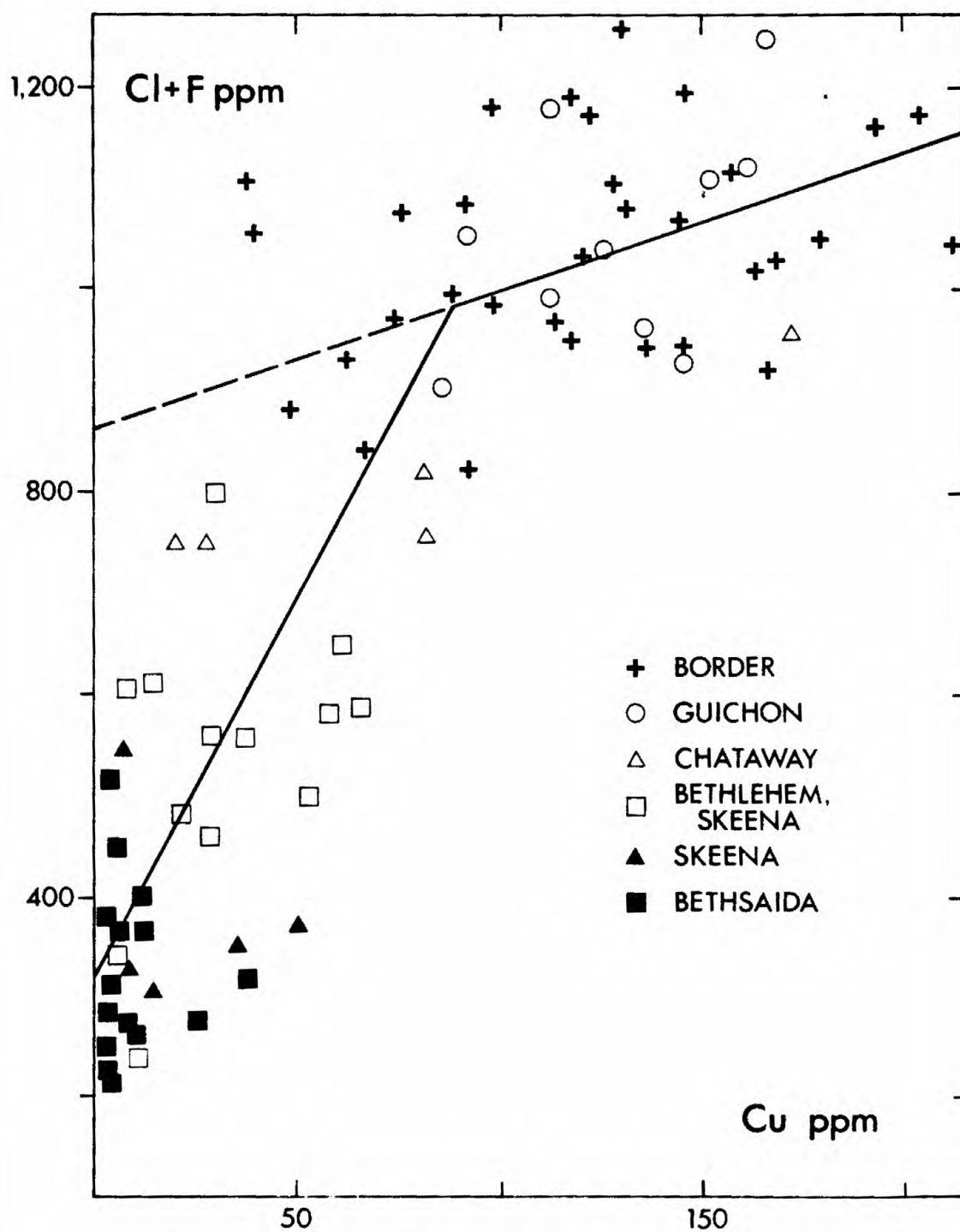


Figure 8 Copper plotted versus Cl plus F for intrusive phases of the batholith. Two distinct trends are defined by the older and younger phases.

change suddenly, that is, they are discontinuous between the older and younger phases. Plagioclase textures reflect the effects of early crystallization at depth and, in the younger phases, separation of a fluid phase. Similarly, lower abundances of more mobile elements in the younger phases reflect their selective removal and concentration into a fluid phase. At less than 8 kbars pressure, chlorine is preferentially taken up in the fluid phase if one is present. Chlorine in biotites from the batholith decreases sharply between the older and younger phases. The decrease in chlorine, the change in plagioclase character and the discontinuity in mobile element abundances reflect the separation of a fluid phase.

Geologically, this hypothesis is supported by the timing of mineralization, and by dike swarms in the batholith that were injected after Bethlehem phase and during and after Bethsaida phase emplacement. Explosion breccias (Carr, 1960) associated with the dikes attest to high volatile pressures.

Separation of a fluid phase at depth would impoverish the magma in Cu, Cl, Rb and probably B and Hg (Olade, 1977). The parallel behavior of Zr is unexplained. Similarly, lower Ni/Co ratios in the younger phases along with minor amounts of cobalt and nickel sulphides and tellurides in the ore deposits, show the presence of these transition elements in the fluid. Apparently, transfer of Na into the fluid phase raised K/Na ratios in the melt and initiated biotite crystallization in the cumulates. This separation of biotite caused lower than expected K_2O values in the Bethlehem phase fluid and a discontinuity in the evolutionary path (Figures 5 and 6). Molybdenite distribution in the ore deposits is similar but not the same as that for copper (Reed and Jambor, 1976; McMillan, 1978) but its concentration in the magma was too low to delineate evolutionary patterns (Brabec, 1971).

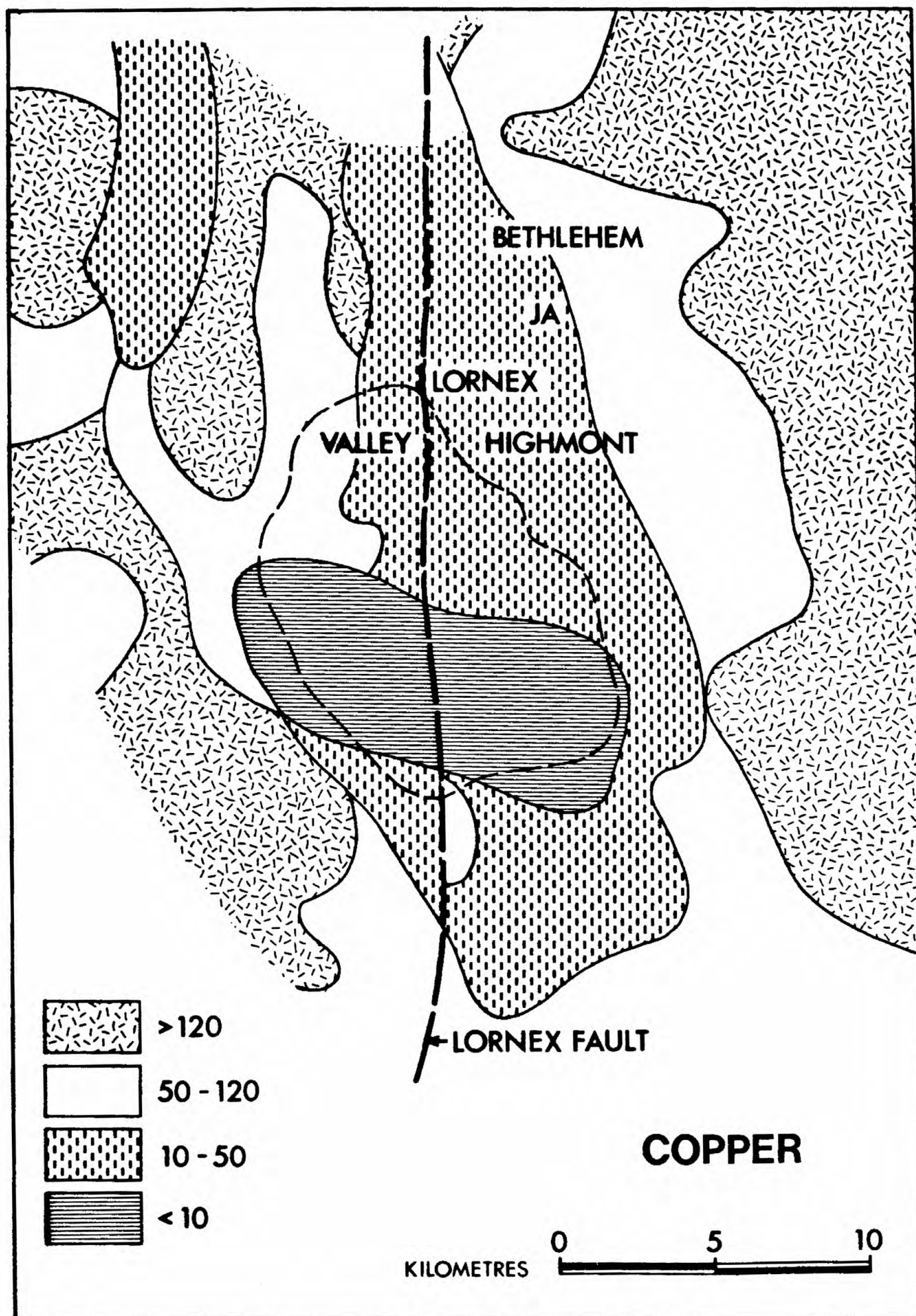
Relationship to Ore Forming Processes

Metals in Highland Valley ore deposits were deposited from a fluid phase that separated during crystallization of the batholith. Crystallization of the source magma took place at depth, under relatively high partial pressure of water, a factor that was probably instrumental in formation of the fluid phase.

The batholith was localized by basement structure and subsequently fractured during periodic reactivation of these regional structures. A strong pattern of northerly and northwesterly faults and fracture swarms and northerly dike swarms resulted. Early ore deposition, such as that at Bethlehem Copper, was controlled by faults and porosity caused by brecciation during dike swarm emplacement. As

the copper distribution map shows (Figure 9), younger ore deposits, such as Highmont, Lornex and Valley Copper, were deposited in structural traps north of the depleted source magma from which the ore fluids were derived.

Figure 9 Distribution of copper in the Guichon Creek batholith. To make distribution patterns easier to interpret, lateral offset on the northerly Lornex fault has been removed. The youngest phase of the batholith has a markedly Cu-impo-
verished zone south of the major Highland Valley ore deposits.



References

- Ager, C.A., McMillan, W.J. and Ulrych, T.J., 1973, Gravity, Magnetism and Geology of the Guichon Creek Batholith: B.C. Ministry of Energy, Mines and Pet. Res., Bulletin 62.
- Armstrong, R.L., 1978, Pre-Cenozoic Phanerozoic Time Scale Computer File of Critical Dates and Consequences of New and In-progress Decay Constant Revisions: American Assn. of Petroleum Geologists, Studies in Geology No.6, p.73-91.
- Brabec, D., 1971, A Geochemical Study of the Guichon Creek Batholith, British Columbia: Unpublished Ph.D. Thesis, Univ. of B.C., 147p.
- Briskey, J.A., 1980, Bethlehem Copper: Unpublished Ph.D. Thesis, Oregon State University, Corvallis, Oregon.
- Briskey, J.A. and Bellamy, J.R., Bethlehem Copper's Jersey, East Jersey, Huestis and Iona Deposits: Cdn. Institute of Mining and Metallurgy, Special Volume 15, p.105-119.
- Carr, J.M., 1960, Porphyries, Breccia and Copper Mineralization in Highland Valley, B.C.: Canadian Mining Journal, Vol.81, p.71-73.
- _____, 1962, Geology of the Princeton, Merritt, Kamloops area: Western Miner, Vol.75, February, p.46-49.
- Gabrielse, H. and Reesor, J.E., 1974, Nature and Settings of Granitic Plutons in the Central and Eastern Parts of the Canadian Cordillera: Pacific Geology, Vol.8, p.109-138.
- Johan, Z. and McMillan, W.J., 1980, Chapitres 3, 4 et 5 en: Mineralisations Type Porphyres Cuprifères Dans Leur Contexte Magmatique: 26th International Geological Congress, Paris, in preparation.
- Kuno, H., 1968, Differentiation of Basalt Magma: in Basalts, Vol.2, H.H. Hess and A. Poldervaart, editors, J. Wiley, New York, p.624-688.
- McMillan, W.J., 1978, Highland Valley Cu-Mo Porphyries: in Sutulov, A., editor, International Molybdenum Encyclopaedia, p.194-206.
- Olade, M.A.D., 1976, Geochemical Evolution of Copper-Bearing Granitic Rocks of Guichon Creek Batholith, British Columbia: Canadian Journal of Earth Sciences, Vol.13, p.199-209.
- _____, 1977, Nature of Volatile Element Anomalies at Porphyry Copper Deposits, Highland Valley, B.C.: Chemical Geology, Vol.20, p.235-252.

- Reed, A.J. and Jambor, J.L., 1976, Highmont: Linearly Zoned Copper-Molybdenum Porphyry Deposits and Their Significance in the Genesis of the Highland Valley Ores: Canadian Institute of Mining and Metallurgy, Special Vol.15, p.163-181.
- Wells, P.R.A., 1977, Pyroxene Thermometry in Simple and Complex Systems: Contributions to Mineralogy and Petrology, Vol.62, p.129-139.

Geology, petrology, and geochemistry of the Jersey, East
Jersey, Heustis, and Iona porphyry copper-molybdenum
deposits, Highland Valley, British Columbia

J. A. Briskey, U.S. Geological Survey

C. W. Field, Oregon State University

J. R. Bellamy, Bethlehem Copper Corporation

GEOLOGY, PETROLOGY, AND GEOCHEMISTRY OF THE JERSEY, EAST JERSEY,
HEUSTIS, AND IONA PORPHYRY COPPER-MOLYBDENUM DEPOSITS,
HIGHLAND VALLEY, BRITISH COLUMBIA

By

Joseph A. Briskey¹, Cyrus W. Field², and John R. Bellamy³

ABSTRACT

The Bethlehem porphyry copper-molybdenum deposits are near the center of the 200-m.y.-old (million year) Guichon Creek batholith, a concentrically zoned, chemically primitive calc-alkaline and trondhjemitic pluton that intrudes oceanic (melange) assemblages of the Pennsylvanian to Late Triassic Cache Creek Group and volcanic-arc lithologies of the Late Triassic to perhaps Middle Jurassic Nicola Group. The deposits, especially the Jersey ore body, display features having significant implications for porphyry copper exploration in volcanic-arc terranes, including: (1) intimate association in time and space with silicic, highly potassium deficient dacite porphyries; (2) dominance of fracture-controlled copper mineralization; (3) formation in a wrench-fault tectonic setting; (4) low abundances of lead, zinc, silver, and gold; (5) well-defined zonation of iron-bearing metallic minerals (bornite-chalcopyrite-pyrite-specularite); (6) low total sulfide content (<2 volume percent) and sparse pyrite (<1 volume percent in the halo zone); (7) high bornite/chalcopyrite ratios (>1); (8) molybdenite peripheral to the central parts of the ore zones; (9) restriction of significant hydrothermal alteration to the ore zones; (10) scarcity of potassium feldspar alteration; (11) marked instability of primary potassium feldspar; (12) loss of K₂O in the propylitic, phyllic, and potassic zones; (13) prominent occurrences of actinolitic to tremolitic amphiboles; (14) widespread prehnite intimately associated and intergrown with copper sulfides; and (15) ubiquitous occurrences of largely postmetallization zeolites, especially laumontite.

ACKNOWLEDGMENTS

The Jersey, East Jersey, Huestis, and Iona porphyry copper-molybdenum deposits are owned and operated by Bethlehem Copper Corporation, Ltd. The authors are extremely grateful to company personnel, particularly to vice-president-exploration Henry G. Ewanchuk, whose cooperation and encouragement made this study possible. The manuscript has benefitted substantially from review by Miles L. Silberman.

¹U.S. Geological Survey, 345 Middlefield Road, Menlo Park, CA 94025

²Oregon State University, Department of Geology, Corvallis, OR 97331

³Bethlehem Copper Corp., Ltd., 1055 W. Hastings St., Vancouver, B.C., Canada, V6E 2H8

INTRODUCTION

The deposits are located 400 km by highway northeast of Vancouver near the geographic center of the 200-m.y.-old Guichon Creek batholith (fig. 1), and on the north slope of west-northwest-trending Highland Valley. In aggregate the ore bodies originally contained in excess of 120 million metric tons of ore averaging nearly 0.5 percent copper, about half of which was in the Jersey deposit.

PETROTECTONIC SETTING AND METALLOGENY

At the time of emplacement of the Guichon Creek batholith the early Mesozoic continental margin of North America had become, beginning in the Late Triassic, the locus of similar, penecontemporaneous magmatism, metamorphism, and sedimentation, resulting from oblique(?) convergence and subduction of oceanic crust beneath the continent (e.g., Davis and others, 1978). Composite, Late Triassic to Early to Middle Jurassic arc magmatism in central and southern British Columbia is manifest in alkaline and calc-alkaline suites of the Late Triassic Takla-Nicola arc, containing the comagmatic Guichon Creek batholith, and in the calc-alkaline assemblages of the Early Jurassic Hazelton arc (e.g., Davis and others, 1978). Late Triassic to Early Jurassic calc-alkaline and alkaline plutons hosting porphyry copper deposits are conspicuously restricted to a contemporaneous volcanic arc terrane (fig. 1).

GUICHON CREEK BATHOLITH

The Guichon Creek batholith (fig. 2) is a concentrically zoned calc-alkaline pluton in which the major intrusive phases become progressively younger and change in composition inward from quartz diorites and diorites of the peripheral Hybrid Phase; through quartz diorites and granodiorites of the Guichon Variety, and granodiorites of the Chataway Variety, the Bethlehem Phase, and the transitional Skeena Variety; to a core of granodiorite and quartz monzonite of the Bethsaida Phase (McMillan, 1976, 1978).

Modal mineralogies and textures of the plutonic units of the Guichon Creek Batholith are typical of calc-alkaline series plutonic suites described for the Coast Plutonic Complex of British Columbia (Roddick and Hutchinson, 1974) and in island-arc and continental-marginal-arc tectonic settings in the northern Caribbean (Kesler and others, 1975), Panama (Kesler and others, 1977), and the Papua New Guinea-Solomon Islands region of the southwest Pacific (Mason and McDonald, 1978). Characteristic features include the widespread presence of oscillatory zoned plagioclase, typical occurrence of potassium feldspar in the interstitial groundmass and its virtual absence as phenocrysts, presence of amphiboles and biotite in all suites, and the sporadic occurrence of clinopyroxene and rare orthopyroxene.

The batholith intrudes "eugeosynclinal" assemblages of the Late Triassic to perhaps Middle Jurassic Nicola Group and the Pennsylvanian to Late Triassic Cache Creek Group (McMillan, 1976, 1978). It is unconformably overlain by sedimentary rocks of the Lower and Middle Jurassic Ashcroft Formation, and by volcanic and sedimentary rocks of the Cretaceous(?) Spences Bridge and Kingsvale Groups and the Eocene Kamloops Group.

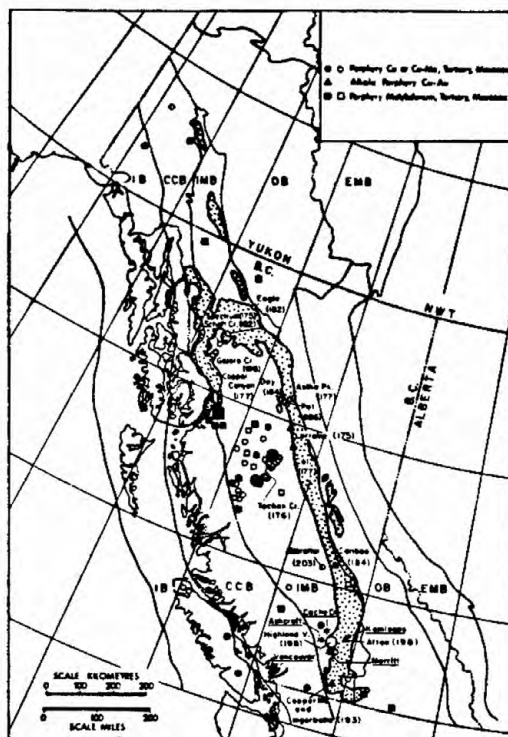


Figure 1. Distribution of porphyry deposits in petrotectonic belts and Upper Triassic to Lower Jurassic island arc volcanic and related rocks (stippled) in the Canadian Cordillera. IB- Insular belt; CCB- Coast Crystalline belt; IMB- Intermontane belt; OB- Omineca belt; EMB- Eastern Marginal belt. Major, known, Late Triassic to Early Jurassic deposits are identified. Numbers in parentheses are ages in millions of years. Each age has a range of ± 5 to 8 m.y., except Copper Canyon (± 9 m.y.) and Day (± 11 m.y.). Modified from Christopher and Carter (1976), McMillan (1976), and Barr and others (1976).



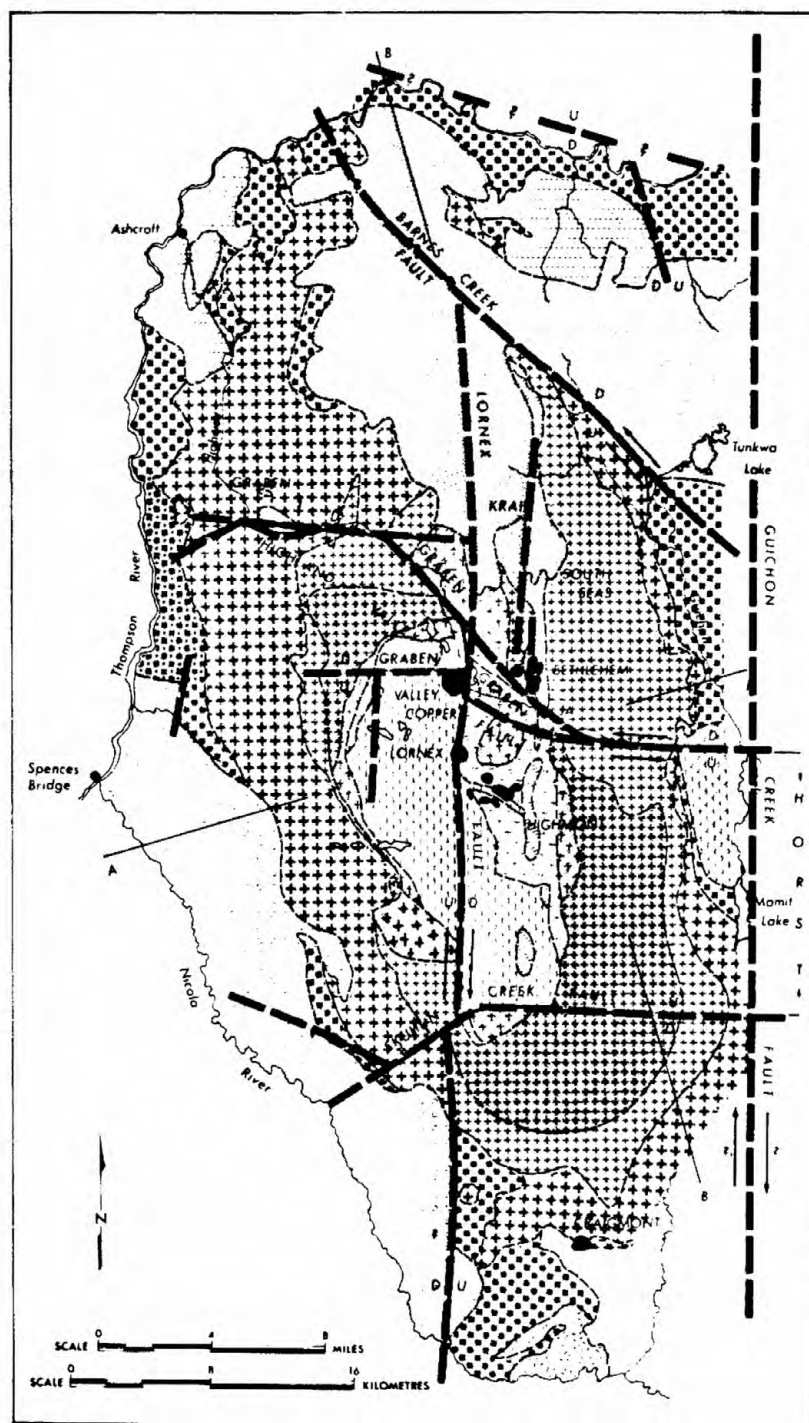


Figure 2. Geologic map of the Guichon Creek Batholith. Stippled, Upper Triassic volcanic and sedimentary rocks (Nicola Group) were originally mapped as Cache Creek Group by Duffell and McTaggart (1952), Carr (1962), and Northcote (1969). Modified from McMillan (1976).

The tectonic fabric of the batholith was established following intrusion of the Bethsaida Phase, but prior to formation of the mineral deposits (McMillan, 1976, 1978). The Lornex and Guichon Creek faults are the important north-trending structures. Major northwesterly to westerly striking faults are the Barnes Creek, Highland Valley, and Skuhun Creek faults (fig. 2).

The batholith is interpreted from geologic, gravity, and magnetic data by Ager and others (1972) to be shaped like a flattened funnel, with the spout underlying Highland Valley and plunging about 80° to the northeast (fig. 3).

The AFM diagram (fig. 4) demonstrates that the units of the batholith show progressive enrichment of alkalis with respect to iron and magnesium. This calc-alkaline trend generally follows the temporal order of intrusion from early diorite and quartz diorite to late silicic granodiorite. The alkali enrichment trend shown by the AFM diagram is further defined by the NKC diagram ($N=Na_2O$, $K=K_2O$, $C=CaO$) (fig. 5). The early major phases and varieties of the batholith display an apparently normal progressive enrichment of K_2O relative to Na_2O and especially CaO , and closely follow the trend of calc-alkaline magma series (solid line). In contrast, the later major units follow a trondhjemitic magmatic trend (dashed line) that extends from CaO -rich to relatively Na_2O -rich lithologies, and probably reflects the low overall K_2O content of the batholith (fig. 6). Comparably low K_2O abundances are recorded for plutonic sequences in Panama (Kesler and others, 1977) and in the Papua New Guinea-Solomon Islands area (Mason and McDonald, 1978).

JERSEY, EAST JERSEY, HUESTIS, AND IONA ORE DEPOSITS

The Bethlehem deposits formed along an irregular intrusive contact separating two major plutonic units of the Guichon Creek batholith (fig. 7). Rocks of the younger Bethlehem granodiorite form a digitated northward-elongated apophysis that is intrusive into rocks of the older Guichon granodiorite. This apophysis apparently followed the north-trending zone of structural weakness that subsequently localized the intrabatholith porphyry dike swarm that transects the property. Intrusive breccias; dacite porphyry dikes; small masses of "granite," granodiorite, and porphyritic quartz latite; dikes of silicic aplite; faults and fractures; and hydrothermal mineralization and alteration have been localized along digitations in the contact of the apophysis. Mining operations removed thin cappings of Guichon granodiorite from parts of the Huestis, Jersey, and East Jersey ore bodies. These cappings indicate that the current level of exposure is near the roof of the apophysis.

The ore deposits are most closely associated in time and space with the silicic, highly potash-deficient dacite porphyries (Briskey and Bellamy, 1976) (fig. 6; 20 analyses; range 0.05-1.98 percent K_2O ; avg 0.36 percent K_2O), which have close textural, mineralogical, and chemical affinities to plagioclase-quartz-hornblende porphyries associated with island-arc deposits in such regions as Panama (Kesler and others, 1977), Puerto Rico (Cox and others, 1973), and Papua New Guinea (Hine and Mason, 1978).

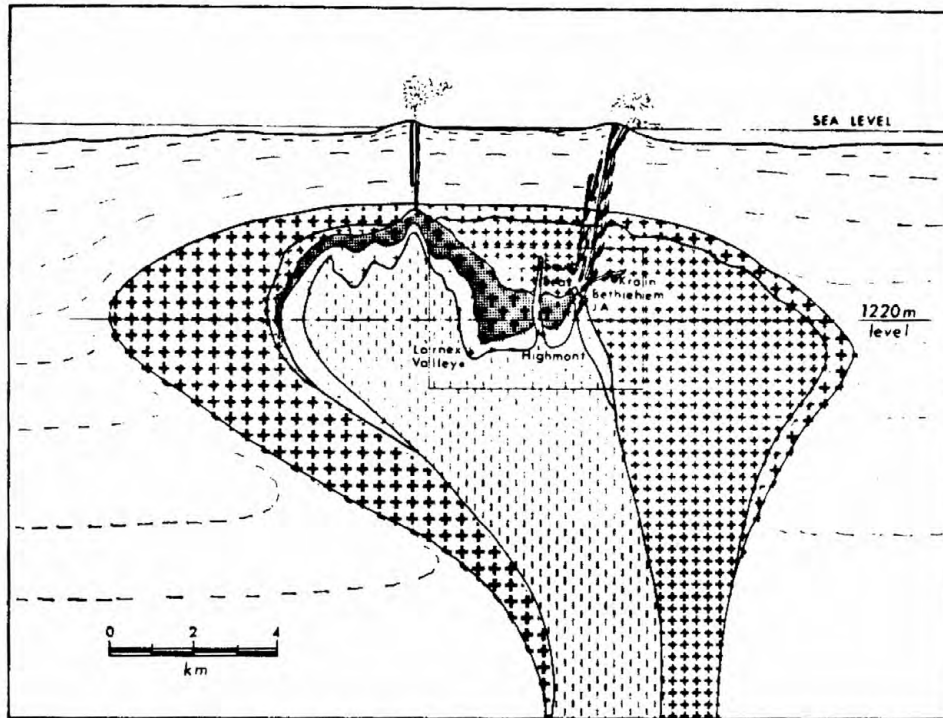


Figure 3. Schematic cross section of the Guichon Creek Batholith showing relative positions of emplacement of the Highland Valley deposits. Looking approximately northeast at section A, Figure 2. From McMillan (1976).

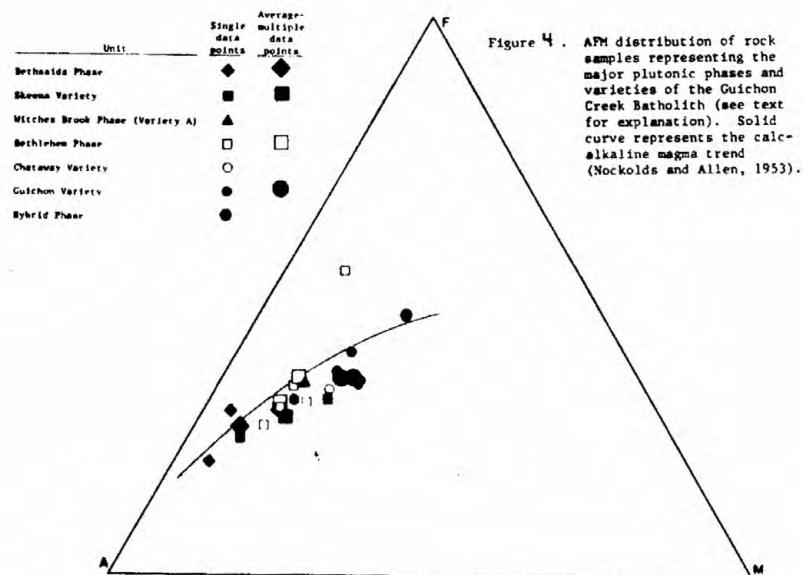
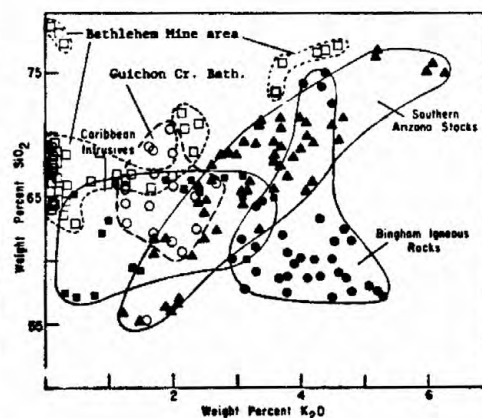
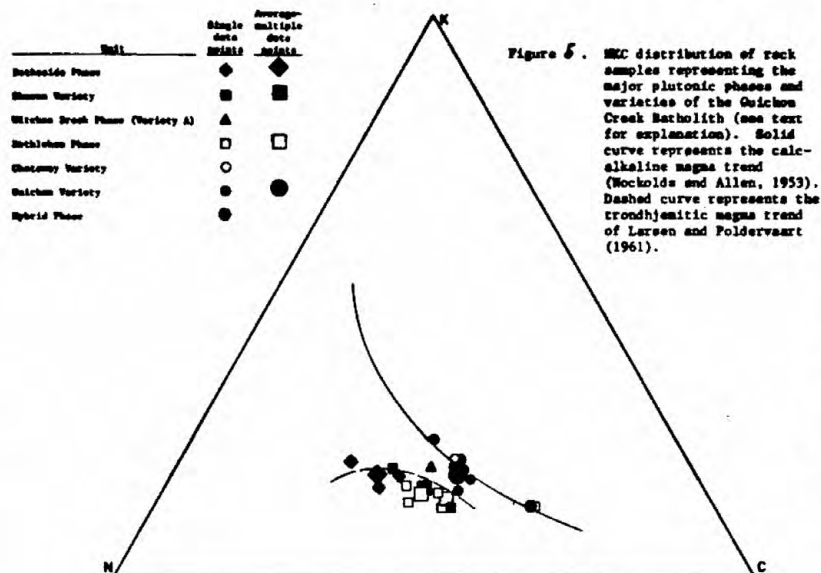


Figure 4. AFM distribution of rock samples representing the major plutonic phases and varieties of the Guichon Creek Batholith (see text for explanation). Solid curve represents the calc-alkaline magma trend (Nockolds and Allen, 1953).



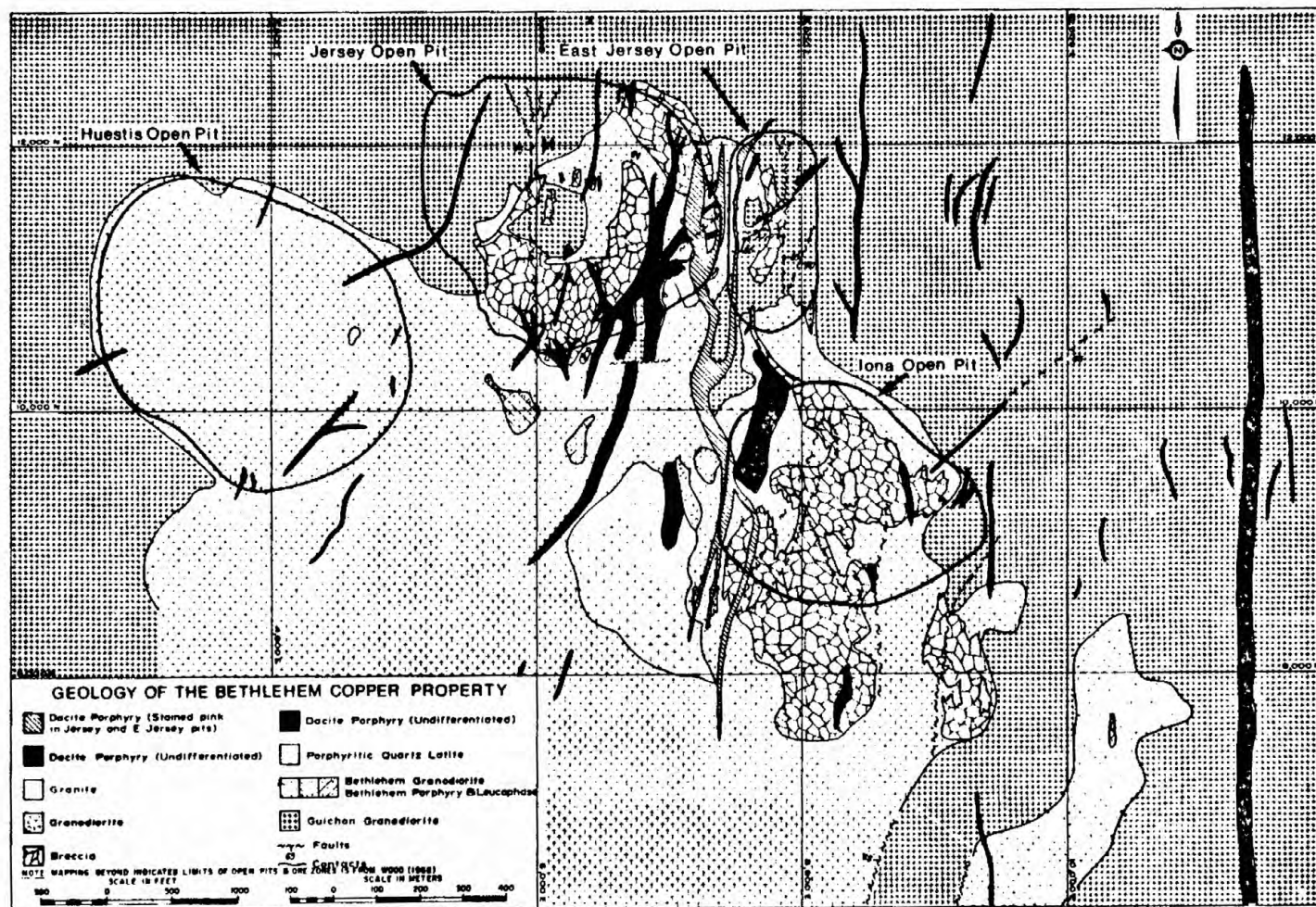


Figure 7. Geology of the Bethlehem Copper property. Mine coordinates in feet.

Structural Geology

Detailed examinations of over 1,600 faults, joints, and zones of closely spaced mineralized fractures were made in the Jersey ore body, and the results are illustrated on contoured Schmidt equal area projections (figs. 8-10) using a computerized technique recommended by Kamb (1959) that allows the extraction of information having statistical significance. As opposed to standard contouring methods employing a one percent counting circle, Kamb's method uses a variable circle size that is a function of the total number of data points and the level of significance chosen. As shown in the following illustrations, structures measured in the Jersey pit dominantly strike north-northeast and dip steeply west, with subordinate northeast-trending vertical attitudes also prominent.

A simplified regional stress pattern of wrench fault tectonics involving a regional, subhorizontal, right-lateral shear couple adequately explains the orientation, magnitude, and sense of displacement of preferentially oriented faults, joints, and mineralized fractures in the Bethlehem ore bodies, and of similarly oriented structures in the Lornex and Valley Copper deposits, and in the Guichon Creek batholith. A stress pattern such as this conforms to that expected from the oblique, northeast-directed plate convergence that is believed to have existed along the nearby coastal margin of Late Triassic British Columbia (e.g. Davis and others, 1978).

Many randomly oriented faults, joints, and fractures also occur in the Jersey ore body. However, the contouring technique utilized in the construction of the stereograms ignores these attitudes in preference for those having statistically preferred orientation. A large number of these randomly oriented structures probably resulted from dilational stresses attendant on intrusion of a rising, expanding batholith, which was periodically being enlarged by injections of melt from an underlying, differentiating magma chamber. Consequently, a tensional tectonic regime must have periodically existed, at least locally, in the upper parts of the pluton during its emplacement. These conditions would have been conducive to the intrusion of dikes, the formation of breccias, and volcanic venting, as well as deep circulation of hydrothermal fluids.

Mineralogy and Geochemistry of Hydrothermal Mineralization

Epigenetic minerals in the Bethlehem ore deposits occur in veins, veinlets, stringers, irregular blebs, and disseminations. Stringers and veinlets predominate. Veins typically contain variable proportions of specularite, quartz, carbonate, epidote, chalcopryite, bornite, pyrite, and tourmaline. They occur in a zone peripheral to the central parts of the Jersey and Huestis ore bodies, but, in contrast, they are more centrally located in the East Jersey and Iona ore zones.

Detailed studies of hydrothermal mineralization and alteration were performed in the Jersey deposit. Copper mineralization in this and the Huestis ore bodies are concentrically zoned; a central core of high-grade copper metallization is surrounded by a peripheral zone of progressively diminishing copper grade (fig. 11). At depth, the high-grade core splits into downward-extending roots. All rock types exposed within zones of minerali-

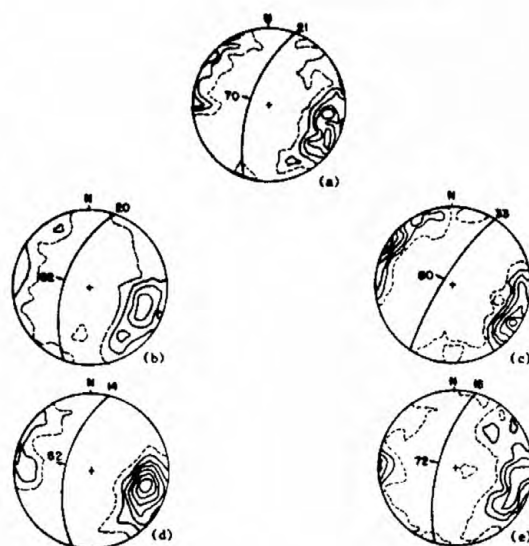


Figure 8. Contours of poles to fault planes in quadrants of the Jersey orebody.

- (a) All faults; $n = 630$
- (b) NW quadrant; $n = 145$
- (c) NE quadrant; $n = 160$
- (d) SW quadrant; $n = 145$
- (e) SE quadrant; $n = 182$

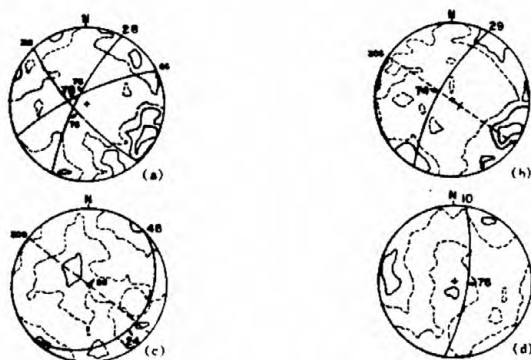


Figure 9. Contours of poles to joint planes in the Jersey orebody.

- (a) Primary joints; $n = 397$
- (b) Secondary joints; $n = 361$
- (c) Tertiary joints; $n = 251$
- (d) Quaternary joints; $n = 64$

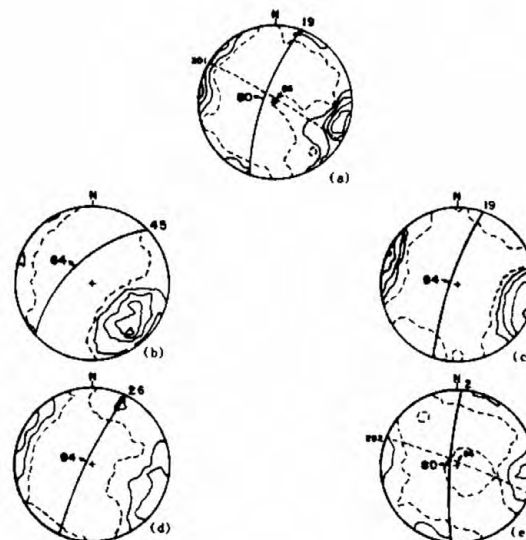


Figure 10. Contours of poles to mineralized fracture planes in quadrants of the Jersey orebody.

- (a) All mineralized fractures; $n = 144$; $ca = 2.72$; $e = 3.89$; $f = 1.95$
- (b) NW quadrant; $n = 41$
- (c) NE quadrant; $n = 28$
- (d) SW quadrant; $n = 40$
- (e) SE quadrant; $n = 35$

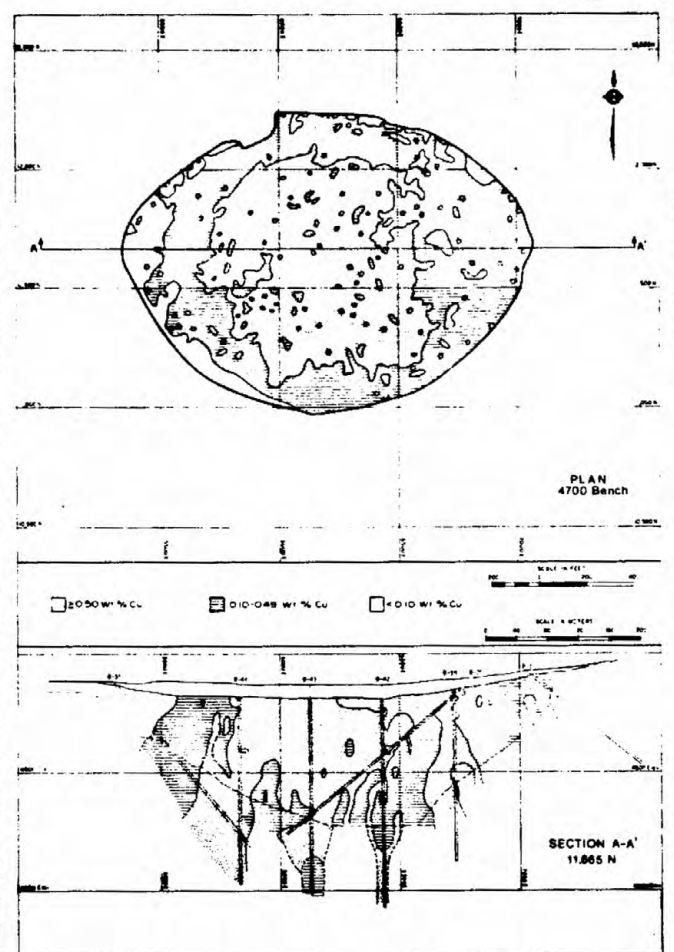


Figure 11. Copper distribution in the Jersey ore body. Mine coordinates in feet.

zation are mineralized. Copper metallization is commonly higher in grade and more uniformly distributed in the breccias, which probably reflects their higher initial porosity and their greater ease of fracturing relative to surrounding granitic host rocks. Faults have only a secondary influence on overall disposition of ore. Although they locally provided channelways for ore deposition and seepage of mineralizing fluids into the peripheral vein system, they do not appear to have been a primary control of copper metallization in the central part of the Jersey and Huestis ore bodies. In contrast, the East Jersey and Iona deposits are elongate northward, reflecting control by breccias and major shear zones.

Hypogene metallic minerals

The only common hypogene metallic minerals on the Bethlehem property are chalcopyrite, bornite, pyrite, specularite, molybdenite, and minor magnetite and chalcocite. There is a well-defined zonation of iron-bearing metallic minerals in the Jersey deposit (fig. 12). Specularite occurrences are chiefly vein controlled and are peripheral to those of pyrite. Together, the distributions of both these minerals form crudely concentric zones about a bornite-rich core. The outer zone of low-grade copper mineralization approximately coincides with the pyrite halo, and the high-grade core is largely contained within the bornite-rich central zone. Chalcopyrite is present throughout the deposit and is most abundant within the outer limits of the pyrite zone. The total sulfide content of the deposit averages less than about 2 volume percent. Pyrite is sparse, averaging less than about 1 volume percent in the halo zone. Reconnaissance work suggests similar zonal patterns in the Huestis ore body, and also that specularite is present peripherally to the Iona ore zone. Molybdenite traditionally is considered to be a relatively deep, centrally located mineral, which generally correlates with high copper grades. Although it is now being recovered from Iona ores (0.0125 weight percent Mo), it is usually sporadically distributed and commonly peripheral to the central parts of the other Bethlehem ore zones.

Hypogene nonmetallic alteration and vein minerals

Common hypogene nonmetallic minerals include white mica, chlorite, epidote, quartz, carbonate, kaolinite, montmorillonite, actinolite, zeolites, secondary biotite, secondary plagioclase, and prehnite. Smaller amounts of tourmaline, sphene, leucoxene, rutile, mixed-layer clays, secondary potassium feldspar, gypsum, and probably vermiculite are also present.

Zonal development of hydrothermal alteration in the Jersey ore body is similar to that described for most porphyry copper deposits. Distributions of epidote and secondary biotite form a roughly concentric zonal pattern, with epidote defining the zone of propylitic alteration peripheral to a central biotite-rich potassic alteration core (fig. 13). The intervening area, dominated by white mica and chlorite, is equivalent to a zone of phyllic alteration. Significant hydrothermal alteration is restricted to the immediate area of the ore body. Only zeolite mineralization, and the epidote zone and associated chlorite, extend beyond the limits of conspicuous copper sulfide mineralization.

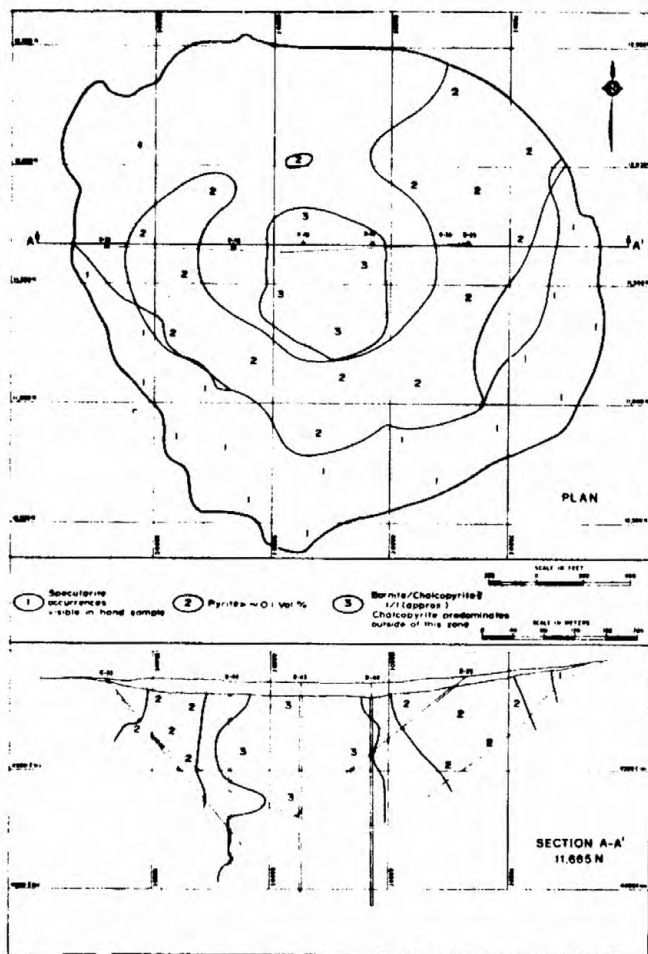


Figure 12. Specularite, pyrite, chalcopyrite, and bornite distribution in the Jersey ore body. Mine coordinates in feet.

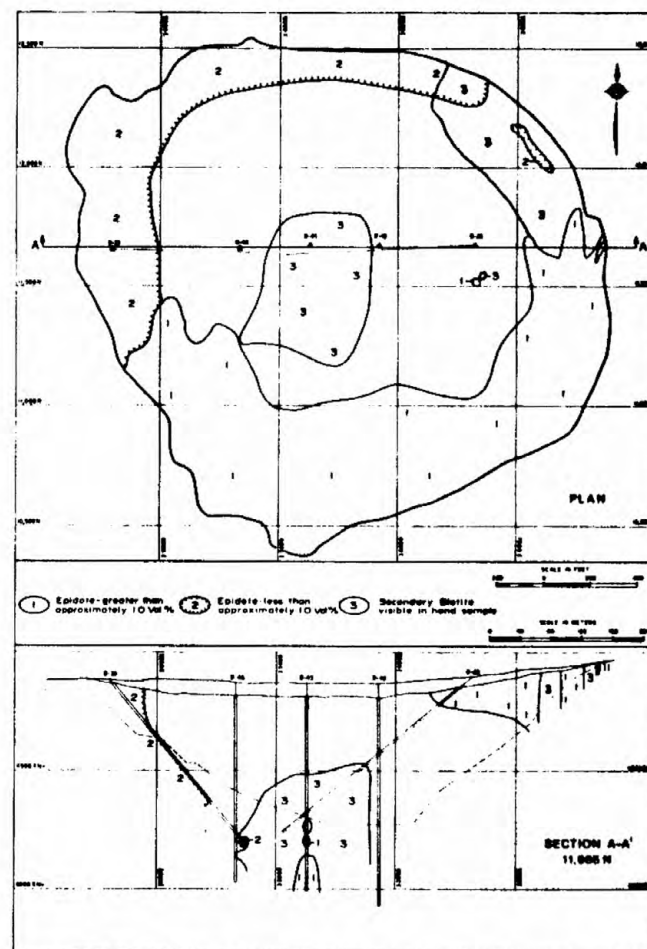


Figure 13. Epidote and secondary biotite distribution in the Jersey ore body. Mine coordinates in feet.

Epidote is most abundant at the outer margins of the Jersey and Huestis ore bodies, but is common in small amounts both peripheral to, and throughout, all of the Bethlehem ore bodies.

Abundances of montmorillonite and kaolinite, as determined semiquantitatively from X-ray diffraction studies, show no systematic or consistent changes between zones of alteration and metallization. However, these minerals predominate over the small quantities of white mica present in the epidote zone, which may therefore be considered a zone of mixed propylitic and poorly developed argillic alteration.

Significant quantities of white mica in the Jersey deposit roughly coincide with areas of greater than 0.1 weight percent copper, even though zonal distributions are not obvious. In the Iona zone, white mica is predominantly restricted to breccias and pervades host rocks only near areas of quartz flooding. Reconnaissance studies of the East Jersey ore body indicate that white mica alteration accompanies significant copper metallization.

Secondary biotite, with or without unusually minute quantities of secondary potassium feldspar, is the diagnostic indicator of potassic alteration in all of the Bethlehem deposits. In the Jersey ore body, secondary biotite is largely restricted to the lower parts of the bornite-rich core zone. However, minor amounts persist somewhat beyond the biotite zone where they are usually largely or completely replaced by chlorite. These remnant occurrences may record retrograde phyllic overprinting of an originally more extensive potassic zone. A slightly earlier episode of biotitization is associated with the breccia at the northeast edge of the Jersey pit. Secondary biotite is widespread in near-surface localities of the Iona breccias, but is only a minor component of rocks in the East Jersey ore body. Microscopic traces of secondary biotite were identified in a few samples from the Huestis pit.

Actinolitic to tremolitic amphiboles, prehnite, and zeolites are unusually abundant at Bethlehem. Actinolitic to tremolitic amphiboles typically occur in fractures and are especially abundant alteration products of hornblende, some biotite, and locally plagioclase. Prehnite, in amounts up to 4 percent, is a common, widely dispersed hydrothermal mineral in the Bethlehem ore zones. It typically forms bladed aggregates replacing plagioclase, but is most abundant in stringers, and as disseminated intergrowths with chalcopyrite and bornite. The calcium- and sodium-rich zeolites laumontite, stilbite, heulandite, and chabazite are the youngest expressions of hydrothermal activity and are ubiquitous throughout all of the Bethlehem ore bodies. Numerous veinlets of pale pink to orangish laumontite that generally contain smaller amounts of carbonate, stilbite, locally heulandite, and rare epidote crosscut all rock types and hypogene mineralization. However, chalcopyrite and traces of bornite are rarely overgrown on zeolite crystals indicating that zeolite and copper sulfide deposition overlapped slightly in time.

Actinolite and late-stage zeolites are not commonly recognized in porphyry copper deposits of continental derivation (see Lowell and Guilbert, 1970; W. J. Moore and S. C. Creasey, oral commun., 1978), but are prominent among vein and alteration mineralogies at Bethlehem, J. A. (McMillan, 1976a), and Highmont (Reed and Jambor, 1976) in Highland Valley; as well as at other

island-arc porphyry copper deposits (e.g. Cox and others, 1973; Chivas, 1978; Ford, 1978; Gustafson, 1978; Kosaka and Wakita, 1978; Mason, 1978; Mason and McDonald, 1978).

Paragenesis

Mineralization is somewhat arbitrarily separated into five depositional stages relative to the main period of sulfide precipitation (fig. 14). The early stage is defined by the crystallization of magnetite and much of the observed tourmaline, perhaps in a partially transitional magmatohydrothermal environment. During the early main stage the important hydrothermal alteration assemblages began to form. Main-stage mineralization is dominated by the deposition of sulfide minerals, specularite, and massive, white to rarely colorless quartz. Coarsely cleavable, massive to euhedral, whitish carbonate, and pale amber to clear, commonly euhedral (dogtooth) carbonate were widely deposited during the late main-stage mineralization event. Hypogene chalcocite is restricted to this period and usually occurs associated with, and slightly later than, the whitish carbonate. Zeolites and closely associated whitish carbonate, both of probable hot springs origin, are the dominant products of late-stage mineralization.

Alteration and minor element geochemistry

There seems to have been little significant change in the amounts of major oxides initially present in the plutonic host rocks of the ore deposits. Except for obvious additions of sulfur, copper, molybdenum, and probably silica, and the removal of potash, hydrothermal circulation has mainly acted to redistribute preexisting chemical elements between central and peripheral zones of alteration and mineralization (fig. 15). Potash is depleted in most hydrothermally altered rocks, being lost in the zones of propylitic alteration, and lost rather than gained in the phyllic and potassic zones. This is primarily a reflection of the marked instability of primary potassium feldspar in all of the zones of hydrothermal alteration at Bethlehem. It is typically completely to partially replaced by mixtures of secondary plagioclase, white mica, montmorillonite, kaolinite, and some quartz. Potassium liberated from altered, primary potassium feldspar and biotite has been partially retained in white mica in the phyllic zone, and by white mica, secondary biotite, and rare secondary potassium feldspar in the potassic zone. Propylitized rocks contain little of these minerals and therefore are the most depleted in K_2O .

The consistently low trace abundances of lead, zinc, and silver measured in 50 samples, particularly between "unaltered" and equivalent altered and mineralized lithologies, further emphasize the simplicity of the metallic mineral assemblage. Lead (<50 ppm (parts per million)) is usually present in amounts near or below the 10 ppm limit of detection. Zinc contents (5-45 ppm) typically range between 15 and 30 ppm. Silver abundances (1-4 ppm) are commonly at or below 1 ppm. The gold content of Bethlehem ores is estimated from production figures to be in or slightly above the range 0.008 to 0.014 ppm. These low minor element analyses are consistent with the absence of significant lead-zinc-silver-gold deposits fringing porphyry ore in the Highland Valley, or occurring in or near the contact aureole of the batholith.

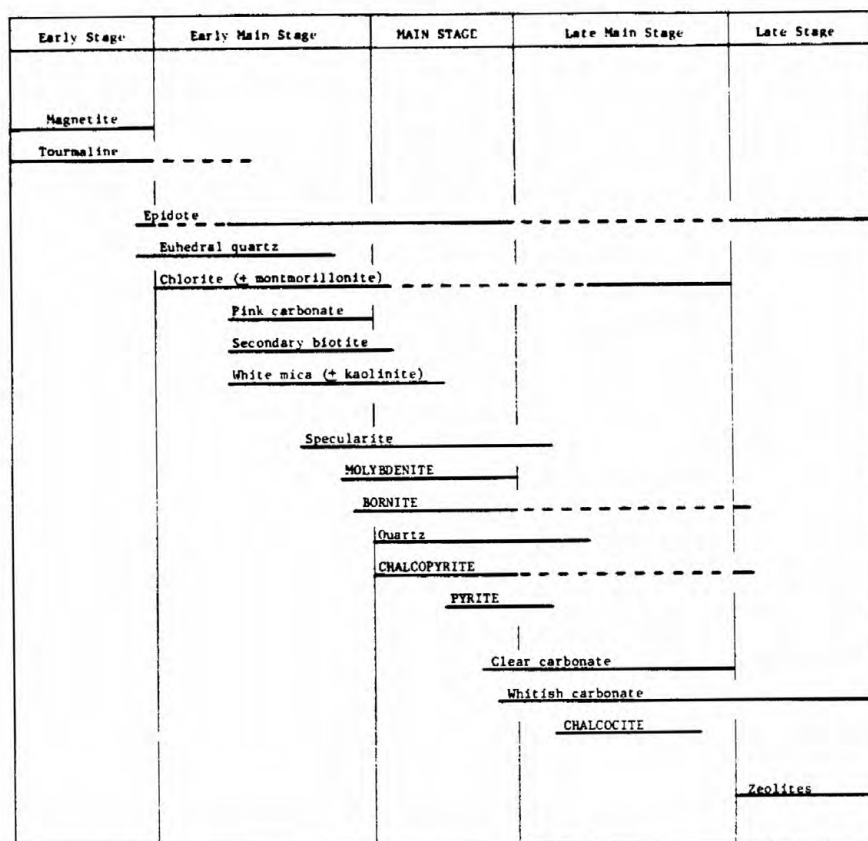


Figure 14. Relative paragenetic sequence of mineral deposition in the Jersey ore body.

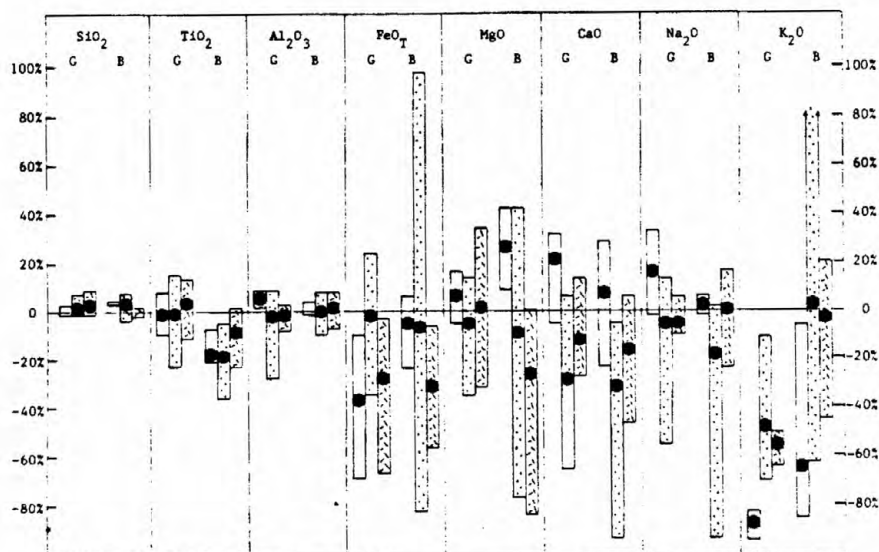


Figure 15. Gains and losses of major oxide components (in percent) in altered and mineralized Guichon and Bethlehem granodiorites from Bethlehem mine. Bars represent ranges, and black dots are averages. Unpatterned, stippled, and herringbone bars are for rocks containing propylitic-argillic, phyllic, and potassic alteration assemblages, respectively. Within each major oxide column, bars are grouped by rock type; G = Guichon granodiorite, B = Bethlehem granodiorite.

Summary of Characteristics

The Bethlehem orebodies generally possess geologic, mineralogic, and geochemical features that are similar to those described for other porphyry copper-molybdenum deposits of continental western North America (e.g. Creasey, 1959, 1966, 1972; Burnham, 1962; Titley and Hicks, 1966; Meyer and Hemley, 1967; Sutherland Brown, 1966, 1969, 1976; Sutherland Brown and others, 1971; Lowell and Guilbert, 1970; Rose, 1970; James, 1971; and DeGeoffroy and Wignall, 1972), and especially in volcanic island-arc terranes (e.g. Cox and others, 1973; Field and others, 1974; Kesler and others, 1975; Titley, 1975; Field and others, 1975; Kesler and others, 1977; and Econ. Geology, 1978). However, in detail the Bethlehem deposits, especially the Jersey orebody, differ in the degree to which many of these features are developed, and have serious implications for porphyry copper exploration in island-arc terranes, especially those in western North America. Distinctive characteristics include: (1) temporal and spatial coincidence with continental margin volcanic island-arc magmatism; (2) an intrabatholith location; (3) occurrence in a relatively silicic, low potash, calc-alkaline to calcic pluton displaying progressive sodium enrichment typical of a trondhjemitic magma differentiation trend; (4) intimate association in time and space with silicic, highly potash deficient dacite porphyries; (5) relatively old mineralization (200 m.y.); (6) dominance of fracture-controlled copper mineralization; (7) formation in a demonstrable wrench fault tectonic setting, possibly relatable to regional plate-margin tectonics; (8) mineralogical simplicity of the metallic constituents; (9) absence of significant lead, zinc, and silver associations; (10) low trace abundances of lead, zinc, silver, and gold, even in high-grade ore; (11) well-defined zonation of iron-bearing metallic minerals; (12) low total sulfide content (average <2 percent) and sparse pyrite (<1 percent in the halo zone); (13) high bornite:chalcopyrite ratios (>1); (14) molybdenite peripheral to the central parts of the ore zones; (15) association of chalcopyrite and bornite with epidote; (16) restriction of significant hydrothermal alteration to the ore zones; (17) scarcity of potassium feldspar alteration; (18) general instability of primary potassium feldspar throughout the deposits; (19) loss of K_2O in the propylitic alteration zone, and loss rather than gain of K_2O in the phyllic and potassic zones; (20) abundance of fault and fracture zones containing abundant greenish-colored white mica that may be comprised of appreciable ferric iron; (21) prominent occurrences of actinolitic to tremolitic amphiboles as both alteration and vein minerals; (22) widespread presence of prehnite intimately associated and intergrown with copper sulfides; (23) ubiquitous occurrences of largely postmetallization zeolites, especially laumontite; and (24) absence of significant supergene enrichment.

REFERENCES

- Ager, C. A., McMillan, W. J., and Ulrych, T. J., 1972, Gravity, magnetics, and geology of the Guichon Creek batholith: British Columbia Department of Mines and Petroleum Resources Bulletin 62, 17 p.
- Barr, D. A., Fox, P. E., Northcote, K. E., and Preto, V. A., 1976, The alkaline suite porphyry deposits--a summary, in Sutherland Brown, A., ed., Porphyry deposits of the Canadian Cordillera: Canadian Institute of Mining and Metallurgy Special Volume 15, p. 359-367.
- Briskey, J. A., and Bellamy, J. R., 1976, Bethlehem Copper's Jersey, East Jersey, Huestis, and Iona deposits, in Sutherland Brown, A., ed., Porphyry deposits of the Canadian Cordillera: Canadian Institute of Mining and Metallurgy Special Volume 15, p. 105-119.
- Burnham, C. W., 1962, Facies and types of hydrothermal alteration: Economic Geology, v. 57, p. 768-784.
- Carr, J. M., 1962, Geology of the Princeton, Merritt, Kamloops area of southern B.C.: Western Miner, v. 35, February, p. 46-49.
- Chivas, A. R., 1978, Porphyry copper mineralization at the Koluola igneous complex, Guadalcanal, Solomon Islands: Economic Geology, v. 73, p. 645-677.
- Christopher, P. A., and Carter, N. C., 1976, Metallogeny and metallogenic epochs for porphyry mineral deposits in the Canadian Cordillera, in Sutherland Brown, A., ed., Porphyry deposits of the Canadian Cordillera: Canadian Institute of Mining and Metallurgy Special Volume 15, p. 64-71.
- Cox, D. P., Larson, R. R., and Tripp, R. B., 1973, Hydrothermal alteration in Puerto Rican porphyry copper deposits: Economic Geology, v. 68, p. 1329-1334.
- Creasey, S. C., 1959, Some phase relations in the hydrothermally altered rocks of porphyry copper deposits: Economic Geology, v. 54, no. 3, p. 351-373.
- _____, 1966, Hydrothermal alteration, in Titley, S. R., and Hicks, C. L., eds., Geology of the porphyry copper deposits, southwest North America: The University of Arizona Press Publication, p. 51-73.
- _____, 1972, Hydrothermal alteration of silicate rocks--general principles, in Fairbridge, R. W., ed., The encyclopedia of geochemistry and environmental sciences: Stroudsburg, Van Nostrand Reinhold Company, p. 561-571.
- _____, 1977, Intrusives associated with porphyry copper deposits: Geological Society of Malaysia Bulletin 9, p. 51-66.
- Davis, G. A., Monger, J. W. H., and Burchfiel, B. C., 1978, Mesozoic construction of the Cordilleran "collage," central British Columbia to central California, in Howell, D. G., and McDougall, K. A., eds., Mesozoic paleogeography of the western United States: Society of Economic Paleontologists and Mineralogists, Pacific Coast Paleogeography Symposium 2, p. 1-32.
- DeGeoffroy, J., and Wignall, T. K., 1972, A statistical study of geological characteristics of porphyry-copper-molybdenum deposits in the Cordilleran belt: Application to the rating of porphyry prospects: Economic Geology, v. 67, p. 656-668.
- Duffell, S., and McTaggart, K. C., 1951, Ashcroft map area, British Columbia: Geological Survey of Canada Memoir 262, 122 p.
- Economic Geology, 1978, Porphyry copper deposits of the southwestern Pacific Islands and Australia: Lancaster, Pennsylvania, The Economic Geology Publishing Company, v. 73, p. 597-981.

- Field, C. W., Briskey, J. A., Henricksen, T. A., Jones, M. B., Schmuck, R. A., and Bruce, W. R., 1975, Chemical trends in Mesozoic plutons associated with porphyry-type metallization of the Pacific northwest: American Institute of Mining, Metallurgical, and Petroleum Engineers, Society of Mining Engineers, preprint no. 75-L-359, 25 p.
- Field, C. W., Jones, M. B., and Bruce, W. R., 1974 Porphyry copper-molybdenum deposits of the Pacific northwest: Transactions of the American Institute of Mining, Metallurgical, and Petroleum Engineers, v. 256, p. 9-22.
- Ford, J. H., 1978, A chemical study of alteration at the Panguna porphyry copper deposit, Bouganville, Papua, New Guinea: Economic Geology, v. 73, p. 703-720.
- Gustafson, L. B., 1978, Some major factors of porphyry copper genesis: Economic Geology, v. 73, p. 600-607.
- Hine, R., and Mason, D. R., 1978, Intrusive rocks associated with porphyry copper mineralization, New Britain, Papua, New Guinea, in Gustafson, L. B., and others, eds., Porphyry copper deposits of the southwestern Pacific islands and Australia: Economic Geology, v. 73, no. 5, p. 749-760.
- James, A. H., 1971, Hypothetical diagrams of several porphyry copper deposits: Economic Geology, v. 66, p. 43-47.
- Kamb, W. B., 1959, Ice petrofabric observations from Blue Glacier, Washington, in relation to theory and experiment: Journal of Geophysical Research, v. 64, p. 1891-1909.
- Kesler, S. E., Jones, L. M., and Walker, R. L., 1975, Intrusive rocks associated with porphyry copper mineralization in island arc areas: Economic Geology, v. 70, p. 515-526.
- Kesler, S. E., Sutter, J. F., Issigonis, M. J., Jones, L. M., and Walker, R. L., 1977, Evolution of porphyry copper mineralization in an oceanic island arc: Panama: Economic Geology, v. 72, p. 1142-1153.
- Kosaka, H., and Wakita, K., 1978, Some geologic features of the Mamut porphyry copper deposit, Saboh, Malaysia: Economic Geology, v. 73, p. 618-627.
- Larsen, L. H., and Poldervaart, A., 1961, Petrologic study of Bald Rock Batholith, near Bidwell Bar, California: Geological Society of America Bulletin, v. 72, p. 69-92.
- Lowell, J. D., and Guilbert, J. M., 1970, Lateral and vertical alteration-mineralization zoning in porphyry ore deposits: Economic Geology, v. 65, p. 373-408.
- Mason, D. R., 1978, Compositional variations in ferromagnesian minerals from porphyry copper-generating and barren intrusions of the western highlands, Papua, New Guinea: Economic Geology, v. 73, p. 878-890.
- Mason, D. R., and McDonald, J. A., 1978, Intrusive rocks and porphyry copper occurrences of the Papua New Guinea-Solomon Islands region: A reconnaissance study: Economic Geology, v. 73, p. 857-877.
- McMillan, W. J., 1976, Geology and genesis of the Highland Valley ore deposits and the Guichon Creek Batholith, in Sutherland Brown, A., ed., Porphyry deposits of the Canadian Cordillera: Canadian Institute of Mining and Metallurgy Special Volume 15, p. 85-104.
- _____, 1976a, J.A., in Sutherland Brown, A., ed., Porphyry deposits of the Canadian Cordillera: Canadian Institute of Mining and Metallurgy Special Volume 15, p. 144-162.
- _____, 1978, Notes and legend to accompany preliminary map no. 30: Geology of the Guichon Creek batholith: British Columbia Ministry of Mines and Petroleum Resources, 17 p.

- Meyer, Charles, and Hemley, J. J., 1967, Wall rock alteration, in Barnes, H. L., ed., *Geochemistry of hydrothermal ore deposits*: New York, Holt, Rinehart, and Winston, Inc., p. 166-235.
- Nockolds, S. R., and Allen, R., 1953, The geochemistry of some igneous rock series: *Geochimica et Cosmochimica Acta*, v. 4, p. 105-142.
- Northcote, K. E., 1969, Geology and geochronology of the Guichon Creek Batholith: British Columbia Department of Mines and Petroleum Resources Bulletin, no. 56, 73 p.
- Reed, A. J., and Jambor, J. L., 1976, Highmont: Linearly zoned copper-molybdenum porphyry deposits and their significance in the genesis of the Highland Valley ores, in Sutherland Brown, A., ed., *Porphyry deposits of the Canadian Cordillera*: Canadian Institute of Mining and Metallurgy Special Volume 15, p. 163-381.
- Roddick, J. A., and Hutchinson, W. W., 1974, Setting of the Coast Plutonic Complex, British Columbia: *Pacific Geology*, v. 8, p. 91-108.
- Rose, A. W., 1970, Zonal relations of wallrock alteration and sulfide distribution at porphyry copper deposits: *Economic Geology*, v. 65, p. 920-936.
- Sutherland Brown, A. S., 1966, Tectonic history of the Insular belt of British Columbia, in Gunning, H. C., ed., *Tectonic history and mineral deposits of the western Cordillera*: Canadian Institute of Mining and Metallurgy, Special Volume 8, p. 83-100.
- _____, 1969, Mineralization in British Columbia and the copper and molybdenum deposits: *Transactions of the Canadian Institute of Mining and Metallurgy and of the Mining Society of Nova Scotia*, v. 72, p. 1-15; *Canadian Institute of Mining and Metallurgy Bulletin*, v. 62, no. 681, p. 26-40.
- _____, ed., 1976, *Porphyry deposits of the Canadian Cordillera*: Canadian Institute of Mining and Metallurgy Special Volume 15, 510 p.
- Sutherland Brown, A. S., Cathro, R. J., Panteleyev, A., and Ney, C. S., 1971, *Metallogeny of the Canadian Cordillera*: Canadian Institute of Mining and Metallurgy Bulletin, v. 64, p. 37-61.
- Titely, S. R., 1975, Geological characteristics and environment of some porphyry copper occurrences in the southwestern Pacific: *Economic Geology*, v. 70, p. 499-514.
- Titely, S. R., and Hicks, C. L., eds., 1966, *Geology of the porphyry copper deposits, southwestern North America*: University of Arizona Press, Tucson, Ariz., 287 p.

The Island copper porphyry copper-molybdenum deposit,
Vancouver Island, British Columbia

P. L. Fahey, University of Washington

THE ISLAND COPPER PORPHYRY COPPER-MOLYBDENUM DEPOSIT,
VANCOUVER ISLAND, BRITISH COLUMBIA

FAHEY, Patrick L., Department of Geological Sciences,
University of Washington, Seattle, Washington
98195

The Island Copper deposit occurs in hornfelsed andesites and is related to a northwest-trending, granodiorite porphyry dike of the Jurassic Island Intrusions. The northwesterly-trending End fault cuts the deposit on the south and may have controlled emplacement of the dike. It and other faults probably were active during and after alteration and mineralization.

The dike has two distinct phases. Massive porphyry is relatively unfractured, has few xenoliths, and commonly is intensely brecciated, mineralized, and altered. Breccia porphyry probably was an autobrecciated intrusive margin, rebrecciated by synformational faults and fractures. The ore zones are in Breccia porphyry and adjacent andesite.

Early stage alteration has quartz veins with silicified envelopes, and small qtz-cpy-py veinlets that contain most of the copper mineralization. Middle stage qtz-py-mo-cpy veins caused extensive hydrolytic alteration. A pervasive cap of middle stage pyrophyllite-sericite-dumortierite alteration occurs on top of the dike in Breccia porphyry. Below the cap, middle stage alteration is confined to veins. Hydrothermal biotite or feldspar have not been found at Island Copper; middle stage alteration may have obliterated them, or they may be present at depth. Late stage veins contain ferroan dolomite, or carbonate, laumontite, pyrite, and minor galena and sphalerite.

(Courtesy of the Geological Society of America, 1980)

Lead isotope models for the genesis of carbonate-hosted
Zn-Pb, shale-hosted Ba-Zn-Pb, and silver-rich deposits in
the northern Canadian Cordillera

C. I. Godwin, University of British Columbia
A. J. Sinclair, University of British Columbia
B. D. Ryan, University of British Columbia

ABSTRACT

Isotope analyses of galena from syngenetic barite-zinc-lead and epigenetic Zn-Pb and Ag-rich deposits from northern Canadian Cordillera are subdivided into four distinct fields and lines on $^{207}\text{Pb}/^{204}\text{Pb}$ and $^{208}\text{Pb}/^{204}\text{Pb}$ versus $^{206}\text{Pb}/^{204}\text{Pb}$ plots. These lines used in conjunction with constraints imposed by stratigraphy, by K-Ar isotopic dates, and by minor element analyses in sphalerite, define three metallogenic events of about 0.52 b.y., 0.37 b.y., and 0.09 b.y., which are summarized as follows:

1. "Old Carbonate" hosted Zn-Pb deposits formed in the Lower Cambrian (about 0.52 b.y.) define closely a maximum source age of 1.9 b.y. This is the first lead isotopic indication of Hudsonian basement in the northern Canadian Cordillera. Spatial association of these deposits to unconformities and generation of lead in an upper crustal but generally uranium-poor environment supports a karstic model for their origin.
2. Shale-hosted Ba-Zn-Pb mineralization from Upper Devonian to Lower Mississippian (about 0.37 b.y.) rocks is indistinguishable in lead isotope composition from the majority of post Lower Ordovician to Devonian "Young Carbonate" hosted zinc-lead deposits. These deposits formed near 0.37 b.y., from brines dewatered from the Selwyn shale basin, where solutions were guided by faults, either within the basin (e.g. shale-hosted Ba-Zn-Pb deposits formed along grabens near hinge lines close to the margin of the basin), or peripheral to and away from the basin (e.g. carbonate-hosted Zn-Pb deposits). Lead for these deposits evolved in an upper crustal, uranium-rich, carbonaceous, shale basin environment from which highly radiogenic lead was extracted.
3. Although most Ag-rich deposits occur as veins not directly associated with plutons, some veins occur within, or are directly associated with, Cretaceous plutons, indicating a general age of mineralization of 0.09 b.y. An apparent Hudsonian source is indicated. Highly radiogenic leads, characteristic of the silver deposits, were probably formed by preferential leaching of lead from uranium-rich minerals.

INTRODUCTION

Lead isotope data have been used effectively in the past to define details of metallogenic evolution for mineral deposits on district and regional scales (e.g. LeCouteur, 1973; Zartman, 1974). Depending on the nature and extent of independent geological controls, lead isotopic data can provide a variety of information on mineral deposits, such as: 1) age of mineralization, 2) the definition of genetically related groups of lead-bearing deposits, 3) details of the history of evolution of lead isotopic compositions, 4) Th, U, and Pb attributes of some of the source rocks of the radiogenic component of common lead. Invariably, certain assumptions must be made in the interpretation of lead isotope data, but the uncertainty of these assumptions can be minimized where adequate geological data exist. In particular, it is useful to have independent evidence for ages of mineralization and/or ages of source rocks of the radiogenic component of ore leads.

This project was designed to provide further insight into metallogenic models for:

1. epigenetic, stratabound, Zn-Pb deposits in carbonate rocks, of Helikian to Devonian age, extending from the Ogilvie Fold Belt in central-western Yukon Territory to the Eastern Fold Belt in British Columbia,
 2. stratiform, shale-hosted, Ba-Zn-Pb deposits of Upper Devonian-Mississippian age in the Selwyn Basin, and
 3. epigenetic, Ag-rich deposits in the northern Canadian Cordillera which are dominantly of vein type but include skarn deposits, porphyry deposits, and replacement deposits.
- Lead isotope analyses, from 73 deposits classified as above and located in Figure 1, are in Tables 1, 2, 3, and 4. All analyses were done in the Geology-Geophysics Laboratory, The University of British Columbia.

ANALYTICAL TECHNIQUES

Lead in galena from the samples was dissolved using HCl. Purified lead as obtained using anion columns and anodic electro-deposition. Samples were analysed using single filament silica gel techniques on a 90 degree, 12 inch mass spectrometer. In run precision, reported in the tables as percent standard deviation within the brackets following mean isotopic ratios, is generally better than 0.1 percent at one standard deviation. Multiple analyses of Broken Hill No. 1 standard shows that the reproducibility of sample analyses is about 0.1 percent at one standard deviation. All data in the tables have been normalized to the Broken Hill No. 1 standard; normalizing procedures assumed the following composition for this standard: $^{207}\text{Pb}/^{206}\text{Pb} = 16.003$, $^{208}\text{Pb}/^{206}\text{Pb} = 15.389$, $^{208}\text{Pb}/^{207}\text{Pb} = 35.657$.

Figure 1: Location of lead isotope analyses in Tables 1, 2, 3, and 4. Deposits located with: 1) circles are "Old Carbonate" hosted, 2) squares are "Young Carbonate" hosted, and 3) triangles are silver rich. Deposits numbered in the 10000 range are in Y.T., 20000 range are in N.W.T.; deposits marked by 2 letters are from B.C. Thick solid lines define tectonic belts where: CPC = Coast Plutonic Complex, YCC = Yukon Crystalline Complex, I = Intermontane Belt, O = Omineca Crystalline Belt, SB = Selwyn Basin, OFB = Ogilvie Fold Belt, WFB = Wernecke Fold Belt, RFB = Richardson Fold Belt, MPB = Mackenzie Fold Belt, and EFB = Eastern Fold Belt. Plutonic rocks are stippled; dotted line defines approximate northern and eastern boundary of plutonic activity.

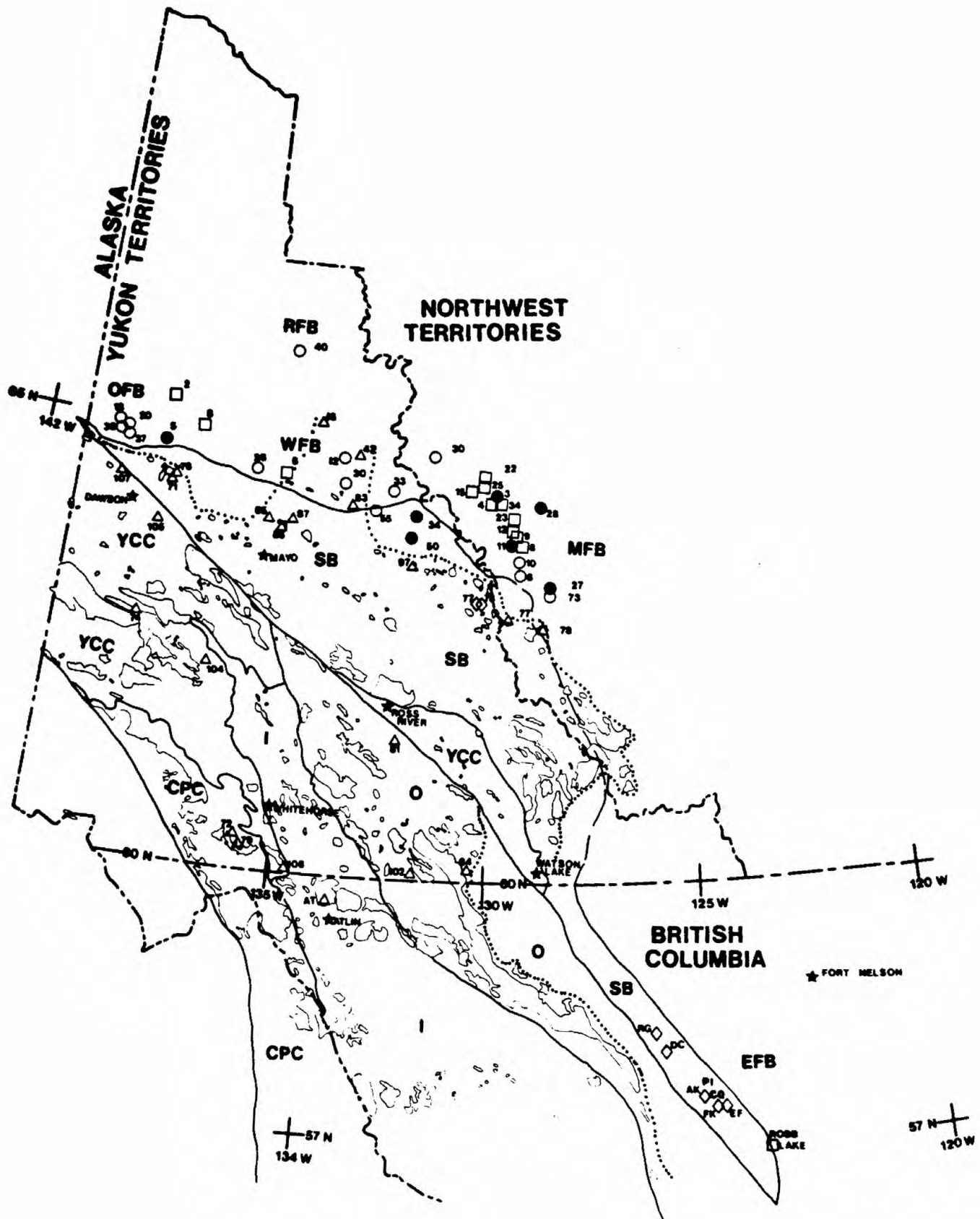


TABLE 1: LEAD ISOTOPE ANALYSES¹ ON GALENA² FROM MINERAL DEPOSITS

Deposits Hosted in "Old Carbonate" Rocks, Eastern Fold Belt, Y.T.

Sample Number	Deposit Name ³	Map Name	Lat. ^o North	Long. ^o West	Lead Isotope Data (Relative 1 σ Error as %)			Remarks
					²⁰⁶ Pb/ ²⁰⁴ Pb	²⁰⁷ Pb/ ²⁰⁴ Pb	²⁰⁸ Pb/ ²⁰⁴ Pb	
10005-001	Kivi ²	05	64.75	138.75	19.205 (.05)	15.728 (.10)	39.565 (.05)	Hel DOLN
10010-017	Economic	10	64.33	131.22	18.425 (.08)	15.631 (.08)	38.351 (.12)	L-Cam DOLN
10010-020	Economic	10	64.33	131.22	18.463 (.07)	15.728 (.07)	38.549 (.08)	
10010-278	Economic	10	64.33	131.22	18.432 (.08)	15.649	38.208 (.09)	
10010-045	Economic	10	64.33	131.22	18.426 (.07)	15.716 (.09)	38.647 (.09)	
	Average for Economic ¹	10	64.33	131.22	[18.437 (.08)]	[15.680 (.08)]	[38.459 (.09)]	
10012-100	Gillespie ¹	12	64.77	133.93	16.532 (.06)	15.451 (.08)	36.188 (.11)	Had DOLN
10013-002	UG ¹	13	64.87	140.03	17.096 (.07)	15.542 (.06)	36.729 (.10)	Hel DOLN
10020-100	Tart ¹	20	64.83	139.83	16.805 (.08)	15.446 (.10)	36.410 (.07)	Hel DOLN
10026-001	Vug ¹	26	64.57	136.28	16.283 (.07)	15.417 (.07)	36.019 (.09)	Hel DOLN
10030-001	Showing ¹	30	64.49	133.83	18.289 (.08)	15.681 (.06)	38.670 (.08)	Hel DOLN
10033-009	Goz ¹	33	64.43	132.55	18.469 (.06)	15.683 (.10)	38.681 (.08)	L-Cam DOLN
10034-009	Birkeland	34	64.15	131.92	18.825 (.02)	15.708 (.05)	38.524 (.07)	Had DOLN
10034-010	Birkeland	34	64.15	131.92	18.790 (.05)	15.706 (.06)	38.451 (.08)	
	Average for Birkeland ²	34	64.15	131.92	[18.808 (.04)]	[15.707 (.06)]	[38.488 (.08)]	
10037-048	Oz ¹	37	64.75	139.75	16.274 (.10)	15.411 (.09)	35.907 (.09)	Hel DOLN
10038-016	Monster	38	64.82	139.97	16.264 (.05)	15.416 (.06)	35.030 (.11)	Prot DOLN
10038-100	Monster	38	64.82	139.97	16.857 (.03)	15.478 (.05)	36.537 (.08)	
	Average for Monster ¹	38	64.82	139.97	[16.560 (.04)]	[15.447 (.06)]	[35.814 (.10)]	
10040-003	Tuku ¹	40	65.97	135.42	18.071 (.11)	15.674 (.04)	38.321 (.06)	L-Cam LINS
10050-001	Odd ²	50	63.91	132.00	18.813 (.09)	15.696 (.07)	38.476 (.03)	Had DOLN
10055-100	Tara ¹	55	64.20	132.98	18.817 (.09)	15.748 (.09)	38.571 (.09)	L-Cam
20003-002	Palm ²	03	64.40	129.80	18.879 (.08)	15.695 (.08)	38.771 (.04)	L-Cam DOLN
20006-001	Pau ¹	06	63.52	129.12	18.758 (.09)	15.733 (.09)	39.902 (.10)	L-Cam DOLN
20010-002	Emily ¹	10	63.67	129.12	18.695 (.05)	15.761 (.06)	39.923 (.07)	L-Cam DOLN
20011-001	Lan ²	11	63.85	129.35	18.800 (.05)	15.692 (.06)	38.807 (.07)	L-Cam DOLN
20027-001	Climax ²	27	63.35	128.38	19.660 (.05)	15.770 (.08)	39.924 (.06)	Had DOLN
20028-001	Vic ²	28	64.30	128.62	18.420 (.10)	15.629 (.08)	38.002 (.07)	Hel DOLN
20030-001	Zie ¹	30	64.87	131.48	18.510 (.07)	15.687 (.09)	38.267 (.05)	L-Cam DOLN

1. All analyses done in the Geology - Geophysics Laboratory, The University of British Columbia.

2. All analyses done on galena samples unless otherwise noted.

3. Data used in determining arith. average and slope of best fit line for "Old Carbonate" are marked with a superscript "1". Data used with "Young Carbonate" in Table 2 are marked with a superscript "2".

TABLE 2: LEAD ISOTOPE ANALYSES¹ ON GALENA² FROM BIFERAL DEPOSITS

Deposits Hosted in "Young Carbonate" Rocks, Carbonate Fold Belts, Y.T., B.C., and N.W.T.

Sample Number	Deposit Name ³	Map Name	Lat. ^o North	Long. ^o West	Lead Isotope Data (Relative 1 σ Error as %)			Remarks
					²⁰⁶ Pb/ ²⁰⁴ Pb	²⁰⁷ Pb/ ²⁰⁴ Pb	²⁰⁸ Pb/ ²⁰⁴ Pb	
G79KN-001	Kicking Horse ²	KN	51.34	116.34	18.558 (.08)	15.697 (.11)	38.857 (.11)	N.Can DOLM
G79NZ-001	Nonarch ²	NZ	51.34	116.34	18.557 (.07)	15.629 (.04)	38.756 (.15)	N.Can DOLM
G79RB-001	Robb Lake	RB	57.00	123.75	20.161 (.09)	15.872 (.09)	41.049 (.06)	
G79RB-002	Robb Lake	RB	57.00	123.75	20.327 (.07)	15.856 (.07)	41.017 (.11)	
G79RB-003	Robb Lake	RU	57.00	123.75	20.310 (.04)	15.851 (.07)	40.993 (.08)	
G79RB-004	Robb Lake	RB	57.00	123.75	20.247 (.04)	15.858 (.05)	41.139 (.01)	
Average for Robb Lake ²		RB	57.00	123.75	[20.261 (.06)]	[15.859 (.07)]	[41.050 (.06)]	
10002-002	Bilbo ²	02	65.25	138.67	22.825 (.03)	16.047 (.07)	42.715 (.05)	L.Pal DOLM
10006-001	Newt ²	06	64.53	135.47	20.362 (.11)	15.848 (.03)	42.560 (.04)	Ord DOLM
10008-002	Hot ²	08	64.98	137.77	20.468 (.14)	15.856 (.07)	39.667 (.10)	Ord DOLM
20004-002	Jude ²	04	64.37	129.87	18.892 (.05)	15.710 (.07)	38.925 (.12)	Ord-Sil DOLM
20008-009	Backbone ²	08	63.85	129.17	18.739 (.07)	15.647 (.05)	38.460 (.09)	Dev LIMS
20009-002	Weather ²	09	63.97	129.28	18.761 (.06)	15.700 (.09)	38.574 (.13)	Dev DOLM
20012-006	Twitya ²	12	64.03	129.27	18.691 (.05)	15.652 (.09)	38.564 (.09)	N.Dev DOLM
20015-001	Jin ²	15	64.48	130.45	19.180 (.05)	15.719 (.06)	38.920 (.04)	Ord-Dev DOLM
20022-001	Guild ²	22	64.63	130.10	18.798 (.08)	15.680 (.12)	38.761 (.05)	Ord-Dev? DOLM
20023-014	Rev:Main ²	23	64.13	129.33	18.762 (.22)	15.675 (.08)	38.537 (.29)	Ord-Sil DOLM
20023-098	Rev:Waterfall ²	23	64.13	129.33	18.747 (.09)	15.662 (.02)	38.498 (.09)	
20023-137	Rev:Cirque ²	23	64.13	129.33	18.767 (.06)	15.653 (.08)	38.509 (.05)	
Average for Rev		23	64.13	129.33	[18.759 (.12)]	[15.663 (.06)]	[38.515 (.14)]	
20025-008	Teyart ²	25	64.53	130.17	18.770 (.10)	15.680 (.09)	38.823 (.08)	Ord-Sil DOLM
20034-007	Kind ²	34	64.37	129.73	18.779 (.10)	15.684 (.08)	38.846 (.06)	Ord-Sil DOLM
20073-001	Majesty	73	63.28	128.45	19.145 (.09)	15.704 (.13)	38.579 (.02)	Nad-Can? DOLM
20073-002	Majesty	73	63.28	128.45	19.204 (.07)	15.727 (.06)	38.881 (.09)	
Average for Majesty ²		73	63.28	128.45	[19.174 (.08)]	[15.716 (.10)]	[38.730 (.06)]	
Pinepoint	Pine Point	75	61.67	114.50	18.187 (.11)	15.604 (.09)	38.083 (.04)	N.Dev DOLM
20075-001	Pine Point: K53	75	61.67	114.50	18.168 (.06)	15.568 (.02)	38.174 (.06)	
20075-002	Pine Point: J69	75	61.67	114.50	18.162 (.05)	15.589 (.06)	38.241 (.04)	
20075-003	Pine Point: S65	75	61.67	114.50	18.162 (.09)	15.587 (.07)	38.129 (.06)	
Average for Pine Point ²		75	61.67	114.50	[18.170 (.08)]	[15.587 (.06)]	[38.157 (.05)]	

1. All analyses done in the Geology - Geophysics Laboratory, The University of British Columbia.

2. All analyses done on galena samples unless otherwise noted.

3. Data used in determining arith. average and slope of best fit line for "Young Carbonate" are marked with a superscript "2"; other "2's" used for these calculations are in Table 1.

TABLE 2: LEAD ISOTOPE ANALYSES¹ ON GALENA² FROM MINERAL DEPOSITS

Selwyn Basin, B.C. and Y.T.

Sample Number	Deposit Name ³	Map Name	Lat. ^o North	Long. ^o West	Lead Isotope Data (Relative 1 σ Error as %)			Remarks
					²⁰⁶ Pb/ ²⁰⁴ Pb	²⁰⁷ Pb/ ²⁰⁴ Pb	²⁰⁸ Pb/ ²⁰⁴ Pb	
Devonian - Mississippian								
G78AK-001	Alcock ³	AK	57.67	125.42	18.984 (.09)	15.764 (.08)	39.561 (.09)	Dev-Mis SHAL, B.C.
G79BT-001	Boya Prospect ³	BT	59.25	127.50	19.560 (.07)	15.710 (.08)	39.689 (.08)	QIMZ PORP, B.C.
G78CQ-001	Cirque ³	CQ	57.52	125.12	18.795 (.08)	15.689 (.08)	39.166 (.08)	Dev-Mis SHAL, B.C.
G78DC-001	Driftpile Creek	DC	58.07	125.92	18.864 (.07)	15.666 (.07)	39.093 (.05)	Dev-Mis SHAL, B.C.
G78DC-002	Driftpile Creek	DC	58.07	125.92	18.860 (.09)	15.686 (.06)	39.202 (.10)	
G78DC-003	Driftpile Creek	DC	58.07	125.92	18.852 (.08)	15.655 (.06)	39.043 (.13)	
Average for Driftpile Creek ³					[18.859 (.08)]	[15.669 (.06)]	[39.113 (.09)]	
G78ZF-001	Elf ³	ZF	57.42	124.72	18.834 (.09)	15.661 (.09)	39.310 (.04)	Dev-Mis SHAL, B.C.
G78FK-001	Fleke ³	FK	57.42	124.87	18.846 (.08)	15.714 (.04)	39.477 (.06)	Dev-Mis SHAL, B.C.
G79PI-001	Pie Shoving ³	PI	57.45	124.78	18.888 (.03)	15.739 (.10)	39.526 (.09)	Dev-Mis SHAL, B.C.
G79RG-001	Rough ³	RG	58.27	126.17	18.709 (.03)	15.617 (.07)	38.548 (.11)	Dev-Mis SHAL, B.C.
10077-001	Jason N. Zone	77	63.15	130.25	18.737 (.10)	15.646 (.12)	39.651 (.30)	Dev-Mis SHAL, Y.T.
10077-002	Jason N. Zone	77	63.15	130.25	18.667 (.07)	15.649 (.09)	38.501 (.08)	
10077-003	Jason N. Zone	77	63.15	130.25	18.661 (.08)	15.664 (.10)	38.609 (.02)	
10077-004	Jason S. Zone	77	63.15	130.25	18.696 (.09)	15.693 (.08)	38.820 (.10)	
10077-005	Jason S. Zone	77	63.15	130.25	18.705 (.03)	15.678 (.05)	38.732 (.02)	
Average for Jason ³					[18.695 (.07)]	[15.666 (.09)]	[38.863 (.10)]	
10078-001	Tom	78	63.17	130.15	18.654 (.09)	15.639 (.08)	38.771 (.02)	Dev-Mis SHAL, Y.T.
10078-002	Tom	78	63.17	130.15	18.655 (.08)	15.666 (.05)	38.656 (.05)	
10078-003	Tom	78	63.17	130.15	18.633 (.08)	15.636 (.07)	38.536 (.12)	
10078-004	Tom	78	63.17	130.15	18.673 (.07)	15.691 (.04)	38.704 (.06)	
10078-005	Tom	78	63.17	130.15	18.695 (.08)	15.727 (.06)	38.892 (.10)	
Average for Tom ³					[18.662 (.08)]	[15.672 (.06)]	[38.712 (.07)]	
Number of deposits (n) = 10 with 11 errors = \bar{x}					[18.883 (.07)]	[15.690 (.08)]	[39.191 (.08)]	
Number of analyses = 20 std. error = s/\sqrt{n}					0.081	0.013	0.122	

1. All analyses done in the Geology - Geophysics Laboratory, The University of British Columbia.

2. All analyses done on galena samples unless otherwise noted.

3. Data used in determining arith. average and std. error of the mean are marked with a superscript "3".

TABLE 2a LEAD ISOTOPE ANALYSES¹ ON GALENA² FROM MINERAL DEPOSITSSilver Bearing Deposits, Selwyn Basin, Wernecke Fold Belt, Omineca Crystalline, and Yukon Crystalline Platforms³

Sample Number	Deposit Name ¹	Map Name	Lat.° North	Long.° West	Lead Isotope Data (Relative to 207Pb/204Pb)			Error as %	Remarks ⁴
					206Pb/204Pb	207Pb/204Pb	208Pb/204Pb		
10016-001	Grosila ^a	16	65.18	134.63	19.477 (.20)	15.692 (.10)	39.208 (.40)		Hel CONG, SAND; WFB
10042-014	Profeit ^a	42	64.82	133.55	19.182 (.08)	15.671 (.04)	39.566 (.09)		U. Had DOLB; WFB
10063-001	Angie ^a	63	61.85	132.53	19.122 (.12)	15.680 (.05)	39.020 (.15)		Dev LINS; 0
10068-001	Nat Cr.	68	61.53	132.63	19.477 (.10)	15.711 (.07)	39.683 (.04)		U. Dev-Min VOLC; 0
10068-002	Nat Cr.	68	61.53	132.63	19.495 (.10)	15.679 (.09)	39.646 (.09)		
Average for Nat Cr. ^a		68	61.53	132.63	[19.486 (.10)]	[15.695 (.08)]	[39.664 (.06)]		
10071-001	Spotted Fawn ^a	71	64.37	138.70	19.216 (.04)	15.681 (.07)	39.071 (.05)		Pal-Mes QZIT; SB
10072-001	Deb ^a	72	60.35	135.85	19.101 (.06)	15.644 (.08)	38.852 (.09)		SKARN; YCP
10074-001	Casino:C-Trench	74	62.73	138.82	19.212 (.06)	15.612 (.06)	38.765 (.06)		PuHP Cu-Mo-W-Ag-Au
10074-002	Casino:C-Trench	74	62.73	138.82	19.282 (.08)	15.668 (.09)	39.101 (.08)		system related to
10074-003	Casino:C-Trench	74	62.73	138.82	19.046 (.04)	15.617 (.09)	38.746 (.09)		K-Ar 70 Ma
10074-004	Casino:Womber	74	62.72	138.83	19.203 (.10)	15.648 (.06)	38.840 (.14)		intrusive; YCP
10074-005	Casino:Porphyry	74	62.73	138.84	19.239 (.06)	15.626 (.05)	38.761 (.04)		
10074-006	Casino:Porphyry	74	62.73	138.84	19.266 (.07)	15.631 (.06)	38.804 (.05)		
10074-007	Casino:Womber	74	62.72	138.83	19.240 (.06)	15.625 (.07)	39.910 (.06)		
Average for Casino ^a		74	62.72	138.83	[19.212 (.07)]	[15.632 (.07)]	[38.990 (.07)]		
10075-001	Mosquito ^a	75	63.92	140.72	19.190 (.07)	15.712 (.10)	39.214 (.18)		Vein in SCHS; YCP
10076-001	Tombstone I ^a	76	64.40	138.69	19.329 (.10)	15.700 (.07)	39.260 (.11)		K-Ar SYEN, 85 Ma
10076-002	Tombstone II ^a	76	64.40	138.66	19.055 (.07)	15.666 (.10)	38.920 (.04)		50 ppm U, 50 ppm Th;
10076-003	Tombstone III ^a	76	64.39	138.64	19.483 (.08)	15.706 (.05)	39.606 (.09)		Vein in QZIT; SB
Average for Tombstone		76			[19.279 (.08)]	[15.691 (.07)]	[39.262 (.08)]		
10079-001	Ras	79	60.20	135.73	19.176 (.10)	15.634 (.10)	38.857 (.12)		SKARN, Zn-Pb-Ag
10079-002	Ras	79	60.20	135.73	19.151 (.09)	15.737 (.05)	39.327 (.06)		near 54 Ma K-Ar
Average for Ras ^a		79	60.20	135.73	[19.164 (.10)]	[15.686 (.08)]	[39.092 (.09)]		stock. Host SCHS
									>1200 Ma (Rb-Sr);
									YCP
10081-001	Ketza R. (K-18B)	81	61.55	132.19	19.502 (.09)	15.731 (.09)	39.765 (.10)		Dev-Min SHAL; 0
10081-002	Ketza R. (K-18B)	81	61.55	132.19	19.392 (.19)	15.745 (.09)	39.873 (.20)		
10081-003	Ketza R. (A-1)	81	61.53	132.16	19.516 (.10)	15.740 (.09)	39.694 (.18)		
10081-004	Ketza R. (Canyh)	81	61.55	132.18	19.478 (.09)	15.725 (.09)	39.621 (.11)		
10081-005	Ketza R. (K-18C)	81	61.55	132.19	19.481 (.11)	15.729 (.05)	39.673 (.11)		
10081-006	Ketza R. (F-3)	81	61.54	132.17	19.451 (.09)	15.718 (.09)	39.679 (.11)		
10081-007	Ketza R. (F-1)	81	61.55	132.18	19.468 (.11)	15.726 (.10)	39.770 (.18)		
10081-008	Ketza R. (Float)	81	61.55	132.19	19.469 (.09)	15.710 (.06)	39.655 (.11)		

10081-009	Ketza R. (STF)	81	61.55	132.19	19.482 (.08)	15.726 (.11)	39.632 (.05)	
10081-010	Ketza R. (STF)	81	61.55	132.19	19.468 (.11)	15.756 (.07)	39.700 (.09)	
10081-011	Ketza R. (K-18)	81	61.55	132.15	19.360 (.06)	15.618 (.11)	39.432 (.09)	
10081-012	Ketza R. (K-18)	81	61.55	132.15	19.440 (.10)	15.733 (.04)	39.636 (.10)	
Average for Ketza R. *		81			[19.459 (.10)]	[15.721 (.08)]	[39.678 (.12)]	
10083-001	Prism:Val,Tetrah'	83	64.26	133.69	20.903 (.10)	15.844 (.08)	41.000 (.15)	Hel DOLA; WFB
10083-002	Prism:Val,Billa'd	83	64.25	133.69	20.983 (.08)	15.828 (.10)	42.184 (.15)	
10083-003	Prism:Val,Lit'rd'	83	64.26	133.71	21.207 (.06)	15.844 (.13)	42.594 (.11)	
Average for Val (n=3) *		83			[21.033 (.08)]	[15.852 (.10)]	[42.193 (.14)]	
10083-004	Prism:North Val	83	64.27	133.71	21.994 (.07)	15.958 (.07)	43.722 (.09)	Hel DOLA; WFB
10083-005	Prism:Vera	83	64.44	133.68	21.055 (.05)	15.846 (.08)	42.263 (.07)	
10083-006	Prism:Vera 1c.2	83	64.26	133.69	21.152 (.03)	15.907 (.05)	42.490 (.10)	
Average for Vera (n=2) *		83			[21.104 (.07)]	[15.876 (.06)]	[42.376 (.08)]	
10083-007	Prism:Zap *	83	64.27	134.03	20.263 (.07)	15.844 (.08)	41.074 (.14)	Hel DOLA; WFB
Average for Prism (n=4)		83			[21.098 (.07)]	[15.582 (.08)]	[42.341 (.11)]	
10084-001	A+B *	84	60.12	130.43	19.516 (.08)	15.714 (.07)	39.657 (.11)	Can PNTL; 0
10085-001	Peso: Veia *	85	64.00	135.95	19.245 (.10)	15.698 (.09)	39.421 (.07)	P.Can? SCNS; SB
10085-002	Peso: Rex *	85	64.00	135.90	21.090 (.08)	15.853 (.10)	41.109 (.08)	
Average for Peso		85	64.00		[20.168 (.09)]	[15.776 (.10)]	[40.265 (.08)]	
10086-001	Caluset	86	63.92	135.39	19.146 (.08)	15.684 (.07)	39.209 (.04)	Galena Hill. Pal-Mes
10086-010	Hector-Caluset	86	63.92	135.39	19.085 (.10)	15.670 (.11)	38.960 (.20)	QZIT-SCNS; K-Ar
Average for Hector-Caluset		86			[19.116 (.09)]	[15.677 (.09)]	[39.084 (.12)]	BS Ha; SB
10086-002	Elsa	86	63.91	135.48	19.144 (.09)	15.672 (.09)	39.116 (.04)	
10086-007	Elsa:Ftval Eray	86	63.91	135.48	19.155 (.09)	15.662 (.11)	39.157 (.09)	
10086-008	Elsa:Hnval Eray	86	63.91	135.48	19.136 (.07)	15.650 (.05)	39.214 (.05)	
Average for Elsa		86			[19.145 (.08)]	[15.661 (.08)]	[39.162 (.06)]	
10086-004	Silver King	86	63.90	135.57	19.144 (.04)	15.713 (.10)	39.445 (.08)	
10086-005	Silver King	86	63.90	135.57	19.093 (.09)	15.656 (.06)	39.126 (.11)	
10086-016	Silver King	86	63.90	135.57	19.218 (.05)	15.646 (.08)	39.214 (.08)	
Average for Silver King		86			[19.153 (.06)]	[15.672 (.08)]	[39.330 (.09)]	
10086-006	Paddy	86	63.9A	135.4A	19.038 (.12)	15.705 (.07)	38.980 (.14)	
10086-009	Ruby	86	63.91	135.43	19.111 (.06)	15.648 (.09)	39.004 (.18)	
10086-011	Birmingham Pit	86	63.91	135.43	19.132 (.09)	15.712 (.09)	39.375 (.13)	
10086-012	Husky	86	63.92	135.48	19.136 (.06)	15.626 (.04)	39.073 (.08)	
10086-013	Husky	86	63.92	135.48	19.118 (.05)	15.645 (.02)	39.193 (.10)	
10086-014	Husky	86	63.92	135.48	19.126 (.03)	15.651 (.05)	39.145 (.07)	
10086-015	Husky	86	63.92	135.48	19.152 (.11)	15.664 (.08)	39.188 (.06)	
Average for Husky		86			[19.133 (.06)]	[15.646 (.05)]	[39.157 (.06)]	
Average for Galena Hill area *		86			[19.118 (.08)]	[15.674 (.08)]	[39.156 (.11)]	

10086-017	Keno	86	63.94	135.94	19.187 (-.04)	15.648 (-.07)	39.191 (-.13)	Keno Hill. Pal-Mes QZIT-SCHS-GREN, K-Ar GRDR 85 Ma; SB
10086-018	Stone	86	63.96	135.23	19.179 (-.10)	15.655 (-.12)	39.260 (-.12)	SCHS-GREN
10086-019	Ladue	86	63.96	135.28	19.320 (-.05)	15.675 (-.06)	39.380 (-.14)	SCHS-GREN
10086-020	Shanrock	86	63.94	135.24	19.234 (-.08)	15.684 (-.10)	39.346 (-.03)	QZIT
10086-021	Keno	86	63.9A ^a	135.9A ^a	19.179 (-.05)	15.682 (-.06)	39.274 (-.08)	QZIT Veinlets
10086-022	Keno	86	63.9A ^a	135.9A ^a	19.140 (-.07)	15.661 (-.04)	39.225 (-.10)	QZIT Dissect.
Average for Keno Hill area ^a		86			[19.206 (-.07)]	[15.668 (-.08)]	[39.279 (-.10)]	
10087-001	Stand-To Mtn. ^a	87	64.03	135.17	19.545 (-.05)	15.739 (-.02)	39.820 (-.10)	QZIT; SB
10097-001	Plata:No.2	97	63.58	132.03	19.397 (-.09)	15.716 (-.07)	39.513 (-.07)	Had QZIT; SB
10097-002	Plata:No.6	97	63.58	132.03	19.403 (-.07)	15.707 (-.07)	39.510 (-.08)	
10097-005	Plata:No.2	97	63.58	132.03	19.418 (-.09)	15.701 (-.08)	39.395 (-.07)	
Average for Plata:No. 2 & 6		97			[19.406 (-.08)]	[15.708 (-.07)]	[39.473 (-.07)]	
10097-003	Plata:Thrust	97	63.58	132.03	19.199 (-.03)	15.674 (-.10)	39.300 (-.09)	In thrust:Had-W.Dev
10097-004	Plata:Inca	97	63.58	132.03	19.425 (-.06)	15.686 (-.05)	39.482 (-.14)	Had QZIT; SB
Average for Plata (n=5) ^a		97			[19.368 (-.07)]	[15.697 (-.07)]	[39.440 (-.09)]	
10102-001	Logtung Darva Ven	102	60.02	131.63	19.195 (-.07)	15.641 (-.06)	38.857 (-.06)	1.7km NE main show;0
10102-002	Logtung W Deposit	102	60.02	131.63	19.328 (-.07)	15.714 (-.09)	39.495 (-.06)	0.7km NE main show;0
Average for Logtung Area ^a		102	60.02	131.63	[19.262 (-.07)]	[15.678 (-.08)]	[39.176 (-.06)]	
10103-001	Red Fox ^a	103	62.30	137.16	19.120 (-.07)	15.579 (-.10)	38.766 (-.10)	GSC Sample: YCP
10104-001	Tinta Hill	104	62.28	136.97	19.200 (-.10)	15.650 (-.10)	38.814 (-.10)	Vein, Au-Ag-Pb-Zn
10104-002	Tinta Hill	104	62.28	136.97	19.162 (-.09)	15.607 (-.11)	38.808 (-.08)	Trs GRDR;
Average for Tinta Hill ^a		104	62.28	136.97	[19.181 (-.10)]	[15.628 (-.10)]	[38.811 (-.09)]	GSC Sample; YCP
10105-001	Orekon Syndic ^a	105	63.88	138.92	19.814 (-.10)	15.745 (-.08)	39.328 (-.16)	King Sol Dome GSC Sample; SCHS; YCP
10106-001	Connaught ^a	106	63.92	140.72	19.303 (-.06)	15.559 (-.12)	39.028 (-.09)	GSC Sample: vein of
10107-001	Silver City ^a	107	64.32	139.83	19.197 (-.05)	15.681 (-.11)	39.110 (-.10)	Pb-Zn in QZCU; YCP
10108-001	Venus ^a	108	60.02	134.64	19.116 (-.09)	15.617 (-.08)	38.642 (-.10)	Au-Ag vein in 70 Ma GRNT; YCP
20077-001	Mt. Christie ^a	77	63.03	129.53	19.611 (-.07)	15.708 (-.10)	39.093 (-.06)	GSC; vein in GRNT; SB
20078-001	O'Grady ^a	78	62.92	128.84	19.192 (-.08)	15.684 (-.09)	39.239 (-.09)	GSC; vein in GRNT; SB

1. All analyses done in the Geology - Geophysics Laboratory, The University of British Columbia.
2. All analyses done on galena samples unless otherwise noted.
3. Data used in determining arith. average and slope of best fit line are marked with a superscript "a".
4. Approximate location only.
5. remarks identify regional setting of deposits (see Fig. 1).

CARBONATE-HOSTED DEPOSITS

A framework for the age of mineralization for epigenetic, stratabound, carbonate-hosted, Zn-Pb deposits was developed by McLaren and Godwin (1979) from an extensive study of minor elements in sphalerite. Deposits were divided into two groups:

- 1) those hosted by "Old Carbonate" rocks of Helikian to Lower Cambrian age; sphalerites from these deposits are characterized by relatively high amounts of minor elements (Ag, Fe, Sn, etc.);
- 2) those hosted by "Young Carbonate" rocks of Middle Ordovician to Devonian age; sphalerites from these deposits contain relatively low minor element levels.

The stratigraphic separation of these two groups is emphasized by the occurrence of an essentially barren unit, the Franklin Mountain formation, between Lower Cambrian and Middle Ordovician rocks. Geochemical evidence of two fundamentally different mineralizing episodes combined with other geological considerations led to the suggestion that one mineralizing episode might be Lower to Middle Cambrian in age and related, in part, to karstic processes. A later mineralizing event during or shortly after Upper Devonian, might have resulted from dewatering shales in the Selwyn Basin. Precise ages of basement rocks in the region are uncertain. Lithostratigraphic correlations by Young et al. (1979) indicate that Proterozoic supracrustal rocks in Central Y.T. might be as old as 1.7 b.y. Certainly the terrane is older than a 1.5 b.y. K-Ar age obtained from phlogopite in alteration associated with a brecciated diatreme that crosscuts Helikian strata (e.g. Archer et al., 1977). This framework therefore provides age constraints that can be tested with lead isotope data.

Lead isotope data for "Old Carbonate" hosted deposits are in Table 1; those for "Young Carbonate" hosted deposits are in Table 2. Deposits are located in Figure 1 and data are plotted in Figure 2 as a $^{207}\text{Pb}/^{204}\text{Pb}$ and $^{208}\text{Pb}/^{204}\text{Pb}$ versus $^{206}\text{Pb}/^{204}\text{Pb}$ plot. The two different groups, noted above, are plotted as circles and squares for "Old" and "Young" types respectively. Seven solidly filled-in circles represent deposits hosted in "Old Carbonate" rocks but characterized by lead isotopes similar to deposits hosted by "Young Carbonate" rocks.

Assignment of the "Old Carbonate" deposits to the "Young Carbonate" deposit group is supported by sphalerite geochemistry and is explained by the model developed in the conclusions.

It is apparent that the two groups have significantly different distribution patterns in Figure 2. "Old" and "Young" deposits both define straight lines with specifications, as listed in Table 5, defined by using a York II least squares fitting procedure (York, 1969), and by error analysis after Ludwig (1980).

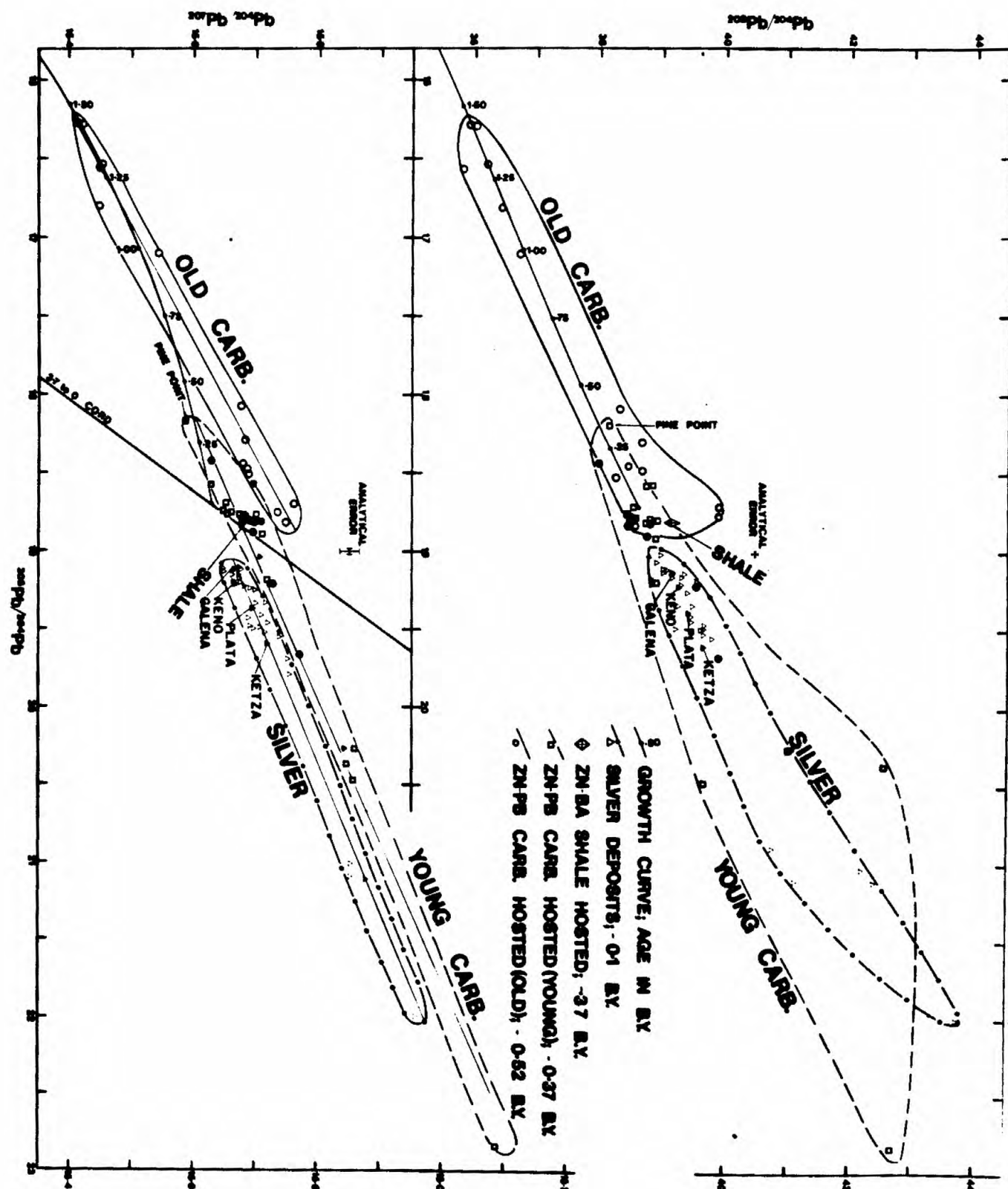


Figure 2: Plot of isotopic ratios for deposits located on Figure 1 and listed in Tables 1 to 4.

We interpret the lines to be secondary isochrons or anomalous lead lines (Russell *et al.*, 1966). This interpretation contains fundamental implications regarding genesis of the deposits, because it requires that 1) lead for each group of deposits be derived from sources that experienced a contemporaneous lead isotope homogenization at the time of formation (t_1), and 2) all deposits in each group formed during the same mineralizing episode of relatively short duration (t_2).

Accepting the secondary isochron interpretation allows us to test whether or not the underlying assumptions are realistic in geological terms. Because a secondary isochron is defined by addition of radiogenic lead to a starting lead, the slope (m) is an estimate of the ratio $^{207}\text{Pb}/^{206}\text{Pb}$ of the radiogenic component. This radiogenic component was generated in the interval between isolation in a source rock (t_1 = age of source rocks) and extraction from the source rocks (t_2 = age of mineralization) according to the equation:

$$m_{t_1-t_2} = \frac{1}{137.8} \left[\frac{e^{\lambda_2 t_1} - e^{\lambda_2 t_2}}{e^{\lambda_1 t_1} - e^{\lambda_1 t_2}} \right]$$

Where: t_1 = age of basement source,

t_2 = metallogenic event,

λ_1 = decay constant of ^{238}U = $0.155125 \times 10^{-9}\text{yr}^{-1}$, and

λ_2 = decay constant of ^{235}U = $0.98485 \times 10^{-9}\text{yr}^{-1}$.

Note that for any given slope both t_1 and t_2 are unknowns in the equation. If one of these ages can be estimated by independent means, the other can be calculated.

"Old Carbonate" hosted deposits (Table 1) occur in Lower Cambrian or older rocks below a marked unconformity formed near Lower to Middle Cambrian time. Thus, if these deposits all formed at about the same time, the Lower-Middle Cambrian boundary at about 0.52 b.y. must be close to the age of mineralization (t_2). Using this for t_2 indicates a basement source age of 1.89 b.y. This age is significantly older than the 1.5 b.y. restriction imposed by the K-Ar date and the about 1.7 b.y. lithostratigraphic age limit noted above. Furthermore, this is the first lead isotopic indication of Hudsonian basement in the northern Canadian Cordillera.

Leads that define the "Old Carbonate" line in Figure 2 lie close to the average crustal growth curves of Stacey and Kramers (1975), suggesting generations of the "Old Carbonate" lead in an upper crustal environment not enriched in uranium. Several galenas (e.g. Oz: 10037 and Monster: 10038) must have resided in an environment that contributed very little radiogenic lead to the original source composition. Such environments are rare in nature, but could be expected where lead evolves in carbonates. This, plus the spatial association of these deposits with unconformities, supports the karstic model espoused by McLaren and Godwin (1979).

The age of shale-hosted Ba-Zn-Pb deposits is known to be very close to the Devonian-Mississippian boundary (0.37 b.y.) from fossils preserved in the barite-sulphide horizon (W. Roberts, 1979, pers. comm.). Lead isotopes from this type of deposit (Table 3) are tightly clustered and their mean coincides with the location of most "Young Carbonate" leads in Figure 2. Since the lead isotopes are generally identical, a similar source for and age of mineralization is implied. Thus the metallogenic event (t_2) responsible for the formation of "Young Carbonate" hosted Zn-Pb deposits and stratiform, shale-hosted, Ba-Zn-Pb deposits is probably near 0.37 b.y.

In addition to the pronounced cluster of "Young Carbonate" and stratiform shale-hosted Ba-Zn-Pb isotopic ratios in Figure 2, there are a series of ratios highly enriched in radiogenic lead plotting along the anomalous lead line to the right of the cluster. These leads either developed in an abnormally high U/Pb environment (i.e. high even for crustal rocks) or developed by contamination of a more normal crustal lead by radiogenic lead. The cluster of analyses can be interpreted easily in terms of more-or-less normal upper crustal evolution of lead isotopic compositions because it is concentrated close to but just above the mean evolutionary curve for crustal leads and coincides with average stratiform, shale-hosted Ba-Zn-Pb deposits. It is our opinion that the radiogenetically enriched leads can be attributed to characteristics of the process of mineralization. Specifically, we envisage the radiogenic-rich leads as originally having had the composition of the cluster, but on moving through a great length of source rocks they became contaminated with relatively large quantities of radiogenic lead generated in the interval t_1 to t_2 . This explanation is reasonable geologically, based on the abundant evidence that even low temperature acidic leaching of rocks will result in preferential extraction of the radiogenic component of leads relative to the component tied up in potassium positions in the lattices of common rock-forming silicates (Doe *et al.*, 1966; Doe and Delevaux, 1972).

Lead for "Young Carbonate" hosted deposits evolved in upper crustal, uranium rich, carbonaceous shale - mainly in the Selwyn Basin. We suggest that the calculated basement age (t_1) of 1.55 b.y. ($t_2 = 0.37$ b.y.) in Table 5 is younger than the true, probably Hudsonian, basement age, due to an increase of ($^{238}\text{U}/^{206}\text{Pb}$) with time in the shale basin source (Ryan and Duncan, 1979).

SILVER DEPOSITS

Lead isotope data from silver-rich deposits, located in Figure 1, are in Table 4 and are plotted in Figure 2. A secondary isochron is clearly defined, and lead isotope analyses plot in fields that are highly radiogenic but distinctly different from fields for "Young Carbonate" deposits. Highly radiogenic leads probably formed from preferential leaching of lead from uranium-rich minerals in crustal rock.

Spatial distribution of silver-rich mineralization in Figure 1 closely follows that of Cretaceous (0.10 to 0.07 b.y.) plutons. Most silver deposits occur as veins not directly associated with plutons. The Keno-Galena Hills (10086) silver camp is one such example, although K-Ar dating of alteration associated with veins by Sinclair *et al.* (in press) give ages equivalent to those in granitic plutons from the general area. A direct relationship between plutons and silver mineralization in the Ketz (10081) and Plata (10097) areas have not been established. However, in some areas silver veins occur within, or are directly associated with, plutons. For example:

1. veins occur within the Cretaceous (Tempelman-Kluit, 1970) Tombstone stock (10076),
2. veins occur within and surrounding the Cretaceous (Godwin, 1975) Casino deposit (10074); and
3. Zn-Pb-Ag bearing skarn at the Ram deposit (10079) formed adjacent to Cretaceous (or Eocene) intrusive rocks (Watson *et al.*, in press).

Since the age of plutonism and associated mineralization is mainly Upper Cretaceous (about 0.09 b.y.), and Hudsonian source age of 1.71 b.y. is calculated in Table 5.

CONCLUSIONS

A summary of ages of metallogenic events and ages of apparent basement source, from Table 5, is presented in Figure 3.

"Old Carbonate" hosted deposits formed at about 0.52 b.y. Minor elements in sphalerite, stratigraphic relationships to unconformities, textural and geometric relations at some deposits (e.g. Goz: 10033), and lead isotope characteristics support a karstic model, depicted in Figure 4, for their origin.

Epigenetic "Young Carbonate" hosted Zn-Pb deposits and syngenetic stratiform Ba-Zn-Pb deposits formed at about 0.37 b.y. from brines dewatered from the Selwyn Basin. Figure 5 suggests that solutions that formed the deposits were guided by faults, either within the basin (e.g. the stratiform, shale-hosted Ba-Zn-Pb deposit formed along graben near hinge lines close to the margin of the basin, c.f. Smith, 1978, and Carne, 1979), or peripheral to and away from the basin (e.g. stratabound, carbonate-hosted, zinc-lead deposits, c.f. Beales and Jackson, 1968). Note that some "Old Carbonate" hosted deposits were also formed by this event; this accounts for some lead in "Old Carbonate" hosted deposits which has the isotopic character of "Young Carbonate" hosted lead (represented by filled circles in Figure 2).

Epigenetic, silver-rich deposits formed in response to about 0.09 b.y. Cretaceous plutonism. Figure 6 shows a model which is particularly appropriate for the Keno-Galena Hill area (c.f. Boyle, 1965). Silver-rich veins are deposited from hydrothermal solutions mobilized by and possibly contributed to by

TABLE 5

Line and Age Calculations¹ for Old and Young Carbonate Hosted and Silver Deposits

Deposit Type ¹	Centroid ²		Slope ²	Intercept ²	Ages ³ (B.Y.)					
	$^{206}\text{Pb}/^{204}\text{Pb}$	$^{207}\text{Pb}/^{204}\text{Pb}$			t_2	t_{2+s}	t_{1-s}	t_1	t_{2-s}	t_{2+s}
Old Carbonate (14 points)	17.642	15.598	0.13441	13.227	0.520	0.556	0.484	1.887	1.843	1.931
Young Carbonate (26 points)	19.147	15.712	0.10772	13.650	0.37	0.403	0.340	1.548	1.492	1.601
Silver (33 points)	19.554	15.713	0.10743	13.618	0.09	0.043	0.137	1.708	1.633	1.778

1: Data in Tables 1 to 3 and Figure 2.

2: Calculated using York II fit (York, 1969)

3: Errors calculated by method of Ludwig (1980)

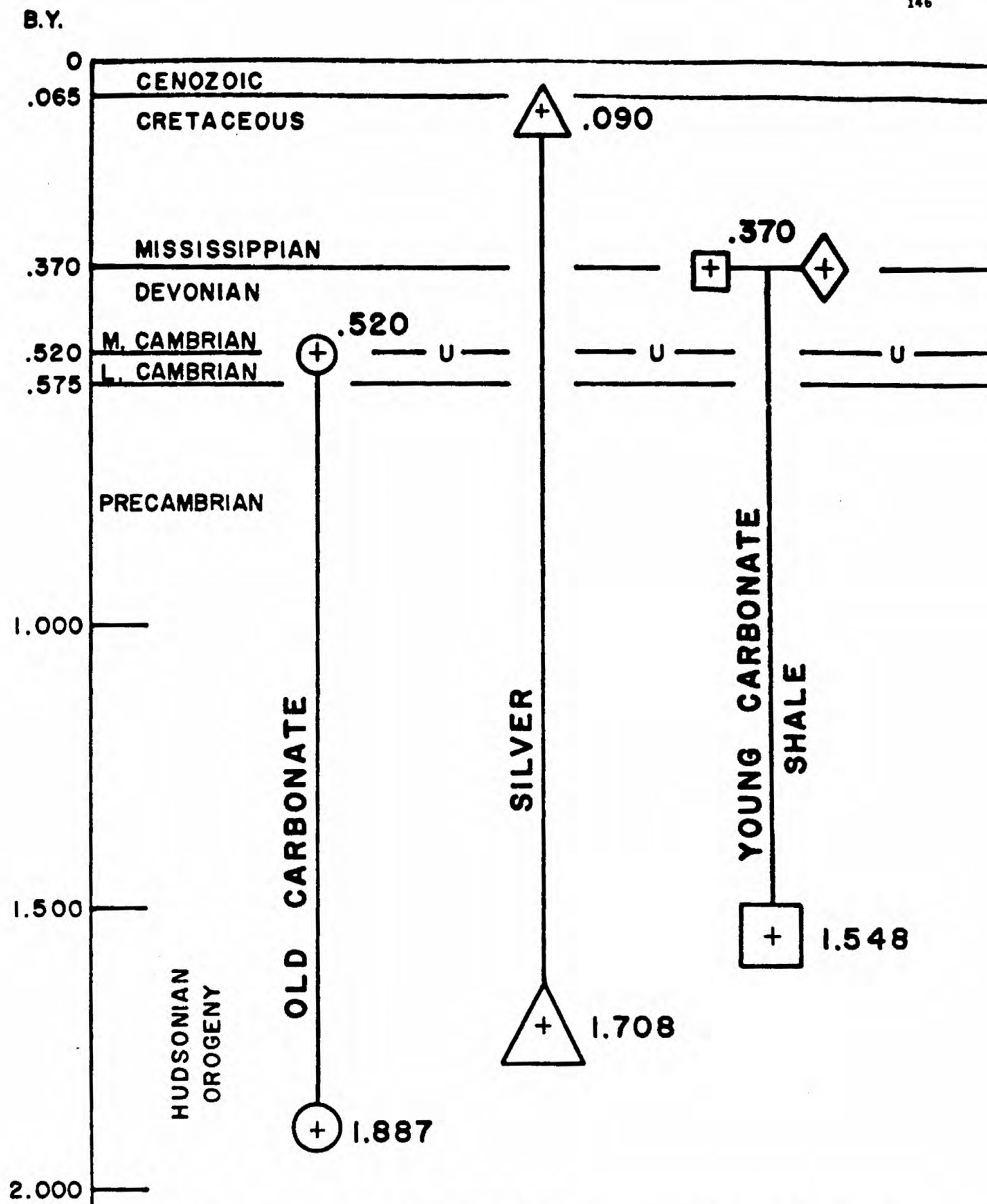


Figure 3: Three ages of mineralization (solid symbol) in the northern Canadian Cordillera related to apparent age of basement source (open symbol). Error or age estimates is illustrated by the height of the symbols (Table 5).

OLD CARBONATE HOSTED

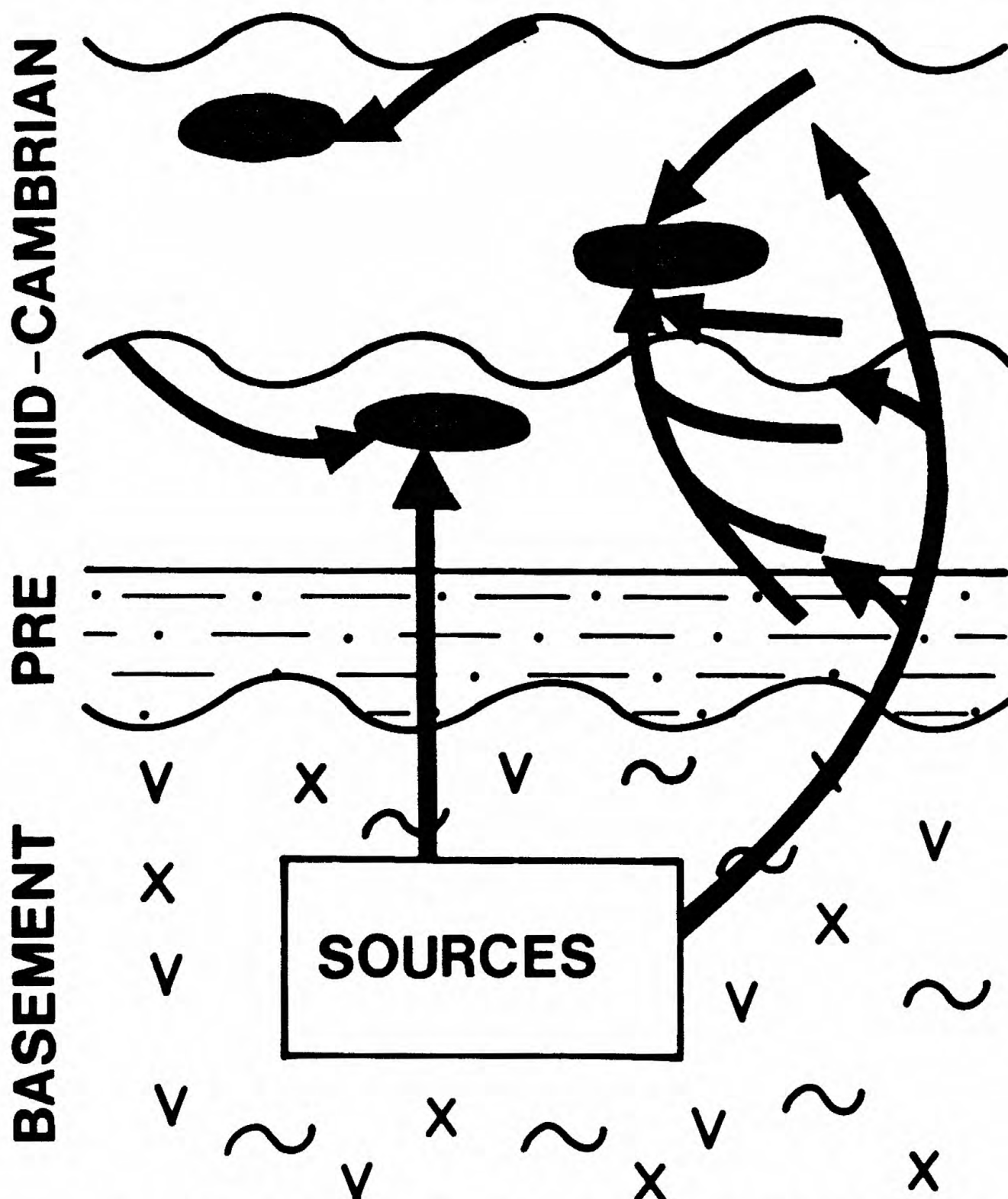


Figure 4: Model for the genesis of many "Old Carbonate" hosted Zn-Pb deposits in the northern Canadian Cordillera. Karstic processes were significant in generation of this type of deposit.

YOUNG CARBONATE AND SHALE HOSTED BA-ZN-PB

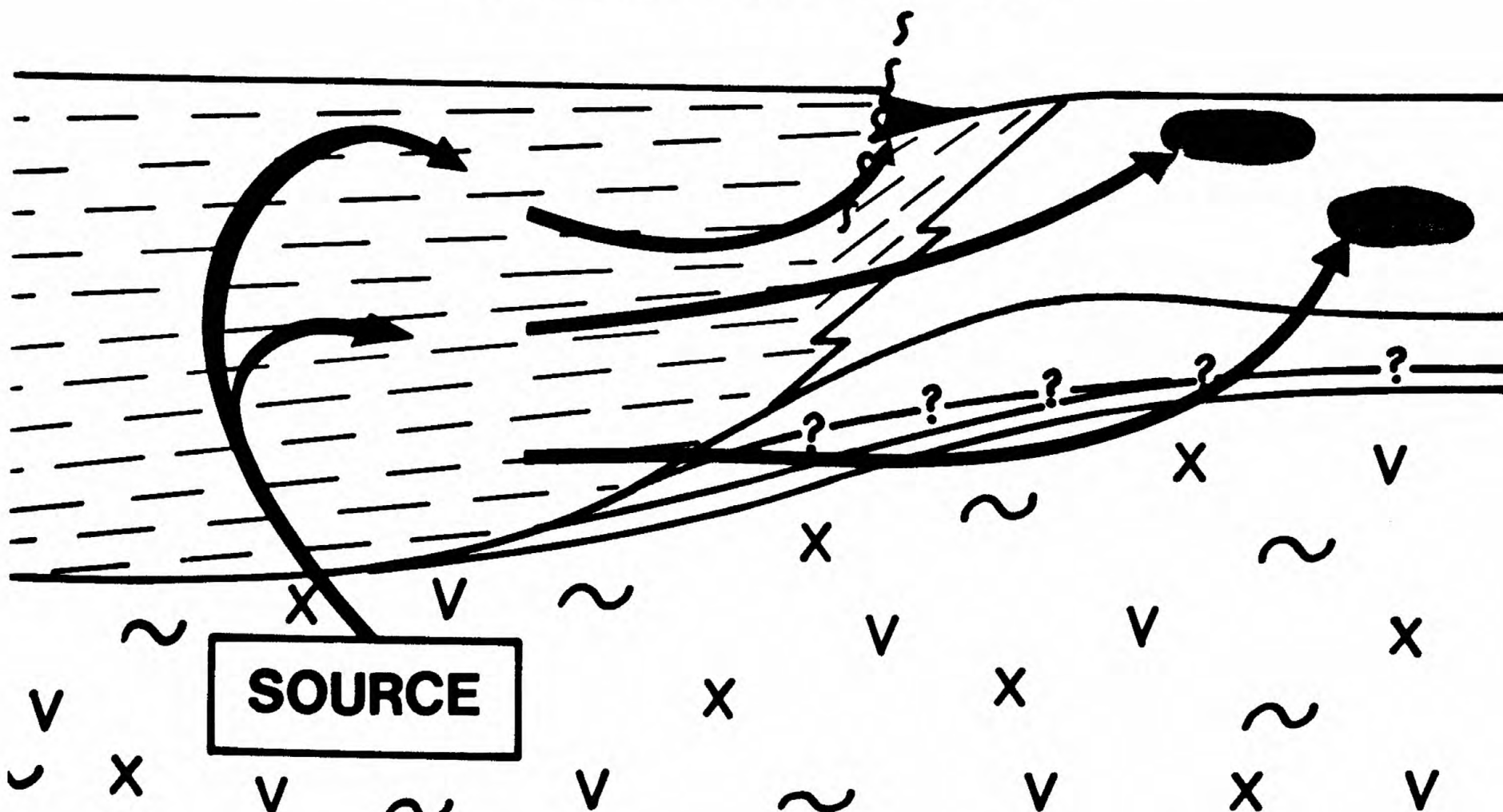


Figure 5: Model for the genesis of "Young Carbonate" hosted Zn-Pb and shale-hosted Ba-Zn-Pb deposits. Mineralizing fluids, generated in the Selwyn Basin, formed deposits within the shale basin or within the platform, depending upon presence of structural and/or stratigraphic traps.

SILVER VEINS

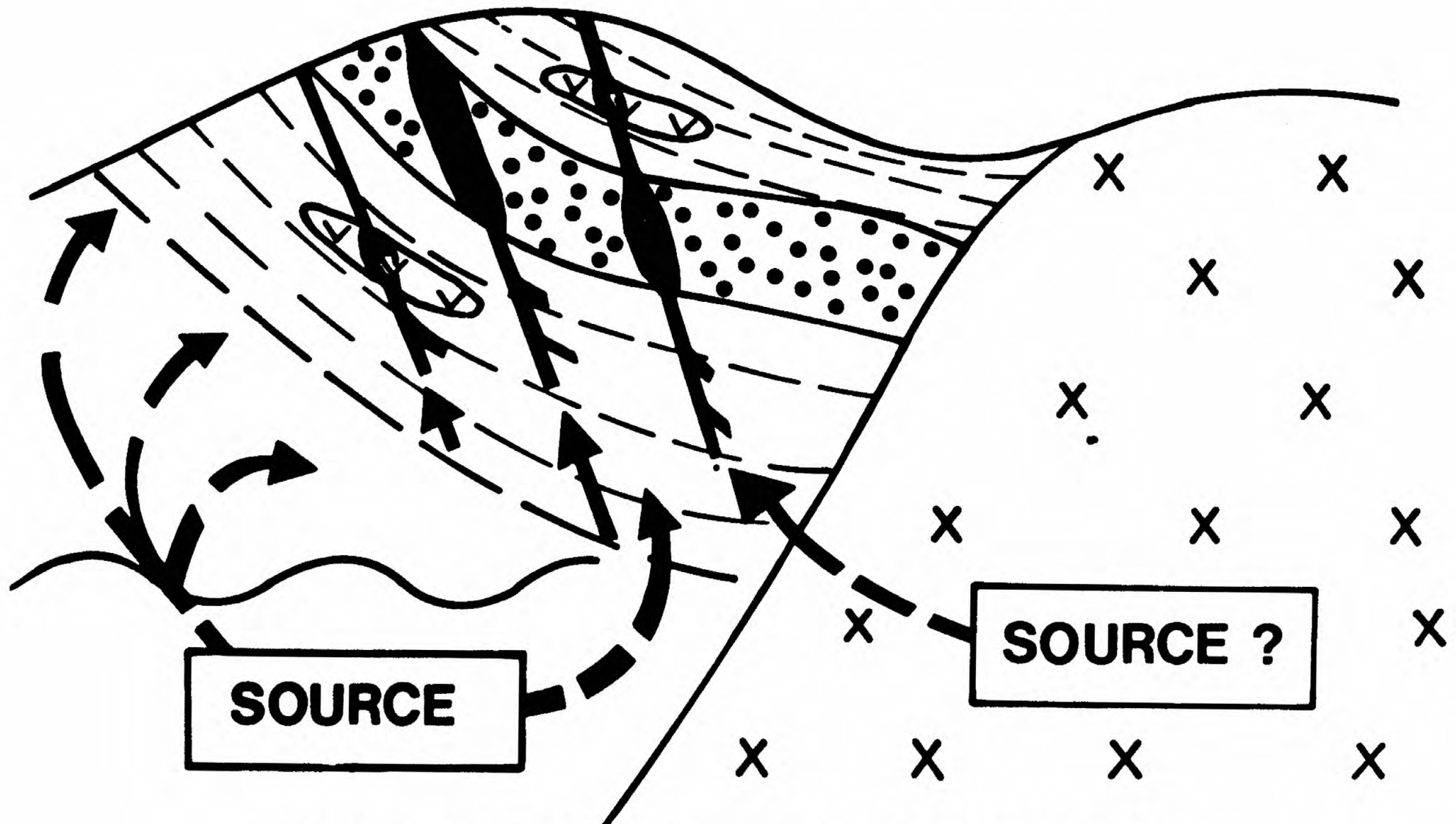


Figure 6: Model for silver rich veins, replacements, or skarns deposited from hydrothermal solutions mobilized by and possibly contributed to by Cretaceous plutons.

Cretaceous plutons.

Models of these metallogenic events form a strong framework for detailed analysis of regional metallogeny in the northern Canadian Cordillera. Exploration can also be focused by the application of such models.

ACKNOWLEDGEMENTS

This work was supported financially by a grant from the Department of Indian and Northern Affairs to A.J. Sinclair and C.I. Godwin, and a COOP grant of the National Research Council to R.D. Russel, W.F. Slawson, and R.L. Armstrong. Cominco Ltd., Cyprus Anvil Mining Corporation, and Rio Tinto Canadian Exploration also provided major funds and some samples used in this study. Critical comments on an earlier version of the manuscript by R.I. Thope, W.A. Padgham, and W.W. Gibbins have improved the manuscript, but the authors accept full responsibility for the interpretations presented. The cooperation of many companies and individuals who helped in the acquisition of the extensive sulphide sample collection is gratefully acknowledged.

REFERENCES

- Archer, A.R., and U. Schmidt, 1978. Mineralized Breccias of Early Proterozoic Age, Bonnet Plume River District, Yukon Territory. *Can. Inst. Min. Met. Bull.*, vol. 71, no. 796, pp. 53-58.
- Beales, F.W., and S.A. Jackson, 1968. Pine Point - a Stratigraphical Approach. *Can. Inst. Min. Met. Bull.*, vol. 61, no. 675, pp. 867-878.
- Boyle, R.W., 1965. Geology, Geochemistry, and Origin of the Lead-Zinc-Silver Deposits of the Keno Hill-Galena Hill Area, Yukon Territory. *Geol. Surv. Can., Bull.* 111, 302 p.
- Carne, R.C., 1979. Geological Setting and Stratiform Mineralization Tom Claims, Yukon Territory. E.G.S. 1979-4, Department of Indian and Northern Affairs, 30 p.
- Doe, E.P., G.E. Hedge, D.E. White, 1978. Preliminary Investigation of the Source of Lead and Strontium in Deep Geothermal Brines Underlying the Salton Sea Geothermal Area. *Econ. Geol.*, vol. 61, pp. 462-483.
- Doe, E.P., and M.H. Delevaux, 1972. Source of Lead in Southern Missouri Galena Ores. *Econ. Geol.*, vol. 67, pp. 409-425.
- Godwin, C.I., 1975. Alternative Interpretations for the Casino Complex and Klotassin Batholith in the Yukon Crystalline Terrane. *Can. Jour. Earth Sci.*, vol. 12, no. 11, pp. 1910-1916.
- Le Couteur, P.C., 1973. A Study of Lead Isotopes from Mineral Deposits in Southeastern British Columbia and in the Anvil Range, Yukon Territory. Unpublished Ph.D. thesis, The University of British Columbia, 142 p.
- Ludwig, Kenneth B., 1980. Calculation of Uncertainties of U-Pb Isotope Data. *Earth Planet. Sci. Lett.*, vol. 5, pp. 320-324.
- McLaren, G.P., and C.I. Godwin, 1979. Minor Elements in Sphalerite from Carbonate-Hosted Zinc-Lead Deposits, Yukon Territory and Adjacent District of Mackenzie, Northwest Territories. Mineral Industry Report 1977, Yukon Territory, EGS 1978-9, pp. 5-21.
- Russell, F.D., E.F. Kanasevich, and J.M. Ozard, 1966. Isotopic Abundances of Lead From a Frequently-Mixed Source. *Earth Planet. Sci. Lett.*, vol. 1, pp. 85-88.
- Ryan, Barry D., and J. Ian Duncan, 1979. U-Th-Pb Systematics: A New Interpretation for Stratabound Pb-Zn Deposits. Program and Abstracts, Geol. Soc. Amer. Annual Meeting, p. 508.

- Sinclair, A.J., C.J. Tessari, and J.E. Harakal, 1980. Age of Ag-Pb-Zn Mineralization, Keno Hill-Galena Hill Area, Yukon Territory. *Can. Jour. Earth Sci.*, vol. 17, no. 9, pp. .
- Smith, C.I., 1978. Geological Setting of Jason and Tom Deposits, Macmillan Pass Area, Eastern Yukon. Sixth Geoscience Forum, Whitehorse, Y.T., December.
- Stacey, J.S., and J.D. Kramers, 1975. Approximation of Terrestrial Lead Isotope Evolution by a Two Stage Model. *Earth Planet. Sci. Lett.*, vol. 26, pp. 207-221.
- Tempelman-Kluit, 1970. Stratigraphy and Structure of the "Keno Hill Quartzite" in Tombstone River - Upper Klondike River Map-Areas, Yukon Territory (116 B/7, B/8). *Geol. Surv. Can., Bull.*, Bull. 180, 102 p.
- Watson, P.H., C.I. Godwin, and R.L. Armstrong, 1980. Geology Mineralization, and K-Ar and Rb-Sr Isotopic Study of the Ram Zinc-Lead-Silver Property. In press, Mineral Industry Report, Yukon Territory, Department of Indian and Northern Affairs.
- York, Derek, 1968. Least Squares Fitting of a Straight Line with Correlated Errors. *Earth Planet. Sci. Lett.*, vol. 5, pp. 320-324.
- Young, G.M., C.W. Jefferson, G.D. Delaney, and G.M. Yeo, 1979. Middle and Late Proterozoic Evolution of the Northern Canadian Cordillera and Shield. *Geology*, vol. 7, March, pp. 125-128.
- Zartman, R.E., 1974. Lead Isotopic Provinces in the Cordillera of the Western United States and their Geologic Significance. *Econ. Geol.*, vol. 69, pp. 792-805.

Possible nonsubduction associated porphyry ore deposits,
Pacific Northwest

T. L. Robyn, Anaconda Copper Company

L. F. Henage, Mobil Energy Minerals

V. F. Hollister, Hollister Geological Consultants

Introduction

Copper mineralization related to Late Tertiary calc-alkaline volcanism is common in central Washington. It has been generally assumed that the calc-alkaline magmas were generated in a subduction zone and that the metals in the copper deposit were also derived from the subduction zone. Recent detailed geologic studies in the Cascades discount any contribution to or control of calc-alkaline magma by subduction processes. Geophysical data do not exhibit patterns characteristic of modern subduction processes. Moreover, available gravity data from on-shore and off-shore studies exhibit patterns characteristic of Basin and Range structures.

Copper porphyry bodies in Washington are localized on the intersections of a major NNE gravity discontinuity and subsidiary NW trending lineaments. Similarly, essentially all copper porphyry systems in the western United States are localized on the margins of major gravity discontinuities (indicating significant crustal discontinuities) where intersected by second order zones of crustal weakness.

Existing data do not support the concept that subduction processes contributed to the formation of these copper porphyries; rather, that the most important aspect of global tectonics is the creation of structurally favorable sites in cratonic blocks. The relative proportions of metals in a given porphyry are dictated by regional crustal composition.

Calc-alkaline Magmas and Subduction

The origin of calc-alkaline magmas is a debated issue. However, data from detailed geologic and geochemical studies are becoming available that provide constraints on models regarding the origin of calc-alkaline magmas. Robyn and Hollister (in press) reviewed these data and concluded that subduction is not a necessary process in the formation of calc-alkaline magmas. Their review is summarized below to illustrate concepts important to our conclusions regarding copper mineralization in central Washington.

The often-quoted, apparent systematic increase inland from trenches of average K_2O contents at a given SiO_2 value has been used to suggest a subduction-controlled process for calc-alkaline magma generation (e.g., Dickinson and Hatherton, 1967). However, White and McBirney (1978) reported data from behind the Cascade axis that show K_2O contents of Pliocene basalts decrease inland from the coast, which is a contradiction of the supposed K_2O vs. SiO_2 - depth to Benioff zone - magma generation relationship. Carr et al.'s (1979) data on Guatemalan Quaternary volcanic rocks illustrate that, when examined in detail, no such relationship exists. Moreover, Cawthorn's (1977) theoretical analysis of K_2O - SiO_2 variations and their supposed relationship with depth to Benioff zone demonstrates that there is no reason why such a relationship should exist.

Robyn and Hollister (in press) concluded that calc-alkaline compositional trends of the rock suites developed after the magmas were extracted from their source region, and that subduction did not contribute to the development of the calc-alkaline compositional trend. Rather, fractionation of dominantly amphibole and plagioclase from basaltic magma generated the calc-alkaline compositional trend in several calc-alkaline suites.

When considered in detail, there is considerable variation in compositions and proportions of rock types in any modern volcanic axis. The variations correspond with changes in the composition and thickness of the crust underlying the axis.

The lack of control or influence on the minor element content of calc-alkaline magmas by subduction processes suggests that the metals of porphyry ore deposits are not derived from subducted oceanic crust.

Calc-alkaline Magmas and Porphyry Ore Deposits

The fractionation of water-bearing parental basaltic magmas to yield andesitic residue must occur at depths of 15 to 30 km, because calcic plagioclase is unstable at pressures greater than 10 kbar (Wyllie, 1970) and amphibole in calc-alkaline magmas is unstable at pressures less than about 5 kb (Cawthorn and O'Hara, 1976). The magnetite rims that surround amphibole (hornblende) in most calc-alkaline rocks indicate that the amphibole was not in equilibrium with its enclosing liquid at low pressure. Hence, the amphibole crystallized at some higher pressure. The strong compositional zoning of plagioclase in calc-alkaline rocks is best explained by variations in magmatic water pressure, because feldspar phase-volumes are very sensitive to changes in water pressure.

A third, low-pressure (1-2 km depth), residence level is required to explain certain petrographic and trace-element characteristics of these rocks (Robyn, 1977; White and McBirney, 1978). Hypabyssal intrusions in eroded calc-alkaline volcanic terranes (western Cascades, Central America), usually associated with mineralization, represent the low-pressure residence level.

The heat of crystallization that is released in the multi-stage process must be transferred to the surrounding wall rock. What effect this heat transfer would have at the intermediate residence level (15 to 30 km) is speculative. However, the low-pressure heat transfer is demonstrably a heat engine which drives large-volume groundwater convection cells.

Evidence for such a convective system is given by several studies. Oxygen-isotope studies demonstrate that the waters of hot springs associated with Quaternary volcanism are almost entirely meteoric water. In addition, analyses of Salton Sea brines show high concentrations of metals being transported by hot saline water (White, 1965). Taylor (1973) concluded that meteoric water was the major component of the hydrothermal

mineralizing system in several Nevada mining districts. Dickson et al. (1979) present stable isotope data that show that the metals in the Carlin gold deposit were leached from the country rock by hydrothermal fluid of meteoric origin.

It should be emphasized that juvenile magmatic water is not an important constituent of the convection system. Rather, high water concentrations in a magma dictate a particular magmatic crystallization history that releases substantial heat into surrounding rocks; this heat transfer is the controlling process in development of a groundwater convection cell. However, such heat transfer processes will occur only where the density differences between the magma and crust is such that magma is ponded at shallow levels in the crust. Such density effects have been described by Bradley (1965), who noted that the density contrast between magma and crust would cause mafic magma to be trapped at shallow levels in an area underlain by thick sialic crust, but would cause the same magma to be erupted to the earth's surface in areas underlain by thin mafic crust. Basalts are not volumetrically dominant in regions of thick continental crust (White and McBirney, 1978; McBirney, 1969), an observation that supports Bradley's model. This observation also leads to the conclusion that areas underlain by sialic crust are more likely to contain porphyry ore deposits because water-bearing magmas intruded there are forced to undergo crystallization at shallow depths where convective water cells are generated by the heat of crystallization.

The differentiation and crystallization histories summarized above illustrate the important genetic link between crustal thickness and composition and the occurrence of porphyry ore bodies. The importance of crustal composition is illustrated by the movement of metals from surrounding rocks into an intrusion, thereby affecting the composition of ore in a developing porphyry ore body. The change in type of ore deposits from western Nevada to eastern Nevada has been noted by several workers (e.g., Hollister, 1978), and is coincident with the Proterozoic crustal limits. Mo-Cu ore bodies occur in terranes underlain by Proterozoic crust, while Au-Cu ore bodies occur to the west. These observations, combined with the structural control of ore deposits, suggest that areas underlain by relatively thick crust and cut by major structures are favorable areas for the formation of porphyry ore deposits. Moreover, because calc-alkaline magma generation can be independent of Benioff zone activity (Robyn, 1979), subducted oceanic crust cannot be demonstrated to be an important contributor to the metal content of porphyry ore deposits.

Structural Setting of Copper Porphyries

The control of global tectonics on igneous activity and sedimentation has been an on-going and documentable process since the Archean. Recurrent influence of major structural lineaments or discontinuities on tectonic, sedimentation and igneous events is well accepted (Tooker, 1979). For example, the Wasatch Line delineated the eastern margin of Lower Cambrian, Ordovician, and Silurian sedimentation and subsequently comprised the eastern margin of the Basin and Range.

The recognition of mineral belts and postulation of lineaments as controls for mineralization is not new; e.g., Roberts (1966), Jerome and Cook (1967). It is not our intent to recapitulate the work of earlier authors, but to re-emphasize the importance of major zones of crustal weakness in controlling major mineralizing systems, particularly the copper porphyry.

The tectonic and Bouguer gravity maps of the western United States (Woolard and Joesting, 1964) present a simplified understanding of the regional structural fabric and allow one to delineate major geologic provinces (Figure 1). Intra-continental geologic provinces such as the Basin and Range and Colorado Plateau are represented on the Bouguer map as areas in which the milligal contours form distinctive textures or patterns. Province margins are typified by a regional shift in the gravity gradient; the western margin of the Colorado Plateau is a good example. Major structural lineaments both form the margins of these provinces and dissect individual provinces. The intersection of a major structural lineament and a province boundary generates an inflection in the gravity contours and creates a secondary texture within the province. Obvious examples are the Midas Trench which strikes northeast across the Basin and Range province, and the Uinta Arch, an east-west structure which dissects the Colorado Plateau and Basin and Range Provinces.

We have traced the geologic province boundaries and major structural lineaments which lie between the Rocky Mountains and Cascade-Sierra Nevada Range, utilizing the Bouguer gravity data. These structural discontinuities are often loci of igneous activity; the northeast trending portion of the Snake River Rift is coincident with the Midas Trench lineament, and the Absaroka volcanic field lies on the southern branch of the Lewis and Clark lineament eastern extremity.

The same Bouguer gravity base was used to plot major and minor porphyry copper deposits and several significant mineral deposits of other types. Essentially all of these deposits are situated on major structural discontinuities in the continental crust.

Recurrent mineralization along these structural discontinuities is exemplified by the localization of Stillwater (2.7 b.y.) on the northern branch of the Lewis and Clark lineament, and Jerome (1.7 b.y.) on the southwest extension of the Colorado Mineral Belt where it intersects the margin of the Colorado Plateau.

The presence of the Coeur D'Alene and Wallace districts and the Butte porphyry on the Lewis and Clark lineament indicates that these structural discontinuities are important for economic mineral deposits other than porphyry systems.

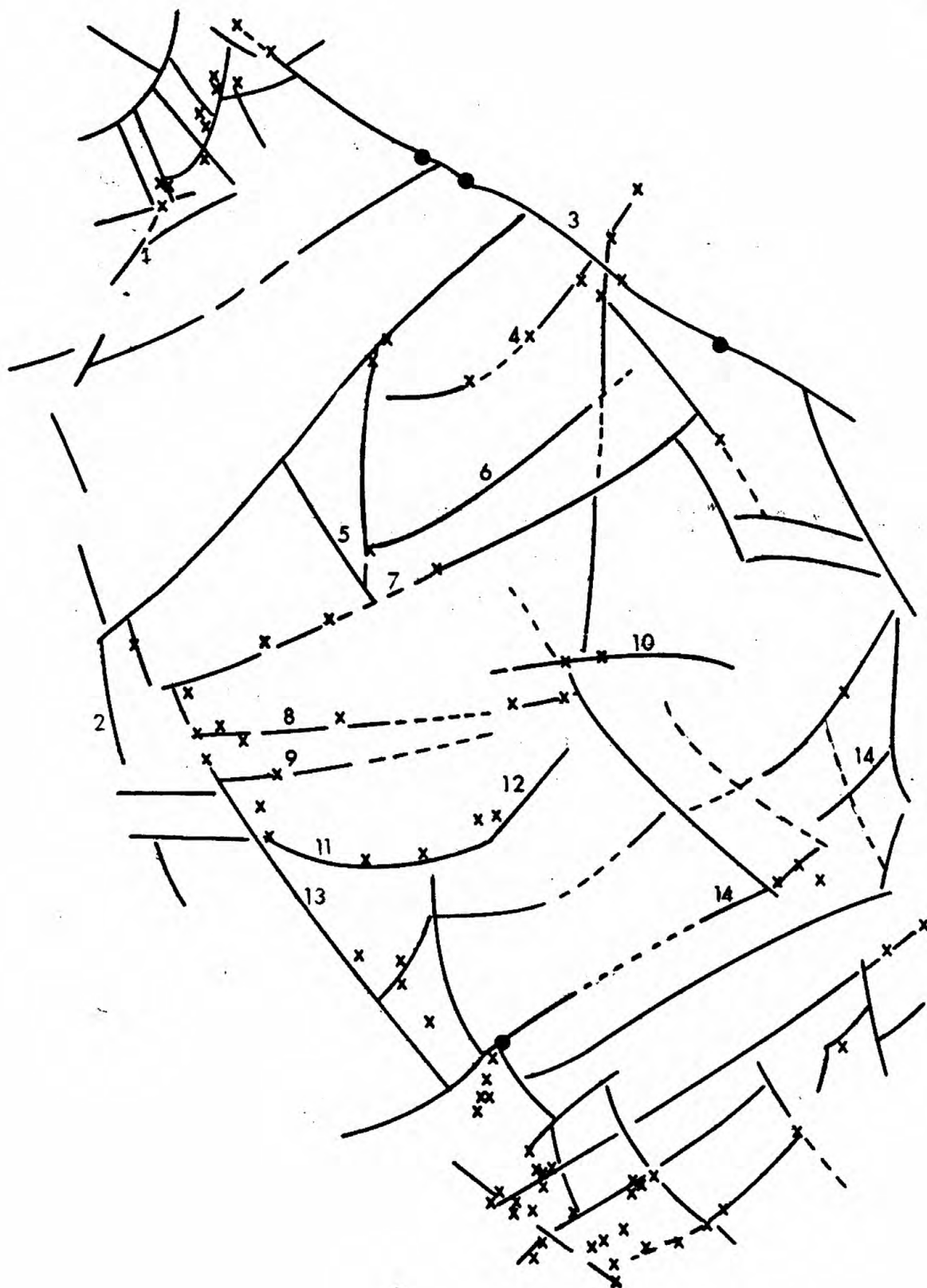


Fig. 1. Generally recognized lineaments of the western U. S.
 1, Cascade; 2, Mother Lode; 3, Lewis and Clark; 4, Transverse Porphyry Belt; 5, North Nevada Rift; 6, Snake River-Yellowstone; 7, Midas Trench; 8, Pancake-Towanta; 9, Warm Springs; 10, Uinta Arch; 11, Pahrnagat; 12, Wasatch Line; 13, Walker Lane; 14, Colorado Mineral Belt. Gravity base from Woolard and Joesting (1964). X's represent major copper porphyry deposits, solid circles represent other types of major ore deposits.

The largest of the porphyry systems are located at the intersection of two structural discontinuities. Examples are: Butte, Bingham, Yerington, Lights Creek, Ithaca Peak, Ray, Inspiration, Morenci, Bisbee, Pima, Esperanza, Twin Buttes, and Tyrone. A significant number of these are located along the gravity inflection which marks the margin of the Colorado Plateau.

Regional crustal composition can dictate the relative abundance of metals which accompany an igneous event. The known western limit of the Late Precambrian - Early Paleozoic continent strikes NNE across Nevada, roughly between 117° - 115° longitude (Burchfiel and Davis, 1972). This same zone was described as a metallogenic province boundary between a western province characterized by gold-silver-mercury-antimony, and an eastern province characterized by deposits of lead-zinc and peripheral gold-silver (Roberts, 1966).

Porphyry Copper Deposits and the Cascade Volcanic Arc

The Cascade volcanic arc in British Columbia and Washington coincides with a linear group of porphyry copper deposits. No deposit which has a potential greater than 50,000,000 tons of 0.5% Cu or more has a radiometric age greater than 22 m.y. (Armstrong et al., 1976). Radiometric ages of 22.0-6.2 m.y. are known for porphyry copper prospects in the arc, and the large solfataric field on Mt. Baker's dormant volcano contains sparse chalcopyrite (Hollister, 1978). Porphyry-type deposits are most common in the Cascade arc from 46° N to 51° N (Hollister, 1979). Calc-alkaline magmatism preceded, accompanied, and followed deposition of the porphyry copper deposits (Wise, 1970; McBirney, 1975). Young deposit ages and current geologic and geophysical data permit inferences to be made concerning porphyry copper formation, calc-alkaline magmatism and subduction in the Cascade volcanic arc.

That portion of the Cascade volcanic arc in which the porphyry copper deposits are found is distinct from many other arcs because the Cascade Range is not underlain by an active Benioff zone, nor is it fronted by a trench, nor does it have the gravity signature typical of active subduction zones.

Seismic activity in the Cascade arc and west, implies current tectonic activity. Offshore seismicity generally occurs on major right-lateral faults such as the Queen Charlotte, as well as on ridge systems. Specific active structures in the North American Plate are commonly identified as vertical strike-slip or dip-slip type faults (Milne et al., 1976). No epicenters deeper than 30 km have been found. Most epicenters occur within the Juan de Fuca Ridge, an active spreading center, or on transform faults normal to the ridge.

No characteristic Benioff array of epicenters, steeply dipping beneath the Cascade arc, has been found. Active faults east of the continental rise are part of a fault pattern typically developed during distensional tectonics.

Active subduction zones around the globe are characterized by linear gravity anomalies over the trench and parallel, linear gravity anomalies near the arc, some 100 km inland. The positive gravity anomaly is not present (Figure 2). Moreover, inspection of gravity for the Cascadia Plain fails to identify any linear negative feature that may be assigned the role of the trench low and no accompanying gravity positive is present to the east. Gravity configuration over both the Juan de Fuca and North American Plates seems to be typical of that developed over a Basin and Range tectonic setting. The gravity data support the interpretation of the seismic data that a distensional tectonic regime had developed and now persists over much of the Juan de Fuca and North American Plates. Note that major porphyry copper deposits are known only in the area characterized by distensional tectonics (Washington), but are not known where the gravity data support a subduction tectonic regime (southern Oregon). Similar gravity data from major copper porphyry provinces are needed to test if this type of mineralization is characteristic of this structural setting.

Atwater (1970) recognized the thick and flat-lying sedimentary accumulations, the lack of a trench at the base of the continental slope, and the absence of a Benioff zone. These features were attributed to a coupling of the North American plate with the Juan de Fuca Plate in the Tertiary. The coupling inhibited subduction in the Upper Tertiary during the period when the younger porphyry copper deposits formed. Upper Tertiary calc-alkaline magmatism of this period also developed in an arc that was free of subduction.

White and McBirney (1978) summarized available volumetric and compositional data from the Cascade Range. They interpret their data to indicate progressive depletion of an upper mantle source region by repeated partial melting at increasing depth. Therefore, the discrepancy in timing between plate movements and pulses of volcanic activity combined with the steady depletion of the magma's source region indicates no control on the magma generation process by external processes (e.g., subducted oceanic crust) for the last 22 m.y. Note that no porphyry copper deposit in Washington is older than 22 m.y.

Interpretation of regional summaries of the Cascade porphyries (Grant, 1969, 1976; Hollister, 1978) shows that deposits with highest Mo:Cu ratios are associated with intrusions that penetrated older, pre-Mesozoic crystalline crust. These include most deposits in the northern part of the province. Deposits with the highest Au:Cu ratios are associated with intrusions that penetrated mafic volcanic rocks. Deposits rich in molybdenum normally are poor in gold, and the reverse is also true.

The importance of crustal thickness and composition on controlling proportions and compositions of volcanic rocks in the calc-alkaline suite is also reflected in specific features of

porphyry ore deposits in other volcanic arcs. In general, island-arc deposits tend to have high Au and low Mo content (Kesler, 1972). The absence of Cu/Mo porphyry deposits in island arcs lacking sialic crust is more than coincidence.

Structural pre-disposition for localizing porphyry systems in the western United States is a valid concept for understanding emplacement of mineralizing systems in the Cascade volcanic arc of Washington. All known copper porphyry systems in Washington lie along a major NNE crustal discontinuity at intersections with NW trending lineaments as defined by the Bouguer gravity contours (Figure 2).

The NNE gravity discontinuity is coincident with the eastern margin of the Mesozoic Okanogan Highlands in north-central Washington and with the eastern margin of the Cascade volcanic province in south-central Washington. The NW-trending faults are second order distensional overprints and are expressed at the surface by post-Mesozoic strike slip fault zones. The result is a general NNE trend to the mineralization.

Conclusions

Porphyry copper deposits in Washington younger than 22 m.y. developed in a non-subduction tectonic setting. Detailed geologic and geochemical studies done in central Oregon discount any contribution by subduction to calc-alkaline magmas generated there. The porphyry copper deposits of Washington formed where a major NNE-trending crustal discontinuity is cut by NW-trending faults. Gravity data indicate that a Basin and Range structural setting occurs in western Washington. Similar tectonic settings controlled the location of major porphyry deposits in the western U.S. The lack of control by subduction on calc-alkaline magma generation in the northern Cascades indicates that the metals of the deposits were not derived from subducted oceanic crust, but are inferred to have been scavenged from the upper crust.

Acknowledgements

The Anaconda Copper Company kindly allowed the presentation and publication of this manuscript. Blair Hay typed the manuscript.

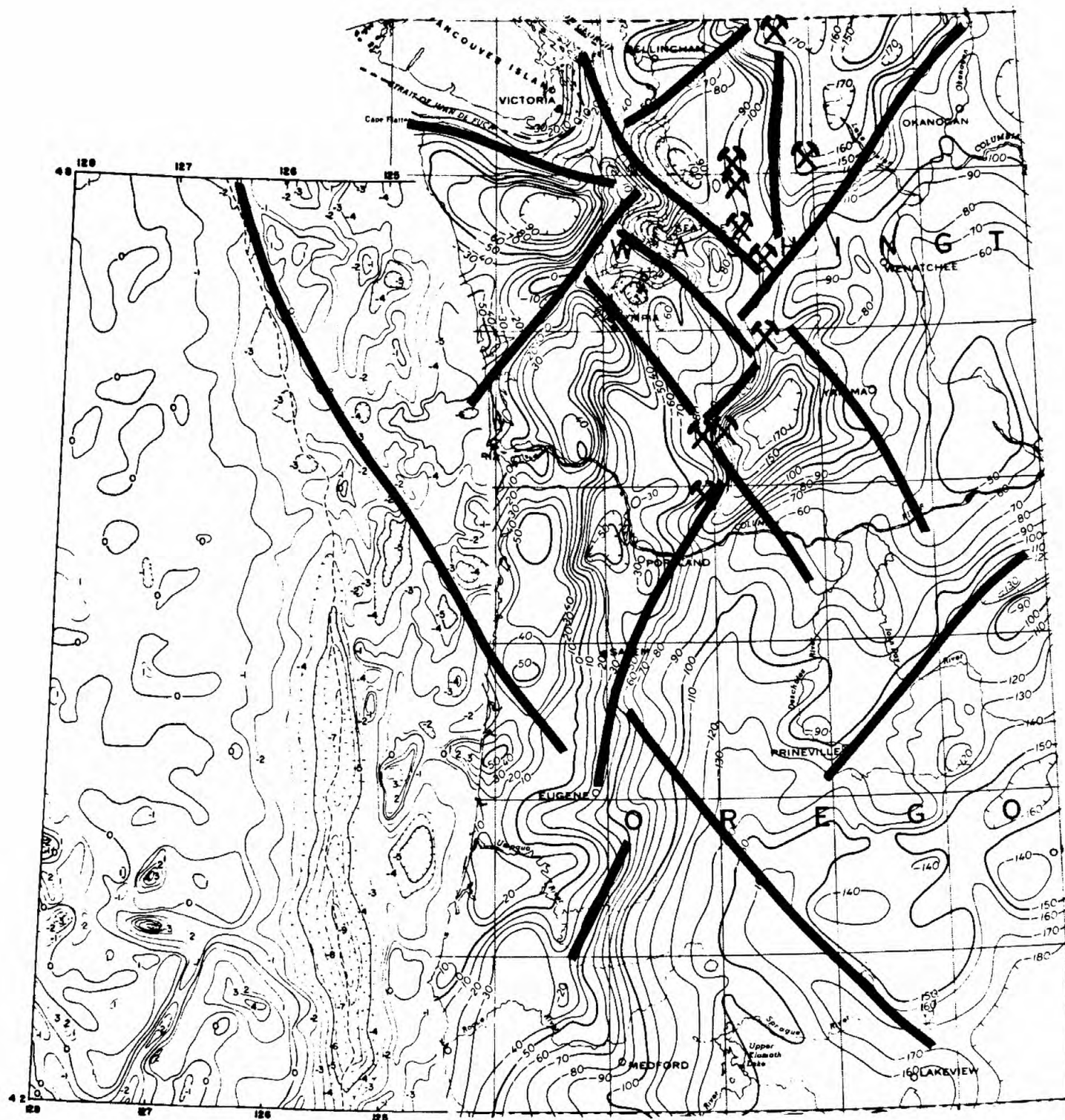


Fig. 2. Locations of porphyry copper deposits of Washington plotted on Bouguer gravity map of the U. S. (Woollard and Joesting, 1964), offshore gravity data are from Silver (1978). Mine symbols represent major copper porphyry deposits of the Pacific Northwest, heavy lines represent easily-recognized lineaments. See text for details.

REFERENCES

- Armstrong, R. L., Harakal, J. E., and Hollister, V. F., 1976, Late Cenozoic porphyry copper: Transactions, Can. Inst. Min. Metall. 85.
- Atwater, T. A., 1970, Implications of plate tectonics for the Cenozoic tectonics of western North America: Geol. Soc. America Bull. 81, p. 3513.
- Bradley, J., 1965, Intrusion of major dolerite sills: Trans. Roy. Soc. N. Z. Geol. 3, p. 27.
- Burchfield, B. C., and Davis, G. A., 1972, Structural framework and evolution of the southern part of the Cordilleran orogen, western United States: Am. J. Sci. 272, p. 97.
- Carr, M. J., Rose, W. I., and Mayfield, D. G., 1979, Potassium content of lavas and depth to the seismic zone in Central America: J. Volc. Geothermal Rsch. 5, p. 387.
- Cawthorn, R. G., 1977, Petrological aspects of the correlation between potash content of orogenic magmas and earthquake depth: Min. Magazine 41, p. 173.
- Cawthorn, R. G., and O'Hara, M. J., 1976, Amphibole fractionation in calc-alkaline magma genesis: Am. J. Sci. 276, P. 309.
- Dickinson, W. R., and Hatherton, T., 1967, Andesitic volcanism and seismicity around the Pacific: Science 157, p. 801.
- Dickson, F. W., Rye, R. O., and Radtke, A. S., 1979, The Carlin gold deposit as a product of rock-water interactions: Nevada Bur. Mines & Geology Rpt. 33, p. 101-108.
- Grant, A. R., 1969, Chemical and Physical Controls for Base Metal Deposition in the Cascade Range, Bulletin No. 58, Washington Div. of Mines and Geology.
- Grant, A. R., 1976, Mineral Resource Analysis Study on US Forest Service Land, Washington, Contract No. 004724N, US Forest Service, Washington, D.C.
- Hollister, V. F., 1978, Geology of the Porphyry Copper Deposits of the Western Hemisphere: Publ. by the Society of Mining Engineers of the American Institute of Mining, Metallurgical and Petroleum Engineers Inc., 219 p.
- Hollister, V. F., 1979, Porphyry copper-type deposits of the Cascade volcanic arc, Washington: Minerals Sci. Engng. 11, No. 1, p. 22.
- Jerome, S. E., and Cook, D. R., 1967, Relation of some metal mining districts in the western United States to regional tectonic environments and igneous activity: Nevada Bur. Mines Bull. 69.

- Kesler, S. E., 1972, Copper, molybdenum, and gold abundances in porphyry copper deposits: Econ. Geol. 67, p. 106.
- McBirney, A. R., 1969, Compositional variations in Cenozoic calc-alkaline suites of Central America: Oregon Dept. Geol. Min. Ind. Bull. 65, p. 185.
- McBirney, A. R., 1975, Volcanic evolution of the Cascade Range, Abstracts, Geological Society of America, Vol. 7, p. 1192.
- Milne, W. G., Hyndman, R. D., Lee, K., Riddibough, R. P., and Rogers, G. D., 1976, Map, seismicity of western Canada: Earth Physics Branch MS.
- Roberts, R. J., 1966, Metallogenic provinces and plate tectonics: Nevada Bur. Mines Rpt. 13, Pt. A, p. 47.
- Robyn, T. L., 1977, Geology and petrology of the Strawberry Volcanics, NE Oregon: PhD. Dissertation, Univ. of Oregon, Eugene, OR, 197 p.
- Robyn, T. L., 1979, Miocene Volcanism in eastern Oregon: An example of calc-alkaline volcanism unrelated to subduction: J. Volc. Geoth. Roch. 5, p. 149.
- Robyn, T. L., and Hollister, V. F., in press, Origin of calc-alkaline magmas associated with porphyry copper deposits: Proc. Int. Union Geol. Aci. Symp., Mexico City, February 4-6, 1980, in press.
- Silver, E. A., 1978, Geophysical studies and tectonic development of the continental margin off the western United States, lat 34° to 48°N: Geol. Soc. America Mem. 152, p. 251.
- Taylor, H. P., Jr., 1973, $^{18}\text{O}/^{16}\text{O}$ evidence for meteoric-hydrothermal alteration and ore deposition in the Tonopah, Comstock Lode, and Goldfield Mining Districts, Nevada: Econ. Geology 68, p. 747.
- Tooker, E. W., 1979, Metal provinces and plate tectonics: Nev. Bur. Mines Geol. Rpt. 33, p. 33.
- White, D. E., 1965, Metal contents of some geothermal fluids: Symposium on problems of ore deposition 2, p. 432.
- White, C. M., and McBirney, A. R., 1978, Some quantitative aspects of orogenic volcanism in the Oregon Cascades: Geol. Soc. America Mem. 152, p. 369.
- Wise, W. S., 1970, Cenozoic volcanism in the Cascade Mountains of southern Washington: Bull. Wash. Div. Mines Geol. 60, 45 p.

Woollard, G. P., and Joesting, H. R., 1964, Bouger gravity anomaly map of the United States: U. S. Geol. Survey Map G64121.

Wyllie, P. J., 1970, Ultramafic rocks and upper mantle: In Fiftieth Anniversary Symposia (editor B.A. Morgan), Min. Soc. America Sp. P. No. 3.

Geology and ore deposits of the St. Helens mining district,
Washington

R. P. Ashley, U.S. Geological Survey

R. C. Evarts, U.S. Geological Survey

GEOLOGY AND ORE DEPOSITS OF THE ST. HELENS MINING DISTRICT,
WASHINGTON

ASHLEY, R. P., and EVARTS, R. C., U.S. Geological Survey, Menlo
Park, CA 94025

The St. Helens mining district includes 35 or more small copper-lead-zinc-gold-silver vein deposits scattered through an area 10-15 km in diameter centered about 15 km NNE of Mount St. Helens, in the southern Washington Cascade Range. Most of the veins occur in a composite stock of probable Miocene age that intrudes andesites, rhyolites, tuffs, and volcanoclastic rocks of Eocene age (Ohanapocosh Fm.). The earliest plutonic phase is a seriate granodiorite that forms the north end of the stock. The next phase is a granodiorite porphyry that forms a partial shell around the south side of the seriate granodiorite. A seriate quartz diorite then intruded the granodiorite porphyry, forming the main mass of the south end of the stock. Finally, quartz monzonite, quartz monzonite porphyry, and granite porphyry, invaded the east side of the previous intrusions and produced numerous dikes scattered through the entire pluton and nearby wallrocks.

Mineralization includes a cluster of NNW-trending veins in quartz diorite, quartz monzonite, and hornfels at the southeast margin of the stock. A second cluster of veins with diverse orientations appears in the middle of the stock, in quartz diorite. The Earl deposit, a porphyry copper ore body currently being explored by Duval Corporation, is located near the east end of this mineralized area. Hydrothermal tourmaline is most common in this part of the stock. The north end of the stock has few vein occurrences, but widespread argillization and silicification suggest that at least two major hydrothermal systems in addition to the one that formed the Earl deposit affected the rocks, mainly at deeper levels.

(Courtesy of the Geological Society of America, 1980)

Geology and mineralization of the Washougal mining district,
Skamania County, Washington

Alexander Shreiner, Jr., Union Oil Company of California
R. J. Shepard, Anaconda Copper Company

GEOLOGY AND MINERALIZATION OF THE WASHOUGAL
MINING DISTRICT, SKAMANIA COUNTY, WASHINGTON

Schriener, Jr., Alexander, Union Oil Company of California, Geothermal Division, P.O. Box 6854, Santa Rosa, CA. 95406; and Shepard, Richard J., Anaconda Copper Company, 555 17th Street, Denver, Co. 80217.

The Washougal Mining District and the associated Silver Star plutonic complex are the southernmost mineral district and intrusion of the Washington Cascades (Figure 1). The district has produced only \$573.00 in copper and silver since 1903 (Moen, 1977). However, the presence of hydrothermal alteration and base metal mineralization, porphyritic intrusions, and breccia pipes typical to many porphyry copper-molybdenum deposits signifies an above average exploration potential for the area.

Bedrock in the district consists of gently folded basalt and andesite flows, and volcanoclastic breccias of the East Fork formation. Flat-lying basalt and basaltic andesite flows of the Skamania formation overlie the East Fork units unconformably. These two informally named formations are of probable late Eocene to early Miocene age and are intruded by the Silver Star plutonic complex (Figure 2). The intrusion consists of small outlying plugs or stocks of intrusive andesite, diorite, and granodiorite, and a larger mass containing quartz diorite, granodiorite, granodiorite porphyry, quartz diorite porphyry, and granite aplite, in probable order of emplacement. At least 30 tourmaline-bearing breccia pipes are associated primarily with the granodiorite phase. They were probably formed by late-stage magmatic fluids. Chemical analyses of twenty-one intrusive rock samples are listed in Table 1. The phases of the plutonic complex show chemical similarities with the calc-alkalic rock suite by systematic distributions on partial Harker variation diagrams (Figure 3), and AFM and NKC ternary diagrams (Figure 4).

The rocks of the Washougal District were gently folded and fractured by a series of northwest trending folds and faults (Hammond and others, 1977, Figure 5). The shape of the pluton suggests emplacement was influenced by deep seated regional structures. Correlation between joint plane orientations and lineaments determined from aerial photographs suggest that pre-existing north-northeast and northwest regional structures controlled the emplacement of the plutonic complex and localized the mineralization (Figure 6).

The mining district contains both epithermal vein and breccia pipe-type mineralization. Vein deposits exist primarily in the south and west parts of the district and the breccia

mineralization is found in the north (Moen, 1977). Metalization is present as sulfides of copper, lead, zinc, and molybdenum with minor amounts of iron, silver, gold, and tungsten. The district is marked by a crude zonation of metals. Anomalously high concentrations of copper and molybdenum are broadly antipathetic with those of silver, lead, and zinc.

The hydrothermal alteration assemblages display an irregular distribution pattern throughout the district. A widespread aureole of propylitic alteration (chlorite + epidote + calcite + quartz, albite, magnetite, zinc) occurs around the main granodiorite intrusion. The phyllic assemblage (quartz + sericite + pyrite + tourmaline, copper, silver) is restricted to breccia pipes, metalized veins, and shear zones. Mineralized breccia pipes in the northern half of the district contain tourmaline (quartz + tourmaline + pyrite) and potassic (biotite + potassium feldspar + chalcopyrite + tourmaline, actinolite, molybdenum, silver, tungsten) alteration assemblages.

Based on the models of Sillitoe (1973), Field and others (1974), Gilbert and Lowell (1974), and Gilmour (1977), the Washougal Mining District is considered to be a porphyry copper-molybdenum system that is eroded to a depth above the level of pervasive disseminated mineralization. The inferred high level of exposure for the Silver Star plutonic complex is consistent with 1) the numerous stocks, cupolas, and dikes of the complex; 2) the predominately fracture-controlled phyllic alteration assemblages; 3) the occurrence of peripheral vein-type mineralization 4) the irregular zonations of hydrothermal sulfide and alteration mineral assemblages and 5) the presence of mineralized breccia pipes. The potential for future base-metal discoveries within the mining district is considered good.

Acknowledgements: This study is part of two masters graduate programs completed at Oregon State University under Dr. Cyrus W. Field.

REFERENCES:

- Field, C.W., Jones, M.B., and Bruce, W.R., 1974, Porphyry copper-molybdenum deposits of the Pacific Northwest: A.I.M.E., Trans., v.255, p. 9-22.
- Gilbert, J.M., and Lowell, J.D., 1974, Variations in zoning pattern in porphyry ore deposits: Can. Inst. Mining Metall., v.67, no.742, p.99-104.
- Gilmour, P., 1977, Mineralized intrusive breccias as guides to concealed porphyry copper systems: Econ. Geol., v.72, p.290-303.

- Hammond, P.E., Bentley, R.D., Brown, J.C., Ellingson, J.A., and Swanson D.A., 1977, Volcanic Stratigraphy and Structure of the Southern Cascade Range, Washington, in Brown, E.H., and Ellis, R.C., eds; Geological excursions in the Pacific Northwest: Geol. Soc. America 1977 Annual Meeting field trip guide; Western Wash. Univ., Bellingham, Washington, p.127-169.
- Moen, W.S., 1977, St. Helens and Washougal Mining district of the Southern Cascades of Washington: Wash. Dept. Natural Res. Infor. Cir. 60, 71p.
- Schriener, A., Jr., 1978, The geology and mineralization of the north part of the Washougal Mining District, Skamania County, Washington: Unpub. M.S. Thesis, Ore. St. Univ., 135p.
- Shepard, R.J., 1979, Geology and mineralization of the Southern Silver Star Stock, Washougal Mining District, Skamania County, Washington: Unpub. M.S. Thesis, Ore. St. Univ., 113p.
- Sillitoe, R.H., 1973, The tops and bottoms of porphyry copper deposits: Econ. Geol., v.68, p.799-815.

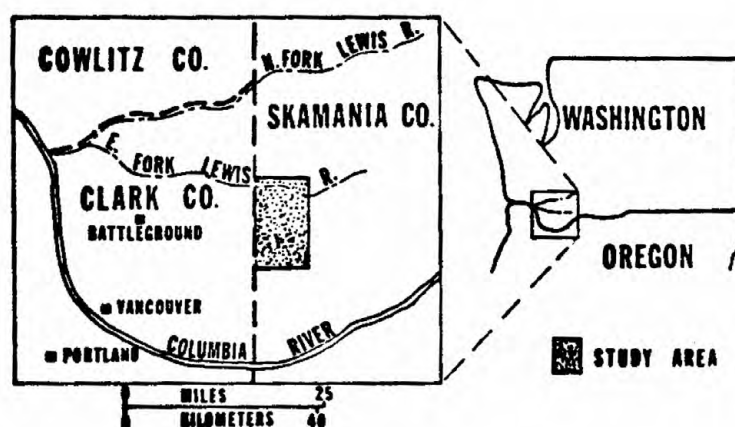


Figure 1: Index Map

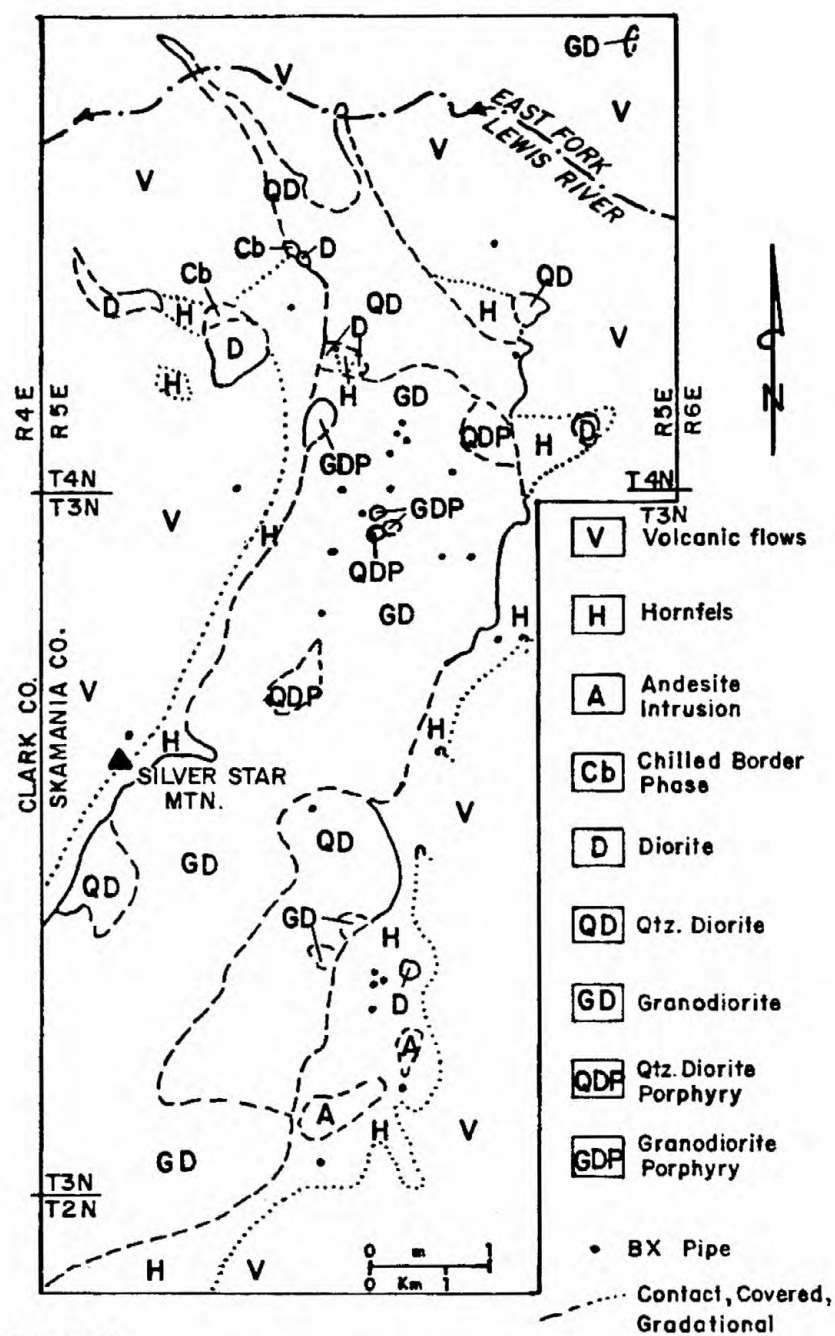


Figure 2:
Preliminary Geology of the Silver Star Plutonic Complex

	SILVER STAR PLUTONIC COMPLEX		SILVER STAR PLUTONIC COMPLEX		SILVER STAR PLUTONIC COMPLEX		SILVER STAR PLUTONIC COMPLEX		SILVER STAR PLUTONIC COMPLEX		SILVER STAR PLUTONIC COMPLEX		SILVER STAR PLUTONIC COMPLEX		SILVER STAR PLUTONIC COMPLEX		SILVER STAR PLUTONIC COMPLEX		SILVER STAR PLUTONIC COMPLEX		SILVER STAR PLUTONIC COMPLEX	
	878-5 ₂	882 ₁	878-97 ₂	134 ₁	Basic Phase 3	118 ₁	NO-4 ₁	878-70 ₂	878-124 ₂	878-816 ₂	309 ₁	88-1 ₁	878-120 ₂	835 ₁	205 ₁	878-94 ₂	Acid Phase 3	834-A ₁	881-A ₁	878-116 ₂	838-B ₁	
SiO ₂	54.9	52.6	50.5	56.5	58.1	58.2	58.2	58.3	60.3	58.9	59.1	61.7	61.8	64.0	63.2	65.9	65.9	68.0	66.5	67.2	72.4	
TiO ₂	1.2	1.25	0.6	1.0	0.6	0.8	1.0	1.1	0.9	0.8	1.0	0.8	1.0	0.98	0.65	0.8	0.45	0.45	0.45	0.6	0.4	
Al ₂ O ₃	16.1	18.2	15.9	19.2	16.5	18.0	16.7	17.0	17.2	16.8	16.1	17.3	15.9	14.0	14.6	14.9	15.72	13.3	16.7	14.5	11.0	
Fe ₂ O ₃	1.7	—	2.7	—	—	—	—	3.2	2.9	2.4	—	—	2.4	—	—	1.6	1.11	—	—	1.3	—	
FeO	5.8	—	4.5	—	—	—	—	3.1	3.4	4.2	—	—	3.4	—	—	2.6	3.05	—	—	2.3	—	
FeO as Total Fe	—	0.6	—	6.7	6.7	6.3	7.6	—	—	—	6.4	5.7	—	4.3	5.2	—	—	4.0	4.0	—	3.0	
MgO	4.9	5.5	3.7	3.5	4.9	4.0	3.0	3.6	3.2	3.6	4.3	2.7	2.7	1.8	1.8	1.9	2.39	2.4	1.5	1.8	0.4	
CaO	7.8	0.5	6.8	8.6	7.3	6.6	5.8	6.6	6.2	4.0	6.6	5.3	5.1	4.6	4.2	4.9	4.78	4.2	4.2	3.9	1.7	
MnO	2.3	3.9	3.2	4.3	3.3	4.2	4.0	4.3	4.0	4.4	5.5	4.3	3.6	4.4	4.4	3.5	3.62	4.3	4.3	3.6	3.8	
K ₂ O	1.3	0.6	1.6	0.6	0.6	1.15	1.0	1.4	0.9	1.7	0.4	2.0	1.9	2.0	2.25	2.5	1.94	2.4	2.0	2.5	4.2	
Na ₂ O	0.14	—	—	—	0.17	—	—	0.14	0.11	0.092	—	—	0.1	—	—	0.085	0.06	—	—	0.049	—	
H ₂ O	1.9	—	—	—	0.7	—	—	0.4	0.5	1.2	—	—	0.6	—	—	0.4	0.76	—	—	0.3	—	
TOTAL	97.04	99.15	97.5	99.8	98.0	99.25	98.10	99.14	99.61	98.092	99.8	99.8	98.5	95.85	100.0	98.885	98.96	98.75	99.85	97.749	98.78	
Ag	0.7	0.3	-0.2	0.3	—	0.7	0.3	0.4	0.3	0.3	0.4	0.3	0.3	0.3	0.3	0.4	—	0.4	0.5	0.3	0.9	
Cu	130	45	95	95	—	55	75	50	18	390	670	50	125	12	50	75	—	100	1670	95	40	
Pb	2	1	4	2	—	1	2	2	1	2	2	2	1	2	2	2	—	2	3	3	3	
Zn	25	11	5	7	—	7	8	20	8	25	6	10	7	9	30	20	—	5	8	4	20	
Sn	75	30	60	35	—	35	20	65	30	60	25	20	30	20	20	45	—	12	15	30	10	

1. From Silver Star, 1970. 2. From Silver Star, 1970. 3. From Silver Star, 1970.

Table 1: Major oxide and trace element analyses for intrusive rocks from the Silver Star Plutonic Complex

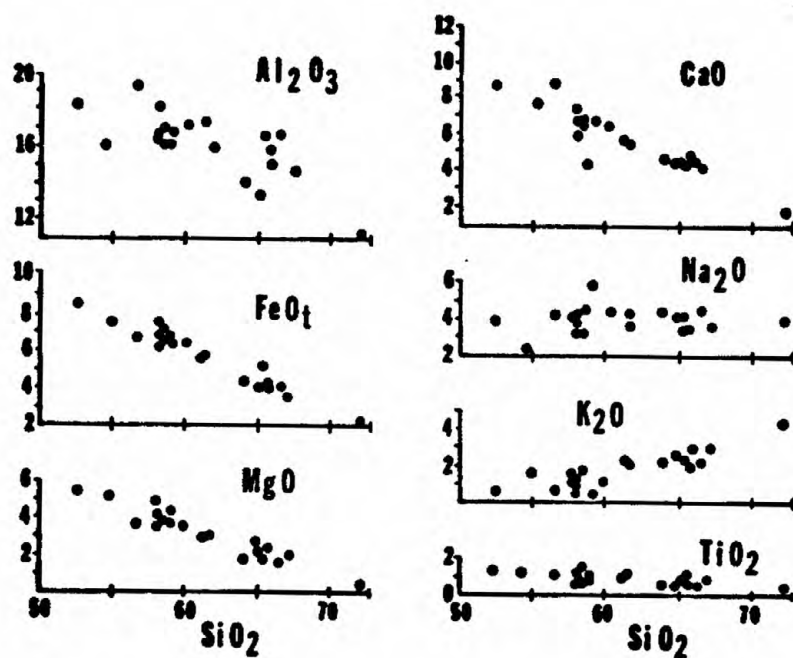


Figure 3: Partial Harker variation diagram for intrusive rocks

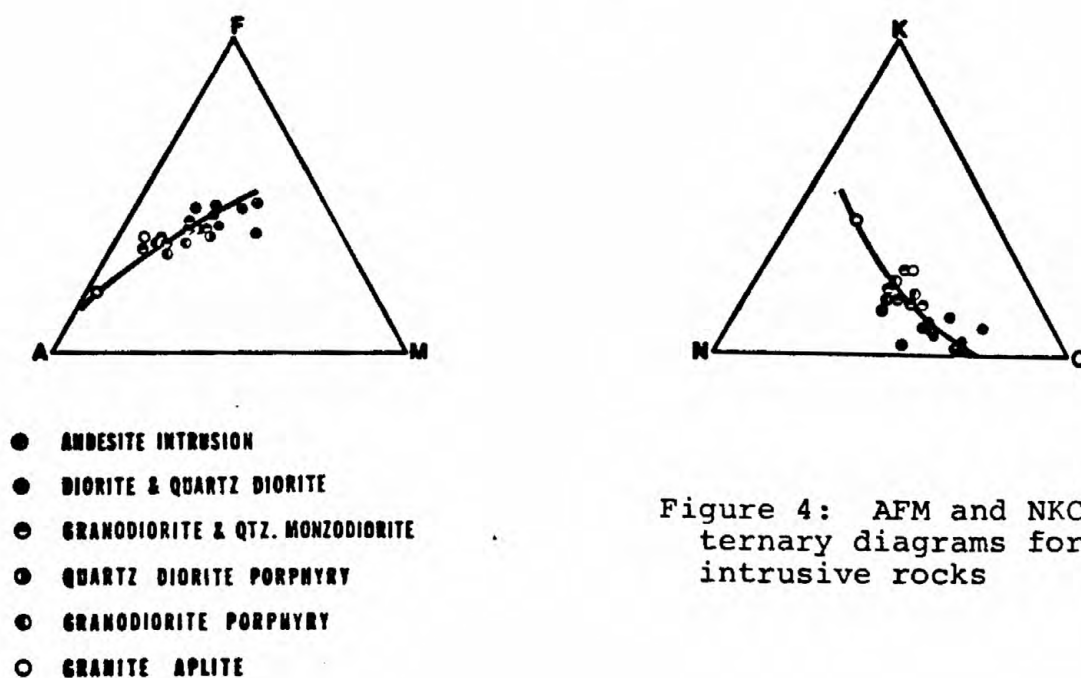


Figure 4: AFM and NKC ternary diagrams for intrusive rocks

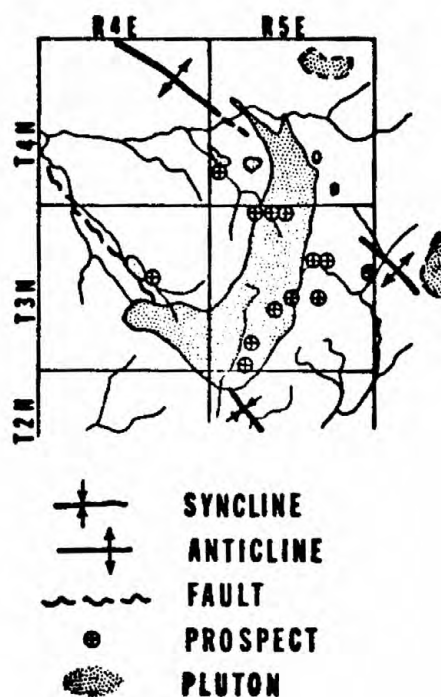


Figure 5:

Regional Structure of
 the Washougal Mining
 District (after Hammond
 and others, 1977, and
 Moen, 1977).

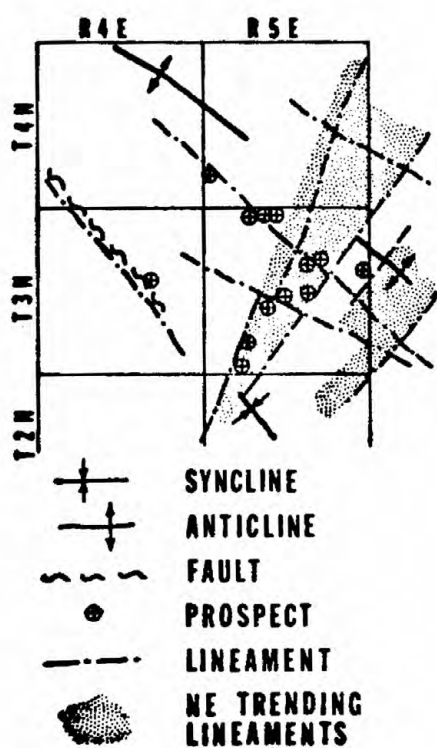


Figure 6:

Lineament analysis for
 Washougal Mining District

New concepts of regional geology and uranium exploration
in northeastern Washington

E. S. Cheney, University of Washington

NEW CONCEPTS OF REGIONAL GEOLOGY AND URANIUM EXPLORATION IN NORTHEASTERN WASHINGTON

CHENEY, Eric S., Department of Geological Sciences, AJ-20,
University of Washington, Seattle, Washington 98195.

INTRODUCTION

Uranium deposits in northeastern Washington (Figure 1) include Rössing-type deposits in the metamorphic rocks and the secondary types shown in Figure 2. No announcement of a commercial uranium discovery has been made since 1975. The purposes of this paper are to suggest how new geological concepts that have evolved since 1975 might be useful in discovering previously unknown uranium deposits and to stress that our knowledge of the regional geology is still too incomplete to efficiently explore for deposits related to Tertiary unconformities and in Tertiary strata.

The new geological concepts are (1) the demonstration by Pearson and Obradovich (1977) that the Tertiary formations are of regional extent and (2) my suggestions (Cheney, 1980b) that (a) the high grade metamorphic rocks are not Mesozoic gneiss domes, as commonly supposed (Okulitch and others, 1977; Fox and others, 1976, 1977), but probably are pre-Paleozoic basement rocks in the cores of Tertiary anticlines, (b) the supracrustal rocks, ranging age from Beltian to Tertiary commonly are separated from the basement by low-angle faults, and (c) the present distribution of the Tertiary rocks is due to their preservation in structural lows rather than in numerous basins of deposition.

The reader is referred to Cheney (1980b) for a more detailed development of the geological concepts; only a brief review will be given here. This will be followed by a discussion of the pegmatites in the Kettle dome, the potential for unconformity and structural traps (Figure 2) marginal to the domes, and, lastly, a discussion of stratigraphic and unconformity traps in or associated with Tertiary strata.

GEOLOGICAL SETTING

The uranium potential of northeastern Washington is related to the nature of the metamorphic rocks and Tertiary sedimentary and volcanic rocks outlined on Figure 2. A more detailed map of the regional geology occurs as Figure 3 in Cheney (1980b). The regional geology is dominated by three metamorphic core complexes or domes. Figure 2 of Cheney (1980b) is a reconnaissance geological map of the Kettle dome.

The Kettle dome is underlain by sillimanite-grade rocks of the Tenas Mary Creek sequence. Two >800 m-thick sheets of augen gneiss occur above and below feldspathic quartzite, biotitic gneiss, and minor marble. Polyphase deformation (including mylonites) and slightly uraniferous aplitic to pegmatitic bodies are common. Cataclasis post-dates the mylonitization, and the Tenas Mary Creek rocks appear to be in tectonic contact with overlying late Paleozoic phyllitic rocks.

Foliation and contacts in the Tenas Mary Creek rocks rarely dip >25° and define the flat-topped dome (which is >65 km long north-south, 27 km wide, and has about 3 km of structural relief). The Okanogan dome consists primarily of orthogneisses and granitic plutons of Mesozoic(?) age. Rocks in the flat-topped Spokane dome are similar to the Tenas Mary Creek and may be pre-Beltian.

The Sanpoil syncline between the Kettle and Okanogan domes and a syncline on the northeastern margin of the Kettle dome contain Eocene rocks. Because the axes and structural reliefs of the Okanogan dome, the Sanpoil syncline, and the Kettle dome are similar, the present structural relief (as opposed to the internal structure and high-grade metamorphism) of the Kettle dome probably is due to post-Eocene folding. The gently synformal Tertiary Newport fault straddling the Washington-Idaho border may be a related structural feature. Other low-angle faults, three of which cut Tertiary rocks, occur between the domes.

The low-angle faults commonly are cataclastic zones more than 100 m thick. Cataclasis evidently occurred as the basement of Mesozoic and Tertiary batholiths and pre-Beltian(?) metamorphic rocks became decoupled from overlying Precambrian to Tertiary layered rocks. Whether this decoupling represents one or more zones of Tertiary décollement of regional extent is not yet known. These faults do not appear to cut the Columbia River basalt. Arching of the Columbia River basalts over the northerly trending Cascade Mountains to the west may indicate that the smaller northerly trending Okanogan, Kettle and Spokane domes owe their present structural relief to doming younger than the Columbia River basalts. Where the intervening synclines, such as the Sanpoil syncline, are bounded by domed, low-angle faults, they have been called grabens (Republic "graben" of Figure 1).

RÖSSING-TYPE DEPOSITS IN THE KETTLE DOME

Most of the uraniferous pegmatites in the Kettle dome appear to be spatially related to the lower sheet of orthogneiss, labelled GPPG in Figure 2 of Cheney (1980b). Pegmatites in the orthogneiss commonly have dimensions of a meter or two, usually grade outward

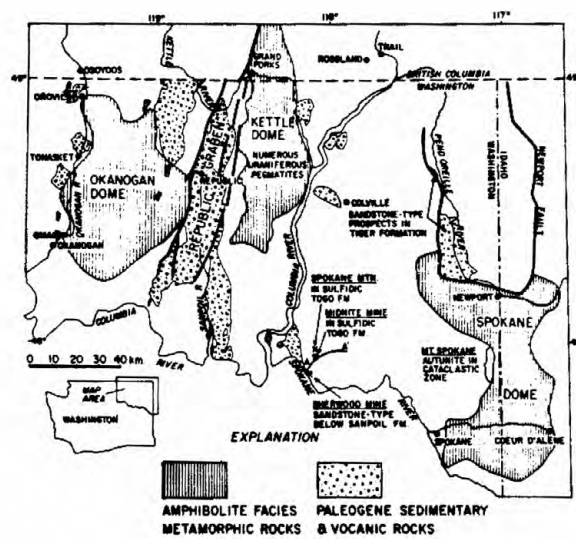


Figure 1

INDEX MAP

into the orthogneiss, and rarely are more radioactive than the gneiss. Pegmatites in the sillimanite-bearing biotitic schists and gneisses above and below the orthogneiss appear to be more radioactive than those in the 650 m-thick quartzite above the gneiss. Most of the pegmatites are concordant or nearly so. The largest pegmatites, with horizontal dimensions up to a hundred meters and with thicknesses up to tens of meters, occur in the 650 m-thick quartzite overlying the orthogneiss. The amount of radioactivity generally appears to be inversely proportional to the size of the pegmatitic body.

The uranium-bearing minerals have not yet been identified, but otherwise, the pegmatites are biotitic and range from aplitic to pegmatitic like those of Rössing described by Berning and others (1976). However, the potential for Rössing-type deposits in the Kettle dome appears to be slight for the following reasons: (1) Few localities exist in which the pegmatites constitute half (or more) of the rock. (2) Rössing is economic, in part, because 40% of the uranium values appear to be due to supergene enrichment in an arid climate (Cheney, 1980a), but the climate in northeastern Washington is sufficiently humid and Pleistocene glaciation was sufficiently recent that the probability of such enrichment is slight. (3) Virtually all of the pegmatites are boudinaged; this metamorphism (and later cataclasis in some areas) may have leached uranium minerals that originally were along the grain boundaries of the silicate minerals.

Radioactive pegmatites also occur in the amphibolites along the eastern margin of the dome. Although these pegmatites commonly are more radioactive than those associated with the GPPG orthogneiss, they are more widely spaced and rarely more than a meter or two thick.

SECONDARY URANIUM DEPOSITS

The true significance of the uraniferous pegmatites of the Kettle and other domes may be that they could have provided uranium for subsequent concentration in the types of secondary uranium traps shown in Figure 2. The stratigraphic and unconformity deposits are well known types of deposits. The structural variant proposed in Figure 2 may exist along the margins of the domes. Mineralogically, all three types of deposits are pyrite (or pyrrhotite) deposits with smaller, but commercially interesting amounts of uranium. Granger and Warren (1969) showed that under limited conditions of oxidation, sulfide minerals oxidize not to sulfate but to sulfite, that this sulfite disproportionates to sulfate and bisulfide ions, and that the bisulfide ion effectively reduces soluble hexavalent uranium to insoluble quadravalent uranium minerals. Thus, any oxidizing sulfide deposit is a potential geochemical trap for uranium.

STRUCTURAL TRAPS

The metamorphic core complexes are rimmed, at least locally, by low-angle faults (Cheney, 1980b). These faults might be the sites of the type of structural trap shown in Figure 2. Thus, any evidence of sulfidic deposits or of radioactivity along the low-angle faults is significant. Wright (1949) suggested that the epithermal gold mineralization at Republic is related to the Bacon Creek fault. Miller (1974) described a part of the Newport fault as being pyritic or pyrrhotitic. Weissenborn and Weiss (1976) noted that most of the autunite along the western side of the Spokane dome occurs in flat faults in a cataclastic zone. Thus, known and inferred faults marginal to the metamorphic core complexes are worthy of exploration.

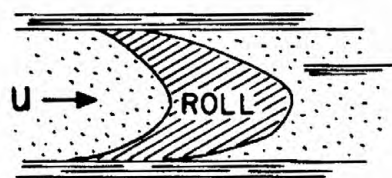
PROTEROZOIC UNCONFORMITY TRAPS

Several of the world's giant uranium deposits occur as veins beneath and within middle Proterozoic strata unconformably overlying graphitic and sulfidic lower Proterozoic metasedimentary rocks (Derry, 1973; Langford, 1978). Two such favorable localities may occur in northeastern Washington. The middle Proterozoic Beltian rocks are in contact with high-grade metamorphic rocks along the northeastern edge of the Spokane dome (Cheney, 1980b, Figure 3). Beltian rocks also appear to overlie the metamorphic rocks of the southern portion of the Spokane dome; if this contact is not a low-angle fault, it is a Proterozoic unconformity. Exploration along the southern edge of the Spokane dome will be hampered by overlying Columbia River basalt and the urban area of Spokane.

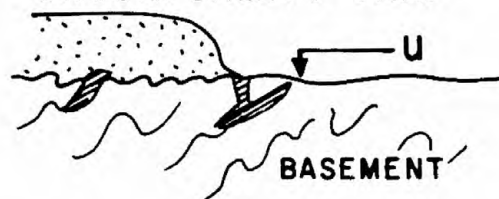
STRATIGRAPHIC TRAPS

Exploration for stratigraphic deposits is hampered by an inadequate understanding of the Tertiary stratigraphy. Although Pearson and Obradovich (1977) recognized that the Tertiary strata and volcanic rocks are of regional extent, they adhered to the

STRATIGRAPHIC TRAP



UNCONFORMITY TRAP



STRUCTURAL TRAP

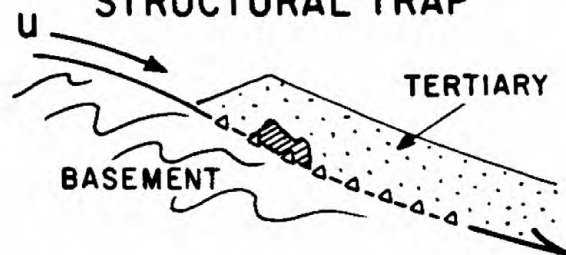


Figure 2

TYPES OF SECONDARY URANIUM TRAPS

concept that the formations were deposited in local basins. Conversely Cheney (1980b) suggested that the Tertiary formations are preserved in structural lows. The facies control of stratigraphic deposits is widely appreciated (Cheney and Trammell, 1973). However, a geologist who believes that the formations are of local extent is likely to conduct a different exploration program than the geologist who believes that the formations and their facies are of regional extent.

A number of stratigraphic uranium prospects have been drilled in the Tertiary Tiger formation of the Pend Oreille valley. Whether the Tiger formation and its facies are of regional extent is not known, but this possibility probably has not been considered, especially in exploration programs initiated prior to Pearson and Obradovich's paper (1977). Significantly, the Tiger formation contains different kinds of clasts in various areas, and Miller (1974) has suggested that the formation may represent deposition during more than one epoch of the Tertiary. Locally the Tiger formation rests upon the Sanpoil dacitic rocks (Pearson and Obradovich, 1977). However, if the Tiger were deposited in more than one epoch, one might speculate that the arkosic portion is correlative with the O'Brien Creek or some other formation below the Sanpoil; whereas, the part containing volcanic clasts might be equivalent to part of the Klondike Mountain formation, which overlies the Sanpoil. With the present lack of data other interpretations are possible. Thus, an evaluation of the uranium potential of the Tiger may be critically dependent upon whether two or more formations exist, and whether the uraniferous interval or facies in the Pend Oreille valley occur elsewhere in northeastern Washington.

The stratigraphic deposit at the Sherwood mine occurs in a conglomerate (Figure 3) that was thought to be the basal unit of the Gerome andesite (Becraft and Weiss, 1963; Weissenborn and Moen, 1974). Pearson and Obradovich (1977) showed that the Gerome is correlative with the Sanpoil and suggested that name Gerome be abandoned. In the Sherwood mine the mineralized conglomerate is overlain by up to a hundred meters of unmineralized arkosic and tuffaceous sandstones with interbedded lignitic siltstones. Eikelberg (1979) suggested that the unmineralized sandstones and siltstones unconformably overlie the mineralized conglomerate. Thus, instead of a single formation, previously called Gerome, three formations may exist (Figure 3). The volcanic rocks apparently are equivalent to the Sanpoil. The unmineralized sandstones and siltstones resemble, at least superficially, and may be equivalent to, the O'Brien Creek formation described by Muessig (1976) and by Pearson and Obradovich (1977). If so, the mineralized conglomerate may be an older, heretofore unrecognized, unit. Between the unmineralized unit and the Columbia River basalt is a lacustrine unit about 6 meters thick of uncertain age (Eikelberg, 1979), which is not shown in Figure 3.

If the mineralization at the Sherwood mine does occur in a heretofore unrecognized unit below the O'Brien Creek formation, previous prospecting in presumed "Gerome"-equivalent rocks (O'Brien Creek and Sanpoil formations) was of limited value. Clearly, studies of the Tertiary stratigraphic relationships in the Sherwood area and any correlation of the units with parts of the Tiger formation are of more than academic interest.

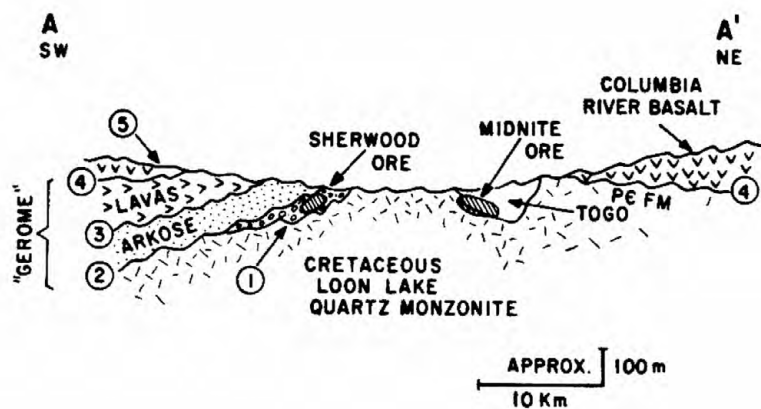


Figure 3

SCHEMATIC CROSS SECTION THROUGH THE SHERWOOD AND MIDNITE URANIUM MINES

The section is along A - A' of Figure 1. The sedimentary and volcanic units are Tertiary. The circled numbers refer to unconformities.

PHANEROZOIC UNCONFORMITY TRAPS

Pitchblende deposits in the Proterozoic Togo argillite and adjacent Cretaceous Loon Lake quartz monzonite occur at the Midnite mine (Nash, 1977a, 1977b) and in an unmined ore body on Spokane Mountain (Robbins, 1978). The majority of the mineralization in both deposits is along fractures in the sulfidic and graphitic Togo formation. Thus, the geology of these deposits is similar to the geology of unconformity deposits (Nash, 1977a, Robbins, 1978), which are thought to be at least partly supergene in origin (Derry, 1973; Langford, 1978).

Except that mineralization does occur in the Cretaceous Loon Lake quartz monzonite, the age of the Midnite and Spokane Mountain deposits is not well known. Analyses prior to 1960 suggested $^{206}\text{Pb}/^{238}\text{U}$ and $^{207}\text{Pb}/^{235}\text{U}$ ages of 102 and 108 million years for the Midnite deposit (Becraft and Weis, 1963). Nash (1977a) and Robbins (1978) interpreted these ages to mean that a Tertiary supergene origin for the deposits either was unlikely or of minor significance. However, unconformity deposits characteristically yield a variety of U/Pb dates (Langford, 1978). Furthermore, as Ludwig (1978) has noted, it is difficult to assess the significance of one or two Pb/U apparent ages from deposits that (1) may have been caused by the migration of ground water and (2) are much younger than the 0.7 b.y. half-life of ^{235}U .

Nash (1977a) suggested that the Midnite deposit was exhumed by the Eocene and that the area has been stable and little modified since then. Accordingly, both Nash (1977a) and Robbins (1978) suggested that the deposits could have originated, in part, by Tertiary supergene enrichment. The schematic cross section of Figure 3 shows that the area has not been as stable as Nash supposed; at least five unconformities occur in the area. Until modern radiometric or other dates are available, the uranium deposits could equally well be related to any or all of these unconformities, and the age and genesis of the deposits relative to the Sherwood deposit must remain speculative. Alternatively, if the stratigraphy were known, all five unconformities could be prospected in an attempt to determine if one is the mineralized horizon.

CONCLUSIONS

The metamorphic core complexes contain low grade pegmatitic uranium deposits that probably have limited commercial potential but which may have been the source of uranium for secondary deposits formed by oxidizing sulfide deposits. Because Davis and Coney (1979) have shown that metamorphic core complexes occur from British Columbia to northwestern Mexico, the guides to exploration suggested here for northeastern Washington may have a wider applicability. Exploration for sulfidic deposits in or below Tertiary sedimentary and volcanic rocks currently is limited by (1) our imperfect knowledge of Tertiary stratigraphy, regional unconformities, regional facies patterns, and post-depositional deformation and erosion, and (2) by the lack of definitive radiometric or other dates of the known deposits. When these problems are solved, exploration for uranium should be more fruitful.

REFERENCES

- Becraft, G. E., and Weis, P. L., 1963, Geology and mineral deposits of the Turtle Lake quadrangle, Washington: U.S. Geological Survey Bulletin 1131, 73 p.
- Berning, J., Cooke, R., Hiemstra, S. A., and Hoffman, U., 1976, The Rössing uranium deposit, Southwest Africa: *Economic Geology*, v. 71, p. 351-368.
- Cheney, E. S., 1980a, A model for the genesis of surficial uranium deposits (abs.): *Geological Society of America Abstracts with Programs*, v. 12, p. 109.
- Cheney, E. S., 1980b, Kettle dome and related structures of northeastern Washington in Crittenden, M., Jr., Coney, P. J., and Davis, G. H., eds., *Cordilleran metamorphic core complexes: Geological Society of America Special Paper 153*, in press.
- Cheney, E. S., and Trammell, J. W., 1973, Isotopic evidence for inorganic precipitation of uranium roll ore bodies: *American Association of Petroleum Geologists Bulletin*, v. 57, p. 1297-1304.
- Davis, G. H., and Coney, P. J., 1979, Geologic development of the Cordilleran metamorphic core complexes: *Geology*, v. 7, p. 120-124.
- Derry, D. R., 1973, Ore deposition and contemporaneous surfaces: *Economic Geology*, v. 68, p. 1374-1380.
- Eickelberg, J. M., 1979, Geology of the Sherwood uranium mine: unpublished report on file at Sherwood Mine, Western Nuclear, Inc., Wellpinit, Washington, 13 p.

- Fox, K. F., Jr., Rinehart, C. D., Engels, J. C., and Stern, T. W., 1976, Age of emplacement of the Okanogan gneiss dome, north-central Washington: Geological Society of America Bulletin, v. 87, p. 1217-1224.
- Fox, K. F., Jr., Rinehart, C. D., and Engels, J. C., 1977, Plutonism and orogeny in north-central Washington -- timing and regional context: U.S. Geological Survey Professional Paper 989, 27 p.
- Granger, H. C., and Warren, C. G., 1969, Unstable sulfur compounds and the origin of roll-type uranium deposits: Economic Geology, v. 64, p. 160-171.
- Langford, F. F., 1978, Origin of unconformity-type pitchblende deposits in the Athabasca basin of Saskatchewan, in Kimberley, M. M., (ed.), Short course in uranium deposits: their mineralogy and origin, Mineralogical Association of Canada, Toronto, p. 485-499.
- Ludwig, K. R., 1978, Uranium-daughter migration and U/Pb isotope apparent ages of uranium ores, Shirley Basin, Wyoming: Economic Geology, v. 73, p. 29-49.
- Miller, F. K., 1974, Preliminary geologic map of the Newport Number 2 quadrangle, Pend Oreille and Stevens Counties, Washington: Washington Division of Geology and Earth Resources Map GM-8.
- Nash, J. T., 1977a, Geology of the Midnite uranium mine area, Washington -- maps, description, and interpretation: U.S. Geological Survey Open-File Report 77-592, 39 p.
- Nash, J. T., 1977b, Speculation on three possible modes of emplacement of uranium into deposits of the Midnite mine, Stevens County, Washington: U.S. Geological Survey Circular 753, p. 33-34.
- Okulitch, A. V., Price, R. A., Richards, T. A. (eds.), 1977, Geology of the southern Canadian Cordillera -- Calgary to Vancouver: Geological Association of Canada Field Trip 8 Guidebook, 135 p.
- Pearson, R. C., and Obradovich, J. D., 1977, Eocene rocks in northeast Washington -- radiometric ages and correlation: U.S. Geological Survey Bulletin 1433, 41 p.
- Robbins, D. A., 1978, Applied geology in the discovery of the Spokane Mountain uranium deposit, Washington: Economic Geology, v. 73, p. 1523-1538.
- Weissenborn, A. E., and Moen, W. S., 1974, Uranium in Washington: Washington Division of Geology and Earth Resources Information Circular No. 50, p. 87-97.
- Wright, L. B., 1949, Geologic relations and new ore bodies of the Republic District, Washington: American Institute of Mining and Metallurgical Engineers Transactions, v. 178, p. 264-284.

Hydrothermal alteration and mineralization at the Blackbutte
mercury mine, Lane County, Oregon

R. E. Derkey, University of Idaho

HYDROTHERMAL ALTERATION AND MINERALIZATION AT THE BLACKBUTTE MERCURY MINE, LANE COUNTY, OREGON

Robert E. Derkey
Department of Geology, University of Idaho, Moscow, Idaho

ABSTRACT

Mercury mineralization at the Blackbutte mine occurs in a sequence of Eocene-Oligocene western Cascades andesitic volcanoclastic tuffs and tuff breccias. Hydrothermal alteration zones are defined by type, texture, and abundance of mineral and the relative amount of bleached host rock. The inner zone is characterized by abundant hydrothermal quartz; local brecciation followed by emplacement of pyrite, siderite, calcite, and cinnabar; completely bleached host rock; and destruction of volcanic textures. The intermediate zone is characterized by lesser amounts of hydrothermal quartz, abundant kaolinite, minor siderite, less intensely bleached host rock, well-preserved relict textures, and irregular-shaped disseminated ore bodies. The outer zone is characterized by the absence of cinnabar, presence of kaolinite but only minor bleached rock, and well-preserved relict textures. Veinlet and disseminated cinnabar mineralization is present at Blackbutte. Fracture-controlled veinlets occur 60 to 90 meters below the crest of the butte in the upper mine levels, and disseminated and minor veinlets of cinnabar occur 300 to 330 meters below the butte on the lower mine levels. Exsolution blebs of a phase Zn_6HgS_9 (phase x) and grains of mercurian tetrahedrite have been identified by microprobe.

Introduction

The Blackbutte mercury deposit, discovered in 1890, is located 65 kilometers south of Eugene, Oregon in Tertiary volcanic rocks of the western Cascades province (Figure 1). Since its discovery, ten mining levels have been developed over a vertical distance of 400 meters. Access to the mining levels is by adit on the north face of Black Butte. Active mining progressed during the periods 1897 to 1908, 1916 to 1919, 1927 to 1942, 1956 to 1957, and 1964 to 1969. The average ore grade from the mine over its last years of operation was between two and three pounds of mercury per ton of ore.

Various reports on the Blackbutte mine include Wells and Waters (1934), Schute (1938), Waters (1943), Brooks (1963), and Derkey (1973). Regional geologic mapping has been done by Wells and Waters (1934) and Hoover (1963).

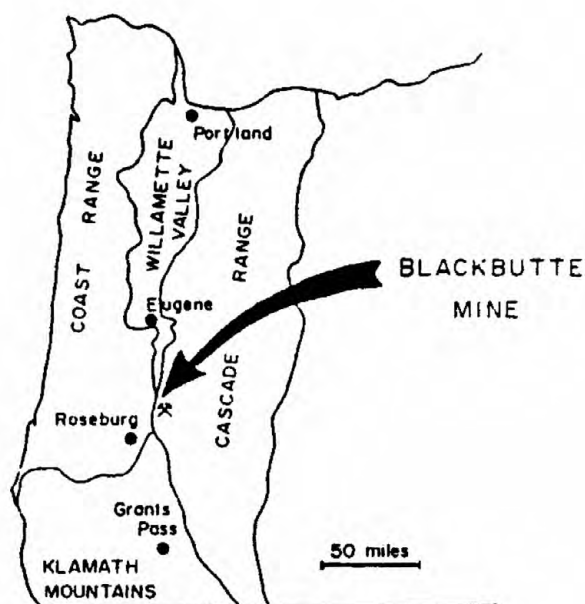


Figure 1. Location map.

Stratigraphy

The Blackbutte mine is in a diverse sequence of pyroclastic and volcanic rock types which belong to the Eocene-Oligocene Fisher Formation (Hoover, 1963). Rocks at Black Butte (Figure 2) include crystal tuffs and abundant volcanic breccias and conglomerates intercalated with andesite flows. The original nature of rocks from the mine can be determined from relict textures usually visible in thin section for the finer-grained tuffs and on slabbed surfaces for the coarser fragmental units. Additional details concerning these westernmost Cascade province volcanics can be found in Hoover (1963).

Structure

The Blackbutte fault zone (Figure 2) trends N70W and dips 50 to 75NE. Its existence is apparent only in the underground workings, and its continuation has not been identified beyond Black Butte itself. Two parallel fault planes one to two meters apart on the upper levels were the focus of the richest and earliest ore mined. Later mining progressed to a wider, lower grade zone in the footwall where only a single fault was apparent. Figure 3 illustrates the nature of the fault in cross-section.

Hydrothermal Alteration Zones

Three alteration zones are defined at Blackbutte based upon the nature and quantity of quartz, kaolinite, calcite,

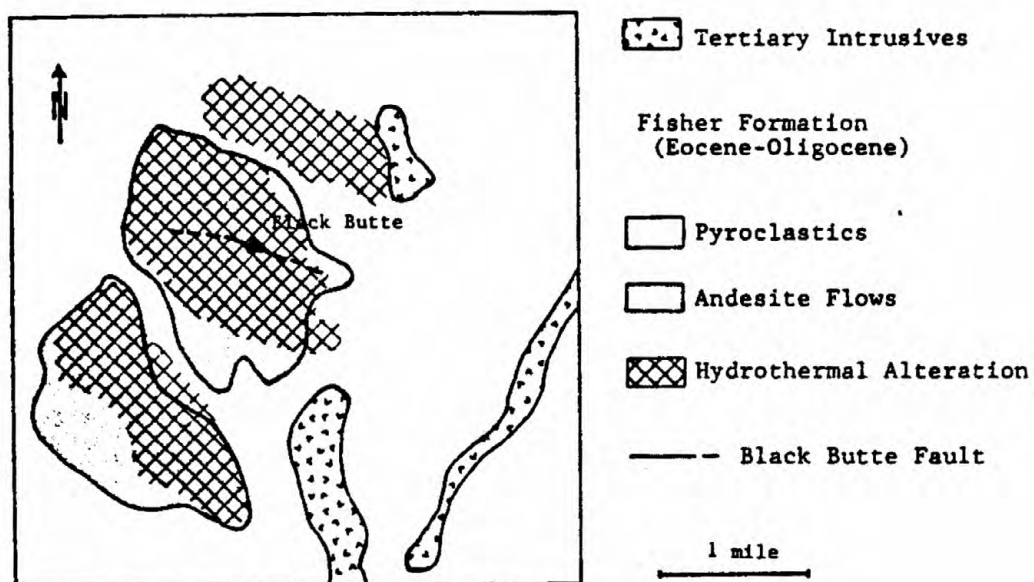


Figure 2. Geologic map of the Blackbutte mine and vicinity. (after Hoover, 1963)

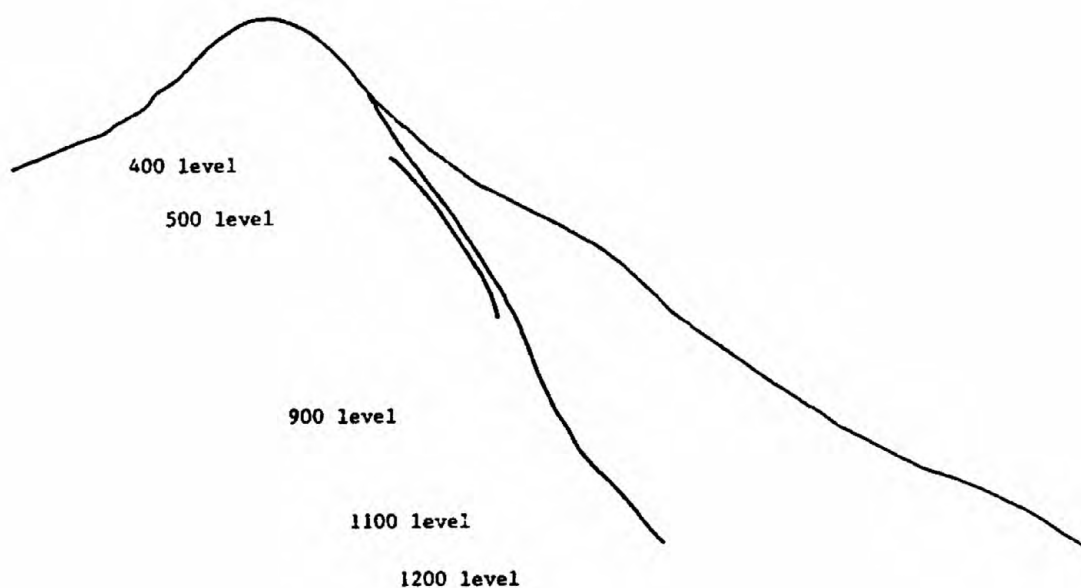


Figure 3. Cross-section of Blackbutte looking east illustrating the relative position of mining levels and the Blackbutte fault.

and siderite. Inner zone silicification consists of a fine-grained (up to 0.01 mm) aggregate of quartz grains which predominate over a lesser quantity of kaolinite. This inner zone alteration is most evident from the silicic ribs which form the crest of the butte. Intermediate zone alteration is characterized by kaolinite predominating over quartz. The typically soft rocks from this zone are indicative of the greater kaolinite content. Portal cross-cuts of the upper mine levels are in the intermediate zone and much of the ore from the 900, 1100, and 1200 levels came from the intermediate zone. The inner and intermediate zones are characterized by intense and nearly complete bleaching-discoloration, and in the field are white or pale shades of pink, gray, maroon, and tan. Rocks from the outer alteration zone, while being extensively altered to quartz and kaolinite, also have remnant plagioclase and pyroxene. Minor bleaching-discoloration occurs in this zone and rock coloration is typically dark gray or dark brown.

Siderite occurs as fine-grained spherulites in the outer zone and as recrystallized spherulites and fracture fillings in the inner zone. Its presence in the intermediate zone is minor and consists of small grains fringed by hematite. Calcite occurs as disseminated grains replacing plagioclase and as fracture fillings in the outer zone and as minor fracture fillings in the intermediate zone. An outline of the nature of the alteration is presented in Table 1.

The alteration zones are illustrated in Figure 4, which shows the 1200 crosscut driven in the late 1960's and Figure 5 which presents a diagrammatic cross-section of the mine. The sporadic nature of the alteration illustrated in these figures is characteristic of epithermal ore deposits such as Blackbutte.

Ore Minerals

Sulfide minerals identified at Blackbutte include cinnabar, mercurian tetrahedrite, pyrite, chalcopyrite, and an isotropic phase (phase x) which optically resembles sphalerite. Pyrite occurs as disseminated grains in all alteration zones and as veinlets in the inner and intermediate alteration zones. Cinnabar occurs as veinlets and as larger disseminated grains up to 3.0 mm in diameter associated with the Blackbutte fault zone from the surface to the 400 mine level (Figure 3). Cinnabar from the 900, 1100, and 1200 mine levels consists of disseminated grains less than 1.0 mm in diameter and minor discontinuous veinlets. Mercurian tetrahedrite, chalcopyrite, and phase x are found only in cinnabar veinlets and large disseminated cinnabar grains.

Possible exsolution blebs less than 0.05 mm in size were initially identified by optical methods as sphalerite. This appeared reasonable, because sphalerite and cinnabar form a continuous series at elevated temperatures (Kremheller, et al., 1960). However, microprobe analysis indicated the blebs were not sphalerite, but were a more complex phase (phase x)

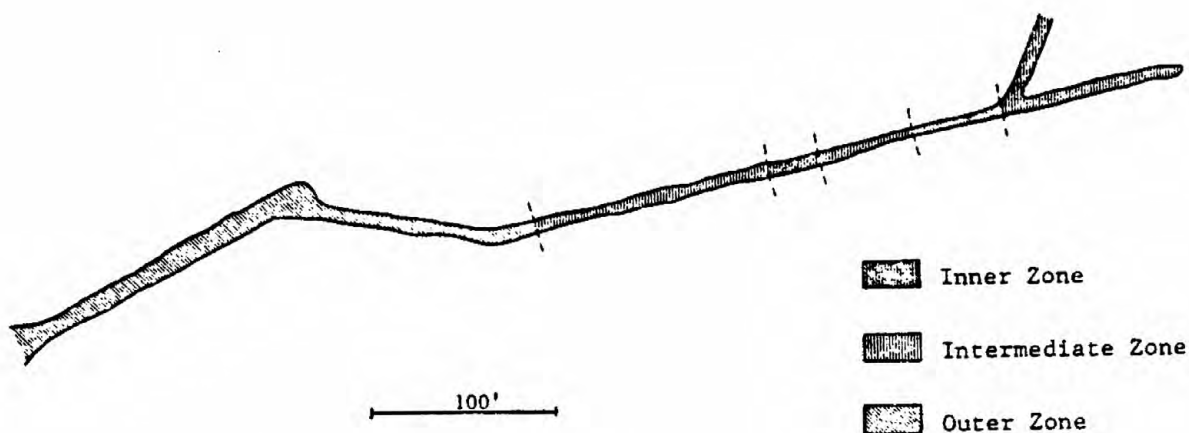


Figure 4. 1200 level, portal cross-cut illustrating hydrothermal alteration zones at Blackbutte.

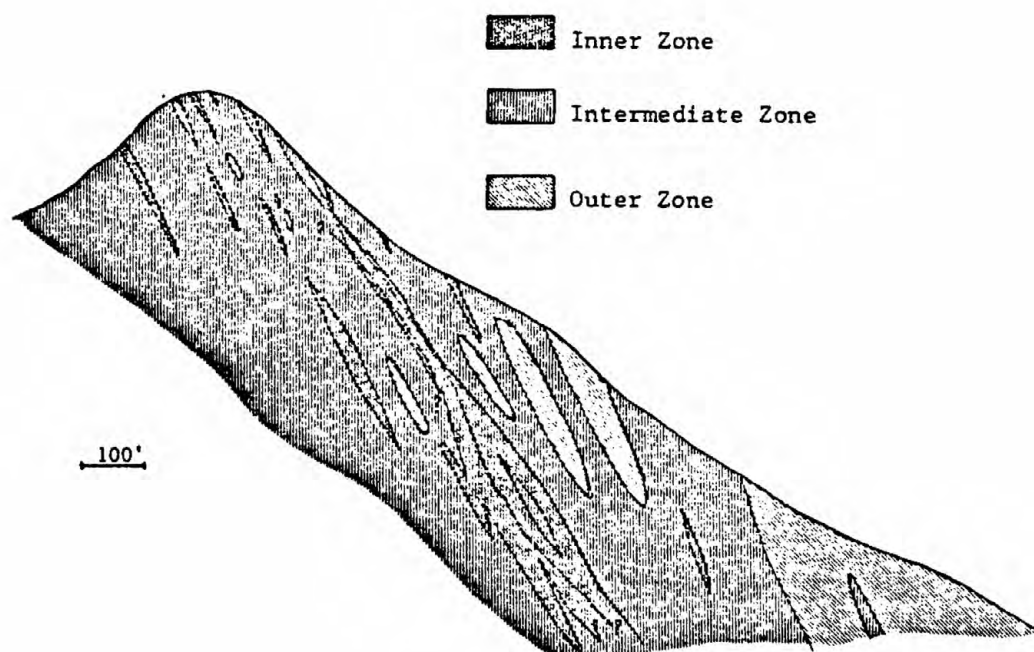


Figure 5. Cross-section of figure 3 with diagrammatic representation of the hydrothermal alteration zones at Blackbutte.

OUTER ZONE	INTERMEDIATE ZONE	INNER ZONE
Incomplete alteration	Kaolinite predominant over quartz	Quartz predominant over kaolinite
Bleaching-discoloration is minor	Bleaching-discoloration is near complete	Bleaching-discoloration is complete
Excellent relict textures	Numerous relict textures	Relict textures destroyed
Fine grained aggregate of siderite, forms spherulites	Disseminated siderite grains with hematite along margins	Veinlet siderite and recrystallized siderite spherulites
Calcite replacing plagioclase and filling fractures	Calcite as scattered fracture fillings	Calcite absent
No cinnabar mineralization	Disseminated cinnabar predominant, sparse and varied	Cinnabar veinlets in brecciated and silicified rocks

Table 1. Hydrothermal alteration zone characteristics.

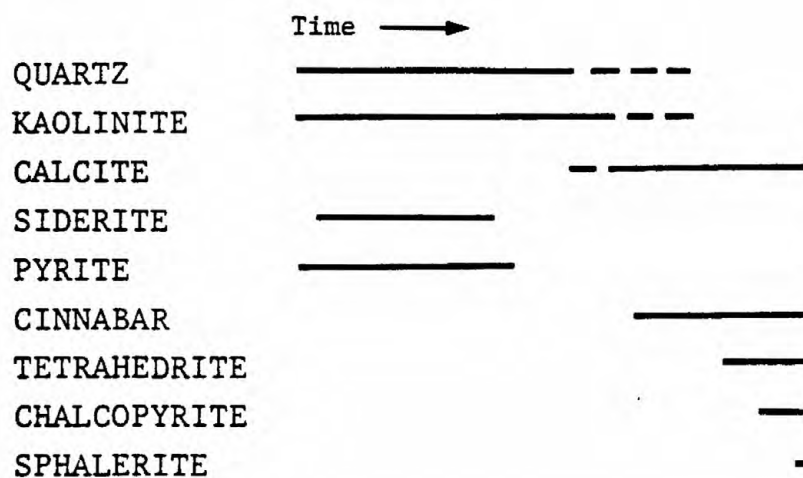


Figure 6. Blackbutte paragenetic sequence.

consisting of mercury, zinc, sulfur, and trace amounts of iron. Zn_6HgS_9 was the structural formula computed from several microprobe analyses.

Leonard, et al. (1978) describes a microscopic Hg-Zn mineral, polhemusite, in Mercury-Antimony ores from Idaho. The mineral has limiting composition equivalent to $\text{Hg}_{0.10}\text{Zn}_{0.92}\text{S}_{0.99}$ and $\text{Hg}_{0.22}\text{Zn}_{0.83}\text{S}_{0.95}$ and contains small amounts of iron. Unlike phase x, polhemusite is anisotropic; however, the strong anisotropy of cinnabar surrounding the small phase x blebs may mask a weaker anisotropy in phase x. The polishing hardness of phase x is similar to cinnabar while that of polhemusite is greater than cinnabar and stibnite. The color of phase x under the ore microscope is similar to sphalerite and descriptively is similar to polhemusite. From the limited amount of available data, phase x blebs can be interpreted as 1) polyhemusite, 2) mercurian sphalerite, or 3) a separate phase.

Mercurian tetrahedrite was identified optically and also analyzed by electron microprobe. The mercury content varied from 18 to 20 weight percent and copper varied from 34 to 36 weight percent. Antimony and arsenic content in mercurian tetrahedrite was variable; however, available analyses indicated near equal atomic amounts of these two elements. Every example of mercurian tetrahedrite in polished section was intimately associated with cinnabar veinlets or large groups of disseminated cinnabar.

Paragenesis

Quartz and kaolinite are the initial products of hydrothermal activity preserved at Blackbutte. Siderite and pyrite appear to be slightly later to contemporaneous with the quartz-kaolinite as indicated by cross-cutting veinlets of pyrite and siderite in the silicified ribs exposed at the crest of the butte. Calcite is later than most of the quartz and kaolinite and appears to be a product of less intense hydrothermal activity or contemporaneous alteration peripheral to the quartz-kaolinite alteration. Cinnabar crystals occur enclosed in calcite crystals and cinnabar veinlets cut calcite. Thus, cinnabar was emplaced late during the depositional cycle of calcite. The remaining copper, zinc, and mercury sulfides appeared later than initial cinnabar. Mercurian tetrahedrite appears as euhedral to anhedral grains in cinnabar and as a cross-cutting veinlet in cinnabar. Tetrahedrite, therefore, appears late during deposition of cinnabar. Phase x, believed to be an exsolution product in cinnabar, is the last sulfide to appear. The paragenetic sequence is represented diagrammatically in Figure 6.

References

- Brooks, H. C., 1963, Quicksilver in Oregon: Oregon Dept. of Geol. and Min. Industries, Bulletin 55, 223 p.
- Derkey, R. E., 1973, Geology of the Blackbutte Mercury Mine, Lane County, Oregon: unpublished M. S. thesis, University of Montana, 66 p.
- Hoover, Linn, 1963, Geology of the Anlauf and Drain Quadrangles, Douglas and Lane Counties, Oregon: U. S. Geol. Survey Bulletin 1122-D, 62 p.
- Kremheller, A., Levine, A. K., and Gashurov, G., 1960, Hydrothermal preparation of two component solid solutions from II-VI compounds: J. Electrochem. Soc., v. 107, p. 12-15.
- Leonard, B. F., Desborough, G. A., and Mead, C. W., 1978, Polhemusite, a new Hg-Zn sulfide from Idaho: Am. Mineralogist, v. 63, p. 1153-1161.
- Schutte, C. N., 1938, Quicksilver in Oregon: Oregon Dept. of Geol. and Min. Industries, Bulletin 4, 172 p.
- Waters, A. C., 1943, The Blackbutte Quicksilver Mine, Lane County, Oregon: U. S. Geol. Survey Strategic Minerals Report.
- Wells, F. G., and Waters, A. C., 1934, Quicksilver deposits of southwestern Oregon: U. S. Geol. Survey Bulletin 850, 58 p.

Volcanogenic massive sulfide deposits in ocean-crust and
island-arc terranes, northwestern Klamath Mountains, Oregon

R. A. Koski, U.S. Geological Survey

ABSTRACT

Numerous massive Fe-Cu-Zn sulfide deposits in the northwestern Klamath Mountains of Oregon and California represent submarine volcanogenic mineralization in accreted ocean-crust and island-arc terranes. The deposits occur within two major lithotectonic assemblages separated by an eastward-dipping thrust fault: the upper-plate western Paleozoic and Triassic belt, and the lower-plate western Jurassic belt.

In the Takilma area near the western margin of the western Paleozoic and Triassic belt, ophiolitic melange hosts a north-south-trending zone of massive sulfide mineralization. Blocks of massive pyrrhotite and (or) pyrite with subordinate chalcopyrite and sphalerite are tectonically intermixed with metadiabase, metagabbro, basalt, and sheared serpentinite. At the Turner-Albright deposit to the west, tholeiitic basalt flows and breccias of the western Jurassic belt contain pyritic massive sulfide and underlying quartz-chlorite-stockwork mineralization.

A thick sequence of island-arc volcanic rocks and arc-derived flysch in the western Jurassic belt contains the Silver Peak and Almeda sulfide deposits. The presence of calcalkaline fragmental volcanic rocks, barite, polymetallic sulfide assemblages, lateral-vertical sulfide-barite zonation, and feeder-zone mineralization indicates a proximal kuroko-type environment. Conversely, well-banded auriferous massive sulfide in fine-grained, carbonaceous greenschists at the Gray Eagle mine in northern California probably formed in a distal, basinal environment within a Jurassic island arc.

The recognition of ocean-crust and island-arc terranes is a key factor in developing base- and precious-metal resources in the region.

INTRODUCTION

Numerous massive Fe-Cu-Zn sulfide deposits occur in accreted ocean-crust and island-arc terranes of the northwestern Klamath Mountains in Oregon and California (Fig. 1). These terranes are parts of the two major lithotectonic assemblages separated by an eastward-dipping thrust fault: the upper-plate western Paleozoic and Triassic belt and the lower-plate western Jurassic belt. Irwin (1960, 1966) first presented and fostered the concept of multiple north-south-trending, arcuate lithic belts juxtaposed in the Klamath Mountains. Subsequently, the geologic and tectonic setting of coherent terranes within these belts have been identified (for example, Irwin, 1972, 1977; Garcia, 1979) and a plate-tectonic model for Klamath evolution through plate convergence, eastward-directed subduction, and accretion has evolved (Hamilton, 1969, 1978; Burchfiel and Davis, 1975,; and Davis and others, 1978).

The massive sulfide deposits described in this report are considered in this recently established plate-tectonic framework. The deposits, located in Figure 1, include: 1) the Queen of Bronze, Cowboy, and others in serpentinite melange of the western Paleozoic and Triassic belt; 2) the Turner-Albright in ophiolite of the western Jurassic belt; 3) the Silver Peak and Almeda in fragmental island-arc volcanic rocks of the western Jurassic belt; and 4) the Gray Eagle in schistose metavolcanic-metasedimentary strata assigned to the western Jurassic belt.

DEPOSITS IN OCEANIC-CRUST TERRANES

Takilma-area deposits

Near Takilma, Oregon, at the western edge of the western Paleozoic and Triassic belt, small masses of pyritic and pyrrhotitic massive sulfide are

Figure 1

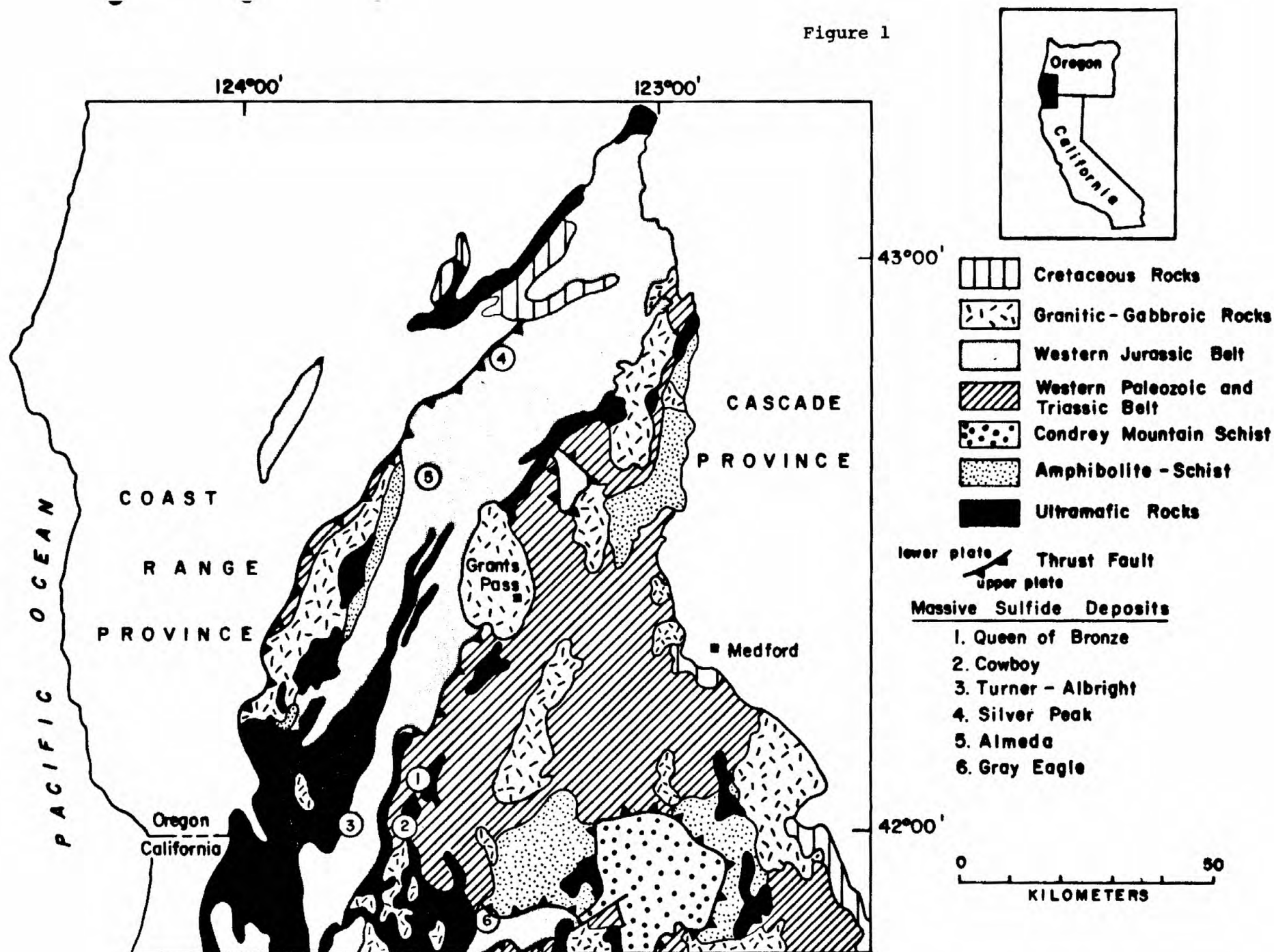


Figure 1. General geologic map of northern Klamath Mountains showing location of major massive sulfide deposits. Geology modified from Hotz (1971).

dispersed within tectonic melange comprised of mafic and ultramafic rocks (Fig. 2). The mafic rocks are largely diabase, diabase breccia, gabbro, and minor(?) basalt, all showing varying degrees of greenschist-facies metamorphism. Exposures at the Queen of Bronze mine and along the E. fork of the Illinois River show that diabasic and gabbroic rocks form dike or sill aggregates. The mafic assemblage is in apparent fault contact with and overlain by a sequence of thinly-bedded gray chert, argillite, graywacke, and intercalated mafic lava flows.

The mafic rocks and overlying strata are intruded and engulfed by large irregular masses of highly serpentized peridotite. Subrounded blocks of diabase, gabbro, and chert-argillite less than a meter to hundreds of meters across are incorporated within the ultramafic bodies. Contacts between large inclusions and serpentinite are typically sheared. The rock assemblage in the Takilma area is lithologically similar to that in the Preston Peak ophiolite described by Snoke (1977) 15 km to the south.

More than 40,000 tons of plus five percent copper ore have been mined from at least six locations in the Takilma district (Shenon, 1933a). Discontinuous sulfide mineralization occurs within a 4-km-long north-south-trending belt which follows the irregular contact between mafic and ultramafic rocks. Deposits in diabasic wallrocks (Queen or Bronze, Waldo, Lilly, and Lytle) form sharply-defined pods, flattened lenses, and thin, discontinuous seams; these bodies are often fault-bounded or are truncated by faults. Breccia or massive-granular textures predominate, but banded and colloform features are also present.

Deposits in ultramafic rocks (Cowboy and Mabel) consist of lenticular aggregates of rounded massive sulfide "boulders" (Shenon, 1933a) in highly-sheared serpentinite. Sulfide aggregates are coarse-grained massive or foliated. These textures appear to have resulted from recrystallization and deformation by flowage.

The principal sulfide minerals at the Queen of Bronze deposit (both the north and south workings) are, in decreasing abundance, pyrite, chalcopyrite, sphalerite, and pyrrhotite. At the Waldo deposit, pyrite, pyrrhotite and chalcopyrite are all abundant; sphalerite and arsenopyrite are minor constituents. Pyrrhotite and chalcopyrite are the major phases in massive sulfide from the Lytle, Mabel, and Cowboy deposits, but sphalerite and cubanite are abundant in some samples. Pyrite is very minor. Shenon (1933a) also reported the presence of cobaltite in "boulder" ore from the Cowboy mine. Sulfide minerals are accompanied by varying amounts of interstitial quartz, chlorite, calcite, and serpentine minerals.

The Takilma deposits appear to represent a discontinuous zone of sulfide mineralization within a subvolcanic diabase-gabbro dike and breccia complex analogous to the mafic complex in the Preston Peak ophiolite described by Snoke (1977). Subsequent movement and serpentization of peridotite has resulted in disruption, deformation, and metamorphism of the sulfide bodies.

Turner-Albright deposit

The Turner-Albright copper-gold deposit occurs in basaltic lavas and lava breccias of the Josephine Ophiolite which is located in the western Jurassic belt (Fig. 1). Recent studies by Vail (1977) and Harper (1980) have resulted in the recognition of a complete ophiolite section above the basal Josephine Peridotite. Basal peridotite tectonite is overlain by ultramafic and gabbroic cumulates, isotropic gabbro, sheeted diabase dikes, mixed pillow lavas and pillow-lava breccias, and a thin layer of metalliferous chert and mudstone. A thick flysch sequence containing interbedded

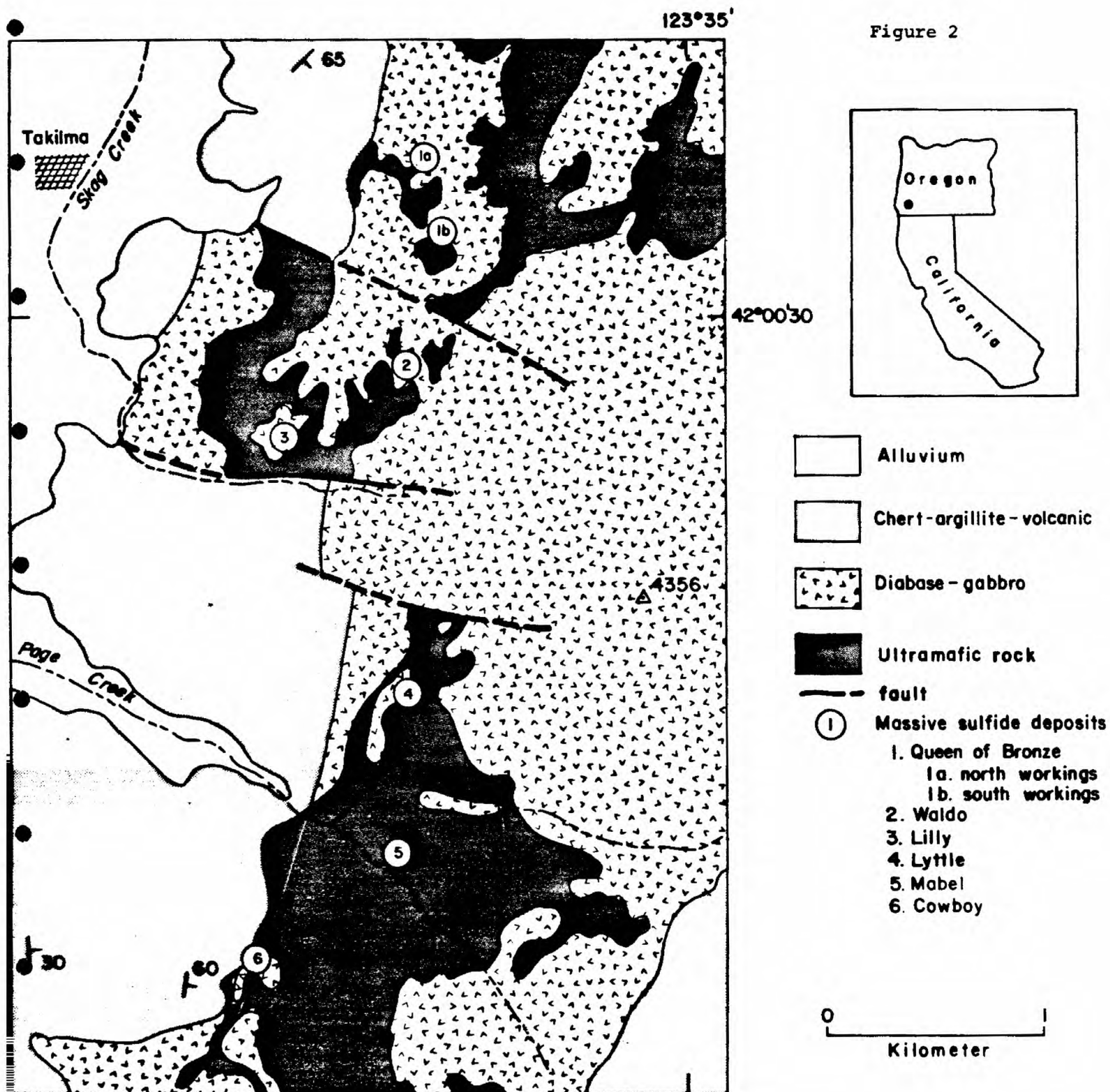


Figure 2. Geologic map of the Takilma area, Oregon, showing location of massive sulfide deposits.

graywacke, slate, conglomerate, and rare limestone conformably overlies the ophiolitic section (Harper, 1980). A diagrammatic section through the Josephine Ophiolite is shown in Figure 3. Field relationships and petrographic and geochemical data indicate that the Josephine Ophiolite and overlying flysch formed in a marginal basin west of the North American plate margin during Jurassic time (Dick, 1977; Harper, 1980).

The basalts hosting massive and stockwork sulfides are widely spilitized and lie within the upper plate of an east-dipping thrust. The footwall of the thrust is barren peridotite (see Fig. 4a from Cunningham, 1979). Comagmatic diabase and gabbro intrusions and intercalated tuffaceous beds within the volcanic pile are weakly pyritized.

The geometry of the deposit is shown in Figure 4b. The steeply-dipping northwest-trending layer of massive sulfide breccia, expressed by prominent linear gossans at the surface, grades northward into a roughly pipeshaped zone of mixed volcanic, sulfide, and chert breccia. Sulfide veinlets and disseminations are common in the mixed breccia and lithic fragments are often replaced by sulfide along their margins. Volcanic material in the pipe-like breccia zone, probably a feeder system for the massive zone, is strongly chloritized and silicified. Hematitic jasper veinlets are also common within the breccia.

Pyrite greatly exceeds other sulfides, but chalcopyrite and sphalerite are widespread and locally abundant. Although coarse breccia textures predominate, individual sulfide fragments frequently display thin alternating bands of pyrite and sphalerite. Pyrite-, chalcopyrite-, and sphalerite-bearing veinlets crosscutting massive pyrite and banded pyrite-sphalerite fragments are evidence for multiple episodes of sulfide deposition.

The configuration of the feeder zone and tabular massive sulfide body indicate that the Turner-Albright deposit is overturned to the southwest. The geologic setting, geometry, and composition of the Turner-Albright deposit are characteristic of Cyprus-type cupreous pyrite deposits. No production of copper ore has been reported from the Turner-Albright, but the gossans have been treated for small amounts of gold.

DEPOSITS IN ISLAND-ARC TERRANES

Stratiform volcanogenic massive sulfide deposits occur in calc-alkaline volcanic rocks of the Rogue-Galice island-arc assemblage (Garcia, 1979) in the western Jurassic belt of southwestern Oregon. Much of the mineralization is located within pyroclastic units along two northeast-trending zones, a northern zone southwest of Canyonville, and a southern zone crossing the Rogue River near Galice. The Silver Peak and Almeda are the most important deposits in the north and south zones, respectively (Fig. 1).

Silver Peak deposit

The geology and mineralization at the Silver Peak mine are described in detail elsewhere in this volume (see Derkey); thus, only a brief summary is presented here. Jurassic metavolcanic rocks hosting the Silver Peak deposit are part of the upper plate of the Coast Range thrust and structurally overlie sedimentary rocks of the Dothan Formation. Johnson and Page (1979) have subdivided the greenschist-facies volcanic rocks near Silver Peak (previously, the Rogue Formation) into a predominantly southeast-dipping sequence of rhyodacitic to andesitic flows, tuffs, tuff breccia, and agglomerates, and pillow basalt. Lavas and tuffs higher in the section are

Figure 3

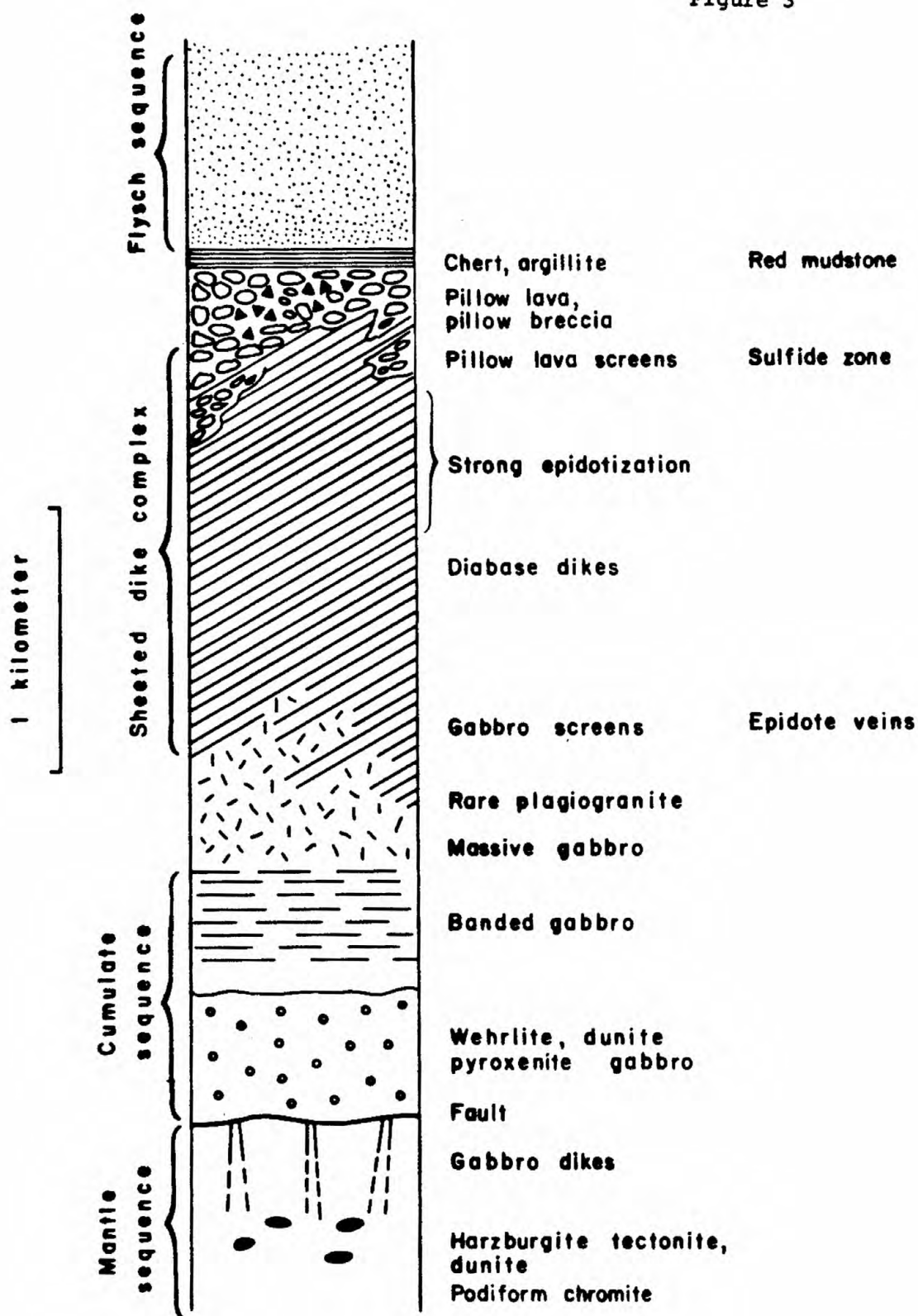


Figure 3. Geologic section of the Josephine Ophiolite (after Harper, 1980).

Figure 4a

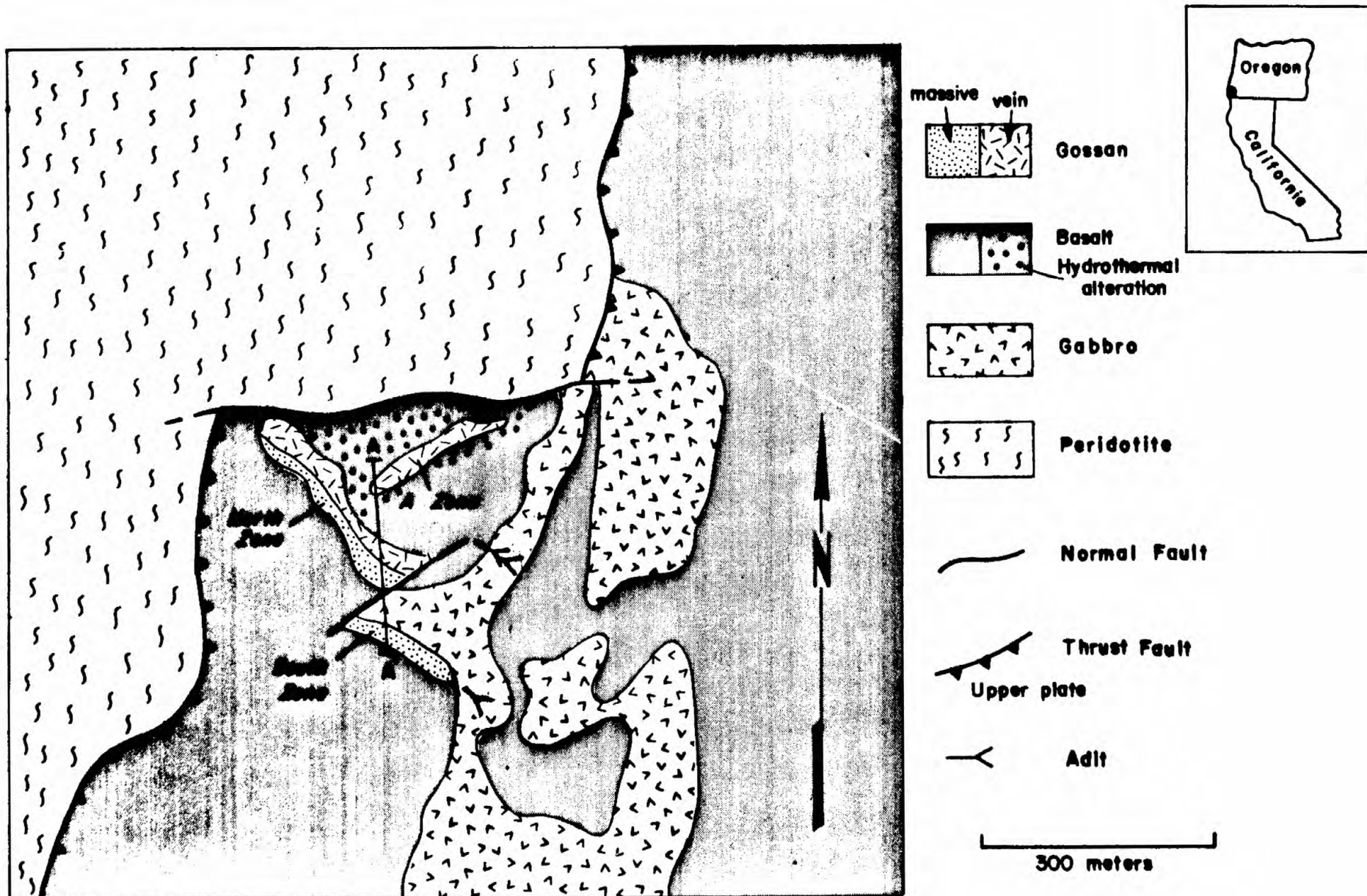
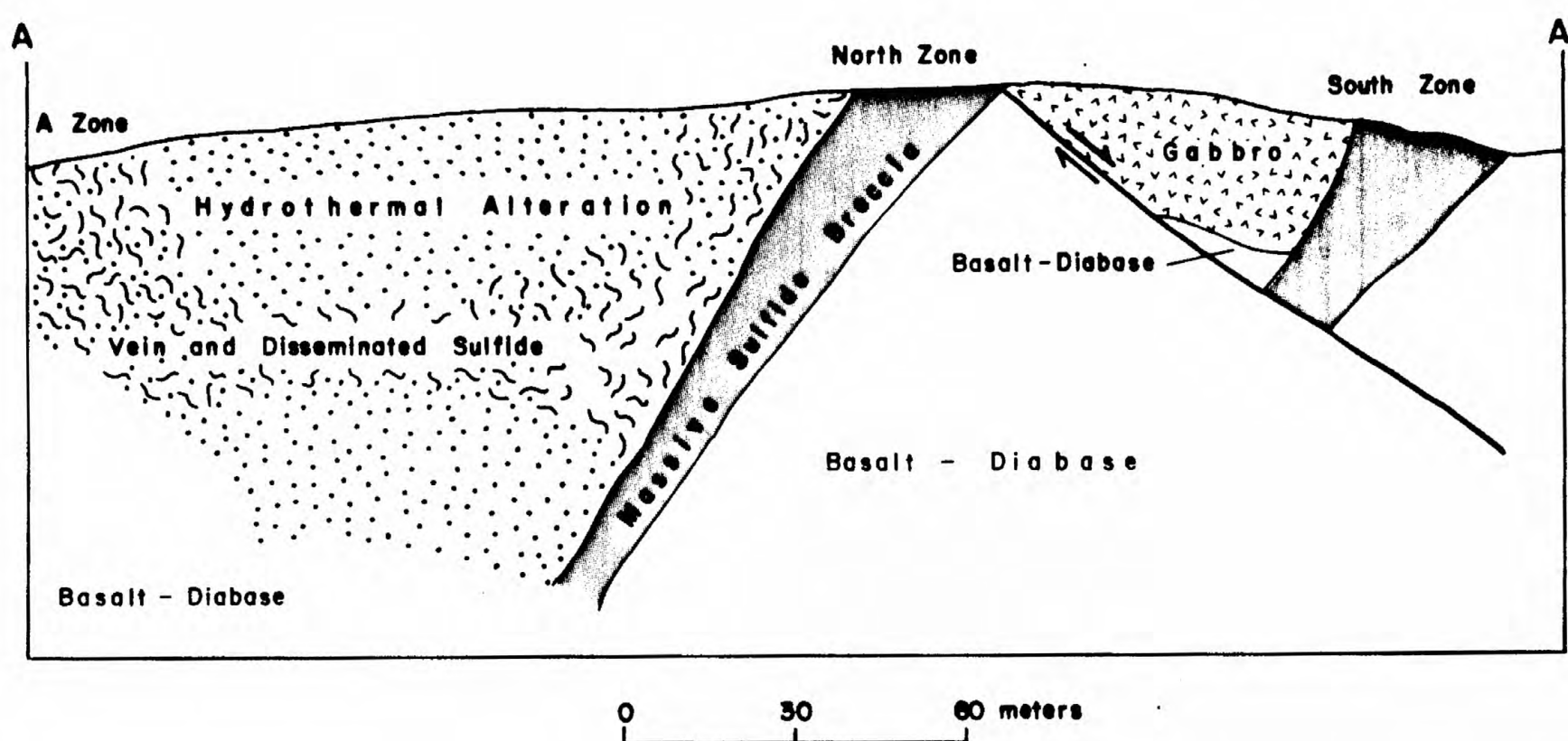


Figure 4. Geologic map (4a) and cross section (4b) of the Turner-Albright mine (after Cunningham, 1979) area.

Figure 4b



interbedded with thinly-bedded gray shale. The sequence is disrupted by southeast-dipping thrust faults and narrow slivers of serpentinite. On the regional map of Johnson and Page (1979), the mineralized zone at Silver Peak lies within the basal metavolcanic unit composed of rhyodacite flows and bedded tuffs.

According to Derkey (1980; and personal communication, 1979) stratiform massive and disseminated sulfide and barite mineralization at Silver Peak is closely associated with foliated pyroclastic rocks containing abundant secondary quartz and sericite. Up to 4 m of massive bedded sulfide containing pyrite, chalcopyrite, sphalerite, bornite, tennantite, and barite with Kuroko-type vertical zonation appears to stratigraphically overlie a silicified volcanic center. The estimated total production at Silver Peak, for the years of operation 1926-1937, is 6,620 tons from which 735,600 pounds of copper, 21,980 oz. silver, and 490 oz. of gold were recovered (Ramp, 1972).

Almeda deposit

The Almeda mine is situated on the north bank of the Rogue River approximately 30 km southwest of Silver Peak. The mineralized horizons occur in highly altered fragmental metavolcanic rocks immediately below the depositional contact with overlying slate and graywacke of the Galice Formation (Fig. 5). The metavolcanic rocks are rhyolitic to dacitic tuffs, tuff breccias, and agglomerates assigned by Wells and Walker (1953) to the Rogue Formation. Sill-like masses of dacite porphyry are emplaced along the Rogue-Galice boundary. The volcanic-sedimentary sequence occurs east of and in fault contact with an ophiolitic assemblage of amphibolite, metagabbro, and ultramafic rocks. Garcia (1979) suggests that this mafic-ultramafic complex may represent oceanic crust upon which the Rogue-Galice island-arc was constructed.

At the Almeda mine, a 60-m-wide, steeply-dipping zone of intensely silicified fragmental rock interstratified between Galice strata and coarse rhyolitic agglomerate, known as the "Big Yank lode", hosts lenses and fragments of massive sulfide and barite. Lenses of massive sulfide are commonly fragmental with clasts of sulfide, barite, and altered volcanic rock. Locally, alternating sulfide and barite layering may represent bedded deposits. Disseminated and vein sulfides are present in and between massive barite lenses and lithic fragments, and form an extensive stockwork in volcanic breccia stratigraphically below the "Big Yank lode". Quartz-sericite alteration and pyritization decrease in intensity with depth below the Almeda deposit, but extend southward from the Rogue River along the Rogue-Galice contact. Sill-like masses of hornblende-bearing porphyry, emplaced near the contact (Fig. 5), are locally altered to fine-grained quartz and sericite accompanied by disseminated pyrite.

The principal hypogene sulfide is pyrite, but chalcopyrite and sphalerite are locally abundant and galena is present in the stratiform ores. Diller (1914) noted two main ore types: 1) "copper ore with barite" (the high-grade stratiform mineralization); and 2) "siliceous gold-silver ore" (the low-grade stockwork mineralization). Shenon (1933b) stated that, between 1911 and 1916, 16,619 tons of ore produced from the Almeda deposit yielded 259,800 pounds of copper, 7,197 pounds of lead, 1,540 ounces of gold, and 48,387 ounces of silver.

The stratiform polymetallic sulfide-barite ore bodies and underlying stockwork at the Almeda mine appear to represent volcanogenic mineralization of the Kuroko-type within the Rogue-Galice volcanic arc.

Gray Eagle deposit

The Gray Eagle massive sulfide deposit, located 8 km north of Happy Camp,

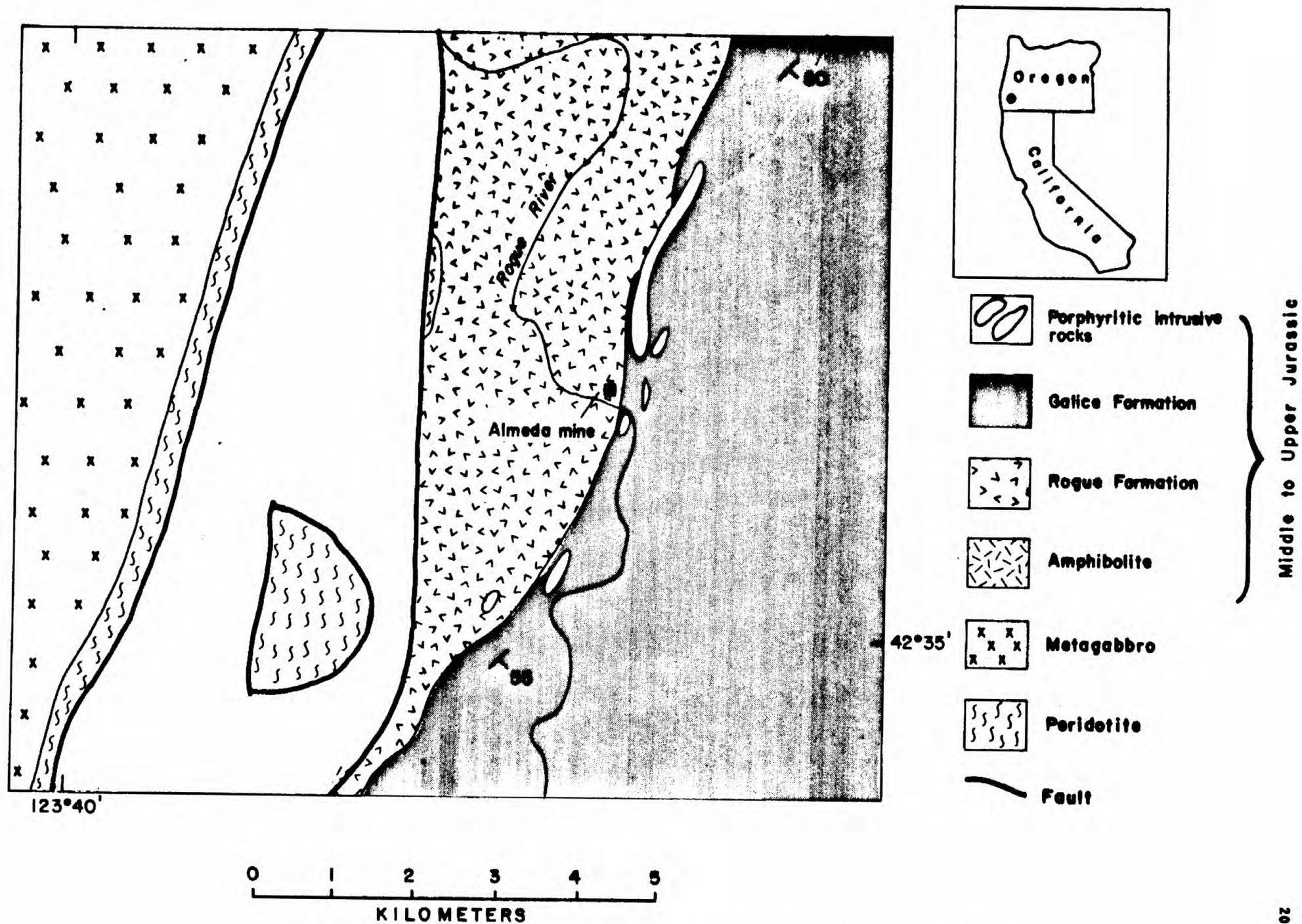


Figure 5. Geology of the Alameda mine area (after Wells and Walker, 1953; and Garcia, 1976).

California, occurs within a gently-dipping sequence of fine-grained meta-volcanic and metasedimentary rocks which structurally underlie amphibolites of the western Paleozoic and Triassic belt along an east-dipping thrust fault of regional extent (Figs. 1 and 6). Klein (1977) refers to these strata as Galice Formation and correlates them with the Condrey Mountain schist to the east. In this report they are considered part of the western Jurassic belt. The greenschist-facies metavolcanic-metasedimentary sequence includes fine-grained greenstone and greenschist interbedded with slate, phyllite, and siliceous and pelitic schist; minor amounts of metarhyolite and marble are also present (Klein, 1975).

The northeast-dipping stratiform and stratabound Gray Eagle deposit consists of banded massive and disseminated sulfide interbedded with and enclosed by chloritic schist. The protolith for the latter may be mafic tuff or tuffaceous sedimentary rocks. The sulfide-bearing chlorite schist is conformably overlain and underlain by unmineralized carbonaceous phyllite.

Sulfide bands, a few mm to 5 cm in thickness, consist largely of pyrite, chalcopyrite, and sphalerite intergrown with quartz. Quartz-rich zones often enclose or border sulfide layers. Within the bands pyrite generally occurs as a network of anhedral to subhedral or subrounded grains in a matrix of chalcopyrite or quartz. Mafic interbands consist of chlorite+sphene or chlorite+quartz+sphene with disseminated fine-grained sulfide, mostly pyrite. Some samples from the Gray Eagle show alternating sphalerite-rich and chalcopyrite-rich bands without intervening mafic layers. The rhythmic, fine-scale silicate-sulfide banding, graded pyrite clasts, and Bouma-type layer sequences all suggest a clastic sedimentary origin for the sulfide deposit, perhaps by turbidity currents.

The mineralized horizon has a thickness of nearly 20 m at the surface where a stratiform auriferous gossan has developed. Down dip from the gossan, copper-bearing sulfide grades laterally into disseminated pyrite which extends for several hundred meters beyond the limit of ore. Past production from the 250 m-long, 125-m wide orebody is reported to be 465,000 tons averaging three percent copper (O'Brien, 1947). Noranda Exploration, Inc., is currently developing the near-surface gossan as a low-grade gold deposit.

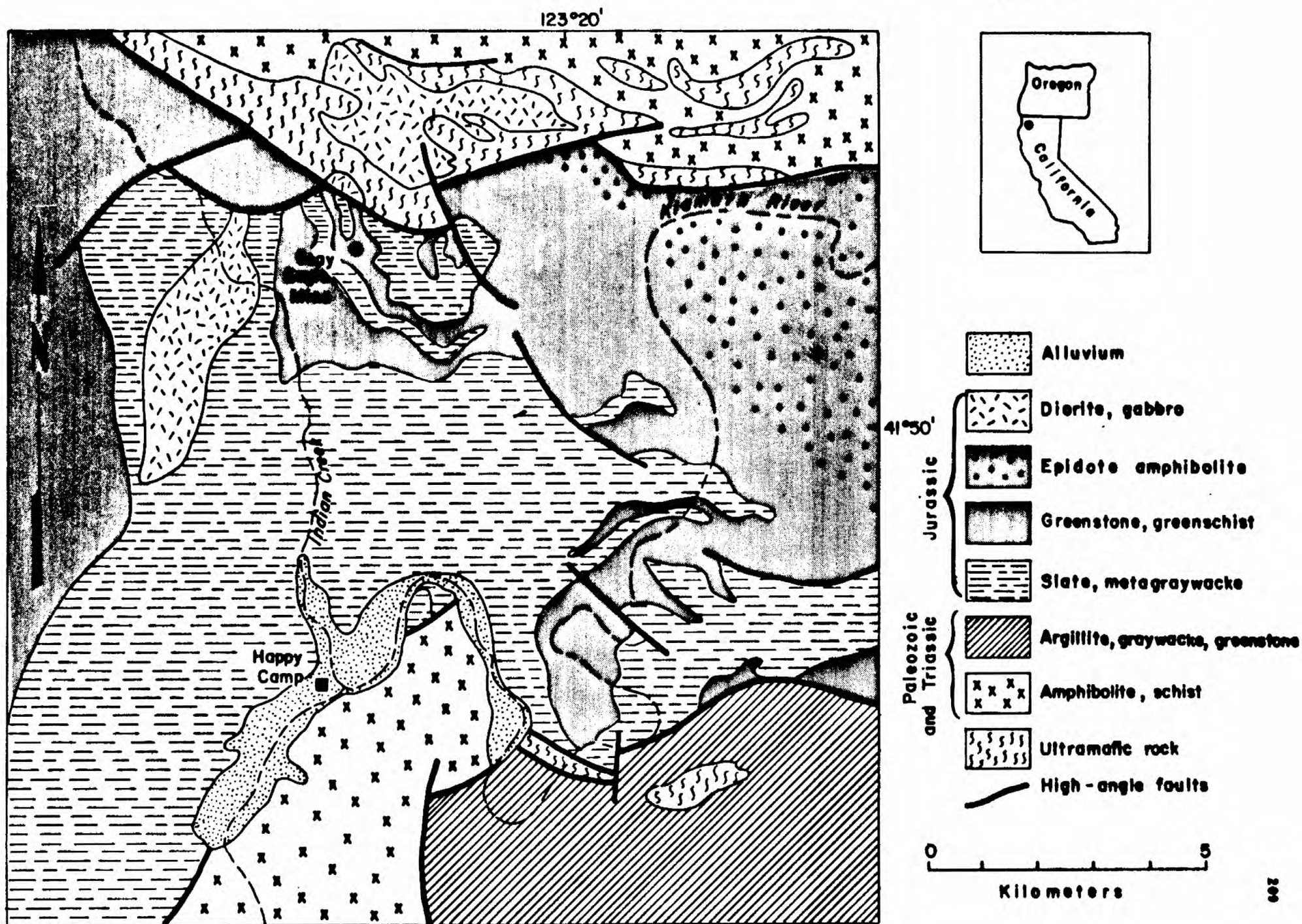
The presence of delicately banded stratiform and stratabound sulfide, fragmental or clastic textures, carbonaceous metasedimentary units, and the apparent absence of a stockwork system, barite mineralization and coarse pyroclastic deposits all indicate deposition away from a volcanic center, possibly within a closed basin. These features are consistent with Colley's (1976) Type IV to Type V Kuroko mineralization formed in intervolcanic or deep-sea (near-arc) basins, respectively. Although the distance from a volcanic vent or feeder zone is uncertain, the quartz-rich bands accompanying sulfide accumulations may represent exhalative precipitates.

CONCLUSIONS

The Takilma-area and Turner-Albright massive sulfide deposits are interpreted as volcanogenic mineralization in ophiolitic terrane. In both cases, the ophiolitic sequence is thought to represent oceanic crust formed in marginal basin environments. Whereas the Turner-Albright mineralization in basalt is analogous to Cyprus-type deposits, the deposits in diabasic and ultramafic rocks near Takilma are disrupted components of tectonic melange.

The Silver Peak and Almeda deposits have numerous Kuroko-type characteristics and probably formed in a proximal position with respect to volcanic

Figure 6



centers in the Jurassic Rogue-Galice island arc. In contrast, the Gray Eagle sulfides were deposited in a basinal environment within or near the arc, and in a relatively distal position from a volcanic vent.

The recognition and interpretation of ocean-crust and island-arc terranes are key factors in developing base- and precious-metal resources in the Klamath region.

REFERENCES

- Burchfiel, B. C., and Davis, G. A., 1975, Nature and controls of Cordilleran orogenesis, western United States: Extensions of an earlier synthesis: *Am. Jour. Sci.*, v. 275-A, p. 363-396.
- Colley, H., 1976, Classification and exploration guide for Kuroko-type deposits based on occurrences in Fiji: *Inst. Mining Metallurgy Trans.*, v. 85, Sec. B., p. B190-B199.
- Cunningham, C. T., 1979, Geology and geochemistry of a massive sulfide deposit and associated volcanic rocks, Blue Creek District, southwestern Oregon: unpublished M.S. thesis, Oregon State Univ., 165 p.
- Davis, G. A., Monger, J. W. H., and Burchfiel, B. C., 1978, Mesozoic construction of the Cordilleran "collage", central British Columbia to central California, in Howell, D. G., and McDougall, K. A., eds., *Mesozoic paleogeography of the western United States: Soc. Econ. Paleontologists and Mineralogists Pacific Coast Paleogeography Symp. 2*, p. 1-32.
- Derkey, R. E., 1980, The Silver Peak volcanogenic massive sulfide, northern Klamath Mountains, Oregon: *Geological Society of America Abstracts with Programs*, v. 12, no. 3, p. 104.
- Dick, H. J. B., 1977, Partial melting in the Josephine Peridotite I. The effect on mineral composition and its consequence for geobarometry and geothermometry: *Am. Jour. Sci.*, v. 277, p. 801-832.
- Diller, J. S., 1914, Mineral resources of southwestern Oregon: *U.S. Geol. Survey Bull.* 546, 147 p.
- Garcia, M. O., 1976, Petrology of the Rogue River area, Klamath Mountains, Oregon: Problems in the identification of ancient volcanic arcs: unpublished Ph.D. dissertation, University of California, Los Angeles, 185 p.
- Garcia, M. O., 1979, Petrology of the Rogue and Galice Formations, Klamath Mountains, Oregon: Identification of a Jurassic island-arc sequence: *Jour. Geol.*, v. 86, p. 29-41.
- Hamilton, W., 1969, Mesozoic California and the underflow of Pacific mantle: *Geol. Soc. America Bull.*, v. 80, p. 2409-2430.
- Hamilton, W., 1978, Mesozoic tectonics of the western United States, in Howell, D. G., and McDougall, K. A., eds., *Mesozoic paleogeography of the western United States: Pacific Coast Paleogeography Symp. 2*, p. 33-70.

- Harper, G. D., 1980, The Josephine Ophiolite: remains of a Late Jurassic marginal basin in northwestern California: *Geology*, v. 8, p. 333-337.
- Hotz, P. E., 1971, Geology of lode gold districts in the Klamath Mountains, California and Oregon: U.S. Geol. Survey Bull. 1290, 91 p.
- Irwin, W. P., 1960, Geologic reconnaissance of the northern Coast Ranges and Klamath Mountains, California, with a summary of the mineral resources: California Div. Mines Bull. 179, 80 p.
- Irwin, W. P., 1966, Geology of the Klamath Mountains province, in Bailey, E. A., ed., *Geology of northern California*: California Div. Mines and Geology Bull. 190, p. 19-38.
- Irwin, W. P., 1972, Terranes of the western Paleozoic and Triassic belt in the southern Klamath Mountains, California: U.S. Geol. Survey Prof. Paper 800-C, p. C103-C111.
- Irwin, W. P., 1977, Ophiolitic terranes of California, Oregon, and Nevada, in Coleman, R. G., and Irwin, W. P., eds., *North American ophiolites*: Oregon Dept. Geology and Mineral Industries Bull. 95, p. 75-92.
- Johnson, M. G., and Page, N. J., 1979, Preliminary geologic map of the meta-volcanic and associated rocks in parts of the Canyonville, Days Creek, and Glandale Quadrangle, Oregon: U.S. Geol. Survey Open-file Report 79-283.
- Klein, C. W., 1975, Structure and petrology of a southeastern portion of the Happy Camp Quadrangle, Siskiyou County, northwest California: unpublished Ph.D. dissertation, Harvard University, 288 p.
- Klein, C. W., 1977, Thrust plates of the north-central Klamath Mountains near Happy Camp, California, in Short Contr. to California Geology: California Div. Mines and Geology Spec. Rept., p. 23-26.
- O'Brien, J. C., 1947, Mines and mineral resources of Siskiyou County: *California Journal of Mines and Geology*, v. 43, p. 413-462.
- Ramp, Len, 1972, Geology and mineral resources of Douglas County, Oregon: State of Oregon Dept. of Geology and Mineral Ind. Bull. 75, 106 p.
- Shenon, P. J., 1933a, Copper deposits in the Squaw Creek and Silver Peak districts and at the Almeda mine, southwestern Oregon, with notes on the Pennell and Farmer and Banfield prospects: U.S. Geol. Survey Circ. 2, 35 p.
- Shenon, P. J., 1933b, Geology and ore deposits of the Takilma-Waldo district, Oregon, including the Blue Creek district, U.S. Geol. Survey Bull. 846, p. 141-194.
- Snoke, A. W., 1977, A thrust plate of ophiolitic rocks in the Preston Peak area, Klamath Mountains, California: *Geol. Soc. America Bull.*, v. 88, p. 1641-1659.

Vail, S. G., 1977, Geology and geochemistry of the Oregon Mountain area, southwestern Oregon and northern California: Corvallis, Ore., Oregon State Univ., Ph.D. thesis, 159 p.

Wells, F. G., and Walker, G. W., 1953, Geologic map of the Galice quadrangle, Oregon: U.S. Geol. Survey Map GQ-25.

The Silver Peak volcanogenic massive sulfide, northern
Klamath Mountains, Oregon

R. E. Derkey, University of Idaho

THE SILVER PEAK VOLCANOGENIC MASSIVE SULFIDE, NORTHERN KLAMATH MOUNTAINS, OREGON.

Robert E. Derkey

Department of Geology, University of Idaho, Moscow, Idaho

ABSTRACT

The Silver Peak mine is 800 meters stratigraphically above the Coast Range Thrust in Jurassic metavolcanics of the Klamath Mountains, Western Jurassic belt. Mineralization is associated with silicic volcanoclastic rocks which are surrounded by and intercalated with calc-alkaline basaltic andesites and andesites. The stratigraphic sequence from bottom to top is: 1) pyroxene-rich andesite, 2) dacite tuffs/flows, and 3) a complex foliated tuff-tuff breccia unit which includes intensely foliated quartz-sericite-pyrite (Q-S-P) tuff, silicified tuff, massive sulfide, and flow banded sulfide lapilli tuff. The massive sulfide parallels both local and regional bedding. Q-S-P tuff and silicified tuff are altered and mineralized equivalents of foliated tuff-tuff breccia believed to have been altered during massive sulfide deposition. Graded bedding, disrupted bedding, flame structures, load structures, and sedimentary slump features indicate subaqueous deposition of the massive sulfide. The zoning sequence of mineralization from bottom to top consists of: 1) friable pyrite, 2) massive pyrite-chalcopryrite (yellow ore), 3) pyrite-chalcopryrite-sphalerite-bornite-tennantite-barite (black ore), 4) barite, and 5) ferruginous chert-sulfide lapilli tuff. This zoning is analogous to that observed in Japanese Kuroko deposits. A plume model is proposed to explain the sedimentary structures and textures of the massive sulfide.

Introduction

The Silver Peak mine is located on Silver Butte nine kilometers south of Riddle, Oregon at the northern end of the Klamath Mountains (Figure 1). The mine recorded production during the years of 1926, 1928-31, and 1936-37; 6,620 short tons of ore yielded 635,600 pounds of copper, 21,980 ounces of silver, and 490 ounces of gold (Ramp, 1972).

The mine has been described and mapped by Shenon (1933). His map (p. 17) calls the Lower Umpqua level the "Main Cross-cut Umpqua Consolidated Mining Company" and the Lower Silver Peak level the "Main Cross-cut Silver Peak Copper Company." Production came only from these two mine levels.

General Geology

Jurassic metavolcanics of the Silver Butte area host volcanogenic massive sulfide mineralization. These island

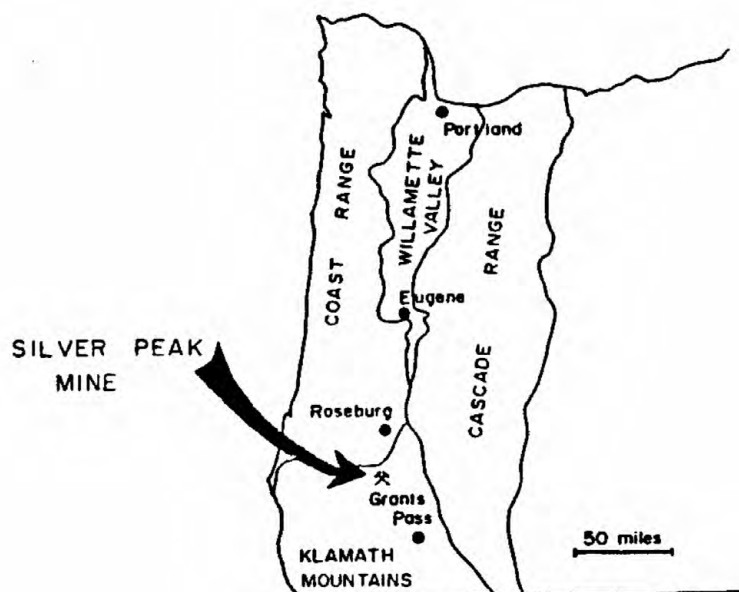


Figure 1. Location map.

arc volcanics (Garcia, 1978, 1979) extend from the Galice area on the Rogue River northeast to Canyonville (Wells and Walker, 1953; Hotz, 1969; Johnson and Page, 1979). The metavolcanics are part of Irwin's (1964) western Jurassic belt. The Silver Peak mine is approximately 800 meters east of the Coast Range Thrust (Figure 2). Stratabound mineralization and bedding in the volcanics at Silver Butte parallels the trend of the Coast Range Thrust and dips 50SE.

Stratigraphy

The lowermost unit exposed in the Silver Peak mine (Figure 3) is an andesite flow with scattered vesicles. The andesite is overlain by dacitic to rhyodacitic tuffs and/or flows which grade upward into foliated tuff and tuff breccia. Massive sulfide mineralization occurs in the foliated tuff-tuff breccia. These three units, andesite, dacite tuff, and foliated tuff-tuff breccia, are all exposed in the Lower Umpqua portal cross-cut of the Silver Peak mine.

The complex, foliated tuff-tuff breccia unit is characterized by diverse color, foliation, type of fragments, pumice content, and local mineralization variations. The unit is believed to have been subaqueously deposited based upon graded bedding in the interbedded massive sulfide and overlying bedded tuffs, load structures where massive sulfide rests on foliated tuff, and massive sulfide flame structures projecting into the overlying tuff. The poorly sorted nature of this unit indicates rapid deposition. Flattened pumice

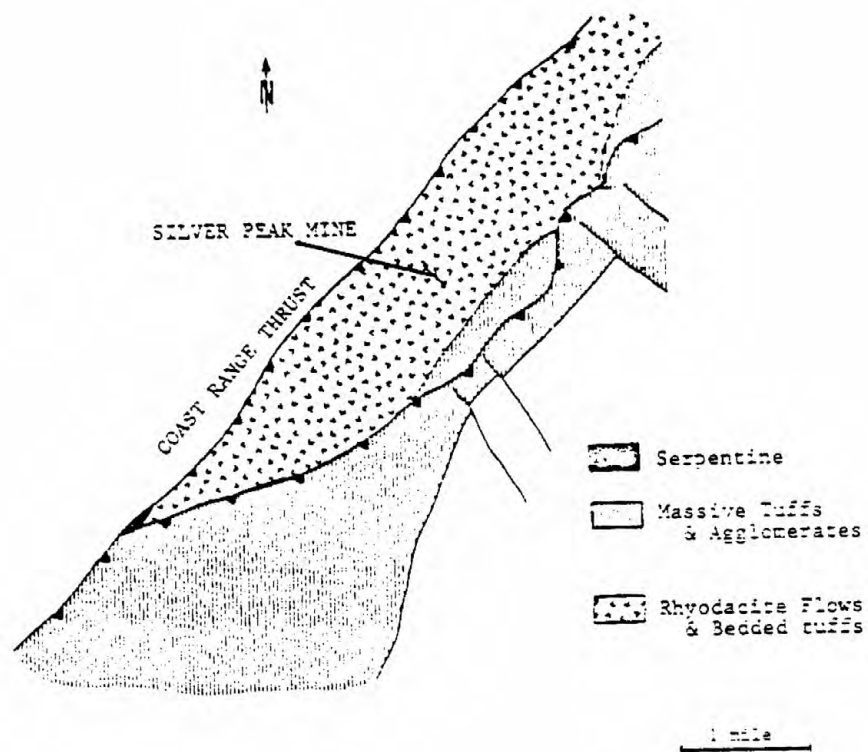


Figure 2. Geologic map of the Silver Peak mine and vicinity (Johnson and Page, 1979). Bar locates cross-section of Figure 3.

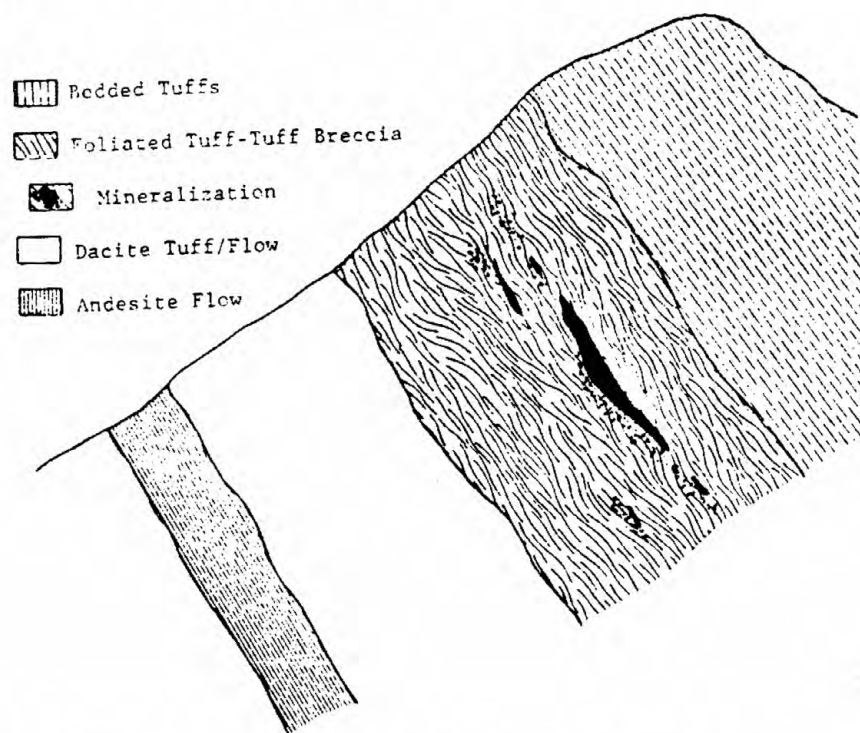


Figure 3. Diagrammatic cross-section of the Silver Peak mine looking northeast.

and volcanoclastic fragments "float" in a matrix of finer tuff. Portions of the tuff-tuff breccia unit are texturally similar to subaerially deposited pyroclastic tuffs and the unit is believed to be a subaqueously deposited pyroclastic tuff.

Mineralogically, the foliated tuff portion of the tuff-tuff breccia unit varies from chlorite-talc-sericite to quartz-sericite-pyrite (Q-S-P). Sequences of Q-S-P tuff up to 75 meters thick underlie beds of massive sulfide at Silver Peak. Textural characteristics of large, slabbed hand specimens of tuff breccia are identical from both the mineralized and non-mineralized portions of the unit. The fine tuffaceous matrix surrounding fragments of non-mineralized tuff has been replaced by pyrite and quartz in the mineralized breccia.

Thin bedded tuff and tuffaceous sandstone overlie foliated tuff-tuff breccia as exposed in drill roads immediately above the mine workings. Outcrops along the crest of Silver Butte, northeast of the mine, consist of massive to thin bedded siliceous tuff which is laterally equivalent to the thin bedded tuff above the mine but differs because of its dense siliceous nature (porcelaneous tuff of Johnson and Page, 1979). The thin bedded tuffs have graded bedding which assists in determining stratigraphic top.

Massive Sulfide

Massive sulfide at Silver Peak consists predominantly of pyrite and varying amounts of chalcopyrite, zincian tennantite, bornite, sphalerite, barite, and quartz. Bodies of massive sulfide parallel the foliation of the enclosing foliated tuff unit; bedding or banding in the massive sulfide also parallels the foliation. Numerous disturbed structures disrupt the bedding continuity of the massive sulfide and suggest that the submarine hydrothermal activity was in part explosive and that deposition of sulfides was on a slope rather than horizontally in a small, quiet basin. Additional sedimentary structures in the massive sulfide include load structures on the underlying tuff, graded bedding, and flame structures into the overlying tuff. Lenses of foliated tuff up to a meter thick are common in the massive sulfide. The massive sulfide sequence (including barite) exposed in the mine is up to four meters thick with an average of approximately one meter and an exposed strike length of 90 meters.

Zoning Sequence

The similarity of Silver Peak to Kuroko deposits is evident from the ore horizon zoning as outlined in Table 1. Silicified tuff one to two meters thick and containing veinlet and disseminated pyrite, chalcopyrite, and bornite underlies the massive ore in both lower mine levels. A feeder system with associated vein sulfides has not been identified at Silver Peak; however, the silicified tuff may



Figure 4. Outline of a single pyrite grain (polished section 205). Small blebs within the pyrite grain are chalcopyrite, tennantite, and bornite. The pyrite grain is surrounded by chalcopyrite.

Ferruginous chert-sulfide lapilli tuff.

Massive white barite.

Black ore-consists of pyrite grains surrounded by chalcopyrite, sphalerite, tennantite, bornite, and barite. Contains thin silica interbeds.

Yellow ore-dense, cemented pyrite. Contains varying amounts of chalcopyrite.

Friable yellow ore-weakly cemented granular pyrite.

Siliceous tuff-locally contains up to 10% disseminated and veinlet pyrite, chalcopyrite, and bornite.

Foliated, sericitic tuff-locally contains up to 40% disseminated pyrite.

Table 1. Zoning sequence at the Silver Peak mine.

be a lateral equivalent to a feeder system. The silicified tuff is overlain or flanked by loosely consolidated massive pyrite (friable yellow ore), dense massive pyrite-chalcopyrite (yellow ore), massive pyrite-chalcopyrite-sphalerite-bornite-tennantite-barite (black ore), massive white barite, and ferruginous chert-sulfide lapilli tuff. Though numerous exceptions can be found, the general sequence (Table 1) is readily apparent at Silver Peak. Zoning is best observed on the Lower Umpqua main drift. In addition to the vertical zoning, a lateral zoning with more abundant yellow ore to the southwest and more abundant black ore to the northeast is observable on the Lower Umpqua main drift.

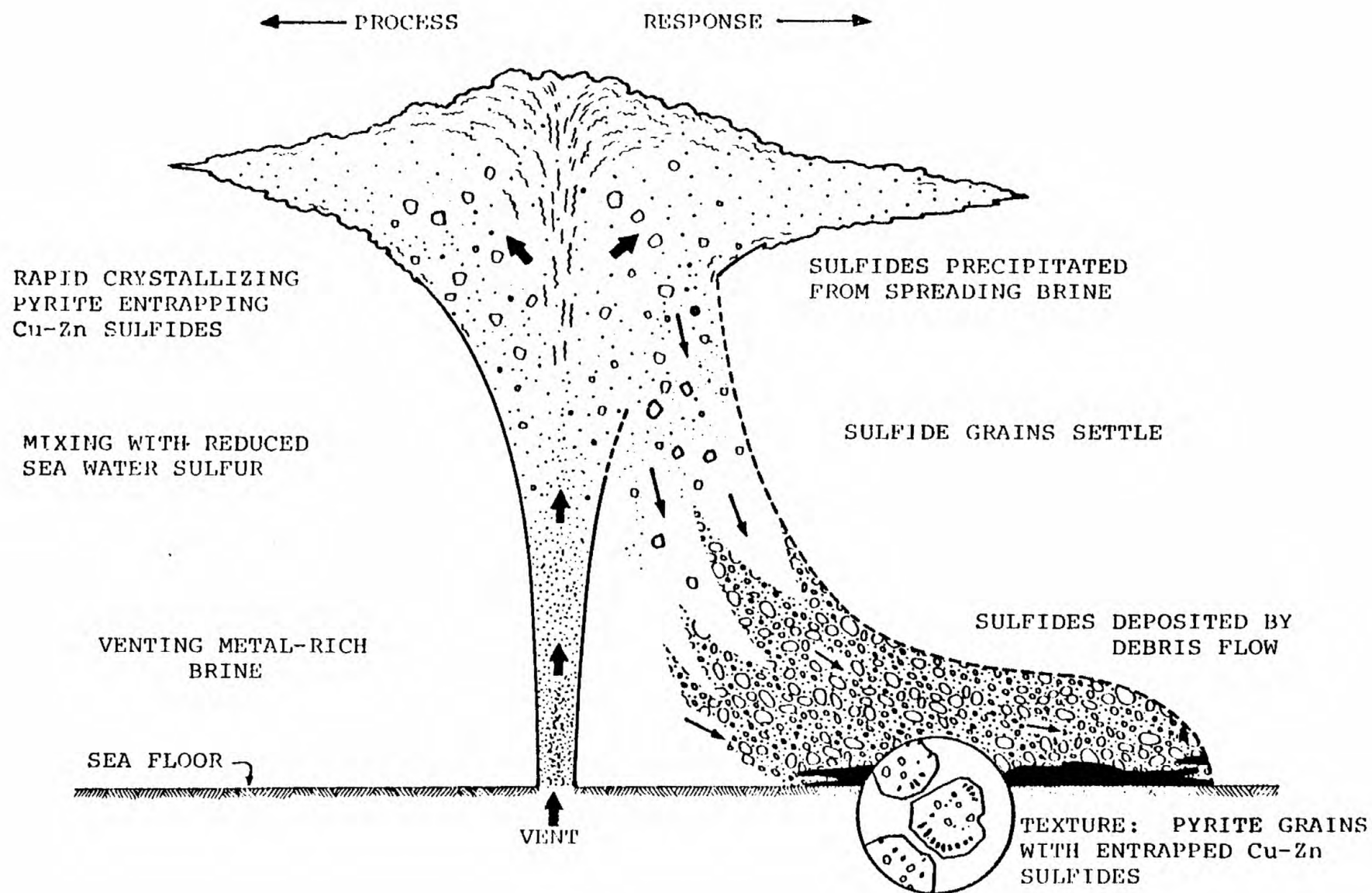
Friable yellow ore consists of a loosely bound aggregate of sub-rounded pyrite grains. No copper or zinc minerals were observed in this zone. Yellow ore consists of a dense aggregate of sub-rounded pyrite grains which often contain locally abundant blebs of chalcopyrite and occasional tennantite. Sub-rounded pyrite grains in black ore from Silver Peak contain blebs of all the Cu-Zn sulfides identified at the mine. Figure 4 is an illustration of a single pyrite grain which contains blebs of bornite, tennantite, and chalcopyrite. The sub-rounded grains of pyrite in massive sulfide at Silver Peak are surrounded and appear to be cemented by the various Cu-Zn sulfides and barite.

Massive white barite overlies black ore on the northeast end of the Lower Umpqua drift. A ferruginous chert bed overlying massive barite similar to those described in Kuroko deposits is not present at Silver Peak; however, ferruginous chert fragments up to three centimeters in diameter are present in flow banded tuff which overlies massive sulfide and massive barite on the northeast end of the Lower Umpqua level. This flow banded tuff also contains up to ten percent disseminated sulfides which are predominantly pyrite and chalcopyrite. The flow banding wraps around individual lapilli size sulfide grains or groups of grains often with associated quartz grains, thus, the name "sulfide lapilli tuff" for this unit.

Plume Model for Mineralization at Silver Peak

A preliminary plume model which integrates recent discoveries of venting and rapidly precipitating sulfide brines on the sea floor is presented to explain textures found in the massive sulfide at Silver Peak. It is similar to experimental modeling by Solomon and Walshe (1979) or Turner and Gustafson (1978) and analogous to vents found at 21 degrees north in the Pacific Ocean (Spiess, et al., 1980; Hekinian, et al., 1980).

Metal rich brines high in iron with variable amounts of copper, zinc, and barium vented onto the sea floor as depicted in Figure 5. Rapid mixing with sea water containing reduced sea water sulfur resulted in rapidly crystallizing



pyrite with copper and zinc being entrapped in the pyrite. The brine which included precipitated sulfide grains either settled slowly from a spreading plume or was rapidly deposited from a sulfide debris flow as depicted in Figure 5.

Numerous disrupted beds, fragments of barite floating in a matrix of black ore, load structures, and graded bedding are features in the massive sulfide all of which could be developed during debris flow. Sub-rounded pyrite grains could also be indicative of attrition during debris flow, or they may be indicative of rapid precipitation and attrition in the vent area.

The texture of sub-rounded pyrite grains which contain blebs of Cu-Zn sulfides can be attributed to rapid precipitation from a venting brine as depicted in Figure 5. A brine with relatively high iron concentration compared to copper and zinc could rapidly precipitate pyrite and entrap copper and zinc to form the blebs found at Silver Peak. Following deposition, the granular pyrite could have been permeated by Cu-Zn brines which surrounded and then cemented the pyrite grains.

References

- Garcia, M. O., 1978, Criteria for the identification of ancient volcanic arcs: *Earth Sci. Rev.*, v. 14, p. 147-165.
- , 1979, Petrology of the Rogue and Galice Formations, Klamath Mountains, Oregon: Identification of a Jurassic island arc sequence: *Jour. Geol.*, v. 86, p. 29-41.
- Hekinian, R., Fevrier, M., Bischoff, J. L., Picot, P., and Shanks, W. C., 1980, Sulfide deposits from the East Pacific Rise near 21°N: *Science*, v. 207, p. 1433-1444.
- Hotz, P. E., 1969, Relationships between the Dothan and the Rogue Formations, southwestern Oregon: *U. S. Geol. Survey Prof. Paper* 650-D, p. D131-D137.
- Irwin, W. P., 1964, Late Mesozoic orogenics in the ultramafic belts of northwestern California and southwestern Oregon: *U. S. Geol. Survey Prof. Paper* 501-C, p. C1-C9.
- Johnson, M. G. and Page, N. J., 1979, Preliminary geologic map of the metavolcanic and associated rocks in parts of the Canyonville, Days Creek, and Glendale quadrangles, Oregon: *U. S. Geol. Surv., Open File Report* 79-283, 1 sheet, map with explanation.
- Ramp, Len, 1972, Geology and mineral resources of Douglas County, Oregon: *Oregon Dept. of Geol. Mineral Indus. Bull.* 75, 106 p.

- Shennon, P. J., 1933, Copper deposits in the Squaw Creek and Silver Peak districts and at the Almeda mine, southwestern Oregon, with notes on the Pennell and Farmer and Banfield prospects: U. S. Geol. Survey Circ. 2, 35 p.
- Solomon, M. and Walshe, J. L., 1979, The formation of massive sulfide deposits on the sea floor: Econ. Geol., v. 74, p. 797-813.
- Spiess, F. N., et al., (RISE Project Team), 1980, East Pacific Rise: Hot springs and geophysical experiments: Science, v. 207, p. 1421-1432.
- Turner, J. S. and Gustafson, L. B., 1978, The flow of hot, saline solutions from vents in the sea floor--some implications for exhalative sulfide deposits: Econ. Geol., v. 73, p. 1082-1100.
- Wells, F. G., and Walker, G. W., 1953, Geologic map of the Galice quadrangle, Oregon: U. S. Geol. Survey Map GQ-25.

Kuroko type mineralization at the Red Ledge deposit, Idaho

A. P. Juhas, Texasgulf Inc.

T. P. Gallagher, Texasgulf Inc.

KUROKO TYPE MINERALIZATION AT THE
RED LEDGE DEPOSIT, IDAHO

Juhas, Allan P., Gallagher, Thomas P.,
Texasgulf Inc., 5934 McIntyre St., Golden, Colorado 80401

INTRODUCTION

The Red Ledge Deposit is located in the Seven Devils mining district in Adams County, Idaho, about 100 miles northwest of Boise near Hells Canyon Dam on the Snake River (Fig. 1). It is a complex zinc-copper-silver deposit of the eugeosynclinal volcanogenic massive sulphide affiliation. Although it occurs in a package of Permian strata it possesses the sulphate minerals and the stratiform and stockwork styles of mineralization which are most characteristic of the Kuroko type deposits of Miocene Age. The deposit is believed to have formed by submarine hot spring processes associated with explosive felsic volcanism.

The authors were involved in the exploration of the Red Ledge Deposit and wish to thank senior management of Texasgulf Inc., especially Drs. Leo Miller and George Mannard for their support and for the opportunity to make this presentation. R. Fredericksen was involved in some of the early drilling.

The emphasis of this paper will be on the various types and styles of mineralization in the deposit, their shapes, distribution patterns, and their relationships to host and associated rocks. Rock types, mineralization types and alteration patterns are based mainly on observations at the hand specimen and drill core level. It is hoped that the framework presented here can be used as a basis for more detailed research by others.

EXPLORATION HISTORY

The first adits were driven into the Red Ledge Deposit in the early 1900's. High grade silver-zinc mineralization was discovered but no production ensued; perhaps because of the rugged topography and complexity of the ores. The Butler Ore Company acquired the property during the depression years and did some exploration during the late 1930's and early 1940's. The property remained dormant until the early 1960's when it was explored as a porphyry copper-molybdenum prospect by a succession of mining companies. The volcanogenic massive sulphide nature of the deposit was recognized in 1972 during a Texasgulf regional reconnaissance program. Texasgulf Inc. optioned the property in 1974, drilled it extensively in 1975 and 1976, and purchased it in 1979.

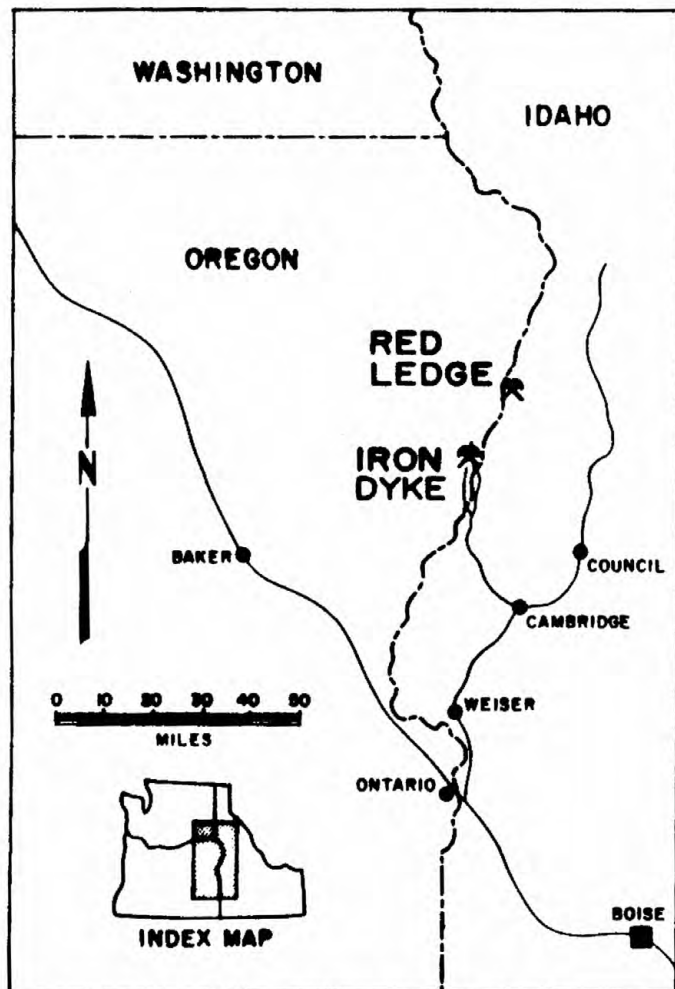


Fig. 1: Location map

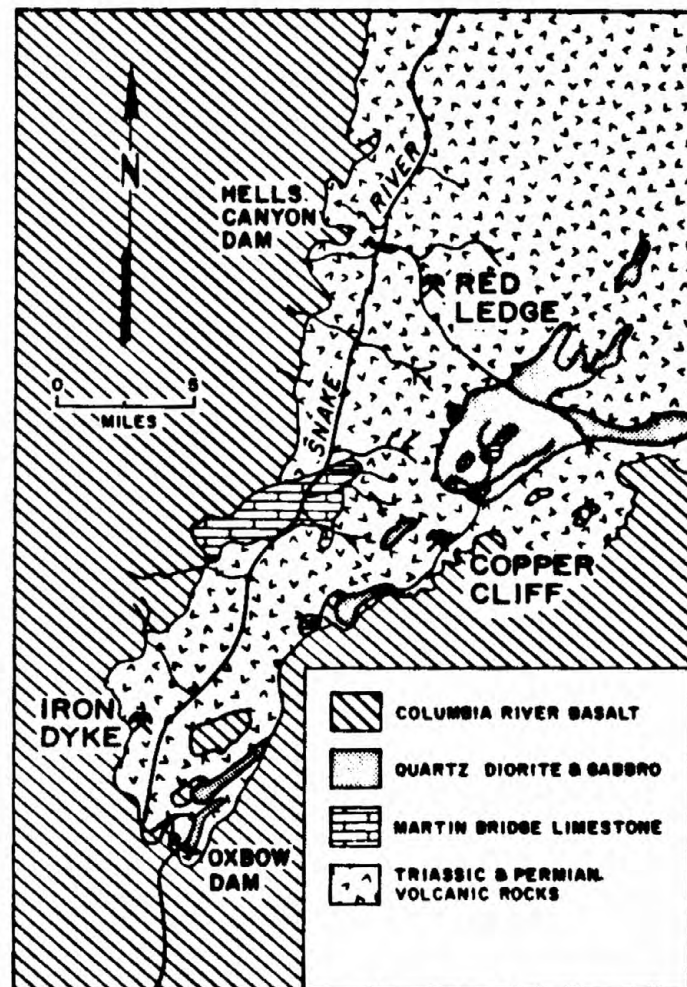


Fig. 2: Regional geology after Vallier 1973, Cook, 1954 and Cannon et. al, (unpublished) 1940.

GEOLOGY

Phanerozoic rocks in the Seven Devils district occur as a window within the Columbia River Basalt of Tertiary age exposed by incision of the Snake River and tributaries (Fig. 2). The oldest units are island arc type volcanic, volcanoclastic and sedimentary rocks of Permian and Triassic age known as the Seven Devils Group. The volcanic and volcanoclastic rocks are comprised of flows, ash flows, tuffs and pyroclastic debris of rhyolitic, dacitic, andesitic and basaltic composition. Plugs, dikes and sills of equivalent composition are also present. Sedimentary rocks are mainly argillites and greywackes with subordinate limestone. They are intercalated with and/or grade into the volcanic units. The above units are capped by a regional marker, the Martin Bridge Limestone of Upper Triassic Age. North of the area shown in figure 2 some Jurassic shales and sandstones are found above the Martin Bridge Formation.

The above units have been complexly modified and deformed. Volcanic rocks, particularly the oldest ones, have been altered to quartz keratophyres, keratophyres and spilites, depending on original composition, and all have suffered lower greenschist facies metamorphism. Folding is complex although difficult to detect for lack of marker horizons. It is especially obvious in the limestones. Major northwest and northeast trending faults transect the area. Much of the deformation and metamorphism may be synchronous with the Triassic and/or Jurassic quartz diorite, gabbro and norite plutons present in the district.

The Red Ledge Deposit (Fig. 3) occurs in a complex pile of Permian calc-alkaline andesitic through rhyolitic volcanic and volcanoclastic rocks, correlative with Vallier's (1974) Hunsaker Creek Formation. Units include flows, flow breccias, ash flows, lapillae tuffs, and derived sedimentary rocks. Complex intrusive - extrusive felsic domes penecontemporaneous with felsic volcanism occur at several levels in the formation. Andesitic dikes cut all units. Folding has rotated the Red Ledge Deposit and environs approximately 90 degrees such that units originally horizontal are now nearly vertical, striking northeast, and some previously vertical fissure systems and related alteration pipes are now sub-horizontal (Fig. 4). Several younger northwest and southeast trending shear zones are present. The deposit has been exhumed by erosion since Pliocene time.

MINERALIZATION

The Red Ledge Deposit is comprised of both epigenetic and syngenetic mineralization displaying gradational concentric and telescoped patterns of metal distribution and alteration. Two main zones are present, a discordant stockworks type system of feeder mineralization and an overlying cap of stratabound and stratiform mineralization.

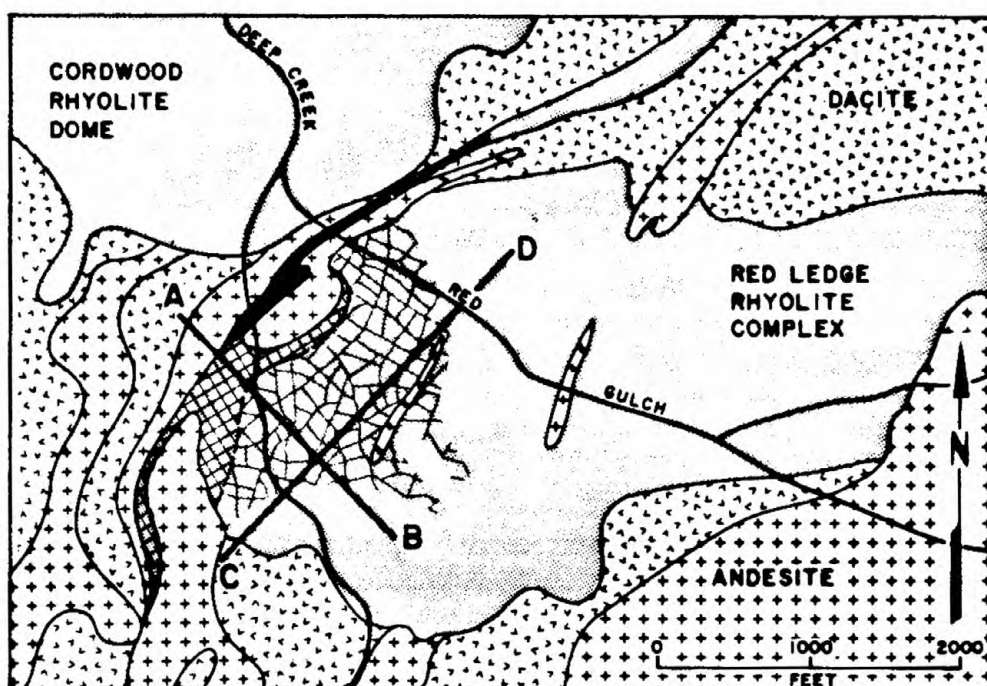





Fig. 3: General surface geology, and distribution of types of mineralization:  massive sulphides  stringer sulphides  feeder sulphides

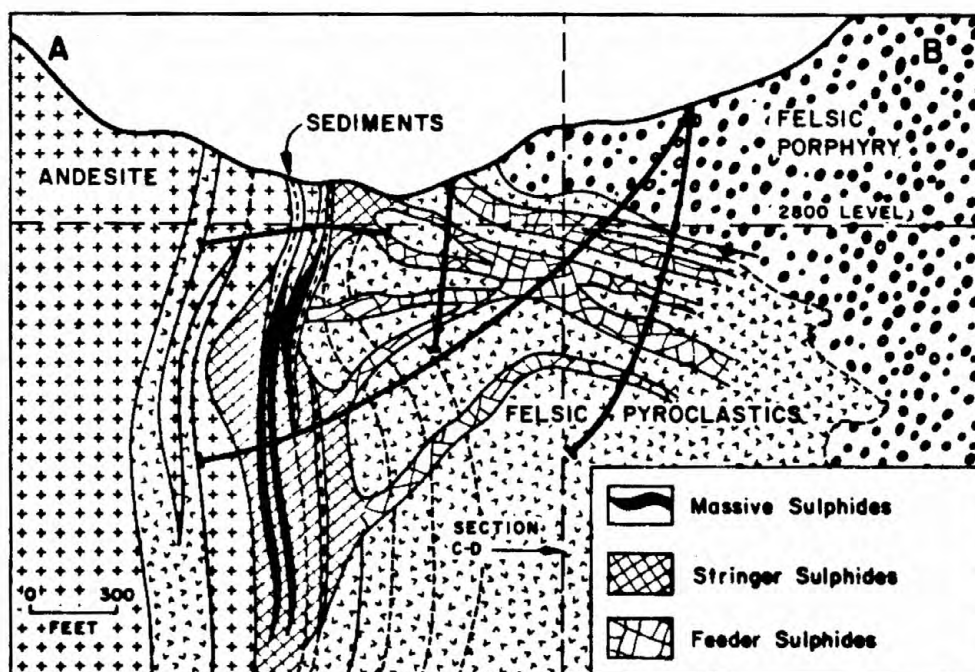


Fig. 4: Geological cross section A-B

The stratiform mineralization occurs at the top of the thickest section of a major felsic sequence and reflects a change in the character of the Hunsaker Creek Formation. The overlying units are comprised mainly of andesitic flows and flow breccias, subordinate sedimentary rocks derived mainly from dacites, and a few interbeds of felsic pyroclastic rocks. Many, but not all, of the andesitic units are of a high oxidation state suggesting a shallow submarine, if not a subaerial origin. The thickest portion of stratiform mineralization is located directly above a presently sub-horizontal fissure system composed of three and possibly four separate, sub-parallel, en echelon fissures. This fissure system occurs in the contact area between a dome-like body of quartz feldspar porphyry and beds of felsic pyroclastic rocks oriented essentially perpendicular to the fissure system. Similar pyroclastic units overlie the dome, are intercalated with the uppermost parts of the dome, and host some of the stratabound mineralization. The intensity and extent of mineralization in the fissure system seems to die out where the fissures appear to become rooted in the porphyry body some 1200 feet below the stratabound zone.

The zone of feeder mineralization controlled by the fissure system is as much as 500 feet wide, over 1000 feet long and cuts across some 1200 feet of strata. It is composed of anastomosing quartz-sulphide veins within silicified felsic host rocks. The roots of the system contain pyrite and minor chalcopyrite. At a depth of about 700 feet stratigraphically below the base of stratiform mineralization chalcopyrite becomes the dominant sulphide. Abundances of 2% to 3% copper over thicknesses of several tens of feet are common. This unique zone is called "deep-throat mineralization." (See Figure 5, a vertical section oriented essentially parallel to the stratabound zone.) Upward and outward chalcopyrite diminishes (although it is still the dominant valuable sulphide mineral) and sphalerite and tetrahedrite become more abundant. Correspondingly, barite becomes progressively more common in the matrix. The feeder mineralization is bordered by a halo of disseminated pyrite, associated with quartz-sericite alteration.

The zone of stratiform mineralization is as much as 400 feet thick and over 1500 feet in diameter (Figs. 4 and 6). It is made up of massive sulphides, breccia sulphides and stringer sulphides that were deposited in three major cycles that correspond to three and possibly four generations of brecciation and quartz-sulphide cementation recognized in the feeder system. (It should be noted that a fourth cycle of felsic volcanism is represented by a thick blanket of pyroclastic rocks in the immediate hanging wall of the zone of stratiform mineralization. It is likely consanguineous with the underlying felsic volcanic rocks of the mineralized zone but has not suffered the same alteration and epigenetic mineralization of the lower units - at least not where explored to date. It characteristically contains abundant disseminated knots and veinlets of pyrite in a quartz-sericite matrix.) Lithologies

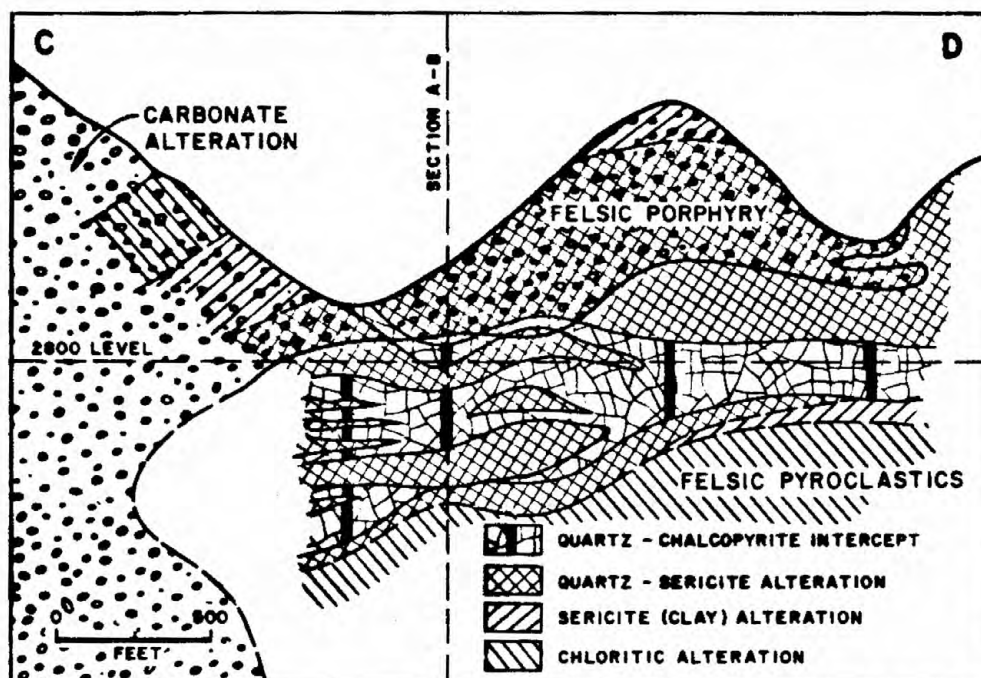


Fig. 5: Vertical geological section C-D looking northwest; "deep throat" mineralization and associated alteration.

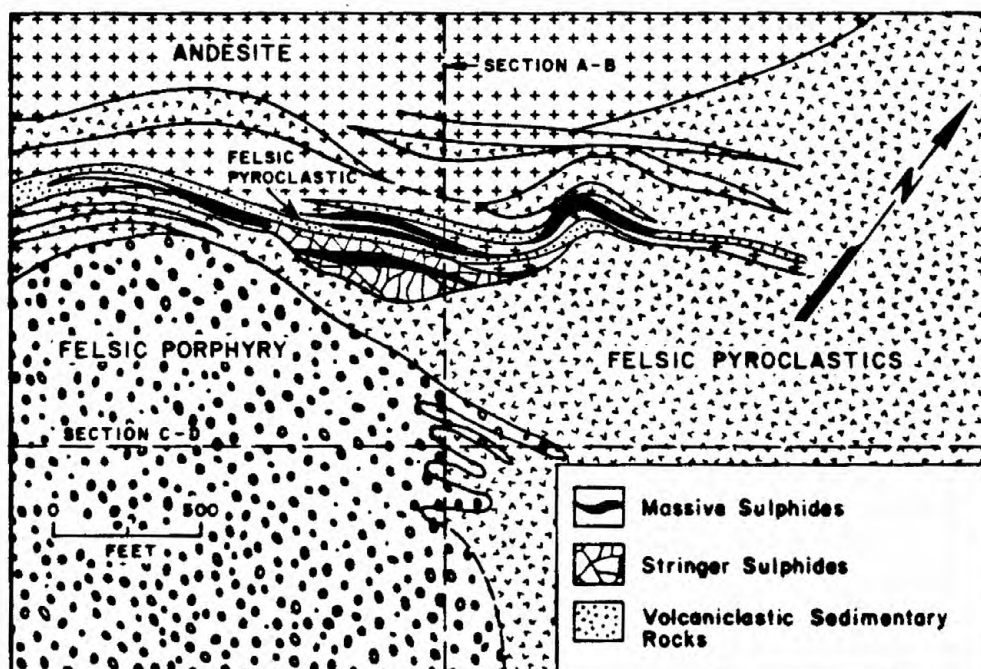


Fig. 6: Geology of the 2800 level. The subhorizontal feeder mineralization and associated alteration halos are omitted.

associated with the stratiform portion of the deposit include rhyolite and dacite fragmental rocks; dark grey to purple to green andesite flows and flow breccias; and layers of epiclastic rocks and tuffs. Each cycle generally commenced with felsic pyroclastic rocks containing stringer mineralization followed by massive sulphides. Andesitic rocks, tuffs and/or volcanoclastic sedimentary rocks are commonly associated with the massive sulphides, or take their position.

Stringer mineralization is the most common type. It occurs in internally monotonous blankets as much as 200 feet thick wherein silicified felsic fragmental rocks are replaced by fine aggregates of barite, pyrite, quartz, sphalerite, chalcopyrite, and tetrahedrite. Sulphides comprise 5% to 25% of the stringer zone and barite 10% to 20%. Where they are in contact, stringer and feeder mineralization are indistinguishable. The barite-quartz-sulphide aggregate cuts across the felsic fragments and fills voids between them. Several episodes of brecciation, mineralization and rehealing are indicated.

Massive sulphides occur in lenses as much as 85 feet thick but average less than 40 feet. They are massive to delicately laminated, and are comprised of pyrite, barite, sphalerite, chalcopyrite, galena, tetrahedrite and minor gold.

Breccia mineralization is a type that is transitional in time and space between stringer and massive sulphide mineralization and is characterized by discrete felsic fragments within massive sulphides. Quartz-barite veins and/or silicification are absent. It is a minor type and has been lumped in with the massive sulphides in the illustrations. The massive and breccia sulphides tend to form in depressions around the edges of zones of stringer mineralization.

Figure 7 illustrates the stacked distribution of the successive massive (and breccia) sulphide cycles. Figures 8 through 11 demonstrate the distribution of metals over the entire stratabound zone irrespective of type of mineralization. Copper has two zones of maximum concentration (Fig. 8). The lower one is a typical bull's-eye type and is due mainly to the copper content of cycle 3 stringer mineralization. The upper zone, with a flat bottom, near the 2800 level, is due to earlier cycles of stringer and massive sulphide mineralization, plus some supergene enrichment. Gold (Fig. 9) has a strong central tendency which parallels copper in its distribution. Zinc (Fig. 10) has a doughnut type distribution pattern. The highs surrounding a central low largely reflect the distribution of massive sulphides as opposed to stringer mineralization. Silver mineralization (Fig. 11) generally parallels the distribution of zinc.

Taken as a whole, the zone of stratabound mineralization at Red Ledge does not demonstrate the classical massive sulphide type metal zoning characterized by copper and gold concentrations near the footwall with zinc, lead and silver concentrations near the hanging wall. In fact, the reverse is true. Copper and gold tend to be richest near the hanging wall, and zinc and silver are concentrated near the middle and lower parts of the zone.

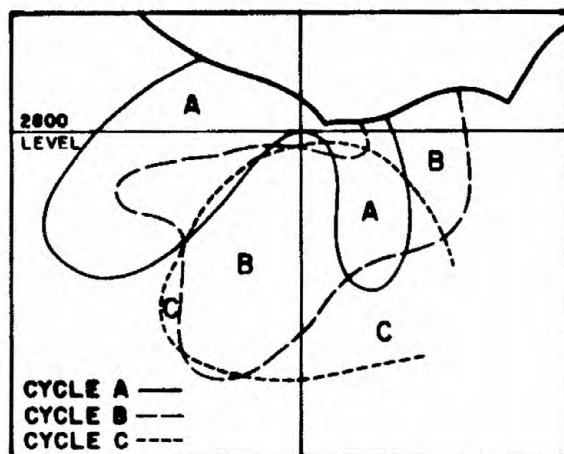


Fig. 7: Distribution of successive massive sulphide cycles.

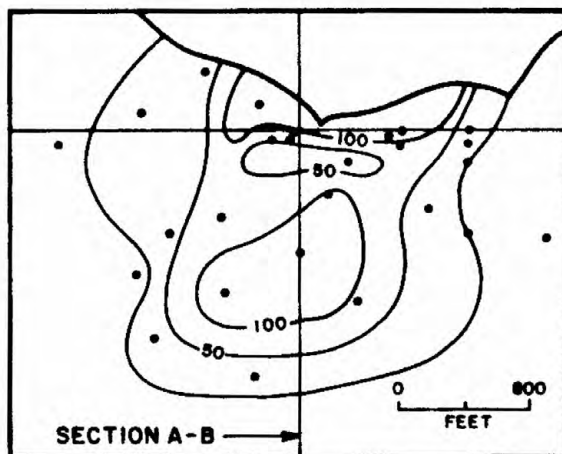


Fig. 8: Copper distribution.
% Cu x feet.

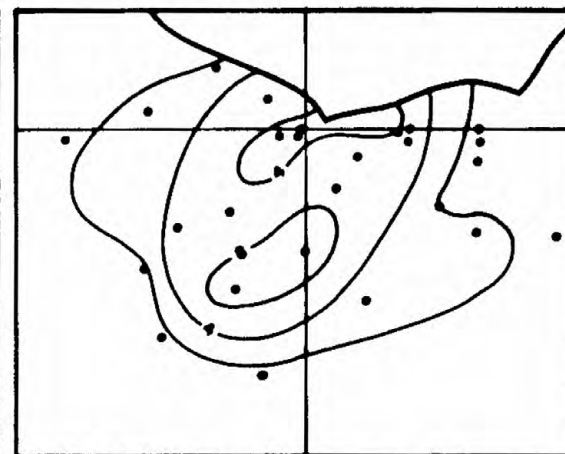


Fig. 9: Gold distribution.
Oz/ton Au x feet.

Note: All figures on this page are of the same vertical longitudinal projection drawn essentially parallel to the plane of strataform mineralization, looking northwest. The metal distribution values represent grade times horizontal thickness in feet across the entire zone of massive plus stringer mineralization. Dots are adits or centers of drill intercepts.

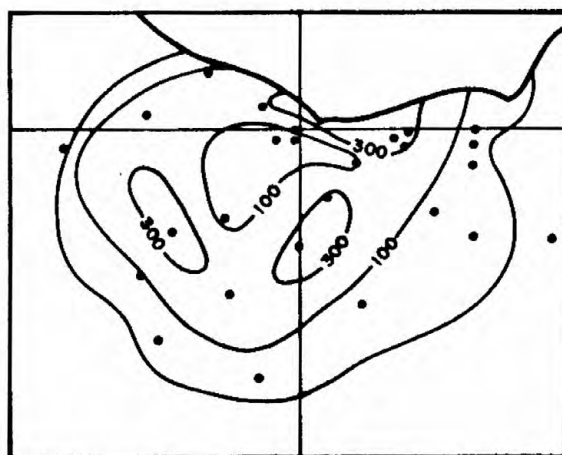


Fig. 10: Zinc distribution.
% Zn x feet.

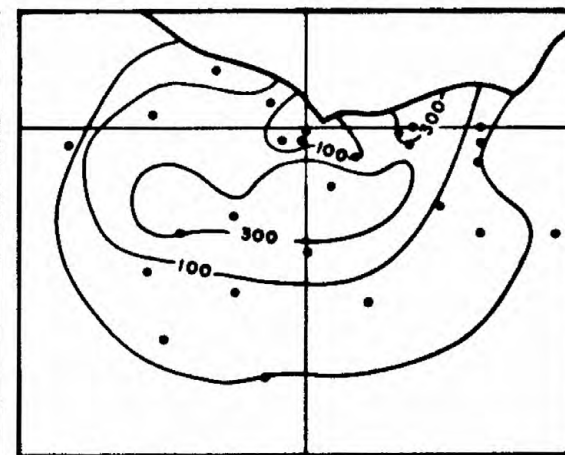


Fig. 11: Silver distribution.
Oz/ton Ag x feet.

This contradiction is explained by the fact that the Red Ledge stratabound zone is comprised of 3 major cycles of stringer-massive sulphide type mineralization and that the earliest were richest in silver, lead and zinc whereas the latest was richest in copper and gold, and did not develop much massive sulphide. Individual stringer-massive sulphide cycles do, however, indeed show much higher zinc/copper or silver/gold ratios near their hanging walls.

Figure 12 is an idealized representation of the distribution patterns of the various important minerals in the Red Ledge system. Taking the stockwork and stratabound portion as a whole and recognizing that the richest copper mineralization is several hundred feet below the zinc-lead-silver zone, the deposit does possess the classical metal distribution patterns. Another feature that has not been commented on, but which should be mentioned is that replacement type barite tends to concentrate near the outer margins of the zone of stratabound mineralization and locally beneath it. Disseminated and stringer type pyrite tends to envelope all other types of mineralization.

ALTERATION

Mineralization at Red Ledge is associated with a broad spectrum of alteration types, most of them progressively and concentrically zoned (Fig. 13). The feeder and stringer mineralization are associated with zones of quartz flooding and pervasive silicic alteration which characteristically weather reddish brown. This grades into quartz-sericite zones and/or zones characterized by intense development of sericite and clay minerals which weather yellowish brown. This is commonly, but not always, bordered by zones in which the felsic rocks take on a greenish color due to the development of chlorite. Farther away the chloritic rocks locally become impregnated with fine, rusty-weathering ferruginous carbonates.

Chlorite and epidote minerals are commonly developed in intermediate volcanic rocks bordering the Red Ledge rhyolite. This is interpreted as propylitic alteration, and is probably of the same rank as the chloritic alteration in the more felsic rocks.

Another type of chlorite alteration (Fig. 13) occurs within the stratabound zone wherein solid dark green chlorite occurs as the matrix to felsic fragments in certain horizons, and rarely as irregular veinlets cutting various horizons, including massive sulphide zones.

Hematitic alteration related to oxidizing post-ore solutions is prominent in several places within the zone of stringer and breccia mineralization. It occurs as hematitic veins and impregnations in felsic fragmental rocks and intercalated andesite flows. Elsewhere stringer sulphides and sulphides interstitial to felsic fragments are altered to solid hematite.

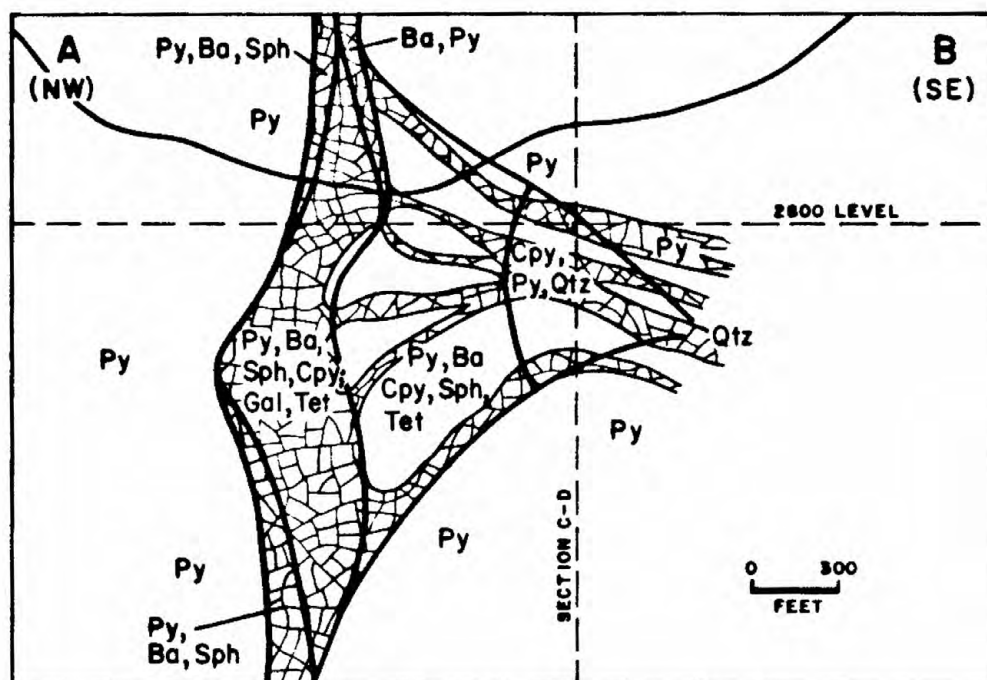


Fig. 12: Patterns of mineralization, cross section A-B.

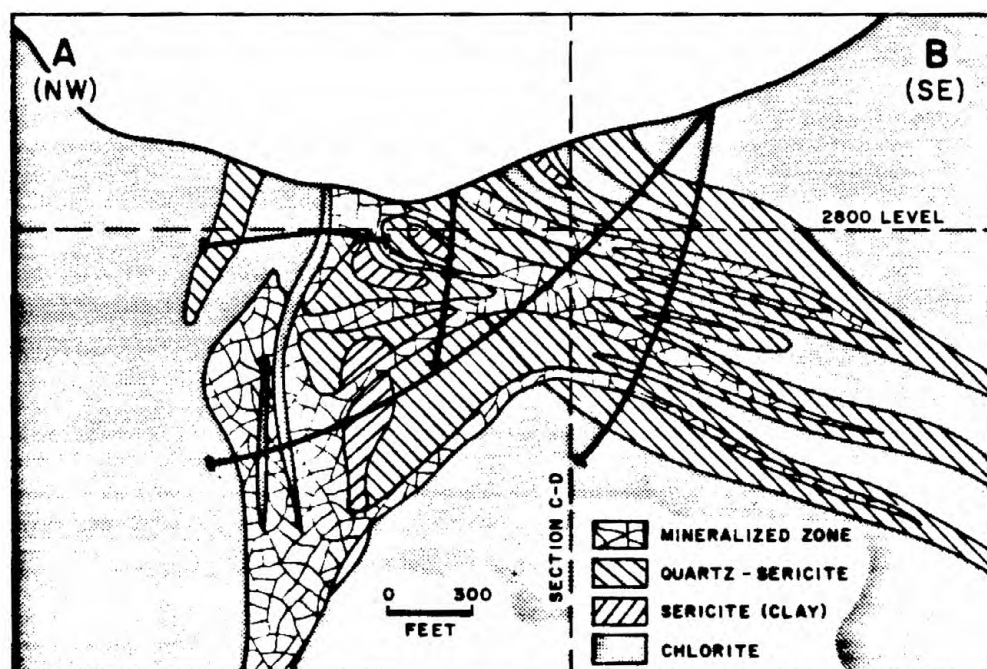


Fig. 13: Alteration patterns, cross section A-B.

CONCLUSIONS

It is interpreted that mineralization at Red Ledge formed in at least three pulses following episodes of dome formation and explosive felsic volcanism. Pyroclastic materials came from one or more vents whereas mineralization formed nearby in basins or on the flanks of the volcanoes by hot spring activity over zones brecciated by steam explosions above ruptured endogenous felsic domes. Feeder mineralization formed by replacement in and about brecciated fissure zones. Stringer mineralization formed by replacement and chemical precipitation in voids within initially porous and/or rebrecciated pyroclastic blankets which periodically swept over the hot spring area. Massive sulphide layers formed by submarine chemical precipitation on top of and in depressions beside the pyroclastic layers during periods of quiescence. Andesite flows and tuffs came from nearby competing volcanoes; the vents of some of which were above sea level. The epiclastic rocks were deposited in depressions with material derived from erosion of earlier rocks and by the re-working of tuffs and breccias.

The Red Ledge lithologies, mineralization, alteration and their zonal relationships are most similar to the Japanese Kuroko type massive sulphide deposits of Tertiary age. The copper-dominant feeder mineralization and associated alteration patterns deep within the Red Ledge rhyolite have similarities to porphyry copper systems. This similarity is due to the unusual size of the Red Ledge system and because the feeder system has formed by a similar genetic mechanism. It would be premature, however, to imply that porphyry copper deposits and massive sulphide deposits are necessarily gradational or compatible.

SELECTED REFERENCES

- Cook, E. F., 1954: Mining geology of the Seven Devils region. Pamphlet 97, Idaho Bureau of Mines and Geology.
- Juhas, A. P. and Gallagher, T., 1978: Final report on Texasgulf's Red Ledge exploration project, Idaho. Private Texasgulf report.
- Juhas, A. P., Freeman, P. S., Gallagher, T. P., and Fredericksen R. S., 1980: Kuroko type mineralization at the Iron Dyke Mine, Oregon and the Red Ledge Deposit, Idaho. GSA Abstracts with Program, Vol. 12, No. 3.
- Livingston, D. C. and F. B. Laney, 1920: The copper deposits of the Seven Devils and adjacent districts. Bull. 1, State of Idaho, Bureau of Mines and Geology.
- Long, R. C., 1975: Geology and mineral deposits of the Red Ledge Mine area, Adams County, Idaho. Unpublished M.Sc. thesis, Oregon State University.
- Vallier, T. L., 1967: The geology of part of the Snake River Canyon and adjacent areas in northeastern Oregon and Western Idaho. Unpublished Ph.D. thesis, Oregon State University.
- Vallier, T. L., 1974: A preliminary report on the geology of part of the Snake River Canyon, Oregon and Idaho. State of Oregon, Dept. of Geology and Mineral Industries, CMS-6.

Kuroko type copper-gold mineralization at the Iron Dyke mine,
Oregon

A. P. Juhas, Texasgulf Inc.

P. S. Freeman, Texasgulf Inc.

R. S. Fredericksen, W.G.M. Inc.

KUROKO TYPE COPPER - GOLD MINERALIZATION AT THE
IRON DYKE MINE, OREGON

Juhas, Allan P.; Freeman, Patrick S.; Texasgulf Inc., 5934 McIntyre St., Golden, Colorado 80401 and Fredericksen, Rick S.; W.G.M. Inc., 1101 W. 7th Ave., Anchorage, Alaska 99501

INTRODUCTION

The Iron Dyke Mine is located at Homestead in Baker County, Oregon, about 100 miles northwest of Boise (Fig. 1). It occurs within the main valley of the Snake River about 15 miles southwest of the Red Ledge Deposit. It is a copper-gold deposit of the eugeosynclinal volcanogenic massive sulphide affiliation. It occurs in the same package of Permian strata as the Red Ledge Deposit described elsewhere in this publication, and is believed to have formed similarly by submarine hot spring processes associated with explosive felsic volcanism. The Iron Dyke is a smaller mineralized system than Red Ledge, and does not have the same spectrum of zones. It is, nevertheless, considered to be of the Kuroko type because of its setting, lithologies, geometry and apparent genetic mechanism.

The authors were involved in various phases of the exploration and evaluation of the Iron Dyke Mine and wish to thank senior management of Texasgulf Inc., especially Drs. Leo Miller and George Mannard for their support and for the opportunity to make this presentation. The emphasis of this paper will be on the general types of mineralization in the deposit, their shape, distribution patterns, and their relationships to host and associated rocks. Rock types, mineralization types and alteration patterns are based mainly on observations at the hand specimen and drill core level made during the course of exploration.

EXPLORATION AND MINING HISTORY

The Iron Dyke still holds the record of being Oregon's largest copper producer. Between 1916 and 1928 about 239,000 tons of ore grading 3.02% copper, 0.146 oz/ton gold and 1.07 oz/ton silver, were produced. The operator, Thayer Lindsley, one of the giants of North American economic geology, went on to Canada to establish the Ventures and Falconbridge empires. The Butler Ore Company acquired the property during the depression years and prepared it for production during the Second World War. The government denied them miners and the property remained dormant until Texasgulf began exploration. Texasgulf's interest was aroused in 1972 during a regional reconnaissance program when the volcanogenic nature of the deposit was recognized.

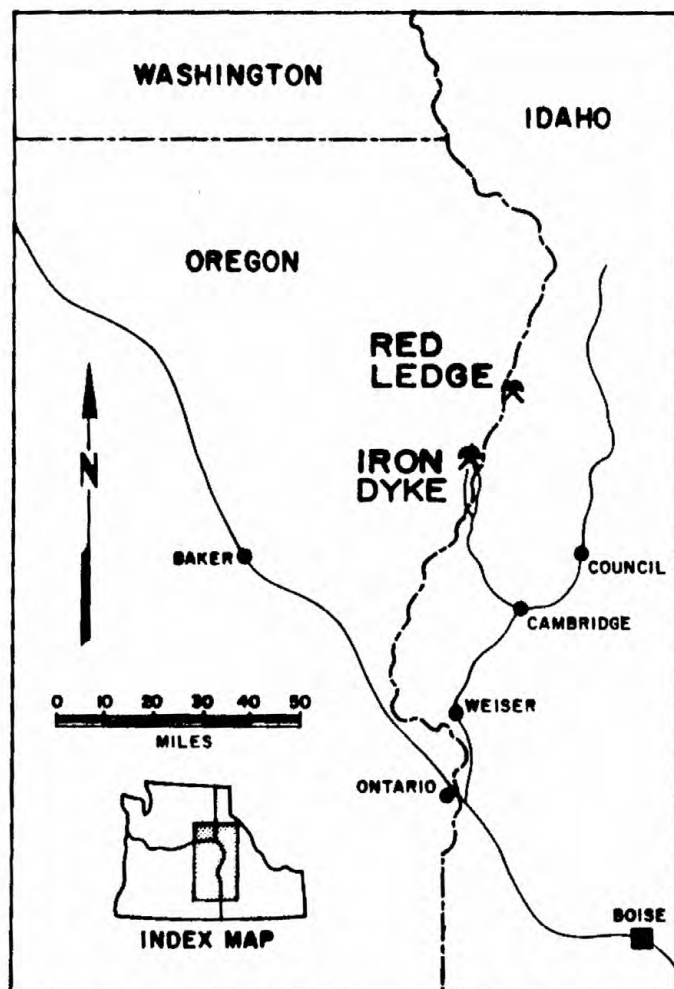


Fig. 1: Location map

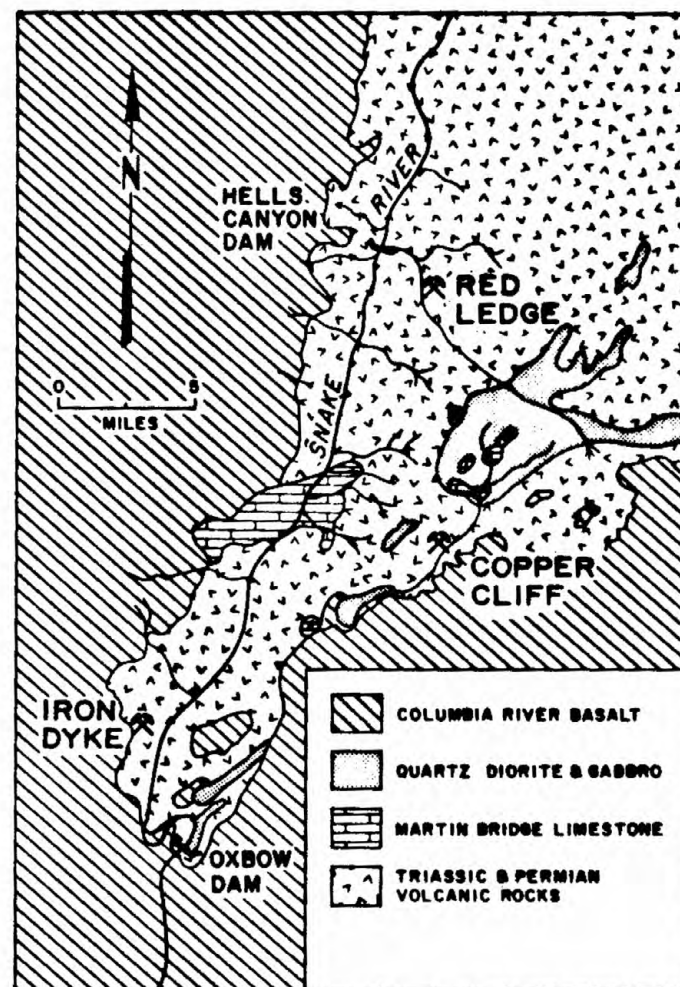


Fig. 2: Regional geology after Vallier 1973, Cook, 1954 and Cannon et. al, (unpublished) 1940.

The property was optioned in 1974 and extensively drilled in 1975 and 1976. This resulted in the discovery of a small ore-body with announced reserves of 325,000 tons of 2.7% copper, .25 oz/ton gold and .7 oz/ton silver. In 1979 the property was purchased by Texasgulf and a joint venture agreement made with Silver King Mines Ltd. to mine the deposit and to treat the ore in their Copper Cliff mill located at Cuprum, Idaho, some 20 miles away by road.

GEOLOGY

The Iron Dyke is in an area within the Columbia River Basalts of Tertiary age that has been exposed by incision of the Snake River. (Fig. 2 - Regional Geology.) The pre-Tertiary rocks are mainly comprised of island arc volcanic and sedimentary rocks of Permian and Triassic age known as the Seven Devils Group. The Iron Dyke deposit occurs within a sequence of volcanoclastic sediments, flows, tuffs, and pyroclastic debris of rhyolitic, dacitic, andesitic, and basaltic composition known as the Hunsaker Creek Formation (Vallier, 1974). Plugs, dikes and sills of equivalent composition are also present. These are overlain elsewhere in the region by volcanoclastic sandstones, argillites, and minor limestone and basaltic flows of the Wild Sheep Creek Formation; maroon and green basic flows and associated volcanoclastic sedimentary rocks and minor limestones of the Doyle Creek Formation; and massive limestones and dolomites of the Martin Bridge Formation.

The above units have been complexly modified and deformed. Volcanic rocks, particularly the oldest ones have been altered to quartz keratophyres, keratophyres and spilites, depending on original composition, and all have suffered lower greenschist facies metamorphism. Folding is complex although difficult to detect for lack of marker horizons. It is especially obvious in the limestones. Major northwest and northeast trending faults transect the area. Much of the deformation and metamorphism may be synchronous with the Triassic and/or Jurassic quartz diorite, gabbro and norite plutons present in the district.

The Iron Dyke Mine occurs in severely dissected terrain on the west bank of the Snake River. The property is underlain by a sequence of rocks (Fig. 3) which from the base upward consists of:

1. Dacitic pyroclastic flows;
2. Sulphide-bearing rhyolite ash flows and tuffs;
3. A lahar or debris flow;
4. Cherty argillites, siltstones, graywackes, and minor fossiliferous limestones;
5. Intrusive andesitic plugs, sills and dikes and;
6. A young capping sequence, the Columbia River Basalt.

The dominant structural feature on the Iron Dyke property is a syncline. This open fold plunges 20 to 30 degrees to the northeast and its axial plane tends to dip steeply to the southeast. Folding is tightest in the southwestern portion and becomes gradually more open to the northeast. Numerous post-mineral faults transect the area. Offsets are a few to over a hundred feet.

The lahar is the main ore host. It is composed of angular to rounded blocks and boulders of rhyolite, andesite and sedimentary rocks several feet to a few inches in diameter the average sizes of which dramatically decrease to the east. It has formed in at least three pulses. The lowest is intercalated with the rhyolite unit. The uppermost is intercalated with the graywacke-argillite sequence and contains a bed of limestone rich in brachiopods. One drill hole encountered several feet of thinly bedded gypsum-talc rock beneath the ore horizon. It is not known if it represents an interbed or simply a large fragment in the lahar.

MINERALIZATION AND ALTERATION

Based on gross relationships to their host rocks; two geometric styles of mineralization occur, forming a continuum linked in time and space (Fig. 4). Both are predominantly comprised of anastomosing networks of quartz-chalcopyrite veinlets. The first type, feeder mineralization, occurs in discordant pipe-like bodies approximately 200 feet in diameter cutting the uppermost portion of the rhyolite sequence. Where revealed by erosion these bodies form resistant knobs. The second type, stringer mineralization, is confined to discrete horizons within the lower lahar unit as shown in longitudinal section (Fig. 5). Stringer mineralization is restricted to within 1000 feet of the feeder zone. At the general scale of exploration, the stringer mineralization is blanket-like in form and statistically continuous. Within this blanket (Fig. 6), the intensity and grade of mineralization is extremely variable if not erratic over distances as little as a few tens of feet. This, in conjunction with faulting, predictably creates mining problems.

The mineralogy of the ore-bearing zones is rather simple, consisting of chalcopyrite and pyrite with minor amounts of sphalerite and trace amounts of gold, silver, galena, pyrrhotite, and bornite. The gangue is mainly quartz, chlorite and some barite. Gold occurs with the chalcopyrite and there is a direct correlation between gold and copper content as shown in the graph based on data from a high grade portion of the stringer zone (Fig. 7). It should be noted that the line does not pass through the origin. This is because a certain amount of the gold reports with a slightly earlier quartz-pyrite-chlorite assemblage, as opposed to the younger chalcopyrite-quartz-barite assemblage.

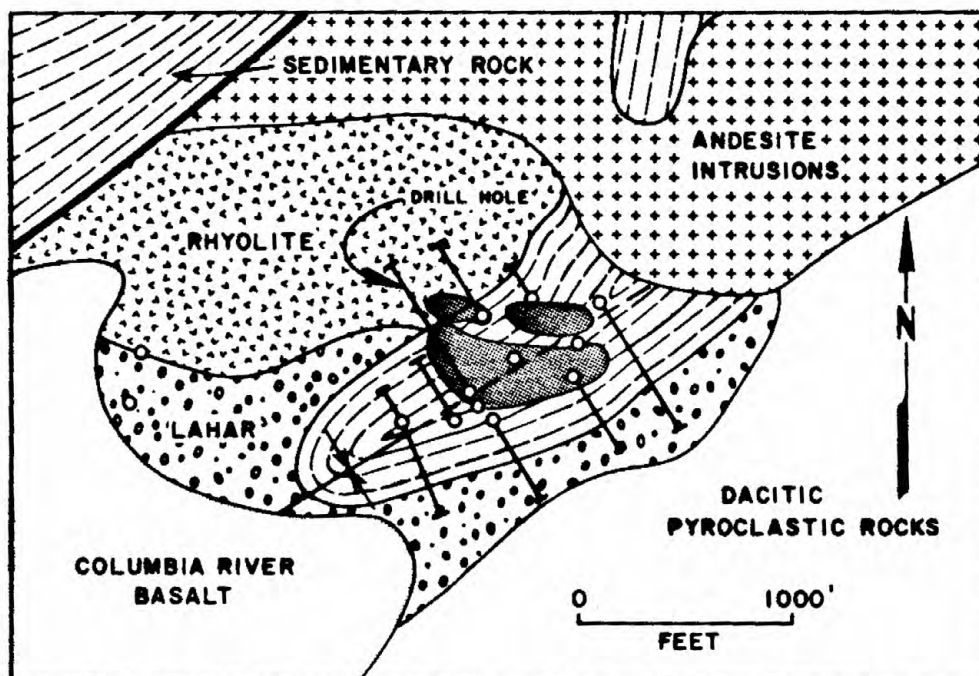


Fig. 3: General surface geology. Strata controlled mineralized zones have been projected to the surface (dark shaded ares).

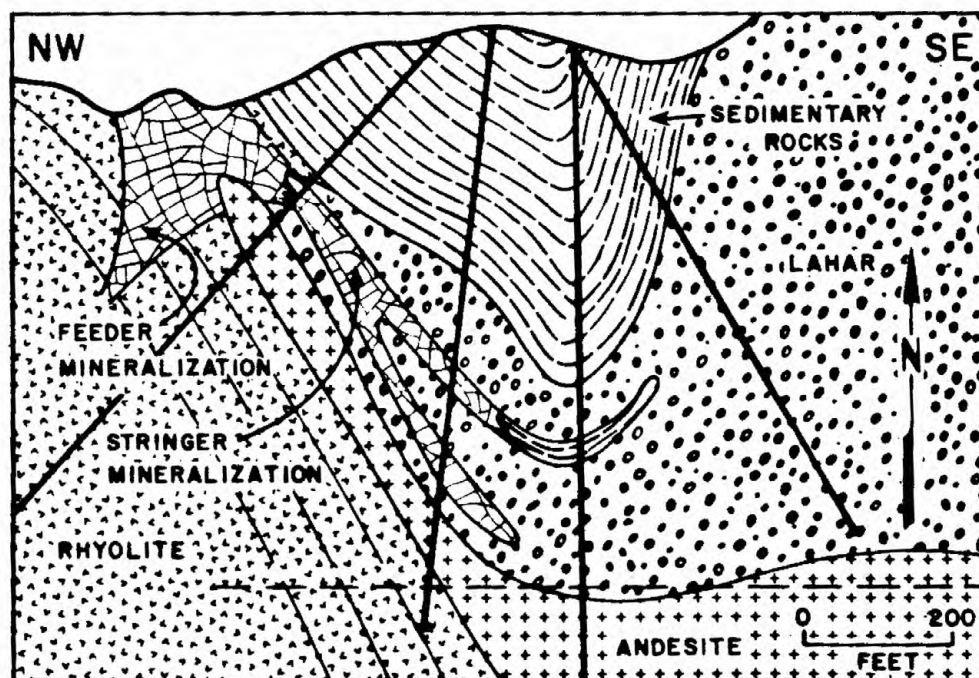


Fig. 4: Geological cross section 0.

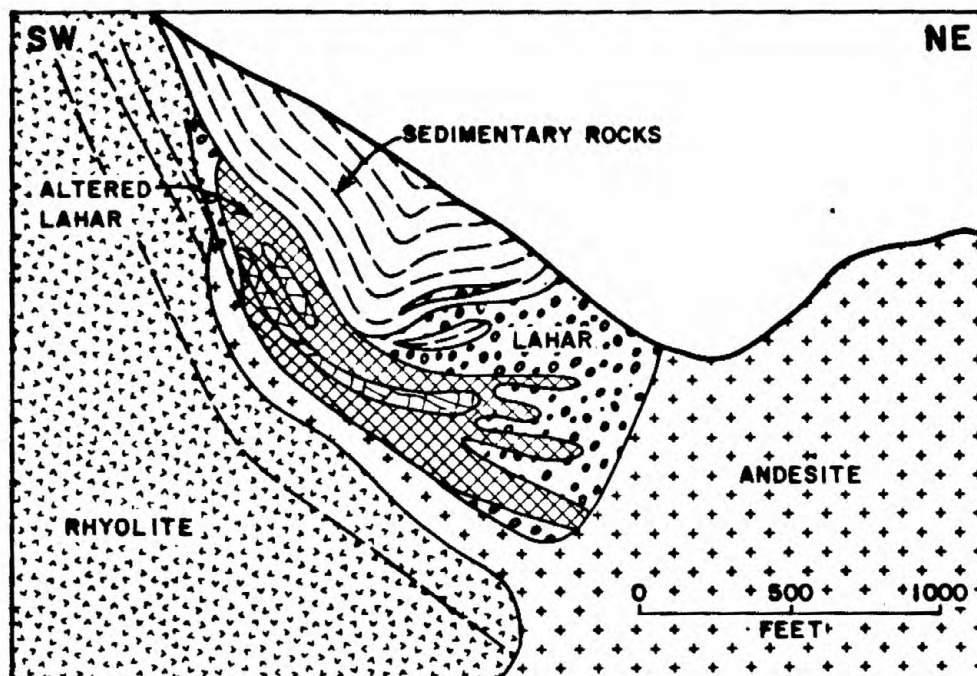


Fig. 5: Longitudinal geological section showing mineralization and alteration halo.

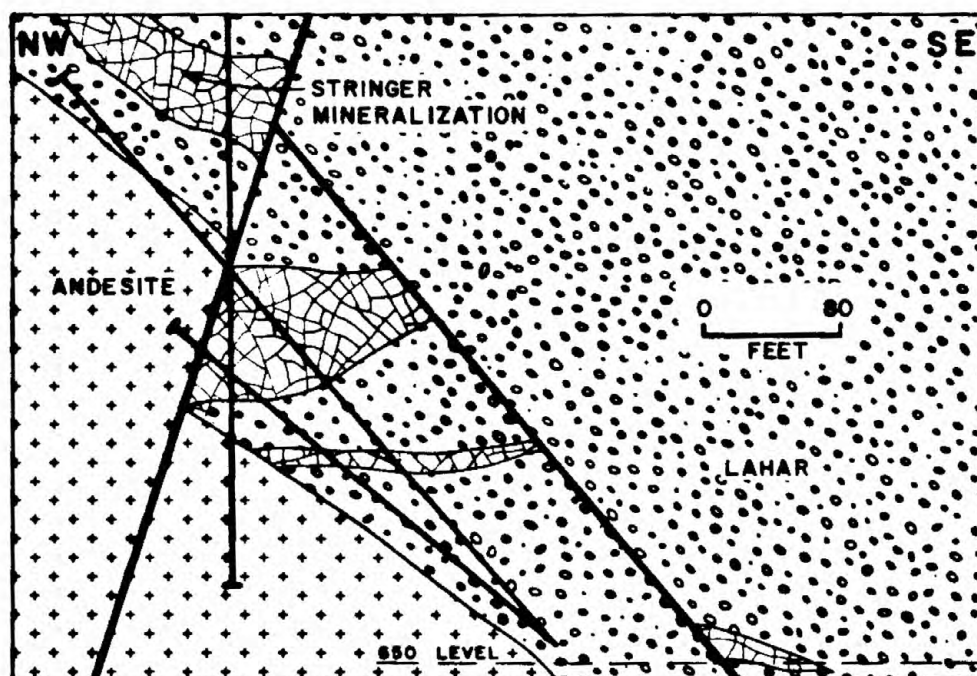


Fig. 6: Distribution of mineralization in detail.

In some places within the lahar unit, rounded cobble and boulder sized fragments of massive chalcopyrite characterized by low gold values are found. These are not connected to quartz-chalcopyrite veinlets. It is believed that these chalcopyrite masses were derived elsewhere and were transported and emplaced with the lahar.

Subtle zonal patterns exist in the stringer zone. Silver is more uniformly and more broadly distributed than the gold. Sphalerite tends to occur peripheral to copper-gold rich zones; both laterally and above them. No zinc rich mineralization has been encountered below the copper rich horizons.

The feeder mineralization within the rhyolite tends to contain appreciably lower gold and copper values and higher silver values than the stringer mineralization within the lahar.

The Iron Dyke Deposit displays concentrically zoned silicic, sericitic and argillic alteration (Fig. 8). Ore is restricted to the silicic zone. This is characterized by a hard, pervasive mixture of quartz and minor chlorite and pyrite which replaces the rock fragments and matrix; the pyrite and chlorite being largely in the matrix areas. Veinlets and knots of quartz, chalcopyrite and minor barite cut through this. The latter are commonly in sharp contact with a halo of quartz-sericite alteration which grades into a widespread argillic halo. Fresh rocks (albeit regionally metamorphosed) are found beyond the argillic zone.

Where altered, the lahar is bleached light grey to white in contrast to its more normal darker green color. Where alteration is pervasive, only a ghost-like fragmental texture is discernible.

The zone of feeder mineralization in the rhyolite sequence is highly silicic, although chloritic haloes surround individual quartz-sulphide veinlets. Chloritic alteration is pervasive only where the quartz-sulphide veinlets are closely spaced (one to three inches). The rhyolitic rocks surrounding the mineralized silicic zone are altered to quartz and sericite.

CONCLUSIONS

It is concluded that the Iron Dyke lahar formed from a vent explosion during the final stages of felsic volcanism. The lahar unit moved as a submarine debris flow and came to rest on the flanks of the volcano. Subsequently, volcanic exhalations passed through fracture controlled feeder systems in the rhyolitic pile and migrated from hot springs into the proximal, porous lahar unit. This resulted in widespread alteration which caused the unit to become indurated. Renewed phreatic explosions brecciated the lahar and allowed emplacement of the majority

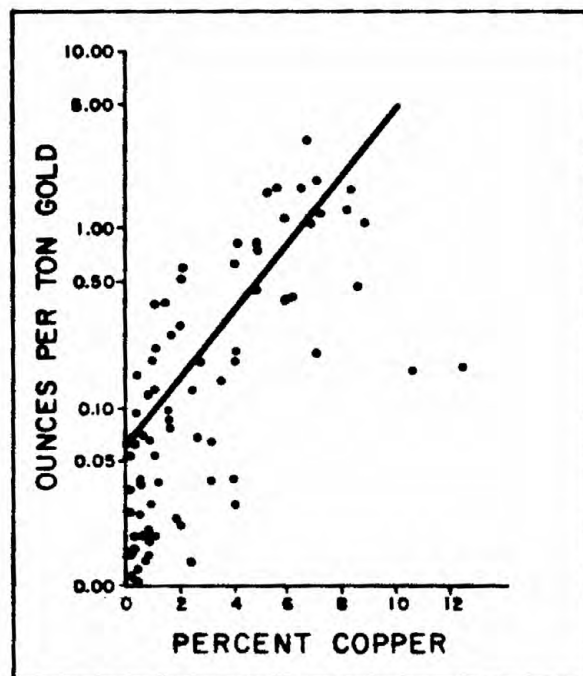


Fig. 7: Distribution of gold.

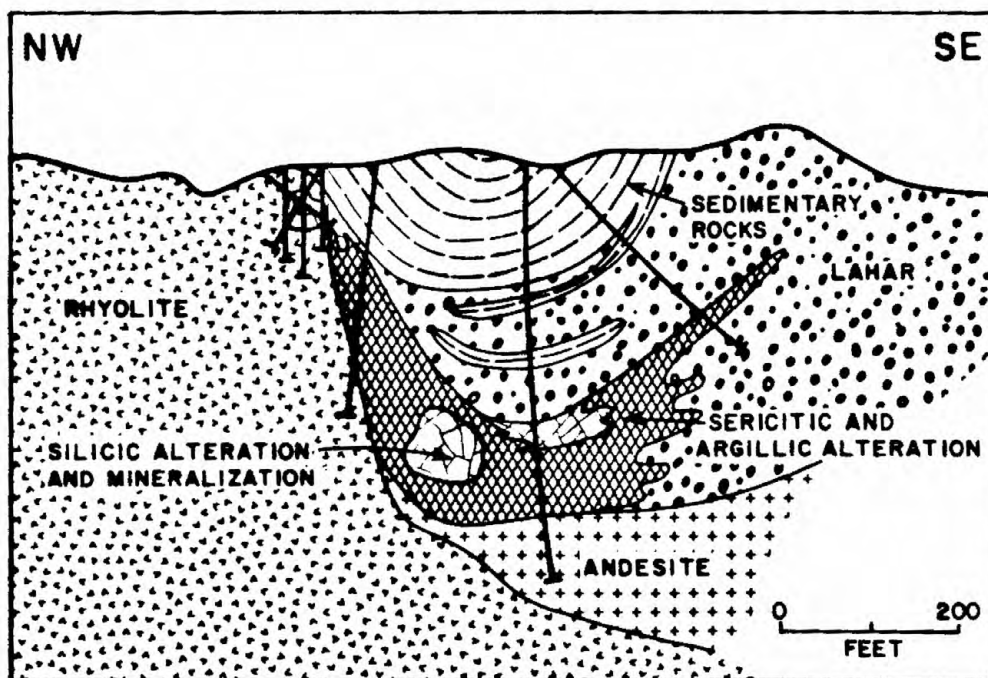


Fig. 8: Geological cross section 400N. with alteration patterns.

of chalcopyrite-gold-barite mineralization. Mineralization took place below the water-rock interface of the lower lahar pulse. Why massive sulphides are not found at that interface or higher in the section is not known. Perhaps the environment was too shallow and too oxidizing for the precipitation of massive sulphides, or perhaps they did form but were subsequently swept away by subaqueous slumping. In any event, the downslope portion of the geological section has been lost due to recent erosion.

REFERENCES

- Brooks, H. C., and Ramp, 1968, Gold and silver in Oregon: Ore. Dept. Geol. and Mineral Indus., Bull. 61.
- Fredericksen, R. S., 1977, Final exploration report, Iron Dyke project, Baker County, Oregon. Private Texasgulf report.
- Juhas, A. P., Freeman, P. S., Gallagher, T. P., and Fredericksen R. S., 1980: Kuroko type mineralization at the Iron Dyke Mine, Oregon and the Red Ledge Deposit, Idaho. GSA Abstracts with Program, Vol. 12, No. 3.
- Lindgren, Waldemar, 1901, The gold belt of the Blue Mountains of Oregon: U. S. Geol. Survey Annual Report 22.
- Swartlye, A. M., 1914, Ore deposits of northeastern Oregon, Corvallis. (Oregon Bur. Mines and Geology, Mineral Resources of Oregon, Vol. 1, No. 8.)
- Vallier, T. L., 1967, Geology of part of the Snake River Canyon and adjacent areas in northeastern Oregon and western Idaho: Unpublished Ph.D. thesis, Oregon State University.
- Vallier, T. L., 1974, A preliminary report on the geology of part of the Snake River Canyon, Oregon and Idaho: State of Oregon, Dept. of Geol. and Mineral Indus., Geol. Map Series #6.
- Vallier, T. L., and Brooks, H. C., 1970, Geology and copper deposits of the Homestead area, Oregon and Idaho: Ore Bin, V. 32, No. 3.

SPECIAL ACKNOWLEDGEMENT

The illustrations for this paper and the related paper on the Red Ledge deposit plus the slides for companion oral presentations were drafted by Dave Montoya, Larry Phillips and Mike Asplund of Texasgulf's exploration division.

Geology of the Little Boulder Creek deposit, Custer County,
Idaho

J. C. Balla, ASARCO

R. G. Smith, ASARCO

GEOLOGY OF THE LITTLE BOULDER CREEK DEPOSIT
CUSTER COUNTY, IDAHO

BALLA, John C., ASARCO, Spokane, Washington 99207;
SMITH, Russell G., ASARCO, Spokane, Washington 99207

The Little Boulder Creek molybdenum deposit is located in central Idaho, adjacent to the southeastern margin of the White Cloud stock. The White Cloud stock is a composite granitic stock of Late Cretaceous Age which intrudes the Wood River Formation (Pennsylvanian-Permian). Adjacent to the White Cloud stock is the Little Boulder Creek quartz monzonite, which has intruded calcareous quartzite units of the Wood River Formation. Calcsilicate skarn alteration and mineralization has been developed adjacent to the Little Boulder Creek quartz monzonite. The more intensely altered diopside-bearing skarn is the host for the major portion of the molybdenum mineralization.

The diopside-bearing skarn is intruded by numerous aplite dikes, simple granitic pegmatite dikes, and quartz veinlets. Molybdenum mineralization occurs as very fine grained molybdenite in veinlets in the skarn. An analysis of the geology of the deposit suggests that the deposit is allochthonous.

(Courtesy of the Geological Society of America, 1980)

Stratiform mineralization and origin of some of the vein
deposits, Bunker Hill mine, Couer d'Alene district, Idaho

M. R. Vulimiri

E. S. Cheney, University of Washington

Abstract

The Coeur d'Alene district, Idaho is well known for its vein deposits. However, several years ago mine geologists of the Bunker Hill Company noted stratiform deposits of sphalerite and argentiferous galena in thin-bedded impure quartzites of the St. Regis-Revett transition zone. This mineralization occurs in cross bedding, current ripple laminations, Bouma sequences, and structures produced by soft sediment deformation.

Stratiform mineralization is impoverished adjacent to vein-lets in hand specimens. On a larger scale, impoverished zones that border veins in the "J" area of the mine are approximately twice as wide as the vein ore. Vein orebodies occur only where faults cut stratiform mineralization. Pb:Zn of samples from veins vary from 5 to 3000, but ratios of stratiform mineralization vary from 5 to 40. Pb:Ag of vein and stratiform samples are virtually the same. Evidently, stratiform Pb and Ag were preferentially mobilized into the veins.

The stratiform Newgard ore is richer in zinc than the stratiform "J" mineralization. In the Newgard Pb:Zn increases stratigraphically upwards. The stratiform orebody that currently is being mined, is about 1100 feet long, approximately 200 feet thick, and extends about 1400 feet downdip.

The stratiform sulfide units can be used, at least locally, within the mine to delineate stratigraphy and structure, thereby enhancing the discovery of new orebodies.

Introduction

The Bunker Hill mine is located in the Coeur d'Alene mining district, northern Idaho. Virtually all of the geological literature on the district has been on the vein-type deposits. Most authors concluded that the veins are magmatic hydrothermal, but Long, Silverman and Kulp (1959, 1960) showed from lead isotopic studies that the vein leads are Precambrian in age. Stratiform lead-zinc deposits were recognized in the "J" area of the Bunker Hill mine as early as 1970 (Meyer, personal communication 1973). Zartman and Stacey (1971) concluded from lead isotopic studies that "J" stratiform mineralization to be Precambrian in age.

The purpose of the present study is to:

1. describe these stratiform lead-zinc deposits.
2. determine the stratigraphic, structural and geochemical relationships of the stratiform ores to the vein-type ores because these might help in exploration for new orebodies.

Stratiform Mineralization and Sedimentary Structures

Sphalerite-rich stratiform ores tend to occur in thicker bedded impure quartzites; whereas galena-rich stratiform deposits of

the "J" area occur in thinner bedded impure quartzites (Ramalingaswamy 1975, Figures 10,11,12 and 13). Dark layers are mainly argentiferous galena, brown layers are mainly sphalerite. Figure 1 shows that mineralization participated in a variety of sedimentary structures. The thick-bedded pure quartzites contain very few sulfides.

The host rocks mainly consist of quartz and sericite. In thin section the stratiform sulfides appear to be associated with finer grained and more sericitic laminae. Individual sulfide blebs are not parallel to bedding and do not have any recognizable sedimentary structures; the lack of any sedimentary features of individual grains probably is due to recrystallization during metamorphism. The sulfides do not appear to replace sericite or quartz.

Stratiform Mineralization and Its Relationship to Vein-type Ores

In some hand specimens sulfides in fractures occur at the intersections of bedding planes containing sulfides with the fractures (Figure 3). A zone of impoverishment of stratiform mineralization commonly borders the fractures (Figures 2 and 4). The vein sulfides are considerably coarser grained than the stratiform sulfides (Figure 2).

The same characteristics occur on an orebody scale in the "J" area. Stratiform sulfides in the country rock become discontinuous, spotty and are absent adjacent to a fracture or a vein (Figure 4 and Ramalingaswamy 1975, Figures 10,11,12 and 13). If mining operations were not almost always restricted to the "J" veins more continuous stratiform deposits probably would be found. The impoverished zones are considerably richer in sericite than the original host rock. This suggests that the quartz originally present may have migrated to the veins.

Of course, historically, the sericite zones with low values of metal have been considered hydrothermal alteration envelopes. The presence of relict stratiform sulfides and the forementioned smaller scale examples in hand specimens show that this is not the case.

In contrast to the "J" area, well bedded, richer stratiform sphalerite deposits occur in the Newgard area (Ramalingaswamy 1975, Figures 13,14 and 15). The tabular orebody is approximately 1100 feet long, stratigraphically 200 feet wide and extends approximately 1400 feet downdip (Figure 5). Even in large fault zones, sphalerite bearing veinlets are more common than minable veins.

The stratigraphy in the Bunker Hill mine consists of a monotonous sequence of thick-bedded and thin-bedded impure quartzites. The stratiform sulfide units appear to be unique marker beds in the St.Regis-Revett transition zone and can help in delineating the stratigraphy at least locally (Ramalingaswamy 1975, Figures 23,24,25 and 26).

Figure 1.

- a. Galena and Sphalerite in Tacde division of Bouma sequences. a - a lower graded layer, b - a lower zone of parallel lamination, c - a zone of current ripple lamination, and e - an upper most clay layer. 9.1 level Newgard area, 27 stope.
- b. Galena in parallel lamination. 23.5 level, "J" area, 23 stope, floor 4.
- c. Galena and Sphalerite in current ripple lamination. 9.1 level, Newgard area, 27 stope.
- d. Galena in cross bedding. 23.5 level, "J" area.
- e. & f. Galena and Sphalerite in soft sediment deformation. 9.1 level Newgard area, 25 stope, and 23 level, "J" area.



a.



b.



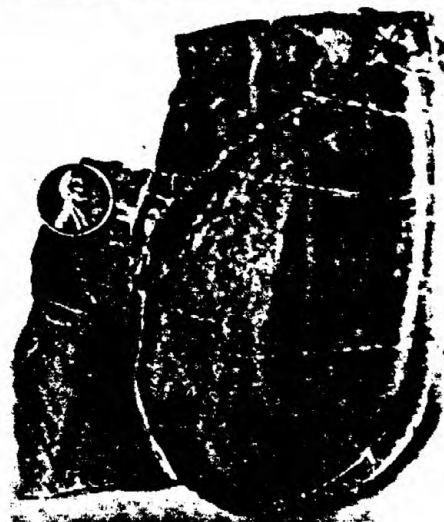
c.



d.



e.



f.



Figure 2 a. & b. Impoverishment of stratiform sulfides bordering 21 level, "J" area, 21 stope, and 23.5 level, 23 stope, floor 4.

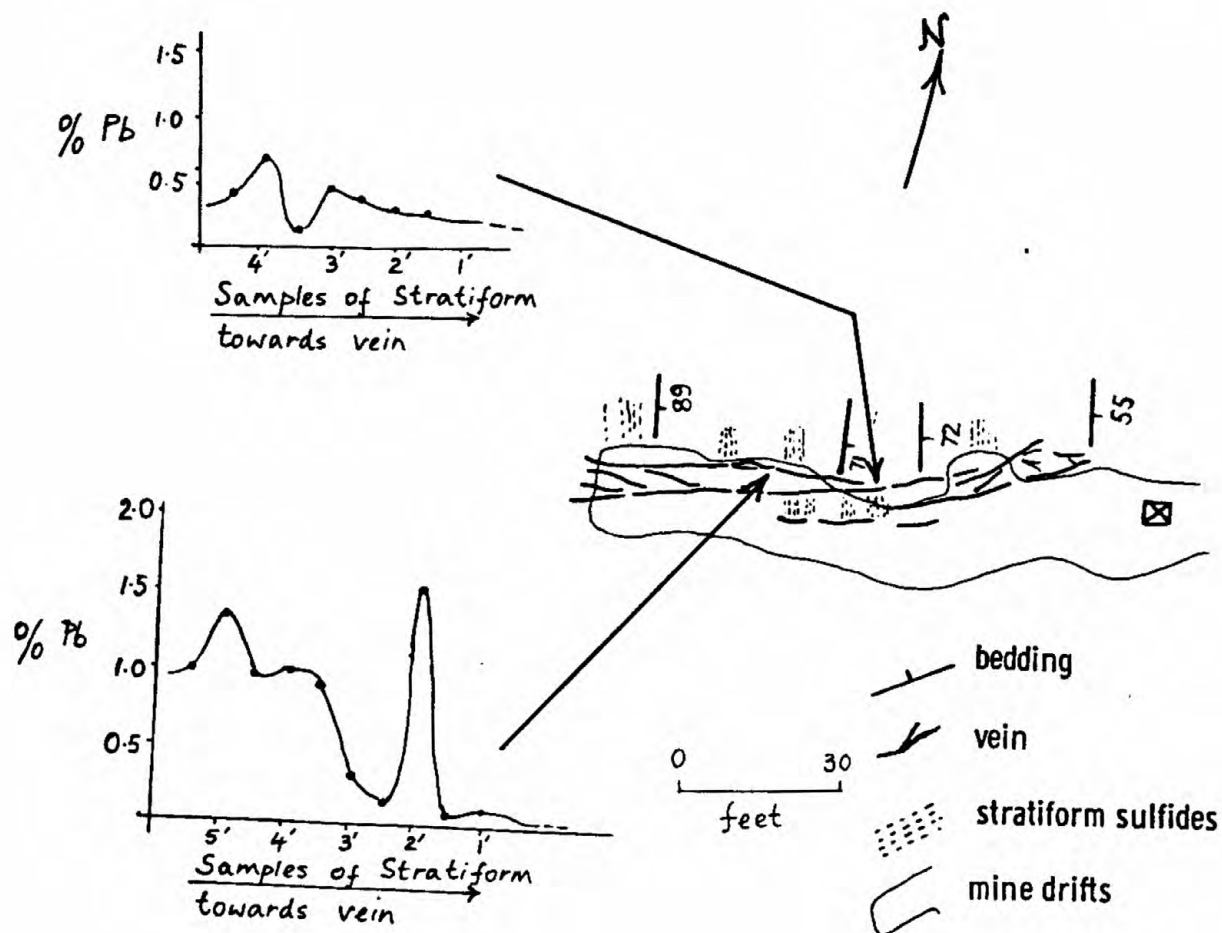
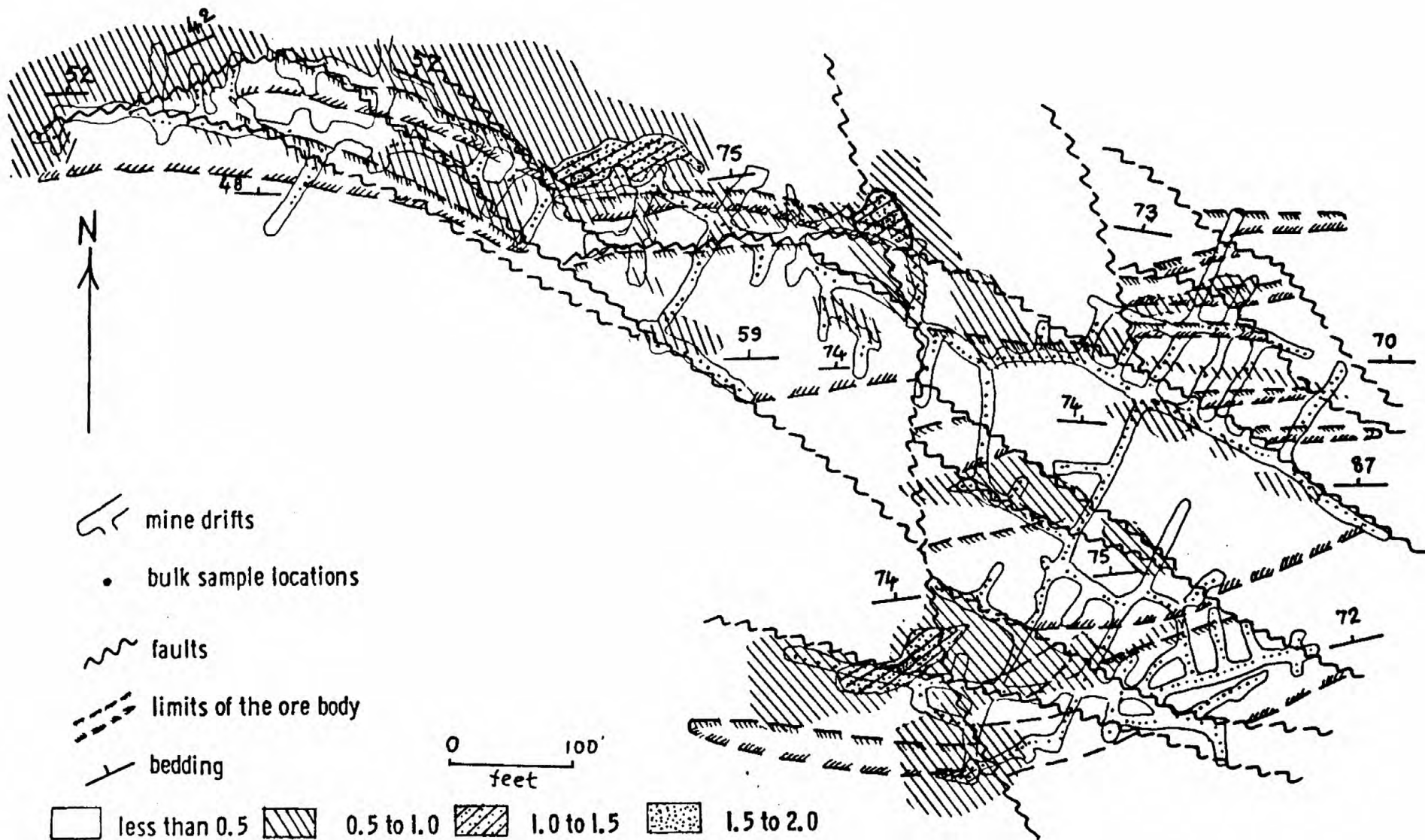


Figure 3. Sulfides occurring at the intersections of bedding planes with the fracture. 23.5 level, "J" area, 23 stope, floor 4.

Figure 4. 23.5 level, 23 stope, "J" area. Pockets of stratiform sulfides in impoverished zones bordering vein. Profiles show decrease of lead in stratiform sulfides towards vein.

Figure 5. Newgard orebody showing geology and zonation of Pb:Zn. 9.1 level, Newgard area.



Metal Ratios of the Ore Bodies

The Pb:Zn of individual samples of the stratiform deposits of the "J" area vary from 5 to 40, the impoverished and semi-impoverished zones generally vary from 5 to 200 (Table 1 and 2 and Ramalingaswamy 1975, Tables 6 and 7). Pb(%):Ag(oz/ton) in both the stratiform and impoverished zones usually vary from 1:1 to 2:1.

Stratiform samples of the Newgard orebody are considerably richer in zinc than those of the "J" area. The Pb:Zn of bulk samples generally are less than 1 (Figure 5) and Pb(%):Ag(oz/ton) vary from 1:1 to 2:1. In the Newgard orebody Pb:Zn increases stratigraphically upwards (Figure 5). Where cut by faults, the orebody tends to have lead to zinc ratios greater than 2 (Figure 5 and Ramalingaswamy 1975, Figures 16 and 18); perhaps lead preferentially migrated into faults in the Newgard orebody as it did in the "J" area.

The main difference between stratiform mineralization and "J" vein ores is not mineralogical but is the absolute and relative amounts of sulfides present. The vein ores have lead to zinc ratios from about 5 to greater than 3000, whereas, lead to silver ratios are virtually same as those of the stratiform sulfides (Table 2 and Ramalingaswamy 1975, Tables 8 and 9).

In the "J" area amount of lead, silver and in some cases copper decrease close to a vein (Figure 4 and Table 1 and Ramalingaswamy 1975, Figure 6 and Tables 4 and 5). The higher Pb:Zn, Ag:Zn and Cu:Zn evidently is due to preferential migration of lead, zinc and copper into fractures and faults.

Genesis of Coeur d'Alene Ore Deposits

Because the stratiform sulfides participated in deformation of soft sediment, they must have been introduced quite early in the history of the strata.

Furthermore, the characteristics of stratiform ores in the Bunker Hill mine are similar to three of the four characteristics described by Renfro (1974) for Sapkha type ores:

1. associated with sandstones interbedded with muds with some carbonates. These carbonate beds contain stromatolites.
2. laterally and vertically zones with respect to metal content.
3. underlain by clastic sediments.
4. overlain by strata that contain evaporite sequences of colomite, gypsum anhydrite and halite.

Furthermore, Rezac (1957) and Harrison (1972) mention the occurrence of stromatolites in the less metamorphosed part of the Ravalli group in Montana. So far no evaporites have been recognized in the St. Regis-Revelt rocks. If they ever were present, they must have been destroyed prior to or during greenschist facies metamorphism. Incidentally, Clarke (1971), Harrison (1972), Trammel (1975) and Lutz (1977) have described stratiform copper deposits in the Revelt and Empire of the Belt Series of Western Montana.

The impoverished zones, the coincidence of vein ores within or adjacent to stratiform deposits in the "J" area and the lead isotopic data (Long, Silverman and Kulp, 1959, 1960, Zartman and Stacey, 1971) suggest that at least some of the vein deposits of the Coeur d'Alene district were derived from the Beltian stratiform deposits.

Sometime after the vein ores formed, they were plastically deformed (Caddey, 1974). We have seen examples of stratiform sulfides in the Lucky Friday, Sunshine, Galena, Morning-star and Crescent mines in the Silver Belt of the district. Although the ores of these mines are richer in silver and copper than Bunker Hill, the host rocks are the same St.Regis-Revett transition zone. It is tempting to speculate that the vein-type ores of many of the Coeur d'Alene mines might have been derived from a single, laterally zoned, sulfide-bearing stratigraphic interval that rivalled in tonnage but not in grade of the sulfides of Adirich formation (equivalent to the Prichard formation of the U.S.) of the Sullivan mine at Kimberley, B.C.

Table 1. Stratiform samples collected along strike towards vein. 21.5 level, "J" area, 22 stope.

Sample No.	Distance from vein in feet	Pb %	Zn %	Ag oz/ton	Cu %	Pb:Zn	Pb:Ag
5480	8.5	0.14	.030	0.11	.008	4.6	1.27
5481	8.0	1.00	.008	0.48	.003	125.0	2.08
5482	7.5	1.50	.008	2.00	.004	187.0	.75
5483	7.0	0.58	.008	0.27	.004	72.6	2.14
5484	6.5	1.10	.008	0.48	.003	137.5	2.29
5485	6.0	2.20	.320	1.00	.005	6.8	2.20
5486	5.5	2.90	.040	1.30	.003	72.5	2.23
5487	5.0	1.50	.008	0.65	.002	187.5	2.30
5488	4.5	1.30	.008	0.60	.003	162.5	2.16
5489	4.0	1.40	.010	0.61	.002	140.0	2.29
5490	3.5	1.60	.008	0.71	.003	200.0	2.25
5491	3.0	0.48	.008	0.17	.003	60.0	2.82
5492	2.5	0.48	.008	0.22	.003	60.0	2.18
5493	2.0	0.52	.010	0.24	.007	52.0	2.16
5494	1.5	0.14	.008	0.05	.005	17.5	2.80
5495	1.0	0.18	.008	0.07	.005	22.5	2.57
5496	0.5	0.16	.008	0.08	.003	20.0	2.00

Table 3. Samples collected of a vein. 21.5, "J" area, 22 stope.

Sample No.	Pb %	Zn %	Ag Oz/Ton	Cu %	Pb:Zn	Pb:Ag
7502	36.5	.023	28.4	.25	1586.9	1.28
7503	30.3	.016	12.4	.11	1893.7	2.44
7504	65.6	.023	28.4	.17	2839.1	2.30
7505	57.4	.018	24.8	.22	3188.9	2.31

REFERENCES

- Barton, P.B., and Skinner, B.J., 1967, Sulfide Mineral Stabilities, in Barnes, H.L., editor, Geochemistry of Hydrothermal Ore Deposits: Holt, Rinehart and Winston, Inc., N.Y., p. 236-333.
- Caddey, S., 1974, Deformation of the "J" Vein. Univ. Idaho Unpub. Ph.D. Thesis.
- Clarke, A.L., 1971, Stratabound Copper Sulfides in the Precambrian Belt Supergroup, Northern Idaho and Northwestern Montana. Mining Geol. Japan Spec. Issue 3, p. 261-267.
- Fryklund, V.C., 1964, Ore Deposits of the Coeur d'Alene District, Shoshone County, Idaho. U.S. Geol. Survey Prof. Paper 478.
- Harrison, J.E., 1977, Precambrian Belt basin of north western United States: its geometry, sedimentation and copper occurrences. Geol. Soc. Amer. Bull. V.83, p. 1215-1240.
- Hobbs, S.W., Griggs, A.B., Wallace, R.E., and Campbell, A.B., 1965, Geology of the Coeur d'Alene District, Shoshone County, Idaho. U.S. Geol. Survey Prof. Paper 478.
- Long, A., Silverman, A., and Kulp, J.L., 1959, Precambrian Mineralization of the Coeur d'Alene District, Idaho. Jour. Geophys. Res., V. 64, no. 8.
- _____, 1960, Isotopic Composition and Precambrian Mineralization of the Coeur d'Alene District, Idaho. Econ. Geol., V. 55, p. 645-658.
- Lutz, R., 1978, Geology of the Spar Lake Stratabound Silver-copper Deposit (abs.): Program with Abstracts, Geol. Assoc. Canada, V. 2, p. 34.
- Ramalingaswamy, V.M., 1975, Stratiform Mineralization and Origin of Vein Deposits, Bunker Hill Mine, Coeur d'Alenes, Idaho. Unpub. M.S. Thesis. Univ. Wash.
- Ransome, F.L., and Calkins, F.C., 1908, Geology and Ore Deposits of the Coeur d'Alene District, Idaho. U.S. Geol. Survey Prof. Paper 294-D.
- Renfro, A.R., 1974, Genesis of Evaporite Associated Stratiform Metalliferous Deposits - A Sabkha Process. Econ. Geol. V.69, p. 33-45.
- Rezak, R., 1957, Stromatolites of the Belt Series in Glacier National Park and vicinity in Montana: U.S. Surv. Prof. Paper. 294 D, p. 111-154.
- Shenon, P.J., and McConnel, R.H., 1939, The Silver Belt of the Coeur d'Alenes. Idaho Bur. Mines and Geology. Pamph. 50.

- Trammel, J.W., 1975, Strata-bound Copper Mineralization in the Empire Formation and Ravalli Group, Belt Supergroup, Northwest Montana. Unpub. Ph.D. thesis, Univ. Wash.
- Zartman, R.E., and Stacey, J.S., 1971, Lead Isotopes and Mineralization Ages in Belt Supergroup Rocks, Northwestern Montana and Northern Idaho. Econ. Geol. V. 66, p. 849-860.

Stable isotopic investigation of hydrothermal ore fluids
in massive sulfide deposits of the West Shasta Cu-Zn district,
California

W. H. Casey, Union Geothermal

B. E. Taylor, University of California at Davis

Stable Isotopic Investigation of Hydrothermal Ore Fluids in
Massive Sulfide Deposits of the
West Shasta Cu-Zn District, California

William H. Casey* and Bruce E. Taylor
Department of Geology, University of California
Davis, California 95616

Introduction

Research on the origins and processes of formation of volcanogenic massive sulfide deposits has been given great impetus by recent observations on present day oceanic hydrothermal systems (e.g. RISE Project Group, 1980; Hekinian et al., 1980; Bischoff, 1980) which are associated with sulfide ore mineral deposition. In this study we report on some of the mineralogical and light stable isotopic systematics associated with massive and locally bedded sulfide ore bodies in the West Shasta district, Shasta Co., California (Fig. 1). Studies by Kinkel et al. (1956), Reed (1977), and Casey (1980) have contributed to the geology and geochemistry of deposits in the district. We are particularly interested in the nature of the geothermal system(s) which formed these ore bodies as suggested by temperature of formation, extent of isotopic exchange, and extent of alteration. The present study is part of a larger, district-wide study now in progress which will allow comparisons to be made with the results of studies of modern oceanic geothermal systems.

Geologic Setting

The West Shasta mining district is formed near Lake Shasta, California, underlain by Paleozoic basement rocks of the Klamath Mountains. These include a bimodal suite of Devonian island-arc volcanic rocks which have been intruded by a Devonian trondjemite stock, and the Copley Greenstone, the oldest unit in the district, which consists of an 1200+ meter-thick sequence of volcanic breccias, pillowed lavas and tuff beds. This greenstone unit ranges in composition from basalt to dacite, but generally consists of basaltic-andesite which has been metamorphosed to the lower greenschist facies, producing quartz, chlorite, albite, amphibole and epidote; relict pyroxene and olivine may also be present. The Copley Greenstone is conformably overlain by the Balaklala Rhyolite, a northeasterly-trending complex of high-silica dacite, with a tabular shape in plan view. A maximum thickness of about 1000 meters can be estimated for the silicic complex from data of Reed (1977). The Balakala Rhyolite can be subdivided into two units: a lower unit consisting of flows, breccia and tuff of fine to medium-grained, quartz-phyric dacite;

* Present Address: Union Geothermal, P.O. Box 6854, Santa Rosa, California 95406

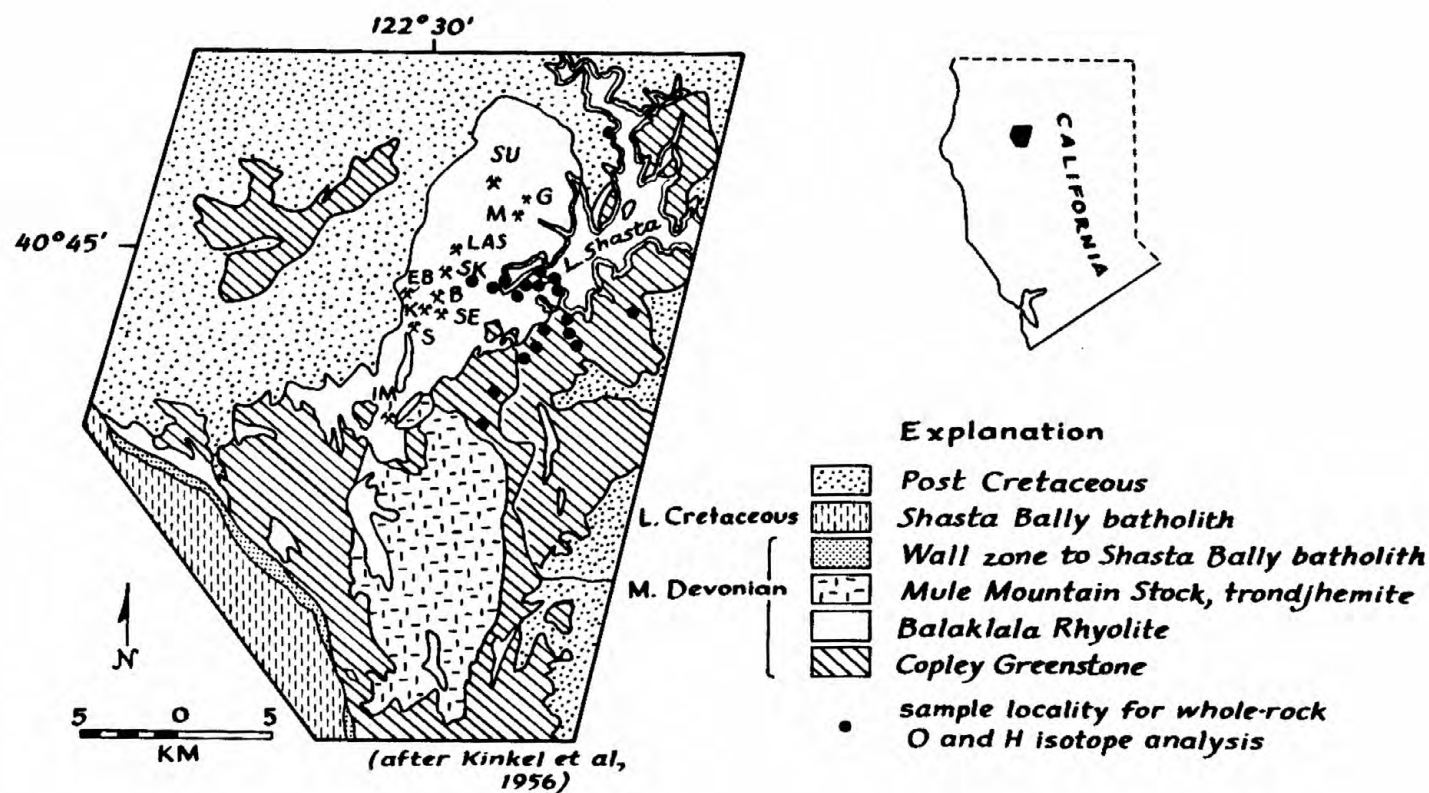


Figure 1. Generalized geologic map of the West Shasta Cu-Zn district showing locations of whole-rock samples analyzed for oxygen and hydrogen isotopes. Deposits indicated are IM, Iron Mountain; S, Stowell; K, Keystone; SE, Spread Eagle, EB, Early Bird; B, Balaklala; SK, Shasta King; US, Uncle Sam; M, Mammoth; G, Golinsky; and SU, Sutro.

and an upper unit consisting of a laterally extensive blanket of coarse-grained crystal tuff. Volcanigenic massive sulfide deposits are hosted by the lower unit within about 200 meters of the contact with the upper unit of the Balakala Rhyolite.

The ore deposits consist of lensoidal stratiform sulfide masses which overly domes, flows or breccia of fine- to medium-grained dacite, and consist of poorly bedded pyrite with subordinate amounts of chalcopyrite and sphalerite. Though sedimentary textures can be observed, much of the ore is a sulfide breccia. Pyrrhotite, sulfate and iron oxide minerals are virtually absent from the primary ore assemblage, and have been reported in only trace amounts throughout the district. Bedded volcanic breccias and tuff layers conformably overly the ore bodies. Hydrothermal quartz, stratiform sulfide beds and disseminated pyrite may be found in the tuff layers.

Ore bodies are infrequently directly underlain by, or adjacent to, a stockwork of quartz + sulfide + sericite + chlorite veins which vertically crosscut and pervasively alter the enclosing dacite. These veins may contain significant amounts of chalcopyrite and sphalerite, and show little evidence for open space filling; rather, they may show evidence of reaction between the hydrothermal fluid and the wall rock. Intervening dacite has been pervasively altered to an assemblage of quartz + sericite + chlorite with abundant disseminated pyrite. The intensity of veining, the variety of sulfide minerals and location of the stockwork relative to massive sulfide deposits indicates that the stockwork was a major conduit for hydrothermal solutions which vented onto the sea floor.

A more subtle and extensive type of alteration, is the metasomatism of the dacite to an assemblage of quartz + chlorite with traces of sericite, pyrite, sphene and leucoxene. The rock has a distinct green color and may be crosscut by structurally-controlled quartz + chlorite veins, having a consistent WNW orientations throughout the central part of the mining district. These veins commonly exhibit open-space-filling textures. Exclusive of the veins, chlorite is present with quartz as pseudomorphic replacement of vitric fragments and in capillary fractures throughout the rock. This alteration is well developed beneath the Shasta King and Balaklala ore deposits and appears sporadically in other parts of the district.

Stable Isotope Geochemistry

Recent workers (e.g. Spooner and Fyfe, 1973; Large, 1977; Parmentier and Spooner, 1978) have proposed that heat-driven convection of seawater through ocean-floor basalt leaches metals and provides a mechanism for the mass transfer required to form volcanigenic massive sulfide deposits. The passage of hydrothermal fluids through the rocks is accompanied by chemical and isotopic exchange reactions, associated with the crystallization of alteration minerals. Ancient convective hydrothermal systems can be detected by shifts in whole-rock hydrogen and oxygen isotope

compositions, governed by time, temperature, permeability, and the initial isotopic compositions of fluid and rock. A large heat convection system around the Balaklala Rhyolite might thus be recorded, and to test this, the Balaklala Rhyolite and Copley Greenstone were both sampled at varying distances away from the central part of the mining district. These samples and others from, and adjacent to, the ore bodies were analysed for isotopes of oxygen, hydrogen and sulfur using standard techniques (Casey, 1980). The water contents of whole rocks ($H_2O + 150^\circ C$) were accurately determined during extraction of hydrogen for isotopic analysis.

Hydrogen isotopes. The hydrogen isotope composition of the Balaklala Rhyolite and Copley Greenstone is characterized by a narrow range of δD_{wr} (whole-rock) values from $-45^\circ/00$ to $-60^\circ/00$ (relative to SMOW). The variation of δD values is neither clearly related to distance from the rhyolite complex, nor systematically associated with weight percent H_2O . With respect to hydrogen, the rocks thus appear to have interacted with a single hydrothermal fluid, and that isotopic exchange between hydrogen-bearing minerals and the fluid was complete. The above range of δD falls within the ranges of δD_{wr} values for rocks which owe their isotopic identity to sea floor hydrothermal alteration, and to metamorphism (Fig. 2). Chlorite separates from two veins in the Balaklala Rhyolite, and an epidote separate from a vein in the Copley Greenstone had δD values of $-48^\circ/00$, $-45^\circ/00$, and $-9^\circ/00$ respectively. Over an assumed temperature range from 200° to $350^\circ C$, these minerals would have been in isotopic equilibrium with a fluid having δD of $0 \pm 5^\circ/00$ (Taylor, 1979; Graham et al., 1980). Hydrogen-bearing mineralogy in these rocks consists dominantly of chlorite (Balaklala and Copley), sericite (Balaklala), with minor amphibole and epidote.

Oxygen isotopes. The oxygen isotope composition of Copley Greenstone and Balaklala Rhyolite compare well with those of similar, sea floor hydrothermally altered rocks (Fig. 3). Mafic rocks from the West Shasta district fall into two groups relative to the value for fresh oceanic basalt and basaltic-andesite: one group is isotopically enriched in ^{18}O by about $2.3^\circ/00$, while the other is isotopically depleted by 1 to $2^\circ/00$. All of the West Shasta samples have higher H_2O contents than fresh oceanic basalt.

Mafic rocks in the West Shasta district now consist dominantly of quartz + chlorite + albite + amphibole, with quartz and chlorite typically the most abundant. As the water-mineral isotopic fractionations for amphibole and albite lie within the range for quartz and chlorite (Bottinga and Javoy, 1973; Taylor, 1974), the whole-rock oxygen isotope geochemistry of our samples can be explained as a result of two general processes: a) precipitation of hydrothermal quartz, at temperatures less than about $350^\circ C$; and b) hydration of mafic minerals and glass to chlorite at temperatures above about $200^\circ C$. These two processes will have had opposite isotopic effects on the Copley Greenstone and similar rocks (Fig. 4). Silicification, accompanied by

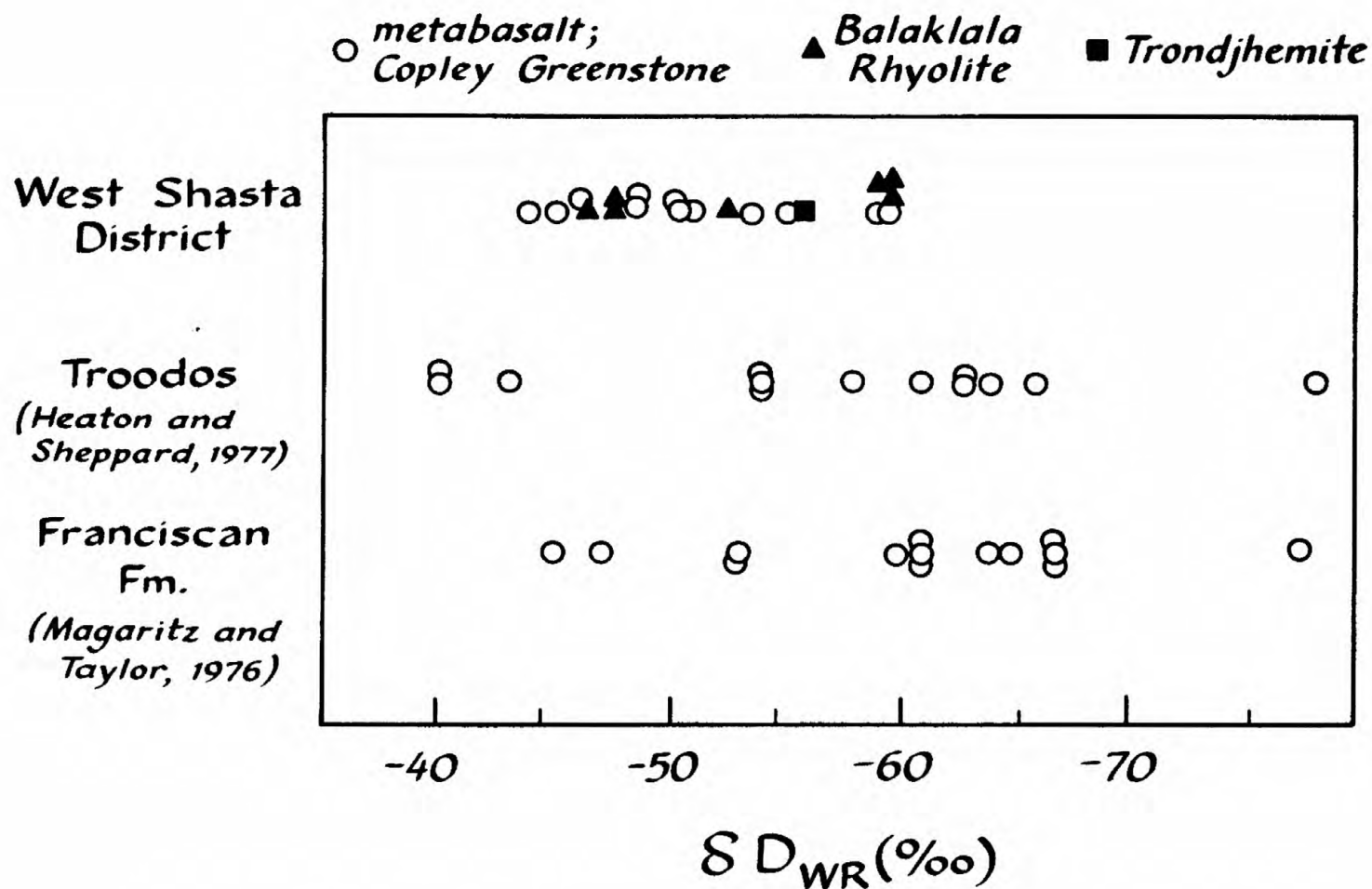


Figure 2. Whole-rock hydrogen isotope compositions of Balaklala Rhyolite, Copley Greenstone, and trondjemite from the West Shasta district. Note that δD values for these rocks are similar to those from the Troodos complex and the Franciscan Formation.

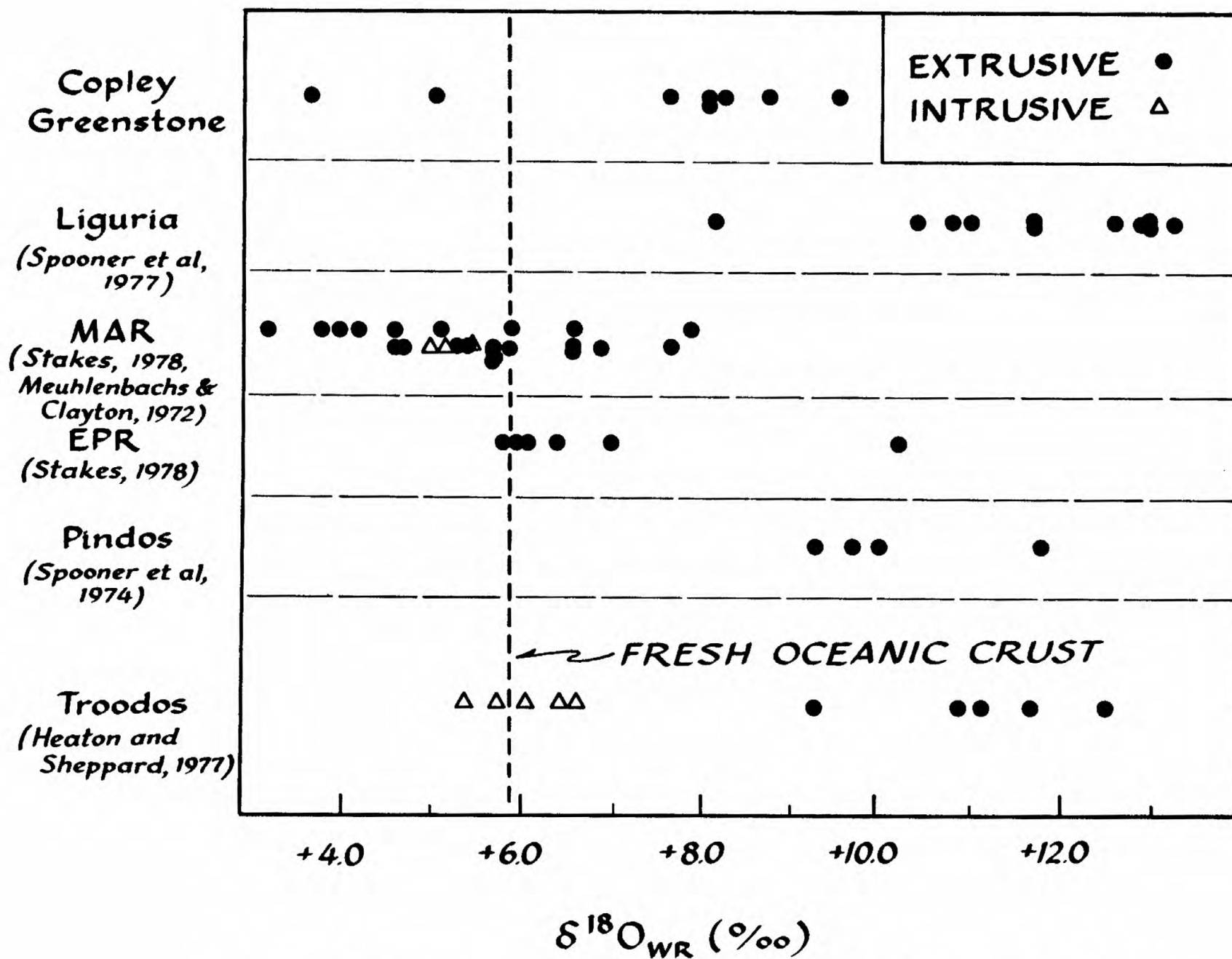


Figure 3. Oxygen isotope compositions of Copley Greenstone compared to other examples of hydrothermally altered oceanic crust.

exchange of oxygen isotopes between hydrothermal fluids and minerals, particularly feldspar, would result in isotopic enrichment of fresh oceanic mafic rock with no increase in water content. Alteration of the primary mineralogy to chlorite causes fresh samples to be depleted in ^{18}O while becoming progressively enriched in H_2O . Most samples of Copley Greenstone have high water contents (2.25 to 5 wt. % H_2O), are enriched in ^{18}O relative to oceanic basalts (Fig. 4), and have mineral assemblages consisting of quartz + chlorite + amphibole + albite. Isotopically depleted samples contain a high percentage of chlorite and amphibole relative to quartz, and tend to have higher water contents.

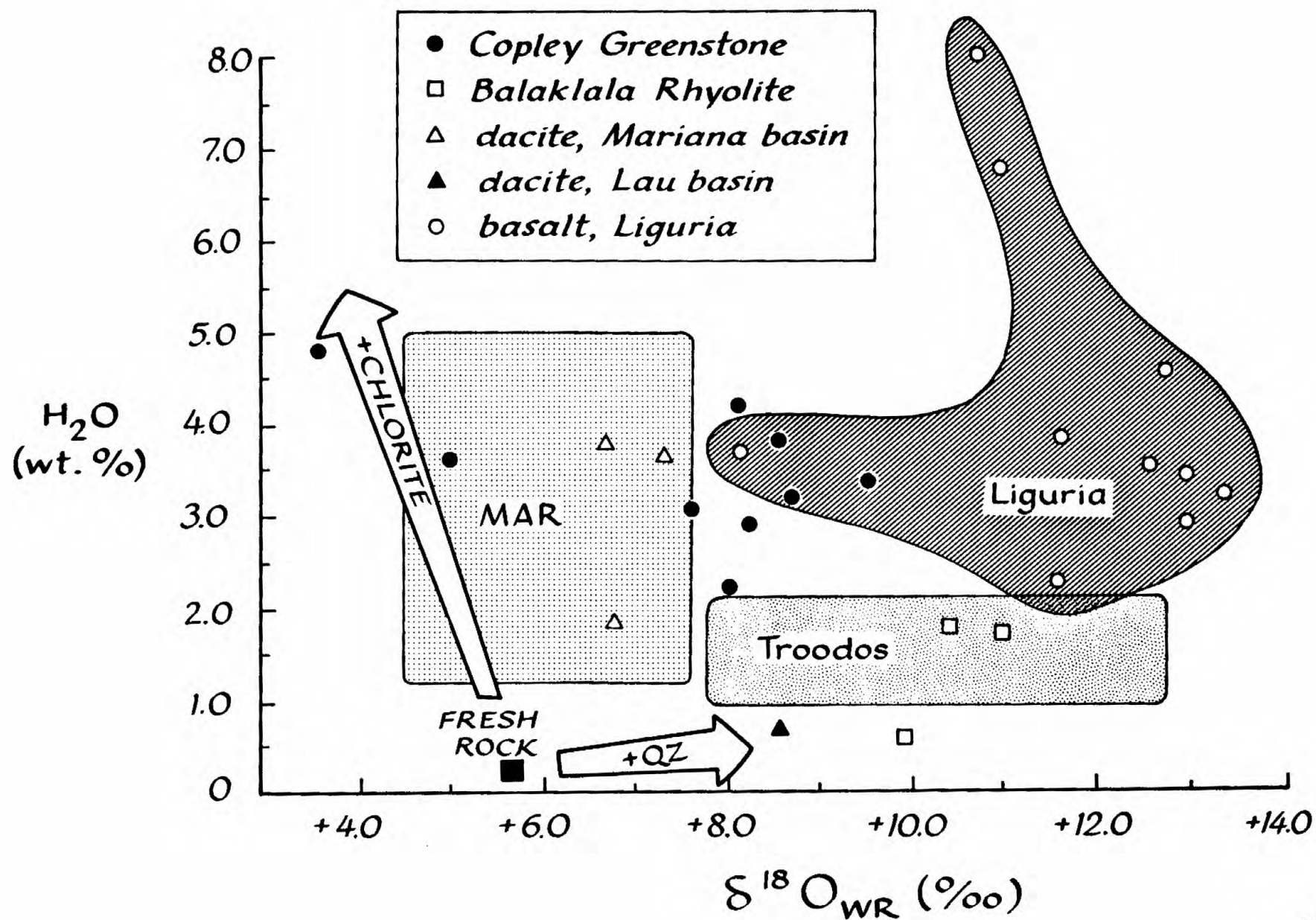
$\delta^{18}\text{O}_{\text{wr}}$ values for the Balaklala Rhyolite are consistently enriched in ^{18}O relative to dacite dredged from the Lau and Marianas basins (Fig. 4). The $\delta^{18}\text{O}$ value of quartz phenocrysts from only slightly-altered Balaklala Rhyolite is +7.6‰, which is also a typical whole-rock value for submarine rocks of intermediate composition (Muehlenbach and Clayton, 1971). $\delta^{18}\text{O}$ values of quartz phenocrysts (+10.0 to +10.3‰) separated from altered dacite beneath the Shasta King ore deposit, however, indicate that the igneous quartz extensively exchanged oxygen with the hydrothermal fluid responsible for quartz + chlorite alteration in these rocks.

In summary, although there is no apparent aureole of isotopically depleted rock around the mineralized portion of the West Shasta district, the hydrogen and oxygen isotope geochemistry of the rocks and minerals consistently indicates that extensive reaction took place between the rocks and a hydrothermal fluid of essentially constant isotopic composition with δD and $\delta^{18}\text{O}$ near 0‰. This fluid was most likely Devonian sea water.

Sulfur isotopes. The chemistry of the hydrothermal fluid can be partially reconstructed by consideration of sulfide mineralogy and the sulfur isotope geochemistry of massive sulfide bodies, stockwork veins and pervasively altered wallrock within a single group of deposits. The West Keystone deposit in the central part of the district was studied in detail because drill core was available which transected all of these features. The West Keystone deposit is a lensoidal mass of about 2 million tons of pyrite lying on the flanks of a rhyolite dome (Reed, 1977). The deposit both overlies, and is crosscut by, a stockwork of quartz + sulfide + sericite veins which undoubtedly comprised part of a feeder zone for this and perhaps other deposits in the area.

Pyrite from the Main Keystone massive sulfide body, associated stockwork veins and intervein wallrock has a uniform $\delta^{34}\text{S}_{\text{py}}$ value of about $+4.6 \pm .46$ ‰ (2 σ), with a total range in $\delta^{34}\text{S}_{\text{py}}$ values from +4.1‰ to +5.3‰ (Fig. 5). With depth, $\delta^{34}\text{S}_{\text{py}}$ increases slightly, by several tenths per mil. Wallrock pyrite does not generally have the same sulfur isotope composition as pyrite from adjacent veins. Also, the $\delta^{34}\text{S}_{\text{py}}$ values of wallrock pyrite do not systematically approach the δ values of pyrite

Figure 4. Oxygen isotope composition and water contents of Balaklala Rhyolite and Copley Greenstone compared to data for samples of Mid Atlantic Ridge basalt (Stakes, 1978), and altered oceanic rocks of the Troodos complex (Heaton and Sheppard, 1977) and Liguria (Spooner et al., 1977). Data for dacite from the Mariana and Lau basins are from Pineau et al. (1976). Two paths are shown for hydrothermal alteration of oceanic crust, one which enriches the rock in quartz and ^{18}O , and a second which results in extensive hydration of the rock, enriching the rock in chlorite and ^{16}O . Most rocks from the West Shasta district exhibit the effects of both alteration processes.



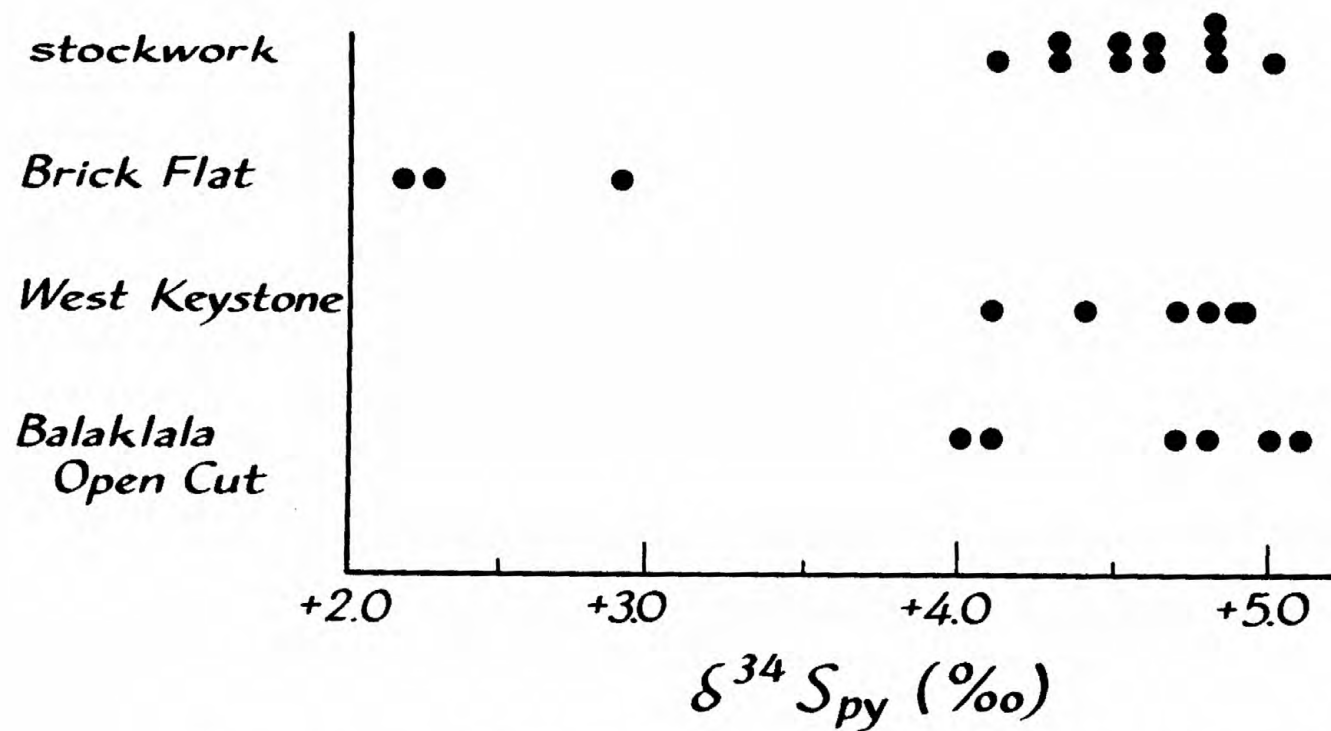


Figure 5. Variation in sulfur isotope composition for pyrite from stockwork and massive sulfide bodies in the West Shasta district.

in the nearest vein, possibly indicating thermal or isotopic disequilibrium between the hydrothermal fluid and the enclosing rock.

In contrast to the rather uniform values for $\delta^{34}\text{S}_{\text{py}}$ from the veins, wall rock and massive sulfide bodies, $\delta^{18}\text{O}_{\text{py}}$ from stockwork veins sampled over the same interval in drill core, varies from + 7.8‰ to + 11.6‰. The absence of sulfate, pyrrhotite and magnetite from ore and alteration mineral assemblages, and uniformity of $\delta^{34}\text{S}_{\text{py}}$ values indicate that the chemical state of the hydrothermal fluids probably remained in the pyrite-stable field (e.g. Ohmoto, 1972) throughout mineralization (although we do not wish to imply that chemical equilibrium generally prevailed!). The sulfur in the hydrothermal fluid was present primarily as aqueous sulfide (e.g. Ohmoto, 1972). Since the fractionation of ^{34}S between H_2S , HS^- and pyrite is less than 3.5‰ over the temperature range of 150°C–400°C, the mean $\delta^{34}\text{S}_{\text{py}}$ value of + 4.6‰ is a good approximation of the $\delta^{34}\text{S}$ value of the total sulfur in the hydrothermal fluid in the Main Keystone deposit.

Other deposits from the West Shasta district exhibit a narrow range in $\delta^{34}\text{S}_{\text{py}}$ values. The Balaklala deposit, a short distance north of the Keystone deposits, also has a mean $\delta^{34}\text{S}_{\text{py}}$ value of about + 4.6‰. Pyrite from the Brick Flat body of the Iron Mountain deposit, however, is less enriched in ^{34}S , with $\delta^{34}\text{S}_{\text{py}}$ value in a narrow range from + 2.2‰ to + 2.9‰. This apparent variation in $\delta^{34}\text{S}_{\text{py}}$ within the district is currently under study.

Sulfur isotope compositions reported for pyrite from sulfide deposits adjacent to hydrothermal vents on the East Pacific Rise at 21°N (Hekinian et al., 1980) vary from + 2.01‰ to + 3.27‰, similar to those reported here. $\delta^{34}\text{S}$ values of sphalerite from the pyrite-bearing samples were also reported by Hekinian et al. (1980), and isotopic disequilibrium between sphalerite and pyrite is indicated.

Geothermometry. The variation in $\delta^{18}\text{O}_{\text{vein quartz}}$ of + 7.8‰ to + 11.6‰ noted above does not correlate with depth in the volcanic pile, but reflects variation in both temperature and probably oxygen isotope composition of the fluids from which the quartz precipitated. Assuming a $\delta^{18}\text{O}$ for the fluid of 0‰, the variation of nearly 4‰ for quartz is compatible with a range of formation temperature of 215°C to 320°C (Bottinga and Javoy, 1973, in Friedman and O'Neil, 1977). Any previous oxygen isotope exchange between wallrocks and the hydrothermal fluid could have shifted the $\delta^{18}\text{O}$ of the fluid in a positive direction, and the estimate of 215°C to 320°C would be too low. Three chalcopyrite-pyrite mineral pairs from the Balaklala massive sulfide and the Main Keystone stockwork indicate temperatures for isotopic equilibration of 340°C to 365°C (Kajiwara and Krouse, 1971). From these temperatures, the $\delta^{18}\text{O}$ of water in equilibrium with the quartz would have been 0 to 4.4‰ (Bottinga and Javoy, in Friedman and O'Neil, 1977); fluids lighter in $^{18}\text{O}/^{16}\text{O}$ than sea water are not indicated. Temperatures of present-day sulfide-

precipitating vent fluids at 21[°]N on the East Pacific Rise have actually been measured to be as high as 380 \pm 30[°]C (RISE Project Group, 1980).

Conclusion

We have shown that the hydrothermal fluid responsible for alteration and mineralization in the central part of the West Shasta district consisted dominantly of sea water. Very minor amounts of a magmatic fluid could have been admixed with the sea water, and meteoric water was not present in any detectable quantity. The temperature of formation of the near-vent alteration and of the massive sulfide bodies was in the range of 215[°]C to 365[°]C, and probably largely near the upper end of this range by comparison with observations on present-day submarine hydrothermal systems.

The temperatures indicated for formation of the massive sulfide deposits and the narrow range in sulfur isotope compositions preclude the involvement of bacteria in reduction of sulfate at the site of formation of the sulfide deposits. The sources for the sulfur are thus magmatic and/or oceanic. A magmatic source for the sulfur cannot be ruled out on the basis of the sulfur isotope data alone. However, since sea water is also a logical source of sulfur (by reduction of sulfate; $\delta^{34}\text{S} > +20\text{‰}$), the narrow range of $\delta^{34}\text{S}$ would seem to preclude the general mixing process which should occur. Of course, if the $\delta^{34}\text{S}$ of aqueous sulfide was very similar to magmatic sulfur ($0 \pm 3\text{‰}$, e.g. Ohmoto and Rye, 1979), then mixing of different proportions of sulfur from each source would go undetected.

Oceanic basalt contains sufficient Fe^{+2} , however, to reduce sea water sulfate at the temperatures indicated for the hydrothermal alteration (Mottl et al., 1979; Seyfried and Mottl, 1977). Taken as a whole, the geologic, mineralogic, and isotopic data support a geothermal system in which Devonian sea water with $\delta^{34}\text{S} = +23\text{‰}$ for sulfate (Holser, 1977) was reduced by interaction with the Copley Greenstone as it was driven by convection along fractures. Partial reduction probably occurred at low temperatures ($\sim 50\text{--}75\text{°C}$; cf. Seyfried and Bischoff, 1979) farther from the actual hydrothermal events, and here the reduction might have been catalyzed by organisms. Large isotope fractionations between reduced sulfur species and sea water would exist. With deeper passage into the basalt, the fluid loses isotopic communication with sea water so that $\delta^{34}\text{S}$ is fixed ($\sim +4.0$ to $+5\text{‰}$), and only its chemical state changes. In this case, the fluid is essentially completely reduced by the time it reaches the actual hydrothermal vent. This process also hydrates the basalt, releases silica to solution, and leaches some of the metals found in the sulfide deposits. The sulfide minerals form upon rapid quenching by sea water of the hot fluids issuing from the vents. Isotopic exchange does not take place between sea water and the hydrothermal fluids, nor would it be anticipated (Sakai and Dickson, 1978). In such a hydrothermal system, the effective water/rock ratios are very high in the

vent areas, but may rapidly decrease away from these sites of intense alteration and ore deposition, due to a large and highly fractured recharge area. This is compatible with our whole-rock isotope data and the dominance of reduced over oxidized sulfur species in the hydrothermal solution (Casey, 1980; c.f. Mottl et al., 1979).

Acknowledgements

We are indebted to Silver King Mines for granting access to their property, and to Dr. John Albers, U.S. Geological Survey, for kindly supplying samples from the Iron Mountain deposit. This research was supported by grants to W. C. from Sigma Xi and ARCO, and by a Thomas W. Todd Fellowship. We are especially grateful to Dr. J. R. O'Neil, U.S. Geological Survey, for use of the mass spectrometers and the extraction facilities in his laboratory.

References

- Barker, Y. F., Millard, H. T. and Knight, R. J. (1979) Reconnaissance geochemistry of Devonian Island arc volcanic and intrusive rocks, West Shasta District, California: In Barker, R. F. (ed.), *Trondjhemites, dacites and Rhyolites*, McGraw-Hill.
- Bischoff, J. L. (1980) Geothermal system at 21°N, East Pacific Rise: Physical Limits on Geothermal Fluid and Role of Adiabatic Expansion: Science 207, 1465-1469.
- Bottinga, Y. and Javoy, M. (1973) Comments on oxygen isotope geothermometry: Earth Planet. Sci. Lett. 20, 250-265.
- Casey, William H. (1980) Geology and geochemistry of mineralization and alteration in the central portion of the West Shasta Cu-Zn district, Shasta County, California: Unpubl. M.S. Thesis, University of California, Davis, 149 pp.
- Friedman, I. and O'Neil, J. R. (1977) Compilation of stable isotope fractionation factors of geochemical interest: Ch. KK in Fleischer, M. (ed.) Data of Geochemistry, 6th ed. U.S. Geol. Survey Prof. Paper 440-KK.
- Graham, C. M., Sheppard, S. M. F. and Heaton, T. H. E. (1980) Experimental hydrogen isotope studies I: Systematics of hydrogen isotope fractionation in the system epidote-water, zoisite-water, and AlO(OH)-water: Geochim. Cosmochim. Acta 44, 353-364.
- Heaton, T. H. E. and Sheppard, S. M. F. (1977) Hydrogen and oxygen isotope evidence for sea water-hydrothermal alteration and ore deposition, Troodos Complex, Cyprus: Geol. Soc. London Spec. Pub. no. 7, 42-57.
- Hekinian, R., Fevrier, M., Bischoff, J. L., Picot, P. and Shanks, W. C. (1980) Sulfide deposits from the East Pacific Rise near 21°N: Science 207, 1433-1444.
- Holser, W. T. (1977) Catastrophic chemical events in the history of the oceans: Nature 267, 403-408.
- Kajiwara, Y. and Krouse, H. R. (1971) Sulfur isotope partitioning in metallic sulfide systems: Canadian Jour. Earth Sci. 8, 1397-1408.
- Kinkel, A. R. Jr., Hall, W. E. and Albers, J. P. (1956) Geology and base metal deposits of West Shasta Copper-Zinc District, Shasta County, California: Geol. Survey Prof. Paper 285, 156 pp.
- Large, R. (1977) Chemical evolution and zonation of massive sulfide deposits in volcanic terrains: Econ. Geol. 72, 549-572.

- Magaritz, M. and Taylor, H. P. (1976) Oxygen, hydrogen and carbon isotope studies of the Franciscan formation, Coast Ranges, California: Geochim. Cosmochim. Acta 40, 215-234.
- Mottl, M. J., Holland, H. D. and Corr, R. F. (1979) Chemical exchange during hydrothermal alteration of basalt by sea water - II. Experimental results for Fe, Mn, and sulfur species: Geochim. Cosmochim. Acta 43, 869-884.
- Muelenbachs, K. and Clayton, R. N. (1971) Oxygen isotope ratios of submarine diorites and their constituent minerals: Can. Jour. Earth Sci. 8, 1591-1595.
- Muelenbachs, K. and Clayton, R. N. (1972) Oxygen isotope geochemistry of submarine greenstones: Can. Jour. Earth Sci. 9, 471-476.
- Ohmoto, H. (1972) Systematics of sulfur and carbon isotopes in hydrothermal ore deposits: Econ. Geol. 67, 551-579.
- Ohmoto, H. and Rye, R. O. (1979) Isotopes of sulfur and carbon: In H. L. Barnes (ed.), The Geochemistry of Hydrothermal Ore Deposits, 798 p., Wiley-Interscience.
- Parmentier, E. M. and Spooner, E. T. C. (1978) A theoretical study of hydrothermal convection and the origin of the ophiolitic sulphide ore deposits of Cyprus: Earth Planet. Sci. Lett. 40, 33-44.
- Pineau, F., Javoy, M., Hawkins, J. W. and Craig, H. (1976) Oxygen isotope variations in marginal basin and ocean ridge basalts: Earth Planet. Sci. Lett. 28, 299-307.
- Reed, M. H. (1977) Calculations of hydrothermal metasomatism and ore deposition in submarine volcanic rocks with special reference to the West Shasta District, California: Unpubl. Ph.D. Thesis, University of California, Berkeley, 201 pp.
- RISE Project Group: Spies, et al. (1980) East Pacific Rise: Hot springs and geophysical experiments: Science 207, 1421-1433.
- Sakai, H. and Dickson, F. W. (1978) Experimental determination of the rate and equilibrium fractionation factors of sulfur isotope exchange between sulfate and sulfide in slightly acid solutions at 300°C and 1000 bars: Earth Planet. Sci. Lett. 39, 151-161.
- Seyfried, W. E. Jr. and Bischoff, J. L. (1979) Low temperature basalt alteration by sea water: an experimental study at 70°C and 150°C: Geochim. Cosmochim. Acta 43, 1937-1947.
- Seyfried, W. E. Jr. and Mottl, M. J. (1977) Origin of submarine metal-rich hydrothermal solutions: experimental basalt--seawater interaction in a seawater-dominated system at 300°C, 500 bars: Proc. 2nd Int. Symposium on Water-Rock Interaction, I.A.G.C., Strasbourg, France, IV, 173-180.

- Spooner, E. T. C. and Fyfe, W. S. (1973) Sub-sea floor metamorphism, heat and mass transfer: Contrib. Mineral. and Petrol. 42, 287-304.
- Spooner, E. T. C., Beckinsale, R. D., Fyfe, W. S. and Smewing, J. D. (1974) ^{18}O enriched ophiolitic metabasic rocks from E. Liguria (Italy), Pindos (Greece) and Troodos (Cyprus): Contrib. Mineral. Petrol. 47, 41-62.
- Spooner, E. T. H., Beckinsale, R. D., England, P. C. and Senior, A. (1977) Hydration, ^{18}O enrichment and oxidation during ocean floor hydrothermal metamorphism of ophiolitic metabasic rocks from E. Liguria, Italy: Geochim. Cosmochim. Acta 41, 857-871.
- Stakes, D. M. (1978) Submarine hydrothermal systems: Variations in mineralogy, chemistry, temperatures, and alteration oceanic layer II: Unpubl. Ph.D. Thesis, Oregon State University, 189 pp.
- Taylor, H. P. (1974) The application of oxygen and hydrogen isotope studies to problems of hydrothermal alteration and ore deposition: Econ. Geol. 69, 843-883.
- Taylor, H. P., Jr. (1979) Oxygen and hydrogen isotope relationships in hydrothermal mineral deposits. In H. L. Barnes (ed.), The Geochemistry of Hydrothermal Ore Deposits, 798 p., Wiley-Interscience.

Genesis of gold-bearing quartz veins of the Alleghany district,
California

A. S. Radtke, Radtke and Associates

R. W. Wittkopp, Helms Exploration Company

Chris Heropoulos, U.S. Geological Survey

GENESIS OF GOLD-BEARING QUARTZ VEINS OF THE ALLEGHANY DISTRICT, CALIF.

RADTKE, Arthur S., Radtke and Associates, Palo Alto, California
94306; WITTKOPP, Raymond W., Helms Exploration Company, Sparks,
Nevada; HEROPOULOS, Chris, U.S. Geological Survey, Menlo Park,
California

Gold-bearing quartz veins in the Alleghany district occur along steeply dipping enechelon faults cutting phyllite, amphibolite, and quartzite. Early hydrothermal fluids moved upward along faults and precipitated quartz plus minor arsenopyrite, pyrite, and gold. Fluid inclusion studies show filling temperatures of 195 to >300°C, salinities of 10 to >20 wt.% NaCl equivalent, and daughter minerals of dawsonite, muscovite, and paragonite. During vein formation all types of wallrock underwent chloritic and sericitic alteration. Sealing of faults by quartz caused later fluids to move upward along contacts between serpentinite and other rock types. These fluids deposited quartz, magnesite-ankerite, and large amounts of arsenopyrite and gold, forming rich ore shoots in veins 50-100 feet from serpentinite contacts. Fluid inclusion data show filling temperatures of 180 to 290°C salinities of 3 to 16 wt.% NaCl equivalent, and a CO₂ content as much as 20%. These fluids altered serpentinite to magnesite and lesser dolomite, chromite to mariposite, and leached silica. Arsenic in the fluids reacted with nickel sulfides to form sulfarsenides. Wallrock alteration along veins by CO₃²⁻-rich solutions is restricted to local formation of ankerite superimposed on the earlier alteration.

Precipitation of gold from late fluids to form high-grade shoots could have been due to (1) reaction between solutions undersaturated with quartz along serpentinite contacts with earlier quartz in veins, and (or) (2) boiling off of CO₂ causing increase in solution pH and lower gold solubilities, or (3) mixing with cool low salinity meteoric water.

(Courtesy of the Geological Society of America, 1980)

Origin of hydrothermal fluids responsible for gold deposition,
Alleghany district, Sierra County, California

Brian Marshall, University of California at Los Angeles

B. E. Taylor, University of California at Davis

ORIGIN OF HYDROTHERMAL FLUIDS RESPONSIBLE
FOR GOLD DEPOSITION, ALLEGHANY DISTRICT,
SIERRA COUNTY, CALIFORNIA

Brian Marshall* and Bruce E. Taylor
Department of Geology, University of California
Davis, California 95616

Introduction

The Alleghany district is located in the northern Sierra Nevada, along the extension of the Mother Lode belt, (Figure 1). The district is known for very high grade gold ore localized as "shoots" in quartz veins. Several of the mines in the district are still in operation today.

Previous work in the district was done by Ferguson and Gannett (1932), Cooke (1947), Carlson and Clark (1956), and Coveney (1972). The reader is referred to these sources for discussions of basement geology and occurrences of gold.

Geology and Petrography

The basement rocks in the district are metamorphosed shale, chert, conglomerate, sandstone, and gabbro. Elongated serpentinite bodies occur in all of the basement rock types, and small granitic stocks intruded the metamorphic rocks in a few localities, (Figure 1). Tertiary gravels and volcanic rocks overlie the basement rocks with angular unconformity (Ferguson and Gannett, 1932). Quartz veins, ranging in thickness from less than 1 cm to over 10 m, occur in all of the basement rock types, including serpentinite and granite.

All of the basement rocks are hydrothermally altered. The mineral assemblages were identified optically and by X-Ray diffraction. What follows are brief descriptions of the granite, serpentinites, and altered wall rocks.

The granite which crops out near the Oriental Mine consists entirely of quartz, feldspar, chlorite, and sulfides. The feldspars are turbid due to fine-grained alteration products and/or fluid inclusions. The granite is fine-grained, and hypidiomorphic-granular in texture.

Serpentinites are 90+% serpentine polymorphs, primarily lizardite and antigorite. Chrysotile occurs as veinlets associated with minute magnetite grains, and lizardite veins cut the serpentinites in places. Bastite and relict olivine are

*Present address: Department of Earth and Space Sciences, University of California, Los Angeles, CA 90024

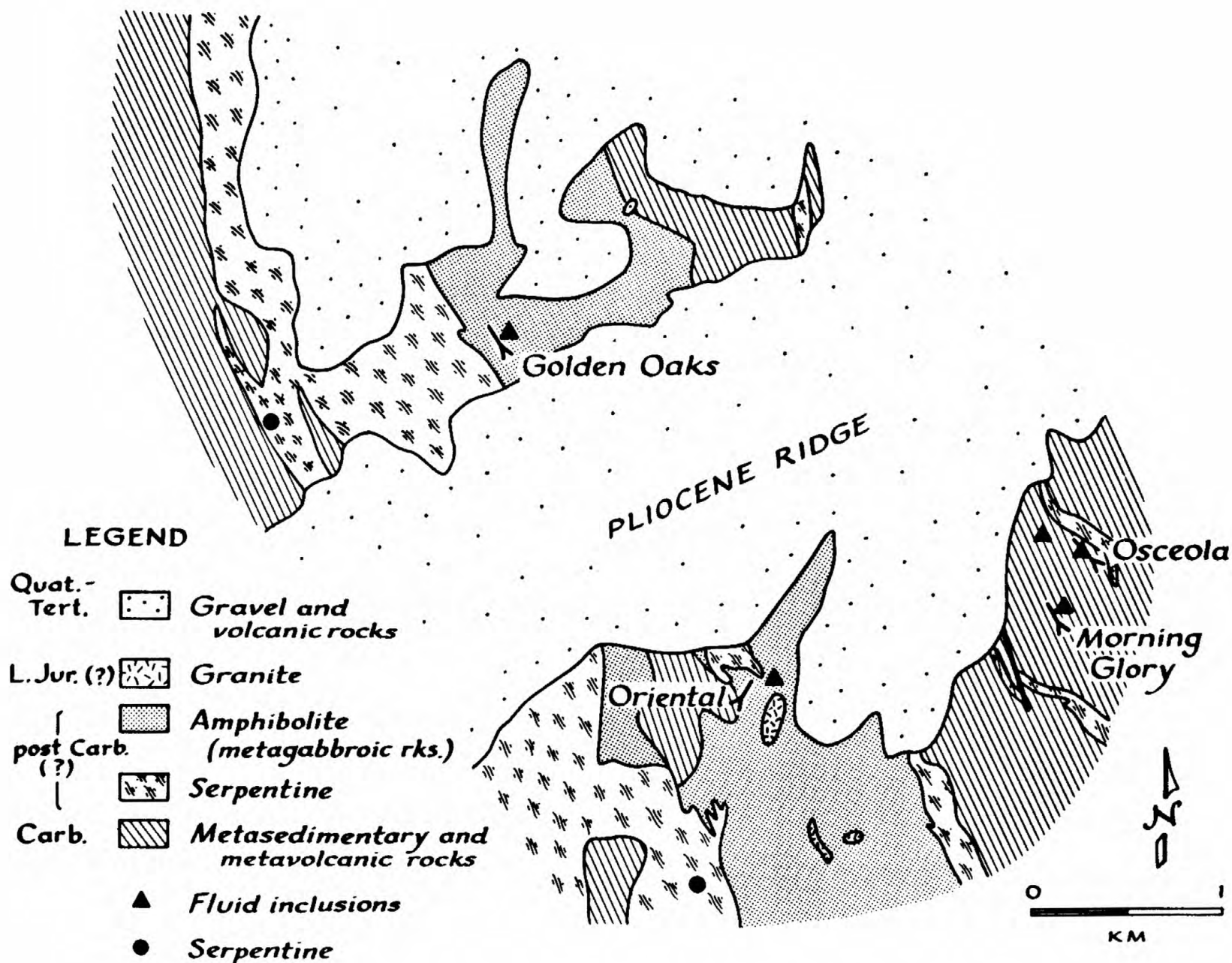


Figure 1. Simplified geologic map of a portion of the Alleghany district (after Ferguson and Gannett, 1932), showing localities of analyzed serpentinite (●) and fluid inclusions (▲). Locations of mines sampled are also shown.

present in samples, where the original texture has been preserved. In more highly altered samples, only embayed relict chromites remain, and no original texture is preserved; magnetite is ubiquitous but very fine-grained. At one locality an inclusion in the serpentinite has been altered to rodingite consisting of hydrogrossular garnet, idocrase, and chlorite. Rarely, quartz and sulfides are observed in the serpentinites.

Closer to quartz veins, serpentinite is partially replaced by veinlets of dolomite and talc, and relict chromite shows even more evidence of chemical reaction (embayment). Adjacent to quartz veins, the wall rock may consist of quartz-dolomite-mariposite+talc+graphite+sulfides. In one locality, the wall rock consists entirely of ankerite. Mariposite, the chromian phengite, showed the presence of nickel in addition to chromium by energy dispersive X-Ray analysis using the microprobe. Sulfide minerals present include pyrite, arsenopyrite, galena, and jamesonite.

Dolomite is frequently observed at the edges of quartz veins, and graphite-pyrite seams, often crenulated, occur in quartz (known as "ribbon quartz") near the edges of veins. The quartz in the veins is generally coarse-grained, often strained, and contains numerous fluid inclusions which give the quartz its gray-white color. Inclusions of wall rock are often present in the veins. Vugs occur occasionally, containing crystals of quartz up to 5 cm across. Vug quartz is usually clear and rarely contains calcite or galena. Gold occurs free in quartz, or associated with arsenopyrite.

Fluid Inclusions

Fluid inclusions in quartz were studied in polished thick (0.5 mm) sections. Two types of inclusions were noted: secondary inclusions which are small and arranged in planes, and primary inclusions which are larger and irregularly spaced. Planes of secondary inclusions often cross grain boundaries proving their secondary origin, related to fracturing or, possibly, strain twinning. Primary inclusions are presumed to have been trapped during crystal growth.

The inclusions range in size from less than 0.8μ to 20μ ; most primary inclusions are from 10 to 15μ across, and usually contain liquid and a vapor bubble which occupies one-tenth to one-quarter of the inclusion volume. Rarely, no gas bubble is present, or an annular ring surrounds the vapor bubble, suggesting the presence of liquid CO_2 ; no daughter mineral were found. Vapor/liquid ratios are fairly constant, indicating that boiling did not occur at the time of quartz deposition.

Coveney (1972) and Radtke et al. (1980) found dawsonite ($\text{NaAlCo}_3(\text{OH})_2$), ankerite, calcite, muscovite, and paragonite daughter minerals as well as liquid CO_2 in fluid inclusions

from the Oriental mine. This indicates that there are inhomogeneities in the chemistry of the vein- and ore-forming fluids. Homogenization temperatures range from less than 200° to over 300°C, (Coveney, 1972 and Radtke et al., 1980).

Stable Isotope Geochemistry

Minerals, rocks, and fluid inclusions were analyzed for their stable isotope ratios ($^{18}\text{O}/^{16}\text{O}$, D/H, $^{13}\text{C}/^{12}\text{C}$) using standard techniques. The data are reported in the delta notation in per mil relative to the SMOW standard for oxygen and hydrogen, or relative to the PDB standard for carbon. Serpentine and quartz samples chosen for fluid inclusion analysis were taken from the localities shown in Figure 2; only serpentinites chosen for isotopic analysis of magnetite are shown. Other samples of serpentine were taken throughout the district. Veins and associated altered rocks were sampled in four mines in the district: the Oriental, Golden Oaks, Morning Glory, and Osceola mines.

Oxygen isotopes. Oxygen isotope compositions of vein quartz range from +16 to +22‰, (Figure 2). The only quartz sample which contained visible gold has the lightest $\delta^{18}\text{O}$ value. A vug quartz crystal from the Oriental Mine is significantly lighter at the apex than at the base, indicating that either the temperature increased as this crystal formed or, more likely, that the $\delta^{18}\text{O}$ of the fluid decreased during crystallization. Quartz from veins in the eastern part of the district is significantly heavier than quartz from the western part of the district; serpentine $\delta^{18}\text{O}$ values range from +9 to +14‰ and show a similar trend in the district. The oxygen isotope composition of the fluid which deposited quartz and serpentinized the ultramafic rocks was probably controlled by the isotopic composition of the basement rocks which contain more ultramafic rocks (now serpentinites) in the west.

The oxygen isotope composition of granite is +16‰, which is much heavier than pristine granitic rocks (cf. Taylor, 1968). The oxygen in the quartz veins may be in part derived from the metasedimentary rocks with which the fluid exchanged.

Geothermometry. Oxygen isotope compositions of mineral pairs were used to determine temperatures of formation. Where possible, coexisting minerals in physical contact were used. Per mil isotopic fractionations are plotted in Figure 3.

The quartz-dolomite isotopic fractionation curve of Figure 3 was constructed from the quartz-water curve of Bottinga and Javoy (1973), the calcite-water curve of O'Neil et al. (1969), and the dolomite-calcite curve of Northrop and Clayton (1966). Two other parallel curves are shown for the fractionation range of our data; these are from two other dolomite-calcite curves,

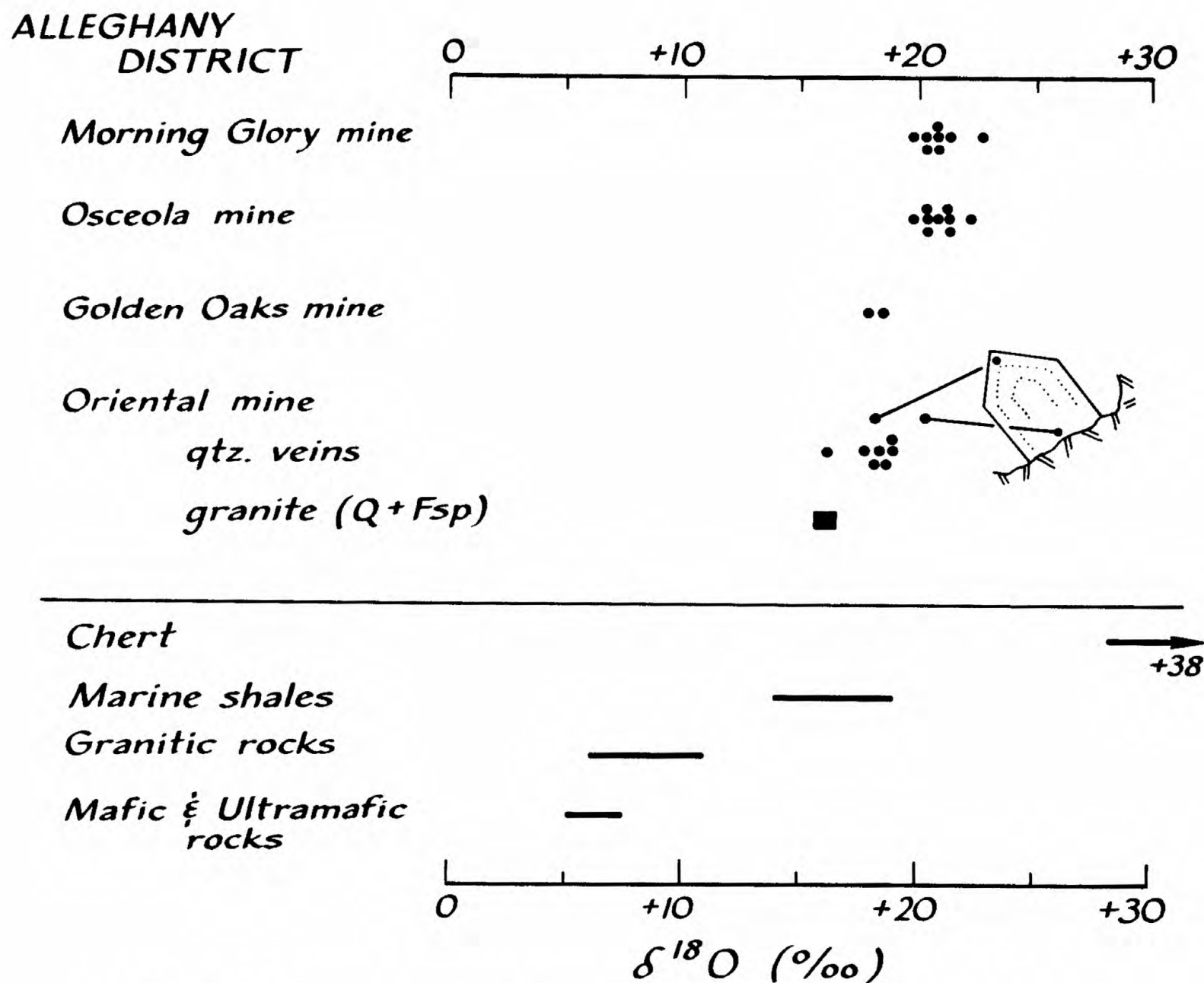


Figure 2. Oxygen isotope compositions of vein quartz and altered granite from the Alleghany district, compared to common ranges in isotopic composition for some crustal rocks. Small sketch schematically shows age relationship of two samples from a late vug quartz crystal.

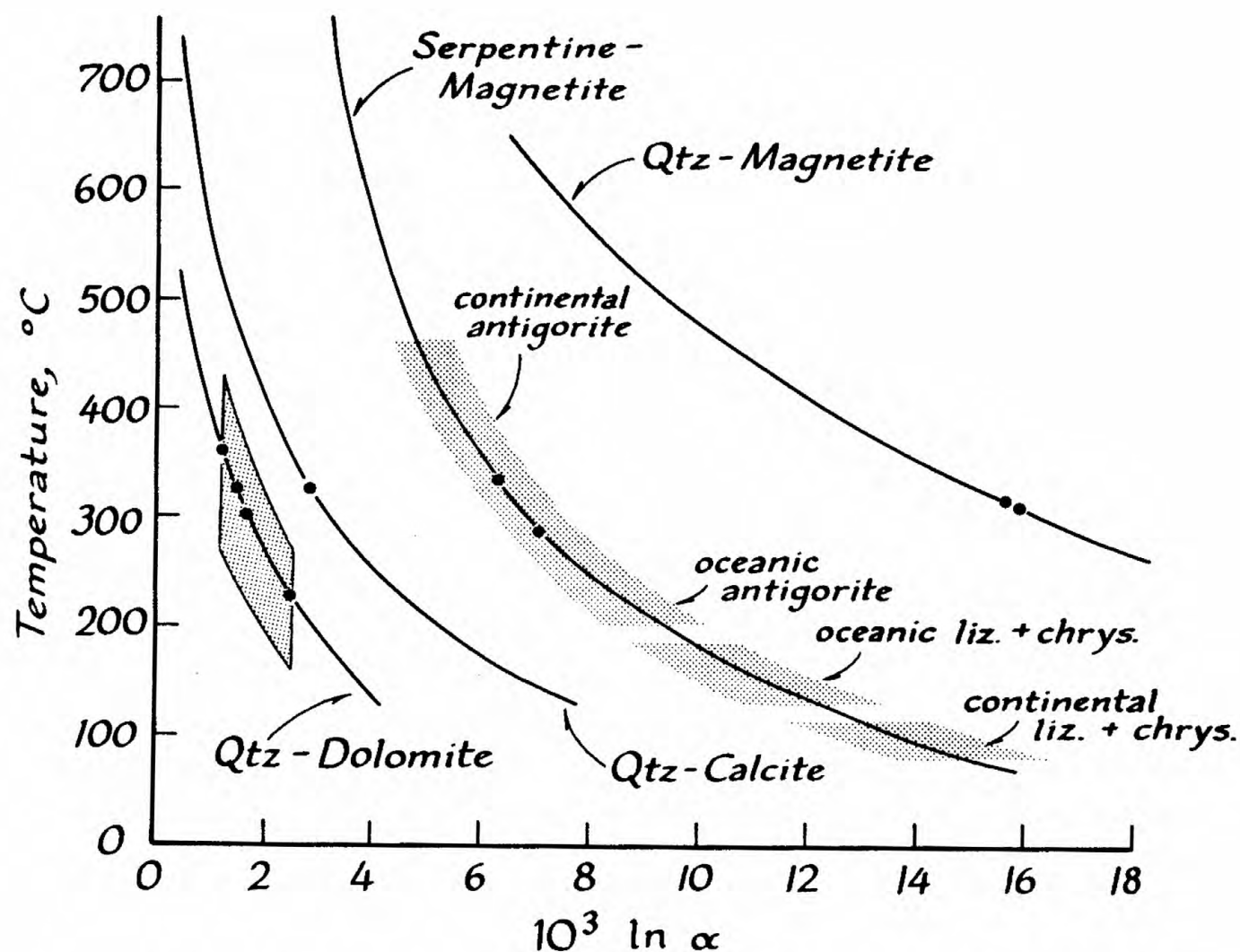


Figure 3. Oxygen isotope fractionation curves for the mineral pairs quartzdolomite, quartz-calcite, serpentine-magnetite, and quartz-magnetite (Bottinga and Javay, 1973; Becker, 1971). Measured fractionations between mineral pairs from the Alleghany district are plotted on their respective curves (•). See text for discussion and sources of data.

(Sheppard and Schwarcz, 1970 and O'Neil and Epstein, 1966). The isotopic temperatures calculated from the curve using Northrop and Clayton's data are 370° , 320° , 300° , and 230°C for measured fractionations between quartz and dolomite. Calcite rhombs, found included in a late vug quartz crystal from the Oriental Mine, are probably the best evidence for contemporaneous deposition of quartz and carbonate. Their oxygen isotope fractionation yields an isotopic temperature of 320°C .

The serpentine-magnetite curve in Figure 3 is from Wenner and Taylor (1971), and yields serpentine-magnetite isotopic temperatures for two samples of 320° and 280°C . Wenner and Taylor (1971) also differentiated temperature ranges for serpentinites of different affinities containing different serpentine polymorphs. Although our data fall within their antigorite field, our samples contain both antigorite and lizardite.

It is thus apparent that quartz vein formation and serpentinization occurred in the same temperature regime. If the fluid that formed the veins was the same fluid that serpentinized the ultramafic rocks, then quartz from the veins should be in isotopic equilibrium with magnetite from the serpentinites. In other words, quartz-magnetite pairs should yield temperatures in agreement with the above results. Two quartz-magnetite pairs yield isotopic temperatures of 310° and 315°C when plotted on the quartz-magnetite curve (Figure 3) constructed from the magnetite-water curve of Becker (1971) and the quartz-water curve of Bottinga and Javoy (1973). Thus, quartz vein formation and serpentinization also occurred in the same hydrothermal system.

Hydrogen isotopes and fluid composition. Hydrogen isotope compositions of granite and serpentinite are -111 and $-114^{\circ}/\text{oo}$, respectively. Quartz was crushed *in vacuo* to yield water for isotopic analysis. δD values of the fluid trapped in the inclusions range from -47 to $-78^{\circ}/\text{oo}$. Each quartz sample was crushed twice to yield water for analysis. Water obtained from the first crushings are all isotopically lighter and less voluminous than water obtained from a second crushing. In addition, the second crushings yielded larger amounts of CO_2 . Thus, we think that the two different crushings represent fluids primarily from quite different generations of inclusions; the first crushings may represent water from the secondary, more easily broken inclusions, while the second crushings may represent mostly primary inclusion fluids. However, it is possible that some isotopic fractionation may be inherent in our analytical technique. Therefore, until more thorough analyses are done, we consider the waters obtained from the second crushings to be representative of the primary fluid inclusions.

$\delta^{18}\text{O}$ Assuming isotopic equilibrium with quartz at 310°C , the $\delta^{18}\text{O}$ of the hydrothermal fluid was $+10$ to $+14^{\circ}/\text{oo}$, based on

Bottinga and Javoy (1973). The oxygen and hydrogen isotope compositions of the fluid are plotted in Figure 4, where it is assumed that the hydrogen isotope composition of fluid trapped in fluid inclusions is that of the hydrothermal fluid.

The ^{18}O -rich nature of the hydrothermal fluid suggests that its oxygen isotope composition must have been controlled by the metasedimentary rocks in the section, and that the water/rock ratios beyond the veins must have been fairly low. The hydrogen isotope composition of the fluid was -45 to -80 ‰, and the chlorite in altered granite, and the lizardite shown in Figure 4 would have been in hydrogen isotope equilibrium with this fluid at about 300°C . The δD values of two data in Figure 4 are clearly lighter than most metamorphic fluids. These values could indicate a small addition of meteoric water to the hydrothermal fluid. However, if large amounts of meteoric water were involved, the oxygen isotope compositions would also be affected. Therefore, the hydrothermal fluid was essentially of metamorphic origin.

Carbon isotopes. Carbon isotope compositions of carbonates (dolomite and calcite) range from -7 to -3 ‰, (Figure 5). CO_2 was obtained from the second crushings of fluid inclusions in quartz; measured $\text{H}_2\text{O}/\text{CO}_2$ molar ratios are about 100^1 . The $\delta^{13}\text{C}$ values of CO_2 range from -2 to -5 ‰ and, based on Bottinga (1968a), the average CO_2 would be in carbon isotope equilibrium with the average carbonate at 310°C .

The carbon dioxide in the inclusions cannot reasonably be derived solely from metamorphic decarbonation reactions (Figure 5). Magmatic or organic sources are more likely. The latter possibility is especially attractive, as there is abundant graphite near the edges of the quartz veins. Assuming an average $\delta^{13}\text{C}$ value of -20 ‰ for marine organic carbon from which the graphite was probably derived, CO_2 in isotopic equilibrium with the graphite at 310°C would have a $\delta^{13}\text{C}$ value of -7 ‰ (Bottinga, 1968b). We consider this value to be at least approximately consistent with the present data, although our conclusions may change when we analyze graphite from the district. CO_2 could, of course, be derived from a mixture of these various sources.

Conclusion

In conclusion, the Alleghany quartz veins formed at temperatures around 310°C . Serpentinization of ultramafic rocks occurred in the same hydrothermal system and at the same temperature. The hydrothermal fluid was essentially metamorphic in nature, and CO_2 in the fluid was derived from oxidation of organic matter, or from a juvenile source.

Gold in the deposits was probably derived from the metasedimentary and/or ultramafic and mafic igneous rocks in the

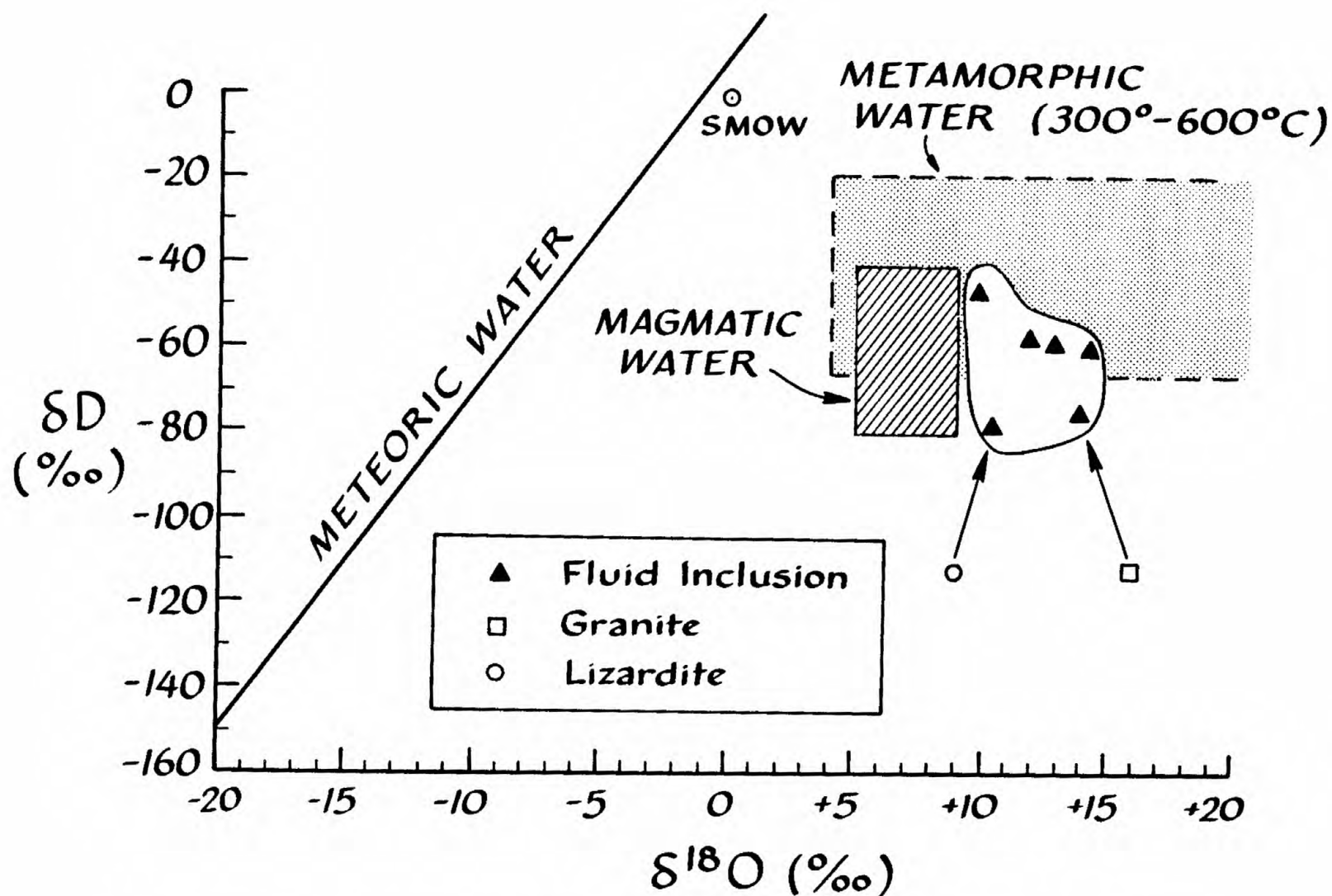


Figure 4. Oxygen (calculated, see text) and hydrogen isotope compositions of water from fluid inclusion in quartz veins, compared to the range of isotopic compositions of meteoric waters (Craig, 1961), magmatic water and metamorphic waters (Taylor, 1974), and Standard Mean Ocean Water (SMOW). Also shown are the isotopic compositions of lizardite and altered granite, each of which could have been in isotopic equilibrium with the range of compositions indicated for the hydrothermal fluids.

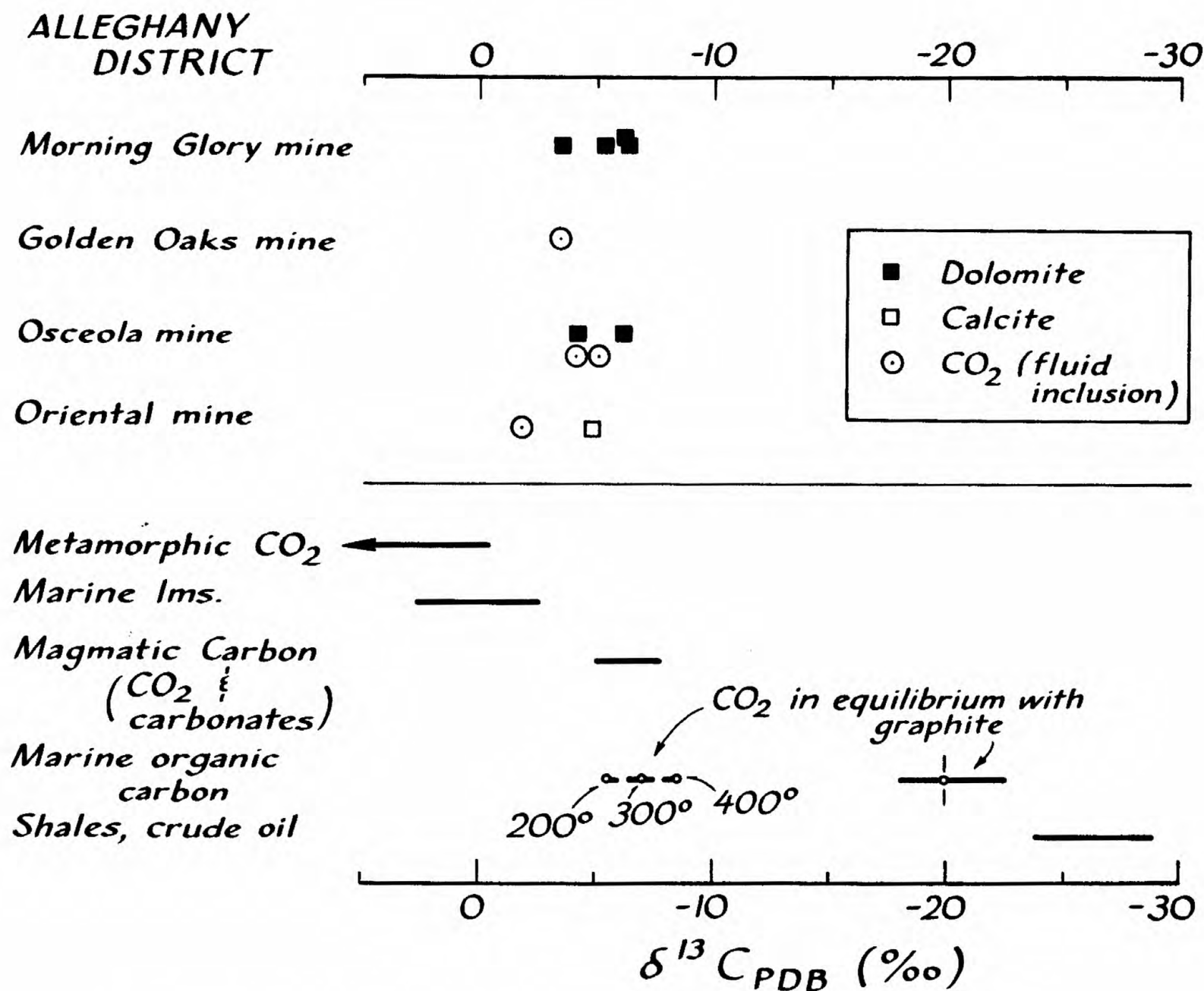


Figure 5. Carbon isotope composition of carbonates and of CO₂ from fluid inclusions in quartz veins, compared to ranges in $\delta^{13}C$ for metamorphic CO₂, marine limestone, magmatic carbon (as CO₂), marine organic carbon, and carbon in shales and crude oil (taken from various sources).

district. The association of serpentinite with gold-quartz veins is common in the Mother Lode belt (Knopf, 1929), and the conclusions arrived at for the Alleghany district may apply to the belt as a whole.

Acknowledgements

We are indebted to Mike Miller and to Don Dickey for permitting access to their mines. Dr. J. R. O'Neil, U.S. Geological Survey, graciously allowed use of his stable isotope laboratory. The support of a President's Undergraduate Fellowship to B. M., and an NSF grant (EAR 79-13238) to B. E. T. is gratefully acknowledged.

References

- Becker, R. H., 1971, Carbon and oxygen isotope ratios in iron-formation and associated rocks from the Hammersley Range of Western Australia and their implications: Univ. of Chicago, Ph.D. thesis, 138 pp.
- Bottinga, Y., 1968a, Calculation of fractionation factors for carbon and oxygen exchange in the system calcite-carbon dioxide-water: Jour. Phys. Chemistry 72, 800-808.
- _____, 1968b, Isotopic fractionation in the system, calcite-graphite-carbon dioxide-methane-hydrogen-water: California Univ. at San Diego, Ph.D. thesis, 126 pp.
- Bottinga, Y., and Javoy, M., 1973, Comments on oxygen isotope geothermometry: Earth and Planetary Sci. Lett. 20, 250-265.
- Carlson, D. W., and Clark, W. B., 1956, Lode gold mines of the AlleghanyDownieville area, Sierra County, California: Calif. Jour. of Mines and Geol. 52, 237-272.
- Cooke, H. R., Jr., 1947, The Original Sixteen-to-One gold-quartz vein, Alleghany, California: Econ. Geol. 42, 211-250.
- Coveney, R. M., Jr., 1972, Gold mineralization at the Oriental Mine, Alleghany, California: Michigan Univ., Ph.D. thesis, 99 pp.
- Craig, H., 1961, Isotopic variations in meteoric waters: Science 133, 1702-1703.
- Ferguson, H. G., and Gannett, R. W., 1932, Gold quartz veins of the Alleghany district, California: U.S. Geol. Surv. Prof. Paper 172, 139 pp.
- Knopf, A., 1929, The Mother Lode system of California: U.S. Geol. Surv. Prof. Paper 157, 88 pp.
- Northrop, D. A., and Clayton, R. N., 1966, Oxygen isotope fractionation in the system dolomite-calcite-carbon dioxide: Science 152, 198-201.
- O'Neil, J. R., and Epstein, S., 1966, Oxygen isotope fractionation in the system dolomite-calcite-carbon dioxide: Science 152, 198-201.
- O'Neil, J. R., Clayton, R. N., and Mayeda, T. K., 1969, Oxygen isotope fractionation in divalent metal carbonates: Jour. Chem. Physics 51, 5547-5558.

- Radtke, A. S., Wittkopp, R. W., and Heropoulos, C., 1980, Genesis of goldbearing quartz veins of the Alleghany district, California: Geol. Soc. America Abst. with Prgms. 12, 148.
- Sheppard, S. M. F., and Schwarcz, H. P., 1970, Fractionation of carbon and oxygen isotopes and magnesium between metamorphic calcite and dolomite: Contr. Mineral. and Petrol. 26, 161-198.
- Taylor, H. P., Jr., 1974, The application of oxygen and hydrogen isotope studies to problems of hydrothermal alteration and ore deposition: Econ. Geol. 69, 843-883.
- Wenner, D. B., and Taylor, H. P., Jr., 1971, Temperatures of serpentization of ultramafic rocks based on $^{18}\text{O}/^{16}\text{O}$ fractionation between coexisting serpentine and magnetite: Contr. Mineral. and Petrol. 32, 165-185.

Subsurface intrusive rocks at The Geysers geothermal area,
California

Alexander Shreiner, Jr., Union Oil Company of California
G. A. Suemnicht, Union Oil Company of California

SUBSURFACE INTRUSIVE ROCKS AT THE GEYSERS

GEOHERMAL AREA CALIFORNIA

Schriener, Jr., Alexander and Suemnicht, Gene A., Geothermal Division Union Oil Company of California, P.O. Box 6854, Santa Rosa, CA 95406

INTRODUCTION

The Geysers, the worlds largest commercial, vapor-dominated geothermal system is located in the Northern California Coast Range about 150 km north of San Francisco (Figure 1). Bedrock in the area consists of the Franciscan assemblage, described by McLaughlin (1978). Wells within the field commonly bottom in and produce steam from fractured Franciscan graywacke. The Clear Lake volcanics of Pliocene to Recent age are adjacent to the steam field (Anderson, 1936, Hearn, Donnelly and Goff, 1976). Major eruptive centers with dacite and rhyolite composition include Mt. Konocti, Mt. Hannah and Cobb Mountain (Figure 1). Of these centers, Cobb Mountain is located adjacent to the Geysers production area. The biotite rhyolite eruptive phase of Cobb Mountain has a K-Ar age of 1.12 m.y., whereas the dacite summit and flank flows have K-Ar ages of 1.06 and 1.08 m.y. respectively. In addition to the Cobb Mountain volcanics, a 2.04 m.y. rhyolite flow and a 1.64 m.y. olivine basalt crop out near the steam field (Donnelly, 1977). Despite this proximity to the Clear Lake volcanics, no related intrusive rocks have been reported within the Geysers field. Recently, a well northeast of Burned Mountain (Figure 1) bottomed in about 120 m of quartz normative, biotite-bearing felsite. Cuttings from several other wells indicate that up to 900 m of chemically and mineralogically similar rock is penetrated locally.

DISCUSSION

Grain mounts and thin sections prepared from drill cuttings show the felsite generally displays porphyritic to equigranular texture. The porphyritic rocks have phenocrysts up to at least 2 mm in size. The major constituents of the rock are, in order of decreasing abundance, plagioclase feldspar, quartz, potassium feldspar (orthoclase), sanidine, and biotite. Minor minerals include orthopyroxene, clinopyroxene, apatite, zircon, oxides and sulfides.

Quartz and orthoclase are commonly found as anhedral interstitial phases. Both of these minerals, which average 1/4 mm in diameter, often form a mosaic texture in the groundmass. Quartz is found as subhedral phenocrysts. The plagioclase feldspar is albitic in composition. It occurs as at least 2 mm long laths with common polysynthetic twins and zoning. Although brown pleochroic biotite is the primary mafic mineral, minor amounts of pyroxene are present in selected samples. The biotite occurs as anhedral crystals less than 1 mm in diameter.

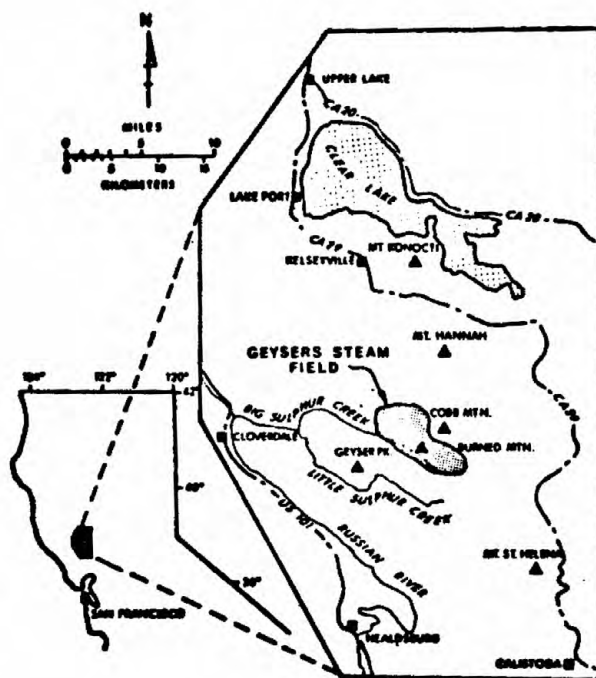


Figure 1. Location map for the Geysers Geothermal steam field.

Chemical analyses of representative felsite samples are listed in Table 1. In addition, major oxide percentages of selected Cobb Mountain volcanic flows and Franciscan graywackes are listed for reference. When plotted on partial Harker variation diagrams (Figure 2), the data display a nearly continuous increase in K_2O , constant Na_2O , and decreasing Al_2O_3 , CaO , Fe_2O_3 , MgO , MnO , and P_2O_5 and TiO with increasing SiO_2 . Similar trends are seen in the Cobb Mountain volcanic samples. AFM ternary plots of felsite values establishes a distinct calc-alkaline trend. A range of values occurs in the NKC plot (Figure 3). The AFM and NKC trends are similar to the observed Cobb Mountain trends are within the range of compositions for rhyolites and dacites for the Clear Lake volcanic field (Figure 4). In general, however, Franciscan assemblage graywackes are dissimilar in composition from the volcanic rocks (Figure 5).

There is a crude mineralogic and chemical zonation within the felsite intrusions. Samples show a decrease in concentrations of mafic minerals accompanied by lower percentages of Al_2O_3 , CaO , Fe_2O_3 , MgO , Na_2O and P_2O_5 and greater percentages of SiO_2 and K_2O inward from the margins of the intrusions. In addition, the felsite grades inward to a coarsely grained and equigranular texture away from the margins of the intrusions.

Potassium-Argon analyses of these cuttings yield calculated ages of 1.6 ± 0.4 m.y. on sanidine, 2.7 ± 0.3 m.y. on biotite, and 2.5 ± 0.4 m.y. whole rock. These discordant ages may be due to some contamination in the cuttings. Donnelly (1977) found that for the Clear Lake volcanics sanidine separates gave the most reliable K-Ar age. Biotites were found to act as "sponges" for atmospheric argon and often produced ages with large analytical errors. Thus, although the precise radiometric age is not known, this intrusion beneath the Geysers is young and within the age range for Clear Lake volcanism.

The Sr^{87}/Sr^{86} ratio for the felsite is 0.708 which is slightly higher than the 0.704 ratio for dacites and rhyolites in the Clear Lake volcanic field (Donnelly, pers comm). This is interpreted as evidence for assimilation of strontium from the Franciscan host rocks.

The presence of a magma chamber or cupola has been inferred beneath the Geysers field. Isherwood's (1976) residual Bouguer gravity map (Figure 6) shows the predominate Clear Lake gravity low centered about Mt. Hannah and localized lows within the central Geysers field. Isherwood suggests that the local gravity lows can not be accounted for by vapor-filled, fractured graywacke alone. Gravity and filtered aeromagnetic data led Isherwood to postulate the existence of a magma chamber above the Curie Point at a 5-7 km depth. Iyer and others (1979) suggests that a magmatic cupola at greater than 10 km depth exists because teleseismic P wave delays (Figure

FELSITE			COBB MTN. VOLCANICS		FRANCISCAN GRAYWACKES ^{1*}	
(Ave. 13 Samples)			RHYOLITE	DACITE	Sonoma County	
			Ave. (2 Samples)	(1 Sample)	(Ave. 8 Samples)	
		Range				Range
SiO ₂	76.87	(71.68 - 80.0)	75.37	65.89	67.3	(58.4 - 72.2)
Al ₂ O ₃	11.36	(9.61 - 12.36)	12.32	14.56	13.5	(11.7 - 14.6)
Fe ₂ O ₃	2.75	(1.58 - 5.09)	2.08	3.80	5.1	(2.1 - 6.2)
CaO	1.29	(0.67 - 2.43)	1.22	4.30	2.7	(0.6 - 8.2)
MgO	0.31	(0.00 - 0.62)	0.26	1.19	1.9	(1.2 - 2.7)
Na ₂ O	3.21	(2.46 - 3.53)	3.22	3.42	4.0	(3.2 - 6.0)
K ₂ O	3.37	(2.84 - 4.62)	4.05	2.98	1.7	(1.1 - 2.4)
TiO ₂	0.13	(>0.001 - 0.36)	0.20	0.65	0.5	(0.4 - 0.6)
MnO	0.06	(0.01 - 0.11)	0.04	0.06	0.1	(>0.1 - 0.2)
P ₂ O ₅	0.08	(0.01 - 0.23)	0.09	0.14	0.1	(0.1 - 0.2)
LOI	0.29	(>0.01 - 0.61)	0.57	0.74		

* 1. Samples 3 & 6-12 on
Table 1, p.33, Bailey
and others, 1964

FELSITE (Ave. 13 Samples)			COBB MTH. VOLCANICS		FRANCISCAN GRAYWACKES ¹	
			MIYOLITE Ave. (2 Samples)	BACITE (1 Sample)	Sonoma County (Ave. 8 Samples)	
	Range				Range	
SiO ₂	76.87	(71.68 - 80.0)	75.37	65.89	67.3	(58.4 - 72.2)
Al ₂ O ₃	11.36	(9.61 - 12.36)	12.32	14.56	13.5	(11.7 - 14.6)
Fe ₂ O ₃	2.75	(1.58 - 5.09)	2.08	3.80	5.1	(2.1 - 6.2)
CaO	1.29	(0.67 - 2.43)	1.22	4.30	2.7	(0.6 - 8.2)
MgO	0.31	(0.00 - 0.62)	0.26	1.19	1.9	(1.2 - 2.7)
Na ₂ O	3.21	(2.46 - 3.53)	3.22	3.42	4.0	(3.2 - 6.0)
K ₂ O	3.37	(2.84 - 4.62)	4.05	2.98	1.7	(1.1 - 2.4)
TiO ₂	0.13	(>0.001 - 0.36)	0.20	0.65	0.5	(0.4 - 0.6)
MnO	0.06	(0.01 - 0.11)	0.04	0.06	0.1	(>0.1 - 0.2)
P ₂ O ₅	0.08	(0.01 - 0.23)	0.09	0.14	0.1	(0.1 - 0.2)
LOI	0.89	(>0.0 - 0.61)	0.87	0.76		

¹ 1. Samples 3 & 4-12 on
Table 1, p.33, Bailey
and others, 1964

Table 1. Major oxide analyses for selected felsite, Cobb Mountain volcanic and Graywacke samples.

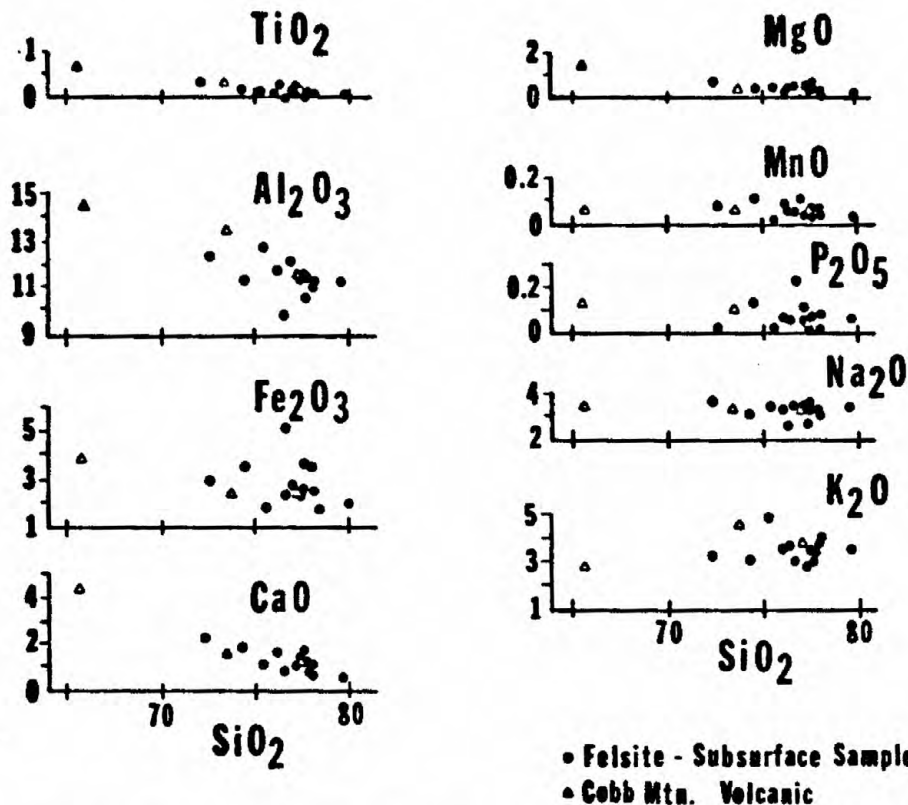


Figure 2. Partial Harker variation diagrams for felsite and Cobb Mountain volcanic samples.

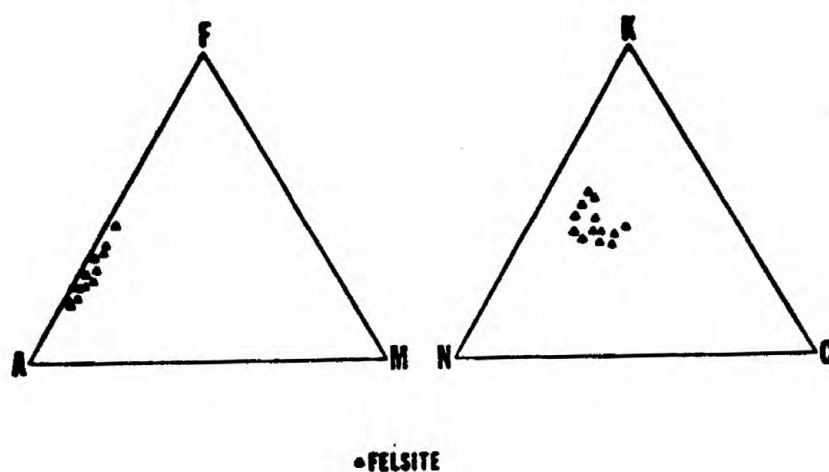


Figure 3. AFM and NKC ternary diagrams for felsite samples.

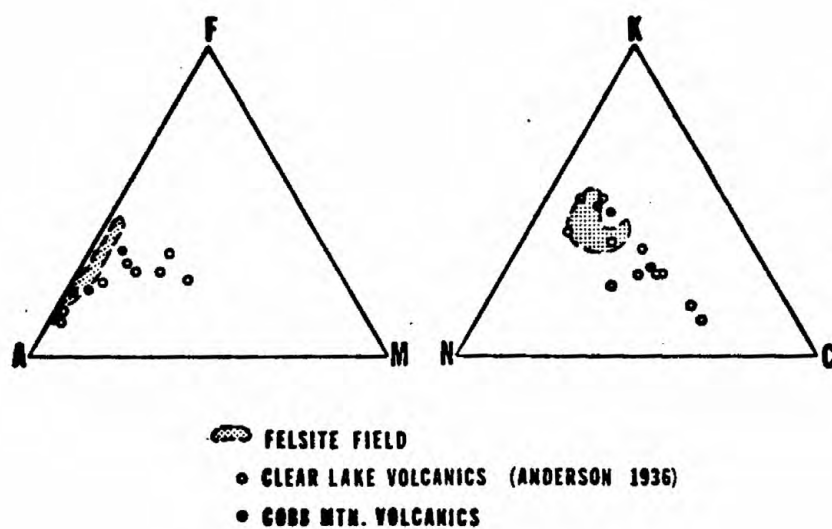


Figure 4. AFM and NKC ternary diagrams for felsite, Clear Lake volcanics and Cobb mountain volcanics samples.

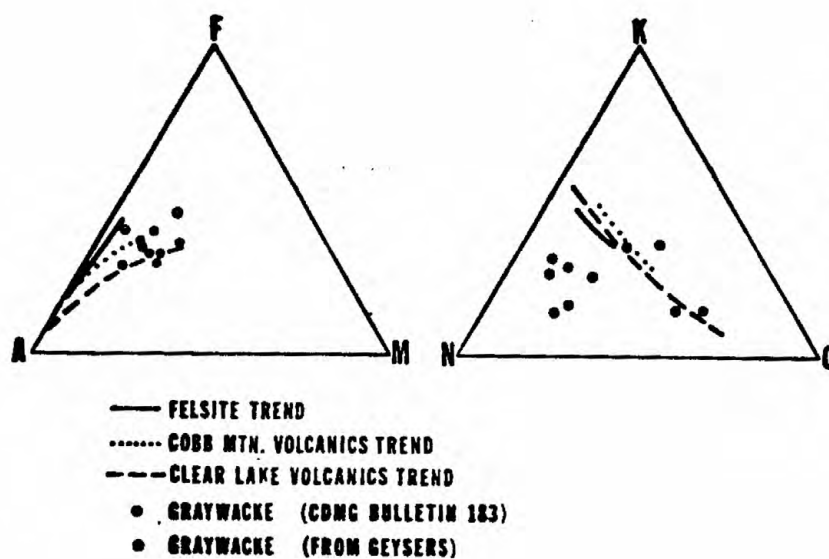


Figure 5. AFM and NKC ternary diagrams comparing felsites, volcanic rocks and graywackes.

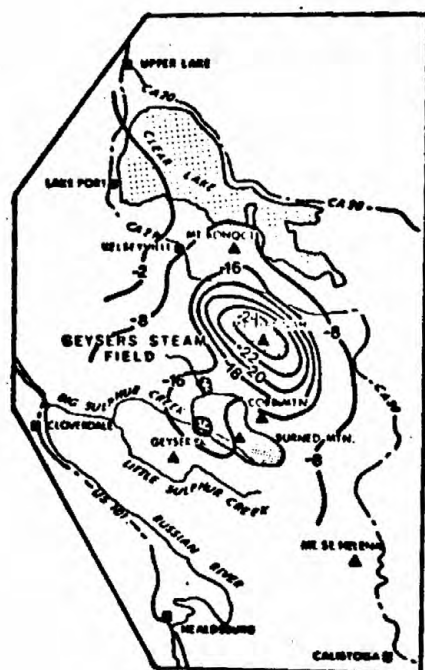


Figure 6. Residual Bouguer gravity of the Geysers-Clear Lake area (Isherwood, 1976).

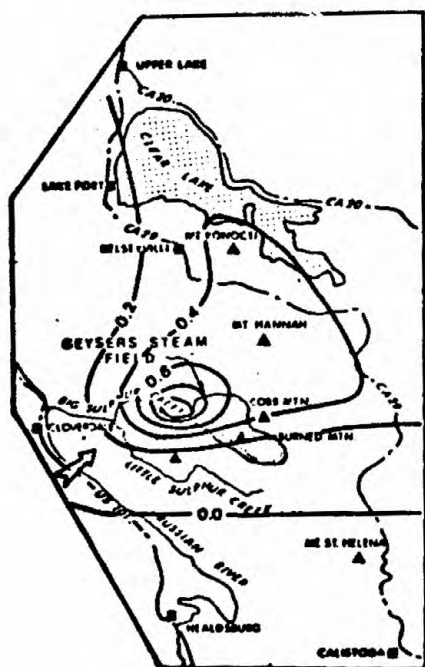
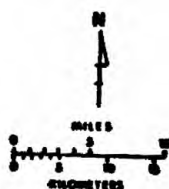
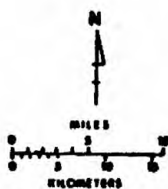


Figure 7. Relative teleseismic p-wave residuals for southwest events near the Geysers (Iyer and others 1979).



7) greater than one second occur through the Geysers field.

CONCLUSIONS

The results of our work establishes the physical presence of subsurface intrusive rocks within the Geysers field. These rocks are temporally and chemically related to Clear Lake volcanism located near the steam field. The age of these felsite intrusions precludes them being the heat source of the present day geothermal system. Nevertheless, the intrusions could be related to the magmatic cupola postulated beneath the Geysers steam field.

ACKNOWLEDGEMENT: The authors thank Union Oil Company of California for permission to publish.

REFERENCES CITED:

- Anderson, C.A., 1936, Volcanic history of the Clear Lake area, California: Geol. Soc. America Bull., v.47, No.3, p.629-664.
- Bailey, E.H., Irwin, W.P., and Jones, D.L., 1964, Franciscan and related rocks, and their significance in the geology of Western California: California Div. of Mines and Geol. Bull. 183, 177p.
- Donnelly, J.M., 1977, Geochronology and evolution of the Clear Lake Volcanic Field: Unpublished Ph.D. dissertation, University of California, Berkeley, 48 pp.
- Hearn, B.C., Jr., Donnelly, J.M., and Goff, F.E., 1976, Preliminary geologic map and cross-section of the Clear Lake Volcanic Field, Lake County, California: U.S.G.S. Open-File Map 76-751.
- Isherwood, W.F., 1976, Gravity and Magnetic studies of The Geysers-Clear Lake Geothermal Region, California: Proceedings, Second United Nations Symposium on the Development and use of Geothermal Resources, 20-29 May, 1975, Lawrence Berkeley Laboratory, v.2, p.1065-1077.
- Iyer, H.M., Hitchcock, T. and Oppenheimer, D.H., 1979, Abnormal P-wave delays in The Geysers-Clear Lake Geothermal Area, California: Science, v.204, May 4, 1979, p.495-497.
- McLaughlin, R.J., 1978, Preliminary geologic map and structural sections of the Central Mayamas Mountains and The Geysers Steamfield, Sonoma, Lake and Mendocino Counties, California: U.S.G.S. Open File Report 78-389.

An overview of tungsten, copper and zinc-bearing skarns
in western North America

L. D. Meinert, Stanford University
Rainer Newberry, Stanford University
M. T. Einaudi, Stanford University

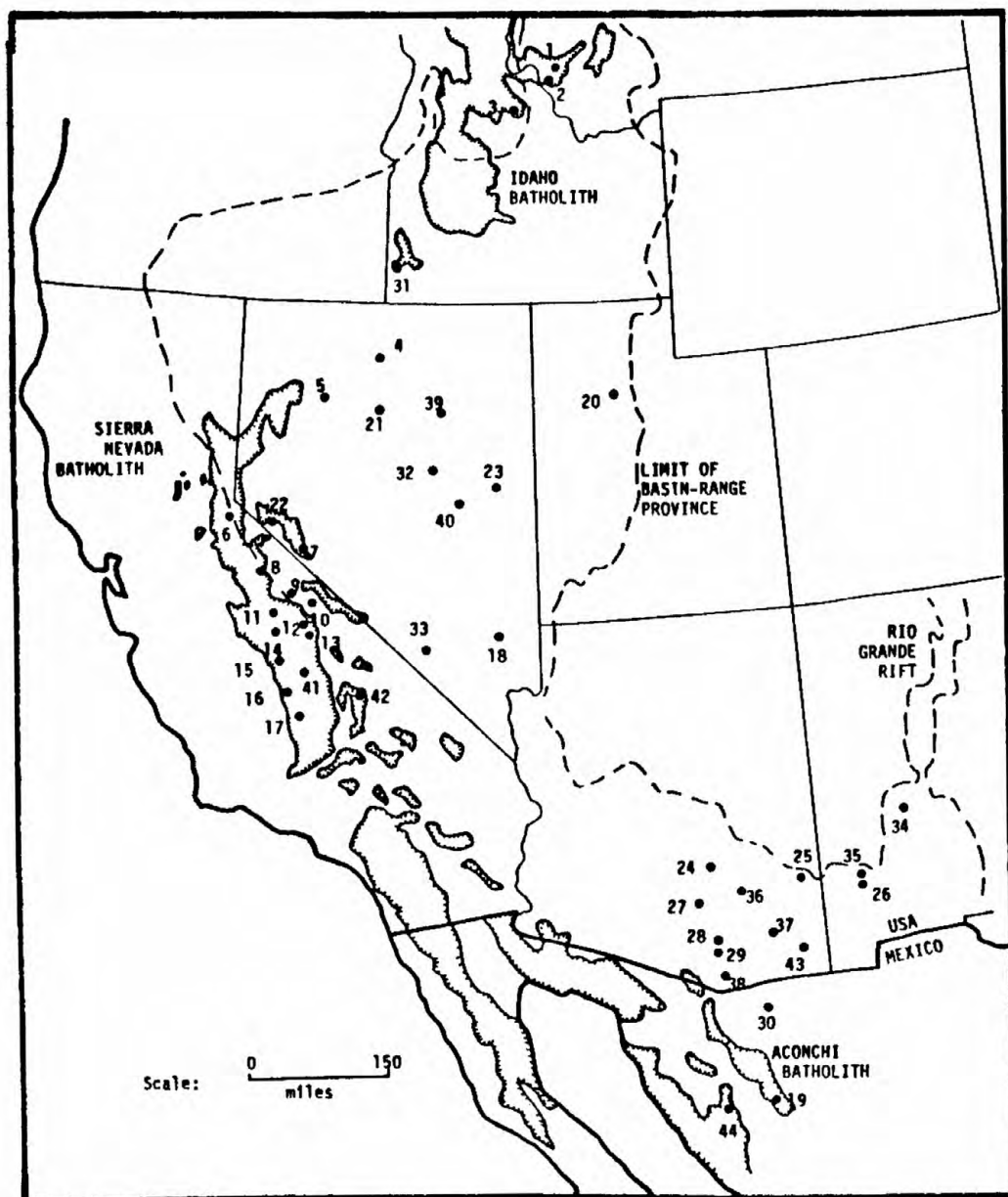
INTRODUCTION

Skarn deposits are important high-grade sources of copper, zinc, iron, tungsten, and a host of by-product base and precious metals. Skarns containing these ore metals are known throughout western North America (Fig. 1). Certain geographical distribution patterns (e.g. tungsten skarns in eastern California, western Montana, and the Selwyn basin, Canada; copper skarns in Arizona) have prompted theories concerning metallogenic provinces. These theories have relied upon mantle inhomogeneties (Noble, 1970), local crustal concentration of critical elements (Krauskopf, 1971) or variable modes of subduction-related magma genesis (Sillitoe, 1976) to explain metal distributions. We suggest instead that differences in ore and calc-silicate mineralogy of calcic skarns associated with calc-alkaline intrusives are due to differences in the environments of skarn formation including tectonic setting, depth, temperature, and wall rock composition.

Zharikov (1970) and Burt (1972) first demonstrated patterns in the relationships between ore and calc-silicate mineralogy in skarn deposits. Other recent workers (Shimazaki, 1975; Einaudi, 1977; Fonteilles et al., 1978) have suggested general relationships between certain skarn types and broad aspects of geologic environment. Overviews of skarn formation in the porphyry-copper environment (Einaudi, in press), in the Sierran tungsten skarn environment (Newberry, 1980) and in the zinc skarn environment (Meinert, 1980) have recently been completed. It is the purpose of this paper to briefly summarize these findings and to suggest a general correlation between environment of formation and metal deposition in skarns.

TUNGSTEN-BEARING SKARNS

Tungsten skarns occur throughout the world; they occur in host rocks of Precambrian to Jurassic ages; and they are associated with calc-alkalic intrusives of mid-Devonian to late Cretaceous ages. Throughout this range in time and space, consistencies in the geology and mineralogy of tungsten skarns suggest that their origin can be accounted for by formation in a common environment of deposition. This common environment is the mesabyssal levels of the crust associated with batholithic complexes (Fig. 1). Stratigraphic



- KEY:**
- | | |
|--------------------------------|------------------------------|
| TUNGSTEN-BEARING SKARNS | COPPER-BEARING SKARNS |
| 1 Brown's Lake | 20 Bingham |
| 2 Lost Creek | 21 Battle Mountain |
| 3 Yellow Pine | 22 Yerington |
| 4 Osgood Mountains | 23 Ely |
| 5 Mill City | 24 Christmas |
| 6 Alpine | 25 Morenci |
| 7 Pilot | 26 Santa Rita |
| 8 Saddlebag Lake | 27 Silver Bell |
| 9 Hardpoint | 28 Pima-Mission |
| 10 Black Rock | 29 Twin Buttes |
| 11 Strawberry | 30 Cananea |
| 12 Pine Creek | ZINC-BEARING SKARNS |
| 13 Tungsten Hills | 31 South Mountain |
| 14 Garnet Dike | 32 Mount Hope |
| 15 Consolidated | 33 Paymaster |
| 16 Tulare County | 34 Linchburg |
| 17 Tungstore | 35 Empire-Groundhog |
| 18 Tem Plute | 36 Aravaipa |
| 19 Baviacora | 37 Dagon |
| | 38 Washington Camp |
| POLYMETALLIC SKARNS | |
| 39 Railroad district | 40 Monte Cristo |
| 41 Mineral King | 42 Darwin |
| 43 Johnson Camp | 44 Tecolote |
- MESOZOIC BATHOLITH COMPLEXES
 LIMIT OF BASIN-RANGE PROVINCE

FIGURE 1: Skarn Location Map

reconstructions and mineralogical data (e.g. sphalerite-pyrite-pyrrhotite geobarometer) indicate a depth of formation of 3 to 15 km below the surface (e.g. Soloman, 1965; Dick, 1976; Evernden and Kistler, 1970; Taylor, 1976). In addition, a considerable amount of geologic data (Table 1), including mig-matic contacts, coarse-grained unaltered intrusives, widespread thermal metamorphism, locally graphitic-pyritic wallrocks, and "reduced" mineral assemblages, suggests that tungsten skarns form in a relatively deep, high temperature, reducing environment.

The process of water exsolution from magma is very different in the tungsten skarn system from that of the porphyry copper related skarns. The typically coarse grained, hypidiomorphic-granular texture of the associated igneous rocks, the associated pegmatite dikes, and the lack of crackle or other breccias suggests that the plutons cooled slowly and did not pressure quench; an y release of aqueous fluid occurred gradually, rather than catas-trophically. The great depth of emplacement suggests that the plutons may not have vented. The general lack of hydrolytic alteration of the intrusives next to skarn suggests that the exsolved hydrothermal fluids were in thermal and chemical equilibrium with the igneous phases and that large-scale convective entry of lower temperature hydrothermal fluids did not occur. Fluid inclusion data of Tan and Kwak (1979), Kerrick (1977) and Milovski et al. (1978) indicates that these solutions were initially at temperatures of 500°C to 700°C.

Skarn formation is intrinsically an evolving process: fluids change from predominantly magmatic to predominantly meteoric, the system cools, and the solubilities/stabilities of minerals change. This evolution causes the appear-ance of different mineral assemblages and compositions superimposed in a complex temporal and spatial pattern. The overall process can be approximated by discreet stages: 1) prograde metamorphism, 2) high temperature garnet-pyroxene-scheelite (CaWO_4) metasomatism, 3) lower temperature amphibole-biotite-sulfide metasomatism and 4) chlorite-calcite-epidote-quartz retrograde metamorphism and metasomatism. Differences between individual tungsten skarns are largely functions of differences in composition of host and wallrocks and intensities of these stages.

Most tungsten skarn provinces are characterized by an abundance of so-called "barren tactites" which generally are thought of as fringes produced by metasomatic systems exhausted in tungsten but are in fact not caused by

TABLE 1:
Conditions of tungsten skarn formation as deduced from geologic evidence

	<u>Geologic characteristic</u>	<u>Typical occurrence in tungsten skarns</u>	<u>Significance/explanation</u>
intrusive rocks	<ul style="list-style-type: none"> grain size texture brecciation syngenetic dikes alteration of intrusive 	<ul style="list-style-type: none"> medium to coarse grained hypidiomorphic-granular virtually absent pegmatites; no porphyries potassic alt'n minor to absent 	<ul style="list-style-type: none"> slow cooling of magma at depth without explosive release of water hydrothermal fluids at high temperatures; in equilibrium with igneous minerals
wall rocks	<ul style="list-style-type: none"> intrusive contacts dike relationships vein skarns skarn localization skarn thickness metamorphic aureole bi-metasomatic zones 	<ul style="list-style-type: none"> sharp to migmatic dikes rarely penetrate carbonates rare to absent along hornfels and intrusive contacts .5 to 6 m large: wall rocks within several km of intrusive frequently converted to hornfels 1-5 cm wide; comparable to zones developed during granulite regional metamorphism 	<ul style="list-style-type: none"> high temperatures cause partial melting massive carbonates too plastic at high P,T to permit access by dikes and metasomatic solutions inhibiting effect of CO₂-buildup in rocks of low permeability; effect of large P_T on calc-silicate reactions wallrock at high temperatures before/ during skarn formation small amounts of hydrothermal fluid: water more soluble in melt at high P; water is taken up by intrusive mafics
skarn rocks	<ul style="list-style-type: none"> size fluid inclusions compositions of calc-silicates retrograde mineralogy sulfides oxides 	<ul style="list-style-type: none"> small: .01 -10 million tons of skarn main stage: 700°- 500°C garnets: often rich in Al, Fe²⁺, poor in Fe³⁺; pyroxenes: rich in Fe²⁺ biotite, hornblende (high Al, Fe²⁺) po+py, bn + py absent; no high-S sulfides magnetite common, hematite absent 	<ul style="list-style-type: none"> relatively reducing environment (deep) relatively low sulfur environment relatively low oxygen environment

igneous-derived metasomatism. Rather, these "barren" calc-silicates are largely caused by initial metamorphism and local metasomatism of impure marbles and interbedded carbonates/non-carbonates. Because fluid flow and escape of CO_2 is limited by the high pressures, large thicknesses of massive "skarnoid" beds are not characteristic; rather, abundant thin reaction skarns are typical.

The main stage of skarn formation begins by overprinting the metamorphic calc-silicates, both by depositing new minerals and by depositing overgrowths on metamorphic ones. Scheelite is typically precipitated as fine-grained sub-hedral crystals during this stage. With time the system evolves to higher iron and manganese activities and sub-calcic garnets (i.e. significant almandine-spessartine components present; Fig. 3) replace earlier grandite garnets. Under highly reducing conditions, essentially pure almandine-spessartine-grossularite may be deposited (Newberry, 1980). The iron-manganese enrichment is a gradual process, with low-iron calc-silicates and scheelite precipitated at the marble front and low-calcium calc-silicates rimming and replacing high-calcium calc-silicates near the intrusive contact. Pyroxenes behave similarly, with early iron-poor pyroxenes replaced and rimmed by iron- and manganese-rich pyroxenes (Newberry, 1980). This general pattern may be interrupted by structural zones of high-iron alteration producing a non-systematic variation in calc-silicate compositions as a function of distance from intrusive contacts. Because calcium activity is lowered by the iron enrichment, high scheelite concentrations tend to be found closer to the marble front and generally low scheelite concentrations are found near intrusive contacts. This phenomena has caused some (Burchard, 1972) to suggest that the intrusives are unrelated to tungsten deposition.

A break in the skarn-forming process occurs with the deposition of sulfides (mostly pyrrhotite, pyrite, and chalcopyrite) accompanied by alteration of pyroxene to amphibole (hornblende to actinolite in composition; Fig. 5) and locally biotite. The destruction of calc-silicates releases large amounts of calcium and characteristically this alteration style is associated with redeposition of scheelite in coarse euhedral bunches.

Final cooling and influx of meteoric waters (as suggested by isotopic data of Taylor, 1976) causes retrograde alteration of grandite garnet to amphibole and/or epidote \pm calcite-quartz; pyroxene to amphibole \pm calcite-quartz-sulfide,

amphibole and biotite to chlorite, and locally total destruction of skarn to zeolite + orbicular calcite + quartz. Scheelite is commonly redistributed or lost during this episode. Retrograde alteration is frequently minor in extent in the deeper skarns and may not appear at all.

Variations in environment of formation can be expressed as a function of a) depth of formation and b) reducing capacity of the wallrocks. At shallower depths, skarns become larger due to 1) increasing amounts of water exsolved by intrusives as pressure decreases, 2) increasing amounts of meteoric water in the system, and 3) increasing fracture porosity in marbles and hornfelses. Shallower tungsten skarns are characterized by increasing size, amount of base metals present, and oxidation state of the calc-silicates. Because tungsten skarns form predominantly in interbedded marble/pelite units (due to the greater effective permeability of such units relative to massive marble at high pressures) the reducing capacity of such rocks varies with the graphite contents of the pelites. Skarns formed in increasingly graphitic/pyritic wallrocks are characterized by more-reduced calc-silicates and frequently abundant pyrrhotite + base metal sulfides. Figure 2 is a classification scheme for tungsten skarns expressed in terms of the depth of emplacement and reducing capacity of the wallrocks. In other words, tungsten skarns possess common features suggesting deep, high temperature skarn formation; perturbations are caused by variations in composition of host and wallrocks and some variations in depth of formation.

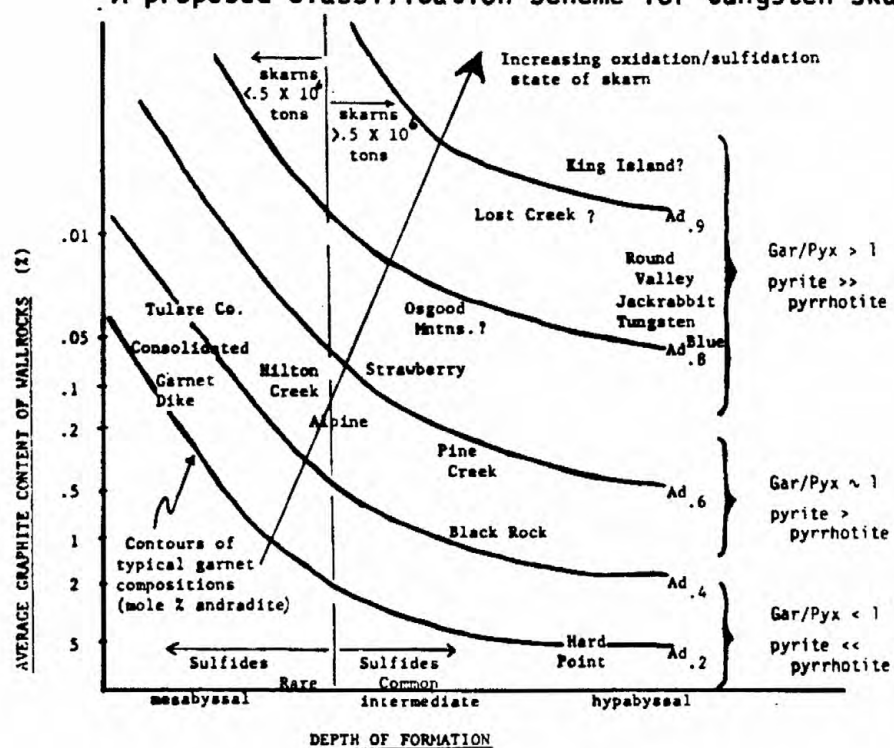
COPPER-BEARING SKARNS

Copper-bearing skarns typically are associated with porphyry-copper deposits which display potassium-silicate alteration. More than a dozen such deposits are known in the western United States, ranging in age from 150 m.y. (Yerington, Nevada) to 38 m.y. (Bingham, Utah), with the majority of Laramide age (70-50 m.y.). A recent review article (Einaudi, in press) describes some of these deposits, sets out their common features, and proposes a general genetic model. The salient features are summarized here.

The copper-bearing skarns considered here are related to highly fractured, sub-volcanic granodiorite to quartz monzonite porphyry stock complexes and associated breccia pipes. The stocks display varying degrees of potassium-

FIGURE 2:

A proposed classification scheme for tungsten skarns



silicate and sericitic alteration associated with disseminated and veinlet copper-iron sulfide mineralization. Vertical extent of mineralized rocks is on the order of 1 to 2 km and depths below the original surface range from 1 to 2 km for shallowest sericitic ore zones to 3 to 5 km for deepest postassium silicate ore zones. These depths are equivalent to lithostatic pressures of 0.2 to 1 kbar or hydrostatic pressures of 0.17 to 0.3 kbar.

The high level of emplacement of porphyry-copper plutons is reflected in their small size, highly fractured states, and fine-grained porphyritic textures. Alteration-mineralization style also reflects their near-surface conditions: relatively high oxidation-sulfidation states characterize even the early high temperature potassic assemblages, with high Mg^{2+}/Fe^{2+} phlogopite, pyrite rather than magnetite, and anhydrite rather than calcite. Copper-bearing skarns reflect this environment, with ferric-rich garnet and ferrous-poor clinopyroxene (Figures 3 and 4). Because fluid flow and escape of CO_2 is enhanced by high fracture permeabilities at low pressure, large thicknesses of skarn are characteristic. Low pressures and low XCO_2 also allow skarn formation to proceed at lower temperatures than in deeper environments. Fluid inclusion studies and mineral equilibria suggest that skarn formation in porphyry environments occurs at 500 to 400°C; these temperatures may be too low for large-scale scheelite deposition (scheelite may be locally present at immediate pluton contacts) and too high for sphalerite deposition. Copper is deposited as chalcopyrite during the late stage of skarn formation, presumably due to decrease in temperature and increase in pH as the fluid reacts with increasingly carbonate-rich rocks near the skarn-marble interface.

The time-evolutionary trend of alteration-mineralization in the porphyry stocks from early pot assium silicate to late sericite and the parallel changes in alteration in carbonate wallrocks have been documented by several workers; the correlations are summarized in Table 2. Potassium silicate alteration typically occurs during initial cooling of the pluton from 600°C to 400°C, as deduced from field evidence (Gustafton and Hunt, 1975), fluid inclusion data (Roedder, 1971; Moore and Nash, 1974) and elemental and isotope partitioning between mineral phases (Sheppard and Taylor, 1974; Brimhall, 1977). Oxygen and hydrogen isotope studies suggest the fluid was magmatic, although its ultimate origin is not clear (Taylor, 1974). During the potassium silicate

TABLE 2

Correlation of events in intrusive and sedimentary rocks at Bingham, Utah
(Einaudi, in press)

Intrusive Rocks	Sedimentary Rocks
1. <u>Intrusion and crystallization of monzonite stock.</u> Partial alteration of augite to actinolite releases Mg & Si to fluid?	Heating and contact metamorphism (possibly some woll in cherty marble). Fluids from monzonite affect first Mg-Si metasomatism: diopside forms in quartzite and calc-siltstone.
2. <u>Intrusion of quartz monzonite porphyry melt and partial crystallization:</u> alteration of more augite to act releases additional Mg & Si? Beginning of biotitic alt'n of act and augite consumes Mg, releases Fe.	Increased Mg-Si metasomatism forms diopsidic hfls and quartzite up to 2 km from stock; woll (diop) in marble. Transition to Fe-Si metasomatism.
3. <u>Potassic alteration and ore deposition attends final crystallization,</u> hydrofracturing, release of magmatic hydrothermal fluid from qmp stock and underlying crystallizing magma: intense bio-kspars alt'n, Qtz veining, and deposition of cp-bn, & moly. 616-303, ave 450°C.	Skarn formation and ore deposition, intense fracturing of hfls and Qtzite. Fe-Si metasomatism: act-cp-Qtz vnits in diop hfls and Qtzite; andradite-cp-py replaces woll and marble; magnetite replaces andradite near stock. Interstitial sulfides.
4. <u>Intrusion and crystallization of latite and Qtz-latite porphyry dikes and plugs;</u> less intense potassic alteration and sulfide deposition. 480°C.	Beginning of skarn destruction (?): gar + mag, py, cal, Qtz, (act); diop + act, cal, Qtz; early cp remobilized into veins.
5. <u>Influx of meteoric water:</u> Late quartz-sericite alteration forms along pyrite (cp) veinlets in NW portion of qmp stock; Pb-Zn-Ag fissures with sericite envelopes in peripheral monzonite.	Late alteration of skarn to py, chlor, mont, talc, ser, and of diop-woll rock to talc + saponite along Pb-Zn-Ag fissures. 330-294°C.

Temperatures based on fluid inclusion homogenization (Roedder, 1971; Moore and Nash, 1974; Wilson, 1978).

Table 3
Main Stage Mineral Zoning in Deep Skarn at
Carr Fork, Bingham, Utah

	Distance from Bingham stock, meters						
	0-50	50-100	100-300	300-350	350-400	400-600	> 600
Gangue	Ad-Cc-Qtz-Di	Ad	Ad(Di)	Ad-Di	Wo (Ad,Di)	Wo-Di-Qtz, Wo-Cc, marble	marble, limestone
Garnet Color	red	red	red, yellow in patches	yellow, red in veins	yellow, yellow-green	---	---
Gap Gar+Di	0.7	1.0	0.9-0.8	0.6	highly variable	0	---
vol % magnetite	1-2	2-5	5-10	2	0	0	0
vol % sulfides	1-2	2-5	15	5	1	0.5	tr
Sulfide Assoc.	cp, (cp-bn)	cp-py	cp-py	cp-py	bn, cp, sl.(py)	bn, cp, sl, gl	sl, gl, py
py/cp	0	0.2	0.5-1.0	5	0	0	---

Data from Atkinson and Einaudi (1978).

stage, the fluid deposits a significant amount of copper in sulfide assemblages displaying relatively low S/Cu + Fe ratios. Oxidation states are relatively high and sulfidation states are moderate.

The overall path with time and toward the peripheries of porphyry copper plutons is toward lower temperature and pressure, higher oxidation-sulfidation states, and probably lower alkali/hydrogen ion ratios. This trend is expressed by the appearance of sericitic alteration accompanied by high-sulfur sulfide assemblages. Temperatures close to 300°C for sericitic alteration are suggested by fluid inclusion data (Roedder, 1971; Nash and Cunningham, 1973) and a high meteoric water component is implied by oxygen and hydrogen isotope data (Sheppard and Taylor, 1974). Although decreasing temperature and increasing dilution of the ore fluid tends to decrease sulfide solubilities, the competing shift toward increasing fO_2 and decreasing pH and total reduced sulfur locally dominates during this stage. Early chalcopyrite, deposited during potassic alteration, is leached and redeposited in structural openings or in chemical traps (potassic-sericitic interface; marble; reducing environments such as carbonaceous beds or hedenbergitic hornfels).

Given a pluton displaying potassium silicate alteration, the mineral associations in carbonate rocks can be predicted solely on the basis of original sedimentary lithology. Limestone develops andraditic garnet and diopsidic clinopyroxene with pyrite, chalcopyrite, and magnetite; outer zones may or may not contain wollastonite, but consistently are depleted in pyrite and enriched in bornite (without pyrite), sphalerite, pyrrhotite and tennantite relative to the garnet zones. Dolomite develops forsterite-serpentine-magnetite-chalcopyrite skarn. Pyroxene hornfels are altered to actinolite and biotite along pyrite-chalcopyrite-magnetite veinlets. The conclusion is that the physiochemical characteristics of hydrothermal fluids associated with potassium silicate alteration in porphyry copper plutons are remarkably similar in known deposits. Table 3 describes a typical zonation pattern as illustrated at Carr Fork, Utah.

Variability between porphyry-related skarn deposits largely involves the degree of retrograde alteration, a variability which is expressed in porphyry copper deposits in general by the degree of sericitic alteration (e.g., the "variation on a theme" of Gustafson and Hunt, 1975). Early stages of retrograde alteration of anhydrous skarn silicates probably are correlatable with the waning of potassic alteration and beginning of sericitic; the dominant

alteration products are quartz-magnetite+pyrite+calcite after andradite and actinolite after salite. Sulfides are dominantly chalcopyrite with lesser pyrite. Later stages of retrograde alteration, correlated with main sericitic alteration in the pluton, involve increasing amounts of montmorillonoids, chlorite, siderite, calcite, and hematite, accompanied by increasing pyrite and lesser chalcopyrite, tennantite, and sphalerite. The retrograde event overprints the early skarn along zones of high permeability which tend to occur along contacts with the pluton.

ZINC-BEARING SKARNS

Zinc-bearing skarns have been described in many countries, including Japan (Shimazaki, 1975), U.S.S.R. (Zharikov, 1970), Korea (Yun, 1979), Norway (Goldschmidt, 1911), Italy (Schaller, 1938), Peru (Burt, 1972), Mexico (Allen and Fahey, 1957), Canada (Dawson and Dick, 1978), and in the United States (Allen and Fahey, 1957; Burt, 1972; Meinert, 1980). The environment of formation of zinc-bearing skarns is not as well understood as that of other skarn types but the general features are summarized in Table 4. Some zinc-bearing skarns are associated with intermediate size granodiorite stocks, whereas others seem to be related to structural pathways, such as major faults, where the existence of a causative pluton can only be inferred. Many zinc-bearing skarns occur in districts which contain major ore deposits mined for metals other than zinc (Central mining district, Hernon and Jones, 1968; Crescent Lake, Dawson and Dick, 1978; Railroad district, Gillerman, in preparation). Although in many ways zinc-bearing skarns appear to be intermediate between or associated with other skarn types, they are invariably characterized by a distinctive manganese- and iron-rich calc-silicate mineralogy (see general reviews by Zharikov, 1970; Burt, 1972; 1978) which suggests that the metasomatic fluid which forms zinc-bearing skarns differs from that which forms other skarn types. This difference could be due to a number of factors, such as original compositional differences at the source or changes in fluid composition related to cooling and travel paths away from the source.

The absence of a well defined metamorphic aureole surrounding most zinc-bearing skarns implies that the environment of skarn formation was far removed from an intrusive heat source. This implication is supported by the common

TABLE 4

GENERAL FEATURES OF ZINC-BEARING SKARNS

<u>INTRUSIVES</u>	generally not exposed or located distal to skarn bodies, typically of intermediate size and composition, equigranular to porphyritic, with locally abundant dikes and sills
<u>STRUCTURAL SETTING</u>	rarely located along main intrusive contact, usually formed along lithologic, fault, or dike contacts
<u>METAMORPHIC AUREOLE</u>	absent to small and low grade, chert nodules typically unreacted near skarn
<u>SKARN SIZE/SHAPE</u>	skarns tend to be small (< 5 million tons) and elongate along structural pathways, length:width typically > 10:1
<u>SILICATE MINERALOGY</u>	iron and manganese-rich pyroxene is the dominant calc-silicate mineral, andraditic garnet occurs closer to source whereas rhodonite, bustamite occur at marble front
<u>SULFIDE MINERALOGY</u>	dominantly sphalerite associated with pyroxene, also minor galena, chalcopyrite, pyrite, and pyrrhotite
<u>RETROGRADE ALTERATION</u>	minor sub-calcic actinolite, ilvaite, and chlorite but most prograde minerals are fresh, abundant epidote endoskarn in nearby intrusive rocks

occurrence of zinc-bearing skarns along structural pathways (Knopf, 1942). Zinc-bearing skarns occur as veins along faults or lithologic contacts near intrusives at Tepezala (Wardke and Moore, 1935), San Antonio (Hewitt, 1943), South Mountain (Sorenson, 1927), and at several mines in the Central mining district (Hernon and Jones, 1968; Jones et al., 1967). At Aravaipa (Simons and Jones, 1963), Paymaster Canyon (Gulbrandsen and Geilow, 1960), and the Groundhog mine (Hernon and Jones, 1968), zinc-bearing skarn occurs at distances up to several miles from the probable source intrusive. The most extreme cases occur at Hidalgo (Schmitt, 1928), Naica (Stone, 1959), and Linchburg (Titley, 1961), where, despite extensive underground mining, no intrusive has been found.

The large distance between igneous source and the site of deposition could have several important effects: 1) components of the metasomatic fluid which are relatively insoluble may be precipitated prior to skarn formation as the fluid cools along a travel path which does not cross carbonate rocks, thus concentrating elements such as manganese and iron which have relatively high solubilities (Helgeson, 1969); 2) the large ratio of carbonate wallrock to skarn in a zinc-bearing skarn relative to a skarn formed at an intrusive contact might result in higher values of X_{CO_2} at a given stage of alteration; and 3) carbonate wallrocks would be largely² insulated from the igneous heat source, resulting in relatively low temperatures of skarn formation. This implies that the relatively high regional temperatures encountered in a very deep environment of formation would not be conducive to zinc-bearing skarn formation unless components such as Mg, Al, W, and Cu could be removed by a proximal carbonate horizon. Also, because temperatures have to be high enough to stabilize skarn minerals, a very shallow environment of emplacement would also not be conducive to zinc-bearing skarn formation. Thus, an environment at intermediate pressure and temperature would be best suited for zinc-bearing skarn formation.

Zinc-bearing skarns differ from most other skarn types in that pyroxene is usually the dominant prograde calc-silicate mineral; in copper-bearing skarns garnet is typically predominant (Soji, 1978). Furthermore, the dominant ore sulfides in zinc-bearing skarns are associated with pyroxene whereas in copper-bearing skarns they are associated with garnet (Burt, 1972). The calc-silicate minerals in zinc-bearing skarns are also unusual in that they contain significant amounts of both ferrous and ferric iron (Zharikov, 1970; Burt, 1972, Meinert, 1980); pyroxenes tend to be manganoan-hedenbergite

(ferrous), garnets tend to be andradite (ferric), and other phases such as ilvaite, contain both ferrous and ferric iron (Fig. 3, 4, 5). Rare manganese-rich minerals such as rhodonite, bustamite, and manganobabingtonite have also been reported (Burt, 1972; Burt and London, 1978). Retrograde alteration, although not as extensive as that in porphyry-copper-related skarns, is characterized by rhodonite, ilvaite, amphibole, chlorite, and zinc or manganese-rich clay (Allen and Fahey, 1957; Burt, 1972). Although the amphibole phase in zinc-bearing skarns is usually described as actinolite (Spurr et al., 1912; Spur, 1932; Laughlin and Korschmann, 1942; Hewitt, 1943), chemical analyses by Allen and Fahey (1957) of amphibole from the San Antonio, Kearny, and Pearson mines, and optical determinations by Titley (1961) on amphiboles from the Linchburg mine, indicate that some of the amphiboles are part of the sub-calcic anthophyllite-cummingtonite series rather than actinolite.

In contrast to silicate mineralogy, the sulfide mineralogy of zinc-bearing skarns is fairly simple. In almost all cases, sphalerite is the dominant sulfide with lesser galena. Chalcopyrite is present in some zinc-bearing skarns in minor amounts. As pointed out by Titley (1961) and Gulbrandsen and Gielow (1960), iron sulfides are usually not abundant in zinc-bearing skarns. Magnetite is the dominant iron oxide in zinc-bearing skarns such as Central mining district (Hernon and Jones, 1968), Paymaster Canyon (Gulbrandsen and Gielow, 1960), and South Mountain (Sorenson, 1927) although Titley (1961) reports large amounts of hematite, possibly of late hydrothermal or supergene origin, at Linchburg.

MINERAL COMPOSITIONS

Figures 3, 4, and 5 are presented as a summary of relationships between ore and calc-silicate mineralogy. Figure 3 illustrates metasomatic garnet, Figure 4 illustrates metasomatic pyroxene, and Figure 5 illustrates metasomatic amphibole compositions for tungsten-, copper-, and zinc-bearing skarns. The systematic differences in calc-silicate compositions, in part first noted by Zharikov (1970), are reflections of significant differences in environments of formation. Calc-silicate minerals from tungsten skarns are relatively rich in ferrous iron and poor in ferric iron, implying a relatively reduced environment. Calc-silicate minerals from copper skarn are typically rich in ferric iron and poor in ferrous iron, suggesting a relatively oxidized

FIGURE 3

Compositions of metasomatic garnets from W, Cu, and Zn skarns

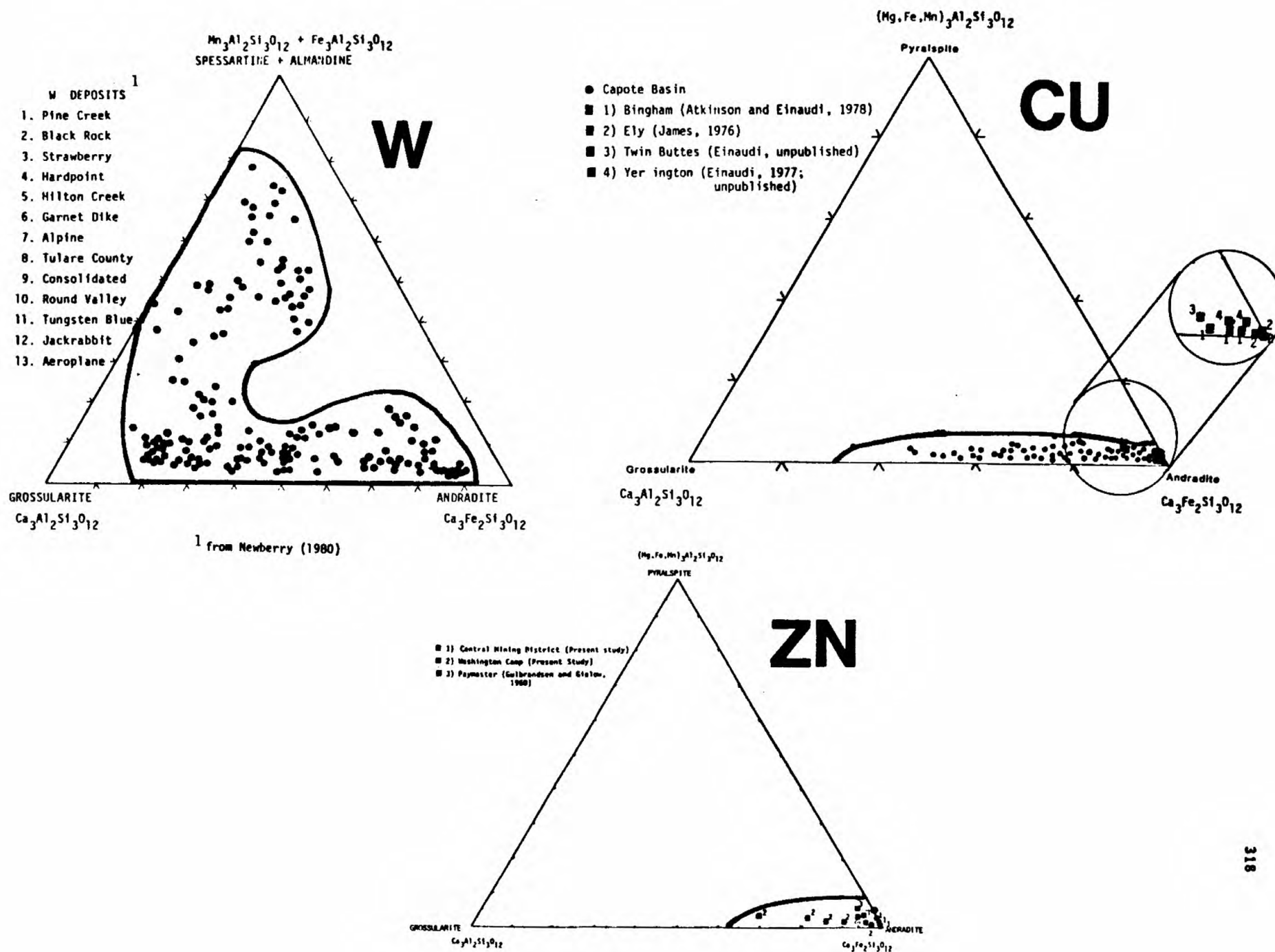


FIGURE 4

Compositions of metasomatic pyroxenes from W, Cu, and Zn skarns

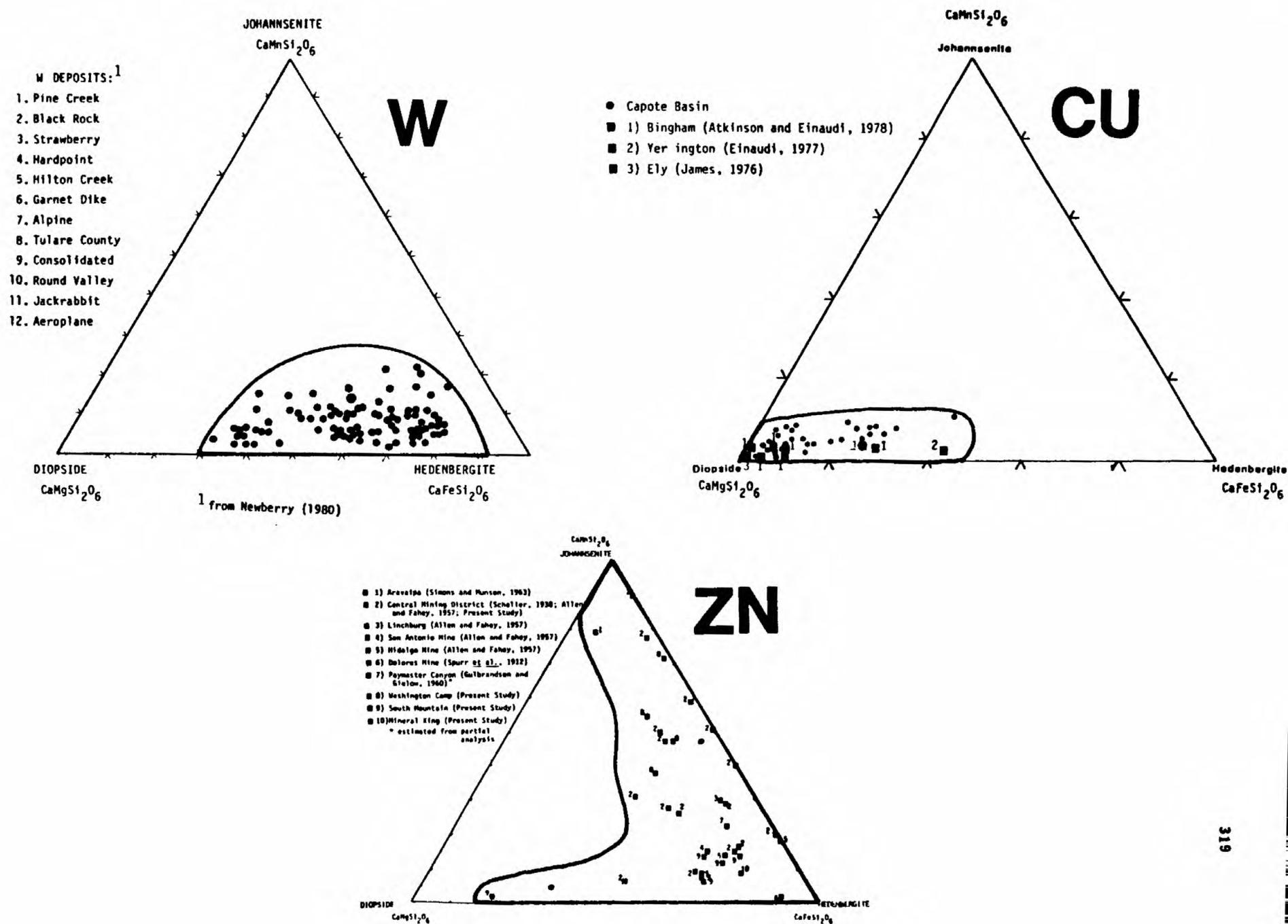
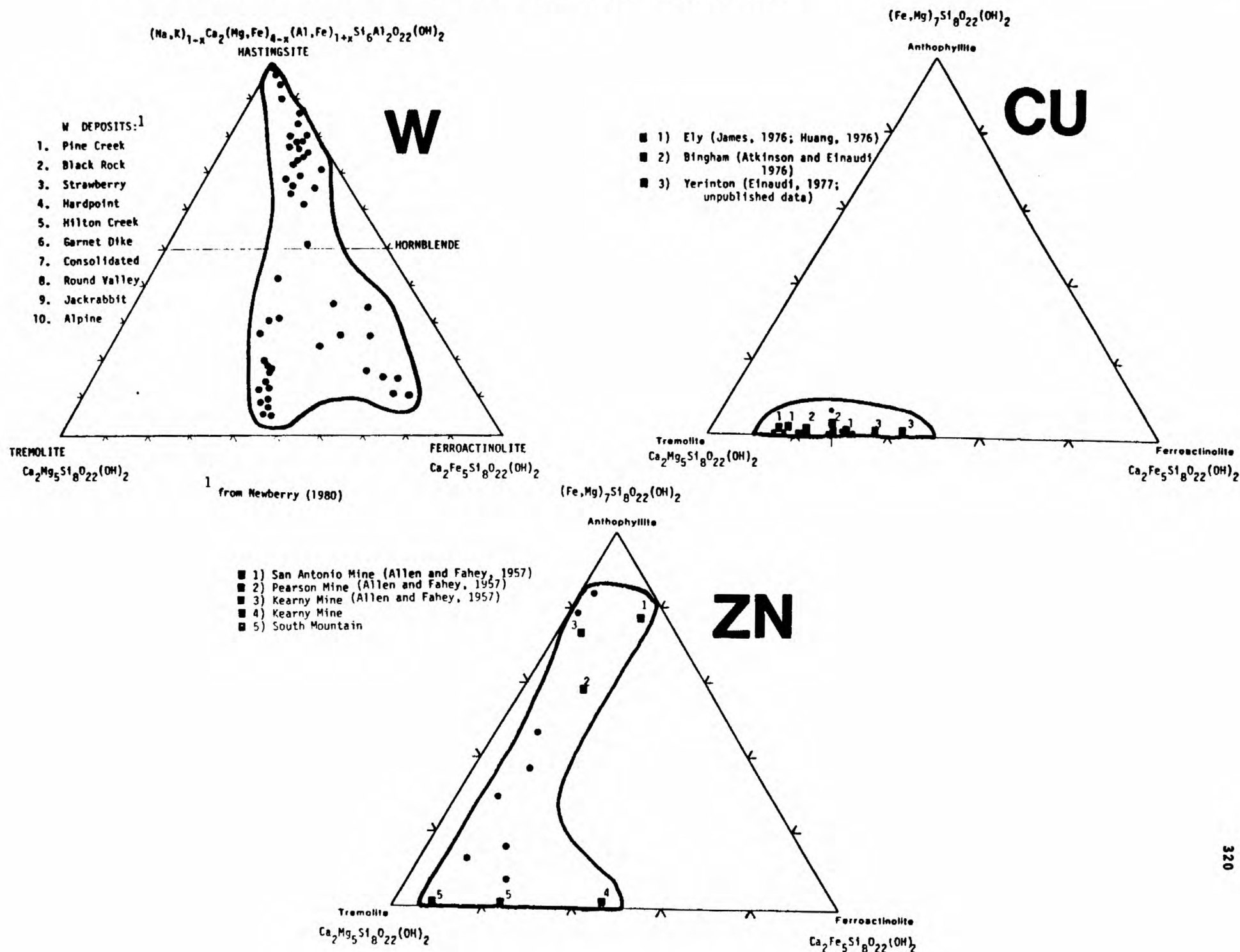


FIGURE 5

Compositions of metasomatic amphiboles from W, Cu, and Zn skarns



environment. Calc-silicate minerals from zinc skarns are both iron and manganese-rich, with typically ferric-rich garnets and ferrous-manganese-rich pyroxenes suggesting an intermediate oxidizing environment. Most striking are differences in amphibole composition: tungsten skarns contain aluminous (high temperature?) ferroactinolites, copper skarns contain tremolitic actinolite, and zinc skarns contain sub-calcic manganiferous actinolites.

SUMMARY

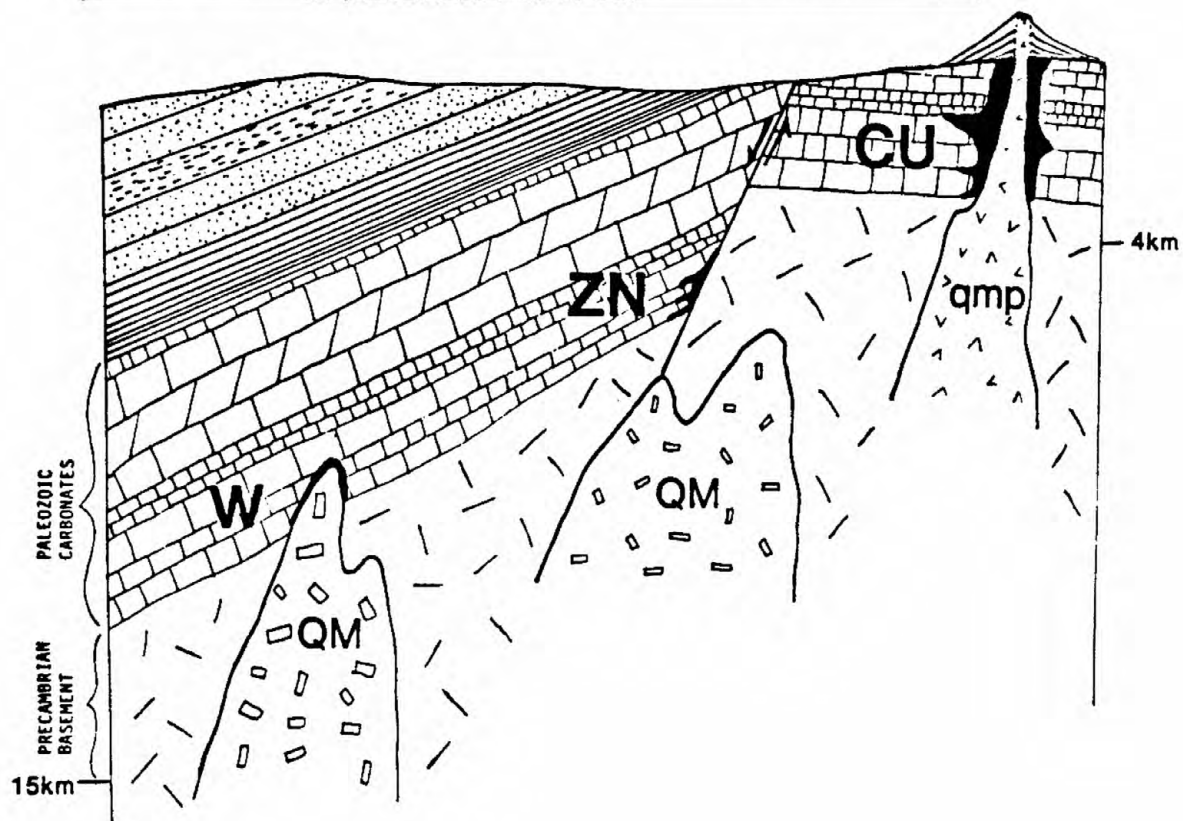
Although skarns occur in a variety of geographic and geologic locations there are regularities of size, mineralogy, structure, and alteration stages which indicate that three general "end member" models are adequate to predict and explain the salient features of most calcic skarns in western North America. The three main skarn types, tungsten, copper, and zinc skarns, form in different geologic environments which are illustrated schematically in Figure 6.

Tungsten skarns are typified by generally deep, reduced settings as deduced from the presence of migmatitic contacts, coarse-grained intrusives, widespread thermal metamorphism, locally graphitic-pyritic wall rocks, and low $\text{Fe}^{3+}/\text{Fe}^{2+}$ ratios. Skarns are usually small (<10 m.t.) and contain relatively minor retrograde alteration. Metasomatic garnets are intermediate grandites with up to 50 mole % almandine+spessartine. Associated pyroxenes contain 30-80 mole % hedenbergite with up to 20 mole % johannsenite. Garnet and pyroxene are both altered to hornblende, often associated with sulfides.

Copper skarns are typified by generally shallow, oxidized settings, as evidenced by the porphyritic texture of intrusives, cogenetic extrusives, limited thermal aureoles, and high $\text{Fe}^{3+}/\text{Fe}^{2+}$ ratios. Skarns are large (up to 300 m.t.) and exhibit extensive retrograde alteration. Metasomatic garnets are andraditic whereas associated pyroxenes are salite with less than 10 mole % johannsenite. Retrograde alteration of garnet consists of quartz-calcite- FeO_x , whereas pyroxene is altered to quartz-actinolite+sulfides. Significant amounts of chlorite-clay-quartz-calcite occur during late alteration.

Zinc skarns appear to occur in transitional environments associated with stocks of intermediate size and composition, or related to structural pathways where causative plutons are not exposed. Skarns are usually small (<5 m.t.) with limited thermal aureoles or retrograde alteration. Metasomatic garnets

FIGURE 6
IDEALIZED SKARN-FORMING ENVIRONMENTS



are andraditic whereas associated pyroxenes are largely johansenite-hedenbergite with less than 40 mole % diopside. Iron (both ferrous and ferric) and manganese also are typically high in retrograde minerals including amphiboles and pyroxenoids.

These general models for tungsten, copper, and zinc skarns show that differences in both ore mineralogy and calc-silicate mineralogy reflect differences in the environment of formation. The variables thought to be important include the depth and temperature of emplacement of causative plutons, the reducing capacity of wall rocks, and the spatial relations between ore fluid source and carbonate host rocks. Depth is a key variable not only in terms of its effect on temperature, total pressure, and X_{CO_2} , but also in terms of the extent of interaction with the oxidized, near-surface environment. Geochemical analysis (Newberry et al., in preparation) of metal solubilities including calculations of tungsten solubility (Newberry, 1980) suggest that these differences in geologic environment (P, T, X_{CO_2} , etc.) are in large part responsible for differences in ore mineralogy² of calcic skarns, rather than initial differences in metal content of hydrothermal fluids. Current work focuses on establishing the chemical relationships between geologic environment and metal deposition and on understanding the genesis of certain poly metallic skarns in the western United States.

- Allen, V.T., and Fahey, J.J., 1957, Some pyroxenes associated with pyrometasomatic zinc deposits in Mexico and New Mexico: *Bull. Geol. Soc. Amer.*, 68, p. 881-896.
- Atkinson, W.W., Jr., and Einaudi, M.T., 1978, Skarn Formation and Mineralization in the Contact Aureole at Carr Fork, Bingham, Utah, *Econ. Geol.*, v. 73, 1326-1365.
- Brimhall, G.A., 1977, Early fracture-controlled disseminated mineralization at Butte, Montana: *Econ. Geol.*, v. 72, p. 37-59.
- Burchard, U., 1972, Geologische untersuchungen zur genese der scheelit-lagerstatte King Island, Tasmania: unpub. Ph.D. Dissertation, Univ. of Munich, FDR.
- Burt, D.M., 1972, Mineralogy and geochemistry of Ca-Fe-Si skarn deposits: Unpub. Ph.D. Dissertation, Harvard Univ., 256 pp.
- Burt, D.M., 1978, Mineralogy and petrology of skarn deposits: *Rendiconti Soc. Ital. Mineral. Petrol.*, v. 33, p. 859-873.
- Burt, D.M., and London, D., 1978, Manganobabingtonite and ilvaite from Hd-Jo skarns, Aravaipa, Arizona: *Geol. Soc. Amer.*, abstr w/progr. v. 10, no. 3, p. 98.
- Dawson, K.M. and Dick, L.A., 1978, Regional metallogeny of the northern cordillera: tungsten and base metal-bearing skarns in southeastern Yukon and southwestern Mackenzie, *Curr. Res., Pt. A, Geol. Surv. Can.*, paper 78, 1A, p. 287-292.
- Dick, L.A., 1976, Metamorphism and metasomatism at the MacMillan Pass Tungsten Deposit, Yukon and District of MacKenzie, Canada: Unpubl. M.S. Thesis, Queens Univ., Kingston, Canada, 226 pp.
- Einaudi, M.T., 1977, Petrogenesis of the copper-bearing skarn at the Mason Valley Mine, Yerington district, Nevada: *Econ. Geol.*, v. 72, p. 769-795.
- Einaudi, M.T., (in press), Contact alteration and mineralization of sedimentary rocks in porphyry copper deposits, in Titley, S.R., ed., *Geology of the porphyry copper deposits, SW North America*, v. 2: Univ. Ariz. Press, 200 pg. mscpt.
- Evernden, J.F., and Kistler, R.W., 1970, Chronology and emplacement of Mesozoic batholithic complexes in California and Western Nevada, U.S. *Geol. Survey Prof. Paper* 623, 42 pp.
- Fonteilles, M., Guy, B., and Soler, P., 1978, The influence of wall rock on skarn mineralization at the Salu and Costabonne tungsten deposits (Pyrenees, France): *Geol. Soc. Amer.*, abstr. w/progr., v. 10, p. 105.
- Goldschmidt, V.W., 1911, Die Kontaktmetamorphose im Kristianlagebiet: *Videnskap. Skrifter I Mat. Nat. Classe*, No. 1, p. 483.

- Gulbrandsen, R.A., and Gielow, D.G., 1960, Mineral assemblage of a pyrometasomatic deposit near Tonapah, Nevada: U.S. Geol. Survey Prof. Paper 400B, p. B20-21.
- Gustafson, L.B., and Hunt, J.P., 1975, The porphyry copper deposit at El Salvador, Chile: Econ. Geol., v. 70, p. 857-912.
- Helgeson, H.C., 1969, Thermodynamics of hydrothermal systems at elevated temperatures and pressures: Am. Jour. Sci., v. 267, p. 729-804.
- Hernon, R.M. and Jones, W.R., 1968, Ore deposits of the CMD, Grant County, New Mexico: In Ridge, J.D., ed., Ore deposits of the U.S. 1933-1967, v. 2, AIME, New York, p. 1211-1237.
- Hewitt, W.P., 1943, Geology and mineralization of the San Antonio mine, Santa Eulalia District Chihuahua, Mexico: Geol. Soc. Amer., Bull., v. 54, p. 173-204.
- Jones, W.R., Hernon, R.M., Moore, S.L., 1967, General geology of Santa Rita quadrangle, Grant County, New Mexico: U.S. Geol. Survey Prof. Paper 555, 144 pp.
- Kerrick, D.M., 1977, The genesis of zoned skarns in the Sierra Nevada, California: J. Petrol. v. 18, p. 144-181.
- Knopf, A., 1942, Ore deposition in the pyrometasomatic deposits, In Newhouse, W.H., ed., Ore deposits as related to structural features: p. 63-72.
- Krauskopf, K.B., 1971, The source of ore metals: Geochim. et Cosmochim. Acta, v. 35, p. 643-659.
- Laughlin, J.L., and Koschmann, A.H. 1942, Geology and ore deposits of the Magdalena mining district, New Mexico: U.S. Geol. Survey Prof. Paper 200, 168 pp.
- Meinert, L.D., 1980, Skarn, manto, and breccia pipe formation in sedimentary rocks of the Cananea district, Sonora, Mexico: Unpubl. Ph.D. Dissertation, Stanford University, 232 pp.
- Milovskiy, G.A., Zlenko, B.F., and Gubanov, A.M., 1978, Conditions of formation of scheelite ores in the Chorukh Dayron Mineralized Area (as revealed by a study of gas-liquid inclusions): Geochem. Int'l., v. 12, pp. 45-52.
- Moore, W.J., and Nash, J.T., 1974, Alteration and fluid inclusion studies of the porphyry copper ore body at Bingham, Utah: Econ. Geol., v. 69, p. 631-645.
- Nash, J.T., and Cunningham, C.G., 1973, Fluid-inclusion studies of the fluor-spar and gold deposits, Jamestown District, Colorado: Econ. Geol., v. 68, p. 1247-1262.
- Newberry, R.J.J., 1980, The Geology and chemistry of skarn formation and tungsten deposition in the central Sierra Nevada, California: Unpubl. Ph.D. Dissertation, Stanford University, 325 pp.

- Noble, J.A., 1970, Metal provinces of the western United States: *Geol. Soc. Amer. Bull.*, v. 81, p. 1607-1624.
- Roedder, Edwin, 1971, Fluid inclusion studies on the porphyry-type ore deposits of Bingham, Utah, Butte, Montana, and Climax, Colorado: *Econ. Geol.*, v. 66, p. 98-120.
- Schaller, W.T., 1938, Johannsenite, a new manganese pyroxene, *Am. Mineral.*, 23, p. 575-582.
- Schmitt, H., 1928, Geologic notes on the Santa Barbara area of the Parral district of Chihuahua, Mexico: *Eng. and Min. Jour.*, v. 126, p. 407-410.
- Sheppard, S.H.F. and Taylor, H.P., 1974, Hydrogen and Oxygen isotope evidence for the origins of water in the Boulder batholith and the Butte ore deposits, Montana: *Econ. Geol.*, v. 69, p. 926-946.
- Shimazaki, H., 1975, The ratios of Cu/Zn-Pb of pyrometasomatic deposits in Japan and their genetical implications: *Econ. Geol.*, v. 70, p. 717-724.
- Sillitoe, R.H., 1976, Andean mineralization: a model for the metallogeny of convergent plate margins, in Strong, D.F., *Metallogeny and plate tectonics*: *Geol. Assoc. Can., Spec. Paper 14*, p. 59-100.
- Simons, F.S., and Munson, E., 1963, Johannsonite from the Aravaipa mining district Arizona: *Am. Mineral.*, 48, p. 1154-1168.
- Soji, T., 1978, Genetical problems of skarn formation, in Imai, H., ed., *Geological studies of the mineral deposits of east Asia*, Univ. of Tokyo Press, p. 201-212.
- Solomon, M., 1965, Geology and mineralization of Tasmania, in McAndrew, J., ed., *Geology of Australian ore deposits*, 2nd ed.: 8th Comm. Mining & Metall. Congr., Melbourne, p. 464-477.
- Sorenson, R.E., 1927, The geology and ore deposits of the South Mountain Mining District, Owyhee County, Idaho: *Idaho Bureau of Mines and Geology*, Pamphlet No. 22, p. 47.
- Spurr, J.E., 1923, *The ore magmas*, McGraw-Hill, New York, p. 728-730.
- Spurr, J.E., Garrey, G.H., and Fenner, C.N., 1912, Study of a contact metamorphic ore deposit, the Dolores mine at Matchuala, S.L.P., Mexico: *Econ. Geol.*, v. 7, p. 444-484.
- Stone, J.G., 1959, Ore genesis in the Naica district, Chihuahua, Mexico: *Econ. Geol.*, 54, p. 1002-1034.
- Tan, T.H. and Kwak, T.A.P., 1979, The measurement of the thermal history around the grassy granodiorite, King Island, Tasmania by the use of fluid inclusion data: *J. Geol.*, v. 87, p. 43-54.
- Taylor, B.E., 1976, Origin and significance of C-O-H fluids in the formation of Ca-Fe-Si skarn, Osgood mtns., Humbolt Co., Nevada: Unpubl. Ph.D. Dissertation, Stanford University, 149 pp.

- Taylor, H.P., 1974, The application of oxygen and hydrogen isotope studies to problems of hydrothermal alteration and ore deposition: Econ. Geol., v. 69, p. 483-883.
- Titley, S.R., 1961, Genesis and control of the Linchburg orebody, Socorro County, New Mexico: Econ. Geol., v. 56, p. 695-722.
- Wardke, A. and Moore, T.G., 1935, Pyrometasomatic vein deposits at Tepezala, Aguascalientes, Mexico: Econ. Geol., v. 30, p. 765-782.
- Wilson, J.C., 1978, Ore fluid-magma relationships in a vesicular quartz latite porphyry dike at Bingham, Utah: Econ. Geol., v. 73, p. 1287-1307.
- Yun, S., 1979, Geology and skarn ore mineralization of the Yeonhwa-Ulchin zinc-lead mining district, SE Tagbaggsan region Korea: Unpubl. Ph.D. Dissertation, Stanford University, 184 pp.
- Zharikov, V.A., 1970, Skarns: Internat. Geol. Rev., v. 12, p. 541-559, 619-647, 760-775.

Paleozoic stratabound lead-zinc-copper deposits in the
western United States

Half Zantop, Dartmouth College

Paleozoic Stratabound Pb-Zn-Cu Deposits in the Western United States?

ZANTOP, Half, Department of Earth Sciences, Dartmouth College
Hanover, N.H. 03755

Abstract

Stratabound and stratiform Pb-Zn-Cu deposits of Precambrian to Mesozoic age have in the last decade been discovered in the Canadian and Alaskan segments of the North American Cordillera. Types of deposits and genetic interpretations range from volcanogenic proximal and distal to carbonate-hosted dia/epigenetic, shale-hosted syn/diagenetic, and sabhka type.

These discoveries raise the question as to whether or not some of the stratabound and stratiform deposits in Paleozoic rocks of the western and southwestern United States, traditionally referred to as Laramide "bedded replacement deposits", may also have formed by volcanic-distal, sedimentary, diagenetic or basin forming processes prior to Laramide magmatism. The stratigraphic control of some of these deposits, their conformity with surrounding sediments, and their setting in rocks formed in transgressive, shallow marine environments, are analogous to the settings of some non-magmatic, carbonate-hosted and shale-hosted base metal deposits of Mississippi Valley/Alpine and Kupferschiefer/Zambian Cu-type affinity.

A re-interpretation of the mode of formation of stratabound and stratiform deposits in the western and southwestern United States is made difficult by the intense tectonic and intrusive overprint such deposits would have received, particularly during the Laramide orogeny. However, a detailed examination of their stratigraphic and sedimentologic setting, composition, and zoning may well provide the evidence needed to determine whether they are Laramide, formed during magmatic-hydrothermal activity, or Paleozoic, formed during sedimentary basin formation, with or without volcanic contributions.

Introduction

Precambrian to Mesozoic, stratabound and stratiform deposits of Pb-Zn-Cu have in recent years been discovered in the North American Cordillera from Alaska southward to Montana and Idaho. Types of deposits include volcanogenic (Hitzman, 1980; Lange et al., 1980), carbonate-hosted epigenetic (Macqueen, 1976; McLaren and Godwin, 1978; Godwin et al., 1980; Mackevett et al., 1980), shale-hosted syn/diagenetic (Godwin et al., 1980), and sabkha-type (Ruelle, 1978).

The discovery of stratabound and stratiform deposits in the northern Cordillera has awakened an intense interest in deposits

not directly associated with intrusive-magmatic activity in western North America. This paper is an attempt to apply the types of criteria used to interpret the mode of formation of the deposits in the northwestern Cordillera to the interpretation of some stratabound and stratiform ore deposits in the western and southwestern United States.

Ever since mining began in the western United States, the bulk of Cu production came from porphyry copper, skarn and vein deposits, and most of the Pb-Zn-Ag production from veins and tabular bedded deposits or "mantos". The spatial and genetic relationship of many major mining districts to intrusive rock is striking and was convincingly presented e.g. by Stringham (1958). Loughlin (1941) and, more recently, Robyn et al. (1980) suggested a structural control of both igneous activity and mineralization, and it is apparent that both tectonics and intrusive activity were essential to the formation and present makeup of most base metal deposits in the western United States. It remained - and remains - a puzzle why many compositionally and texturally favorable intrusives are not mineralized, and why some mining districts do not appear to be spatially related to intrusive rock.

In addition to the structural and intrusive controls, a strong stratigraphic control of mineralization is apparent in the western and southwestern United States. In individual mining districts, this control has been used as a guide in exploration for many years. The nature of this control, its significance for exploration, and its possible genetic implications have been stressed recently, e.g. by Callahan (1977) for the Cordilleran deposits from Alaska southward to northeastern Mexico, by Wertz (1971), Eyde (1972), and Gilmour (1978) for some districts in Arizona and New Mexico, and by James et al. (1979) for the Pioche district in Nevada. As a world-wide phenomenon, such stratigraphic control lead Knight (1957) to develop and present his "source bed concept".

Stratabound and stratiform mineralization in the western and southwestern United States has traditionally been thought of as Laramide, magmatic hydrothermal replacement of favorable sedimentary host rocks, even though it was not always apparent why a particular sedimentary horizon should be replaced in preference of another, or why some stratabound mineralization is found far from any intrusive center to which it might be genetically related. The question arising here is: are there chemical, textural, or paleogeographic factors which have made some sedimentary units particularly receptive for replacement, or may some deposits be pre-intrusive, related to Paleozoic exhalative, sedimentary and/or basin-forming processes similar to those held responsible for the formation of Mississippi Valley/Alpine-type and Kupferschiefer/Zambian-type deposits? If there are pre-Laramide stratabound/stratiform deposits, they would have been so profoundly affected by Laramide structural and intrusive overprint, and by renewed

skarn- and vein-type ore formation in the same metallogenic province (cf. Rye and Rye's discussion of Precambrian and Tertiary mineralization in the Homestake Gold Mine, South Dakota) that their original characteristics and mode of formation would be difficult to reconstruct unequivocally.

Two types of stratabound deposits are of primary interest in the discussion of Laramide and possibly pre-Laramide deposits: (a) skarn deposits, closely associated with intrusives, and (b) "bedded replacement deposits" or "mantos", for which the relationship to intrusives is not so apparent. To contrast the two types of deposits: the skarn deposits are adjacent to intrusives (or to tectonic channels for hydrothermal solutions), and are zoned outward from them. The copper-rich aureole around the Bingham stock, e.g. at the Carr Fork mine in Utah (Atkinson and Einaudi, 1978; Reid, 1978) shows the characteristic setting of skarn mineralization. The sulfide aureole has a large vertical extent, over 5000 feet, and a smaller lateral extent, about 2000 feet away from the intrusive. Intense hydrothermal alteration is evident and affects all rocks in the section. Mineralization is best developed in recrystallized, massive, clean limestones and dolomites. The manto-type deposits, on the other hand, tend to be tabular, elongate or ribbon-shaped, and they are less distinctly zoned. Rocks stratigraphically below and above mineralization are often not altered, and mineralization is preferably in thin, impure, argillaceous and carbonaceous limestones and dolomites. The mineralized rocks often overlie basal sandstones and shales, at the base of thick carbonate or carbonate-shale sequences. The Pan-American and Caselton mines in the Pioche district, Nevada, and the Silver King mine in the Park City district, Utah, are good examples of stratabound, "manto" type deposits. These deposits are 1000's of feet long, several 100 feet wide, and only 10's of feet thick. They are in stratigraphic conformity with the surrounding sediments, and there is no clear spatial or genetic relationship of mineralization to intrusive rock.

While mineralization in the skarns is evidently controlled by magmatic-hydrothermal activity and involves replacement, the mineralization in "manto type" deposits is not so easily explained by hydrothermal activity, and textural and compositional evidence for replacement is often lacking. Two major unresolved questions with respect to replacement in mantos are: (a) what rock type has been replaced, and what geochemical processes are involved in the replacement? Compositionally, host rocks for manto mineralization range from limestones and dolomites to sandstones, graywackes and shales; and (b) why are only some, often very thin layers in the stratigraphic section of many mining districts mineralized, while chemically and physically similar layers, which should be equally susceptible to replacement, are barren? These unresolved questions, and the analogies between some mantos in the western U.S. and sedimentary/diagenetic deposits elsewhere, lead to consideration of the working hypothesis presented here: that some of

the "bedded replacement deposits" or "mantos" may not represent "magmatic hydrothermal replacement", but may have formed by non-intrusive (but possibly volcanic), exhalative, sedimentary and basin-forming processes like those responsible for the mineralization in some of the stratabound base-metal deposits found e.g. in the northern Cordillera of Canada and Alaska. Our rapidly growing knowledge of stratabound/stratiform ores, and of their relationships to sedimentary environments, diagenesis and basin formation, can provide the clues which are needed to support or to dismiss this hypothesis as applied to the interpretation of individual manto deposits in the western and southwestern United States.

In order to compare the Pb-Zn-Cu mantos with non-magmatic, stratabound deposits elsewhere, they will be divided into two categories: (a) carbonate-hosted Pb-Zn-(Ag) mantos with minor Cu, i.e. "Mississippi Valley/Alpine-type" analogues, and (b) clastic and carbonate-hosted Cu mantos with minor Pb, Zn and Ag, or "Kupferschiefer/Zambian Cu-Belt-type" analogues.

Carbonate-Hosted Pb-Zn-(Ag) Deposits

The carbonate hosted Pb-Zn deposits comprise a range of settings and compositions, as represented by the Mississippi Valley, Pine Point, Alpine, and Irish deposits. They range from stratabound to stratiform, from coarse-grained to fine-grained, and from low to high Cu and/or Ag. Callahan (1977) has described the stratigraphic setting of Mississippi Valley-type deposits, stressing the relationship of sites of mineralization to unconformities, as shown in Fig. 1: (a) deposits above an unconformity, related to old shorelines, reef complexes, and basement highs, the "Type A sites"; (b) deposits below an unconformity, related to solution cavities, paleokarsts and collapse breccias, the "Type B sites"; and (c) deposits related to facies changes, e.g. limestone-dolomite and limestone-shale, the "Type C sites". Deposits of "Type A" or "Type C" settings are linear, thousands of feet long, tens to hundreds of feet wide, and tens of feet thick, parallel to paleophysiographic features like shorelines, reefs or paleochannels. The "Type A" deposits are stratiform rather than stratabound, and mineralization appears to be syn/diagenetic as shown by sedimentary textures and structures in the ores (Callahan, 1977). Mineralizations in the "Type B sites", and in some "Type C sites" related to limestone-dolomite facies changes, reflect control by subsurface drainage and may be of any age relative to the host rock, early diagenetic to epigenetic. Callahan (1977) suggests that stratabound/stratiform Pb-Zn-(Ag) ores in several mining districts in the western and southwestern United States have formed in "Type B" settings, e.g. ores in the Metaline district in Washington State, the Goodsprings district in Nevada, the East Tintic district in Utah, the Gilman-Leadville district in Colorado, the Johnson Camp district in Arizona, and the Hanover district in New Mexico.

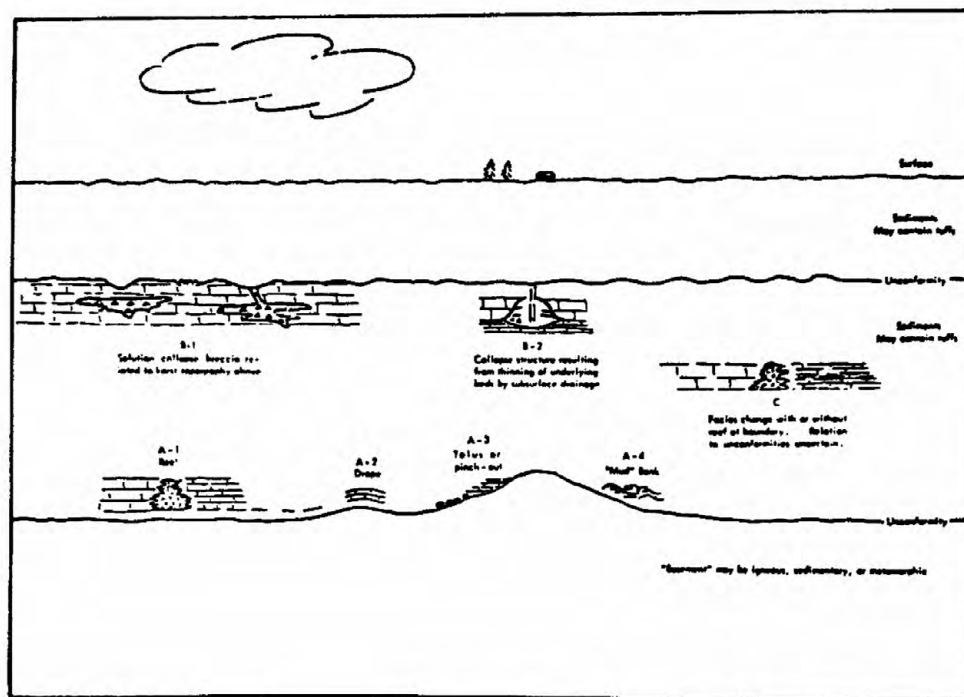


Fig. 1. Idealized vertical section illustrating the features responsible for the localization of Mississippi Valley type mineral deposits (From Callahan, 1977).

This paper emphasizes the possibility of Pb-Zn-(Ag) deposits related to a basal unconformity, the "Type A" sites, in the western and southwestern United States.

Common to non-magmatic ores in this setting is that they formed in shallow marine environment, under reducing conditions, and in areas of slow sedimentation (Bernard and Samama, 1976). It appears that the base metals were introduced in the time interval from sedimentation to late diagenesis, and that their concentration is a result of normal sedimentary basin formation (Macqueen, 1978). The influence of transgression and of basin highs in the genesis of such base metal concentrations is well illustrated in many Mississippi Valley-type and Kupferschiefer/Zambian-type deposits. The transgressive sequences sandstone-shale-carbonate or sandstone-carbonate with attendant Pb-Zn-(Ag) mineralization is common in Mississippi Valley-type deposits above an unconformity. The role of "active basement highs", formed by faulting (e.g. growth faulting), upwarp or reef development, in the formation of stratiform base metal deposits was stressed by Bernard and Samama (1976). The sedimentary succession over the "active" basement high is from clastic to carbonate, as shown in Fig. 2: an upward-fining sequence of clastic rocks, grading into calcareous shales and marls, and finally into dolomites and limestones. A transitional facies often develops between the clastic and the carbonate sedimentation: a facies of bituminous, sulfide-rich shales, marls and dolomites with associated cherts and other colloidal precipitates. Provided an adequate supply of base metals, this sedimentary environment provides an effective trap for ore formation.

Let us compare these sedimentary settings with the settings of some stratabound, carbonate-hosted "mantos" in the western and southwestern United States: the Pan American and Caselton mines in the Pioche district, Nevada, and the Silver King mine in the Park City district, Utah.

The Pioche Zn-Pb-Ag district has been described in much detail by Gemmill (1968), and its genesis has recently been re-interpreted by James and Knight (1979) and by Shanks et al. (1979). Mineralization is largely confined to the "Combined Metals Bed" (Fig. 3) of the Cambrian Pioche Shale, a deltaic shale-limestone sequence (James and Knight, 1979). The Pioche Shale overlies the Prospect Mountain Quartzite unconformably, and is at the base of a limestone-dolomite-shale section of over 6000 feet thickness. The Combined Metals Bed is an impure, carbonaceous limestone less than 100 feet thick. In the Caselton area, continuous mineralization is found within this thin stratigraphic interval over a length of more than 9000 feet and a width of 700 feet. Detailed sections of the Combined Metals Bed show that some of the richest mineralization is restricted to beds less than 3 feet thick (Gemmill, 1968). No hydrothermal alteration is apparent in the associated, non-mineralized beds, and the only igneous rock in the area, the Yuba dike, shows no obvious genetic relationship to mineralization.

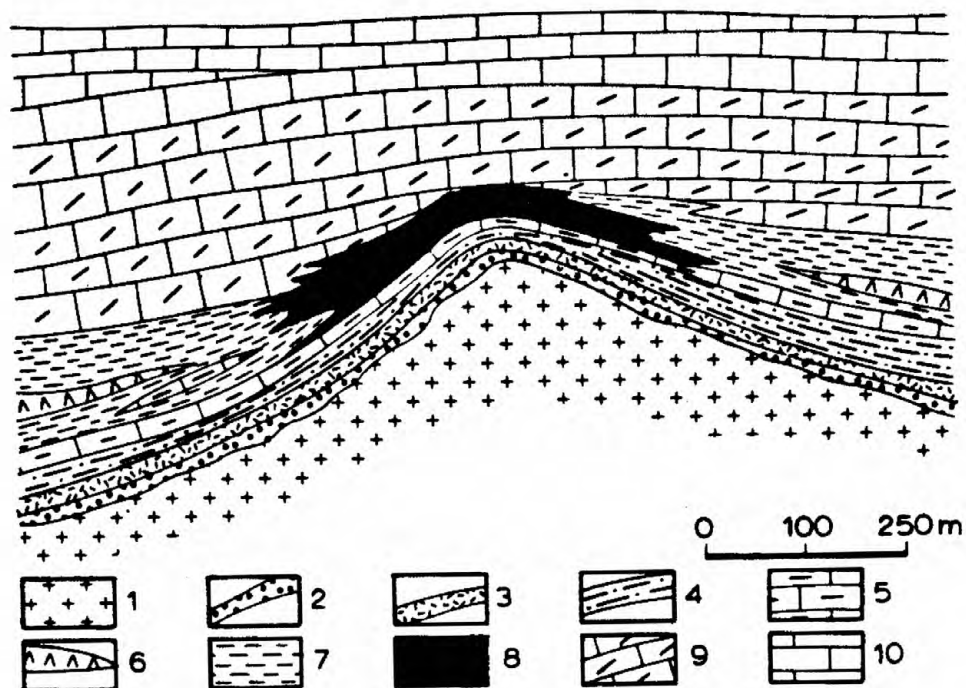
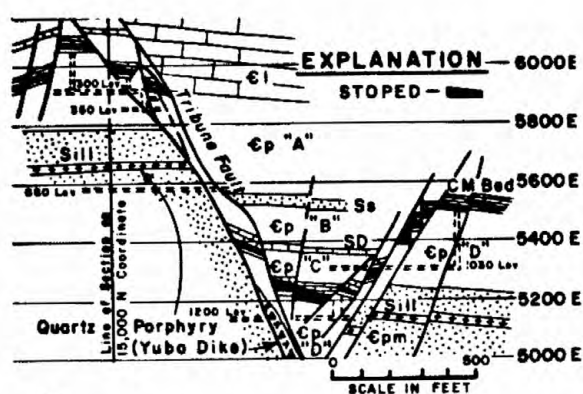


Fig. 2. The St. Felix de Pailleres buried hill at the end of the Sinemurian. 1 = Hercynian basement: granite; 2 = fluvial conglomerate: Buntsandstein; 3 = blanket arkose; 4 = marls and evaporites: Lower Saliferous; 5 = marine dolomite: Muschelkalk; 6 = marls and evaporites: Upper Saliferous; 7 = variegated marls: Upper Keuper and Rhaetian; 8 = bituminous and metalliferous shales and dolomites; 9 = Hettingian dolomites; 10 = Sinemurian limestones. (From Bernard and Samama, 1976).



A

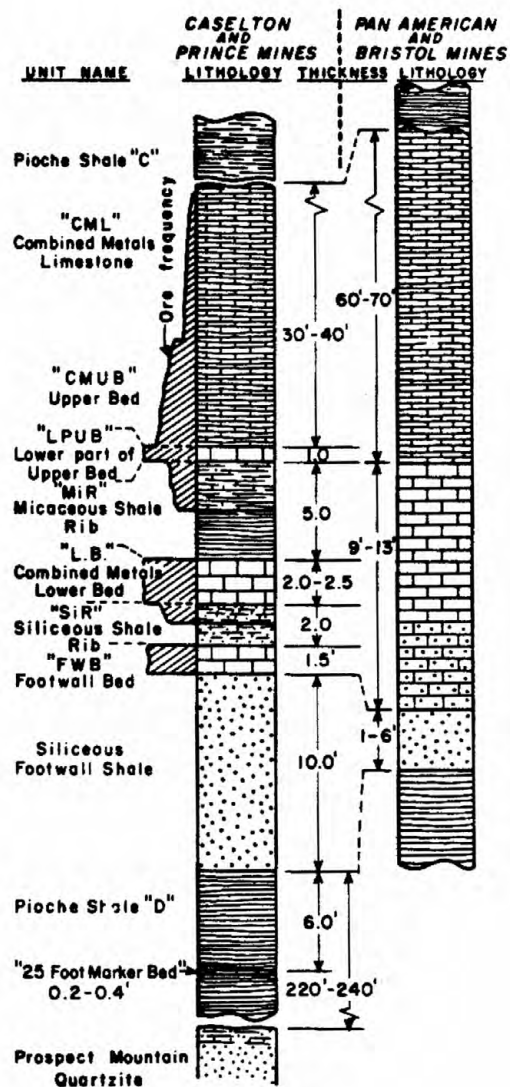


Fig. 3. Geologic cross section and stratigraphic setting of mineralization in the Pioche District, Nevada. (From Gemmill, 1968).

(James and Knight, 1979). Stratigraphically, the mineralization is in carbonaceous carbonates, above a basal clastic sequence, and close to the base of a thick shale-carbonate section. The setting thus conforms to a transgressive, shallow marine sequence as described above. Recent geochemical and paleomagnetic studies (Shanks et al., 1979) suggest that the sulphur in the Pan American sulfides is not of magmatic source, and that mineralization happened not long after deposition of the surrounding sediments. James and Knight (1979) propose that the Pan American mine in the Pioche district may represent "a western variant of the Mississippi Valley ore genesis process", and the Caselton mine a tidal channel mineralized by "upgrading of Pan American type ores by later heated fluids".

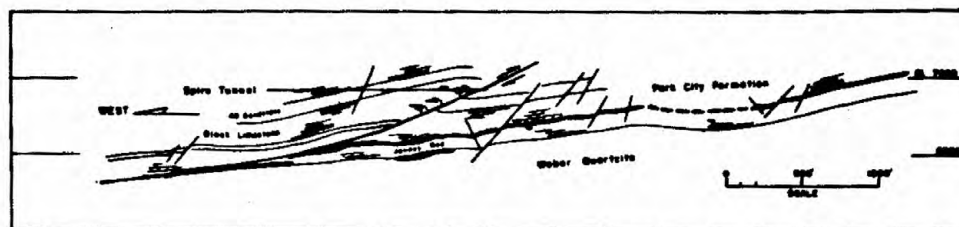
The stratigraphic sequence at the Silver King Pb-Zn-Ag mine in the Park City district, Utah, shows a similarly transgressive setting of mineralization (Fig. 4). Here, the thin Jenny bed of Pennsylvanian age overlies a basal sandstone, the Weber sandstone. Mineralization is confined to the Jenny bed in a narrow, thin belt about 10,000 feet long and in stratigraphic conformity with the surrounding sediments (Barnes and Simos, 1968). The sedimentary rocks that envelope mineralization are fresh and unaltered, even in close proximity to the ore, and the only igneous rock present, a diorite porphyry dike, appears to be unrelated to ore (Barnes and Simos, 1968).

These examples of deposits in apparent "Type A sites" show some characteristics which are common to Cordilleran "mantos" and non-magmatic carbonate-hosted ores elsewhere: (a) ribbon shape or elliptical shape, possibly parallel to paleo-shorelines, basin highs, or tidal channels; (b) stratigraphic setting above unconformities; (c) facies control by shallow-marine, organic-rich dolomites and limestones; (d) Pb and Zn as the main metals, and, in the case of the Cordilleran deposits, Ag as an important by-product; (e) no apparent hydrothermal alteration of over- and underlying rocks, and (f) no clear genetic relationship to intrusive magmatic activity.

The fact that the carbonate-hosted ores as we see them today show the effects of intense Tertiary structural, magmatic and metallogenic overprint in most districts in no way detracts from their stratigraphic and paleogeographic control, and from the exploration- and genetic implications this control may have.

Stratabound/Stratiform Copper Deposits

The carbonate-hosted deposits discussed above contain Pb, Zn and minor Ag as main ore metals. Much more complex because of intense tectonism and magmatism are some Fe- and Cu-bearing mantos in central Arizona. Here, the lower Martin Formation is host to important stratabound/stratiform Cu mineralization with minor Pb, Zn and Ag, e.g. in the Magma mine, Superior (Hammer and Peterson, 1968), and in the Christmas mine, in the southern reaches of the



Geologic cross section

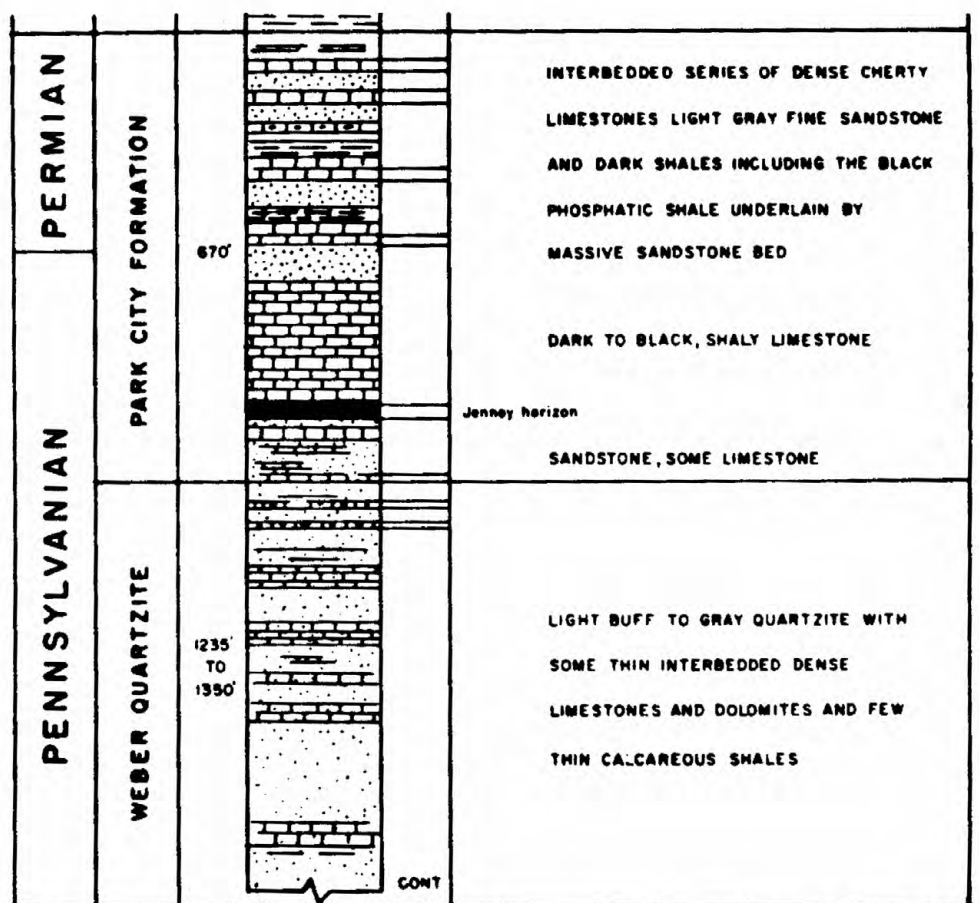


Fig. 4. Geologic cross section and stratigraphic setting of mineralization in the Silver King mine, Utah. (From Barnes and Simos, 1968).

Dripping Springs Mountains (Eastlick, 1968). The lower Martin Formation is of Devonian age and is part of a transgressive, shallow-marine sequence, deposited over Cambrian and Precambrian quartzites (Teichert, 1965). The Devonian sediments unconformably overlie Precambrian and Cambrian quartzites and sandstones; they grade from basal, fine-grained sandy to shaly, calcareous clastics to overlying dolomites and limestones. In both districts, the Cu-mineralization is associated with abundant iron as magnetite, hematite, and pyrite. The presence of sedimentary, hematitic iron oxides in this unit was described by Willden (1960), and old Cu-Ag prospects are common in the lower Martin Formation throughout central Arizona (Eastlick, 1968).

The stratigraphic setting of the Cu mineralization is well illustrated in the Magma mine (Fig. 5), which has both rich veins and stratabound "mantos", the latter mainly in the Lower Martin Formation. The vein- and manto mineralizations were described by Hammer and Peterson (1968), Gustafson (1962), and Sell (1961). The mineralized manto is from 6 to 30 feet thick and lies about 20 feet above a basal unconformity with the Precambrian Troy Quartzite and, locally, Cambrian sandstone. The intervening beds are limy sandstones, quartzites, and limestones. According to Sell (1961), the "replacement horizon" is either completely replaced or completely barren, and no "replacement features" are recognized. Mineralization appears to be controlled by northeast- and east striking normal faults which were active from Precambrian time through the Paleozoic and Mesozoic (Hammer and Peterson, 1968). Where the mineralization abuts against surrounding rock, the contact is sharp. The laterally adjacent rock is a medium grey, fine to medium crystalline limestone (Sell, 1961). The main ore minerals are chalcopryite, bornite, and chalcocite, in a gangue dominated by hematite and pyrite. A clear zoning pattern has not been established, but hematite forms the fringes of some of the mineralization.

The Christmas mine, which lies about 30 miles southeast of the Magma mine, combines several types of mineralization (Fig. 6): porphyry copper and vein mineralization related to dioritic and dacitic intrusives in its upper levels, skarn mineralization in close spatial association with intrusive in Pennsylvanian and Mississippian limestones and dolomites; and stratabound-stratiform mineralization extending farther out from the intrusive, particularly in the O'Carroll bed of the lower Martin Formation. The geology of the Christmas mine is discussed in much detail by Eastlick (1968), Perry (1969), and Koski (1978). The mineralization in the lower Martin Formation has characteristics which are quite distinct from those of the mineralizations higher in the section. The mineralized layer is about 5 to 10 feet thick on average and lies above a basal unconformity with Cambrian quartzites (Eastlick, 1968), at the transition of shaly to dolomitic sedimentation. Close to the intrusive, mineralization spreads upward and affects a greater thickness of the Martin Formation. The

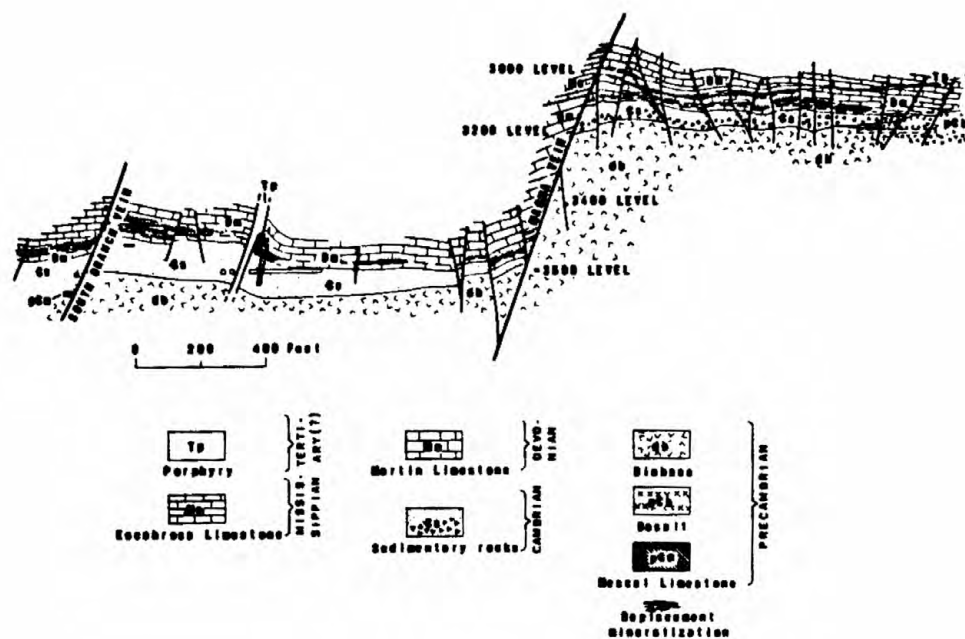


Fig. 5. Vertical North-trending section looking west, Magma Mine, Arizona. (From Hammer and Peterson, 1968).

mineralized unit contains abundant iron oxides, mainly magnetite, and pinches out laterally. Ore minerals are bornite and chalcocopyrite, with minor galena and sphalerite. The gangue is distinct from that higher up in the section in that it has a higher Mg content, reflected by the presence of dolomite, magnesian olivine, and serpentine. This high Mg content may be an indication of a pre-evaporitic setting in the sedimentary environment in which the host rocks to the manto formed. At an outcrop about four miles west of the Christmas mine, the London/Arizona area, the mineralized lower Martin is about 6 feet thick and shows convolute laminations composed of magnetite, silty dolomite, and very minor Cu oxides. These appear to be stromatolites, sedimentary structures which form by biogenic sediment trapping in shallow marine, reefal, pre-evaporitic or evaporitic environments.

In both the Magma and Christmas mines, the composition of the stratabound/stratiform ore in the lower Martin Formation (Fe-Cu with minor Pb, Zn and Ag), its mineralogy (hematite/magnetite, chalcocite, bornite, chalcocopyrite, pyrite), and its stratigraphic setting above a basal unconformity, in a sequence of fine-grained clastics and carbonates, are reminiscent of Kupferschiefer/Zambian-type deposits formed in a pre-evaporitic setting, or in a sabkha-setting as described by Renfro (1974). Because of the structural and intrusive complexities, the suggestion that the high Fe-content of the ores in the lower Martin Formation may correlate stratigraphically with the sedimentary Fe reported by Willden (1960), and that some of the Cu may also be pre-Laramide, is highly speculative at this point, but deserves closer scrutiny.

Conclusions

The examples given above show that some of the stratabound and stratiform deposits in the western and southwestern United States have stratigraphic, sedimentary, and compositional characteristics which are similar to those of Mississippi Valley/Alpine-type and possibly Kupferschiefer/Zambian-type deposits. These types of deposits are not related to intrusive magmatic activity and replacement, but are thought to have formed during basin-forming processes, with or without exhalative contributions of base metals, spanning the time from sedimentation to late diagenesis. Considering that no magmatic-intrusive activity was needed to produce such deposits, and that the strictly stratabound and stratiform mineralization over large areas would be more easily achieved while the sediments were still poorly consolidated, permeable, and water-rich, it is suggested that the primary formation of some of the stratabound deposits in the western United States may be related to Paleozoic sedimentary and basin forming processes rather than to Laramide magmatism. The occurrence of vein- and skarn deposits close to or in association with some of these stratabound ores may be a reflection of (a) tectonic and magmatic-hydrothermal overprint of pre-existing stratabound deposits, and (b) superposition of both pre-Laramide mineralization related to basin development, and Laramide mineralization

related to intrusive activity, both controlled by deep crustal fracture zones which were active from the Precambrian through the Mesozoic. Existence of such fracture zones was suggested by Loughlin (1941) and by Robyn et al. (1980) for the western United States, and for the E-NE set of faults in the Magma mine by Hammer and Peterson (1968).

The evidence given here is permissive rather than compelling. Tectonic zones of weakness may provide channelways for mineralizing solutions and for emplacement of intrusives at different times. Likewise, many of the stratigraphic and sedimentologic characteristics of the ores, e.g. setting above thick sandstone/quartzite units, and shallow-marine deposition and high organic content of the sediments containing mineralization, may be interpreted as indicating favorability of sedimentary conditions for the deposition of the ores during basin formation, or as factors rendering the stratigraphic sequence favorable for migration of hydrothermal solutions and consequent replacement.

In order to assess the hypothesis of Paleozoic formation of some of these ores - not an easy task in view of the structural, metamorphic and magmatic complexities of many of the mining districts - the following investigations are suggested: (a) paleomagnetic timing of the emplacement of the ores, as suggested by Callahan (1977), and as carried out in the Pioche district by Shanks et al. (1979); (b) detailed stratigraphic, sedimentologic, and paleophysiographic studies of the "mantos" and of their host rocks; and (c) compositional and stable isotope studies in which an effort is made to contrast intrusive and tectonically controlled skarn and vein mineralization on one hand, and stratigraphically controlled manto mineralization on the other. Such studies may provide clues as to the timing and mode of emplacement of manto mineralization in individual mining districts, and help to substantiate or to dismiss the working hypothesis presented here.

References

- Atkinson, Jr., W.W., and Einaudi, M.T., 1978, Skarn formation and mineralization in the contact aureole at Carr Fork, Bingham, Utah: *Econ. Geol.*, v. 73, p. 1326-1365.
- Barnes, M.P., and Simos, J.G., 1968, Ore deposits of the Park City District: Graton-Sales Volume, John D. Ridge, ed., p. 1102-1126.
- Bernard, A.J., and Samama, J.C., 1976, Summary of the French school of studies of ores in sedimentary and associated volcanic rocks - epigenesis vs. syngeneses, in: *Handbook of stratabound and stratiform ore deposits*, K.H. Wolf, ed., v. 1, p. 299-333.
- Callahan, W.H., 1977, Some thoughts regarding premises and procedures for prospecting for base metal ores in carbonate rocks in the North American Cordillera: *Econ. Geol.*, v. 72, p. 71-81.
- Eastlick, J.T., 1968, Geology of the Christmas mine and vicinity, Banner Mining District, in: Graton-Sales Volume, John D. Ridge, ed., p. 1191-1210.
- Eyde, T.H., 1972, Stratigraphy is a sometimes overlooked guide to porphyry coppers: *Mining Engineering*, v. 24, No. 4, p. 40-42.
- Gemmill, Paul, 1968, The geology of the ore deposits of the Pioche District, Nevada, in: Graton-Sales Volume, John D. Ridge, ed., p. 1128-1147.
- Gilmour, P., 1978, Some thoughts regarding premises and procedures for prospecting for base metal ores in carbonate rocks in the North American Cordillera - A discussion: *Econ. Geol.*, v. 73, p. 287.
- Godwin, C.I., Sinclair, A.J., and Ryan, B.D., 1980, Lead isotope models for the genesis of carbonate-hosted Zn-Pb, shale-hosted Zn-Pb-Ba, and Ag-rich deposits, Y.T. and adjacent N.W.T., northern Canadian cordillera: This volume.
- Gustafson, L.B., 1961, Petrogenesis and hypogene zoning at the Magma mine, Superior, Arizona, unpublished Ph.D. thesis, Harvard University.
- Hammer, D.F., and Peterson, D.W., 1968, Geology of the Magma mine area, Arizona, in: Graton-Sales Volume, John D. Ridge, ed., p. 1282-1310.
- Hitzman, W.M., 1980, Geology of the B.T. claim group, southwestern Brooks Range, Alaska: This volume.
- James, L.P., and Knight, L.H., 1979, Stratabound Pb-Zn-Ag ores of the Pioche District, Nevada - unusual "Mississippi Valley" deposits?: RMAG UGA - 1979 Basin and Range Symposium, p. 389-395.
- Knight, C.L., 1957, Ore genesis - the source bed concept: *Econ. Geol.*, v. 52, p. 808-817.
- Koski, R.A., 1978, Geology and porphyry copper-type alteration-mineralization of igneous rocks at the Christmas Mine, Gila County, Arizona: Ph.D. thesis, Stanford University.
- Lange, I.M., Nokleberg, W.J., Plahuta, J.T., Krouse, H.R., Doe, B., and Jansons, U., 1980, Geochemistry of volcanogenic Zn-Pb-Ba deposits, NW Brooks, Ak: This volume.

- Loughlin, G.F., 1941, Comments on the origin and major structural control of igneous rocks and related mineral deposits: *Econ. Geol.*, v. 36, p. 671-697.
- Macqueen, R.W., 1976, Sediments, zinc and lead, Rocky Mountain Belt, Canadian Cordillera: *Geosci. Canada*, v. 3, p. 71-81.
- Macqueen, R.W., 1978, Base metal deposits in sedimentary rocks: some approaches: *Geosci. Canada*, v. 6, p. 3-9.
- MacKevett, Jr., E.M., Armstrong, A.K., Potter, R.W., Silberman, M.L., 1980, Kennicott-type copper deposits, Wrangell Mountains, Alaska - an update and summary: This volume.
- McLaren, G.P., and Godwin, C.I., 1978, Minor elements in sphalerite from carbonate-hosted zinc-lead deposits, Yukon Territory and adjacent district of Mackenzie, Northwest Territories.
- Nokleberg, W.J., Plahuta, J.T., and Lange, I.M., 1979, Volcanogenic zinc-lead-barite deposits in pelagic rocks of late Paleozoic and early Mesozoic age, Northwestern Brooks Range, Alaska: *GSA, Abstracts with Programs*, p. 487.
- Perry, D.V., 1969, Skarn genesis at the Christmas mine, Gila County, Arizona: *Econ. Geol.*, v. 64, p. 255-270.
- Reid, J.E., 1978, Skarn alteration of the Commercial Limestone, Carr Fork area, Bingham, Utah: *Econ. Geol.*, v. 73, p. 1315-1325.
- Renfro, A.R., 1974, Genesis of evaporite-associated stratiform metalliferous deposits - a sabkha process: *Econ. Geol.*, v. 69, p. 33-45.
- Robyn, T.L., Henage, L.F., and Hollister, V., 1980, Possible non-subduction associated porphyry ore deposits, Pacific Northwest: This volume.
- Ruelle, J.C.L., 1978, Depositional environment and genesis of stratiform copper deposits of the Redstone copper belt, Mackenzie Mountains, N.W.T.: *Geol. Soc. Am. (Abstracts)*, p. 482-483.
- Rye, D.M., and Rye, R.O., 1974, Homestake Gold Mine, South Dakota: I. Stable isotope studies: *Econ. Geol.*, v. 69, p. 293-317.
- Sell, J.D., 1961, Bedding replacement deposits of the Magma mine, Superior, Arizona: M.S. thesis, The University of Arizona.
- Shanks, W.C., Martin, D.L., and Inden, R.E., 1979, Timing and tectonic setting of ore formation, Pan American Mine, Pioche, Nevada: *Geol. Soc. America, Abstracts with Programs*, p. 515.
- Stringham, B., 1958, Relationship of ore to porphyry in the Basin and Range province, USA: *Econ. Geol.*, v. 53, p. 806-822.
- Teichert, C., 1965, Devonian rocks and paleogeography of central Arizona: *United States Geol. Surv. Prof. Paper* 464, 181 p.
- Wertz, J.B., 1971, Apparent stratigraphic control of some copper mining districts in southeast Arizona: *Mining Engineering*, v. 23, No. 11, p. 53-54.
- Willden, R., 1960, Sedimentary iron formation in the Devonian Martin Formation, Christmas Quadrangle, Arizona: *United States Geol. Survey Prof. Paper*, 400-B, B21-B23.

USGS LIBRARY-RESTON



3 1818 00070416 1